UNITED STATES
SECURITIES AND EXCHANGE COMMISSION

Washington, D.C. 20549

Form 6-K

REPORT OF FOREIGN PRIVATE ISSUER
PURSUANT TO RULE 13a-16 OR 15d-16
UNDER THE SECURITIES EXCHANGE ACT OF 1934

For the month of: March 2026

Commission file number: 001-38350

Lithium Argentina AG

(Translation of Registrant's name into English)

Dammstrasse 19, 6300 Zug,
Switzerland
(Address of Principal Executive Office)

900 West Hastings Street, Suite 310,
Vancouver, British Columbia,
Canada V6C 1E5

(North American Mailing Address)

Indicate by check mark whether the registrant files or will file annual reports under cover:

Form 20-F ☒ Form 40-F ☐

SIGNATURE

Pursuant to the requirements of the Securities Exchange Act of 1934, the registrant has duly caused this report to be signed on its behalf by the undersigned, thereunto duly authorized.

Lithium Argentina AG
(Registrant)

By: *"Samuel Pigott"*
Name: Samuel Pigott
Title: Chief Executive Officer

Dated: March 20, 2026

EXHIBIT INDEX

Exhibit	Description
99.1	S-K 1300 Technical Report at the PPG Salars, Salta Province, Argentina, dated effective December 31, 2025

Exhibit 99.1

LithiumArgentina

S-K 1300 TECHNICAL REPORT
Scoping Study Report
At the PPG Salars,
Salta Province, Argentina

Prepared by:
WSP Golder
Atacama Water

Effective Date: December 31, 2025
Filing Date: March 19, 2026

Distribution List

Table of Contents

1.0	**EXECUTIVE SUMMARY**	**2**
1.1	Introduction	2
1.2	Property Location, Description and Ownership	2
1.3	Accessibility, Climate, Local Resources, Infrastructure and Physiography	2
1.4	Geological Setting and Mineralization	3
1.4.1	Pozuelos	4
1.4.2	Pastos Grandes	4
1.5	Deposit Types	5
1.5.1	Pozuelos	5
1.5.2	Pastos Grandes	5
1.6	Exploration and drilling	6
1.6.1	Pozuelos	6
1.6.2	Pastos Grandes	6
1.7	Metallurgical Testing	7
1.8	Mineral Resource Estimates (Effective Date: December 31, 2025)	8
1.8.1	Pozuelos	8
1.8.2	Pastos Grandes	9
1.8.3	Hydrologic Dynamic Modelling	10
1.9	Mineral Reserve Estimate	11
1.10	Mining Methods	11
1.10.1	LCE Production Schedule	12
1.11	Recovery Methods	13
1.12	Process Description	13
1.12.1	Solar Evaporation Ponds	14
1.12.2	Brine Processing	14
1.13	Site Infrastructure	15
1.14	Market Studies and Contacts	15
1.15	Environmental Studies, Permitting, Social and Community Impact	16
1.15.1	Mine Closure and Reclamation Plans	16
1.16	Capital and Operating Costs	17
1.16.1	Capital Cost Estimate	17

1.16.2 Operating Costs Estimate 18
1.16.3 RIGI Economics 19
1.17 Economic Analysis 20
1.17.1 Sensitivity Analysis 21
2.0 INTRODUCTION 22
2.1 Background 22
2.2 Source of Information 23
2.3 Authorization and Purpose 23
2.4 Report Responsibility Matrix 24
2.5 Property Inspection and Statement of Independence 25
2.6 Special Considerations for Brine Resources 26
2.6.1 Brine Resource Estimation – Porosity 26
2.6.2 Brine Reserve Estimation 27
2.7 Units Of Currency 27
2.8 Reliance On Other Experts 30
3.0 PROPERTY DESCRIPTION 31
3.1 Location 31
3.2 Mineral Tenure 32
3.3 Environmental Liabilities 35
3.4 Permits 35
3.5 Aboriginal Communities 36
3.6 Mining Rights Opinion 36
4.0 ACCESSIBILITY, CLIMATE, LOCAL RESOURCES, INFRASTRUCTURE AND PHYSIOGRAPHY 37
4.1 Accessibility 37
4.1.1 Road Access 37
4.1.2 Air Transport 38
4.1.3 Railway Road 38
4.1.4 Port 38
4.2 Climate 39
4.3 Physiography 42
4.3.1 Pozuelos 42
4.3.2 Pastos Grandes 42

4.4 Local Resources 43
4.5 Local Infrastructure 43
4.5.1 Existing Power Lines 43
4.5.2 Natural Gas 45
4.5.3 Water 45
4.5.4 On-site Facilities 45
4.6 Soils 46
4.7 Vegetation 46
4.7.1 Fauna 46
5.0 HISTORY 47
5.1 Prior Exploration and Ownership - Pozuelos 47
5.1.1 Fresh Water Exploration 48
5.1.2 Past Production 48
5.2 Prior Ownership and History – Pastos Grandes 48
6.0 GEOLOGICAL SETTING, MINERALIZATION, AND DEPOSIT 50
6.1 Regional Geology 50
6.2 Structures 50
6.3 Geological Setting 52
6.3.1 Lithology 53
6.3.2 Local Geology (Pozuelos) 62
6.3.3 Local Geology (Pastos Grandes) 62
6.4 Mineralization 63
6.4.1 Brine Composition (Pozuelos) 64
6.4.2 Brine Composition (Pastos Grandes) 65
6.5 Deposit Types 65
6.5.1 General 65
6.5.2 Pozuelos 67
6.5.3 Pastos Grandes 72
7.0 EXPLORATION 77
7.1 Pozuelos 77
7.1.1 Geophysical Surveys 77
7.1.2 Gravity Survey 77

7.1.3 Magnetotellurics (MT) Survey 77
7.2 Pastos Grandes 80
7.2.1 Surface Brine Sampling 80
7.2.2 Eramet Exploration (2011-2013) 81
7.2.3 Millennial Exploration (2017 – 2019) 81
7.2.4 LSC Exploration (2017 – 2018) 83
7.2.5 Centaur/AMSA Exploration (2018 – 2022) 83
7.2.6 LAR Exploration (2023) 84
7.2.7 Geological Mapping and Geochronology 85
7.3 Drilling 85
7.3.1 Pozuelos 85
7.3.2 Pastos Grandes 101
8.0 SAMPLE PREPARATION, ANALYSES, AND SECURITY 113
8.1 Pozuelos 113
8.1.1 Brine Samples 113
8.1.2 Drainable Porosity Estimate 124
8.1.3 Core Samples (RBRC) 126
8.1.4 Geophysical Hole Logging 127
8.1.5 Analytical Quality Assurance and Quality Control (“QA/QC”) 131
8.2 Pastos Grandes 134
8.2.1 Drainable Porosity 134
8.2.2 Brine Samples 137
8.2.3 Drainable Porosity QA/QC 139
8.2.4 Brine QA/QC 142
8.3 Conclusions and Recommendations 155
9.0 DATA VERIFICATION 156
10.0 MINERAL PROCESSING AND BRINE TESTING 157
10.1 Introduction 157
10.1.1 Process Overview 157
10.2 Brine Evaporation 157
10.3 Purification of Brine 157
10.4 Solvent Extraction Test Work 157

10.4.1 Experimental Principle 157
10.4.2 Experimental Steps 157
10.4.3 Experimental Summary and Data 158
10.5 Lithium Carbonate and Hydroxide 164
10.6 Closing Statement 165
11.0 MINERAL RESOURCE ESTIMATES (EFFECTIVE DATE: DECMBER 31, 2025) 166
11.1 Pozuelos 166
11.1.1 Overview 166
11.1.2 Hydrostratigraphic Model Development 166
11.1.3 Block Model 173
11.1.4 Resource Categorization 175
11.1.5 Resource Estimate 176
11.2 Pastos Grandes 181
11.2.1 Resource Model Domain and Aquifer Geometry 181
11.2.2 Specific Yield 181
11.2.3 Brine Concentrations 182
11.2.4 Resource Category 183
11.2.5 Resource Model Methodology and Construction 186
11.2.6 Resource Estimate 193
11.3 Mineral Resources for the PPG Project 195
11.4 Groundwater Dynamic Modelling at Pozuelos 195
11.4.1 Model Construction 195
11.4.2 Predictive Simulations 199
11.4.3 Summary 209
11.4.4 Limitations 209
11.4.5 Recommendations 209
11.5 Groundwater Dynamic Modelling at Pastos Grandes 210
11.5.1 Model construction 210
11.5.2 Model Calibration 216
11.5.3 Predictive Simulations 220
11.5.4 Model Result 224
12.0 MINERAL RESERVE ESTIMATE 225

13.0 MINING METHODS **226**
13.1 Brine Wellfield 226
13.1.1 Uncertainty Assessment 233
13.1.2 Well Utilization Philosophy 233
13.2 LCE Production Schedule 235
14.0 PROCESSING AND RECOVERY METHODS **236**
14.1 General 236
14.2 Process Description 236
14.3 Pre-concentration Ponds 237
14.3.1 Salt Harvesting 241
14.3.2 Mass Balance 244
14.4 Plant Location and the Plant Layout 246
14.4.1 General 246
14.4.2 Process Description 247
14.4.3 Iron Pre-loading 247
14.4.4 Solvent Extraction Process 247
14.4.5 Raffinate Treatment Process 251
14.5 Primary Purification 253
14.5.1 Primary Purification Plant 253
14.6 Secondary Purification 256
14.6.1 Process Description 257
14.6.2 Carbonate Removal 257
14.6.3 TOC Removal Process 259
14.6.4 Ca Removal 260
14.6.5 Boron Removal 261
14.7 Bipolar Membrane Electrodialysis 263
14.7.1 Process Description 263
14.7.2 Mass Balance 263
14.8 Lithium Carbonate Plant 265
15.0 INFRASTRUCTURE **267**
15.1 General 267
15.2 Utilities 267

15.2.1 Power 267
15.2.2 Natural Gas 271
15.2.3 Water Supply 271
15.2.4 Ancillary Facilities^^ 277
15.2.5 Reagents and Fuels 281
15.2.6 Waste Storage 284
16.0 MARKET STUDIES 285
16.1 Lithium Applications 285
16.2 Lithium Demand 286
16.3 Lithium Supply 289
16.4 Lithium Suppliers Leading Companies and Their Market Shares 291
16.4.1 Competitive Strategies 291
16.5 Lithium Supply Demand Balance 292
16.5.1 Market Projections: Risk Assessment and Identification of Opportunities 292
16.5.2 Economic Factors and Price Volatility 293
16.5.3 Impact of Logistics and Tariff Costs 293
16.6 Price Forecast 293
17.0 ENVIRONMENTAL STUDIES, PERMITTING AND SOCIAL OR COMMUNITY IMPACT 297
17.1 Environmental And Social Studies Performed – Pastos Grandes 300
17.1.1 Baseline 300
17.1.2 Limnology 309
17.1.3 Ecosystem Characterization 310
17.1.4 Social-Economic Characterization 310
17.1.5 Social Perception 312
17.1.6 Archaeological Survey 312
17.1.7 Protected Natural Areas 314
17.2 Environmental And Social Studies Performed – Pozuelos 315
17.2.1 Pozuelos Baseline 315
17.2.2 Social Aspects 317
17.2.3 Social and Community Aspects 317
17.2.4 Archaeological Survey 318
17.2.5 Prevention/mitigation Measures 318

17.3 Ecological and Environmental Aspects 319
17.3.1 Waste and Tailing Disposals 319
17.3.2 TMA and Solid Tailings 319
17.4 Closure and Reclamation Plans 328
18.0 CAPITAL AND OPERATING COSTS 329
18.1 Capital Cost Estimate 329
18.1.1 Basis of Estimate 330
18.1.2 Exclusions and Assumptions 331
18.1.3 Brine Well Field 332
18.1.4 Evaporation Ponds 332
18.1.5 Process Plants 333
18.1.6 Infrastructure and Energy 334
18.1.7 Tailings Management (TMA and Plant Residues) 335
18.1.8 Sustaining Capital 336
18.1.9 Owner's and Indirect Costs 337
18.1.10 Engineering, Procurement and Construction Services 337
18.1.11 Contingency 337
18.1.12 CapEx Summary 337
18.2 Operating Costs Estimate 339
18.2.1 Basis of Estimate 339
18.2.2 Manpower 340
18.2.3 Electric Power 342
18.2.4 Reagents, Fuel and Consumables 344
18.2.5 Ponds Harvesting and TMA 344
18.2.6 Water 344
18.2.7 Camp 345
18.2.8 Product Transportation 345
18.2.9 Other Costs (General and Maintenance Supplies) 346
18.2.10 OpEx Summary 346
19.0 ECONOMIC ANALYSIS 348
19.1 Main Assumptions 348
19.2 Evaluation Criteria 348

19.3 Tax 349
19.3.1 Provincial Royalty 350
19.3.2 Export Refund 350
19.3.3 Tax on Debits and Credits Accounts 350
19.3.4 Aboriginal Programs 350
19.3.5 Capital Allowance 350
19.3.6 Corporate Taxes & VAT 350
19.4 RIGI 350
19.4.1 About the RIGI 350
19.4.2 Beneficiaries 350
19.4.3 Investment 351
19.4.4 RIGI Benefits 351
19.5 Capital Expenditures 351
19.6 Operating Costs 352
19.7 Production Revenues 352
19.8 Cash Flow Projection 352
19.9 Economic Evaluation Results 354
19.10 Sensitivity Analysis 354
19.11 Discussion And Conclusions 357
20.0 ADJACENT PROPERTIES 359
20.1 Other Properties in Pozuelos 359
20.2 Other Properties in Pastos Grandes Salar 359
21.0 OTHER RELEVANT DATA AND INFORMATION 361
21.1 Project Schedule 361
21.2 Management of Depleted Brine 361
22.0 CONCLUSIONS AND RECOMMENDATIONS 363
22.1 Geology and Mineral Resources 363
22.2 Hydrologic Dynamic Modelling 363
22.2.1 Pozuelos 363
22.2.2 Pastos Grandes Salar 364
22.3 Mining Method 364
22.3.1 LCE Production Schedule 365

22.4 Process Information and Design 366
22.4.1 Process Description 366
22.4.2 Solar Evaporation Ponds 367
22.4.3 Brine Processing 367
22.4.4 Evaluation of Process Configurations and Final Product Optionality 367
22.5 Evaluation of Energy Supply Alternatives 368
22.6 Closure and Reclamation Plans 368
22.7 Economic Analysis 368
22.8 Project Risks 370
22.8.1 Process Plant 370
22.8.2 Infrastructure 370
22.8.3 Environmental 371
22.8.4 Time to Market (Schedule) 371
22.8.5 Others 371
23.0 REFERENCES 372
24.0 RELIANCE ON INFORMATION PROVIDED BY THE REGISTRANT 374

TABLES

Table 1: Mineral Resource Estimate for Pozuelos (Effective Date: December 31, 2025) 8
Table 2: Mineral Resources Estimate for Pastos Grandes (Effective Date: December 31, 2025) 9
Table 3: Mineral Resources for the PPG Project (Effective Date: December 31, 2025) 10
Table 4: LCE Production Schedule 13
Table 5: Design Criteria for the Pre-concentration Ponds for All Stages 14
Table 6: 3-year and 5-year Average Spot Price of Battery Grade LCE* 16
Table 7: Capital Cost Summary for the 3 Phases (USD) 18
Table 8: Operating Cost Summary for the 3 Phases 19
Table 9: The Key Inputs to the Economic Analysis (including RIGI benefits) 20
Table 10: Design Criteria for Brine Extraction 22
Table 11: PPG Scoping Study Responsibility Matrix 24
Table 12: Abbreviations Table 27
Table 13: Mining Tenement of PPG Project 33
Table 14: Maximum, Average and Minimum Elemental Concentrations of the Pozuelos Brine 64
Table 15: Average Values (mg/L) of Key Components and Ratios for the Pozuelos 65

Table 16: Maximum, Average and Minimum Elemental Concentrations of the Pastos Grandes Brine 65
Table 17: Average Values (mg/L) of Key Components and Ratios for the Pastos Grandes Brine 65
Table 18: Water Balance for Salar de Pastos Grandes Subbasin 76
Table 19: Location and Total Depth of the Drillholes at Pozuelos 87
Table 20: Summary of Pumping Test Results in Pozuelos 98
Table 21: Boreholes Incorporated in the Geological Model at Pastos Grandes Salar 103
Table 22: Summary of Pumping Test Results in Pastos Grandes Salar 111
Table 23: Number of Samples Sent to Each Laboratory 113
Table 24: Assayed Parameters, Units, Detection Limits and Method References Used by ALS 114
Table 25: Brine Samples Analysis 114
Table 26: Summarizes RBRC Results for Each HSU Unit of the Salar 126
Table 27: Sy Measured with BMR Before and After Processing the Dataset 127
Table 28: Percentages of Sy Before and After Removing the Outliers 128
Table 29: Average of Specific Yield Estimated from the N-Pt 130
Table 30: Drainable Porosities Estimated for Each HSU Using RBRC, Neutron Logging and BMR 130
Table 31: Number of Samples (including QA/QC) 131
Table 32: Summary of Laboratory Tests Conducted by GSA 136
Table 33: Analytical Methods Used by ASANOA and SGS for Brine Assays 138
Table 34: Total Porosity Results for Paired Samples Using GSA Lithologic Classification 140
Table 35: Specific Yield Results for Paired Samples Using GSA Lithological Classification 140
Table 36: Summary of QAQC Insertion Rates for Each Campaign 142
Table 37: Statistical Analysis of Duplicate Samples – ASANOA 143
Table 38: Statistical Analysis of Check Samples – ASANOA & SGS 144
Table 39: Element Concentrations (Best Values) for Standard RR – Millennial 146
Table 40: Statistical Analysis of Duplicate Samples – SGS 148
Table 41: Element Concentrations for Standards 1& 2 - AMSA 150
Table 42: Statistical Analysis of Duplicate Samples – ASANOA 151
Table 43: Element Concentrations (best values) for Standards A & B – Centaur 152
Table 44: Statistical Analysis of Duplicate Samples – Ganfeng 153
Table 45: Statistical Analysis of Check Samples 154
Table 46: Analysis Data of Five-stage Simulated Extraction Experiment 158
Table 47: Analysis Data of Five-stage Simulated Extraction Experiment 158
Table 48: Experimental Data of PPG Li-rich Brine Tank Extraction Operation 160
Table 49: Summary of Experimental Data 162
Table 50: Analysis Result of PPG Brine Feed for Extraction Batch Operation 162
Table 51: Analysis Result of Raffinate from Extraction Batch Operation 163

Table 52: Analysis Result of Stripping Solution 163
Table 53: Percentage of Each Hydrostratigraphic Unit in the Total Volume of the Block Model 170
Table 54: Averages of Sy Used for the Resource Estimate 171
Table 55: Resource Estimated for Each HSU (Effective Date: December 31, 2025) 177
Table 56: Measured, Indicated and Inferred Resource Estimate for the Pozuelos (Effective Date: December 31, 2025) 177
Table 57: Drainable Porosities from Neutron Logs (Source: Bea., Chanampa 2021/2022) 178
Table 58: Historical Resource Estimates for Pozuelos 180
Table 59: Summary Statistics of Drainable Porosity for Geological Units 182
Table 60: Summary of Brine Chemistry Composition 182
Table 61: Summary of Univariate Statistics of Li and K 187
Table 62: Parameters for the Calculation of the Experimental Variograms of the Indicator Variable 189
Table 63: Parameters for the Calculation of the Experimental Variograms of the K and Li Concentrations 189
Table 64: Mineral Resources (LCE) for the Pastos Grandes Salar (Effective Date: December 31, 2025) 194
Table 65: Mineral Resources (LCE) for the PPG Project (Effective Date: December 31, 2025) 195
Table 66: Updated Model Parameters (Source: AW, September 2024) 198
Table 67: Brine Well Extraction Rates 202
Table 68: Freshwater Well Extraction Rates 203
Table 69: Effect of Infiltration on Li Production (Source: AW, September 2024) 206
Table 70: Unsaturated Parameter Values 215
Table 71: Effective Porosity for Transport Simulations 216
Table 72: Steady Sate Calibration Statistics 218
Table 73: Simulated Water Balance 218
Table 74: Pumping Test Maximum Simulated and Observed Drawdown Values 220
Table 75: Simulated Water Balance 224
Table 76: Brine Production for Lithium Carbonate Production (Assuming 75% of Overall Lithium Recovery Efficiency) 224
Table 77: Pozuelos Wells (Phase 1) 227
Table 78: Pastos Grandes Wells (Phases 2) 228
Table 79: Pastos Grandes Wells (Phases 3) 230
Table 80: Design Properties of Wells Piping 233
Table 81: Summary of Well Management Risks and Remedies 233
Table 82: LCE Production Schedule 235
Table 83: Design Criteria for the Pre-concentration Ponds for All Stages 238
Table 84: Preconcentration Ponds Areas for Stage 1** 238
Table 85: Preconcentration Ponds Areas for Stage 2&3 238
Table 86: Salt Quantity for the Three Phased 51 KTPA Production 242

Table 87: Raw Brine Analysis* 244
Table 88: Mass Balance for Phase 1 Pond System 245
Table 89: Summary of Mass Balance for Three Phases 245
Table 90: Mass Balance of the Extraction System 247
Table 91: Basic Parameters of Solvent Extraction 248
Table 92: Analysis of Main Solvent Extraction Streams 248
Table 93: Material Balance Table for Lithium Extraction 250
Table 94: Material Balance of the Raffinate Resin Organic Removal Process 252
Table 95: Boron Removal Mass Balance 254
Table 96: Mass Balance for Ca Removal 256
Table 97: Secondary Purification Feed Specifications 257
Table 98: Material Balance of the Acidizing Process in Carbonate Removal 258
Table 99: Material Balance of Neutralization Process in Carbonate Removal 258
Table 100: Material Balance for TOC Removal Process 259
Table 101: Brine Specification for Ca Ion Exchange 260
Table 102: Mass Balance for Ca Ion Exchange 260
Table 103: Brine Components to Boron Removal Resin 262
Table 104: Mass Balance for Boron Removal 262
Table 105: Bipolar Membrane Electrodialysis 263
Table 106: Mass Balance for Bipolar Membrane Electrodialysis 263
Table 107: Internal Overhead Lines 269
Table 108: Power Consumption for 50K Production and 150K Production 270
Table 109: Saturated Steam Usage 271
Table 110: Fresh Well Coordinates at Pozuelos and Pastos Grandes 273
Table 111: Raw Water Consumption for the Three Phases of Production 274
Table 112: Analyses of the Water Treatment System 277
Table 113: Population in Terrace 2, 3 and 4 in Camp Sectors 281
Table 114: Annual Consumptions of Reagents 281
Table 115: Fuel Distribution for Each Stage 283
Table 116: Estimated Fuel Consumption 284
Table 117: 3-year and 5-year Average Spot Price of Battery Grade LCE 294
Table 118: Benchmark Minerals Market Price Expectations for Battery Quality Lithium 296
Table 119: Main Water Budget in Pastos Grandes 304
Table 120: Solid/semi-solid Effluent for 3 Phases 319
Table 121: Details of Sewage 321
Table 122: Composition of Treated Effluents 322

Table 123: Classification of Wastes National Hazardous Waste Law 24051 327
Table 124: Summary of the Estimate Methodology Used for Main Areas for All Three Phases 331
Table 125: Evaporation Ponds and Wells 332
Table 126: Process Plants for Each Stage 333
Table 127: Infrastructure and Energy Capital Costs 335
Table 128: CapEx for The TMA and Gypsum Disposal 336
Table 129: Sustaining Capital 337
Table 130: Capital Cost Summary for the 3 phases 338
Table 131: Personnel List at Site 340
Table 132: Personnel and Cost During Phase 1 341
Table 133: Electricity Consumption for the 3 Phases of Production 343
Table 134: Reagents Cost Summary 344
Table 135: Water Use 345
Table 136: Annual Operating Cost Summary 346
Table 137: Assumed Production Schedule 348
Table 138: The Key Inputs to the Economic Analysis (including RIGI benefits) 349
Table 139: Capital Expenditures Schedule 351
Table 140: Discounted Cash Flow Summary (including RIGI benefits) 353
Table 141: Economic Evaluation – Base Case (including RIGI benefits) 354
Table 142: Sensitivity Analysis 355
Table 143: Sensitivity Analysis for Different Price Scenarios 357
Table 144: LCE Production Schedule 366

FIGURES

Figure 1: PPG Project Location (Source: Golder, Jan 2025) 31
Figure 2: PPG Mining Properties (Source: Golder, Jan 2025) 33
Figure 3: Local Road Access Map (Source: Ganfeng, 2024) 37
Figure 4: Ground Infrastructure to Reach Chilean Ports (Source: Ganfeng, 2024) 39
Figure 5: Isohyet Map of Puna (Source: Golder, Feb 2024) 41
Figure 6: Weather Data – Santa Rosa de Pastos Grandes, 35NW of Pozuelos, Sep. 2020 – Sep. 2023 41
Figure 7: Physiography of Salar de Pozuelos and Surrounding Area (Source: Golder, Feb 2024) 42
Figure 8: PPG Project Near Infrastructure (Source: LAR, 2025) 44
Figure 9: Main On-site Facilities and Areas (Source: Ganfeng, 2024) 45
Figure 10: Map of the central Andean Mountains and location of the PPG project (Modified from Benson et al., 2026) 51
Figure 11: Geological Map and Stratigraphic Column of the PPG Project and Locations of Cross Section A-A' and B-B' 52

Figure 12: Representative Geological and Structural Cross Sections of Pastos Grandes (upper) and Pozuelos (lower). Note: cross sections are not the same scale. 53
Figure 13: Copalayo Mountain Looking East from Pozuelos (left), and Outcrop of the Metasediments (right) of the Copalayo Formation North of Pastos Grades at Condor Huasi. (Source: LAR, 2025) 53
Figure 14: Outcrops of the Oire Eruptive Complex Showing Varying Granitic Textures from Pastos Grandes basin (left) and the Eastern Margin of the Aguas Calientes Caldera (right). (Source: LAR, 2025) 54
Figure 15: Outcrop of the Geste Formation Conglomerate in Northern Pozuelos. (Source: LAR, 2025) 55
Figure 16: Outcrop of the Pozuelos Formation at Quebrada Seca Comprised of Sandstones and Siltstones, with Minor Mudstones and Tephra. (Source: LAR, 2025) 56
Figure 17: Verde Conglomerate Overlying Sands and Silts of the Pozuelos Formation and Underlying Tajamar Tuff (left) and a Close-up Photograph of the Unit in Outcrop (right) (Source: LAR, 2025) 56
Figure 18: Outcrop of the 10.2 Ma Tajamar Tuff in the Pastos Grandes Basin (Source: LAR, 2025) 57
Figure 19: Example of Dark Glassy, Porphyritic, Lava Flow Material from One of the Quevar Lava Flows Exposed in the Northern Part of Pastos Grandes (Source: LAR, 2025) 58
Figure 20: Lacustrine Interval of the Sijes Formation with Interbedded Siltstones, Mudstones, Borates, and Tephra (Source: LAR, 2025) 59
Figure 21: Outcrop of the Halite Mudstone Core of the Blanca Lila Formation in Blanca Lila Island (left) and Marginal Carbonate Mudstone Facies on the Southwestern Margin of the Pastos Grandes Basin (left) (Source: LAR, 2025) 60
Figure 22: Key Lithologies Present Drill Core in the PPG Project. (Source: LAR, 2025) 61
Figure 23: Schematic Representation of Mineralization at Pastos Grandes Until ~0.2 Ma (Source: LAR, 2025) 63
Figure 24: Annotated Photograph Looking West from the Southern Extent of the Pastos Grandes System into the Canyon Connecting the Two Salars (Source: LAR, 2025) 63
Figure 25: Schematic Representation of Mineralization at Pozuelos and Pastos Grandes during and after the Flooding Event ~200,000 years ago (Source: LAR, 2025) 64
Figure 26: Schematic Illustration for Brine Deposits Environments Where Lithium Occurs (Source Hardie Smooth and Eugster 1978, modified by Imex 2023) 67
Figure 27: Springs Identified in Salar de Puzuelos (Modified from CONHIDRO, 2018) 68
Figure 28: Geologic Cross Section W-E of Salar de Pozuelos (Modified from CONHIDRO, 2018) 69
Figure 29: Hydrology of Salar de Pozuelos - Watershed Definition (Modified from CONHIDRO, 2018) 70
Figure 30: Water Balance Conceptual Model for Endhoreic Basins in Arid Regions Followed for Salar de Pozuelos 71
Figure 31: Summary of Water Balance Estimated for the Period 2020 in Salar de Pozuelos 71
Figure 32: Hydrological Subdivisions of the Pastos Grandes Basin (Source: AW, Dec 2024) 72
Figure 33: Surface Water Features within the Northern Portion of the Pastos Grandes Basin (Source: AW, Dec 2024) 73
Figure 34: Hydrogeological Cross Section in Pastos Grandes Salar (Source: AW, Dec 2024) 75
Figure 35: Magnetotellurics and Highs and Downs of the Gravity Line 1-2 (Proingeo 2021) 77
Figure 36: MT Survey Lines and Stations Conducted by Proingeo in 2021 78
Figure 37: Line 4 MT Vs Lithologies of the Drillholes (Source: Proingeo 2021) 79
Figure 38: Line 1-2 MT Vs Lithologies of the Drillholes (Source: Proingeo 2021) 79

Figure 39: Historical Surface Brine Samples in Salar de Pastos Grandes (Source: AW, Dec 2024) 80
Figure 40: Geophysical Surveys Conducted in Salar de Pastos Grandes (Source: AW, Dec 2024) 82
Figure 41: Location of the Drillholes at Pozuelos (Source: Golder, Jan 2025) 86
Figure 42: Lithologies from the HSU Saline Lake (Source: Golder, Jan 2025) 88
Figure 43: Lithologies from the HSU Mudflat (Source:Golder, Jan 2025) 89
Figure 44: Lithologies from the HSUs Sandy (left photo) and Muddy (right photo) Alluvial and Colluvial Sediments (Source: Golder, Jan 2025) 89
Figure 45: Lithologies of the HGU Fractured Aquifer (Source: Golder, Jan 2025) 90
Figure 46: Lithologies of the HGU Siltstone (Source: Golder, Jan 2025) 91
Figure 47: South-North Cross Section M-M' PZ-2023-26, PZ-2023-24, PZ-2024-28(bis), PZ-2023-14, PZ-2023-12 (Source: Golder, Jan 2025) 91
Figure 48: South-North Cross- Section L-L' PZ-2024-11, PZ-2024-03, PZ-2023-19, PZ-2023-22, PZ-2024-21 (Source: Golder, Jan 2025) 92
Figure 49: Cross Section I-I': PZ-2023-26, SPZ-DDDH17, PZ-2024-25, PZ-2024-03 and Cross Section A-A' (SP-2017-11,SP-2017-12- PZ-2023-04, PZ-2024-11, SP-2017-14) (Source: Golder, Jan 2025) 93
Figure 50: Cross Section E-E' (PZ-2024-28(bis), PZ-2024-13, SP-2017-07, PZ-2024-22, SP-2017-08) and Cross Section H-H' (PZ-2023-24, PZ-2023-20, DDDH-400, PZ-2024-03) (Source: Golder, Jan 2025) 93
Figure 51: Cross Section F-F' (PZ-2024-01, PZ-118-01, PZ-2023-19) and Cross Section D-D' (SP-2017-02, PZ-2024-07, PZ-2024-21) (Source: Golder, Jan 2025) 94
Figure 52: Cross Section B-B' (PZ-2023-12, PZ-2024-16PW, PZ-2024-09) and Cross Section K-K' (PZ-2023-14, PZ-18-02) (Source: Golder, Jan 2025) 94
Figure 53: Borehole Locations in Salar de Pastos Grandes (Source: Golder, Oct 2024) 102
Figure 54: Geological Model and Each Stratum in Pastos Grandes (Source: AW, Dec 2024) 107
Figure 55: Location Map of the Pumping Tests Conducted in Salar de Pastos Grandes (Source: AW, Dec 2024) 108
Figure 56: Lithium Concentrations from all the Exploration Samples (Source: Golder, Jan 2025) 118
Figure 57: Lithium Concentrations in Northern Drillholes (Source: Golder, Jan 2025) 119
Figure 58: Lithium Concentration in the Northern Zone from Pozuelos (Source: Golder, Jan 2025) 119
Figure 59: Lithium Concentrations Central Drillholes (2017-2018 exploration) (Source: WSP Golder, Jan 2025) 120
Figure 60: Lithium Concentrations from the Central Drillholes (2023-2024 Exploration) (Source: Golder, Jan 2025) 121
Figure 61: Lithium Concentration in the Central Zone from Pozuelos (Source: Golder, Jan 2025) 121
Figure 62: Lithium Concentrations from the Southern Drillholes (2017-2018 Exploration) (Source: WSP Golder, Jan 2025) 122
Figure 63: Lithium Concentrations from the Southern Drillholes (2023-2024 Exploration) (Source: WSP Golder, Jan 2025) 122
Figure 64: Lithium Concentrations from the Southern Zone from Pozuelos (Source: Golder, Jan 2025) 123
Figure 65: Histogram for Lithium Concentrations of the Complete Dataset of Samples (Source: Golder, Jan 2025) 123
Figure 66: Location of the Wells with Drainable Porosity Data (Source: WSP Golder, Jan 2025) 125

Figure 67: Penetration Rate from PZ-2024-16PW and PZ-2023-12 (Source: Golder, Jan 2025) 128
Figure 68: Porosity Relationships for Unconsolidated Material (Source: Johnson 1967) 129
Figure 69: Photographs of the Fractured Aquifer (Source: Golder, Jan 2025) 130
Figure 70: Performance of the Reference Sample TDS B 3002 (Source: Golder, Jan 2025) 132
Figure 71: Performance of the Reference Sample TDS D 3001 (Source: Golder, Jan 2025) 132
Figure 72: Performance of the Reference Sample TDS D 3004 (Source: Golder, Jan 2025) 132
Figure 73: Duplicate Vs Original Samples (Source: Golder, Jan 2025) 133
Figure 74: Blanks Performance (Source: Golder, Jan 2025) 133
Figure 75: Pt (top), Sy (middle), Sy and RBR (bottom) Comparison for Check Samples DBSA-GSA (Source: AW, Dec 2024) 141
Figure 76: Max-min Plot for Li (left) and K (right) in Duplicates – ASANOA (Source: AW, Dec 2024) 143
Figure 77: Max-min Plot for Li (left) and K (right) in Duplicates – SGS (Source: AW, Dec 2024) 144
Figure 78: Max-min Plot for Li (left) and K (right) in Check Samples: ASANOA – SGS (Source: AW, Dec 2024) 145
Figure 79: Blank vs Previous Samples for Lithium and Potassium – ASANOA (Source: AW, Dec 2024) 145
Figure 80: Blank vs Previous Samples for Lithium and Potassium – SGS (Source: AW, Dec 2024) 146
Figure 81: Graphical Analysis of Li (top) and K (bottom) within ‘RR’ Standards Assayed y ASANOA (Source: AW, Dec 2024) 147
Figure 82: Graphical Analysis of Li (top) and K (bottom) within ‘RR’ Standards Assayed by SGS (Source: AW, Dec 2024) 147
Figure 83: Graphical Analysis of Li (top) and K (bottom) within ‘INBEMI’ Standards Assayed by SGS (Source: AW, Dec 2024) 148
Figure 84: Max-min Plot for Lithium (left) and Potassium (right) in Duplicates – SGS (Source: AW, Dec 2024) 149
Figure 85: Blank vs Previous Samples for Lithium (left) and Potassium (right) – SGS (Source: AW, Dec 2024) 149
Figure 86: Blank vs Previous Samples for Lithium (left) and Potassium (right) – SGS (Source: AW, Dec 2024) 150
Figure 87: Blank vs Previous Samples for Lithium (left) and Potassium (right) – SGS (Source: AW, Dec 2024) 150
Figure 88: Max-min Plot for Lithium (left) and Potassium (right) in Duplicates – ASANOA (Source: AW, Dec 2024) 151
Figure 89: Blank vs Previous Samples for Lithium (left) and Potassium (right) – ASANO (Source: AW, Dec 2024) 152
Figure 90: Max-min Plot for Lithium (left) and Potassium (right) in Duplicates – ASANOA (Source: AW, Dec 2024) 153
Figure 91: Max-min Plot for Lithium (left) and Potassium (right) in Duplicates – Lab Pozuelos (Source: AW, Dec 2024) 154
Figure 92: Blank vs Previous Samples for Lithium (left) and Potassium (right) – Lab Pozuelos (Source: AW, Dec 2024) 155
Figure 93: Process Flowsheet for Continuous Extraction Process (Source: Ganfeng, 2024) 159

Figure 94: Lithium Yield of PPG Li-rich Brine (Source: Ganfeng, 2024) 161
Figure 95: Lithium Content in Raffinate and Organic Phase (Source: Ganfeng 2024) 161
Figure 96: Continuous Extraction Device Diagram (Source: Ganfeng 2024) 164
Figure 97: Location of the Control Points (Source: Golder, Jan 2025) 167
Figure 98: Resource Area vs Mining Properties (Source: Golder, Jan 2025) 169
Figure 99: Hydrostratigraphic Units from the Hydrostratigraphic Model (Source: Golder, Jan 2025) 170
Figure 100: Histograms of the Sy (PHIEE) for the Muddy Alluvial and Colluvial Sediments (Source: Golder, Jan 2025) 171
Figure 101: Histograms for Porosities of the Saline Lake (Source: Golder, Jan 2025) 172
Figure 102: Histograms of the Sy (PHIEE) for the Sandy Alluvial and Colluvial Sediments (Source: Golder, Jan 2025) 172
Figure 103: Porosity relationships for unconsolidated material (Source: Johnson 1967) 173
Figure 104: Swat Plot Showing the Concentrations of Lithium from the Samples, Kriging and Inverse Distance Estimator (Source: Golder, Jan 2025) 174
Figure 105: Lithium Distribution from the Block Model (Source: Golder, Jan 2025) 175
Figure 106: Measured, Indicated and Inferred Resource Distribution (Source: Golder, Jan 2025) 176
Figure 107: Specific Yield Variogram Showing no Spatial Correlation (Source: AW, Dec 2024) 181
Figure 108: Specific Yield Violin Graph by Different Geological Model Unit (Source: AW, Dec 2024) 182
Figure 109: Histogram of Vertical Sampling Distances (Source: AW, Dec 2024) 183
Figure 110: Schematic Section Illustrating Resource Categories Based on Data Density for Different Zones (Source: AW, Dec 2024) 184
Figure 111: Spatial Distribution of Resource Classification by Depth (Source: AW, Dec 2024) 185
Figure 112: Lithium and Potassium Histograms and Cumulative Distributions (Source: AW, Dec 2024) 188
Figure 113: Lithium and Potassium Histograms and Cumulative Distributions for Region I (Source: AW, Dec 2024) 188
Figure 114: Experimental Variogram and Variogram Model for the Indicator Variable (Source: AW, Dec 2024) 190
Figure 115: Experimental Variogram and Variogram Model for Potassium and Lithium in Region I (Source: AW, Dec 2024) 191
Figure 116: N-S Section through the Resource Model Showing the Lithium Grade Distribution (Source: AW, Dec 2024) 192
Figure 117: W-E Section through the Resource Model Showing the Lithium Grade Distribution (Source: AW, Dec 2024) 192
Figure 118: SW-NE Section through the Resource Model Showing the Lithium Grade Distribution (Source: AW, Dec 2024) 193
Figure 119: Evaporation Function (Source: AW, September 2024) 196
Figure 120: Boundary Conditions for Lateral Recharge and Extraction Wells (Source: AW, September 2024) 197
Figure 121: Generalized Hydrostratigraphic Units (built up from bottom to top in images a to f) (Source: AW, September 2024) 198

Figure 122: Initial Single-density Head and Lithium Concentration Distribution at the top and bottom of Screens of the Simulated Brine Wells (brown plus signs denote brine well locations) (Source: AW, September 2024) 199
Figure 123: Change in Hydraulic Head during 20-year Base Case Simulation (Source: AW, September 2024) 200
Figure 124: Lithium Concentration Distribution at Beginning and End of Base Case Run, Sections A to C (Source: AW, September 2024) 201
Figure 125: Lithium Production Estimate (Source: AW, September 2024) 203
Figure 126: Simulated Drawdown without Infiltration (Source: AW, September 2024) 204
Figure 127: With-recharge Configuration and Drawdown at end of Operations (Source: AW, September 2024) 205
Figure 128: With-infiltration-well Configuration and Drawdown at end of Operations (Source: AW, September 2024) 206
Figure 129: Average Drawdown and Area of Drawdown Impact after Operations (Source: AW, September 2024) 207
Figure 130: Simulated Drawdown after End of Brine Pumping (Source: AW, September 2024) 208
Figure 131: Model Domain and Meshes Element Size (Source: AW, Dec 2024) 210
Figure 132: Mesh Vertical Extension (Source: AW, Dec 2024) 211
Figure 133: Model Boundary Conditions (Source: AW, Dec 2024) 212
Figure 134: Indirect, Lateral Recharge (Left) and Evapotranspiration and Diffuse Groundwater Discharge Zones (right) to Salar Pastos Grandes (Source: AW, Dec 2024) 213
Figure 135: 3D View of the Hydrogeological Units in the Mmodel (Source: AW, Dec 2024) 214
Figure 136: Hydrogeological Units in Cross Sections (Source: AW, Dec 2024) 215
Figure 137: Initial Distribution of Lithium Concentration (Source: AW, Dec 2024) 216
Figure 138: Location of Head Observation Piezometers (left) and Simulated Steady State Water Table and Residuals (right) (Source: AW, Dec 2024) 217
Figure 139: Observed vs. Simulated Water Levels (Source: AW, Dec 2024) 217
Figure 140: PGPW1815 (left) and PW1 (right) Pumping Test Simulated and Observed Drawdowns (Source: AW, Dec 2024) 219
Figure 141: PG-2023-03PW (left) and PGPW16-01 (right) Pumping Test Simulated and Observed Drawdowns (Source: AW, Dec 2024) 219
Figure 142: Layout of the Brine Production Wellfield and Freshwater Wellfield (Source: AW, Dec 2024) 221
Figure 143: Average Lithium Concentration of Wellfield Production (top) (Source: AW, Dec 2024) 222
Figure 144: Predicted Drawdown after Year 20 (Source: AW, Dec 2024) 223
Figure 145: Production Wells for Three Phases 226
Figure 146: Production Wells for Phase 1 227
Figure 147: Proposed Production Wells for Phase 2 228
Figure 148: Proposed Production Wells for Phase 3 230
Figure 149: Construction Drawing of Production Well 232
Figure 150: Simplified Overall Process Flowsheet for Each Phase (Source: Ganfeng, 2024) 237

Figure 151: Ponds Simple Conceptual Configuration** (Source: Ganfeng, 2024) 239
Figure 152: Phase 1 Ponds Layout 240
Figure 153: Phase 2 and 3 Ponds Layouts 240
Figure 154: Proposed TMA and Infiltration Ponds for Phase 1 242
Figure 155: TMA Locations for Phase 2&3 243
Figure 156: Simplified Process Diagram for the Pre-concentration Ponds (Source: Ganfeng 2024) 243
Figure 157: Process Plants Layout for Three Phases (Source: Golder, 2024) 246
Figure 158: Solvent Extraction Flowsheets (Source: Ganfeng, 2024) 250
Figure 159: Process Flow Diagram of Raffinate Resin Organic Removal (Source: Ganfeng, 2024) 252
Figure 160: Process Flow Diagram of Sewage Treatment Station (Source: Ganfeng, 2024) 253
Figure 161: Process Flow Diagram of Boron Removal in Primary Purification Plant (Source: Ganfeng, 2024) 254
Figure 162: Location of the Plant's Solid Waste Deposit (Source: Golder, Jan 2025) 255
Figure 163: Flowsheet for Ca Removal Process (Source: Ganfeng, 2024) 256
Figure 164: Flowsheet for Carbonate Removal Process (Source: Ganfeng, 2024) 259
Figure 165: Flowsheet for TOC Removal Process (Source: Ganfeng, 2024) 260
Figure 166: Flowsheet for Ca Removal Process (Source: Ganfeng, 2024) 261
Figure 167: Flowsheet for Boron Removal Process (Source: Ganfeng, 2024) 262
Figure 168: Flowsheet for Bipolar Membrane Electrodialysis (Source: Ganfeng, 2024) 265
Figure 169: Flowsheet for Lithium Carbonate Plant (Source: Ganfeng, 2024) 266
Figure 170: PPG Project Electric Line from La Puna 269
Figure 171: PPG Project Electric Line to the Plant 269
Figure 172: The Process Flow for LNG (Source: Ganfeng 2025) 271
Figure 173: Location of Fresh Wells at Pastos Grandes 272
Figure 174: Location of Fresh Wells at Pozuelos 273
Figure 175: Northern Aqueduct Wells and Route 275
Figure 176: Southern Aqueduct Wells and Route 276
Figure 177: Simplified Block Flow Diagram for the Purification System (Source: Ganfeng, 2024) 277
Figure 178: Typical Layout of Truck Shop (Source: Ganfeng, 2024) 278
Figure 179: Typical Layout of a 2,160 m^2 Warehouse (Source: Ganfeng, 2024) 279
Figure 180: Typical 1,960 m^2 Warehouse Layout (Source: Ganfeng, 2024) 279
Figure 181: South-west Fuel Plant Location (Source: Ganfeng, 2024) 282
Figure 182: Layout of Waste Warehouse (Source: Ganfeng, 2024) 284
Figure 183: LFP, LMFP, and NCM Comparison (Source: Lithium Quarterly Market Review October 2024 from iLiMarkets.) 285
Figure 184: Battery Raw Materials Cost (Source: Lithium Quarterly Market Review October 2024 from iLiMarkets) 286

Figure 185: Battery Raw Materials Cost (Source: Lithium Quarterly Market Review October 2024 from iLiMarkets.) 286
Figure 186: Lithium Demand in Batteries (2024) (Source: Lithium Quarterly Market Review October 2024 from iLiMarkets.) 287
Figure 187: Lithium EV Main Players (Source: Lithium Quarterly Market Review October 2024 from iLiMarkets.) 287
Figure 188: EV Sales Forecast per Region (Source: Lithium Quarterly Market Review October 2024 from iLiMarkets. Horizontal axis label is in years.) 288
Figure 189: EV Penetration Rate Forecast (Source: Lithium Quarterly Market Review October 2024 from iLiMarkets.) 288
Figure 190: Lithium Production (2023) by Country (Source: U.S. Geological Survey, Mineral Commodity Summaries, January 2024. It excludes US production.) 289
Figure 191: Lithium Supply Forecast per Resource Type (Source: Lithium Quarterly Market Review October 2024 from iLiMarkets.) 290
Figure 192: Lithium Supply Forecast per Country (Source: Lithium Quarterly Market Review October 2024 from iLiMarkets) 290
Figure 193: Market cap/sum LCE Mined (24-28) (Source: Lithium Quarterly Market Review October 2024 from iLiMarkets) 291
Figure 194: Lithium Supply & Demand Forecast (Source: Lithium Quarterly Market Review October 2024 from iLiMarkets) 292
Figure 195: Projected Pricing for Battery-Quality Lithium Carbonate Used in Economic Model (Source: “Lithium Price Forecast,” Benchmark Mineral Intelligence, Q1 2025.) 294
Figure 196: Spot Price Comparison for Li_2CO_3 and $LiOH*H_2O$ (micronized) over the 1-year Period between July 2024 and July 2025 295
Figure 197: Environmental Baseline Study Area (Source: Ausenco, 2018) 301
Figure 198: Salar de Pastos Grandes Basin and Sub-Basins (Source: Ausenco, 2018) 302
Figure 199: Inflows and Outflows Considered in Water Budget (Source: UMAss/UAA, 2024) 305
Figure 200: Areas Sampled for Flora and Floristic Units (Source: Ausenco, 2018) 307
Figure 201: Bird and Mammal Observation Transects and Mouse Trap Locations (Source: Ausenco, 2018) 308
Figure 202: Limnologic Sampling Site Locations (Source: Ausenco, 2018) 309
Figure 203: Location of Social Communities (Source: Ausenco, 2018) 311
Figure 204: General Location of Large Pastures in Pastos Grandes (Source: Ausenco, 2018) 313
Figure 205: Distribution of Natural Protected Areas (Source: Ausenco, 2018) 314
Figure 206: The Fauna Observed at Pozuelos 317
Figure 207: Efluentes Plant Location (Source: Ganfeng, 2024) 320
Figure 208: Pumping Well Details (Source: Ganfeng, 2024) 323
Figure 209: Views of the Wastewater Treatment System (Source: Ganfeng, 2024) 324
Figure 210: Infiltration Duct (Source: Ganfeng, 2024) 325
Figure 211: Acid Effluent Neutralization System (Source: Ganfeng, 2024) 325
Figure 212: Layout of Warehouse and Waste Yard (Source: Ganfeng, 2024) 326
Figure 213: Capital Cost Distribution for Phase 1 338

Figure 214: Operating Cost Distribution Phase 1 347
Figure 215: After-Tax NPV Sensitivity to CapEx, OpEx and Price Variation 356
Figure 216: After-Tax IRR Sensitivity to CapEx, OpEx and Price Variation 356
Figure 217: Sensitivity Analysis for Different Price Scenarios 357
Figure 218: San Mateo Property in Pozuelos (Source: Ganfeng 2024) 359
Figure 219: Other Properties in Pastos Grandes Salar (Source: AW, 2023) 360
Figure 220: Project schedule for 3 Phases 362

APPENDICES

APPENDIX A HYDROGEOLOGY TEST WORK

FORWARD LOOKING STATEMENTS

This Technical Report, including the economics analysis, contains statements or information that constitute forward-looking information (forward-looking statements) within the meaning of applicable Canadian and United States securities laws. Forward looking statements include, but are not limited to project economics, financial and operational parameters such as the timing and amount of future production from the Project, expectations with respect to the NPV and costs of the Project, anticipated mining and processing methods of the Project; proposed infrastructures, anticipated mine life of the Project, expected recoveries and grades, timing of development plans, the estimation of mineral resources; realization of mineral resource estimates; the timing, success and amount of estimated future exploration; costs of future activities; capital and operating expenditures; and success of exploration activities. Generally, forward looking statements can be identified by the use of forward-looking terminology such as “plans”, “expects” or “does not expect”, “is expected”, “budget”, “scheduled”, “estimates”, “forecasts”, “intends”, “continue”, “anticipates” or “does not anticipate”, or “believes”, or variations of such words and phrases or statements that certain actions, events or results “may”, “could”, “would”, “will”, “might” or “will be taken”, “occur” or “be achieved”. Forward looking statements are made based upon certain assumptions and other important facts that, if untrue, could cause the actual results, performance, or achievements of the project to be materially different from future results, performances or achievements expressed or implied by such statements. Such statements and information are based on numerous assumptions, some of which are discussed in this Technical Report. Forward-looking statements are subject to known and unknown risks, uncertainties and other important factors that may cause the actual results, level of activity, performance or achievements of the project to be materially different from those expressed or implied by such forward-looking statements, including but not limited to: there being no assurance that the exploration program or programs for the project will result in expanded mineral resources; risks and uncertainties inherent to mineral resource estimates; the high degree of uncertainties inherent to economic analysis which are based to a significant extent on various assumptions; exchange rate fluctuations; variations in cost of supplies, labor rates and consumable and equipment costs; receipt of necessary approvals; availability of financing for project development; uncertainties and risks with respect to developing mining projects; general business, economic, competitive, political and social uncertainties; future lithium prices; accidents, labor disputes and shortages; environmental and other risks of the mining industry, including without limitation, risks and uncertainties discussed in the Company’s latest Annual Information, Annual Report on Form 20F and other continuous disclosure documents of the Company available under the Company’s profile at www.sec.gov and www.sedarplus.ca. There may be other factors that cause results not to be as anticipated, estimated or intended. There can be no assurance that such statements will prove to be accurate, as actual results and future events could differ materially from those anticipated in such statements. Accordingly, readers should not place undue reliance on forward looking statements.

1.0 EXECUTIVE SUMMARY

1.1 Introduction

This report titled “Scoping Study Report at the PPG Salars, Salta Province, Argentina” (the “Report” or “Technical Report”), was prepared by Golder and Atacama Water Consultants (“AW”) to provide Ganfeng Lithium International Co. (“Ganfeng”) and Lithium Argentina AG (“LAR” or “Lithium Argentina”) with a Technical Report that is compliant with S-K §229.1300 regulations (the “S-K regulations”) on the PPG Salars (the “PPG Project” or “Project”), located in the Salta Province, Argentina.

The work associated with this Technical Report consists of all studies, engineering, cost estimates, and planning services, as well as preparation of a Scoping Study Report for the PPG Project (“the Project”).

The QPs has relied on Ganfeng Lithium International Co. (“Ganfeng”), Lithium Argentina AG (“Lithium Argentina or “LAR”) for legal, political, environmental, and tax matters.

The mineral resources estimate for the Pastos Grandes (“PG”) and the Sal de la Puna (“SdlP”) Projects presented in this report have been prepared by the QP employed by Atacama Water Consultants (“AW”) and reviewed by the QP employed by Golder.

1.2 Property Location, Description and Ownership

PPG Project is located in the “lithium triangle” in the province of Salta, Argentina. The project is surrounded by Salar de Pocitos to the west, Salar de Rincon to the Northwest, Caucharí to the North, and Salar de Centenario to the South.

The Project is owned by Ganfeng Lithium International Co. (“Ganfeng”) and Lithium Argentina AG, formerly Lithium Americas Corp. and Lithium Americas (Argentina) Corp. (“Lithium Argentina” or “LAR”) , and they are currently developing the PPG Project through three projects that are being consolidated into a new Joint Venture (JV). The parties entered into a framework agreement dated August 12, 2025, to establish the JV. On closing of the JV, Ganfeng will hold 67% of the PPG Project with Lithium Argentina holding the remaining 33%, with ownership based on resources, capital contributions and technology inputs. Formation of the JV remains subject to certain conditions and there is no guarantee that the parties will satisfy those conditions and enter into definitive agreements to form the JV.

Project areas cover the following:

- Pastos Grandes Project (“PG Co”): size of 20,095 hectares
- Sal de la Puna Project (“SdlP”): size of 13,852 hectares
- Pozuelos-Pastos Grandes Project (“Pozuelos”): size of 32,314 hectares

The total PPG Project covers 66,261 hectares with mineral rights.

1.3 Accessibility, Climate, Local Resources, Infrastructure and Physiography

Access to the properties from Salta is via National Route 51 (RN51) 170 km west and northeast to San Antonio de los Cobres. From there, the route goes 15 km to the junction with Provincial Route 129 (PR129) and from there 50 km toward Santa Rosa de los Pastos Grandes and then south approximately 11 km to salar de Pastos Grandes. From Pastos Grandes RP129 goes westwards approximately 35 km, where it joins up with the access road southwards to Pozuelos.

Access from Antofagasta, Chile is via the Panamerican Highway 5N 70 km to Baquedano, proceeding east along Routes 365, 367, and 23 for approximately 300 km to the international crossing at Paseo Sico. From Sico the shortest route to the sites is 130 km via routes RN51, RP127 and RP129 through Cauchari and Pocitos. Access from Chile is also possible via Paso Jama on NR52 and then via RN40 to Cauchari and RN 51, RP127 and RP129.

The climate of the Puna varies from semiarid in the eastern border to arid along the western border. Mountains east of the Altiplano-Puna are orographic barriers to humidity, producing the rain shadow desert in the plateau. The paucity of precipitation on the Puna is compounded by the high elevation, producing a harsh climate. The air is extremely dry, winds blow strongly throughout the year, precipitation is scarce, temperatures are low, clouds are normally absent, radiation is intense, and there are large daily temperature fluctuations. These parameters enhance evaporation and reduce detrital input to basins. Perennial streams locally feed sub-basins, but normally the water quickly disappears into alluvial fans. The conditions described above produce high rates of evaporation varying from 2,500 to 3,000 mm in an annual period (7-8 mm per day) generating a considerable hydric deficit.

The primary source of precipitation in this region is associated with Atlantic moisture recycled via the Amazon and moisture related to the South Atlantic Convergence Zone during summer. Minor amounts of precipitation also reach this arid zone via incursions of the southern hemisphere westerlies during winter. 80% of the annual precipitation falls in the summer from November to February. Based on data from the meteorological station at salar de Pocitos, the yearly average is 35 mm, mostly concentrated during the summer.

Based on INTA (National Institute of Agroindustry and Technology) data for the Puna region during the period 1901-1940, the mean annual temperature is 9.5°C. The warmest month is December, which has a monthly mean temperature of 13.2°C, whilst the coldest month is June with 3.7°C. Daily temperature amplitude varies from 30°C to 35°C between day and night, depending on the season. The frost-free period is relatively short, and frost is very common and intense.

Winds can be quite strong in the area, with wind speeds in excess of 80 km/h being recorded. Winds tend to increase during the day, with maximum wind speeds typically reached in the mid-afternoon. Wind speeds vary by season, with higher speeds typically being recorded in the summer months.

The village of Pocitos is located about 36 km northwest of the property. Pocitos is a station on the Antofagasta-Salta Railway, and commercial train service is available three times per week between Pocitos and Antofagasta. Pocitos is the terminus of the Gasoducto de la Puna (Puna gas pipeline) which has an extension running to Mina Fenix lithium operated by Rio Tinto (formerly FMC Lithium) at Salar de Hombre Muerto.

Soils in Pozuelos/Pastos Grandes area are of the aridisol type, with high salt content, very low organic content, low fertility and having a relatively coarse texture. SEGEMAR, the Argentine geological survey, classifies the Salar itself as having a saline soil type “La”, with the immediate surrounding area containing the dunes and wetlands classified as DGtc-7 soil type and the higher elevations consisting of consolidated rock outcrops and natural elevations as EKtc-14 and Eni-6 soils.

1.4 Geological Setting and Mineralization

The PPG Project is in the Puna portion of the Andean Mountain range, a region dominated by the Altiplano-Puna Volcanic Complex flanked by the Western and Eastern Cordillera sequences (De Silva et al., 2006; Kay and Coira, 2009). The Altiplano-Puna Volcanic Complex is a large volcanic province typified by large dacitic to rhyolitic ignimbrites and sources calderas in Bolivia, Chile, and Argentina that formed from the Miocene to Pliocene (De Silva et al., 2006). The Western Cordillera (Cordillera Oriental) forms the western boundary of the Puna Plateau and is dominated by volcanism associated with active subduction of the Nazca Plate beneath the South American plate. The basins that formed during Eastern Cordillera contain primarily clastic material sourced from the basement rocks, sequences of lacustrine rocks with claystones and borates, and halite-dominated evaporitic sequences.

In Pastos Grandes and Pozuelos, two major structural regimes occur: NNE structurally controlled basins and NW-SE lineaments. The NNE structures are primarily reverse faults associated with major Andean uplift events, whereas the NW-SE lineaments are characterized by left-lateral accommodating offsets (Coira et al., 1982; Marret et al., 1994; Allmendinger et al., 1997; Chernicoff et al., 2002).

1.4.1 Pozuelos

The modern salar at Pozuelos is classified as a mature salar. The lithology of the salar reflects this development, with the following general sequence of hydrogeologic units:

- Ephemeral Saline Lake Facies: comprised of halite with mixed textures is the uppermost layer of the salar and contains sediments related the modern hypersaline lake.
- Perennial Saline Lake Facies: comprised of fractures and massive halite with interstitial clays and sand.
- Saline Mudflat Facies: comprised of silt mixed with clays and fine sand, associated with an older, oversaturated lake and quiet environment, likely time-equivalent to the Sijes and Blanca Lila Formations.
- Playa Margin Facies: comprised of gravels representing alluvial and colluvial deposits with some interbedding of more sandy facies, both laterally and vertically, likely corresponding to Geste and Pozuelos Formations, respectively.
- Siltstone: comprised of Cenozoic siltstones likely correlative with the Pozuelos Formation; and
- Fractured Aquifer: comprised of the Copalayo Formation bedrock with varying degrees of fractures.

The brine from Pozuelos are solutions saturated in sodium chloride with an average concentration of total dissolved solids ("TDS") of 316 g/L and an average density of 1.21 g/cm^3. The other components present in the Pozuelos brine are K, Li, Mg, SO_4^{2-}, Cl and B with relatively low Ca. The brine can be classified as a sulphate-chloride type with anomalous lithium. Lithium concentrations in Salar de Pozuelos have an average value of 518 mg/L, with some samples reaching up to 908 mg/L.

1.4.2 Pastos Grandes

The modern salar at Pastos Grandes contains five major hydrogeological units based on drill core, surface mapping, and geophysical information. This includes:

- A Fluvial/Alluvial unit: comprised of gravel and sand around the salar, with thicknesses up to 450 m in the northern sector of the basin.
- An Upper Clay unit: comprised of claystones and siltstones mostly in the centre-south of the basin, roughly correlative with the marginal facies of the Blanca Lila Formation.
- A Saline Lacustrine unit: comprised of thick massive halite beds and minor interbedded claystones, ranging from 200 to over 700 m in thickness, roughly correlative with the indurated halite core of the Blanca Lila Formation typified by the Blanca Lila islands.
- A Central Clastic unit: comprised of clays and clayey sands underneath the halite bodies with thicknesses up to 300 m, roughly correlative with marginal lacustrine facies of the Sijes and/or Blanca Lila Formations; and

- Base Breccia/Gravels unit: comprised of sedimentary breccia with coarse fragments of silicified conglomerate, metasediments, ignimbrite, and intercalated tuff, reaching over 200 m on the western margin of the salar and corresponding mostly to the Pozuelos Formation (and locally Tajamar Tuff, Verde Conglomerate, and marginal facies of the Sijes Formation).

The brine from Pastos Grandes are solutions saturated in sodium chloride with an average concentration of total dissolved solids ("TDS") of 302 g/L and an average density of 1.19 g/cm^3. The other components present in the Pastos Grandes brine are K, Li, Mg, SO_4, Cl and B with relatively low Ca. The brine can be classified as a sulphate-chloride type with anomalous lithium. Lithium concentrations in Salar de Pastos Grandes have an average value of 403 mg/L, with some samples reaching up to 700 mg/L.

1.5 Deposit Types

1.5.1 Pozuelos

According to Alonso et al. (1991), Salar de Pozuelos is a dry salar, characterized by high rates of evaporation and there is sediment starved (fluvial input is restricted to rare flash floods, and groundwater is the most important source of brine). This is consistent with the conceptual model for mineralization, indicating that the main source of water/Li in the system was a one-time input from the catastrophic flooding of the Pastos Grandes basin into Pozuelos less than 200,000 years ago.

The Pozuelos basin covers an area of 384 km^2 including 10 sub-basins that provide lateral groundwater inflows. The Salar nucleus itself covers an area of 84 km^2. No surface water inflows occur into the Salar. The main source of surface water within the Pozuelos watershed are the fourteen springs.

The Salar de Pozuelos basin is an enclosed (endorheic) basin in which recharge occurs through direct infiltration of precipitation and groundwater inflows from the surrounding sub-basins. Discharge occurs mainly through evaporation.

Groundwater recharge is estimated to range between 128 L/s and 707 L/s. Evaporation is estimated at 493 L/s.

In mid-2024, LAR and Ganfeng engaged the UMASS/UAA Lithium Solutions team to initiate an updated water balance study of the Pozuelos basin using the same methodology that was applied in the 2023/2024 Pastos Grandes water balance study (Blin et al., 2024).

1.5.2 Pastos Grandes

The Pastos Grandes basin covers an area of 1,738 km^2 with a Salar nucleus of 36 km^2 comprised mostly of flat sandy-silty salt crust. The general elevation of the salar surface is 3,773 masl, with the "islands" having a typical elevation of approximately 3,785 - 3,790 masl. The surrounding hills range in elevation from approximately 3,825 masl on the south, east and northeast sides of the salar and increase rapidly on the west side to approximately 3,990 masl.

Surface runoff is mainly restricted to the rainy season during summer. A water balance for the Pastos Grandes Subbasin was prepared as part of the conceptual hydrogeological model. In closed endorheic basins such as Salar de Pastos Grandes recharge is in long-term equilibrium with evaporation in the absence of any brine production. Recharge is composed of direct recharge from precipitation and lateral groundwater inflows from adjacent subbasins (Sijes subbasin) and was estimated within a range of 200 - 900 L/s.

A systemic surface monitoring was implemented in 2023 to obtain a better understanding of the flow regimes in these streams throughout the different seasons of the year. Data indicate that inflows into the Pastos Grandes system includes surface and groundwater flow 776 L/s – 2,130 L/s, with a mean 960 L/s of lateral recharge (Blin et al., 2024). Future dynamic models will incorporate the new data from this more comprehensive monitoring program utilizing state-of-the-art measurement, isotopic, and geochemical techniques.

1.6 Exploration and drilling

1.6.1 Pozuelos

Geophysical survey exploration has been carried out in the salar since 2009.

LSC has completed two seismic exploration programs on Salar de Pozuelos: the first program was completed in later 2017 and consisted of a 28.29 km seismic survey comprising three lines with geophones placed at 400 m stations, in order to test depths to 350 m. GEC was subsequently engaged to undertake the second seismic survey along the SW-NE axis of the salar in 2018 to improve the data interpretation. It comprised three profiles, a longitudinal line of 14,280 m and two transvers lines of 7,690 m and 6,320 m running in a NW-SE across the salar in the south and north. GEC redid the seismic profiling of the longitudinal line in mid-2018. The line run in a NE direction from the SE to the NE, with a length of 14,394 m.

Gravity and Magnetotellurics studies were conducted by the company Proingeo in 2021: the gravity from Proingeo (2021) was used to interpret the elevation of the basin's basement; and the Magnetotellurics geophysics survey from Proingeo 2021 was a guide to delineating aquifer continuity.

Lithea completed a program of exploration for fresh water in 2016 (Hidrotec, 2016). The focus of the program was on the northwestern corner of the salar based on the results of the SEV geophysics.

Drilling for lithium at the Pozuelos dates from 2008. Two vertical wells (SPZ RC001 and SPZ RC002) to a depth of approximately 90 m was drilled. One HQ size diamond drillhole (SPZ DDH001) drilled to a depth of 183 m adjacent to SPZ RC001, to collect data on variations in lithology with depth and to collect brine samples.

LSC completed sixteen diamond core drill holes (DDH-400, SP-2017-01 to SP-2017-15) at Pozuelos in 2017. Boreholes were drilled at HQ diameters and with the depths ranging from 51.8 m to 322.7 m. Besides, fourteen pumping wells have been completed at the salar by LSC in 2017.

In 2018, two exploration holes were drilled to test the northern section (PZ-18-02) and the lateral and depth extension of the central depocenter (PZ-18-01). The brine and core samples were collected, and a series of pumping wells and piezometers were developed to evaluate aquifer parameters and brine chemistry.

In each drilling campaign, lithium exploration wells have been successively drilled deeper. Wells PZ-2024-22 and PZ-2023-19, from the latest drilling campaign from 2023/2024, opened new targets to deeper zones of the basin at the east. Recently, in the latest drilling program, wells PZ-2024-11, PZ-2024-25 and PZ-2024-21 opened new deeper targets toward the southeast and northeast of the salar.

1.6.2 Pastos Grandes

70 boreholes for a total 31,485 m have been drilled recovering 12,265 m of core samples. Additionally, 14 pumping wells were drilled and tested to evaluate flow potential, and the results were used to forecast production through a dynamic model.

In 2011 and 2012, Eramine Sudamerica SA, a subsidiary of Eramet SA, carried out surface mapping and sampling, drilling and pump testing at locations across the salar. Drilling was limited to a maximum depth of 160 m. In addition, Eramine also completed a program of geophysical surveys, including TEM, CS-AMT and VES (Eramine, 2016).

Millennial conducted an extensive program of field work across the Salar from 2016 to 2021 known as the Stage Two and Three investigations of the Pastos Grandes Project.

LSC completed six drill holes at Pastos Grandes in 2018. Boreholes were drilled using a combination of diamond bit and tri-cone at HQ diameter. Drilling was completed by Hidrotec (Holes SPG-02, 2B, 4A, 5, 5B) and AGV (Hole PG-18-01).

Centaur Resources ("Centaur") carried out lithium exploration activities on the 'Alma Fuerte' mining claim of its Sal de la Puna Project immediate to the south and east of the LAR mining claims during 2018/2019. This program included drilling of three boreholes including a pumping well to around 600 m depth, pumping tests, and seismic & TEM geophysical surveys.

Recently LAR completed a fourth exploration campaign consisting of two exploration boreholes using Mud Rotary and Diamond Drilling methodology (PGMW23-23 and PGMW23-24).

AMSA and Centaur carried out drilling programs on the Sal de la Puna Project between 2018 and 2022. These programs consisted of two diamond core holes (DD-01 and DD-02), five combination core /rotary holes (PP-01- 2018, PP-02-2018 and R-01 through R-03), two production wells (PP-03-2019 and PW-1), and several piezometer installations.

Ganfeng Lithium drilled five exploration boreholes in 2023 and 2024 with the diamond drilling methodology (PG- 2023-02, 03, 04, 05 and 13) and two production wells (PG-2023-03PW and PG-2024-21PW) were drilled using the mud rotary methodology.

1.7 Metallurgical Testing

Tests have been performed for the solvent extraction technology by Ganfeng. Several approaches to extracting lithium from the brine were investigated, including a novel solvent extraction technology tested by laboratories in China.

The solvent extraction test work was to verify the extractant selectivity for lithium and its efficiency of boron removal and to identify the feasibility of the proposed experimental route and process of extraction method, and the reliability of multi-component synergistic extraction-water stripping. This was achieved with a proprietary and selective solvent formulation.

When the synergistic extractant is contacted with the brine containing high concentration of Cl after being preconditioned with an active agent, lithium can be extracted to form a relatively stable complex. In the stripping stage, due to ion concentration difference, lithium chloride is stripped from the organic phase with water allowing for the regeneration of the organic phase. An aqueous phase rich in lithium chloride is obtained.

The main conclusions and recommendations are as follows:

- Traditional evaporation route to pre-concentrate the brine to approximately 3 g/L was generated by a computer model
- Extraction efficiency was greater than 90% and stripping greater than 94%
- Lithium concentration in raffinate ranged from 0.25 to 0.35 g/L
- Strip solution concentration ranged from 19 to 20 g/L Li
- Boron extraction rate ranged from 40% to 45% calculated by raffinate

The PPG Project's feasibility depends, in part, on developing suitable processing methods aligned with the specific chemistry of the PPG brines. The solvent extraction technology considered for the Project, while still being refined, is not entirely novel, and scaling up solvent extraction generally presents lower risks than other lithium direct extraction approaches. Testwork conducted by Ganfeng indicates that a suitable extractant can be formulated for the PPG brine, and further work is underway to continue advancing the technology.

1.8 Mineral Resource Estimates (Effective Date: December 31, 2025)

1.8.1 Pozuelos

The Resource Estimate was developed using three-dimensional block modelling with Leapfrog Geo (Seequent) software. The modelling was supported by geophysical, geological, and geochemical data and interpretations made by Golder. The resources estimate was prepared in according with the requirements of the S-K §229.1300 and uses the best practices methods specific to brine resources. A 125 mg/l lithium concentration cut-off was applied to the resource estimate.

The modelling method consisted of the following steps:

- The footprint of the resource zone was defined based on the interpreted boundaries of the salt flat and the deposit characteristics.
- The drilling data and MT results were interpreted to identify primary lithologies and their continuity within the resource zone. Data interpolation was conducted to develop a full 3D geological model.
- The 3D geological model was divided into five Hydrostratigraphic Units (HSUs), which are groups of lithologies with similar hydrological properties.
- The drainable porosity data from Neutron logs were used to calculate the amount of lithium-enriched brine available for the Pozuelos project.
- The assays from the brine samples from packer testing were interpolated in the block model to obtain the amount of lithium available to estimate the total resource stated as LCE.

A summary of the Measured, Indicated and Inferred Resource Estimate is shown in following table.

Table 1: Mineral Resource Estimate for Pozuelos (Effective Date: December 31, 2025)

Salar	Resource Category	Aquifer Volume (km^3)	Brine Volume (km^3)	Average Lithium Concentration (mg/L)	Lithium (tonnes)	LCE (tonnes)
Pozuelos	Measured Resource	20.45	2.21	490.5	1,097,038	5,836,244
	Indicated Resource	3.54	0.41	528.7	221,877	1,180,384
	Measured + Indicated	**23.99**	**2.62**	**510.0**	**1,318,915**	**7,016,628**
	Inferred Resource	9.50	1.25	581.0	736,924	3,920,437

Notes:

1) *S-K §229.1300 definitions were followed for Mineral Resources.*
2) *Lithium carbonate equivalent ("LCE") is calculated using the Li: LCE factor = 5.322785 multiplied by the mass of Lithium.*
3) *A cut-off grade of 125 mg/l has been applied to the mineral resource estimates. An FoB price forecast of US$18,000 per metric ton of Li_2CO_3 and US$17,800 per metric ton of coarse particle $LiOH \times H_2O$ for years beyond 2028 is used. A 75% overall lithium recovery efficiency factor has been applied to calculate the final LCE production.*
4) *The Mineral Resource Estimate is not a Mineral Reserves Estimate and has no demonstrated economic viability.*
5) *Comparisons of values may not be equivalent due to rounding of numbers and the differences caused by use of averaging methods.*

6) *The Siltstone unit was not included in the resource estimate.*

7) *Project economics in this report are not based on Inferred Mineral Resource.*

8) *The QPs are not aware of any known legal, political, environmental, or other risks that could materially affect the potential development of the mineral resources.*

1.8.2 Pastos Grandes

The resource estimation for the Pastos Grandes salar was developed using the Stanford Geostatistical Modelling Software (SGeMS) by Atacama Water (AW), and it was prepared in accordance with the requirements of S-K §229.1300 and uses the best practices methods specific to brine resources. A 125 mg/l lithium concentration cut-off was applied to the resource estimate.

The modelling method consisted of the following steps:

- The footprint of the resource zone was defined based on the interpreted boundaries of the salt flat and the deposit characteristics.
- Based on the lithological descriptions of the drill core and cutting together with the interpretation of the available geophysical information and field observations, a 3-D geological model of the Pastos Grandes sub-basin were developed.
- The 3D geological model was divided into five major Hydrostratigraphic Units (HSUs), which are groups of lithologies with similar hydrological properties.
- The specific yield values were derived from 115 valid drainable porosity analyses of undisturbed samples, analysed by GeoSystems Analysis.
- The distribution of lithium concentration in the model domain is based on a total of 530 brine analyses (not including QA/QC analyses) to estimate the total resource stated as LCE.

A summary of the Measured, Indicated and Inferred Resource Estimate is shown in following table.

Table 2 shows the mineral resources for Pastos Grades expressed as lithium carbonate equivalent (LCE).

Table 2: Mineral Resources Estimate for Pastos Grandes (Effective Date: December 31, 2025)

Salar	**Resource Category**	**Aquifer Volume (km^3)**	**Brine Volume (km^3)**	**Li (mg/L)**	Li Resource (tonnes)	**LCE (tonnes)**
Pastos Grandes	Measured Resource	25.28	3.09	451	1,393,000	7,414,640
	Indicated Resource	1.15	0.17	166	28,000	149,038
	Measured + Indicated	**26.43**	**3.26**	**439**	**1,421,000**	**7,563,678**
	Inferred Resource	26.43	3.26	456	525,000	2,794,462

Note:

1) *S-K §229.1300 definitions were followed for Mineral Resources.*

2) *This table includes resources in all areas of PG and SdlP previously owned by Ganfeng and Lithium Argentina separately.*

3) *Lithium carbonate equivalent ("LCE") is calculated using the Li: LCE factor = 5.322785 multiplied by the mass of Lithium.*

4) *A cut-off grade of 125 mg/l has been applied to the mineral resource estimates. An FoB price forecast of US$18,000 per metric ton of Li_2CO_3 and US$17,800 per metric ton of coarse particle $LiOH \times H_2O$ for years beyond 2028 is used. A 75% overall lithium recovery efficiency factor has been applied to calculate the final LCE production.*

5) *The Mineral Resource Estimate is not a Mineral Reserves Estimate and has no demonstrated economic viability.*

6) *Comparisons of values may not be equivalent due to rounding of numbers and the differences caused by use of averaging methods.*

7) *Project economics in this report are not based on Inferred Mineral Resource.*

8) *The QPs are not aware of any known legal, political, environmental, or other risks that could materially affect the potential development of the mineral resources.*

The integrated mineral resources for the PPG Project are shown in Table 3.

Table 3: Mineral Resources for the PPG Project (Effective Date: December 31, 2025)

Salar	Resource Category	Pozuelos		Pastos Grandes (including SdlP)		Subtotal LCE (tonnes)
		Li (mg/L)	LCE (tonnes)	Li (mg/L)	LCE (tonnes)	
PPG	Measured Resource	491	5,836,244	451	7,414,640	13,250,884
	Indicated Resource	529	1,180,383	166	149,038	1,329,421
	Measured + Indicated	**510**	**7,016,627**	**439**	**7,563,678**	**14,580,305**
	Inferred Resource	581	3,920,437	456	2,794,462	6,714,899

Note:

1) *S-K §229.1300 definitions were followed for Mineral Resources.*

2) *Lithium carbonate equivalent ("LCE") is calculated using the Li: LCE factor = 5.322785 multiplied by the mass of Lithium.*

3) *A cut-off grade of 125 mg/l has been applied to the mineral resource estimates. An FoB price forecast of US$18,000 per metric ton of Li_2CO_3 and US$17,800 per metric ton of coarse particle $LiOH \times H_2O$ for years beyond 2028 is used. A 75% overall lithium recovery efficiency factor has been applied to calculate the final LCE production.*

4) *The Mineral Resource Estimate is not a Mineral Reserves Estimate and has no demonstrated economic viability.*

5) *Comparisons of values may not be equivalent due to rounding of numbers and the differences caused by use of averaging methods.*

6) *Project economics in this report are not based on Inferred Mineral Resource.*

7) *The QPs are not aware of any known legal, political, environmental, or other risks that could materially affect the potential development of the mineral resources.*

1.8.3 Hydrologic Dynamic Modelling

1.8.3.1 Pozuelos

In September 2024, Atacama Water Consultants completed the simulation of brine abstraction (960 L/s) from Pozuelos to support an annual production of 50,000 TPA LCE over a 20-year project life, evaluation of water level declines during the operation and water levels recoveries after the operation ceases, and evaluation of the effects of depleted brine infiltration (148 l/s) on lithium concentrations and LCE production targets.

The updated model was built on Ganfeng's original FEFLOW model (spz_reserves_model_2024.fem), prepared in FEFLOW 8.0 and was a single-density flow-and-lithium-transport model designed to produce a preliminary simulation result with and without planned infiltration schemes.

These preliminary models show that, with the conceptual values of hydraulic conductivity, specific yield, and lateral recharge, the proposed total brine pumping rate of 960 L/s for a period of 20 years appears to be feasible.

The preliminary run suggests that the freshwater well locations may not be sufficient to meet the 24 L/s of freshwater required for the project which will have to be sourced from Pastos Grandes. With 960 L/s of total brine extraction, the model predicts drawdowns of greater than 80 m in areas, with an average drawdown on the order of 26 m at the end of operations. The modelling shows that changing the pumping rates at individual wells or including infiltration of 148 L/s (modelled as reinjection) can reduce the drawdown in local areas within the Salar. The infiltration can also improve freshwater capture by reducing drawdown along the Salar margins. The modelling shows that applying infiltration to the Pozuelos does not significantly affect the simulated brine production.

The recovery after operations model predicts approximately 57% recovery by 10 years after the end of operations and 90% recovery by 20 years after the end of operations. The simulated water table recovery after the end of operations is fastest in the south, followed by the north and Salar margins. The low-permeability halite in the centre of the Salar is predicted to recover more slowly that the other areas. However, if there is any direct precipitation onto the Salar, this area could recover more quickly than modelled.

The dynamic model result at Pozuelos as of September 2024 is presented in Table 69 in Section 11.3.

Note that updated resources estimate at Pozuelos (as of March 2025, see Section 11.1) has not been reflected in the September 2024 dynamic model.

1.8.3.2 Pastos Grandes

A numerical groundwater flow and transport model has been developed in December 2024. The modelling work was carried out by DHI in Lima, Peru under close supervision of Atacama Water and the QP.

The numerical model, calibrated to steady state and transient flows and heads, was used to simulate brine extraction over a 20-year period. The simulation utilizes transient groundwater flow and lithium mass transport beginning with the initial steady state head distribution and the initial lithium concentration distribution from the brine resource estimate. The analysis assumes an overall efficiency of 75% to estimate the LCE production. A freshwater wellfield with a total flow rate of 150 L/s (10 wells) is included in the simulation enough to source phase I and II of the Project.

The brine wellfield production rate is 977 L/s for a period of 20 years, distributed among 47 production wells with a constant rate varying between 7 L/s and 25 L/s.

The model simulations predict that 1,395 kt of LCE is contained in the brine pumped to the evaporation ponds over the 20-year period, resulting in a final LCE plant production of 1,045 kt considering a 75% overall lithium recovery efficiency. The yearly average over the 20-year period is 52.3 kt/year. The average lithium concentration is predicted to range between 435 mg/l and 415 mg/l.

The dynamic modelling results at PG as of December 2024 are presented in Table 75 and Table 76 in Section 11.3.

1.9 Mineral Reserve Estimate

No reserve has yet been defined for the PPG Project. Two updated groundwater models have been developed for Pozuelos and Pastos Grandes Salars with the results of drilling and testing to date and this will be used to develop a maiden reserve for the PPG Project.

1.10 Mining Methods

The brine extraction wellfields will be located within the respective Salars and will be accessible by interconnected roads. The production process starts when brine is pumped from the aquifers beneath the Salars, using electrical pumps, placed in bores (wells) that are completed in the Salars. The extracted brine is pumped from each well to a main distribution pipeline and then to the evaporation ponds.

Phase 1 wellfield comprising 34 production wells, while Phases 2 and 3 will include 60 and 61 wells respectively including spares and redundant wells. The brine production wells will be completed with 12 in-diameter stainless steel production casing and be equipped with 380V submersible pumping equipment. The well depth will vary from 420 m to 640 m for the different phases of the project. The power to the wellfield and individual wells will be delivered via a medium voltage power line.

The brine production wellfield will be operated during the three Phases to support a production of approximately 51,000 TPA of LCE for each phase.

Based on the operational experience of similar installations, wells availability of 80-90% can be achieved.

1.10.1 LCE Production Schedule

The project will have the capacity to produce 153,000 TPA LCE of Li_2CO_3 and $LiOH \times H_2O$, and it is planned to be developed and constructed in 3 Phases, each with a capacity of approximately 51,000 TPA LCE:

- **Phase 1:** 40,000 TPA Li_2CO_3 + 12,500 TPA $LiOH \times H_2O$
  - Brine from Pozuelos
  - 34 wells planned in Pozuelos
  - Starting production: Q1 2029
- **Phase 2:** Additional 40,000 TPA Li_2CO_3 + 12,500 TPA $LiOH \times H_2O$
  - Brine from Pastos Grandes
  - 60 wells in Pastos Grandes planned
  - Starting production: Q4 2031
- **Phase 3:** Additional 40,000 TPA Li_2CO_3 + 12,500 TPA $LiOH \times H_2O$
  - Brine from Pastos Grandes + Sal de la Puna + Pozuelos
  - 61 wells in Pastos Grandes + Sal de la Puna planned
  - Starting production: Q4 2035

Golder is comfortable with using 37% of measured and indicated (M+I) resources for production planning. It is common to apply 37% of aquifer efficiency factor to measured and indicated resources to estimate pumpable resources for mine life planning in the lithium brine industry. The predictive groundwater flow and transport model simulations carried out for Pozuelos and Pastos Grandes support that the application of the 37% efficiency factor is reasonable.

Table 4 shows that, if only M+I resources are included and 37% of M+I resources are considered pumpable, the PPG regional lithium development project has a nominal production life of 30 years for Phase 1, 28 years for Phase 2, and 24 years for Phase 3.It is planned that all 3 phases will end in the same year. A 75% overall lithium recovery efficiency factor has been applied to calculate the final LCE production. The recovery is based on test work carried out to date and assumptions provided by Ganfeng.

Table 4: LCE Production Schedule

Items	M+I	Pumpable**	Recovered*	Phase 1 @ 30 years (consumed)	Phase 2 @28 years (consumed)	Phase 3 @ 24 years (consumed)	Remaining resources
Unit	(kt, LCE)	(kt, LCE)	(kt, LCE)	(kt, LCE)	(kt, LCE)	(kt, LCE)	(kt, LCE)
Pozuelos	7,017	2,596	1,947	1,492	-	387	68
Pastos Grandes	7,563	2,798	2,099	-	1,345	754	-

Note:

1. *Units: k (1,000) tons LCE.*
2. ** An overall recovery rate of 75% is used for all phases.*
3. *** Assuming 37% of M+I resources can be pumped out and go into production.*
4. *Annual production rate of ~51,000 TPA of LCE is assumed for each phase (40,000 TPA of Li_2CO_3 plus 12,500 TPA of $LiOH \times H_2O$).*

1.11 Recovery Methods

The plan is to produce during each Phase 40,000 TPA of lithium carbonate and 12,500 TPA of lithium hydroxide monohydrate (LHM) from extracted brine of the Pozuelos and Pastos Grandes wellfields. The brine will be concentrated to approximately 3 g/L Li by standard solar evaporation ponds. A lithium carbonate equivalent (LCE) of 51,000 TPA will be produced for each of the three phases planned for a total of 153,000 TPA LCE at the end of the third phase.

Process engineering and design for the ponds and the process plants were completed by Santiago, Chile based Adinf and Jiangxi, China based Ganfeng Lithium, respectively, based on their respective experience and test work results.

The construction of the PPG Lithium Plant will be in three stages. Each stage (phase) is designed to process 3,383,884 m^3/y of pre-concentrate brine feed and produce a design minimum 51,000 TPA battery grade Li_2CO_3 equivalent.

Phases 2 and 3 involve adding duplicate process trains, to be constructed for production in Years 4 and 8, to treat for a combined production total of 153,000 TPA LCE, at the end of the final phase.

1.12 Process Description

The main activities involved include:

- Pre-concentration of the brine
- Solvent extraction
- Raffinate treatment
- Primary purification
- Secondary purification

- Lithium hydroxide and lithium carbonate processing

The Pozuelos and Pastos Grandes wellfields provide brine feed to the solar evaporation ponds for preconcentration. The evaporation ponds are also located within the Salars. After the brine is concentrated to approximately 3 g/L lithium in the ponds, it's sent to solvent extraction circuits where lithium is selectively extracted and concentrated to 19 g/L.

1.12.1 Solar Evaporation Ponds

The pre-concentration pond systems are divided into four (4) independent strings each with 8 ponds. Once the brine reaches the target lithium concentration, it is pumped to a Buffer-pond for storage, from where it will be transferred to the processing plant designed to process 11,635 tons per day of brine at 0.246% Li over 300 days per year operating time, during each of the 3 Phases of production.

Table 5: Design Criteria for the Pre-concentration Ponds for All Stages

Parameter	Unit	Phase 1	Phase 2	Phase 3
Evaporation rate	mm/day	7 (referred to water)	7 (referred to water)	7 (referred to water)
Seepage	mm/m^2	0.05	0.05	0.05
Entrainment	%w/w	10%	10%	10%
Feed Li Concentration	%w/w	0.0462	0.0355	0.0355
Flow Rate	TPD	67,070	87,347	87,347
Concentrated brine (Li)	%w/w	0.246	0.246	0.246
Flow Rate	TPD	11,635	11,635	11,635
Dilution Water	%	1%	1%	1%
Wells	N	34	60	61

The crystallized salts, mainly sodium chloride, are collected (harvested) every 1 to 2 years to maintain the appropriate volume capacity of the ponds. For this purpose, typical earthmoving machinery will be used, such as bulldozers, front-end loaders, and dump trucks.

All waste salts will be discharged to a Tailing Management Area (TMA) located on the salars.

1.12.2 Brine Processing

The lithium in concentrated brine is extracted by a solvent, and transferred into a rich LiCl solution with a concentration of 19 g/L.

The process consists of a three-step solvent extraction cycle: extraction, washing and stripping. There will be 5 production lines with a capacity of 10,000 TPA each, thus completing a production of ~51,000 TPA.

The lithium rich solution from solvent extraction undergoes primary and secondary purification steps designed to remove excess boron, calcium, and carbonate. The purified and adjusted stream is split and sent to the lithium carbonate plant and the membrane electrodialysis plant to produce the lithium hydroxide feedstock. Lithium hydroxide monohydrate is obtained after further evaporation and crystallization while lithium carbonate is produced with the conventional process by addition of soda ash.

Detailed description and flowsheets are included in Chapter 17.

1.13 Site Infrastructure

Infrastructure proposed for the Project includes:

- Site access roads
- **Accommodation:** modular, camp style accommodation is proposed in close proximity to the processing plant to include construction and operations personnel for Stages 1 through 3.
- **Power Supply:** The Project will have as its main source of electrical energy, a new high voltage line at 345 kV connected to the Argentine interconnection system (SADI) from the ET La Puna located approx. 70 km from the property. The electric company will provide a LAT connection thru a transformer station and from there will enter the project with medium voltage lines.
- **Power Distribution & Electrical:** From the transformer station, two 33kV lines will be installed for internal power distribution, these lines will go the first to the medium voltage distribution centre (CD-MV) in the process plant 15 km from the EETT and the second will travel 12 km to reach the production wells located in Salar de Pastos Grandes. From the CD-MV, a 33 kV line will be installed channelled by trays to the transformation centres of the production plant where the CCM and low voltage distribution systems will be installed for the different terminal circuits; from the same CD-MV the laying of a 33 kV medium voltage overhead line will be carried out. approximately 15 km to energize the production wells and evaporation ponds located in Pastos Grandes.
- As an emergency system, critical equipment will be connected to diesel generators. It is intended that where equipment of similar requirements is to be procured, for the site and camp, that makes and models be standardized where possible.
- **Natural Gas:** Heat and steam for the process will be initially supplied by bracket around Liquefied Natural Gas (LNG) trucked to site, stored, re-gasified and distributed to the respective users.
- **Water Supply:** The water supply system for the project will consist of wells distributed in the salars of Pozuelos and Pastos Grandes. All the wells will be connected to aqueducts to transport water to the points of consumption. To meet the requirements for water for ponds and process plants, services and camp, the pipelines will be distributed taking into account the distances to optimize the routing of pipes.
- **Buildings:** truck shops, plant offices, process plant workshop, warehouse, laboratory and gatehouse.

1.14 Market Studies and Contacts

Lithium is one of the most versatile elements and one of the most sought-after, since its density is approximately half that of water. Therefore, the material is used in a variety of applications, including the production of ceramics, glass and aluminium, and pharmaceutical uses, but it is the use in lithium-ion batteries that has driven the lithium industry's dynamics in recent years. The fast-growing market for hybrids and Electric Vehicles ("EVs") is being driven by regulations and targets on CO_2 emission reductions, falling battery costs, improved driving range and expanding charging infrastructure. All major automotive OEMs have announced aggressive growth plans in battery-powered electric vehicles.

Overall, lithium demand is expected to grow from 0.5 mt of LCE in 2021 to 5.6 mt by 2040, representing a CAGR of 13%. Battery demand already accounts for a significant portion of overall demand, but with the global push towards battery EVs and energy storage needs from renewable power generation sources, battery use is expected to make up substantially most of future lithium demand. Battery demand constitutes 78% of total lithium demand in 2021, but by 2040 it is expected to make up 96% of total demand, growing at a CAGR of 15%.

Golder looked at the trailing 3-year and 5-year average spot price of battery grade LCE as support for projected average LCE price over the next 5 to 10 years. The average prices are shown in Table 6 below.

Table 6: 3-year and 5-year Average Spot Price of Battery Grade LCE*

LCE Price	From	To	LCE (CNY/T)	LCE (USD/T)
Average over the last 5 years	2020-10-31	2025-10-31	150,858	21,629
Average over the last 3 years	2022-10-31	2025-10-31	135,625	19,127

** https://tradingeconomics.com/commodity/lithium*

Golder believes an FoB price forecast of US$18,000 per ton of Li_2CO_3 and US$17,800 per ton of coarse particle $LiOH \times H_2O$ for years beyond 2028 is reasonable for this Scoping Study.

1.15 Environmental Studies, Permitting, Social and Community Impact

There are no known environmental liabilities. Previous owners have prepared baseline studies for Pozuelos and Pastos Grandes and the preparation of the Production Environmental Study update at PPG is in progress (EIR). In addition, the Company already submitted an Environmental Study for the pipeline corridor which allows the transport of brine from Pastos Grandes to Pozuelos. The EIR/EIS for Phase 1 (Pozuelos) was approved by the Province of Salta in November 2025.

Ganfeng and LAR are committed to preserving the natural environment of the Puna region. All exploration activities are under the auspices of an approved Environmental Impact Statement (EIR) by the Provincial Argentine regulator. These are referred to locally as Declaration De Impacto Ambiental (DIA) and are issued for the exploration activities. Resolution 440 for activities at Pastos Grandes was approved in December 2017 and Resolution 034 was passed in February 2018 for advanced exploration activities at Pozuelos.

Ganfeng and LAR have continued to commit to the highest environmental and social standards and maintain a constant and active dialogue with all stakeholders in the provinces, including the local communities, National, Provincial and respective Municipal Administrations, and their representatives in the various government departments. The PPG Project is within the direct influence of the community of Santa Rosa de los Pastos Grandes, located in close vicinity to Salar Pastos Grandes. The community of Pocitos, located approximately 60 km north of Pozuelos is also considered to be within the project as an indirect area of influence.

In general, Pozuelos and Pastos Grandes are relatively unencumbered by communities and, the Pozuelos area, in particular, hosts no people in its vicinity. Nevertheless, Ganfeng and LAR are committed to ensuring a positive impact on local host communities through a range of initiatives.

1.15.1 Mine Closure and Reclamation Plans

Closure and reclamation for the PPG Project have followed legislative requirements and best practice guidance. The legislative requirements for mine closure were outlined under Law 7070 and Decree 3097/00 (as amended by Decree 1587/03) in Salta Province.

A conceptual mine closure plan was included in both the Pozuelos and Pastos Grandes IIAs (Initial Investment Analysis).

On completion of mining operations at the Project, Ganfeng and LAR are committed to restoring the area to its pre-mining use state where practical and applicable. For the purposes of this study, Golder conservatively estimated closure costs by applying a 5% factor to initial CapEx. The closure costs are included in the sustaining CapEx in the technical economics model for the project.

We recommend a detailed mine closure plan within the next 5 years. Development of a mine closure plan is not a one-time event but a continuous process, evolving from a conceptual stage during project development to a detailed plan during operations.

1.16 Capital and Operating Costs

The CapEx is compliant with the American Association of Cost Engineers (AACE) International Recommended Practice with an accuracy of -15% to +25%.

1.16.1 Capital Cost Estimate

Capital and Operating Cost estimates were developed by Golder for the three phases of production with an average capacity of 51,000 TPA LCE divided into 40,000 TPA of lithium carbonate and 12,500 TPA of lithium hydroxide monohydrate. It covers three sites (Pozuelos, Pastos Grandes, and SdlP) where a pre-concentrated brine is produced and processed at a central plant. A simple breakdown structure was developed to facilitate cost allocation of the different elements.

Civil, structural, piping and mechanical costs were partially derived from available engineering, and the remaining costs are factored. Electrical and instrumentation costs were quantified and priced according to the operating philosophy.

Capital Operating Cost estimates developed by Golder are in conformance with the requirements of § 229.601(b)(96).

These estimates incorporate direct and indirect costs for the implementation of the entire Project, including:

- Brine production wellfield and pipeline delivery system
- Evaporation ponds and liners
- Platforms, earthworks and earth movements and concrete
- Lithium Process Plants
- General services
- Infrastructure; and
- Indirect and Owner’s Costs.

No provision has been included to offset future cost escalation since estimated expenses, as well as expected revenue, are expressed in constant dollars. This value excludes interest expense that might be capitalized during the same period. This value includes the following estimates:

- Direct Project Costs
- Indirect Project Costs
- Project Contingencies
- Owners Costs
- Freight and Duties

- Taxes for some of the areas.

The CapEx summary for the three phases of production is presented in Table 7.

Total CapEx for PPG Project, including equipment, materials, indirect costs, contingencies, owners' cost, and VAT has been estimated to be US$3,301,209,207**.**

Table 7: Capital Cost Summary for the 3 Phases (USD)

CAPEX FOR PHASE 1		PHASE 2	PHASE 3	TOTALS
COST AREA_ TOTAL INSTALLED COST				
WELLFIELD	$ 103,431,233	$ 188,999,721	$ 208,999,993	$ 501,430,948
EVAPORATION PONDS	$ 233,942,960	$ 294,869,162	$ 288,074,056	$ 816,886,179
TMA AREAS (Initial)	$ 22,365,351	$ 21,084,083	$ 21,084,083	$ 64,533,517
SOLVENT EXTRACTION	$ 214,871,407	$ 214,871,407	$ 214,871,407	$ 644,614,220
PURIFICATION PLANTS	$ 50,726,301	$ 50,726,301	$ 50,726,301	$ 152,178,902
ELECTRODIALYSIS&LHM PLANTS	$ 85,706,660	$ 85,706,660	$ 85,706,660	$ 257,119,979
UTILITIES PLANTS	$ 16,135,210	$ 16,135,210	$ 16,135,210	$ 48,405,631
LCE PLANT	$ 91,668,862	$ 91,668,862	$ 91,668,862	$ 275,006,586
ENERGY	$ 56,380,653	$ 23,267,387	$ 33,548,551	$ 113,196,591
INFRASTRUCTURE	$ 169,942,333	$ 67,967,715	$ 13,960,185	$ 251,870,232
VAT ADD ON	$ 47,140,956	$ 22,520,849	$ 15,050,802	$ 84,712,607
OWNERS COSTS	$ 31,981,793	$ 30,313,580	$ 28,958,444	$ 91,253,816
TOTAL CAPITAL EXPENDITURES	**$ 1,124,293,717**	**$ 1,108,130,936**	**$ 1,068,784,553**	**$ 3,301,209,207**

1.16.2 Operating Costs Estimate

The operating cost estimate has been made with quantities developed by the QP and unit prices provided by Lithea. The QP considers it to have an accuracy of ±15%. The estimate includes all site-related operating costs associated with the production of high purity lithium carbonate and lithium hydroxide but expressed as a total LCE. The operating costs were developed by the QP in conjunction with Ganfeng.

The operating expenditures (OpEx) have been calculated based on the following breakdown:

- Manpower
- Electric power
- Reagents
- Consumables & miscellaneous
- Camp operation & personnel transport
- Product transportation
- G&As

Annual operating cost summaries for the three stages of production are shown in **Table 8**.

Table 8: Operating Cost Summary for the 3 Phases

OPERATING COST Phase 1		OPERATING COST Phase 2		OPERATING COST Phase 3	
PRODUCTION TPA LCE	51,006	102,012		153,018	
	$/YEAR	$/YEAR		$/YEAR	
LABOUR + CAMP	$ 32,337,683	$	45,106,523	$	58,305,580
REAGENTS	$ 73,623,821	$	147,247,642	$	220,872,345
POWER & ENERGY	$ 72,225,910	$	149,408,298	$	226,590,686
G&A	$ 7,859,050	$	11,453,100	$	15,047,150
MEMBRANE	$ 2,017,000	$	4,034,000	$	6,051,000
SALTS DISPOSAL	$ 15,538,911	$	30,057,790	$	44,576,669
CONSUMABLES	$ 9,705,600	$	17,470,080	$	24,264,000
PRODUCT TRANSPORTATION	$ 10,500,000	$	21,000,000	$	31,500,000
MAINTENANCE	$ 21,888,841	$	43,777,681	$	65,666,522
SERVICES	$ 13,886,999	$	20,584,469	$	39,750,716
CONTINGENCY	$ 12,979,663	$	24,507,924	$	36,632,607
TOTAL ANNUAL COSTS	**$ 272,563,478**	**$**	**514,647,507**	**$**	**769,257,275**
COST/T LCE	**$ 5,344**	**$**	**5,045**	**$**	**5,027**

Dollar inflation has a significant impact on the plant's OpEx, particularly on the local cost components. This OpEx does not account for the effects of inflation. Certain inputs and services required for operations are sourced from the local market, and their prices were presented in U.S. dollars in our OpEx estimate to mitigate the impact of currency exchange rate fluctuations.

A total production cost of US$5,027 per ton LCE is estimated after Phase 3 is in full production. VAT has been included in the cost of reagents, and consumables.

1.16.3 RIGI Economics

This project can benefit from the Incentive Regime for Large Investments (RIGI, for its acronym in Spanish). The RIGI is a special framework introduced in Argentina under the "*Bases and Starting Points for the Freedom of Argentines Act*" (commonly known as the Bases Law), enacted in 2024. Its primary objective is to attract and promote large-scale, long-term investments by providing legal and fiscal stability, along with tax, customs, and foreign exchange incentives.

The application of RIGI results in a US$0.9 billion increase of NPV, compared with the case without RIGI, and an IRR improvement of 7.6%.

There is no guarantee that the PPG Project will secure RIGI eligibility.

1.17 Economic Analysis

The analysis was prepared using an economic model and assesses both before-tax and after-tax cash flow scenarios. Capital (CapEx) and Operational (OpEx) Expenditures presented in previous sections have been used in this analysis. Prices for lithium carbonate and hydroxide was estimated by the Golder. The results include Net Present Values (NPV) for 10% discount rate, Internal Rate of Return (IRR) and sensitivity analysis of key inputs.

The following criteria have been used to develop the economic model:

- Project life: Life of mine (including construction and operation) is estimated to be 33 years.
- Pricing for lithium carbonate of US$18,000 and lithium hydroxide monohydrate (LHM) of US$17,800 per ton was used.
- Final production rate of 153,000 TPA LCE after all three phases of production reach full operation 9 years after the start of phase 1.
- Discounted Cash Flow (DCF) analysis was based upon scheduling of the currently available Measured and Indicated (M+I) Resources with the assumption that 37% of M+I resources are pumpable as brine feed to the evaporation ponds and an overall lithium recovery efficiency of 75%.
- A discount rate of 10% was used.
- The Discounted Cash Flow (DCF) economic evaluation was carried out on a constant money basis so there is no provision for escalation or inflation on costs or revenue.
- For DCF evaluation purposes, it has been assumed that 100% of capital expenditures, including pre-production expenses, are financed with owners' equity.
- Pre-construction costs are not included in DCF analysis.
- VAT is included for both CapEx and OpEx.
- Lithium grades and recoveries stay constant for 30 years with no dilution.
- The key inputs to the economic analysis are shown in Table 9.

Table 9: The Key Inputs to the Economic Analysis (including RIGI benefits)

Economics Overview	Units	Phase 1	After Phase 3
LCE Production (nom)	TPA	51,006	153,018
Li_2CO_3 Production	TPA	40,000	120,000
LHM Production	TPA	12,500	37,500
Mine Life (nominal)	years	30	30
Capital Cost (CapEx)	US$	1,124,293,717	3,301,209,207
Operating Cost (OpEx)	US$/t LCE	5,344	5,027
Average Selling Price (LCE/LHM)	US$/t	18,000/17,800	18,000/17,800
Discount Rate	%	10	10
Net Present Value (NPV) Pre-Tax	US$	-	7,881,378,524
Internal Rate of Return (IRR) Pre-Tax	%	-	37%
Net Present Value (NPV) Post-Tax	US$	-	5,766,032,301
Internal Rate of Return (IRR) Post-Tax	%	-	32.7%

The project is currently estimated to have a payback period of five years. The economic analysis indicates an after-tax Net Present Value (NPV), discounted at 10%, of approximately US$5.77 billion with an Internal Rate of Return (IRR) of approximately 32.7%.

1.17.1 Sensitivity Analysis

Sensitivity analysis indicates that the Project is highly profitable.

Project strengths are as follows:

- Brine: The Project pumps subsurface brine to extract lithium, which is a proven and cost-effective method compared to hard rock mining.
- Lithium: The PPG Project has over 15,077,000 tons of measured and indicated (M+I) LCE resources, enough to support a production rate of 153,000 TPA LCE for a nominal 30-year life.
- Convenient accessibility and available utilization: The Project site is located 70 km away from energy pipeline. The flat and featureless ground over which the feeder pipeline is to be built reduces pipeline construction cost and complexity.
- Pricing Estimate: Sensitivity analysis indicates that the Project is economically viable even under unfavorable pricing conditions.
- Low operation costs.
- SX (DLE) strengths vs conventional process
- The application of RIGI results in a US$0.9 billion increase of NPV, compared with the case without RIGI, and an IRR improvement of 7.6%.

Some project risks list as follows:

- **Location:** Elevation: The Project site is at a high elevation, approximately 4,000 m above sea level, which can result in difficult work conditions for those not accustomed to high altitudes. Medical oxygen tanks are readily available for staff travelling to and working at the mine site.
- **Weather Dependence:** Unpredictable weather, including heavy rains and long winters in recent years, could affect the evaporation cycle in the ponds.
- **Process Implementation:** The process is specialized to the type of brine in the salar and there is no other industrial operation running the same process configuration. Mitigation measures include dedicated steps for removing impurities and purifying the solution.
- **Process System Design and Supplier Expertise:** Equipment and facilities are custom-designed for this unique process and the high-altitude, high-wind environment. Tests at additional suppliers and a pilot plant are recommended before placing equipment orders.

2.0 INTRODUCTION

2.1 Background

Ganfeng Lithium International Co. (“Ganfeng”) and Lithium Argentina AG, formerly Lithium Americas Corp. and Lithium Americas (Argentina) Corp. (“Lithium Argentina” or “LAR”) through their subsidiaries in Argentina are the holders of mining concessions for the extraction of lithium granted by the mining court of the province of Salta that cover the following areas:

- Pastos Grandes Project (“PGCo”): size of 20,095 hectares
- Sal de la Puna Project (“SdlP”): size of 13,852 hectares
- Pozuelos-Pastos Grandes Project (“Pozuelos”): Size of 32,314 hectares

The total PPG Project covers 66,261 hectares.

The project begins with the extraction of lithium-enriched brine from Salar de Pozuelos/Pastos Grandes and ends with the production of lithium carbonate and lithium hydroxide.

The brine extracted from the wells is transported by surface pipes to solar evaporation ponds located in the above mentioned salars where it reaches an approximate lithium concentration of 0.24%; then it is sent to a processing plant where the direct extraction of lithium by solvent extraction is carried out. The liquid rich in lithium, continues through a purification process with reagents and resins to eliminate the impurities of boron, calcium, carbonates and total organic carbon. Subsequently, the purified brine goes through a last stage of calcium removal with resins and then divides into two streams, one that goes directly to the production of lithium carbonate battery grade and industrial technical grade and the other that goes to an additional stage of boron removal, then to an electrodialysis process and to a lithium hydroxide production plant.

The solid residues from the purification stages, mainly Hydrated Calcium Pyroborate ($Ca_2B_2O_5 \cdot H_2O$) and Calcium Carbonate ($CaCO_3$), are separated from the brine by filtration and sent to final disposal.

The other liquids effluents obtained from the elimination of impurities are recirculated in the process or sent for final disposal.

The main steps involved in the production of Li_2CO_3 and $LiOH \times H_2O$ are:

- Extraction of brine from wells.
- Pre-concentration of brine in solar evaporation ponds (0.24% Li).
- Brine purification with reagents (solvent extraction DLE process)
- Brine purification with resins.
- Lithium carbonate plant battery grade and industrial technical grade.
- Lithium hydroxide plant.

Table 10: Design Criteria for Brine Extraction

Design Criteria	Unit	Quantity
Battery Grade Lithium Carbonate	%	99.5
Technical Grade Lithium Carbonate	%	99.0
Lithium Hydroxide Monohydrate	%	99.8

Design Criteria	Unit	Quantity
Production from Each Phase (3)	TPA	51,000
Operating Time (Ponds)	Days/year	365
Operating Time (Plants)	Days/year	300
Wells Phase 1	N total wells	34
Wells Phase 2	N total Wells	61
Wells Phase 3	N total Wells	62
Lithium Concentration in brine	% Each Phase	0.045/0.035
Evaporation Rate	mm/d	7
Overall Recovery (Design)	%	75

2.2 Source of Information

The source of information contained in this report vary depending on the subject. In general, much of the information was developed by different parties during earlier studies and updated accordingly. This information includes the following documents:

- Lithium Resources and Reserves Pastos Grandes Phase 2 Project Salta Province, Argentina, AW, Dec 2024
- Report for LCS Lithium – Preliminary Economic Assessment (PEA) – Pozuelos – Pastos Grandes Project, GHD, Jan 2019
- PG Technical Report Resource Estimate Aug 15, 2024, AW
- Brine Compositions & Flowrates from PG, Lithium Argentina, August 2024
- LIENPZ-0000-GE-MDC-001_B General Description Memo
- LMA 40 kt LCE & 12.55 kt $LiOH.H_2O$ Process flow information-E-0(2024.09.07)
- New Conceptual Geological Models for PZ and PG, Lithium Argentina, Jan 2025
- PG Water Budget: UMass/UAA Lithium Solutions: Salar Water Budget - Pastos Grandes July 2024 Update
- UMass/UAA Lithium Solutions: Preliminary Pozuelos Freshwater Availability Assessment September 2024

2.3 Authorization and Purpose

The following report has been prepared by the QP employed by Atacama Water and the QP employed by Golder at the request of LAR to provide a Scoping Study for the PPG Project, in Salta Province, Argentina, that follows the S-K §229.1300.

The report provides a comprehensive assessment of geological, technical, engineering, operational and commercial aspects (economic analysis) under which the PPG Project in northwest Argentina may be considered potentially economic so that the current development program can continue.

Atacama Water prepared 6.3.3, 6.4.2, 6.5.3, 7.2, 7.3.2, 8.2, 11.2, and 11.4 - 11.5 of this report. Sections 1 – 5, 6.1 – 6.2, 6.3.1 – 6.3.2, 6.4.1, 6.5.1 - 6.5.2, 7.1, 7.3.1, 8.1, 8.3, 9 - 10, 11.1, 11.3, and 12 - 24 were prepared by QP employed by Golder with technical support from Silvio Bertolli, Executive Consultant to Golder.

In addition, the QPs relied extensively on Ganfeng and LAR and on their independent consultants, as cited within the text of the study and the references, for information on costs, prices, legislation and tax in Argentina, as well as for general project data and information.

2.4 Report Responsibility Matrix

Responsibilities for the various sections of the report are shown in Table 11.

Table 11: PPG Scoping Study Responsibility Matrix

CHAPTER	RESPONSIBILITY
1 Summary	Golder
2 Introduction	Golder
3 Property Description	Golder
4 Accessibility, Climate, Local Resources, Infrastructure, and Physiography	Golder
5 History	Golder
6 Geological Setting, Mineralization, and Deposit	Golder, Atacama Water
6.1 Regional Geology	Golder
6.2 Structures	Golder
6.3 Geological Setting	Golder, Atacama Water
6.3.1 Lithology	Golder
6.3.2 Local Geology (Pozuelos)	Golder
6.3.3 Local Geology (Pastos Grandes)	Atacama Water
6.4 Mineralization	Golder, Atacama Water
6.4.1 Brine Composition (Pozuelos)	Golder
6.4.2 Brine Composition (Pastos Grandes)	Atacama Water
6.5 Deposit Types	Golder, Atacama Water
6.5.1 General	Golder
6.5.2 Pozuelos	Golder
6.5.3 Pastos Grandes	Atacama Water
7 Exploration	Golder, Atacama Water
7.1 Pozuelos	Golder
7.2 Pastos Grandes	Atacama Water
7.3 Drilling	Golder, Atacama Water
7.3.1 Pozuelos	Golder
7.3.2 Pastos Grandes	Atacama Water

CHAPTER	RESPONSIBILITY
8 Sample Preparation, Analyses, and Security	Golder, Atacama Water
8.1 Pozuelos	Golder
8.2 Pastos Grandes	Atacama Water
8.3 Conclusions and Recommendations	Golder
9 Data Verification	Golder
10 Mineral Processing and Brine Testing	Golder
11 Mineral Resource Estimates	Golder, Atacama Water
11.1 Pozuelos	Golder
11.2 Pastos Grandes	Atacama Water
11.3 Mineral Resources for the PPG Project	Golder
11.4 Groundwater Dynamic Modelling at Pozuelos	Atacama Water
11.5 Groundwater Dynamic Modelling at Pastos Grandes	Atacama Water
12 Mineral Reserve Estimates	Golder
13 Mining Methods - Well field	Golder
14 Recovery Methods	Golder
15 Project Infrastructure	Golder
16 Market Studies & Contracts	Golder
17 Environmental Studies, Permitting & Social or Community Impacts	Golder
218 Capital& Operating Costs	Golder
19 Economic Analyses	Golder
20 Adjacent Properties	Golder
21 Other Relevant Data and Information	Golder
22 Conclusions and Recommendations	Golder
23 References	Golder
24 Reliance on Information Provided by the Registrant	Golder

2.5 Property Inspection and Statement of Independence

James Wang visited the Salars and project facilities in April 2024. He visited the sites where the lithium process plants and infrastructures etc. will be located.

Frederik Reidel has visited and inspected the project sites on several occasions, with the most inspection taking place in October 2024.

Golder and Atacama Water are independent of Ganfeng and LAR.

2.6 Special Considerations for Brine Resources

The approach used herein to evaluate the Resources of the PPG Project is based on the framework in the S-K §229.1300, with some enhancements to accommodate the special considerations for brine.

The S-K regulations define Mineral Resource as:

"a concentration or occurrence of material of economic interest in or on the Earth's crust in such form, grade and quality, and quantity that reasonable prospects for economic extraction. A Mineral Resource is a reasonable estimate of mineralization, taking into account relevant factors such as cut-off grade, likely mining dimensions, location or continuity, that, with the assumed and justifiable technical and economic conditions, is likely to, in whole or in part, become economically extractable. It is not merely an inventory of all mineralization drilled or sampled."

It is the opinion of the supervising QP and Ganfeng and LAR, that the S-K §229.1300 definition of a Mineral Resource and Mineral Reserve extends to natural solid, inorganic material such as lithium, which is an industrial mineral that happens to be hosted in a liquid brine.

It is also the professional opinion of the supervising QP and Ganfeng and LAR that, subject to taking into consideration certain additional parameters of a brine deposit (including porosity, permeability and boundary conditions), the S-K §229.1300 regulation for evaluating a Mineral Resource is applicable to minerals hosted in a brine.

2.6.1 Brine Resource Estimation – Porosity

Evaluation of the Resource potential of a brine deposit includes estimation of two key components:

- the continuity and distribution of brine grade; and
- the portion of host material that contains the brine (i.e., the drainable porosity).

The first of these is analogous to solid deposits. Brine grade is determined through detailed sampling and an understanding of site geology, conceptually similar to solid deposit exploration. The second component (drainable porosity) does not have a direct analogy to solid deposits. The term "drainable porosity" denotes the ratio of the volume of fluid in the void spaces in a rock or sediment that can drain under gravity conditions to the total volume of the rock or sediment (e.g., Fetter, 1994). It is relevant to brine deposits because brine occurs in the pore spaces of a rock or sediment. However, not all the brine present in the pore space constitutes a Resource. A portion of the brine will not be recoverable due to:

- partial retention of brine by capillary tension within the pore spaces.
- dead-end pores that are not hydraulically connected to the broader pore network; and
- For a brine Resource Estimate, a porosity-related parameter known as Specific Yield ("Sy") or drainable porosity has come into common use to estimate the drainable portion of host material. Sy is defined as the ratio of the volume of water a rock or soil will yield by gravity drainage to the bulk volume of the rock or soil (e.g., Fetter, 1994). Meanwhile, Total Porosity (P) is defined as ratio of the total pore space of a rock or soil to the bulk volume of the rock or soil. Consequently, the difference between P and Sy is that portion of the pore space that will not drain under gravitational forces. Brine Resource Estimates will generally be supported by the development of a hydro-stratigraphic model which, at the Resource Estimate stage, is primarily used to characterize the distribution of Sy throughout the zone of estimation.

2.6.2 Brine Reserve Estimation

No reserve has been defined for the PPG Project yet. Two updated groundwater models have been developed for Pozuelos and Pastos Grandes Salars with the results of drilling and testing to date and this will be used to develop a maiden reserve for the PPG Project.

2.7 Units Of Currency

Unless otherwise stated, all units used in this report are metric. Salt contents in the brine, including lithium, are reported in weight percentages or mass per volume. All monetary values in the report are expressed in constant USA dollars.

The following table shows the meaning of the abbreviations for technical terms used throughout the text of this report, Table 12.

Table 12: Abbreviations Table

%	percentage
°C	temperature in degrees Celsius boron
BG	battery grade
B	boron
Ca	calcium
$CaCO_3$	calcium carbonate
CAGR	Compound annual growth rate
CapEx	capital expenditure
Cl	chlorine
Cl-	chloride ion
cm	centimetre
CO_3	carbonate
DCF	discounted cash flow
E	evaporation
G&A	General and Administration
g/cm^3	grams per cubic centimetre grams per litre
GPS	global positioning system
H_3BO_3	boric acid
ha	hectare
HCl	hydrochloric acid
HCO_3	bicarbonate

HSU	Hydrostratigraphic unit
ICP	Inductively Coupled Plasma
IRR	Internal Rate of Return
K/Li	potassium to lithium ratio kilogram
km	horizontal conductivity kilometre
km^2	square kilometer
ktpy	Kilo tonnes per year
Kv	vertical conductivity
L	litre
LAR	Lithium Argentina AG
LCE	lithium carbonate equivalent lithium
LHM	lithium hydroxide monohydrate
LiOH	lithium hydroxide
Li_2CO_3	lithium carbonate
L/s	litres per second
m	metre
masl	Meters above sea level
M+I	Measured + Indicated
mg	milligram
Mg	magnesium
$Mg(OH)_2$	magnesium hydroxide
mg/L	milligrams per litre
MT	Magnetotellurics
MW	megawatts
Na	sodium
Na_2SO_4	sodium sulfate
NPV	Net Present Value
OEMs	Original equipment manufacture
OpEx	operating costs
P	total porosity
Pe	effective porosity

PFD	process flow diagram
PG	Pastos Grandes
pH	measure of acidity or alkalinity
P&ID	piping and instrumentation diagram
PZ	Pozuelos
QA/QC	quality assurance/quality control
RBRC	relative brine release capacity
RC	reverse circulation
SO_4	sulfate
SO_4/K	sulfate to potassium ratio
SO_4/Li	sulfate to lithium ratio
SO_4/Mg	sulfate to magnesium ratio
SO_4	sulfate ion
MUSD	million US dollars
Ss	specific storage
SX	Solvent extraction
SX-B	solvent extraction - boron
Sy	specific yield
TDS	total dissolved solids
TEM	transmission electron microscope
TMA	tailing management area
TPP	Thermodynamic Property Package
TPA	tonnes per annum
USD	United States dollar
UTM	Universal Transverse Mercator coordinate system World Geodetic System
VEM	vertical electrical sounding
wt%	weight percent

2.8 Reliance On Other Experts

Golder has relied on Ganfeng, LAR, and their independent consultants for matters referring to site topography, site environmental information, exploration, drilling, and general project information.

The mineral resource estimate for the Pastos Grandes ("PG") and the Sal de la Puna ("SdlP") Projects presented in this report have been prepared by the QP, Frederik Reidel from Atacama Water Consultants ("AW") and reviewed by the QP, James Wang from Golder.

James Wang, QP, is responsible for the economics presented in this technical report.

3.0 PROPERTY DESCRIPTION

3.1 Location

PPG Project is located in the “lithium triangle” in the province of Salta, Argentina. The project is surrounded by Salar de Pocitos to the west, Salar de Rincon to the Northwest, Caucharí to the North, and Salar de Centenario to the South (Figure 1).

The Project incorporates two salars that are in close proximity to each other, namely the Pozuelos and Pastos Grandes salars, centred at 24°42′S, 66°49′W, and 24°34′S, 66°42′W, respectively. The salars are located in the Puna (Altiplano) region of northwestern Argentina, Salta Province, Departamento Los Andes. The salars are regarded as one production system for the purposes of this report. Figure 1 illustrates the location of the PPG Project.

Access to the property from Salta is excellent. A high-quality paved highway is available from Salta to San Antonio de los Cobres, the major urban centre in the Puna. The typical driving time from Salta to the property is approximately 4.5 hours.

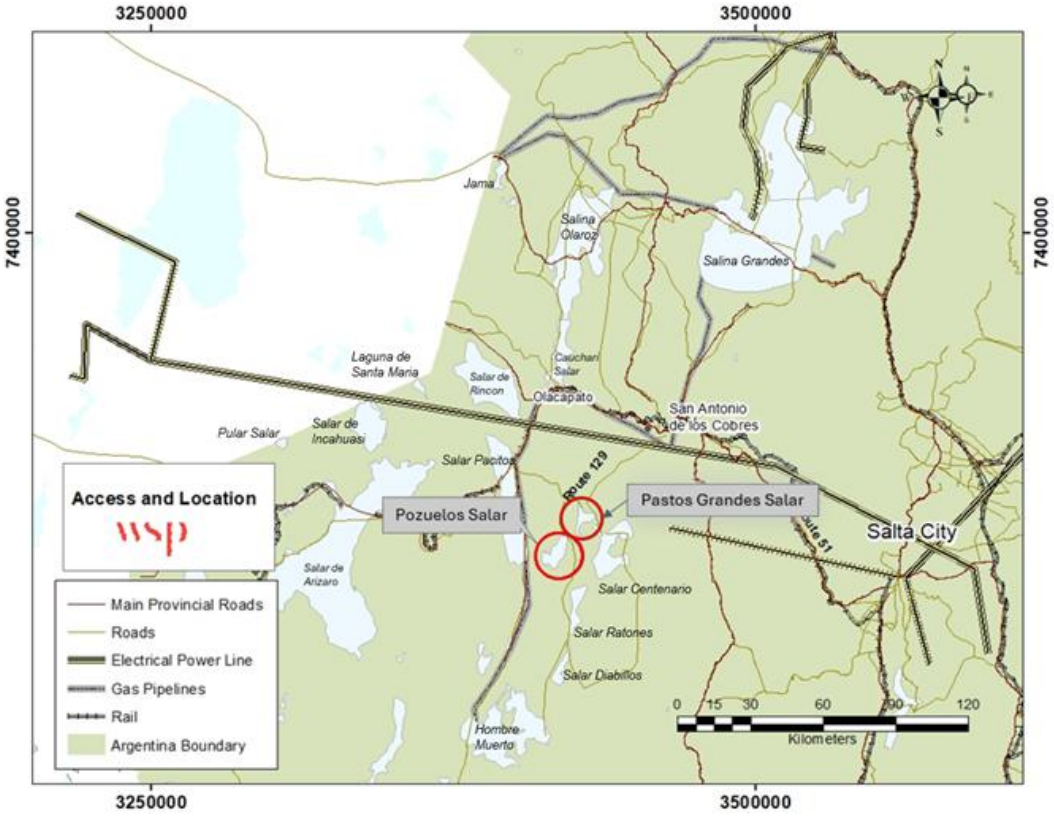

Figure 1: PPG Project Location (Source: Golder, Jan 2025)

3.2 Mineral Tenure

The Project is owned by Ganfeng and Lithium Argentina (the “Client”), and they are currently developing the PPG Project through three projects that are being consolidated into a new Joint Venture (JV). The parties entered into a framework agreement dated August 12, 2025 to establish the JV. On closing of the JV, Ganfeng will hold 67% of the PPG Project with Lithium Argentina holding the remaining 33%, with ownership based on resources, capital contributions and technology inputs. Formation of the JV remains subject to certain conditions and there is no guarantee that the parties will satisfy those conditions and enter into definitive agreements to form the JV.

The project consists of tenements covering Salar de Pozuelos and neighbouring Pastos Grandes. The New JV would make it one of the largest unified lithium brine resources, and one of the few consolidated basins. Ownership of the basins are currently distributed amongst three companies:

- Lithea Project (Pozuelos-Pastos Grandes - “Pozuelos”) is owned 100% by Ganfeng (green area), with the area of 32,314 hectares.
- Pastos Grandes SA (Pastos Grandes - “PGCo”) is owned 15% by Ganfeng Lithium and 85% by LAR (Blue area), with the area of 20,095 hectares.
- Sal de la Puna Project (Pastos Grandes - “SdlP”) is owned 100% by Puna Argentina SAU, whose parent company, Sal de la Puna Holdings S.à r.l., is owned 35% by Ganfeng and 65% by LAR (Orange area), with the area of 13,852 hectares.

The total PPG Project covers 66,261 hectares.

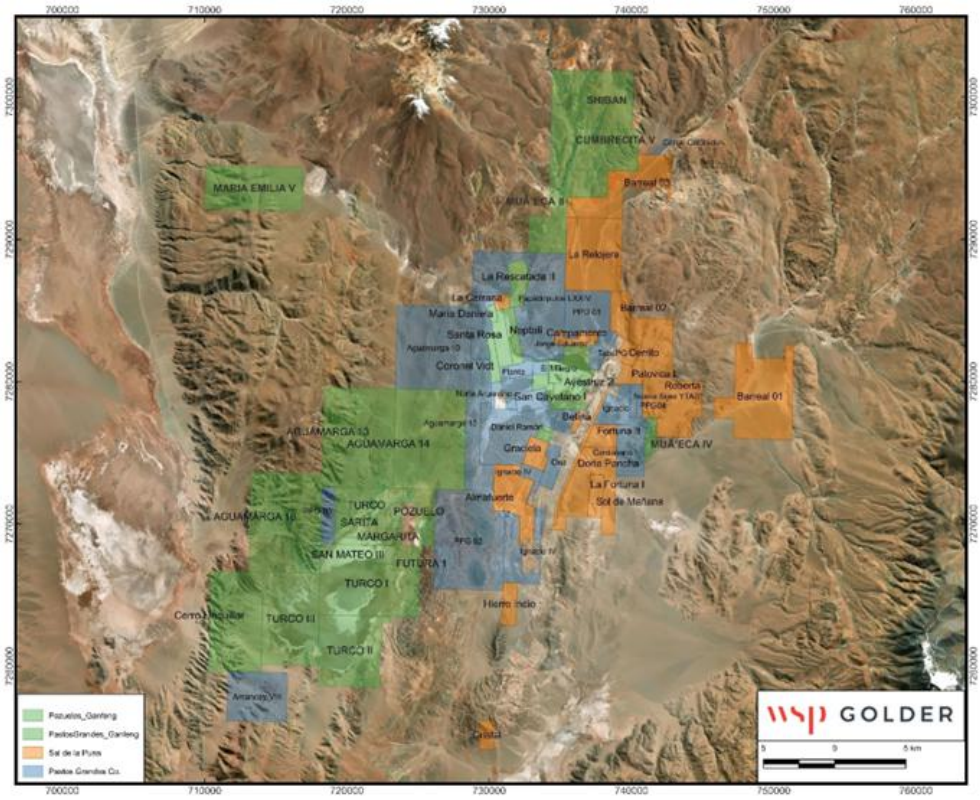

Figure 2: PPG Mining Properties (Source: Golder, Jan 2025)

Table 13: Mining Tenement of PPG Project

No.	Mine property ID	File No.	Area (ha)	Acquisition date	Minerals	Company
1	Turco I	17950	3095	10-Apr	Lithium and Borate	PZ_Ganfeng
2	Turco II	17951	2221	10-Apr	Lithium and Borate	PZ_Ganfeng
3	Turco III	17952	2600	10-Apr	Lithium and Borate	PZ_Ganfeng
4	Turco	17949	1576	10-Apr	Lithium and Borate	PZ_Ganfeng
5	Sarita	1208	194	10-Jul	Lithium and Borate	PZ_Ganfeng
6	Margarita	5569	300	10-Jul	Lithium and Borate	PZ_Ganfeng
7	Pozuelo	4959	200	10-Jul	Lithium and Borate	PZ_Ganfeng
8	San Mateo II	13171	200	10-Jul	Lithium and Borate	PZ_Ganfeng
9	San Mateo III	13172	200	10-Jul	Lithium and Borate	PZ_Ganfeng
10	Futuro I	12815	200	10-Oct	Lithium and Borate	PZ_Ganfeng
11	Aguamarga 13	19095	3500	14-May	Copper spread	PZ_Ganfeng
12	Aguamarga 14	19096	3500	14-May	Copper spread	PZ_Ganfeng

13	Aguamarga 18	19100	3500	14-Aug	Copper spread	PZ_Ganfeng
14	Cerro Unquillar	-	2591	-	-	PZ_Ganfeng
15	Shiban	21252	1498.13	14-Nov-11	Ag, Cu	Others_Ganfeng
16	Cumbrecita V	20026	2599.83	25-Nov-09	Ag, As, Au, Ba, Pb	Others_Ganfeng
17	Munecaa II	24075	1629.64	28-Jun-19	Lithium and Borate	Others_Ganfeng
18	Muneca IV	24220	194.72	27-Nov-19	Lithium and Borate	Others_Ganfeng
19	Maria Emilia V	23673	2077.05	26-Jul-18	Lithium and Borate	Others_Ganfeng
20	Avestruz	17517	460	17-Feb	Borates, Li, K	PG_Ganfeng
21	Leoncia	13533	100	17-Feb	Sodium, Sulfate, Li, K	PG_Ganfeng
22	San Cayetano I	17322	200	17-Dec	Borates, Li, K	PG_Ganfeng
23	María Luisa II	17904	100	17-Feb	Borates, Li, K	PG_Ganfeng
24	La Buscada	17589	88	17-Feb	Sodium, Chloride, Li, K	PG_Ganfeng
25	Calchin	18790	90	16-Dec	Salt, Li, K	PG_Ganfeng
26	La Playosa	18791	344	16-Dec	Salt, Li, K	PG_Ganfeng
27	Coronel Vidt	3445	185	16-Dec	Salt, Li, K	PG_Ganfeng
28	María Daniela	17737	60	16-Dec	Sodium, Sulfate, Li, K	PG_Ganfeng
29	La Rescatada II	17391	396	16-Dec	Borates, Li, K	PG_Ganfeng
30	Neptali I	9606	300	16-Dec	Salt, Borates, Li, K	PG_Ganfeng
31	Santa Rosa	17568	360	16-Dec	Salt, Li, K	PG_Ganfeng
32	El Milagro	17588	99	13-Jul-2016	-	PG Co.
33	Neptali II	18403	165	13-Jul-2016	-	PG Co.
34	Norte Argentino	18550	356	13-Jul-2016	-	PG Co.
35	Jorge Eduardo	18693	599	13-Jul-2016	-	PG Co.
36	Aguamarga 15	19097	1,298.00	19-Oct-2017	-	PG Co.
37	TabaPG	20016	317	19-Oct-2017	-	PG Co.
38	Papadopulos LXXIV	20247	3,038.00	19-Oct-2017	-	PG Co.
39	Ignacio	17606	500.05	20-Dec-2017	-	PG Co.
40	Ignacio IV	17630	1,026.84	20-Dec-2017	-	PG Co.
41	Daniel Ramon	18571	1,833.48	20-Dec-2017	-	PG Co.
42	Aguamarga 10	19092	3,087.28	20-Dec-2017	-	PG Co.
43	Nueva Sijesyta 01	23736	109.4423	20-Dec-2017	-	PG Co.
44	Papadopulos XXXII	19667	300	12-Oct-2016	-	PG Co.
45	PPG 01	24231	968.66	4-Dec-2019	-	PG Co.
46	PPG 02	24255	3,317.50	18-Dec-2019	-	PG Co.
47	PPG 03	24256	394.8	18-Dec-2019	-	PG Co.
48	Quarry Agregates Corral Colorado	24333	50	1-Jun-2020	-	PG Co.
49	PPG 04	734830	94	29-Apr-2021	-	PG Co.
50	Amancay VIII	748926	1,447.56	2-Sep-2022	-	PG Co.
51	ONA	1268	294	5-Jul-2023	-	PG Co.
52	Centenario I	19475	799	1-Mar-2024	-	PG Co.
53	La Relojera	22820	1997.5	-	-	Arena mineral
54	Fortuna II	20120	321.3	-	-	Arena mineral
55	Barreal 03	22880	1456.6	-	-	Arena mineral

56	Barreal 02	22879	413.3	-	-	Arena mineral
57	Barreal 01	22878	2682.9	-	-	Arena mineral
58	Almafuerte	18792	999.9	-	-	Arena mineral
59	Graciela	6189	299	-	-	Arena mineral
60	Patovica I	20902	257	-	-	Arena mineral
61	Roberta	23098	2523	-	-	Arena mineral
62	PPG 05 (ULEX-BORAX-PPG)	741663	231	-	-	PPG-SA-PASA
63	Sol de Manana	11961	299	-	-	PASA (Puna Arg SAU)
64	La serrana	13676	100	-	-	PASA (Puna Arg SAU)
65	La Fortuna 1	19308	1503	-	-	PASA (Puna Arg SAU)
66	Hierro indio	1186	305	-	-	PASA (Puna Arg SAU)
67	Dona Pancha	5879	208	-	-	PASA (Puna Arg SAU)
68	Cristal	5785	199	-	-	PASA (Puna Arg SAU)
69	Cerrito	7544	203	-	-	PASA (Puna Arg SAU)
70	Betina	4896	64	-	-	PASA (Puna Arg SAU)

3.3 Environmental Liabilities

According to current regulations, an environmental impact assessment must be filed prior to commencing field work and must be updated every two years; however, failure to comply with this does not cause the mining concession to expire.

Environmental liabilities include decommissioning and reclamation of the existing raw ponds, lined process ponds, and surface buildings associated with the pilot plant.

There are no known environmental liabilities.

3.4 Permits

In Salta there are Provincial and National environmental regulations: Provincial Constitution (art. 30, 81, 82 y 83), Environmental Protection Provincial Law No. 7070 and Provincial Decree No 3097/00 and 1587/03, Law No. 7017 of Waters Code of Salta Province and its regulatory decree No. 1502/00, 2299/03, among others, Provincial Law No 7141 of the Mining Procedure Code. The applicable authority in Salta is the Mining Secretary of the Province of Salta.

Lithea has an Environmental Impact Statement (“EIS”) approved by Salta’s Mining Secretariat for a 20ktpa lithium carbonate plant. The EIS has been renewed on a biannual basis.

PG Co has had an approved environmental impact declaration for the production of 20,000 TPA of LCE since 2020. Since 2022, the renewed declaration has been submitted every two years.

The Company has already submitted an Environmental Study for the pipeline corridor which allows the transport of brine from Pastos Grandes to Pozuelos. The EIR/EIS for Phase 1 (Pozuelos) was approved by the Province of Salta in November 2025.

3.5 Aboriginal Communities

For Pozuelos, a notarial certificate has been issued stating that no aboriginals live on the tenements and that there are no aboriginal claims on the subject lands.

The QP has not received the related notarial certificate of aboriginal communities in Pastos Grandes Salar.

3.6 Mining Rights Opinion

Argentina's Constitution establishes that natural and mineral resources belong to the provinces. The federal government of Argentina passed a Mining Code which establishes a common ground that each of the provinces should observe when regulating the mining activities. The federal government also established a limit on mining royalties to be paid by mining companies to the provinces, set at a maximum of 3% of the "pithead value" of the extracted mineral.

Individual Argentinian provinces promulgated provincial laws and regulations that govern the exercising of mineral rights. The province of Salta enacted Provincial Law Nº 8229, which adhered to the 3% maximum of "pithead value" of the extracted mineral. The Provincial Law defines the "pithead value" as the value obtained in the first stage of the commercialization process, minus direct and operating costs necessary to achieve that stage.

Lithea's annual fee (canon) obligations are up to date.

Regarding the mining concessions of the Pastos Grandes Co and Sal de la Puna, the following is indicated:

- No key issues have been found.
- All patent (canon) payments are up to date on all those claims where the patent is due.
- All claims are free from any evidence of mortgages, encumbrances, prohibitions, interdictions, or litigation.

4.0 ACCESSIBILITY, CLIMATE, LOCAL RESOURCES, INFRASTRUCTURE AND PHYSIOGRAPHY

4.1 Accessibility

Access to the properties from Salta is via National Route 51 (RN51) 170 km west and northeast to San Antonio de los Cobres. From there, the route goes 15 km to the junction with Provincial Route 129 (PR129) and from there 50 km toward Santa Rosa de los Pastos Grandes and then south approximately 11 km to salar de Pastos Grandes. From Pastos Grandes R129 goes westwards approximately 35 km, where it joins up with the access road southwards to Pozuelos as shown in Figure 3.

Access from Antofagasta, Chile is via the Panamerican Highway 5N 70 km to Baquedano, proceeding east along Routes 365, 367, and 23 for approximately 300 km to the international crossing at Paseo Sico. From Sico the shortest route to the sites is 130 km via routes RN51, RP127 and RP129 through Cauchari and Pocitos. Access from Chile is also possible via Paso Jama on NR52 and then via RN40 to Cauchari and RN 51, RP127 and RP129.

Figure 3: Local Road Access Map (Source: Ganfeng, 2024)

4.1.1 Road Access

Route 51 is mostly paved until it reaches San Antonio de los Cobres, where it continues as a gravel road. All other access roads described in this report are gravel roads, mostly kept in good condition as these roads are used by several mining companies active around Pastos Grandes. These roads are also used to reach several locations, including tourist destinations, around the area. Figure 3 shows the local roads available around the project.

4.1.2 Air Transport

The nearest cities to the project's site are Jujuy and Salta. Both have air connectivity offering regular flights to Chile and other South American countries (via Buenos Aires connection). Domestic flights connecting to other major cities across Argentina are also available on a regular basis.

4.1.3 Railway Road

The Salta-Antofagasta railway links Argentina and Chile, through the Andes. The 1 m gauge, non-electrified, 941 km, single-track railway connects the city of Salta, Argentina with the port city of Antofagasta, Chile. The track distance from Antofagasta to the Socompa Station is approximately 290 km.

The railway is currently being reactivated with agreements between the regional governments, and it undoubtedly will benefit many mining projects in the Puna (Figure 4).

4.1.4 Port

Nearest ports to the project site are the Antofagasta and Mejillones Ports in Chile, both of which serve as large Chilean mining industry ports for import and export activities. These main ports can be reached from the Pozuelos site following the same access route on Route 51, reaching "Paso de Sico" border pass and from there following Route 23 westbound to San Pedro de Atacama, Calama and finally Antofagasta (Figure 4). In this case, the distance from Pozuelos to Antofagasta is approximately 700 km.

Alternatively, Antofagasta can be reached by traveling north of Pozuelos, through San Antonio de los Cobres, and reaching Route 52 and then traveling west to reach the "Paso de Jama" border pass into Chile. This is the most used border pass in the region for international traffic. The distance from Pozuelos to Antofagasta through this route is approximately 800 km.

Additionally, an active railroad is available connecting San Antonio de los Cobres with the Port of Antofagasta in Chile. The train stops at Pocitos, approximately 60 km from Pozuelos, where an existing lithium producer currently loads lithium products onto trains destined for Antofagasta. This is also the preferred logistics route for product export as well as for the import of reagents to the Project site.

Alternative ports of import/export in Argentina are Rosario and Buenos Aires, which lie approximately 1,370 and 1,700 km away from the project site, respectively.

Figure 4: Ground Infrastructure to Reach Chilean Ports (Source: Ganfeng, 2024)

4.2 Climate

The climate of the Puna varies from semiarid in the eastern border to arid along the western border. Mountains east of the Altiplano-Puna are orographic barriers to humidity, producing the rain shadow desert in the plateau. The paucity of precipitation on the Puna is compounded by the high elevation, producing a harsh climate. The air is extremely dry, winds blow strongly throughout the year, precipitation is scarce, temperatures are low, clouds are normally absent, radiation is intense, and there are large daily temperature fluctuations. These parameters enhance evaporation and reduce detrital input to basins. Perennial streams locally feed sub-basins, but normally the water quickly disappears into alluvial fans. The conditions described above produce high rates of evaporation varying from 2,500 to 3,000 mm in an annual period (7-8 mm per day) generating a considerable hydric deficit.

The primary source of precipitation in this region is associated with Atlantic moisture recycled via the Amazon and moisture related to the South Atlantic Convergence Zone during summer. Minor amounts of precipitation also reach this arid zone via incursions of the southern hemisphere westerlies during winter. 80% of the annual precipitation falls in the summer from November to February. Based on data from the meteorological station at salar de Pocitos, the yearly average is 35 mm, mostly concentrated during the summer.

Based on INTA (National Institute of Agroindustry and Technology) data for the Puna region during the period 1901-1940, the mean annual temperature is 9.5 °C. The warmest month is December, which has a monthly mean temperature of 13.2 °C, whilst the coldest month is June with 3.7 °C. Daily temperature amplitude varies from 30 °C to 35 °C between day and night, depending on the season. The frost-free period is relatively short, and frost is very common and intense.

Winds in the Puna region vary considerably in velocity and are strongly controlled by the relief. The Puna region is located within a high-pressure zone originating southwest oriented winds, but its altitude above sea level generates a low-pressure centre with predominating local winds. There is also a seasonal air mass interchange between the Puna and its ranges; during the day the wind blows down from the ranges to the lower regions and during the night the reverse occurs. The maximum speed is registered during spring, remaining uniform the rest of the year. Beginning in September, there is an increase of solar radiation, atmospheric humidity and temperature variation producing more air mass movement compared to other months.

The climatic conditions at Salar de Pozuelos and Salar de Pastos Grandes are very similar due to their proximity to each other. The PPG Project lies close to the 50 mm/year isohyet (see Figure 5). Data for Santa Rosa de los Pastos Grandes, located approximately 35 km to the northeast of Salar de Pozuelos and 11 km north of Pastos Grandes, has been used to illustrate weather trends over the past few years. Figure 6 provides data on precipitation, wind speed, and other factors for Santa Rosa de los Pastos Grandes. Total average annual precipitation is approximately 60 mm/year in the actual salar, with higher elevations receiving somewhat more precipitation, primarily in the form of snowfall. Overall, the estimated average annual precipitation for the basin as a whole is estimated at approximately 75 mm.

Winds can be quite strong in the area, with wind speeds in excess of 80 km/h being recorded. Winds tend to increase during the day, with maximum wind speeds typically reached in the mid-afternoon. Wind speeds vary by season, with higher speeds typically being recorded in the summer months.

While the climate does not impose significant restrictions on exploration, it is normal procedure to not undertake drilling during the peak of the summer rain period in January and February due to problems associated with surficial flooding of the salars. The presence of water on the surface weakens the salt crust, preventing movement of heavy vehicles.

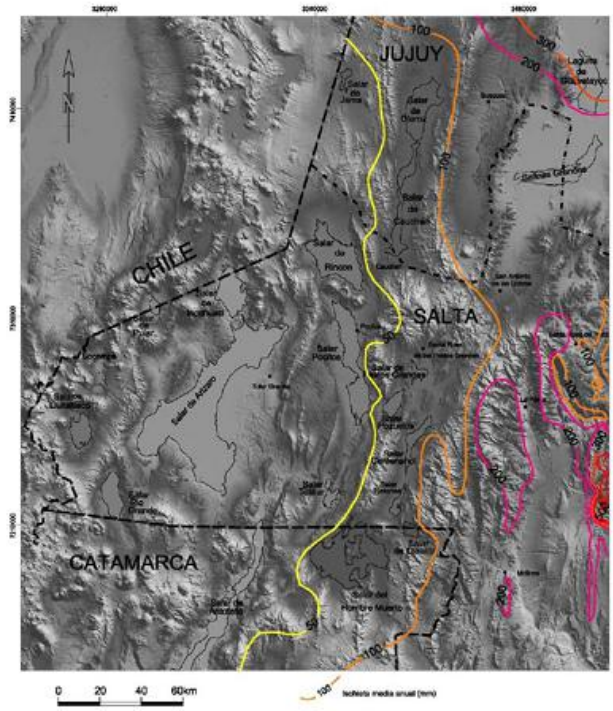

Figure 5: Isohyet Map of Puna (Source: Golder, Feb 2024)

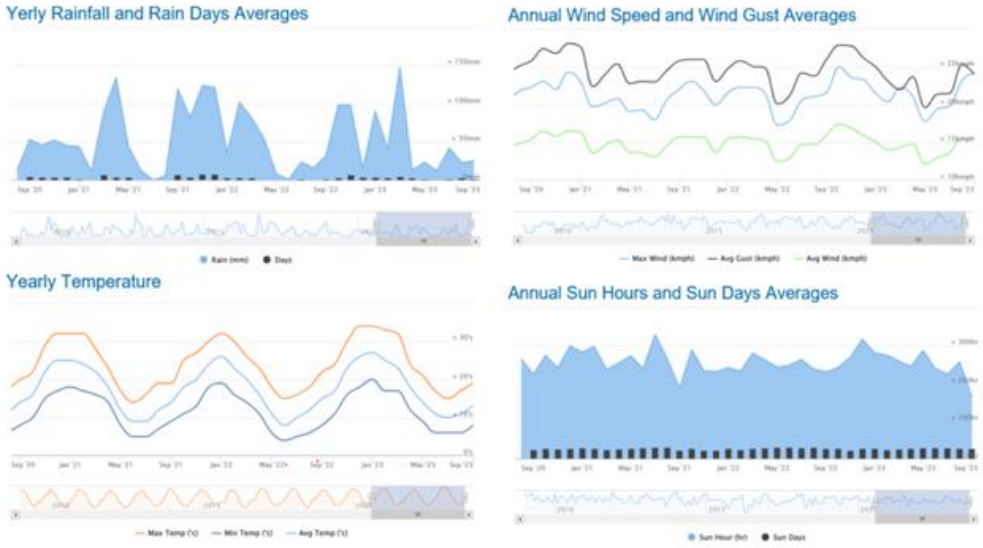

Figure 6: Weather Data – Santa Rosa de Pastos Grandes, 35NW of Pozuelos, Sep. 2020 – Sep. 2023

4.3 Physiography

4.3.1 Pozuelos

As with other evaporite basins throughout the Puna, Salar de Pozuelos has a centripetal drainage and basin-filling composed mainly of halite. It is emplaced between the NNE-SSW trending relatively low mountain chains: Pozuelos and Copalayo range. The average altitude is 3,755 masl. In the centre of the salar, whereas the maximal altitude reaches 4,850 masl. in the Pozuelos range (see Figure 7). The overall basin has a drainage area of approximately 385 km^2, while the salar itself occupies an area of approximately 82 km^2 comprising the core, edge and alluvial fan (Conhidro, 2018).

The salar is roughly ellipse-shaped and is characterized by a NE-SW trending long axis and a short axis slightly displaced southward. The salar is a large fossil salt pan where inflow waters seem to currently stem exclusively from fresh and salty springs from the flanks of the two bounding ranges. However, it is evident that sometime in the geologic past (less than 1.5 MYA) it was connected to Salar de Pastos Grandes by a paleo channel located in the north-eastern end of Pozuelos.

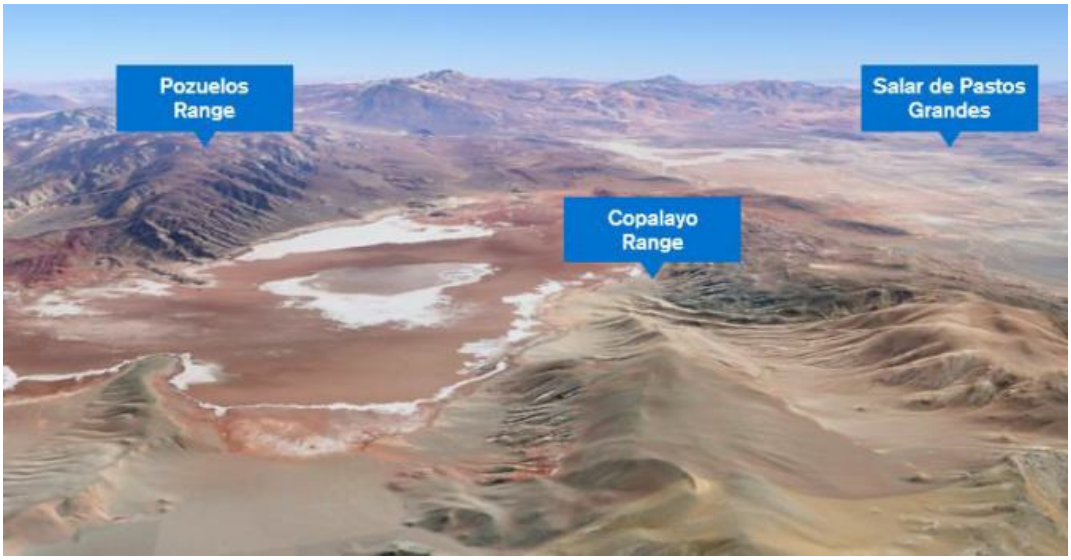

Figure 7: Physiography of Salar de Pozuelos and Surrounding Area (Source: Golder, Feb 2024)

The surface of Salar de Pozuelos is characterized by three types of salt crust with transitions between the three types:

- Hard, rough saline crust with halite pinnacle formations to approximately 30 - 40 cm height.
- Earthy saline crust with rounded surfaces, often with substantial clay and trending to soft conditions during wet periods; and
- Smooth saline crust.

4.3.2 Pastos Grandes

The nucleus of Salar de Pastos Grandes occupies an area of approximately 36 km^2 comprised mostly of flat sandy-silty salt crust. The overall basin of Salar de Pastos Grandes is 1,738 km^2 (drainage area), with the basin floor measuring 48 km^2.

Several remnants of outcropping halite sand-silt-clay sediments are present in the central portion of the salar and represent approximately 15% of the salar surface (Millennial Lithium, 2018). These outcrops, the Blanca Lila Formation, form “islands”. They are, however, hydraulically connected to the salar (Millennial Lithium, 2018).

The general elevation of the salar surface is 3,773 masl, with the “islands” having a typical elevation of approximately 3,785 - 3,790 masl. It reflects the paleotopographic height of the Pastos Grandes lake prior to its drainage into the Pozuelos system. The surrounding hills range in elevation from approximately 3,825 masl on the south, east and northeast sides of the salar and increase rapidly on the west side to approximately 3,990 masl.

4.4 Local Resources

There are no significant local resources at the property. Basic first aid, accommodation and food can be obtained at the village of Santa Rosa de Pastos Grande (population 120). The town of San Antonio de los Cobres, with a population of approximately 5,500, is the regional centre of the Puna and offers more extensive but still somewhat limited services in the form of accommodations, restaurants, basic equipment supplies and repairs, a clinic, primary and secondary schools and communications.

The village of Pocitos with a population of approximately 100 is located about 36 km to the northwest of the Project. It is envisaged that some labor force will be contracted from these localities.

4.5 Local Infrastructure

There is limited infrastructure within the immediate area of Pozuelos and Pastos Grandes. The village of Pocitos, population approximately 100, is located about 36 km northwest of the property. Pocitos is a station on the Antofagasta-Salta Railway and commercial train service is available three times per week between Pocitos and Antofagasta. Pocitos is the terminus of the Gasoducto de Puna (Puna gas pipeline) which has an extension running to Mina Fenix operated by Rio Tinto (formerly FMC Lithium) at Salar de Hombre Muerto. The project has permitting for construction but subject to significant infrastructure.

4.5.1 Existing Power Lines

- InterAnder 345kW Main Powerline and solar PV generation (60 km N).
- Powerline from Rincon Solar Farm transfer station to Pozuelos by YPF Luz & Partners
- High solar radiation makes the Puna a perfect candidate to include solar energy in the supply

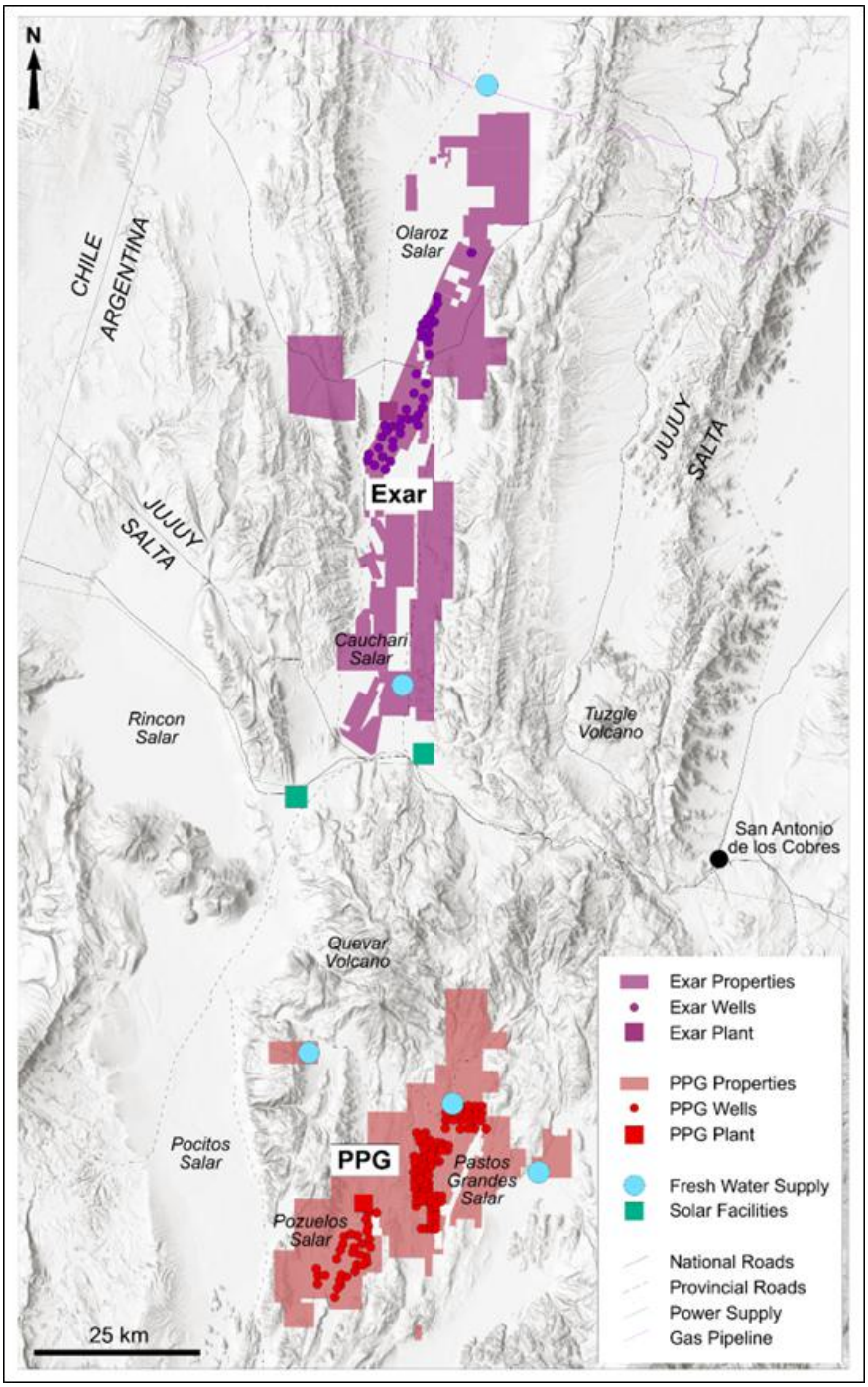

Figure 8: PPG Project Near Infrastructure (Source: LAR, 2025)

4.5.2 Natural Gas

Two (2) main gas pipelines (Nor Andino and Atacama Pipelines) are located between 200 - 250 km from Pozuelos.

Heat and steam for the process have been assumed to be supplied by brackets around Liquefied Natural Gas (LNG) trucked to site, stored, re-gasified and distributed to the respective users.

4.5.3 Water

It is expected that all industrial water supply requirements for the Project can be developed from groundwater resources hosted in the alluvial fans surrounding Salar de Pastos Grandes and Sijes River sub-basin.

4.5.4 On-site Facilities

Pozuelos hosts the Pozuelos exploration camp, which was completed in October 2018. The camp serves as the exploration base for the PPG Project and will be expanded as the Project advances.

PPG Main Camp is located in the northern end of Salar de Pozuelos (Figure 9), 38 km away from Santa Rosa de los Pastos Grandes Village.

Figure 9: Main On-site Facilities and Areas (Source: Ganfeng, 2024)

4.6 Soils

Soils in Pozuelos/Pastos Grandes area are of the ardisol type, with high salt content, very low organic content, low fertility and having a relatively coarse texture. SEGEMAR, the Argentine geological survey, classifies the salar itself as having a saline soil type “La”, with the immediate surrounding area containing the dunes and wetlands classified as DGtc-7 soil type and the higher elevations consisting of consolidated rock outcrops and natural elevations as EKtc-14 and Eni-6 soils.

4.7 Vegetation

Vegetation in the Puna consists of sparse, low shrub steppe-type zerophile and holophile plants. In more humid areas of the Puna such as Salar de Pastos Grandes the dominant grass types are Stipa and Fescue Dolihophila. Drier parts are represented by scattered grasses and low shrubs including: Fabiana sp, Adesmia sp, Parastrephia sp, Bacharis sp, Maihuenopsis and Polylepis sp, Tomentela (endangered), Ferozerable Prosopis (used as firewood), Trichosereus Pascana (endangered and used in construction), Larrea Divaricata ("Jarilla Hembra"), Artemisia Vulgaris ("Ajenjo"), Haplopapus Rigidus (locally "Bailabuena" and endangered due to medicinal use), Alcantholippia Deserticola phil (locally "rica rica" and endangered due to medicinal use), Baccharis Incarum ("Tola"), and Senecio Eriophyton or Escalonia Resinosa ("Chachacoma”) (Millennial Litium, 2018).

4.7.1 Fauna

Fauna in the Puna are adapted to the extreme living conditions of high aridity, intense sunlight during the day and very low night-time temperatures. Many animals are nocturnal or have acquired certain physiological features and behaviors that allow them to survive in the harsh environment. The most significant mammals in the region are the vicuña (Vicugna Vicugna), a camelid species, and llama (Lama Glama), which is domesticated. Fox (Dusicyon, Lycalopex) are present and prey on small rodents such as the mole known as Oculto or Tuco-Tuco (Ctenomys Opimus) and the Puna mouse (Auliscomys Sublimis).

Birds in the region include the Parina or Andean flamingo, living in moist and salty lagoons, and known as the Cerceta de la Puna (Anas Puna), and the Andean Goose, Guayata or Huallata (Chloephaga Melanoptera). The queu or quevo (Tinamotis Pentlandi) inhabits the highlands and is similar to a large partridge. The Nandu enano (Rhea) comparable with the species Pterocnemia Pennata inhabits the lower plains of the region. Small parrots, pigeons and owls also exist as sporadic inhabitants. The donkey (donEquus Africanus Asinuskey) is a feral species introduced by inhabitants of the area.

5.0 HISTORY

5.1 Prior Exploration and Ownership - Pozuelos

The prior exploration history and ownership of Salar de Pozuelos and Salar de Pastos Grandes properties is documented in NI 43-101 technical reports filed by LSC lithium on SEDAR (Hains, 2016; 2017a, b; 2018a, b). A brief summary is provided in the following sections.

- Sampling of brine in Argentine salars by Fabricaciones Militares (an Argentine government agency) during 1970.
- Evaluation of mineral potential of Argentine salars, including Pozuelos, by Igarzábal (1984) as part of the Instituto de Benefico de Minerales (INBEMI) investigation carried out by the National University of Salta.
- Production of borates from surface of northern portion of Salar de Pozuelos (on-going on intermittent basis).
- Acquired by Ekeko S.A. in about 2007. Acquired by LitheA Inc. in 2008 (Ekeko and LitheA were related companies at the time).
- LitheA was acquired by LSC Lithium by way of purchase option dated November 23, 2016. Option exercised March 15, 2017. (See press release issued by LSC Lithium on March 15, 2017, for details).

Details of the exploration by LitheA are described in detail in Hains (2017a, b; 2018a, b). Exploration activity included the following:

- **Surface Sampling**

  Widely spaced surface sampling (40 pits) to maximum depth of 1.8 m and mechanically dug pits (237 on 500 m x 500 m grid). Assay results indicated the presence of two higher grade areas within the salar and a significant area of high-grade brine within the central nucleus of the salar, with decreasing lithium grades towards the margins of the salar.

- **Geophysics**

  2009 Vertical Electrical Sounding (SEV) and magnetotelluric (MT) surveys to determine the presence and distribution of aquifer zones and the shape of the salar basin. The work identified the presence of three resistivity response zones indicating the presence of brine:

  1) Upper Conductive Zone (UCZ) is likely to consist of current or recent evaporite facies and highly porous brine-saturated halite.

  2) Intermediate Resistive Zone (IRZ) mainly formed by massive halite, gypsum, carbonates, borates and interbedded clastic sediments; and,

  3) Lower Conductive Zone (LCZ) or geoelectrical basement composed of buried equivalents of Ordovician and Cenozoic sedimentary outcrops surrounding the salar.

Presence of two depocenters in the salar one greater than 150 m depth with a halite composition and the other, smaller one, greater than 100 m depth and probably of a more clastic nature.

- **Drilling, pump tests, and evaporation tests**

  - Drilling

    Two vertical wells (SPZRC001 and SPZRC002) to a depth of approximately 90 m. A short (20 m deep) uncased piezometer well was drilled approximately 11 m east of SPZ RC001;

One HQ size diamond drillhole (SPZ DDH001) drilled to a depth of 183 m adjacent to SPZ RC001. This hole was drilled to collect data on variations in lithology with depth and to collect brine samples below a massive clay layer encountered at about 90 m depth in the rotary holes.

- Pump Tests

  Pump tests were conducted by Eramine Sudamerica and LitheA from holes SPZ001 and SPZ002. The results of the pumping tests by Conhidro (2011) indicated a transmissivity in the area of hole SPZ001 of 1,001 m^2/day and a storage coefficient of 0.0025 to 20 m depth and a transmissivity of 639 m^2/day and storage coefficient of 0.0000855 to 79.5 m. The pumping test for SPZ002 indicated a substantial drawdown of 55 m and a flow rate of 100 m^3/h over the full depth of the well. Grades (>500 mg/L lithium).

  Eramine Sudamerica (2012) completed step tests at well RC001PZ (ex SPZ RC001) and determined a transmissivity on the order of 400 m^2/day. A long-term pumping test (19 days) showed average lithium content during pumping was about 570 mg/L, with similar stability in other key anions and cations.

- Evaporation Tests

  As part of the work with POSCO, LitheA undertook a series of evaporation tests on brine recovered from the salar. These tests included analyses of evaporation from small test pits, as well as studies of evaporation using both lined and unlined ponds on the salar. It was found that due to the high porosity of the surface halite, pond evaporation using unlined ponds was not possible, but that use of lined ponds could be considered.

5.1.1 Fresh Water Exploration

LitheA completed a program of exploration for fresh water in 2016 (Hidrotec, 2016). The focus of the program was on the northwestern corner of the salar based on the results of the SEV geophysics. A 12” diameter 60 m deep RC hole was drilled near SEV 13 at UTM 3,418,550 Easting, 7,274,830 Northing (Gauss Kruger Posgar 94 datum). The hole was geo-electrically logged and three intervals screened for grain size distribution. The well was completed at 8” internal diameter with open slot casing from 20 to 42 m depth. The pump was set at 38 m depth.

Step and constant rate pumping tests indicated a specific yield for the well of 3.248 m^3/h/m with a yield of 18.936 m^3/h and a maximum operating rate of 35 m^3/h. Geological mapping of freshwater inflow areas around the perimeter of the salar shows major inflow sources are located in the northwestern and southern areas of the salar.

5.1.2 Past Production

There has been no past production of lithium brine at Salar de Pozuelos. The amount of production of borates from surface deposits is unknown.

5.2 Prior Ownership and History – Pastos Grandes

Mining for borates has been conducted in the Pastos Grandes area since the early 1960s. Borax Argentina, a subsidiary of Orocobre Limited, mines colemanite, hydroboracite and ulexite from the Sijes Formation on tenements located on the southern and eastern margins of the Pastos Grandes basin. The minerals are processed at the Sijes borates plant operated by Borax Argentina S.A.

In 1987 Ulex started borate mining operations on the southeastern extension of the Pastos Grandes basin at the Sol de Mañana mine, producing approximately 1,000 ton per annum of colemanite- hydroboracite-ulexite. Tramo SRL has mined colemanite on an intermittent basis at the Quebracho property on the southern border of Pastos Grandes and common salt on the salar surface since 2006. Various other mining groups have recovered salt from the salar using solar evaporation on various properties across the salar.

Initial exploration for lithium at Pastos Grandes was undertaken by the Direcion Generale Fabricaciones Militares (DGFM), an agency of the Argentine government, in 1979 when a program to explore for lithium in many of the salars in the Puna was started (Nicolli et al, 1982). Work at Pastos Grandes included geological mapping and surface sampling, with six brine samples from surface and eight from hand-dug pits and four from stream samples. The samples from the salar showed an average value of 384 ppm Li and 4,066 ppm K for pit samples and 327 ppm Li and 3,518 ppm K for surface samples (Nicolli et al, 1982).

In 2011 and 2012 Eramine Sudamerica SA, a subsidiary of Eramet SA, carried out surface mapping and sampling, drilling and pump testing at locations across the salar. Drilling was limited to a maximum depth of 160 m. In addition, Eramine also completed a program of geophysical surveys, including TEM, CS-AMT and VES (Eramine, 2016). The work by Eramine was summarized in an NI 43-101 technical report filed by Millennial Lithium in 2016 (Rojas, 2016) and updated in 2017 (Rosko, 2017).

LSC, as part of its initial due diligence exploration program related to acquisition of tenements on salar de Pastos Grandes, completed a program of surface sampling under the direction of the author. Details of the results of the due diligence program can be found in Hains (2017a).

LSC completed a program of exploration geophysics, drilling, and brine sampling resulting in an initial resource estimate for Salar de Pastos Grandes tenements dated October 19, 2018, of measured and indicated resources of 344 kt Li and of inferred resources of 58 kt Li.

Millennial conducted an extensive program of field work across the Salar from 2016 to 2021 known as the Stage Two and Three investigations of the Pastos Grandes Project. These programs delineated measured and indicated resources of 4,120 kt of LCE (Montgomery & Associates 2019). A positive NI 43-101 Feasibility Study (FS) was completed (Worley 2019) for a 24,000 TPA battery lithium carbonate production plant with a 40-year mine-life using conventional lithium processing technology based on 943 kt of proven and probable Mineral Reserves. In January of 2022 Lithium Americas Corp completed the acquisition of Millennial including the Pastos Grandes Project. LAR does not treat the mineral reserve estimate as a current mineral reserve estimate and no qualified person has done sufficient work to classify this historical mineral reserve estimate as a current mineral reserve. While the mineral reserve estimate was reported in accordance with CIM categories, the qualified person is unable to verify the relevance and reliability of the estimate at this time.

Centaur Resources (“Centaur”) carried out lithium exploration activities on the ‘Alma Fuerte’ mining claim of its Sal de la Puna Project immediate to the south and east of the LAR mining claims during 2018/2019. This program included drilling of three boreholes including a pumping well to around 600 m depth, pumping tests, and seismic & TEM geophysical surveys. On October 19, 2021, AMSA announced the results of the maiden mineral resource estimate (effective as of September 9, 2021) conducted on its Sal de la Puna Project (SdlP). An Inferred mineral resource consisting of 560,000 t LCE was defined on the Almafuerte property.

In 2023, LAR purchased AMSA (Sal de la Puna project). AMSA is now 65% owned by LAR and 35% owned by Ganfeng.

LAR owns 85% of Pastos Grandes Co Project (PGCo) while Ganfeng Lithium Netherlands Co., B.V. owns the other 15%.

6.0 GEOLOGICAL SETTING, MINERALIZATION, AND DEPOSIT

6.1 Regional Geology

The Central Andean Altiplano-Puna Plateau is the second-highest orogenic plateau globally, averaging 4000 meters above sea level, and the highest associated with extensive arc volcanism (Allmendinger et al., 1997; Pingel et al., 2023). The eastward-propagating fold and thrust belt defines a series of longitudinal tectonomorphic zones relevant to lithium (Li) brine formation, including, from east to west: the Precordillera and Cordillera de Domeyko; the Salar de Atacama (a distinct salt flat separate from the Altiplano-Puna basins), the Western Cordillera; the Altiplano-Puna; and the Eastern Cordillera (Figure 10; Allmendinger et al., 1997; Strecker et al., 2007; Victor et al., 2004; Carrapa et al., 2011; Benson et al., 2026). The Altiplano-Puna Plateau comprises high-elevation internally drained basins, arid climate conditions, and thick sedimentary accumulations conducive to Li brine generation and is geological setting of the PPG system (Figure 10).

6.2 Structures

The current relief of the Puna is characterized by north-south elongated mountain ranges separated by wide valleys often with endorheic depocenters (Figure 10). In most cases, the ranges are dominated by Paleozoic and Paleogene rocks unconformably overlain by Neogene sedimentary and volcanic rocks. Structures in the Neogene rocks are predominantly characterized by open folds and low-displacement thrust faults, contrasting with tight folds and high-displacement thrust faults exhibited by the Paleozoic to Paleogene units (Seggiaro et al., 2017). These basins have formed primarily in the eastern and central sectors of the Puna Plateau, through compressional Miocene-age orogeny (Helvaci and Alonso, 2000), and have been accumulation sites for numerous salars, including Pastos Grandes.

Altiplano-Puna Plateau uplift timing and mechanisms remain debated. Paleoaltimetric, thermochronologic, and palinspastic reconstructions contend either rapid kilometer-scale uplift during the Middle-Late Miocene (Ghosh et al., 2006; Pingel et al., 2023) or a more gradual rise since at least the Eocene (Canavan et al., 2014; Carrapa et al., 2014). Most of the uplift of the Altiplano began in the Late Oligocene, migrating eastward to the Eastern Cordillera of NW Argentina by ~12 Ma, where exhumation continued through ~4 Ma (Allmendinger et al., 1997; Carrapa et al., 2011). Farther south in the Puna, major uplift initiated in the Miocene and lasted until ~1-2 Ma. (Allmendinger et al., 1997).

Eastward migration of the orogen was accompanied by voluminous ignimbrite volcanism covering >500,000 km^2 (Allmendinger et al., 1997). Ignimbrites of the Altiplano-Puna Volcanic Complex (APVC), centered near the Argentina-Bolivia-Chile triple junction (Figure 10) erupted most extensively from large calderas between ~10-4 Ma (De Silva et al., 2006), and are often preserved as intercalated tuffs and tephra in Neogene sedimentary successions throughout the central Andes. Later Pliocene to Quaternary backarc volcanic centers and ignimbrite deposits became more subdued and more localized along NW-SE crustal lineaments such as Archibarca, Culampaja, Ojos del Salado, and Calama-Olacapato-El Toro (COT) lineaments (Figure 10; Richards and Villeneuve, 2002; Chen et al., 2020). These zones - including the Tocomar-Tuzgle area in the eastern Puna and the Cerro Galan Caldera in the Southern Puna (Figure 10) - reflect long-lived magmatism and hydrothermal activity in zones of elevated crustal permeability that likely contributed to Li mobilization and enrichment in adjacent basins.

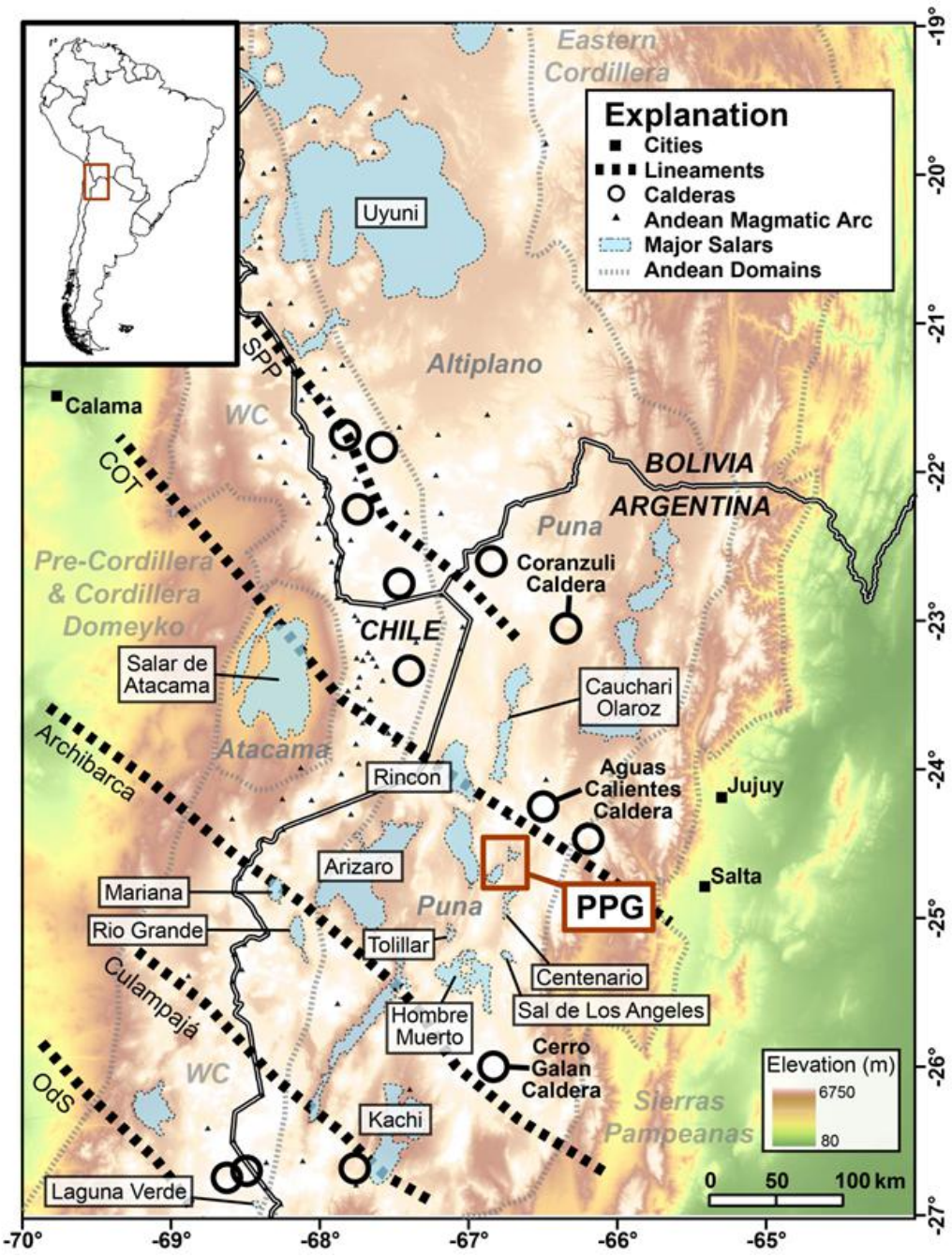

Figure 10: Map of the central Andean Mountains and location of the PPG project (Modified from Benson et al., 2026)

6.3 Geological Setting

The PPG Project spans both the Pastos Grandes and Pozuelos salars, which have intertwined geological histories and lithium mineralization. A geological map of the whole system is presented in Figure 11 and representative cross sections of both salars are presented in Figure 12. Stratum descriptions, outcrop locations, and ages for the major lithologies in the Project are discussed as follows.

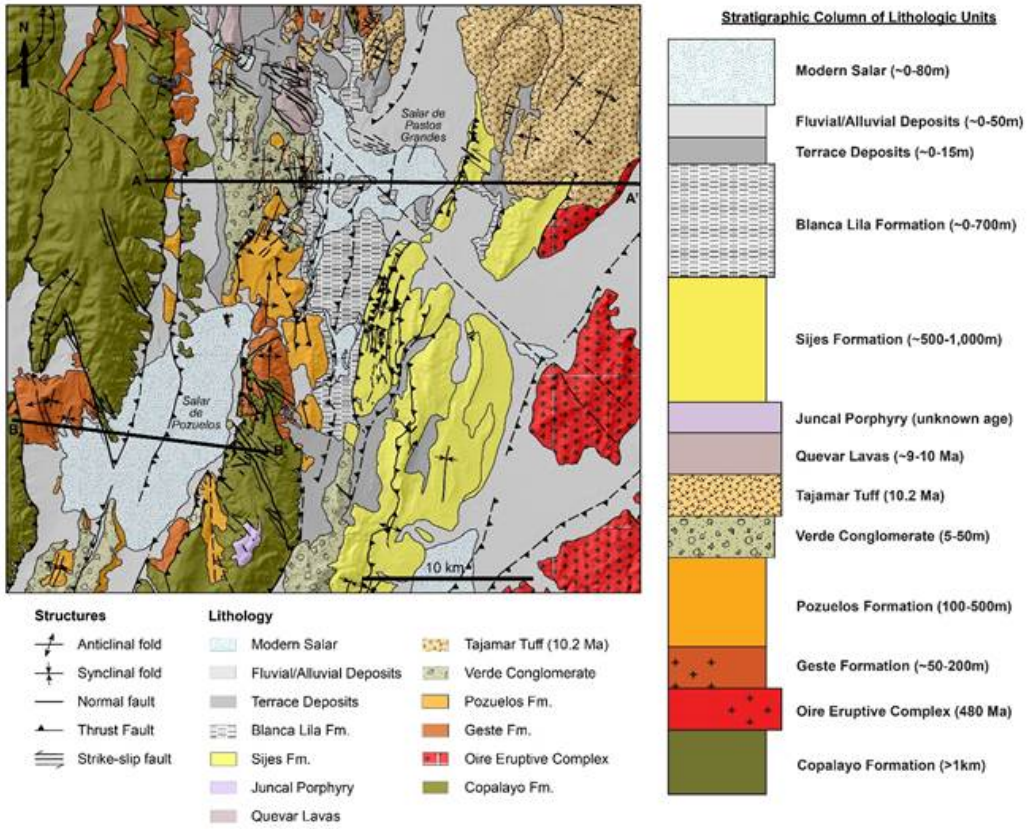

Figure 11: Geological Map and Stratigraphic Column of the PPG Project and Locations of Cross Section A-A' and B-B'

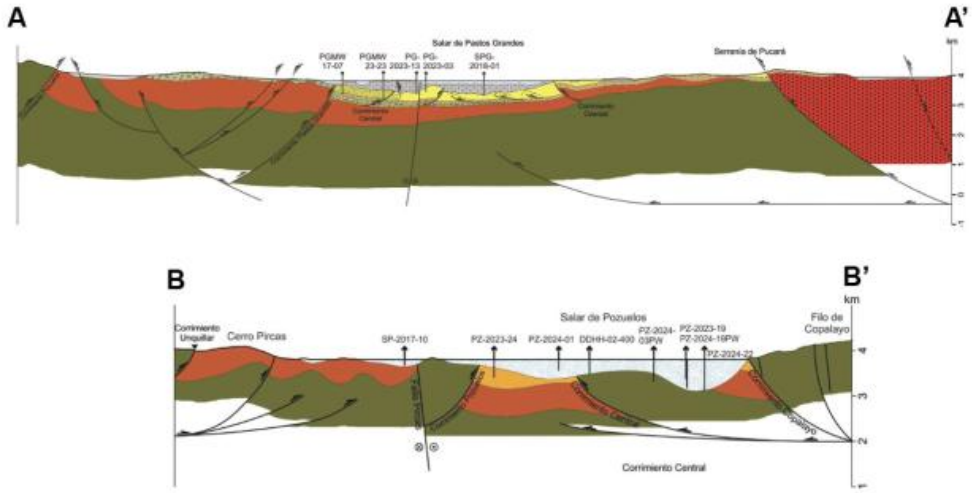

Figure 12: Representative Geological and Structural Cross Sections of Pastos Grandes (upper) and Pozuelos (lower). Note: cross sections are not the same scale.

6.3.1 Lithology

6.3.1.1 Copalayo Formation

The Copalayo Formation outcrops in the Sierra de Pozuelos, the ridge that divides the Centenario-Pastos Grandes basin in the east from the Pocitos basin to the west. Outcrops are also mentioned in the Sierras del Pucara, on the northeastern limit of the basin, and in the vicinity of the town of Santa Rosa de los Pastos Grandes (Cerro Condor Huasi). The formation is comprised of folded and faulted yellow-green shales, siltstones and subordinate sandstones (Figure 13), with evidence of low-grade regional metamorphism, localized hydrothermal alteration. The Copalayo Formation is the oldest outcropping unit in the area, estimated as Lower to Middle Ordovician based on different associations of graptolite fauna. An age of 453 Ma collected south of Quevar is consistent with other ages of ~440 – 460 Ma obtained on the unit in the Puna (Einhorn et al., 2015).

Figure 13: Copalayo Mountain Looking East from Pozuelos (left), and Outcrop of the Metasediments (right) of the Copalayo Formation North of Pastos Grades at Condor Huasi. (Source: LAR, 2025)

6.3.1.2 Oire Eruptive Complex

The Oire Eruptive Complex is a north-south strip of granitic to subvolcanic rocks that form the western foothills of the Palermo snow-capped mountain with slopes towards the Salar de Pastos Grandes basin. The Oire Eruptive Complex contains fine-grained and porphyritic varieties of granodiorite (Figure 14), which are locally intruded by rhyodacite porphyries. A complex of aplitic and lamprophyre dykes completes the sequence (as defined by Blasco et al., 1996). Crystallization ages on U-Pb in monazites from other areas indicate an age of ~470 Ma, roughly similar to the age of the Copalayo Fm (Blasco et al., 1996). New U-Pb zircon ages on granites from the Oire Eruptive Complex in the eastern margin of the Pastos Grandes salar and to the northeast along the margins of the Aguas Calientes Caldera indicate an age of ~480 Ma (Benson et al., 2026).

Figure 14: Outcrops of the Oire Eruptive Complex Showing Varying Granitic Textures from Pastos Grandes basin (left) and the Eastern Margin of the Aguas Calientes Caldera (right). (Source: LAR, 2025)

6.3.1.3 Geste Formation

The Geste Formation consists of conglomerates and sandstones and is interpreted to represent an alluvial depositional environment. Clasts within the conglomerate are dominantly quartzite and metasediments (Figure 15) and were likely derived from the erosion of underlying Copalayo Formation. These clasts are typically between 5-20 cm in size and are sub-angular to sub-rounded but can be up to 70 cm wide in places. Sandstone grain composition is similar to the conglomerates, being dominated by quartzites and metasediments, with a medium-coarse grain size. Both the conglomerate and sandstone have a fine matrix that is heavily altered to give the Geste Formation its characteristic red orange to purple colour (Figure 15). In between the Pastos Grandes and Pozuelos, the Geste Formation has been described as over one kilometre thick, but its thickness within the basins is unknown at this time. Based on mammal ages, this unit was assigned a Middle to Upper Eocene age (Alonso, 1992). DeCelles et al. (2007) obtain a detrital U-Pb zircon age of ~36 Ma on Geste formation from three outcrops collected in the canyon between the Pastos Grandes and Pozuelos.

Figure 15: Outcrop of the Geste Formation Conglomerate in Northern Pozuelos. (Source: LAR, 2025)

6.3.1.4 Pozuelos Formation

The Pozuelos Formation predominantly consists red to brown poorly consolidated sandstones and siltstones with local lenses of conglomerates and subordinate beds of mudstones and intercalated tephra. In the area between the Pastos Grandes and Pozuelos, the contact between the underlying conglomeratic Geste Formation and the Pozuelos formation is not immediately obvious, as this represents an upward fining foredeep basin (DeCelles et al., 2007). In the map, the units are separated based on the dominant lithology into the conglomerate-dominated Geste Formation and the sandstone-dominated Pozuelos Formation. Another discriminating feature is the presence of tephra layers; minimal to no volcanism occurred coincident with the Geste Formation. As time went on, volcanism in the Altiplano-Puna Volcanic Complex began to increase and some of these rocks are preserved in the Pozuelos Formation.

In places, the Pozuelos Formation directly overlies the Copalayo Formation, such as in southern Pozuelos and at Quebrada Seca north of Pastos Grandes. At Quebrada Seca, the strata are exposed as a 200 m thick section of brown to red sandstones and some finely laminated, silty claystones to subordinate waxy mudstones (Figure 16). A new U-Pb zircon age of ~10.7 Ma on a crystal-rich tuff in the upper portion of this sequence (sample TB24-029) is consistent with an age older than the Tajamar Tuff, though it is within error. The Pozuelos Formation is drilled along the western margin of the Pastos Grandes basin (hole PGMW19-21) based on new geochronology of an intercalated ignimbrite, the Verde Ignimbrite, dated at ~14.6 Ma (Benson, T.R., Boutt, D., Butler, K.L., Deshong, T., Gibbons, L., Hatton, K., Jenckes, J., McCaffrey, O., Mesbah, N., Munk, L.A., Rasbury, T., and Wooton, K., in review, The timing and origin of lithium brine deposits in the central Andean Mountains, *Geology*.). The same ignimbrite is found interbedded in red sandstones and siltstones of the Pozuelos Formation to the west of Pastos Grandes and north of Pozuelos, where a U-Pb age of ~14.9 Ma (sample TB-2024-96-SBU) was obtained on zircon minerals. These ages are consistent with previous estimates of ~15-10 Ma for the formation (Vandervoort, 1993).

Figure 16: Outcrop of the Pozuelos Formation at Quebrada Seca Comprised of Sandstones and Siltstones, with Minor Mudstones and Tephra. (Source: LAR, 2025)

6.3.1.5 Verde Conglomerate

The Verde Conglomerate is a mappable unit atop the Pozuelos Formation that likely represents a fanglomerate from the west associated with basinal formation. The distinctive green outcrops owe their color to the primary constituent clasts angular to subangular metamorphic clasts of the Copalayo Formation (Figure 17). The Verde Conglomerate is directly overlain by the 10.2 Ma Tajamar Tuff.

Figure 17: Verde Conglomerate Overlying Sands and Silts of the Pozuelos Formation and Underlying Tajamar Tuff (left) and a Close-up Photograph of the Unit in Outcrop (right) (Source: LAR, 2025)

6.3.1.6 Tajamar Tuff

At 10.2 Ma, the Tajamar Tuff erupted from the Aguas Calientes Caldera (Petrinovic et al., 2006; 2010) ~15 km to the north of the Pastos Grandes project. The tuff blanketed the northern Pastos Grandes area and serves as the key marker bed in the basin. The unit is distinctive in its mineral content, with a crystal-rich cargo of quartz, biotite, and feldspar (~40%) and a pink weathering color (Petrinovic et al., 2006; 2010). Lithic fragments are primarily angular volcanic rock less than a few cm in diameter and range from ~10% of the rock near the caldera margin to <1% of the rock in the Pastos Grandes basin. Where nonwelded obvious white pumice lapilli comprise ~15% of the rock. Pumice is not obvious in welded portions (in some cases incorrectly mapped as Verde Ignimbrite), though in places, flattened crystal-rich fiamme up to 10cm wide can be observed. The Tajamar Tuff (Figure 18) is geochemically distinct from the Verde Ignimbrite, making it easy to distinguish chemically. New U-Pb zircon ages on this unit from outcrop and core confirm that this unit is ~10.2 Ma (Benson et al., 2026).

Figure 18: Outcrop of the 10.2 Ma Tajamar Tuff in the Pastos Grandes Basin (Source: LAR, 2025)

6.3.1.7 Quevar Volcanic Complex

The Quevar Volcanic Complex is a large volcanic pile composed of the output from several lava forming eruptive sequences. Age relationships for the Quevar Volcanic Complex suggest an eruptive age of the volcanics ~8.7-9.9 Ma (Escuder et al., 2022; Pingel et al., 2023), situating it sequentially just after eruption of the Tajamar Tuff from the Cerro Aguas Calientes caldera (Escuder et al., 2022). Hydrothermal activity within the complex occurred until at least ~4 Ma, resulting in the formation of an Ag-Pb (Sb, As, Bi) deposit (Robl et al., 2009; Escuder et al., 2022), and likely providing Li-rich hydrothermal fluids to the Pastos Grandes basin (e.g., Benson et al., 2023) through most of the lifetime of the lake. The pile of lava has several different types and compositions ranging from andesitic lava flows to rhyodacite and perlite. Whole-rock geochemical data reflect this, though all units seem to follow a roughly linear fractionation line noted by higher Nd than the Tajamar Tuff. All the lava though has a dark, dense, glassy texture to it (Figure 19) with a range of phenocrysts including abundant feldspars or quartz depending on the flow. Much of the flow area is also characterized by distinct signs of interaction with fluids; this includes the appearance of perlite on the southern flank where the lavas likely flowed into a paleolake. Flow structures such as flow banding and vesicles are visible in well exposed parts of the flow. In places, the Quevar rocks are pyroclastic in nature. Most of the compositionally highly evolved members of the Quevar volcanics flowed onto the south flank of the volcanoes and into the Pastos Grandes basin. Benson (2024) obtained a new age in well PGMW-23-23 of 8.9 ± 0.2 Ma that we correlate to the Quevar volcanics based on composition and phenocryst assemblage.

Figure 19: Example of Dark Glassy, Porphyritic, Lava Flow Material from One of the Quevar Lava Flows Exposed in the Northern Part of Pastos Grandes (Source: LAR, 2025)

6.3.1.8 Juncal Porphyry

The Juncal porphyry (with epithermal overprint) is a poorly studied copper-gold prospect south of Pozuelos within the Copalayo Formation (Figure 13). The main dacitic intrusive measures approximately 1km x 0.25km, though the quartz-sericite alteration zone with metal enrichments covers an area of ~4.5 km^2 (Arganaraz and Innes, 2002). Mineralization occurs in both quartz veins and disseminates within the intrusive. The rock has not yet been dated, though it is estimated to be Miocene in age based on similarities to other porphyries in the region.

6.3.1.9 Sijes Formation

Sediments that accumulated after the eruption of the Tajamar Tuff have previously been called the Pozuelos, Sijes, and Singuel Formations. Herein, we adopt the Sijes Formation terminology to apply to all sediments that accumulated after the Tajamar Tuff and prior to deposition of the Blanca Lila Formation ~4 Ma. This is because the rocks exhibit vertical and lateral variations that are considerably faulted and folded making their discriminated projections into the subsurface a futile effort at present.

In places over 1km thick, the Sijes Formation outcrops to the east and south of the Pastos Grandes salar and has been intersected at depth in drill holes on the eastern margin of the salar.

Proximal facies of this unit consist of repeated 5-10 m cycles of interbedded clays, silty sands and minor evaporites (halite), with tuff horizons (Figure 20). The clastic layers are typically 3-5 cm thick and have little discernable internal structure. The layers are a brown-red color, and the clays have a waxy sheen and taste of salt, likely secondary. The fine-grained lacustrine lithologies contain borate beds that are the sites of historical and active borate mines (Alonso, 1992). Previous workers have dated the Sijes Formation at ~8-3 Ma (Vandervoort, 1993; Quade et al., 2015; Pingel et al., 2020) and new U-Pb zircon ages on tephra interbedded in the Sijes Formation obtained by are in agreement with this age range (Benson et al., 2026).

Marginal facies of the post-Tajamar sediments include the previously defined Singuel Formation along the eastern margin of the basin. It consists largely of 5-10 m cyclical deposits of pebble conglomerates fining upwards into sandy siltstones, and occasional tuff horizons. The clasts in the Singuel conglomerate are largely quartzite, metasediment, and granitoids derived from the exposures of basement rock along the southeastern flank of the basin. These clasts are sub-rounded to rounded and have an average size of 5-10 cm, with some clasts up to 20 cm. To the west, marginal sediments coeval with the main Sijes depocenter are alluvial to fluvial in nature (conglomerates and sand-siltstones) and have an age of 3.07 ± 0.29 Ma from an interbedded tephra (TB24-009). This age is likely coincident with the onset of thrust faulting that resulted in the formation of the Blanca Lila Lake.

Time-equivalent facies of the Sijes Formation occur as "Tertiary basement" in the Pozeulos salar, where fine-grained lacustrine to coarse-grained marginal facies were deposited atop the Copalayo and Geste Formations (Benson et al., 2026). This area was not the focus of prolonged sediment accumulation, as ages of intercalated tephra are restricted to ~7-9 Ma (Benson et al., 2026). Where observed in outcrops and core, these sediments have an orange to tan color, are finely laminated, and are strongly folded and indurated (Benson et al., 2026), likely due to post-4 Ma thrust faulting.

Figure 20: Lacustrine Interval of the Sijes Formation with Interbedded Siltstones, Mudstones, Borates, and Tephra (Source: LAR, 2025)

6.3.1.10 Blanca Lila Formation

The Blanca Lila Formation is the youngest stratigraphic unit in the Pastos Grandes Basin. The unit consists largely of thick evaporite layers with interbedded silts, clays and tuff horizons (Figure 21). Evaporite layers are halite dominated. Clastic layers are fine grained with little internal structure, tan-grey in color, and typically <5 cm thick. In drill core, this unit varies from 10s of meters thick along the western margin of the salar to >700m thick in the central part of the basin just west of a N-S trending thrust fault (DD-01). Here, the Blanca Lila Formation is dominantly fine to coarse cubic halite and chevron halite with interstitial red, brown, and black clay and silt, with minor sandy intervals. Hole DD-01 did not reach the bottom of the Blanca Lila Fm so the unit could be much thicker than currently appreciated.

The Blanca Lila Formation is typified in outcrop by the halite-rich Blanca Lila islands within the Pastos Grandes Basin, which represented a high stand of the Blanca Lila Lake ~200,000 years ago (Pingel et al., 2020). Marginal facies of this lake are preserved along the north, south, east, and west margins of the Pastos Grandes basin and are dominated by carbonate and gypsum evaporites (Figure 21).

Time-equivalent facies occur in the Pozuelos, ranging from ~1-2 Ma (Benson et al., 2026). These rocks preserve a classic small lacustrine system with coarse grained facies near the modern salar margins and and a fine-grained mixed clay-halite core in the center of the lake.

Figure 21: Outcrop of the Halite Mudstone Core of the Blanca Lila Formation in Blanca Lila Island (left) and Marginal Carbonate Mudstone Facies on the Southwestern Margin of the Pastos Grandes Basin (left) (Source: LAR, 2025)

6.3.1.11 Terrace Deposits

The terrace deposits are developed on Tertiary units in both Pastos Grandes and Pozuelos basins. They consist of alluvial deposits that generally correspond to the outcrops from which they come. Most are comprised of medium to coarse fanglomerates, moderately selected with coarse stratification, and a yellowish color that is well differentiated from the reddish deposits of the Tertiary. Clasts of volcanic and metamorphic rock predominate over the older schists and sediments. The deposits vary in age based on the area, with some likely as young as the Holocene or as old as the mappable Verde Conglomerate shown in Figure 17 (Blasco et al, 1996).

6.3.1.12 Fluvial/Alluvial Deposits

These deposits constitute the modern detrital accumulations and comprise various origins and are widely distributed throughout the project area. They present variable thicknesses and are unevenly distributed over all the underlying units. In general, they are unconsolidated deposits of highly variable granulometry which cover depressions forming alluvial fans or constitute fluvial deposits in various creeks. Locally there are accumulations of dune forming sands with aeolian origin, such as at the southern end of the Salar de Pozuelos. The ejection cones that converge towards the great depressions are composed of clastic elements of variable granulometry, generally sandy silt or fine clastic material. Finally, vertical and horizontal granulometric selection can be observed while superficial and thin layers of angular fragments are common, settled on silt or sand, leaving thick clasts accumulated on the surface (Blasco et al, 1996).

6.3.1.13 Modern Salar

The modern Pastos Grandes and Pozuelos salars contain a variety of similar lithologies, though the stratigraphy and thicknesses very considerably. For example, the halite interval at Pozuelos is relatively uniformly thick across the whole salar (~80m), whereas the halite body at Pastos Grandes thickens drastically to the east.

The uniform thickness of the halite body at Pozuelos and the geomorphology of the margins suggest that the bulk of the Li in the salar was transported via a catastrophic flood from the Blanca Lila lake (Benson et al., 2026). Because the high stand of the former Blanca Lila lake contains tephra as young as 0.2 Ma (Pingel et al., 2020), this flood likely occurred within the past few hundred thousand years through the steep incision of the Pozuelos Canyon.

Because the Pozuelos is a younger and shallower system, Ordovician basement rock (Copalayo Fm.) was intersected in drill core in Pozuelos. The oldest rock drilled at Pastos Grandes is the Pozuelos Fm. Along the western margin of the salar, indicative of the longevity and depth of the Pastos Grandes basin.

Both salars contain key lithologies presented in Figure 22. These lithologies were used as a basis to group the subsurface into key hydrogeological units, which differ in both salars.

Figure 22: Key Lithologies Present Drill Core in the PPG Project. (Source: LAR, 2025)

6.3.2 Local Geology (Pozuelos)

The modern salar at Pozuelos is classified as a mature salar. The lithology of the salar reflects this development, with the following general sequence of hydrogeologic units:

1) Ephemeral Saline Lake Facies, comprised of halite with mixed textures is the uppermost layer of the salar and contains sediments related the modern hypersaline lake.

2) Perennial Saline Lake Facies, comprised of fractures and massive halite with interstitial clays and sand.

3) Saline Mudflat Facies, comprised of silt mixed with clays and fine sand, associated with an older, oversaturated lake and quiet environment, likely time-equivalent to the Blanca Lila Formations.

4) Playa Margin Facies, comprised of gravels representing alluvial and colluvial deposits with some interbedding of more sandy facies, both laterally and vertically, likely corresponding to the Blanca Lila Formation marginal facies, respectively.

5) Siltstone, comprised of Cenozoic siltstones likely correlative with the Sijes Formation; and

6) Fractured Aquifer comprised of the Copalayo Formation bedrock with varying degrees of fractures.

Pictures and further information on these hydrogeological units and their distribution throughout the Pozuelos Basin appear in Chapter 10.

6.3.3 Local Geology (Pastos Grandes)

The modern salar at Pastos Grandes contains five major hydrogeological units based on drill core, surface mapping, and geophysical information. This includes:

1) A Fluvial/Alluvial Unit, comprised of gravel and sand around the salar, with thicknesses up to 450 m in the northern sector of the basin;

2) An Upper Clay unit comprised of claystones and siltstones mostly in the center-south of the basin, roughly correlative with the marginal facies of the Blanca Lila Formation;

3) A Saline Lacustrine Unit, comprised of thick massive halite beds and minor interbedded claystones, ranging from 200 to over 700 m in thickness, roughly correlative with the indurated halite core of the Blanca Lila Formation typified by the Blanca Lila islands;

4) A Central Clastic Unit, comprised of clays and clayey sands underneath the halite bodies with thicknesses up to 300 m, roughly correlative with marginal lacustrine facies of the Sijes and/or Blanca Lila Formations; and

5) Base Breccia/Gravels Unit, comprised of sedimentary breccia with coarse fragments of silicified conglomerate, metasediments, ignimbrite, and intercalated tuff, reaching over 200m on the western margin of the salar and corresponding mostly to the Pozuelos Formation (and locally Tajamar Tuff, Verde Conglomerate, and marginal facies of the Sijes Formation).

Further information on these hydrogeological units and their distribution throughout the Pastos Grandes Basin appears in Chapter 10.

6.4 Mineralization

Mineralization at Pastos Grandes salar occurred beginning ~4 Ma as uplift of the Andes led to folding and faulting of the Sijes Formation and older rocks and the generation of the modern Pastos Grandes basin. Li-rich water accumulated in this basin, having become enriched in Li due to leaching of Li from volcanic glass and/or directly from nearby hydrothermal systems, including that of the Quevar system (Benson et al., 2026). Because of the high elevation and arid climate, the water in the Blanca Lila Lake reached halite saturation and precipitated halite. The residual fluid, a Li-rich brine, migrated laterally and downward into pore spaces in clastic rocks of the Pastos Grandes basin, including Blanca Lila Formation, Sijes Formation, Tajamar Tuff, Pozuelos Formation, Verde Conglomerate, Verde Ignimbrite/Tuff, and Geste Formation (Figure 23).

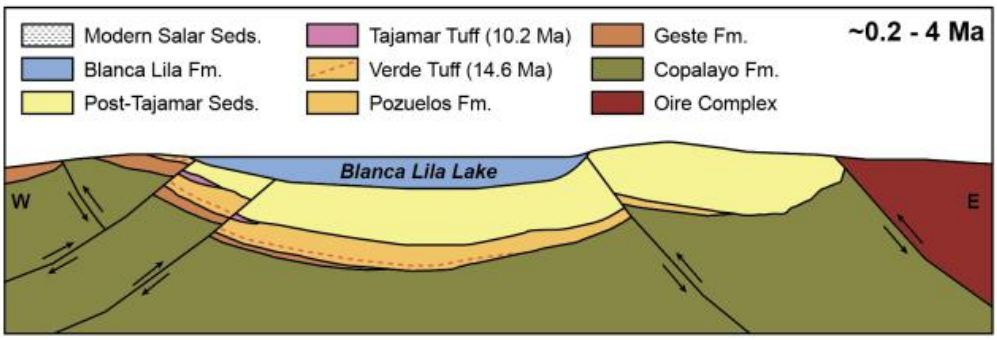

Figure 23: Schematic Representation of Mineralization at Pastos Grandes Until ~0.2 Ma (Source: LAR, 2025)

The Blanca Lila Lake continued to accumulate sediments, halite, and Li-rich brine until ~200,000 years ago, when the lake overflowed and caused a catastrophic flooding event (Benson et al., 2026) This caused the incision of a canyon from the topographically higher Pastos Grandes to Pozuelos as the Blanca Lila Lake drained to modern levels.

Figure 24: Annotated Photograph Looking West from the Southern Extent of the Pastos Grandes System into the Canyon Connecting the Two Salars (Source: LAR, 2025)

The Pozuelos, being a relatively dry and shallow system compared to Pastos Grandes, received this influx of Li-rich lake water to the system with only minor previous lacustrine activity during Blanca Lila time. Since this flooding event ~200,000 years ago (Figure 25), the high modern rates of evaporation led to the precipitation of ~80 meters of massive halite beds and Li enrichment in the residual brine, which spread laterally and downward into the pore spaces of the poorly consolidated alluvial/fluvial sediments, Pozuelos and Geste Formation, and underlying fractured Copalayo Formation.

Following the flooding event, the lake level of the Pastos Grandes basin dropped to modern levels, leaving behind lake high stands where clastic material was affixed to the basin margins or the indurated halite core was preserved in the Blanca Lila islands (Figure 25). Halite precipitation and Li brine accumulation continue to this day in both systems.

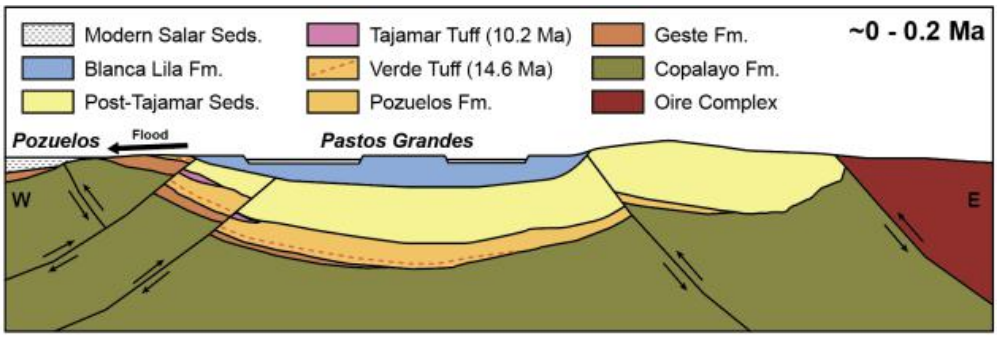

Figure 25: Schematic Representation of Mineralization at Pozuelos and Pastos Grandes during and after the Flooding Event ~200,000 years ago (Source: LAR, 2025)

6.4.1 Brine Composition (Pozuelos)

The brine from Pozuelos are solutions saturated in sodium chloride with an average concentration of total dissolved solids ("TDS") of 316 g/L and an average density of 1.21 g/cm^3. The other components present in the Pozuelos brine are K, Li, Mg, SO_4^{2-}, Cl and B with relatively low Ca. The brine can be classified as a sulphate-chloride type with anomalous lithium. Lithium concentrations in Salar de Pozuelos have an average value of 518 mg/L, with some samples reaching up to 908 mg/L.

Table 14 shows a breakdown of the principal chemical constituents in the Pozuelos brine including maximum, average, and minimum values, based on 397 primary brine samples collected and validated between 2017 and 2024.

Table 14: Maximum, Average and Minimum Elemental Concentrations of the Pozuelos Brine

Units	B	Ca	Cl	Li	Mg	K	Na	SO_4^{2-}	Density
	mg/L	mg/L	mg/L	mg/L	mg/L	mg/L	mg/L	mg/L	g/cm^3
# Samples	397	397	397	397	397	397	397	397	397
Maximum	872.0	3,048.2	195,598.8	908.0	5,565.0	7,479.0	126,612.0	41,070.0	1.26
Average	530.0	934.3	181,378.1	518.0	3,236.1	4,328.8	111,863.7	12,064.0	1.21
Minimum	186.1	177.0	150,191.0	169.0	785.01	2,009.0	96,080.0	2,020.9	1.173

Brine quality is evaluated through the relationship of the elements of commercial interest, such as lithium and potassium, with those components that constitute impurities, such as Mg, Ca and SO_4. The calculated ratios for the averaged chemical composition are presented in Table 15.

Table 15: Average Values (mg/L) of Key Components and Ratios for the Pozuelos

K	Li	Mg	Ca	SO_4^{2-}	B	Mg/Li	K/Li	Ca/Li
g/L	g/L	g/L	g/L	g/L	g/L	-	-	-
4.33	0.52	3.24	0.93	12.06	0.53	6.22	8.32	1.80

6.4.2 Brine Composition (Pastos Grandes)

The brine from Pastos Grandes are solutions saturated in sodium chloride with an average concentration of total dissolved solids ("TDS") of 302 g/L and an average density of 1.19 g/cm^3. The other components present in the Pastos Grandes brine are K, Li, Mg, SO_4^{2-}, Cl and B with relatively low Ca. The brine can be classified as a sulphate-chloride type with anomalous lithium. Lithium concentrations in Salar de Pastos Grandes have an average value of 403 mg/L, with some samples reaching up to 700 mg/L.

Table 16 shows a breakdown of the principal chemical constituents in the Pastos Grandes brine including maximum, average, and minimum values, based on 531 primary brine samples collected and validated between 2017 and 2023.

Table 16: Maximum, Average and Minimum Elemental Concentrations of the Pastos Grandes Brine

Units	B	Ca	Cl	Li	Mg	K	Na	SO_4^{2-}	Density
	mg/L	mg/L	mg/L	mg/L	mg/L	mg/L	mg/L	mg/L	g/cm^3
# Samples	501	501	479	531	501	531	501	487	439
Maximum	2,460.00	15,661.00	196,869.00	701.00	5,130.15	7,221.00	130,032.18	13,998.04	1.22
Average	568.12	868.86	172,164.81	403.52	2,354.34	3,980.64	102,830.68	7,706.25	1.19
Minimum	20.20	11.00	116.00	8.75	23.20	18.00	196.00	12.00	1.00

Brine quality is evaluated through the relationship of the elements of commercial interest, such as lithium and potassium, with those components that constitute impurities, such as Mg, Ca and SO_4. The calculated ratios for the average chemical composition are presented in Table 17.

Table 17: Average Values (mg/L) of Key Components and Ratios for the Pastos Grandes Brine

K	Li	Mg	Ca	SO_4^{2-}	B	Mg/Li	K/Li	Ca/Li
g/L	g/L	g/L	g/L	g/L	g/L	-	-	-
3.98	0.40	2.35	0.87	7.71	0.57	5.83	9.86	2.15

6.5 Deposit Types

6.5.1 General

These reservoirs are accumulations of brine that occur as groundwater in terrigenous lacustrine clastic-evaporite depositional environments, where brine have purportedly gained lithium from different possible sources, but the primary lithium sources of the salar deposits and the mobilization process of lithium are still a matter of speculation. Chemical weathering of volcanic rocks at or near the surface and direct inputs from hydrothermal systems are considered the two main mechanisms of Li enrichment in brine (Benson, 2025).

Lithium, as well as other elements, occurs as a dissolved element in the brine. In the Altiplano and Puna region, most brine contain lithium in concentrations of economic interest.

The lithium is concentrated in the basin because of the natural high evaporation rates that occur in high elevations and arid environments.

Lithium is highly soluble; it does not produce evaporite minerals when concentrated by evaporation. Instead, it accumulates in residual brine in the subsurface of the salars.

Globally, brine reservoirs have the seven following notable features in common (after Munk et al., 2025):

- Arid climate
- Closed basin containing the salar (salt crust), salt lake, or both
- Associated igneous, geothermal, and/or hydrothermal activity
- Tectonically driven subsidence
- Suitable lithium sources
- Sufficient time to concentrate lithium in the brine
- Hydrogeological paths for flow of subsurface water.

The supply of material, basin depth and duration of accumulation all contribute to variations in the thickness of salar deposits. Very thick salar sequences may have alternating layers of lacustrine clays and halite beds. The former generally reflect periods of high floodwater runoff into the closed basins, perhaps induced by higher rainfall (pluvial periods). Saline sediments, or pure evaporite beds, reflect arid climatic phases. The precise climatic interpretation of paleo-lacustrine salar sequences is complex.

A schematic illustration of brine deposits environments where lithium mineralization occurs is depicted in Figure 26.

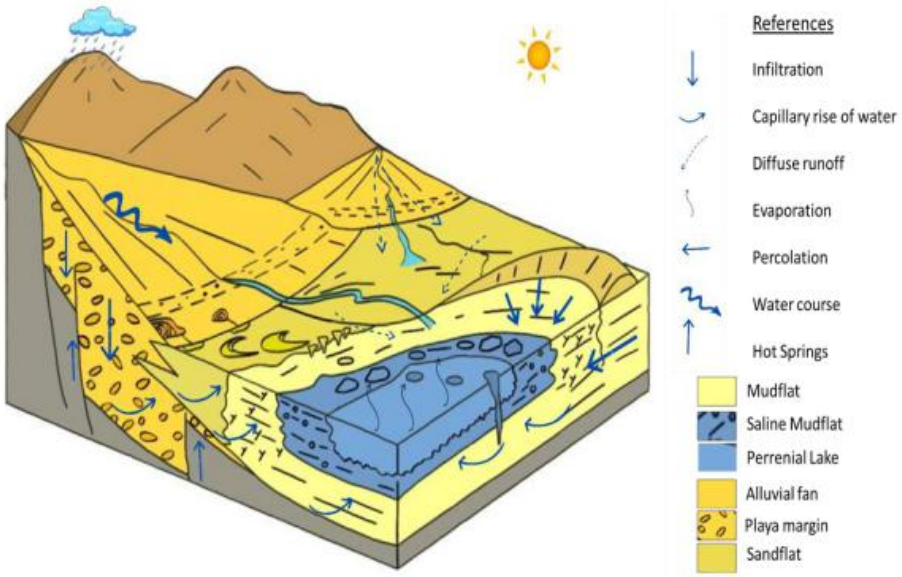

Figure 26:Schematic Illustration for Brine Deposits Environments Where Lithium Occurs (Source Hardie Smooth and Eugster 1978, modified by Imex 2023)

6.5.2 Pozuelos

6.5.2.1 Pozuelos Basin

Salar de Pozuelos is an intramontane endorreic basin composed by evaporitic and clastic sediments. The geographic basin is delimited to the west by the Pozuelos Range and the east by Copalayo Range.

The evaporitic facies that fill the basin are controlled by a typical precipitation sequence: Carbonates - Borates - Chlorides (from the margin to the basin center). This underground mineralization is shown on the salar surface developing several kinds of crusts. The distribution of these crusts is not concentric to the salar depocenter, due to the solute input through several streams and underground water discharge in the northern portion of basin.

Big alluvial fans, unconsolidated or partially cemented by evaporitic phase, are well developed in the transition zone between the ranges and the evaporitic facies on the salar margins. The typical materials of these deposits are known as "detritic-evaporitic" facies. Both the basement and the basin margins are tectonically active, giving rise to folding and fracturing of rocks.

According to Alonso et al. (1991), Salar de Pozuelos is a dry salar, characterized by high rates of evaporation and there is sediment starved (fluvial input is restricted to rare flash floods, and groundwater is the most important source of brine). This is consistent with the conceptual model for mineralization presented in Chapter 7, indicating that the main source of water/Li in the system was a one-time input from the catastrophic flooding of the Pastos Grandes basin into Pozuelos less than 200,000 years ago.

The Pozuelos basin covers an area of 384 km^2 including 10 sub-basins that provide lateral groundwater inflows. The Salar nucleus itself covers an area of 84 km^2.

6.5.2.2 Surface and Ground Water

Unlike Pastos Grandes, the Pozuelos does not contain surficial rivers or streams supplying water to the salar. The main source of surface water are the fourteen springs shown in Figure 27 in the watershed of Pozuelos. Of these springs, M14 (red circle) produces the most freshwater; the others contain brackish to brine water

On the other hand, M14 spring (red circle) is located on the middle to lower slopes of the Ordovician outcrops (Figure 27) in a potential fault zone and it produces the most freshwater, unlike the others located closer to the margin of the salar, which contain brackish to brine water.

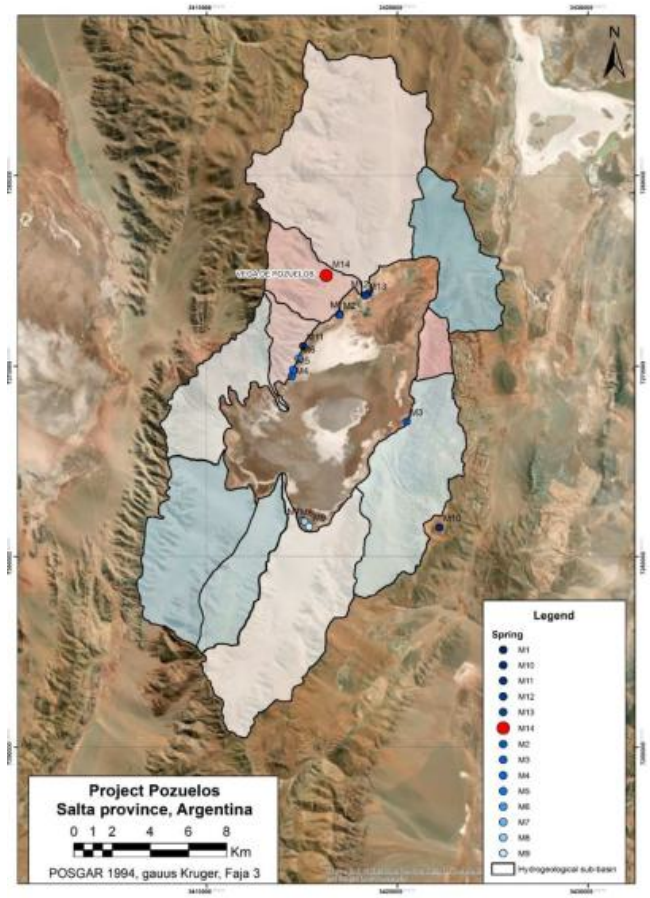

Figure 27: Springs Identified in Salar de Puzuelos (Modified from CONHIDRO, 2018)

The groundwater in Pozuelos basin is characterized by the interaction of two aquifer units (see geologic cross section W-E in Figure 28). A thick detrital aquifer is well developed between the ranges and the salar margins which water is saline, but with densities rounding 1 kg/L. This aquifer is located over the Ordovician sedimentary formations, which is the local geologic basement. To the center of the salar (saline core), the underground waters are brine with densities around of 1.2 kg/L.

The interaction of saline waters from the salar margins and the salt brine is through wedge shaped saline type interphase. The relationship between both contrasted density environments and the topography are the main causes of the occurrence of saline springs from the detrital aquifer reaching the surface flooding several margin portions of the salar. This sector coincides on the surface with the gradient rupture zone generated between distal zones of alluvial cones and the great salt flat. The flooded zones are located closely of the boundary between the detrital and carbonated-borate crust.

These inflow waters become concentrated by evaporation and show a general increase in salinity toward the basin center. Evaporative concentration leads to precipitation of gypsum crusts in the marginal zone of Salar de Pozuelos and precipitation of halite in the subaerial halite nucleus.

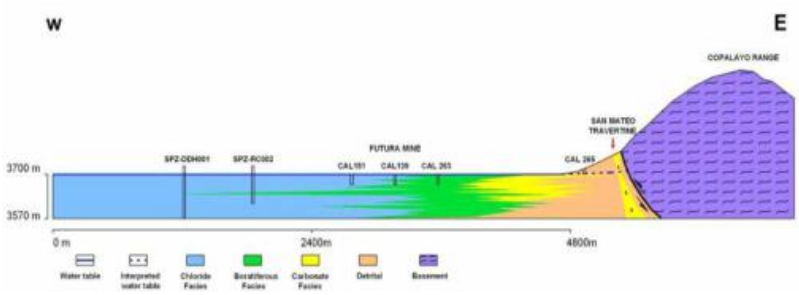

Figure 28: Geologic Cross Section W-E of Salar de Pozuelos (Modified from CONHIDRO, 2018)

6.5.2.3 Hydrology

Associated watersheds in Salar de Pozuelos were defined based on DEM (resolution 30 m) with the support of ARCGIS 10.7. A total of 10 sub-basins were identified, covering in a total of 384 km^2 (300 km^2 of watersheds + 84 km^2 of salar), and they are shown in Figure 29.

The major sub-basins are located on the northern sector of the salar (Figure 29). The drainage density defined as the total streamline lengths divided of the total area (watershed + salar) was 1,573 km/km^2.

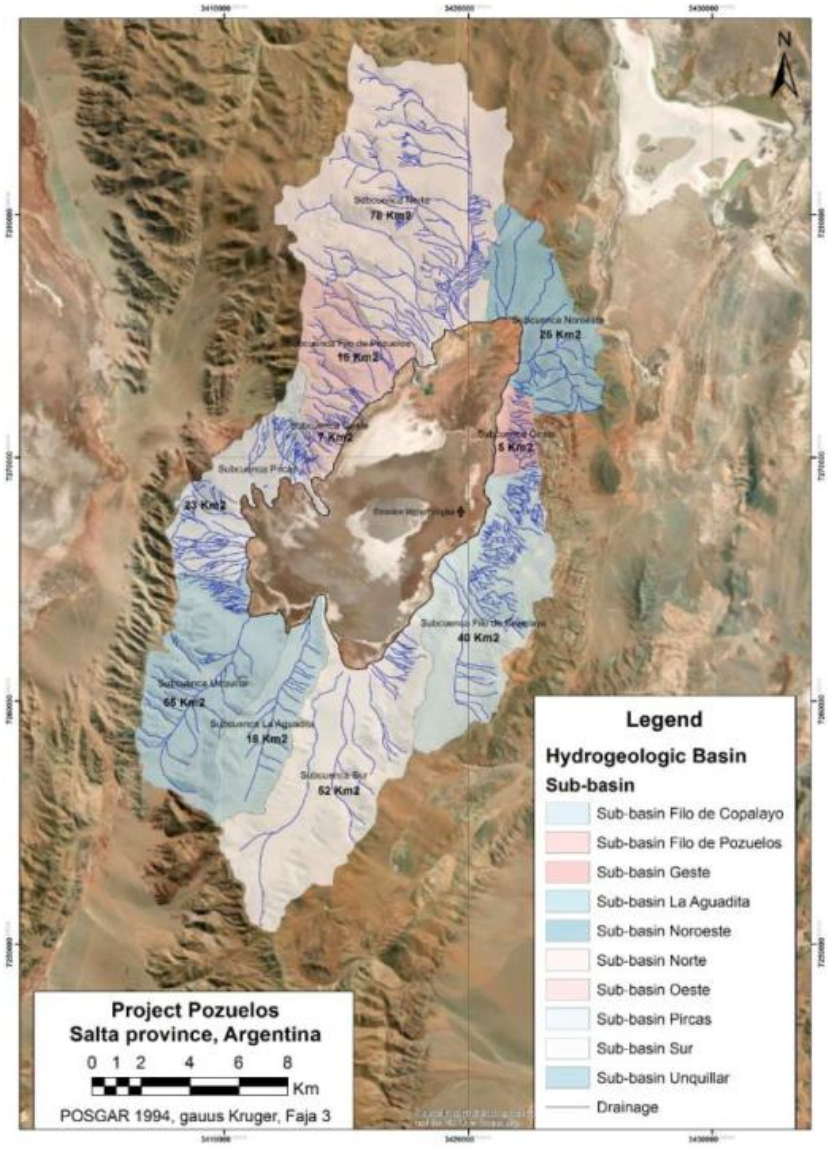

Figure 29: Hydrology of Salar de Pozuelos - Watershed Definition (Modified from CONHIDRO, 2018)

6.5.2.4 Water Balance

A conceptual model of the water balance in a salt flat as Salar de Pozuelos is shown in Figure 30. In a closed basin (endorheic), the water outflows are mainly by evaporation, while the recharge occurs though infiltration of direct precipitation and groundwater inflows from higher ground in the surrounding sub basins.

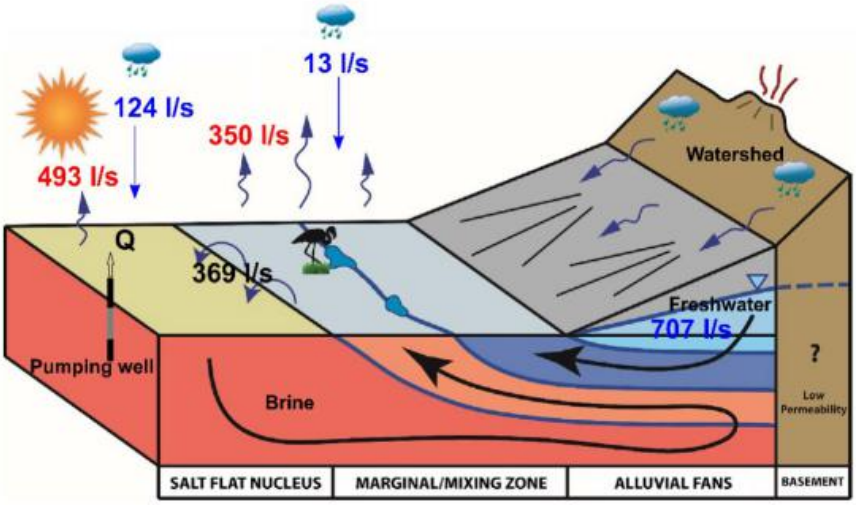

Figure 30: Water Balance Conceptual Model for Endhoreic Basins in Arid Regions Followed for Salar de Pozuelos

Water balance carried out in Salar de Pozuelos for the period 2020 is summarized in Figure 31. Lateral recharge from the associated watersheds was estimated at 707 L/s, whereas the evaporation through the salar crust was estimated at 493 L/s.

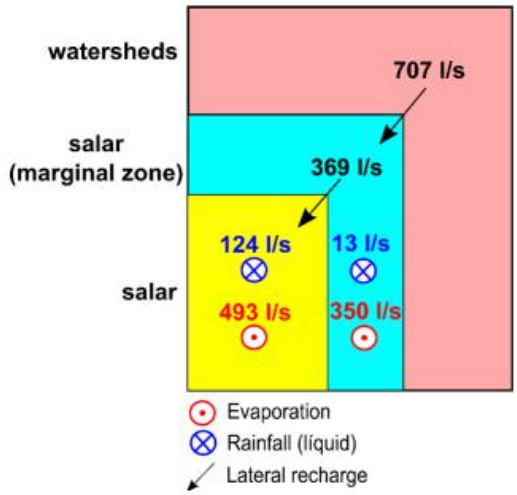

Figure 31: Summary of Water Balance Estimated for the Period 2020 in Salar de Pozuelos

In mid-2024, LAR and Ganfeng engaged the UMASS/UAA Lithium Solutions team to initiate an updated water balance study of the Pozuelos basin using the same methodology that was applied in the 2023/2024 Pastos Grandes water balance study (Blin et al., 2024). Preliminary results indicate that the average groundwater recharge into the whole basin is 128 L/s (Boutt et al., 2024), lower than the estimate used in the present study based on 2020 data. LAR and Ganfeng will continue to monitor the hydrologic system at Pozuelos using advanced techniques to further define this number and use the most accurate values in future dynamic models.

6.5.3 Pastos Grandes

6.5.3.1 Salar Basin

The nucleus of Salar de Pastos Grandes occupies an area of approximately 36 km^2 comprised mostly of flat sandy-silty salt crust. The overall basin of Salar de Pastos Grandes is 1,738 km^2 (drainage area), with the basin floor measuring 48 km^2. The general elevation of the salar surface is 3,773 masl, with the "islands" having a typical elevation of approximately 3,785 - 3,790 masl. The surrounding hills range in elevation from approximately 3,825 masl on the south, east and northeast sides of the salar and increase rapidly on the west side to approximately 3,990 masl.

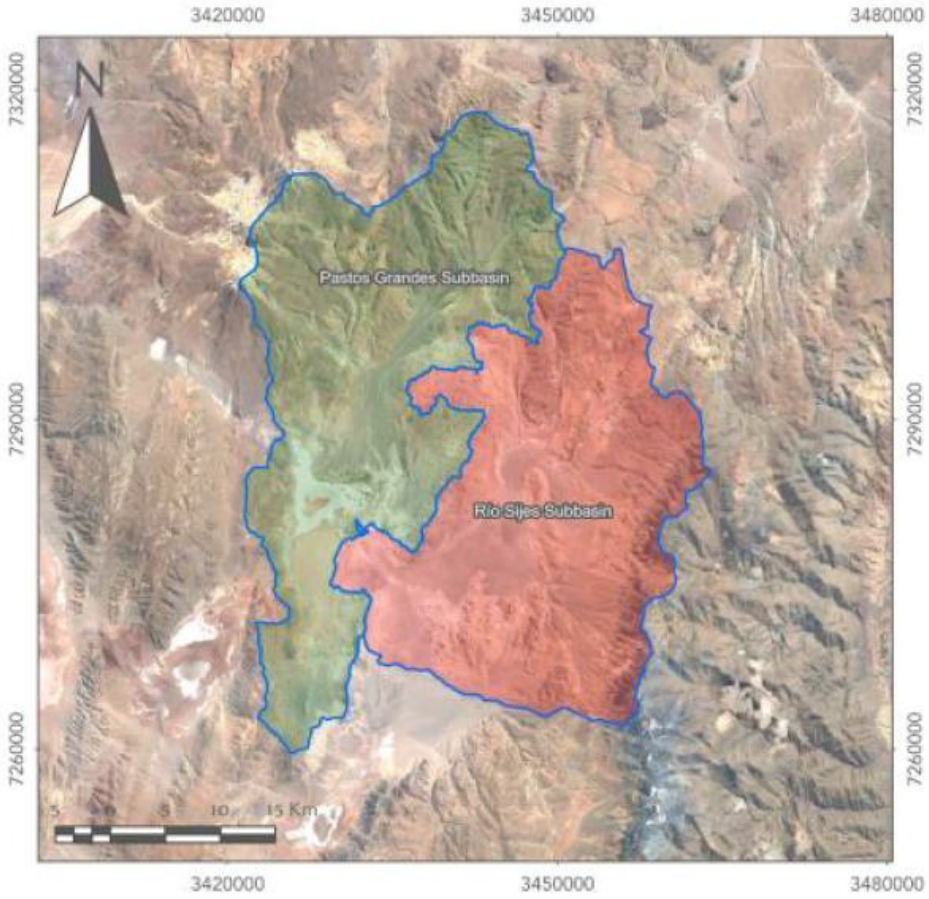

Figure 32: Hydrological Subdivisions of the Pastos Grandes Basin (Source: AW, Dec 2024)

Unlike other salars of the region, the topography of the nucleus of the Salar the Pastos Grandes is irregular. The current saline crust flat is disrupted over approximately 15% of its area by elevated outcrops of Blanca Lila Formation, which have been interpreted as slightly older salar sediments that have been eroded yet remained as more resistant "islands".

6.5.3.2 Surface and Groundwater

Surface runoff is mainly restricted to the rainy season during summer. Three intermittent to ephemeral rivers enter the Salar, Rio Sijes from the east, Rio Pastos Grandes from the north, and Rio Corral Colorado from the northeast (Figure 33). Flow in Rio Sijes may originate from groundwater discharge to the surface system near the exit point of the Sijes subbasin into the Pastos Grandes. Average flow of Río Sijes has been measured at 160 L/s. Flow in Rio Corral Colorado has been measured at 44 L/s and in Rio Pastos Grandes at 38 L/s.

Three semi-permanent lagoons occur near the discharge areas of the three above-mentioned rivers into the nucleus of the Salar. Springs and wetlands occur towards the north of the Salar over the interface between the alluvium and evaporitic crust in the lower parts of the Rio Pastos Grandes and Rio Corral Colorado.

A systemic surface monitoring was implemented in 2023 to obtain a better understanding of the flow regimes in these streams throughout the different seasons of the year. Data indicate that inflows into the Pastos Grandes system are considerably higher than previous estimates; new data estimates including surface and groundwater flow range between 776 L/s – 2130 L/s, with a mean 960 L/s of lateral recharge (Blin et al., 2024). The new data is not included in the present study but will be used in future dynamic models of the salar.

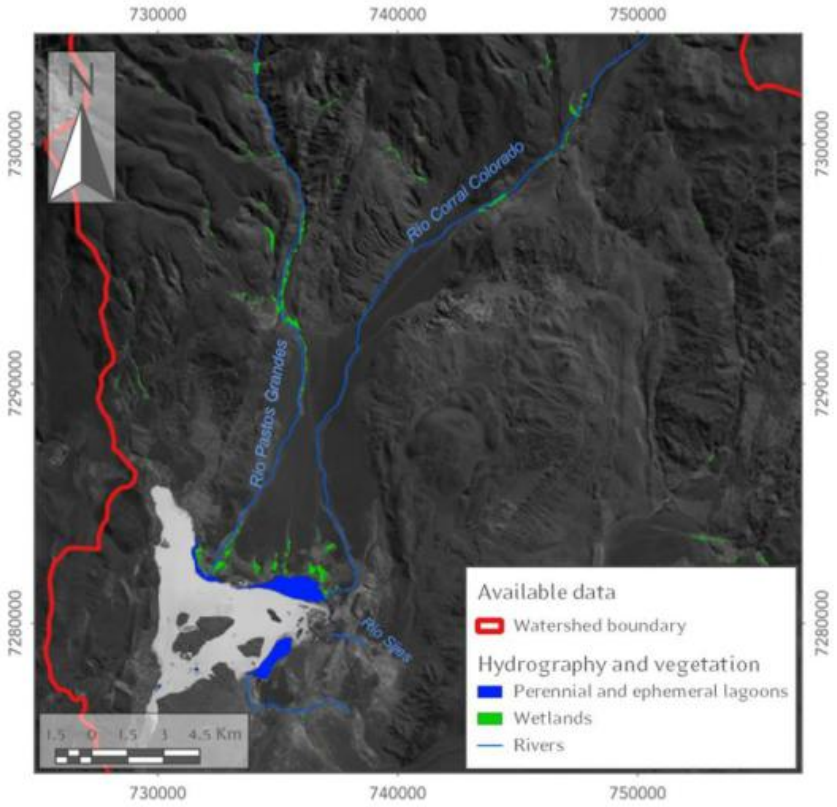

Figure 33: Surface Water Features within the Northern Portion of the Pastos Grandes Basin (Source: AW, Dec 2024)

Subsequent work has highlighted additional sources of water entering the basin through the Rio Sijes.

6.5.3.3 Hydrogeology

The Salar is the lowest topographic point in the Pastos Grandes Basin. The salt flat itself is surrounded by alluvial fans which drain into the Salar and tertiary rocks that may act as impermeable boundaries, although further hydrogeological characterization work of the Tertiary is recommended. The surface of the Salar in the north is composed of mainly chloride facies (halite crust) with active evaporation occurring since the brine level occurs within 5 cm from the surface. The Salar surface in the south is covered by the Blanca Lila Fm with an average thickness of 3 m. Depth to brine in the southern part of the Salar is between 3 m and to 4 m, below the evaporation extinction depth that is estimated around 2.5 m.

Based on the interpretation of drilling and testing work in the basin, four hydrogeological units have been identified as shown in Figure 34 and are described below:

- UH-1 Fine Grained Shallow Deposits (Upper Clay): These sediments belong to the Blanca Lila formation and are in conformity with the underlying Saline Lacustrine Unit, reaching a maximum thickness of 30 m at the northeast of the Salar. Because of the fine texture, permeability and storage properties for this Unit are estimated to be low with a hydraulic conductivity (K) ranging between 0.1 – 0.01 m/d (reaching up to 10 m/d at some specific points), a specific storage (Ss) range between $1x10^{-7}$ 1/m and $1x10^{-5}$ 1/m and drainable porosity between 5.0E-02 and 7.0E-02. Geophysics and field sampling suggests that this Unit is saturated with brine inside the Salar and with brackish water around the margins.

- UH-2 Evaporitic Deposits (Saline/Lacustrine): Massive evaporitic unit, intercalated with lenses of fine- grained sediments that can have a thickness up to 700 m. This relatively homogeneous Unit includes the saline lacustrine material that forms the surface of the salar nucleus and is overlain by the Blanca Lila Fm (UH-1) in the south. Based on drilling and testing results this Unit has a relatively low permeability and could limit hydraulic connectivity between the upper and deeper hydrogeological units in the basin. The hydraulic conductivity ranges between 1.0E-03 and 1.0E-01 m/d, the specific storage ranges between $1x10^{-7}$ 1/m and $1x10^{-5}$ 1/m, and the specific yield ranges between 3.0E-02 and 6.0E-02. Geophysics and field sampling suggests that this Unit is saturated with brine.

- UH-3 Alluvial and Colluvial Deposits (Alluvial): This hydrogeological unit includes the alluvial fans identified at the margins of the Salar which are composed of unconsolidated gravels and sand. This Unit overlies and is in lateral contact with UH-2 and locally appears interfingered with UH-4. The hydraulic conductivity ranges between 1.0E-01 and 1.0E+02 m/d, Ss ranges between 1.0E-05 and 1.0E-03 1/m, the Sy ranges between 1.2E-01 and 1.8E-01. Groundwater flow in the Alluvial and Colluvial Deposits is generally unconfined; however, locally semi- confined to confined flow conditions occur where this unit is overlain by UH-1 and UH-2. The unit hosts freshwater resources in the alluvial fans on higher ground above the margin of the Salar and significant brine resources in the southern portion of the Salar where it is partially overlain by UH-1.

- UH-4 Lower Deposits (Base Gravels and Central Clastics): Overlaying basement rock, this hydrogeological unit includes the Central Clastics and Base Gravels. It is composed of sandy gravels with a high fraction of fine material in a sedimentary matrix and some clayey to silty lenses that decrease the bulk vertical hydraulic conductivity. This unit is constrained to the central portion of the basin, underlies UH-2, and is in lateral contact with the unconsolidated deposits of UH-3. The hydraulic conductivity of this unit is estimated to range between 1.0E-02 and 1.0E+00 m/d, the specific storage range between $1x10^{-7}$ 1/m and $1x10^{-5}$ 1/m, and the drainable porosity ranges between 8.0E-02 and 1.7E-01. This unit forms part of the confined lower brine aquifer from which future brine production will likely not affect the freshwater resources hosted in the alluvial system due to the overlying low-permeability halite unit.

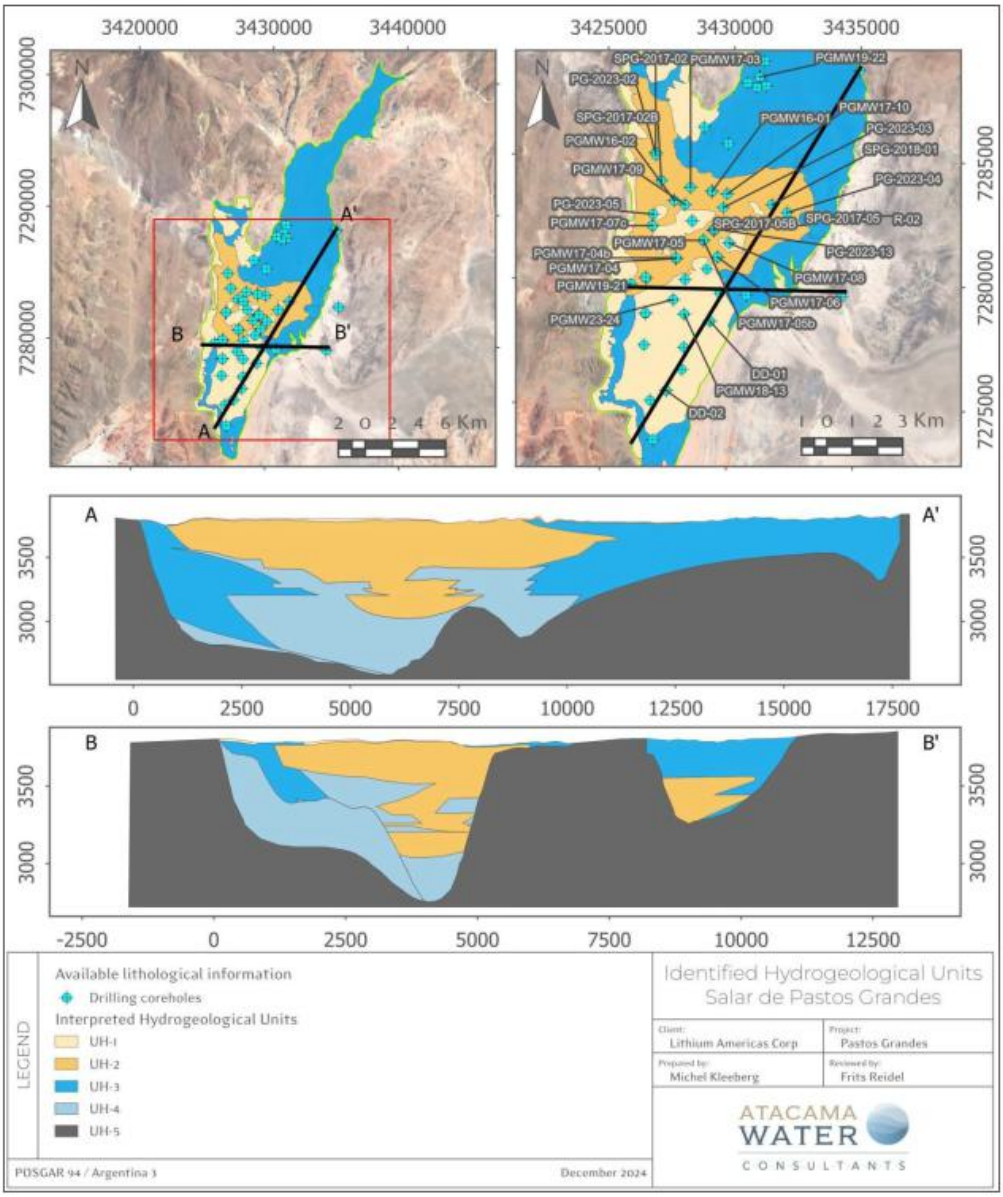

Figure 34**: Hydrogeological Cross Section in Pastos Grandes Salar (Source: AW, Dec 2024)**

6.5.3.4 Water Balance

A water balance for the Pastos Grandes Subbasin was prepared as part of the conceptual hydrogeological model and is summarized in Table 18. The range of the water balance components presented here takes into account the data presented in the following documents:

- "Modelo Hidrogeológico Conceptual de Salar de Pastos Grandes, Proyecto Sal de la Puna", prepared by Atacama Water for AMSA in 2022
- "Salar water Budget-Pastos Grandes", prepared by UMAss/UAA Lithium Solutions for Lithium Americas in 2024

In closed endorheic basins such as Salar de Pastos Grandes recharge is in long-term equilibrium with evaporation in the absence of any brine production. Recharge is composed of direct recharge from precipitation and lateral groundwater inflows from adjacent subbasins (Sijes subbasin) and was estimated within a range of 200 - 900 L/s.

Discharge occurs mainly through evaporation in the form of:

1) soil evaporation where the water table is above the extinction depth.

2) evapotranspiration from wetlands at the margins of the Salar; and

3) free water (or brine) evaporation from perennial or ephemeral lagoons over the surface of the Salar.

Table 18: Water Balance for Salar de Pastos Grandes Subbasin

Inflows (L/s)		
Direct recharge from precipitation		180 - 700
Lateral recharge from Sijes Subbasin		20 – 200
Total inflows		200 - 900
Outflows (L/s)		
Evaporation	Lagoon evaporation	50 – 200
	Evapotranspiration	50 - 200
	Soil evaporation	100 - 500
Total outflows		200 - 900

Ongoing monitoring by LAR in conjunction with the UMASS/UAA Lithium Solutions team in the Pastos Grandes basin indicates that the values in Table 18 are conservative, as they underestimate the lateral recharge from the Sijes subbasin to the east of the project. New data estimates 776 L/s – 2,130 L/s, with a mean 960 L/s of lateral recharge (Blin et al., 2024). Future dynamic models will incorporate this updated data to reflect a more comprehensive monitoring program utilizing state-of-the-art measurement, isotopic, and geochemical techniques.

7.0 EXPLORATION

7.1 Pozuelos

7.1.1 Geophysical Surveys

Geophysical survey exploration has been carried out in the salar since 2009. Gravity and Magnetotelluric studies were conducted by Proingeo in 2021:

- Gravity: previous resource estimates used the gravity survey to extend the basin in-fill at depth and,
- Magnetotellurics: to understand the continuity of the aquifer towards the north and west of the salar.

7.1.2 Gravity Survey

The gravity from Proingeo (2021) was used to interpret the elevation of the basin's basement.

In the QP's opinion, the data interpretation suggests highs, which are forced to correlate with the basement interpreted in wells SPZ-DDH 17, SP-2017-12, and PZ-18-02. In addition, it suggests abrupt lows in sectors where the basement was not reached.

The QPs believe that the interpretation of the basement from gravity 2021 does not represent the basement of the relevant aquifer since the fractured aquifer from PZ-18-02 has been shown to host lithium-enriched brine (Figure 35). Furthermore, it does not correlate with the Magnetotellurics survey, which is further appropriate basin analysis at this scale of relatively small basins.

Figure 35 shows the highs and ups of the gravity survey (Proingeo 2021).

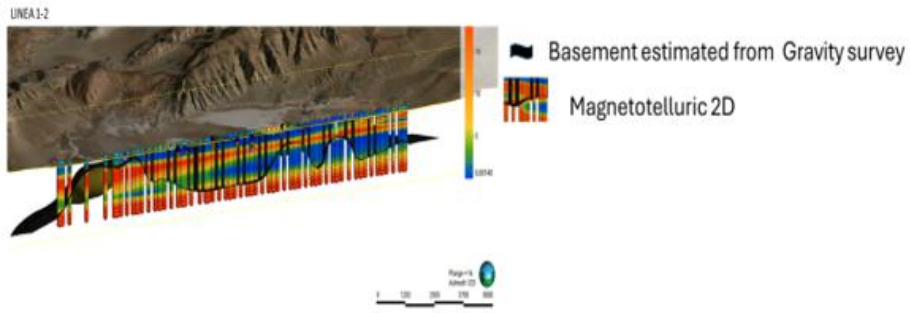

Figure 35: Magnetotellurics and Highs and Downs of the Gravity Line 1-2 (Proingeo 2021)

7.1.3 Magnetotellurics (MT) Survey

The Magnetotellurics geophysics survey from Proingeo 2021 was a guide to delineating aquifer continuity.

The location of the Lines is shown on the map in Figure 36.

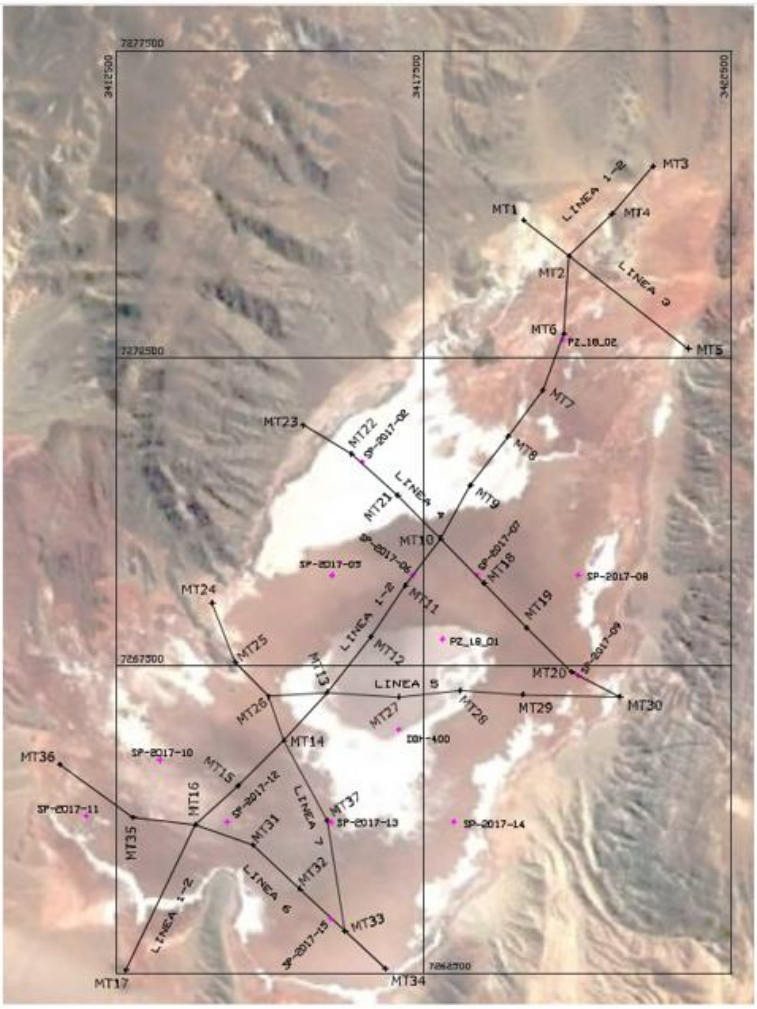

Figure 36: MT Survey Lines and Stations Conducted by Proingeo in 2021

The porous granular aquifer was correlated with the lowest resistivities and the Siltstone with the highest resistivities.

The basement was not identified with the MT as the equipment's calibration seems to have been limited to resistivities characteristic of porous media (the maximum resistivity reading was 20 Ohm×m). The resistivities of the aquifer were similar to those of the bedrock.

Figure 37 and Figure 38 show how the MT suggests the continuity of the aquifer between the exploration wells.

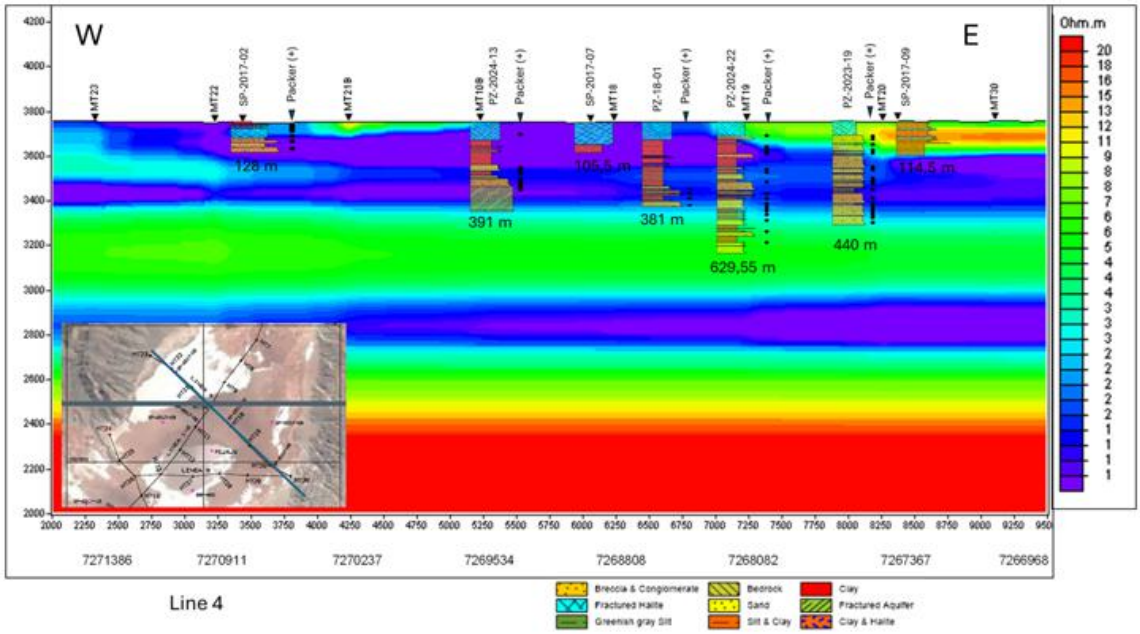

Figure 37: Line 4 MT Vs Lithologies of the Drillholes (Source: Proingeo 2021)

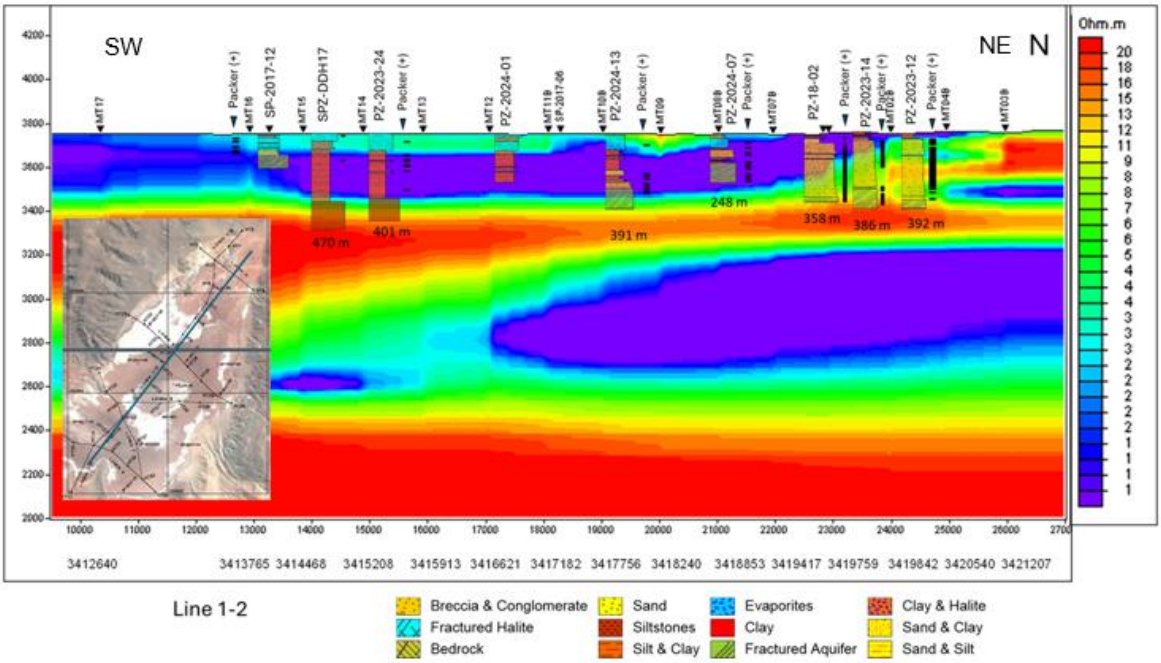

Figure 38: Line 1-2 MT Vs Lithologies of the Drillholes (Source: Proingeo 2021)

7.2 Pastos Grandes

This section provides a description of the exploration work that has been carried out in the Salar between 2011 and 2024 by various owners, including surface brine sampling and geophysical surveys. Sampling distribution is shown in Figure 39, while the location of the geophysical profiles is presented in Figure 40.

7.2.1 Surface Brine Sampling

In 2011, Eramet took a total of nine samples from shallow hand-dug auger holes excavated within the eastern section of the Salar and the wetlands that sit beyond its northern limit. After laboratory analysis, three brine samples toward the west of the Salar had lithium concentrations near 600 mg/L and potassium concentrations near 7,000 mg/L, while samples at the center of the Salar came with lithium and potassium concentrations near 200 and 2,000 mg/L, respectively. On the other hand, LSC completed a second surface program in 2016 which included samples from 11 sites (shallow brine bodies and hand dug pits) with similar results than Eramet achieved in 2011. Lithium concentration reached the highest lithium concentration at the southwest (737 mg/L) and to the center of the salar ranged between approximately 200 - 500 mg/L.

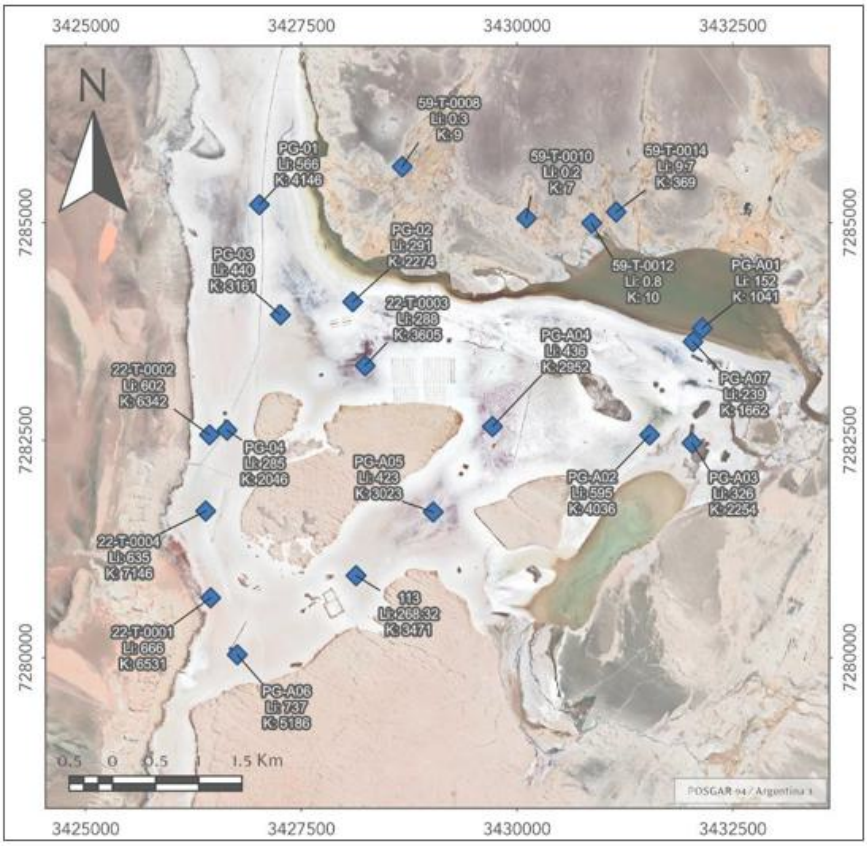

Figure 39: Historical Surface Brine Samples in Salar de Pastos Grandes (Source: AW, Dec 2024)

7.2.2 Eramet Exploration (2011-2013)

7.2.2.1 TEM Survey (2011)

Eramine carried out a TEM survey in the Salar de Pastos Grandes implementing six TEM stations. The primary purpose of the survey was to observe and identify resistivity contrasts that could potentially correspond to variations in groundwater salinity. However, Eramine did not publish or reveal any information about the specifics, outcomes, or implications of the survey, which are therefore omitted from this report.

7.2.2.2 VES Survey (2013)

During 2013, Eramine conducted a VES survey to study the distribution and relations between brine and freshwater at depth, as well as to assess the TEM results from the 2011 survey. This study included 5 original stations, with only two of them currently available for this report. The location of the stations is included in Figure 40.

In general, a prominent contrast between a lower and a higher resistivity zone was observed at a respectively depth between 50-70 m. This contrast has been interpreted to be the limit between unconsolidated sediments (probably related to Blanca Lila) and a massive halite body (with an apparent resistivity ranging between 1 to 110 Ohm×m, where no interpretations were given for these wide intervals).

7.2.2.3 CSAMT Survey (2011)

In 2011, Eramine/Bolera Minera S.A. conducted a controlled source audio-frequency magnetotelluric survey within the Salar, to delineate the distribution of conductive lithologies and its relationship with freshwater/brine, comparing these results with the VES and TEM surveys previously conducted. The location of the CSAMT profiles, generated from the data acquired and interpreted from 11 stations, is shown in Figure 40. In general, these profiles show similar resistivities and patterns as in the VES survey, but for grater depths.

7.2.3 Millennial Exploration (2017 – 2019)

7.2.3.1 VES Survey (2017)

Millennial lithium did a second VES survey in 2017, focused on the alluvial deposits located beyond the northern limit of the Salar. This study included 10 VES stations interpreted in 3 vertical sections, whose locations are shown in Figure 40. The main purpose of this survey was to study the saline interphase, since it had been assumed that the Salar's brine had moved into the clastic sediments north of the salar due to density differences. Therefore, this survey was also conducted to extend the potential inferred resources to the north and to identify potential new drilling locations.

Although the exact boundaries of the unsaturated zone were not perfectly correct, as observed in further drilling works, conceptually they were considered acceptable as a first approach of the saline interphase distribution. As an example, this geophysical survey predicted the existence of enriched-lithium brine at a depth of about 300 m for well PGMW17-11, while during the drilling process of this borehole that enriched-brine was encountered at a depth near 200 m.

7.2.3.2 Seismic Survey (2018-2019)

Millennial Lithium carried out a two-phase seismic investigation program during 2018-2019. The scope of this survey was to provide new evidence of the lithology of the Salar and to help with the design further exploration steps. The location of the seismic profiles is shown in Figure 40.

The seismic tomography survey provided valuable information on the vertical distinction and lateral continuity of lithological layers. Additionally, several structures were interpreted, especially in the longest north to south profile, suggesting north to northwest dipping beds.

7.2.3.3 Downhole Temperature and Electrical Conductivity Surveys

Once the drilling from the 2016-2017 exploration campaign were completed, and the boreholes from the exploration stage 2 were completed as 2-inch PVC screened piezometers, a down-hole electrical conductivity profile was conducted at five wells, as shown in Figure 40 (PGMW16-02, PGMW17-04b, PGMW17-05c, PGMW17-07d, and PGMW17-11). Temperature and electrical conductivity were recorded at 3 m intervals using an In-Situ brand Aquatroll 100 downhole electrical conductivity probe, and laboratory samples were taken to measure laboratory density. The results from this survey showed that there is a reasonably good correlation between the Aquatroll measurements of specific conductivity, and the laboratory measurements of the depth- specific samples.

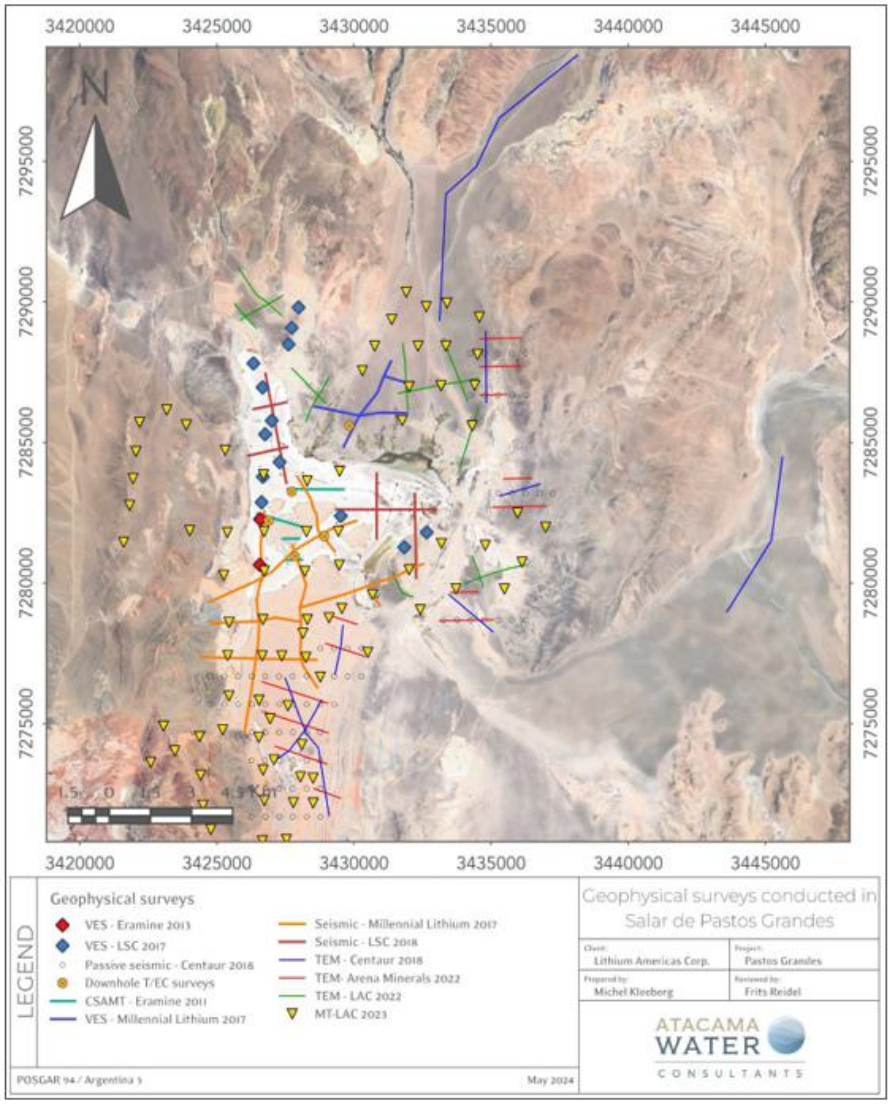

Figure 40: Geophysical Surveys Conducted in Salar de Pastos Grandes (Source: AW, Dec 2024)

7.2.4 LSC Exploration (2017 – 2018)

7.2.4.1 VES Survey (2017b)

To study the lithological distribution in subsurface, and the relationship of geology with freshwater and brine, LSC Lithium carried out a VES study in 2017 over their mining concessions, including 13 surveying stations. 10 of these stations were arranged SW-NE over the northwestern limit of the Salar, one at the center of it and the remaining two of them located at the eastern limit of the Salar, between alluvium deposits and the evaporitic crust.

The results of this study vary, depending on the location of the profiles, but in general the interpreted geoelectrical units from top to bottom are: 1) conductive modern gravels and sands; 2) a semi-conductive fine grained unit (silt and clays and/or halite gypsum and borates), probably related to the Blanca Lila Formation; 3) highly conductive zone of evaporates and mixed halite/clastics saturated with brine; 4) a more resistive layer representing again the Blanca Lila Formation or other Tertiary sequences and; 5) A resistive zone interpreted as the hydrogeological basement composed of thick clastic facies (conglomerates) and/or facies of volcanic rocks (andesites).

7.2.4.2 Seismic Survey (2018)

In 2018, LSC undertook a seismic tomography refraction survey on LSC mining claims, comprising six lines for a total of 15,372 m, as shown in Figure 40. For interpretation, lithologies were assigned according to literature values, regional geologic information and correlated to lithological information observed during the drillings of two boreholes (SPG-2017-02B and SPG-2017-04A).

To the west of the Salar, up to 7 seismic units were identified with no structural features up to the maximum depth of the profiles (600 m). From top to bottom the identified units are: 1) dry alluvial deposits; 2) halite crust; 3) saturated sand, clay and/or organic material; 4) crystalline halite; 5) saturated sand, clay and/or organic material; 6) gravels and 7) breccia.

To the center and east of the Salar, up to 11 seismic units were identified with no structural features up to the maximum depth of the profiles (600 m). From top to bottom the identified units are: 1) dry to partially saturated sediments and alluvial material (saturated sand, clay and/or organic material); 2) halite crust; 3) saturated sand, clay and/or organic material; 4) halite with scarce matrix; 5) halite with abundant matrix; 6) halite with scarce matrix; 7) sand; 8) alternation of halite and sand bands; 9) gravel, sand and/or clay; 10) halite with interbedded sand; 11) gravel and/or sand.

7.2.5 Centaur/AMSA Exploration (2018 – 2022)

7.2.5.1 TEM Survey (2018)

Centaur Resources conducted TEM studies to evaluate the presence of brine beyond the margins of the Salar. Specifically, they implemented TEM lines located to the north (Corral Colorado river valley), east (Sijes subbasin) and south of the Salar's crust. Figure 40 includes the trace of each profile.

For the mining concessions located to the south of The Salar de Pastos Grandes (over Blanca Lila Formation), the survey showed a highly conductive unit close to the surface interpreted as the halite body saturated with brine, based on drilling. At 100 m depth there is a slightly more conductive unit, interpreted as a more porous halite than the one found at surface.

TEM lines to the north and east confirmed the existence of a brine body, part of the saline interface, overlain by brackish to freshwater hosted in the alluvial recent sediments.

7.2.5.2 Passive Seismic Survey (2019)

With the main purpose of identifying basement rocks and confirming interpreted fractures to the south and east of the Salar, a passive seismic survey was conducted by Centaur Resources in 2019. This study included measurements at 78 stations arranged in 10 east-west orientated lines (Figure 40). In general, this survey did not consistently identify a contact with basement rocks, which was explained with the high depth of the Salar and the poor seismic contrast between the massive halite body and basement rocks.

7.2.5.3 TEM Survey (2022)

During mid-2022, Arena Minerals carried out a TEM survey on their SdlP mining concessions, located near the eastern boundary of the Salar. The main purpose of the survey was to refine the delineation of the overburden and hydrogeological basement, and to further investigate the freshwater/brine relationship at this portion of the Salar based on Centaur's 2018 survey. The profile locations are included in Figure 40.

The survey also helped to identify the limit between the unconsolidated sediments and the rocks that conform the basement. These results and interpretations were correlated to lithological information observed during the drillings of boreholes DD-01, DD-02 and DD-03.

7.2.6 LAR Exploration (2023)

7.2.6.1 TEM Survey (2022b)

Finally, during late 2022, with the main purpose of refining the comprehension of the subsurface and verifying the existence of aquifers suitable for industrial water production, a TEM campaign was conducted by LAR. This survey was focused on the alluvial deposits located beyond the northern limit of the Salar, where twelve lines (Figure 40) were surveyed, with a vertical maximum resolution of 160-200 m.

Three geoelectrical units were identified in this report, corresponding to:

- fine grained sediments, saturated in salt water with abundant interstitial clay of high electrical conductivity.
- fine to coarse grained sediments saturated with water; and
- medium to coarse grained sediments partially or not saturated.

7.2.6.2 AMT-MT Survey (2023)

As an integral part of the set of research carried out for Lithium Americas in the Pastos Grandes Project, Proingeo S.A. conducted the geophysics work to understand the subsurface features and the extension of the Salar in depth using Audiomagnetotelluric (AMT) and Magnetotelluric (MT); The secondary objective was to detect those suitable areas with potential to host saturated brine.

In April-March 2023 86 AMT and MT stations were measured in 26 lines (Figure 40), 10 North – South (or approximately N- S), 12 East – West lines (or approximately E – W), 2 Lines with a Southwest direction. Northeast (SO-NE) and 2 lines heading Southeast-Northwest (SE-NO). For interpretation, cross-sections were built based on the measured soundings, and these were projected onto the traces for better representation.

Three geoelectric units have been defined, the first unit corresponds to very low electrical resistivity (less than 1 ohm×m), associated with layers with saturation of brine or layers with abundant content of moist clay or combination of both and/or presence of good petrophysical properties; The second unit corresponds to average electrical resistivity, associated with layers saturated with less brackish water and/or lower clay content (2 to 7 ohm×m approximately); the third unit corresponds to higher values of electrical resistivity (greater than 10 ohm×m), associated with consolidated, poorly fractured rock with low brine saturation or less brackish water and/or poor petrophysical properties.

Up to 1,000 m depth, except for the Center – West, low resistivity horizons are identified throughout the salar, particularly between depths of 300 m and 600 m. No units of interest would be found below 1,000 m depth.

7.2.7 Geological Mapping and Geochronology

Recent geological work (2024) has been carried out by LAR geology team, focused on both the Salar de Pastos Grandes and Pozuelos. These works include geological mapping, surface rock sampling, core sampling, core relogging, geochemistry, and geochronology. The new geologic understanding is supported by background regional geological literature.

The mapping, relogging and geochronological studies are still in progress (Benson T., 2024). A detailed summary of this work can be found in Section 10.2 of this report.

7.3 Drilling

7.3.1 Pozuelos

7.3.1.1 Overview

Drilling for lithium at the Pozuelos dates from 2008. In each drilling campaign, lithium exploration wells have been successively drilled deeper. Wells PZ-2024-22 and PZ-2023-19, from the latest drilling campaign from 2023/2024, opened new targets to deeper zones of the basin at the east. Recently, in the latest drilling program, wells PZ-2024-11, PZ-2024-25 and PZ-2024-21 opened new deeper targets toward the southeast and northeast of the salar.

The drilling program was conducted with the following objectives:

- Obtain depth-specific brine samples for characterising the subsurface brine chemistry,
- Run downhole geophysics to obtain an indication of fluid salinities and the potential correlation with the amount of brine hosted in the porous media,
- Characterize the in-fill of the basin with continuous cores, downhole geophysics, and other drilling information,
- The diamond borehole was completed as a deep observation well for use in subsequent pumping tests,
- Based on the diamond core logs and downhole geophysics, the pumping wells were planned in strategic locations to prove recoverable resources.

Figure 41 shows the location of the drillholes (Coordinate System UTM Zone 19s, WGS 84).

Table 19 shows a summary of the location and total depths reached for the drill holes.

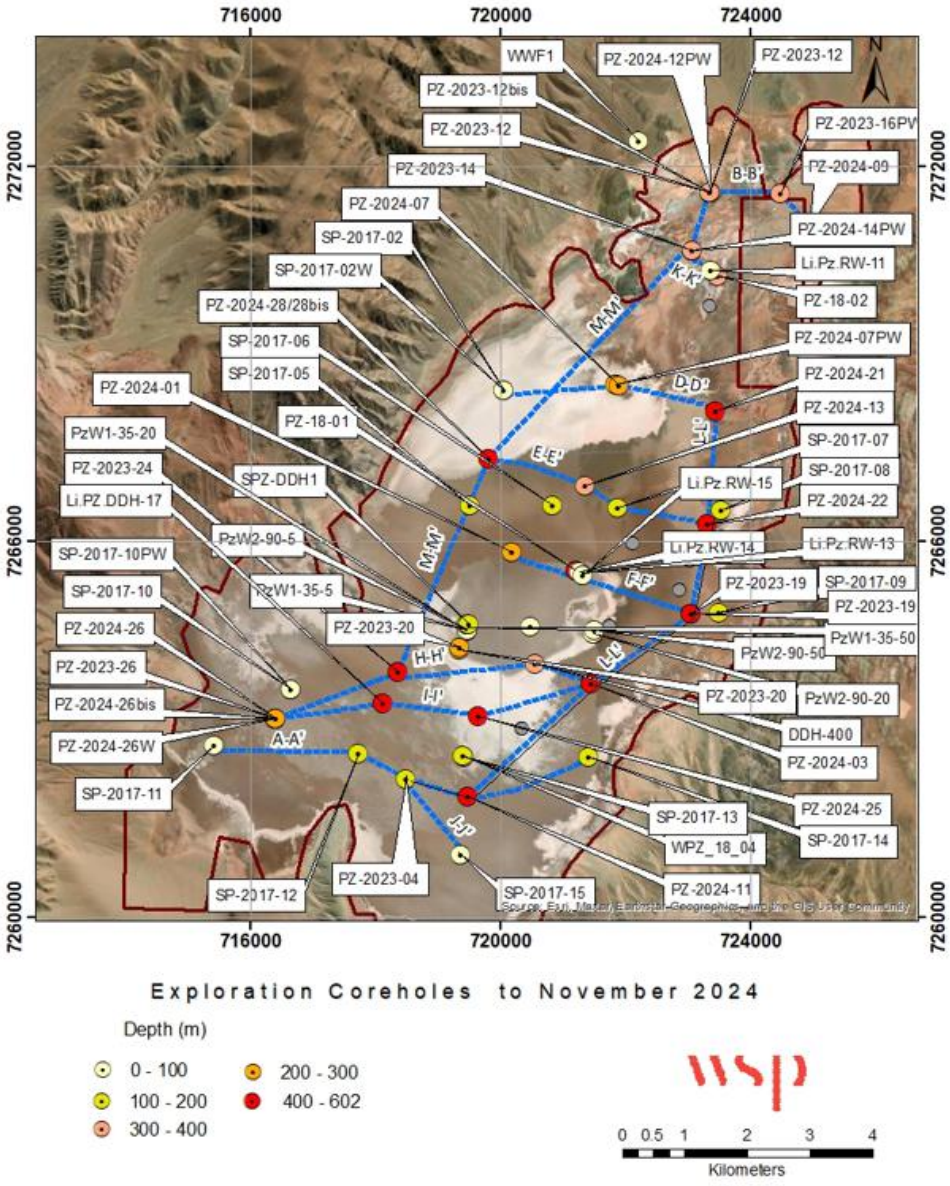

Figure 41: Location of the Drillholes at Pozuelos (Source: Golder, Jan 2025)

Table 19: Location and Total Depth of the Drillholes at Pozuelos

No.	HOLE ID	POINT_X (m)	POINT_Y (m)	Depth (m)	No.	HOLE ID	POINT_X (m)	POINT_Y (m)	Depth (m)
1	PZ-2023-04	718489	7262217	180.0	18	SP-2017-06	720837	7266577	200.0
2	PZ-2023-12	723343	7271587	395.0	19	SP-2017-07	721877	7266539	105.5
3	PZ-2023-14	723060	7270657	386.0	20	SP-2017-08	723528	7266502	125.0
4	PZ-2023-19	723041	7264846	440.0	21	SP-2017-09	723487	7264864	114.5
5	PZ-2023-20	719340	7264278	240.5	22	SP-2017-10	716658	7263641	141.5
6	PZ-2023-26	716410	7263183	206.0	23	SP-2017-11	715433	7262741	52.1
7	PZ-2023-24	718360	7263930	401.0	24	SP-2017-12	717732	7262613	168.5
8	PZ-2024-01	720191	7265839	248.0	25	SP-2017-13	719414	7262572	125.0
9	PZ-2024-03	721457	7263727	488.0	26	SP-2017-14	721413	7262572	123.5
10	PZ-2024-07	721888	7268501	248.0	27	SP-2017-15	719375	7261007	81.5
11	PZ-2024-09	724950	7271050	266.0	28	PZ-18-01	721295	7265504	404.3
12	PZ-2024-13	721354	7266900	391.0	29	PZ-18-02	723359	7270331	358.0
13	PZ-2024-22	723315	7266290	629.6	30	Li.PZ.DDH-17	718125	7263417	470.0
14	DDH-400	720552	7264056	322.7	31	PZ-2024-11	724489	7271560	482.0
15	SPZ-DDH1	719496	7264678	183.0	32	PZ-2024-28-bis	719806	7267352	491.0
16	SP-2017-02	720055	7268425	128.0	33	PZ-2024-21	723450	7268070	600.0
17	SP-2017-05	719517	7266583	101.0	34	PZ-2024-25	719618	7263223	605.0

7.3.1.2 Salar Infill

Pozuelos is a close basin formed within an elevated area of tertiary and Ordovician rocks.

In the basin, geological processes related to the mechanical action of fragmentation and transport of clastic material coexist with evaporitic facies linked to brine accumulation.

The lithologies encountered from the boreholes supported the understanding of the different facies of the sediments filling the depocenter of the basin. The drillhole data was re-logged using photographs of the cores, packer sampling results, and down-hole geophysics provided by the client.

All data collected from the drill holes were correlated in cross-sections to determine the continuity facies (Figure 41).

The facies were used to define the Hydrostratigraphic Units (HSUs) from the Leapfrog Model.

7.3.1.2.1 Ephemeral Saline Lake Facie

The Ephemeral Saline Lake facie is the uppermost layer of the salar. The lithology comprises halite with a mix of textures, saccharoidal and cubic crystals. This facie is often found with interstitial sediments. The formation of these facies is related to a hypersaline lake exposed to environmental conditions.

7.3.1.2.2 Perennial Saline Lake Facie

The Perennial Saline Lake facies is represented by fractured and massive halite with interstitial clays or sand.

A perennial saline lake is formed in an arid climate, resulting in high continuous evaporation rates, concentrating on the brine surface and boosting the nucleation and growth of saline minerals in the brine surface. The newly concentrated brine and the saline minerals precipitated by this process will sink into the lake, and less dense and concentrated fluids will remain above to evaporate. This repetitive process is the leading cause of the stratification of the perennial lake sediments.

For modelling purposes, the perennial and ephemeral saline lake facies were grouped in the Hydrostratigraphic Unit (HSU) “Saline Lake”, which is encountered in the upper portion of the salar, except in the North where the facies are distinctly clastic.

Figure 42 shows cores of Halite interpreted to be from an ephemeral and perennial Saline Lake.

Figure 42: Lithologies from the HSU Saline Lake (Source: Golder, Jan 2025)

7.3.1.2.3 Saline Mudflat Facies

The saline mudflat is formed by silt mixed with clays and fine sand.

This unit is dominant in the west and centre of the salar and usually underlies the Saline Lake unit. It is probably the latest depocenter of the basin.

The mudflat sediments are associated with the old, oversaturated lake and a quiet environment that allowed the deposition of fine sediments over the bottom of the lake. This is probably linked to the major long-term climate change, which caused the dry-up of the region (Reeves, 1968, p.120).

Figure 43 shows cores of clay and silt lithologies interpreted to be formed in facies of a Saline Mudflat.

Figure 43: Lithologies from the HSU Mudflat (Source:Golder, Jan 2025)

7.3.1.2.4 Playa Margin Facies

The facies of the playa margin were formed by fluvial processes, landslides and gravitational slides on the high-angle slopes of the basin margin. Those processes led to the deposition of thick layers of colluvial and alluvial deposits in the main depocenter of the basin.

The Alluvial and Colluvial deposits are accumulations of materials of different sizes resulting from the fractures and fragmentation of mountain rocks. They are characterised by angular gravel distributed chaotically without stratification. They usually present a sandy or silt-clay matrix with lithoclasts with erratic distribution.

The Playa Margin facies are represented in the Hydrostratigraphic Model with the HSUs “Muddy Alluvial and Colluvial Sediments” and “Sandy Alluvial and Colluvial Sediments”. The contact between these units is transitional (Vertically and laterally); However, the sandy beds are predominantly towards the East (PZ-2023-19, PZ-2023-04). The muddy sediments are mainly in the north extreme and southwest of the salar.

Figure 44 shows cores of Alluvial and Colluvial sediments interpreted to be from the Playa Margin Facies.

Figure 44: Lithologies from the HSUs Sandy (left photo) and Muddy (right photo) Alluvial and Colluvial Sediments (Source: Golder, Jan 2025)

7.3.1.2.5 Fractured Aquifer

Several wells, along and across the salar, reached a deep geological unit, densely fractured with a high alteration grade, mixed with chaotic and coarse sediments.

The packer proved that this unit acts hydraulically, similar to granular porous media. Therefore, it was considered part of the brine resource of the salar.

This unit has been represented in the Hydrostratigraphic Model by the HSU “Fractured Aquifer”, and it was described in the drill holes PZ-2024-14, PZ-2023-12, PZ 18-02, PZ-2024-07, PZ-2024-13, DDH-400, and PZ-2024-03, PZ-2024-11 and PZ-2024-25. In all the cases, it is the lowest Unit.

Figure 45 shows cores of the lithologies interpreted as Fractured Aquifer Unit.

Based on the wide distribution of this unit, it was interpreted as an aquifer overlying the Ordovician solid bedrock.

Figure 45: Lithologies of the HGU Fractured Aquifer (Source: Golder, Jan 2025)

7.3.1.2.6 Siltstone

The Siltstone encountered the wells SP-2027-12, DDH-17, PZ-2023-24 and PZ-2023-28bis. It is considered part of the Cenozoic basement, which outcrops the south and southwest margin of the salar. It is unknown if this Unit overlies the Fractured Aquifer Unit.

This unit has been represented by the HSU “Siltstone,” it was excluded from the Resource Estimate because it is considered a hydrological basement.

Figure 46 shows cores of the lithologies interpreted as Siltstone Unit.

Figure 46: Lithologies of the HGU Siltstone (Source: Golder, Jan 2025)

7.3.1.3 Cross-Sections and Continuity of the Hydrostratigraphic Units

The lithological descriptions, interpretations and packer sampling results were schematically analysed in cross-sections to define the continuity of the basin's infill. The location of each section is shown in Figure 41.

Figure 47 to Figure 52 show the continuity of the facies in schematic cross sections.

South-North Sections

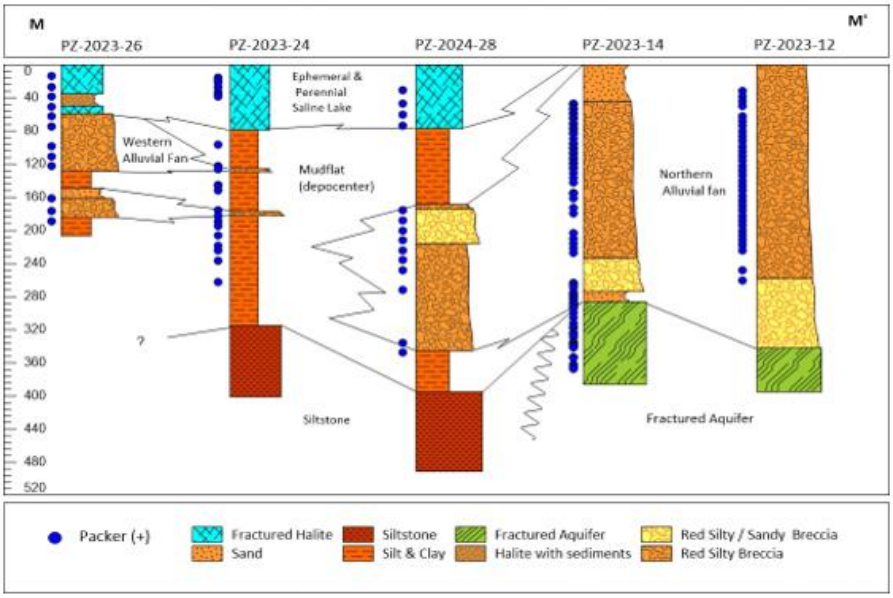

Figure 47: South-North Cross Section M-M' PZ-2023-26, PZ-2023-24, PZ-2024-28(bis), PZ-2023-14, PZ-2023-12 (Source: Golder, Jan 2025)

The Cross-section M-M' shows the siltstone as a basement in the centre and south of the basin and the fractured aquifer (Ordovician) towards the north. This shows the complexity of the faulting and folding in the west side and floor of the salar.

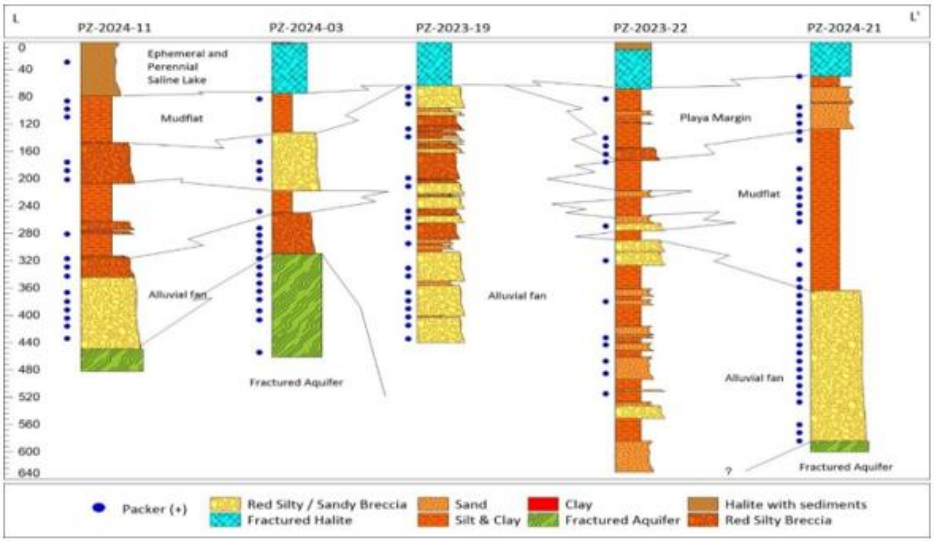

Figure 48: South-North Cross- Section L-L' PZ-2024-11, PZ-2024-03, PZ-2023-19, PZ-2023-22, PZ-2024-21 (Source: Golder, Jan 2025)

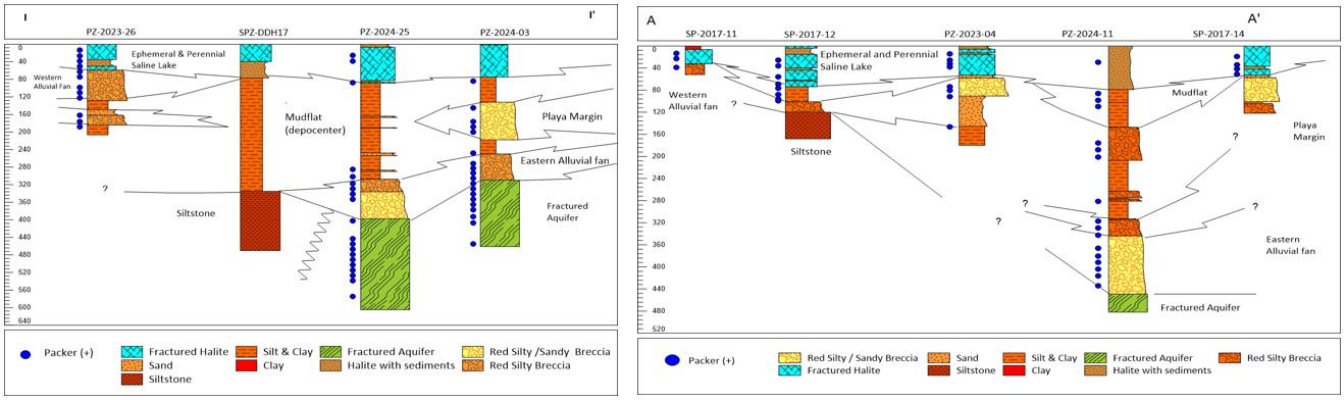

Figure 49: Cross Section I-I': PZ-2023-26, SPZ-DDDH17, PZ-2024-25, PZ-2024-03 and Cross Section A-A' (SP-2017-11,SP-2017-12- PZ-2023-04, PZ-2024-11, SP-2017-14) (Source: Golder, Jan 2025)

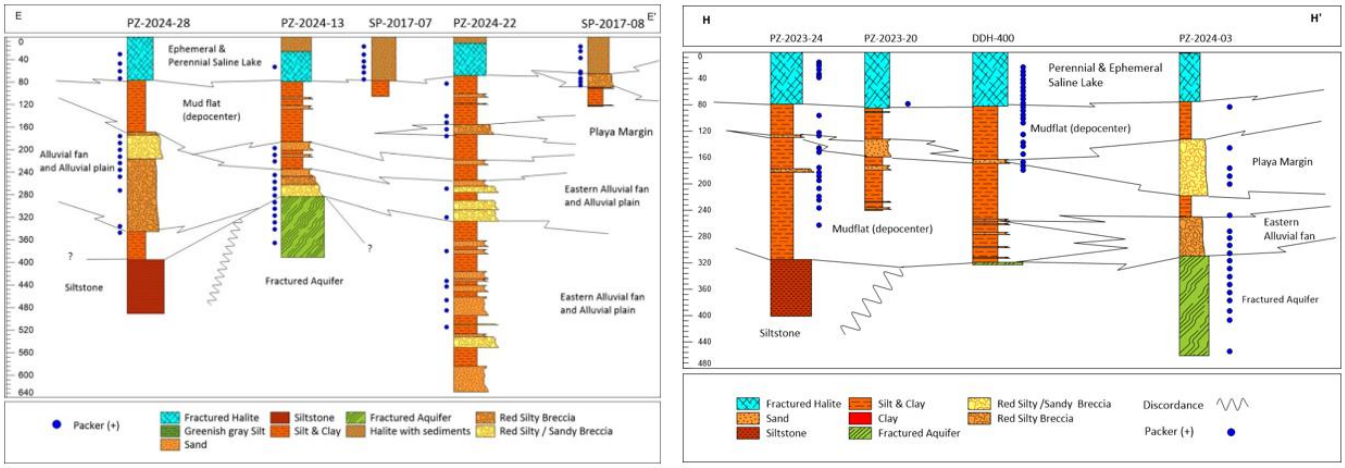

Figure 50: Cross Section E-E' (PZ-2024-28(bis), PZ-2024-13, SP-2017-07, PZ-2024-22, SP-2017-08) and Cross Section H-H' (PZ-2023-24, PZ-2023-20, DDDH-400, PZ-2024-03) (Source: Golder, Jan 2025)

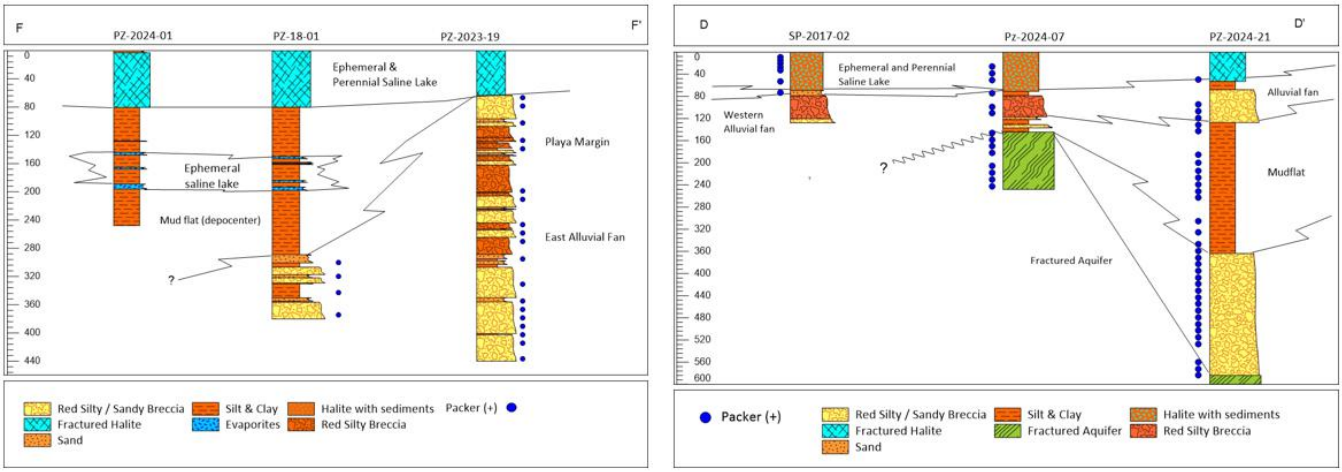

Figure 51: Cross Section F-F' (PZ-2024-01, PZ-118-01, PZ-2023-19) and Cross Section D-D' (SP-2017-02, PZ-2024-07, PZ-2024-21) (Source: Golder, Jan 2025)

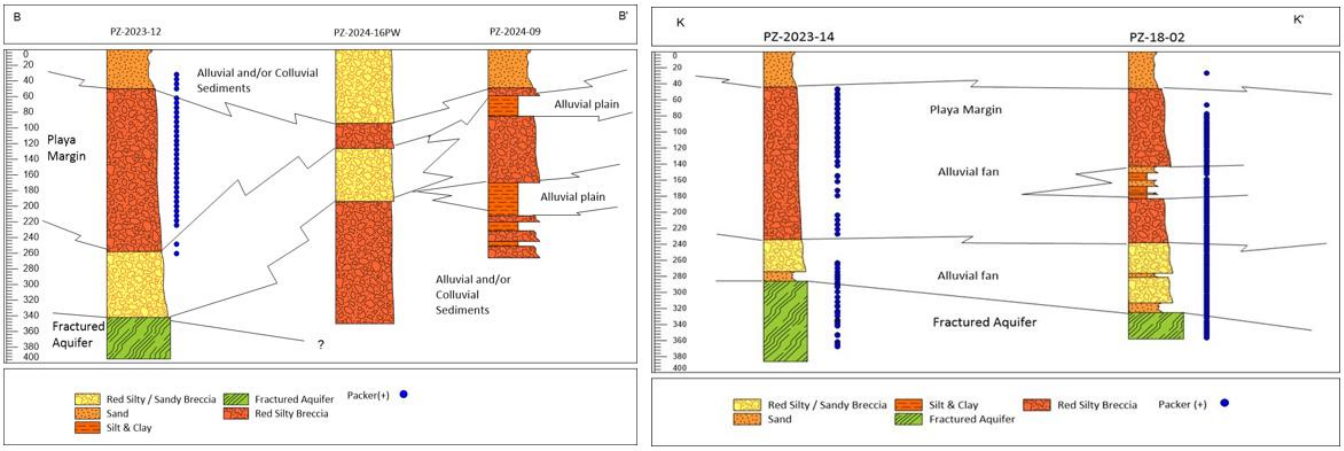

Figure 52: Cross Section B-B' (PZ-2023-12, PZ-2024-16PW, PZ-2024-09) and Cross Section K-K' (PZ-2023-14, PZ-18-02) (Source: Golder, Jan 2025)

7.3.1.4 Hydrogeology Test Work

7.3.1.4.1 2017 Pumping Test

The results of pumping tests from the 2017 exploration program are detailed in Hains (2017b) and summarized in Table 20. Step-tests and long-term pumping tests were run on Wells PW1 (35 m depth) and PW-2 (90 m depth). Both wells were monitored by piezometer wells set at 5 m, 20 m and 50 m in a radial pattern from each well, with piezometers installed at the same depth as the pumping wells.

7.3.1.4.2 2018 Pumping Test

The LSC 2018 pumping well test program was designed to test aquifer properties and evaluate brine chemistry variables across the salar. Pumping tests were conducted based on step tests and 2-day to 7-day constant rate tests. All holes were conventionally developed using compressed air and over pumping and were left open.

- **Well SP-2017-10W**

Pumping well SP-2017-10W was drilled to 141.5 m depth and placed adjacent to exploration hole SP-2017-10 in the southwestern portion of the salar to test the smaller depocenter in that area. Piezometers SP-2017-pz5-10W and SP-2017-pz10-10W were placed at right angles and distances of 5.12 m and 10.23 m from the pumping well, respectively. The screen interval was from 66 m to 99 m, with the pump set at 99 m. The pump discharge was placed 200 m from the well and the flow rate monitored with a weir and flow meter.

Step tests were run at pumping rates of 10.6, 20.4, 40 and 82.16 m^3/hr. Brine samples were collected at 15-minute intervals from 08:15 to 14:00 on March 31, 2018.

A two-day constant rate test was run on April 1, 2018, with samples collected initially at 1-hour intervals and eventually at 3-hour intervals. High pumping rates were achieved with high lithium values exceeding 700 mg/L. As the data were promising, a 7-day constant rate pumping test was run starting August 9, 2018. Brine samples were collected every hour for the first day, every 3 hours the second day and every 8 hours on subsequent days. Lithium values averaged 731 mg/L in the 2-day continuous pumping test and increased to 750 mg/L for the 7-day continuous pumping test, with an overall average assay of 742 mg/L for the combined tests.

The 7-day test was run at a constant pumping rate of 82.16 m^3/h. Well recuperation was achieved in 20 hours. The well performance for the 7-day test is illustrated in Appendix A.

Pumping data were analysed by Walton's method using Starpoint Software Infinite Extent Version 4.1.0.1. Based on the results, the average transmissivity was estimated at 246 m^2/day and the storage coefficient (S) at 6.35E-3 in a semi-confined aquifer. Based on the results of the pumping tests it was concluded that the well was capable of producing at a maximum rate of 130 m^3/h with a drawdown of 51.62 m.

- **Well WPZ-18-04**

This well is located in the south-central part of the salar adjacent to Hole SP-2017-13. The well was finished at 8", screened in sections down to 176 m, and fitted with a 1-3 mm filter gravel pack. Well SP-2017-13 was set up as a piezometer well with screens from 6.5 m to 80 m. Step tests of 2-hour duration were conducted to establish the hydraulic characteristics of the well. The results of the step test showed very fast recovery.

The pumping test indicated well WPZ-18-04 represented an aquifer with evaporite facies from 0 m to 80 m below surface and clastics from 80 m to 182 m. The well is capable of a pumping rate of 70 m^3/h with a drawdown of 56.04 m. Recovery in the well is excellent.

- **Well SP-2017-2W**

This well is located adjacent to Hole SP-2017-2. It was drilled to 70 m depth, with a screen filter installed from 11 m to 66.5 m. The well design included two piezometers installed at right angles to the pumping well at distances of 5.75 m and 11.85 m, respectively. The pumping and piezometer wells were conventionally developed until clear brine was obtained. Piezometer measurements were obtained using both manual and automatic (datalogger) methods. Pump discharge was measured using a flow gauge and a V-notch weir, with the discharge set at 200 m from the well.

A step test to establish hydraulic data and determine suitable pumping rates. The step test was run on March 13, 2018, between 11:15 and 17:00. Samples were collected every 15 minutes. Step test pumping rates were set at 13 m^3/h, 21 m^3/h and 28 m^3/h based on 2-hour runs for each pumping rate.

A 2-day constant rate test was run at a pumping rate of 27.5 m^3/h, with 24-hour recuperation. Based on the analysis, the average transmissivity (T) for the aquifer was calculated as 224 m^2/day and the storage coefficient, S = 4.11E-3 in a semi-confined aquifer system.

- **Well SP-2017-14W**

This pumping well was designed to test aquifer properties in the eastern section of the south end of salar. The pumping well was located adjacent to SP-2017-14. The well was drilled to 123.5 m, with screen filters set at 11 m to 51.5 m. Piezometer holes were drilled to the same depth and screened to the same interval as the pumping well. The piezometers were constructed at right angles to the pumping well at distances of 5.8 m (Pz5) and 11.6 m (Pz10) from the well.

A step test was run at 2-hour duration for each test, with brine samples collected every 15 minutes.

A two-day constant rate test was run at a pumping rate of 17.5 m^3/h. Brine sample assays showed a slight decrease over time, averaging 358 mg/L for the test, but only 350 mg/L towards the end of the test.

Based on the data, the estimated maximum pumping rate for the well is 20 m^3/h with a calculated dynamic level of 25.19 m under the well head. The mean value of the Transmissivity of the aquifer is T = 156 m^2/day and the storage coefficient, S, is 1.44E-3 in a semi-confined aquifer.

- **Well WPZ-18-01**

The well was drilled at 8” diameter using a tricone bit to a depth of 103 m and screened at intervals of 14 - 30 m, 42 - 49 m, 59 - 67 m and 85 - 103 m.

A step test was run at two-hour intervals at pumping rates of 11.5, 19.2 and 39.2 m^3/h. Brine samples were collected every 15 minutes.

A 7-day constant rate pumping test was run from September 11 to September 17, 2018, at a pumping rate of 41.5 m^3/h, with 2 days for recovery. The pumping rate was monitored with a flow meter and a V-notch weir.

Brine assay values over the duration of the constant rate pumping test showed good stability, with an average lithium concentration of 415 mg/L.

The constant rate pumping data was analysed using Starpoint Software Infinite Extent Version 4.1.0.1 software. Good concordance was obtained between the step test results and the constant rate tests. The constant rate pump test gave an average transmissivity value of T = 152 m^2/day with a storage coefficient, S, of 2.80E-4 in a semi-confined aquifer.

7.3.1.4.3 2020 Pumping test

During the 2020 field campaign, in-situ eight (8) long-term pumping tests (72 hours) were carried out in the Pozuelos to obtain hydraulic properties assigned to different hydrostratigraphic units. They allowed capturing an initial spatial distribution of the main hydraulic parameters for the aquifer units defined in SPz. Details about the calibration process was reported in Litica (2020a), and they were carried out with the MODFLOW code (Harbaugh, 2005), and PEST (Parameter Estgimation, Doherty, 2008).

Long-term pumping tests (72 hours) carried out in the unconfined shallow aquifer allowed pumping rates of about 9.5 to 64 m^3/h, involving both halite (Centre and Southern platforms) and clastic units. On the other hand, long-term pumping test carried out in the deeper aquifer (clastic) allowed pumping rates of 12.3 to 74 m^3/h. However, specific pumping flow rates were low (low efficiency) in those pumping wells with window screens in both shallow and deeper aquifers, whereas well efficiencies increase in those pumping wells with windows screens in both aquifers (Li.Pz.RW-11: 16.8 m^3/h/m; Li.Pz.RW-14: 1.9 m^3/h/m, Li.Pz.RW-17: 9.3 m^3/h/m).

The calibrated parameters were the hydraulic conductivity (K), the specific yield (Sy), and the specific storage coefficient (Ss), and they are summarized in Table 20. The pumping test details are shown in Appendix A.

Table 20: Summary of Pumping Test Results in Pozuelos

Pumping test	Well	Pumping test type	Q (m^3/hr)	Duration (day)	Screen depth (m)	Maximum drawdown (m)	Fit	T (m^2/d)	Specific rate (m^3/h/m)	Ss
PW-1 (2017)	PW-1	Step-drawdown	22.79	105 min	0 - 35 m	7.85	-	-	2.903	-
			26.41	90 min		10.6	-	-	2.492	-
			33.75	162 min		20.77	-	-	1.625	-
	PzW1-35-20	Observation well	33.75	30 days	-	0.16	-	-	-	2.44E-02
	PzW1-35-50	Observation well	-		-	0.04	-	-	-	3.61E-02
	PW-1	Pumping well	-		0 – 35 m	-	-	1490	-	-
PW-2 (2017)	PW-2	Step-drawdown	5.29	120 min	35 - 80 m	2	-	-	2.65	-
	PW-2 35		8.87	120 min	-	4.39	-	-	2.02	-
	PW-2 80		13.4	120 min	-	7.775	-	-	1.69	-
	PW-2	constant rate	15 - 27.87	15 days	-	42.88	-	-	-	-
SP-2017- 10W (2018)	SP-2017-10W	Step-drawdown	10.6	-	-	1.815	-	-	5.84	-
			20.4	-	-	3.645	-	-	5.597	-
			40	-	-	8.18	-	-	4.889	-
			82.16	-	-	22.9	-	-	3.587	-
	SP-2017-10W	Pumping well	82.16	7 days	66-99	-	-	408	-	1.82E-02
	Piezo 5	Observation well	-	-	-	-	-	411	-	4.00E-05
	Piezo 10	Observation well	-	-	-	-	-	405	-	8.20E-04
SP-2017-2W (2018)	SP-2017-2W	Step drawdown	13	2 hrs	11-66.5	6.175	-	-	2.1	-
			21	2 hrs	-	11.15	-	-	1.88	-
			28	2 hrs	-	28.94	-	-	0.967	-
	Pz5	Observation well	-	-	-		B-irsoy Summers	121	-	3.53E-03
	Pz10	Observation well	-	-	-		Bi-rsoy Summers	406	-	4.08E-08
	SP-2017-2W	Pumping well	30		-		Re-covery	166	-	
	Pz5	Observation well	-	-	-		Wal-ton	92	-	2.88E-03
			-	--	-		Reco-very	197	-	1.78E-03
	Pz10	Observation well	-	-	-		Walto-n	267	-	1.09E-02
			-		-		Recov-ery	320	-	1.47E-03

Pumping test	Well	Pumping test type	Q (m^3/hr)	Duration (day)	Screen depth (m)	Maximum drawdown (m)	Fit	T (m^2/d)	Specific rate (m^3/h/m)	Ss
SP-2017-14W (2018)	SP-2017-14W	Step drawdown	3.4	2 hrs	11- 51.5	2.18	Jacobs- and Hantush	-	1.559	-
			8.16	2 hrs	-	5.38	Jacobs and Hantush	-	1.515	-
			19.5	2 hrs	-	22.41	Jacobs and Hantush	-	0.87	-
	SP-2017-14W	Pumping well	17.5	-	-		Recovery	82	-	-
	Pz5	Observation well	-	-	-		Walton	46	-	1.01E-03
			-	-	-		Recovery	267	-	
	Pz10	Observation well	-	-	-		Walton	54.5	-	1.46E-03
			-	-	-		Recovery	333	-	-
WPZ-18-01 (2018)	WPZ-18-01	Step drawdown	11.5	-	-	5.09	Jacobs and Hantush	-	2.259	-
			19.2	-	-	10.12	Jacobs and Hantush	-	1.897	-
			39.2	-	-	33.66	Jacobs and Hantush	-	1.164	-
	WPZ-18-01	Pumping well	41.5	7 days	-			-	-	-
	Pz20	Observation well	-	-	-	-	Hantush	159	-	2.89E-04
			-	-	-	-	Recovery	145	-	-

Pumping test	Well	Pumping test type	Q (m^3/hr)	Duration (day)	Screen depth (m)	Maximum drawdown (m)	Fit	T (m^2/d)	Specific rate (m^3/h/m)	Ss
Li.PZ.RW-10 (2020)	-	Constant rate	64	3 days	47-144	17	-	-	3.8	-
Li.PZ.RW-11 (2020)	-	Constant rate	67	3 days	47-341	4	-	-	16.8	-
Li.PZ.RW-12 (2020)	-	Constant rate	12.3	2.35 days	143-341	29	-	-	0.4	-
Li.PZ.RW-13 (2020)	-	Constant rate	9.5	3 days	5-35	24	-	-	0.4	-
Li.PZ.RW-14 (2020)	-	Constant rate	50	3 days	3-38; 300-381; 393-405	26	-	-	1.9	-
Li.PZ.RW-15 (2020)	-	Constant rate	12.4	3 days	300-383; 395-407	-	-	-	-	-
Li.PZ.RW-16 (2020)	-	Constant rate	41	3 days	5-35	17	-	-	2.4	-
Li.PZ.RW-17 (2020)	-	Constant rate	84	3 days	5-35; 83-149	9	-	-	9.3	-
Li.PZ.RW-18 (2020)	-	Constant rate	73	3 days	38 - 149	29	-	-	2.5	-

7.3.2 Pastos Grandes

70 boreholes have been drilled in the PG Salar, for a total of 31,485 m and recovering 12,265 m of core samples. 14 pumping wells were drilled and tested to evaluate flow potential, and the results were used to forecast production through a dynamic model.

Various drilling campaigns have been carried out for the Project since 2011.

- Eramet conducted the first exploration program in 2011 including 11 shallow exploration boreholes ("S" series), two diamond drill holes (D 01PGDDH and DW02PGDDH), four shallow exploration holes completed with 6-inch diameter casing ("PMP" series), and three exploration wells of varying depths completed with 6-inch diameter casing (DW03PG, DW04PG, DW05PG). Detailed information of these boreholes has not been published and is mostly unavailable, although according to Dworzanowski et al. (2018) maximum depths reached at this stage rarely exceeded 100 m.

- LSC completed six drill holes at Pastos Grandes in 2018 (Table 20). Boreholes were drilled using a combination of diamond bit and tri-cone at HQ diameter. Drilling was completed by Hidrotec (Holes SPG-02, 3B, 4A, 5, 5B) and AGV (Hole PG-18-01).

- The two campaigns conducted by Millennial included 32 brine exploration boreholes (PGMW16-01 through PGMW19-22), 6 freshwater exploration wells (PGWW18-01 to PGWW19-06) and 4 brine production wells (PGPW16-01 to PGPW18-17) with drilling depths of up to 600 m. Most of the monitoring wells were completed as piezometers with 2-inch diameter PVC slotted casing, while production wells were constructed with 6 to 8- inch diameter screened casing.

- Recently LAR completed an exploration campaign consisting of two exploration boreholes using Mud Rotary and Diamond Drilling methodology (PGMW23-23 and PGMW23-24).

AMSA and Centaur carried out drilling programs on the Sal de la Puna Project between 2018 and 2022. These programs consisted of two diamond core holes (DD-01 and DD-02), five combination core /rotary holes (PP-01- 2018, PP-02-2018 and R-01 through R-03), two production wells (PP-03-2019 and PW-1), and several piezometer installations.

Ganfeng Lithium drilled five exploration boreholes in 2023 and 2024 with Diamond Drilling methodology (PG- 2023-02, 03, 04, 05 and 13) and two production wells (PG-2023-03PW and PG-2024-21PW) were drilled using Mud Rotary methodology.

The objectives of the drilling program can be broken down into three general categories:

- Exploration drilling to allow the estimation of "in-situ" brine resources: The drilling methods were selected to allow for 1) the collection of continuous cores to prepare "undisturbed" samples from specified depth intervals for laboratory porosity analyses and 2) the collection of depth-representative brine samples at specified intervals. Additional details of the sampling process can be found in the following Chapters 11 of this report.

- Test well installations: 8 rotary holes (PGPW16-01 to PGPW18-17; PGWW18-01 to PGWW19-03, and PW-1) which were drilled and completed as production wells to carry out pumping tests and additional selective brine sampling. Monitoring wells were installed adjacent to most of these production wells for use during the pumping tests as observation points.

- Pumping tests: Eight pumping tests had been completed in the Salar of Pastos Grandes. These tests included three short-term tests (PGWW18-02, PGWW19-02 and PGWW19-03), each lasting about one day and conducted on freshwater wells; three three-day tests conducted on brine wells (PGPW16-01, PGPW18-15 and PGPW18-17); and two long-term pumping tests (PGPW16-01 and PGPW17-04) with 23- and 30-day duration.

Figure 53 shows the location of the drilling carried out in Pastos Grandes salar and Table 21 includes a summary of the construction details of each completed borehole.

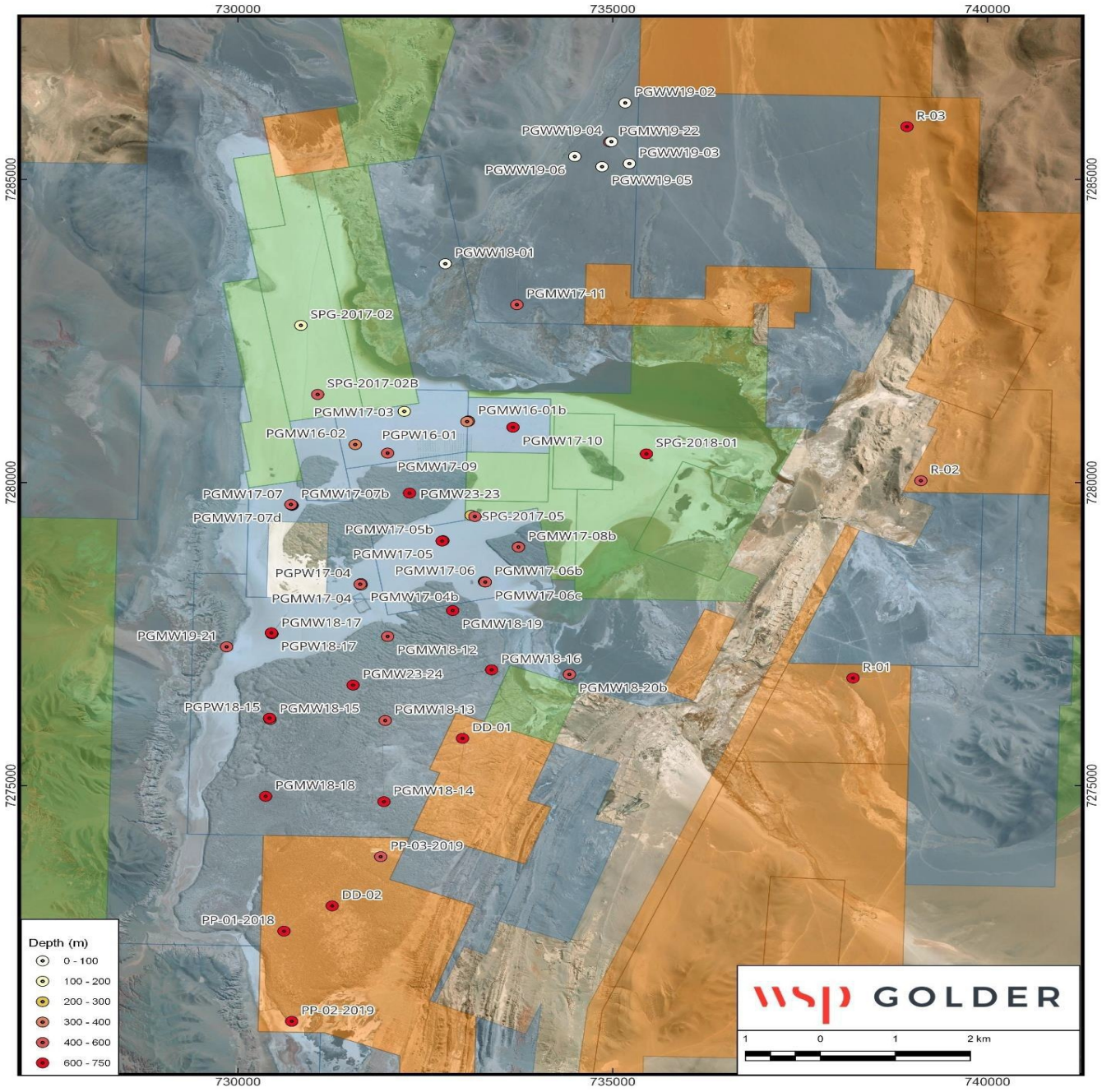

Figure 53: Borehole Locations in Salar de Pastos Grandes (Source: Golder, Oct 2024)

7.3.2.1 Salar Infill

As part of this resource update, geological descriptions were reinterpreted and the redundant information of each platform was consolidated in a single drilling record (for example, different boreholes within a few meters, of different depths and different drilling methodologies). The interpretations originally set forth in the core samples descriptions were reconciled with the observations made from field visits to adjust the lithological descriptions with the interpretation of the units. Currently, geologists from Lithium Argentina and Ganfeng are working on relogging cores from wells drilled with DDH methodology, using photographic guides and a template with new lithological facies codes.

Table 21 lists the detail of the boreholes considered in the reinterpretation while shows their spatial distribution.

Table 21: Boreholes Incorporated in the Geological Model at Pastos Grandes Salar

No.	BH ID	East (m)	North (m)	Elevation (masl)	Final depth (m)	Drilling method	Source
1	PGMW16-01	3429220.36	7283662.47	3773.51	190.0	DDH	Millennial
2	PGMW16-01b	3429223.50	7283656.94	3773.52	355.0	MR	Millennial
3	PGMW16-02	3427722.56	7283239.5	3773.47	400.0	DDH-181-MR	Millennial
4	PGMW17-03	3428364.31	7283801.39	3773.59	154.0	DDH	Millennial
5	PGMW17-04	3427849.60	7280923.97	3773.48	245.5	DDH	Millennial
6	PGMW17-04b	3427848.14	7280949.82	3773.50	564.0	MR-401-DDH	Millennial
7	PGMW17-05	3428920.43	7281678.07	3773.48	121.0	DDH	Millennial
8	PGMW17-05b	3428927.12	7281681.13	3773.46	387.0	DDH	Millennial
9	PGMW17-05c	3428915.71	7281674.94	3773.47	601.0	MR	Millennial
10	PGMW17-06	3429495.98	7281017.41	3773.49	455.0	DDH-387.5-MR	Millennial
11	PGMW17-06b	3429501.98	7281013.41	3773.50	424.0	MR	Millennial
12	PGMW17-06c	3429506.18	7281010.08	3773.48	571.0	MR	Millennial
13	PGMW17-07	3426901.91	7282219.36	3773.48	203.3	DDH	Millennial
14	PGMW17-07b	3426894.32	7282226.27	3773.61	203.3	MR	Millennial
15	PGMW17-07c	3426891.31	7282229.04	3773.63	412.0	DDH-283-MR	Millennial
16	PGMW17-07d	3426886.96	7282232.66	3773.61	510.0	MR	Millennial
17	PGMW17-08	3429936.20	7281600.28	3790.37	425.5	DDH	Millennial
18	PGMW17-08b	3429935.38	7281596.44	3790.31	446.0	MR	Millennial
19	PGMW17-09	3428156.97	7283108.31	3773.50	595.0	DDH-268-MR-475-DDH- 548.5-MR	Millennial
20	PGMW17-10	3429819.91	7283570.78	3773.49	601.0	DDH-178-MR	Millennial
21	PGMW17-11	3429828.42	7285592.86	3814.17	568.0	MR	Millennial

22	PGMW18-12	3428223.79	7280085.04	3805.04	554.0	MR	Millennial
23	PGMW18-13	3428221.75	7278698.22	3793.48	559.0	MR-524-DDH	Millennial
24	PGMW18-14	3428233.29	7277360.1	3798.16	635.0	MR	Millennial
25	PGMW18-15	3426685.37	7278682.07	3794.75	594.0	MR	Millennial
26	PGMW18-16	3429622.29	7279564.99	3789.89	641.0	MR	Millennial
27	PGMW18-17	3426679.33	7280094.81	3773.59	605.0	MR	Millennial
28	PGMW18-18	3426653.97	7277413.4	3800.72	605.0	MR	Millennial
29	PGMW18-19	3429082.17	7280531.59	3788.50	602.0	MR	Millennial
30	PGMW18-20b	3430660.87	7279511.6	3777.94	575.0	MR	Millennial
31	PGMW19-21	3426079.79	7279867.29	3773.63	574.3	MR-180-DDH	Millennial
32	PGMW19-22	3431007.74	7288303.34	3835.00	464.5	MR-102-DDH- 347.5-MR	Millennial
33	PGPW16-01	3429205.29	7283651.25	3773.51	351.0	MR	Millennial
34	PGPW17-04	3427838.48	7280938.71	3774.29	475.0	MR	Millennial
35	PGPW18-15	3426677.60	7278703.09	3794.59	610.0	MR	Millennial
36	PGPW18-17	3426672.41	7280111.44	3773.43	606.0	MR	Millennial
37	PGWW18-01	3428858.61	7286247.57	3817.11	42.0	MR	Millennial
38	PGWW19-02	3431200.48	7288951.92	3840.48	62.0	MR	Millennial
39	PGWW19-03	3431278.44	7287951.85	3831.85	62.0	MR	Millennial
40	PGWW19-04	3431029.59	7288307.87	3835.10	62.0	MR	Millennial
41	PGWW19-05	3430914.39	7287892.93	3832.10	62.0	MR	Millennial
42	PGWW19-06	3430547.09	7288052.35	3830.53	62.0	MR	Millennial
43	PGMW23-23	3428464.00	7282454.00	3792.00	675.5	MR-217-DDH	LAR
44	PGMW23-24	3427780.00	7279273.00	3797.00	701.0	MR- 210-DDH	LAR
45	SPG-2018-01	3431609.00	7283171.00	3776.90	601.0	DDH-50?-MR	LSC
46	SPG-2017-02	3426955.00	7285189.00	3775.50	121.0	DDH	LSC
47	SPG-2017-02B	3427203.00	7284055.00	3769.40	572.5	DDH-50?-MR	LSC
48	SPG-2017-04[a]	3243076.00	7282489.00	3774.20	553.0	MR	LSC
49	SPG-2017-05	3429294.00	7282107.00	3780.80	279.5	DDH	LSC
50	SPG-2017-05B	3429344.00	7282088.00	3778.70	500.5	DDH	LSC
51	PP-01-2018	3426947.42	7275196.05	3806.23	611.0	MR	Centaur

52	PP-02-2019	3427082.04	7273710.57	3784.51	650.0	MR	Centaur
53	PP-03-2019	3428209.84	7276451.69	3804.97	542.0	MR	Centaur
54	DD-01	3429258.90	7278426.26	3801.36	700.0	DDH	AMSA
55	DD-02	3427581.56	7275626.21	3803.30	646.0	DDH	AMSA
56	R-01	3434445.65	7279534.51	3803.34	601.0	MR	AMSA
57	R-02	3435278.95	7282808.61	3803.48	411.0	MR/DDH	AMSA
58	R-03	3434966.77	7288641.75	3828.22	617.0	MR	AMSA
59	PG-2023-02*	730853.00	7282476.00	3782.00	107.2	DDH	Ganfeng Lithium
60	PG-2023-03*	733517.00	7280362.00	3782.00	500.5	DDH	Ganfeng Lithium
61	PG-2023-04*	736048.00	7280160.00	3782.00	404.6	DDH	Ganfeng Lithium
62	PG-2023-05*	730736.00	7280096.00	3782.00	453.5	DDH	Ganfeng Lithium
63	PG-2023-13*	733174.00	7279501.00	3782.00	450.5	DDH	Ganfeng Lithium

Based on the lithological descriptions of the drill core and cuttings together with the interpretation of the available geophysical information and field observations five major hydrogeological units were defined and correlated, these units were incorporated into a 3-D geological model of the Pastos Grandes sub-basin. Figure 54 shows a view of the geologic model from the southwest. The geological units are described below.

7.3.2.1.1 Fluvial/Alluvial Unit

The Fluvial/Alluvial Unit is characterized by a heterogeneous sequence of alluvial and fluvial sediments of variable texture, dominated by clastic sediments formed by gravel and sand that surround the Salar. These fractions may present low proportions of fine sediments (sands or clays) which develop mainly along the northern and southern edges of the Salar de Pastos Grandes, prograding in depth towards the centre, to interfigered with finer sediments, formed by clay and sandy clays with variable proportion of silt from the Central Clastics Unit. In the northern sector of the basin (wells PGMW17-10 and 11) it reaches approximately 450 m in thickness. Figure 54 shows the spatial distribution of this unit.

7.3.2.1.2 Upper Clay Unit (Blanca Lila Formation)

Formed by a superficial sequence of clays with a wide distribution in the centre-south of the basin, as well as in the western margins were, according to field observations. This clay dominated unit interfingers with layers of evaporites, halite, and borates. In the bibliography travertine and tuff horizons were also described (Alonso and Menegatti, 1990, Benson, 2024). Figure 54 shows the spatial distribution of this unit.

7.3.2.1.3 Saline/Lacustrine Unit (Blanca Lila Formation)

Underlaying the Upper clay Unit and in the north-central sector from the surface, a thick halite sequence is recognized. This Unit is characterized by a massive and compact halite body with the presence of interstitial clastic material and occasional intercalations of finer levels of clay. The average thickness of this Unit ranges between 200 m and 300 m, reaching maximum thicknesses of 700 m (DD-01) in the central-eastern sector of the basin, which is interpreted as an ancient depocenter. Figure 54 shows the spatial distribution of this unit.

7.3.2.1.4 Central Clastic Unit

This Unit consists of clay and clayey sands and occurs within the central sector of the basin underneath the halite deposits, as shown in Figure 54. This Unit is poorly characterized due to limited and low-quality borehole information but seems to represent a distal sector of an alluvial fan and its interaction with marginal lacustrine deposits of the Salar. In the central sector of the basin has a thickness of approximately 300 m.

7.3.2.1.5 Base Breccia/Gravels Unit (Pre-Tajamar Sediments)

Based on lithological description, a sedimentary breccia unit of coarse fragments of silicified conglomerate and ignimbrites was recognized in borehole PGMW19-21. New geological framework (Benson, 2024) indicates that this unit is a crystal-rich ignimbrite with an age of ~14.6 Ma interbedded in pre-Tajamar sediments equivalent to the Pozuelos Formation. This Unit is made up of intermixed levels of sand and gravel with a thickness of 200 m on the western edge of the basin and deepening towards the north-central limit of the model where due to limited information its thickness becomes uncertain. Figure 54 shows the spatial distribution of this unit.

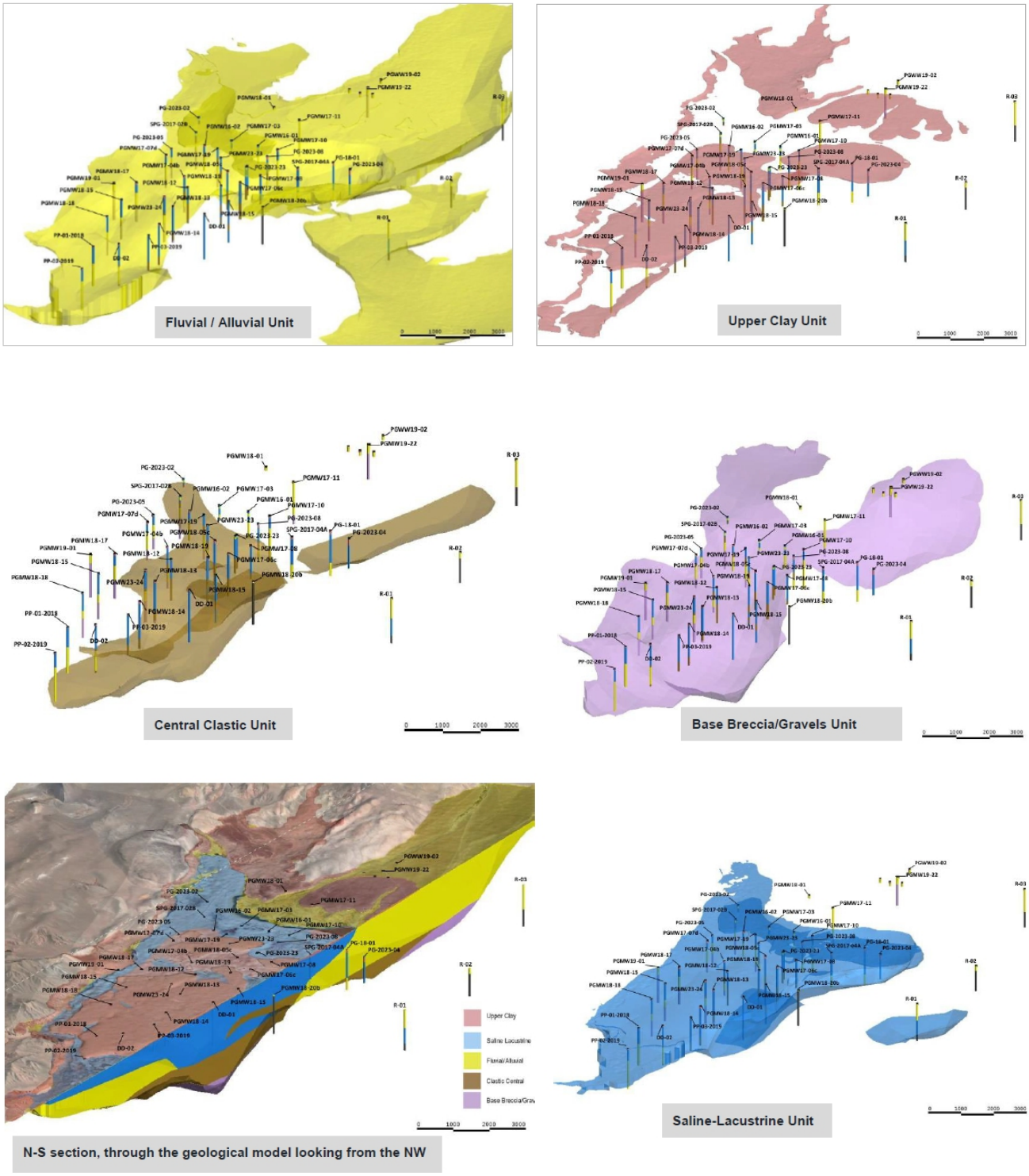

Figure 54: Geological Model and Each Stratum in Pastos Grandes (Source: AW, Dec 2024)

7.3.2.2 Hydrogeology Test Work

Millennial completed eight pumping tests between 2017 and 2019. These tests included three one-day tests on the freshwater wells; three three-day tests on brine wells; and two long-term pumping tests (23- and 30-day duration) also on brine wells. Figure 55 includes the layout of each of these pumping tests.

In 2023 LAR performed one variable rate pumping test in well PW-01. In 2024 Ganfeng performed a pumping test in PG-2023-03PW.

7.3.2.2.1 Brine Well Pumping Tests

- **PGPW16-01 (2017)**

A 3-day pumping test was carried out on well PGPW16-01 at an average pumping rate of 27.7 L/s. The configuration of the test and its results are shown in Table 22 and Appendix A. The production well is screened across the saline halite unit and the underlying brine aquifer. This test included four observation wells but only SW03PG-1 (without completion information) reacted to pumping. Drawdown and recovery data were interpreted, respectively with Cooper & Jacob (1946) and Theis (1935) recovery solutions leading to a hydraulic conductivity (K) estimate of about 3 m/d.

Figure 55: Location Map of the Pumping Tests Conducted in Salar de Pastos Grandes (Source: AW, Dec 2024)

- **PGPW17-04 (2019)**

A 23-day pumping test was completed on PGPW17-04 at a pumping rate of 15.23 L/s in 2019. The production well is screened across halite, sand, and silt; because of the low permeability of the halite, it is believed that the drawdown response is mainly related to the unconsolidated clastic sediments beneath it. Drawdown data during the pumping stage was discarded due to an apparent non-related water level recovery observed during test. Therefore, only recovery data were adjusted to the Theis (1935) recovery solution, leading to a transmissivity estimate of 40 m^2/d, or a hydraulic conductivity 0.12 m/d assuming a saturated thickness of 329 m. The configuration of the test and its results are shown in Table 22 and Appendix A.

- **PGPW18-15 (2019)**

A pumping test (variable and constant rate, and recovery) was carried out in PGPW18-15 during April of 2019. The well was screened in the same lithological unit as PGPW-17-04. The configuration of this test and its results are shown in Table 22 and Appendix A**.** Water levels during the test were also monitored in PGMW18-15. The hydraulic conductivity was estimated to range between 0.15 - 0.22 m/d.

- **PGPW18-17**

A three-day pumping test was conducted on well PGPW18-17 well with an average pumping rate of 19.4 L/s. The configuration of the test and its results are shown in Table 22 and Appendix A**.** Drawdown data was measured only in the pumping well and was adjusted to the Cooper and Jacob (1946) and Theis (1935) recovery solutions. The estimated hydraulic conductivity ranges between 0.17 – 0.22 m/d, which is consistent with previous results for the same lithologies in the Salar.

- **PGPW16-01 (2019)**

A 15-day pumping test was conducted on well PGPW16-01 at an average pumping rate of 23.2 L/s during May 2019. The results of this 2019 test are summarized in Table 22 and Appendix A and they are quite similar to the results of the 2017 test. Drawdown and recovery data were interpreted with the Theis (1935) recovery solution, leading to a hydraulic conductivity estimate of about 2 m/d.

- **PW-01 (2023)**

In September 2023, a preliminary pre-test and a step pumping test were conducted by AMSA. A constant rate, long-term pumping test could not be completed in well PW-01 due to gas appearance during the test.

The step test consisted of 4 stages, over 10 hours, 2.5 hours each stage. The steps tested were: 13.2 L/s, 16.7 L/s, 20.5 L/s, and 24.8 L/s (Table 22). Water levels during the test were monitored in PW-01, as well as in DD-02 and M-01.

PW-01 and DD-02 are screened in the alluvial sediments, while M-01 is screened in the halite. DD-02 showed maximum drawdown of 8.7 m, while M-01 did not react (Appendix A).

- **PG-2023-03PW (2024)**

In April 2024 a constant rate pumping test was performed in well PG-2023-03PW. The observation wells used were PG-2023-03, PG-2023-13, Li.PG.RW-05, and Li.PG.RW-06. The duration of the test was 1 day, with an average discharge of 17.5 L/s (Table 22).

The results of this test are summarized in Table 22 and Appendix A. The pumping well and the observation well PG-2023-03 (both screened in gravel and sands) showed an early recovery, while still pumping, at minute 1400. Observation wells PG-2023-13 and Li.PG.RW-05 (screened in mixed halite and gravel, and gravel respectively) showed initial rapid water level decline (up to minute 1100) with following drawdown rate decrease. On the other hand, observation well Li.PG.RW-06 (screened in halite) showed no drawdown.

Drawdown data (initial 1400 minutes) in the PG-2023-03 observation well was interpreted by Ganfeng, with Cooper and Jacob, and Theis's solutions, leading to a hydraulic conductivity estimate of about 4 m/d.

7.3.2.2.2 Pumping Tests Conducted in Freshwater Wells

- **PGWW18-01 (2019)**

A variable rate and a 1-day constant rate tests with an average flow rate of 0.85 L/s was carried out on well PGWW18-01 in May 2019. No hydraulic parameters could be obtained from this test because of the short test duration and the low pumping rate as shown in Table 22.

- **PGWW19-02 (2019)**

The pumping test in PWGWW19-02 was conducted in 2019 (a variable rate, a constant rate and a recovery). The layout of this test and results are shown in Table 22 and Appendix A. Drawdown and recovery trends were adjusted with the Cooper and Jacob (1946) and Theis (1935) recovery solutions, respectively. Estimated hydraulic conductivity values range from 20 to 60 m/d which is considered reasonable for these types of coarse-grained unconsolidated sediments. The pumping test configuration didn't include observation wells; therefore, no storage estimates could be obtained.

- **PGWW19-03**

A variable rate, constant rate test and recovery test were carried out on Well PWWW19-03. The layout of this test and main results are shown in Appendix A and in Table 22. Drawdown and recovery trends were adjusted with the Cooper and Jacob (1946) and Theis (1935) recovery solutions, respectively. Estimated hydraulic conductivity ranges from 6 to 11 m/d, which is reasonable for this type of coarse-grained unconsolidated sediments with a higher fine fraction. The pumping test configuration didn't include any observation wells; therefore, no storage estimates could be obtained from this test.

Table 22 include summary information on the pumping tests conducted in the Salar.

Table 22: Summary of Pumping Test Results in Pastos Grandes Salar

Test	Well	Type*	Q (L/s)	Duration (days)	Minimum saturated thickness (m)	Maximum drawdown (m)	Fit	T (m^2/d)	K (m/d)	Specific capacity (L/s/m)
PGPW16-01-2017	PGPW16-01	P	27.7	3	224	9.04	C&J (1946)	1.1	4.9	3.1
							Theis Rec. (1935)	500	2.2	-
	PGMW16-01	O			38	0.13	-	-	-	-
	PGMW16-01b	O			189	0.08	-	-	-	-
	SW03PG-1	O			No data	1.19	C&J (1946)	1.1	-	-
							Theis Rec. (1935)	1	-	-
	SW03PG-2	O			No data	0.03	-	-	-	-
PGPW17-04	PGPW17-04	P	15.2	23	329	57.11	Theis Rec. (1935)	40	0.12	0.27
	PGPW17-04b	O			484	3.88	-	-	-	-
	DW05PG	O			No data	0.12	-	-	-	-
PGPW18-15	PGPW18-15	P	24.1	3	456	38.7	C&J (1946)	90	0.2	0.68
							Theis Rec. (1935)	70	0.15	-
	PGMW18-15	O			453	6.5	Theis (1935)	100	0.22	-
PGPW18-17	PGPW18-17	P	19.4	3	589	30.31	C&J (1946)	130	0.22	0.64
							Theis Rec. (1935)	100	0.17	-
PGPW16-01 (2019)	PGPW16-01	P	23.2	15	224	15.15	Theis Rec. (1935)	400	1.8	1.5
	PGMW16-01	O			38	0.12	-	-	-	-
	PGMW16-01b	O			189	0.07	-	-	-	-
	SW03PG-1	O			No data	1.83	-	-	-	-
	SW03PG-2	O			No data	0.14	-	-	-	-

Test	Well	Type*	Q (L/s)	Duration (days)	Minimum saturated thickness (m)	Maximum drawdown (m)	Fit	T (m^2/d)	K (m/d)	Specific capacity (L/s/m)
PW01	PW01	P	13.2-24.8	0.4	-	40.4	-	-	-	-
	DD-02	O			-	8.7	-	-	-	-
	M-01	O			-	0	-	-	-	-
PG-2023- 03PW	PG-2023-03PW	P	17.5	1	-	-	-	-	-	-
	PG-2023-03	O			235	0.54	C&J (1946)	1000	4	
							Theis (1935)			
	PG-2023-13	O			-	-	-	-	-	-
	Li.Pg.Rw-06	O			-	-	-	-	-	-
	Li.Pg.Rw-05	O			-	-	-	-	-	-
PGWW19-02	PGWW19-02	P	15.5	0.8	24	5.32	C&J (1946)	1.6	66.6	2.9
							Theis rec. (1935)	500	20.8	-
PGWW19-03	PGWW19-03	P	3.1	1	36	3.46	C&J (1946)	250	66.6	0.9
							Theis rec. (1935)	400	11.1	-
PGWW18-01	PGWW18-01	P	0.85	1	10.96	5.13	-	-	-	0.2

8.0 SAMPLE PREPARATION, ANALYSES, AND SECURITY

8.1 Pozuelos

LSC oversaw the sampling program (sample collection, QA/QC, and secure transport) until September 2019, followed by Litica Resources until July 2022. Since then, GF Lithium, which owns 100 % of the project, has carried out the sampling program.

This report includes the brine samples from the "POZUELOS EXPLORATION MASTERFILE" File updated to October 2024. It provides a summary of the core samples collected in 2017 for Relative Brine Release Capacity (RBRC) testing, a laboratory measurement of drainable porosity.

The QPs consider it appropriate to include in this section the downhole logging used to estimate drainable porosity measured directly in the field, which has the benefit of measuring the porosity directly from the formation in natural conditions.

8.1.1 Brine Samples

Samples were collected during drilling at specific intervals using packers. It consists of a tool with three inflatable sections. The first is placed inside the drill rod, above the crown, using an HQ3-size seat (inside). The second is positioned below the crown, on the outside of the drilling column and in contact with the formation. This inflatable element isolates the formation above the area to be sampled. Between the second and third inflatable element are the holes that allow the drilling brine to enter the interior of the drill bar. The third inflatable element isolates the lower portion of the area to be sampled. Brine samples are retrieved by airlift inside the HQ drill rod. It is considered an acceptable sample when 3 times the volume of the drill depletion was removed or when the sample is presented free of drilling muds with constant conductivity of density.

8.1.1.1 Samples Analysis

To date, 516 brine samples have been analysed. These were submitted to different laboratories according to the needs of advancing exploration.

The samples collected until 2018 were sent to Alex Steward International Argentina (ASI) Laboratory in Jujuy Province. ASI is certified to ISO 9001, 14001, and OHSAS 18001 standards and is accredited under the international ISO/IEC 17025 technical standards. SGS was used as the check laboratory for QAQC purposes.

Details of the samples sent to each laboratory are shown in Table 23.

The samples after 2018 were assayed in Litica's internal Laboratory on-site (Pozuelos Lab). All the laboratories analysed them using the Induction-Coupled Plasma (ICP).

The samples PPG0116 and PPG0121 from PZ-2024-25 were taken out of the database because those were considered diluted due to sampling procedures.

Table 23: Number of Samples Sent to Each Laboratory

Lithea Exploration 2023-2024		**Litica Exploration 2017-2018**	
Laboratory	# Packer Samples	Laboratory	# Packer Samples
Pozuelos Lab	324	ASI	192
ASI	2	SGS	18

Details of the assays performed by Alex Steward International Laboratory are shown in the Table 24 below.

Table 24: Assayed Parameters, Units, Detection Limits and Method References Used by ALS

Cations/ Anions	Units	Code	Analysis Methodology	Detection Limit
TDS (Dried at 180ºC)	mg/L	LMFQ08	Gravimetry	10
Sulfates SO_4^{2-}	mg/L	LMCI22	Gravimetry	10
Chloride Cl^-	mg/L	0002NLMCI01	Volumetric	10
Alkalinity Total	mg/L	LMFQ15	Volumetric	20
Carbonates CO_3^{2-}	mg/L	LMFQ16	Volumetric	10
Bi-Carbonates HCO_3^-	mg/L	LMFQ17	Volumetric	10
B	mg/L	LMMT03	ICP-OES	1
Be	mg/L	LMMT03	ICP-OES	0.01
Ca	mg/L	LMMT03	ICP-OES	2
Fe	mg/L	LMMT03	ICP-OES	0.3
K	mg/L	LMMT03	ICP-OES	2
Li	mg/L	LMMT03	ICP-OES	1
Mg	mg/L	LMMT03	ICP-OES	1
Mn	mg/L	LMMT03	ICP-OES	0.01
Na	mg/L	LMMT03	ICP-OES	2
Sr	mg/L	LMMT03	ICP-OES	0.5
Conductivity	mS/cm	LMFQ01	Potentiometric	0.05
Density	g/ml	LMFQ19	Picnom	0.001
pH	Ph units	0002NLMCI28	Potentiometric	0.1

The average and general statistics of geochemical results for Li, K, Ca, Mg, SO_4^{2-}, and TDS of the available samples from each individual well, are summarized in Table 25.

Table 25: Brine Samples Analysis

SP-2017-02	Li mg/L	Ca mg/L	Mg mg/L	K mg/L	SO_4^{2-} mg/L	TDS (180°)
Average	446	911	3333	4107	11443	314719
Maximum	507	1281	3625	4764	15669	322100
Minimum	360	502	3024	3312	4700	303800
Standard Deviation	49	278	188	485	4743	5867

SP-2017-05	Li mg/L	Ca mg/L	Mg mg/L	K mg/L	SO_4^{2-} mg/L	TDS (180°)
Average	245	1287	2202	2932	6233	313344
Maximum	290	1412	2426	3241	11236	324950
Minimum	169	1000	2056	2809	4717	295100
Standard Deviation	34	157	109	157	2082	10627
SP-2017-06	**Li mg/L**	**Ca mg/L**	**Mg mg/L**	**K mg/L**	**SO_4^{2-} mg/L**	**TDS (180°)**
Average	283	1519	2350	3029	5235	324642
Maximum	296	1814	2471	3126	5672	328900
Minimum	272	1433	2285	2972	4783	322100
Standard Deviation	9	147	67	53	351	2460
SP-2017-07	**Li mg/L**	**Ca mg/L**	**Mg mg/L**	**K mg/L**	**SO_4^{2-} mg/L**	**TDS (180°)**
Average	279.7	1389.2	1950.0	3169.7	4984.3	319100
Maximum	290.6	1535.1	1968.4	3273.7	5474.1	327300
Minimum	250.9	1319.2	1930.3	2936.4	4297.0	310400
Standard Deviation	15	95	15	125	441	5843
SP-2017-08	**Li mg/L**	**Ca mg/L**	**Mg mg/L**	**K mg/L**	**SO_4^{2-} mg/L**	**TDS (180°)**
Average	294	932	1836	3196	9309	321944
Maximum	426	1159	3152	4324	17402	325700
Minimum	253	435	785	2483	5984	312250
Standard Deviation	61	251	812	634	4216	4300
SP-2017-09	**Li mg/L**	**Ca mg/L**	**Mg mg/L**	**K mg/L**	**SO_4^{2-} mg/L**	**TDS (180°)**
Average	238	1176	1699	2322	5863	318119
Maximum	268	1407	1898	2577	6775	326450
Minimum	218	1049	1482	2077	4750	311500
Standard Deviation	17	110	142	201	767	5663
SP-2017-10	**Li mg/L**	**Ca mg/L**	**Mg mg/L**	**K mg/L**	**SO_4^{2-} mg/L**	**TDS (180°)**
Average	457.77	1814.73	2633.21	4243.56	7110.56	308866.67
Maximum	576.10	2540.86	3427.25	5271.32	12051.24	312100.00
Minimum	370.82	1069.11	2095.52	3500.95	2724.70	307200.00
Standard Deviation	106	736	702	919	4688	2801
SP-2017-11	**Li mg/L**	**Ca mg/L**	**Mg mg/L**	**K mg/L**	**SO_4^{2-} mg/L**	**TDS (180°)**
Average	467	2478	2967	4127	3586	305633
Maximum	557	3106	3398	5097	6211	309300
Minimum	402	1595	2676	3496	1881	302200
Standard Deviation	80	787	381	853	2307	3556
SP-2017-12	**Li mg/L**	**Ca mg/L**	**Mg mg/L**	**K mg/L**	**SO_4^{2-} mg/L**	**TDS (180°)**
Average	409	2801	2564	3505	3054	325175
Maximum	450	3048	2728	3726	5211	329700
Minimum	378	2326	2493	3358	2021	320750
Standard Deviation	26	313	91	152	1361	3263

SP-2017-13	Li mg/L	Ca mg/L	Mg mg/L	K mg/L	SO_4^{2-} mg/L	TDS (180°)
Average	452	2465	2506	3700	4357	315783
Maximum	508	2730	2611	4322	5829	323450
Minimum	430	2332	2412	3517	2314	311500
Standard Deviation	28	140	69	309	1550	5034
SP-2017-14	**Li mg/L**	**Ca mg/L**	**Mg mg/L**	**K mg/L**	**SO_4^{2-} mg/L**	**TDS (180°)**
Average	395	2528	2107	3161	2456	320825
Maximum	444	2951	2333	3565	2823	329700
Minimum	272	1887	1575	2161	2107	313800
Standard Deviation	83	454	357	668	311	6684
SP-2017-15	**Li mg/L**	**Ca mg/L**	**Mg mg/L**	**K mg/L**	**SO_4^{2-} mg/L**	**TDS (180°)**
Average	370	2165	2600	2800	3107	300829
Maximum	385	2267	2698	3041	4075	310900
Minimum	361	1816	2517	2666	2803	285600
Standard Deviation	8	161	77	141	444	11371
DDH-400	**Li mg/L**	**Ca mg/L**	**Mg mg/L**	**K mg/L**	**SO_4^{2-} mg/L**	**TDS (180°)**
Average	522	1644	2466	4833	6138	328709
Maximum	614	1988	2923	5780	13702	335900
Minimum	467	1085	2282	4404	3169	316700
Standard Deviation	33	342	158	290	2920	4983
PZ-18-02	**Li mg/L**	**Ca mg/L**	**Mg mg/L**	**K mg/L**	**SO_4^{2-} mg/L**	**TDS (180°)**
Average	572	1105	3120	4494	9482	314229
Maximum	622	1746	3918	5044	14731	329400
Minimum	386	543	2186	3056	4126	282500
Standard Deviation	44	279	384	383	2889	6892
PZ-2023-26	**Li mg/L**	**Ca mg/L**	**Mg mg/L**	**K mg/L**	**SO_4^{2-} mg/L**	**TDS (180°)**
Average	637	1516	3900	5629	11213	325083
Maximum	908	3283	5547	7479	21415	334000
Minimum	426	383	2608	3870	1904	319000
Standard Deviation	193	1261	1181	1405	8501	5265
PZ-2024-03	**Li mg/L**	**Ca mg/L**	**Mg mg/L**	**K mg/L**	**SO_4^{2-} mg/L**	**TDS (180°)**
Average	606	558	3707	5431	15595	328579
Maximum	710	1104	4046	6764	19941	334000
Minimum	478	394	2893	4934	11400	323000
Standard Deviation	60	157	258	400	2016	2893
PZ-2024-07	**Li mg/L**	**Ca mg/L**	**Mg mg/L**	**K mg/L**	**SO_4^{2-} mg/L**	**TDS (180°)**
Average	483	546	3128	4393	19155	325429
Maximum	620	823	3656	5132	27029	338000
Minimum	299	338	2152	2995	12986	315000
Standard Deviation	106	162	497	681	4111	6630

PZ-2024-13	Li mg/L	Ca mg/L	Mg mg/L	K mg/L	SO_4^{2-} mg/L	TDS (180°)
Average	536	623	3508	4357	15039	315286
Maximum	698	1194	4088	5224	16997	327000
Minimum	266	475	1976	2080	10751	277000
Standard Deviation	145	188	675	983	1900	13842
PZ-2024-22	**Li mg/L**	**Ca mg/L**	**Mg mg/L**	**K mg/L**	**SO_4^{2-} mg/L**	**TDS (180°)**
Average	385	832	3000	3202	10257	315000
Maximum	526	1085	3422	5169	21081	332000
Minimum	230	376	2084	2237	7176	267000
Standard Deviation	70	206	411	728	3681	15389
PZ-2024-11	**Li mg/L**	**Ca mg/L**	**Mg mg/L**	**K mg/L**	**SO_4^{2-} mg/L**	**TDS (180°)**
Average	340	539	2220	2891	11706	219267
Maximum	698	1194	4088	5224	27029	338000
Minimum	60	157	258	400	1900	2893
Standard Deviation	217	353	1374	1841	7930	146811
PZ-2024-25	**Li mg/L**	**Ca mg/L**	**Mg mg/L**	**K mg/L**	**SO_4^{2-} mg/L**	**TDS (180°)**
Average	636	711	4094	4892	14009	325000
Maximum	739	2131	4967	5985	26130	336000
Minimum	336	430	2414	2775	2910	311000
Standard Deviation	129	492	890	872	5477	7841
PzW1-35-5	**Li mg/L**	**Ca mg/L**	**Mg mg/L**	**K mg/L**	**SO_4^{2-} mg/L**	**TDS (180°)**
Average	613	1913	2542	6084	3518	332925
Maximum	627	1999	2592	6617	3634	338300
Minimum	575	1853	2458	4929	3305	324800
Standard Deviation	16	44	39	533	112	5124
PzW2-90-50	**Li mg/L**	**Ca mg/L**	**Mg mg/L**	**K mg/L**	**SO_4^{2-} mg/L**	**TDS (180°)**
Average	499	642	2194	4867	15039	324700
Maximum	509	1408	2525	5060	27687	333600
Minimum	480	307	1960	4641	5071	312000
Standard Deviation	11	383	178	151	7249	6440
PZ-2023-20	**Li mg/L**	**Ca mg/L**	**Mg mg/L**	**K mg/L**	**SO_4^{2-} mg/L**	**TDS (180°)**
One Sample	590	177	2935	5983	41070	356000
PZ_2023_14	**Li mg/L**	**Ca mg/L**	**Mg mg/L**	**K mg/L**	**SO_4^{2-} mg/L**	**TDS (180°)**
Average	559	599	3602	4563	14640	309169
Maximum	694	942	4587	5718	18120	327000
Minimum	287	389	2364	2126	10103	246000
Standard Deviation	94	125	484	816	1806	20561
PZ_2023_24	**Li mg/L**	**Ca mg/L**	**Mg mg/L**	**K mg/L**	**SO_4^{2-} mg/L**	**TDS (180°)**
Average	545	1136	3015	4926	10524	318609
Maximum	739	2425	4580	6307	21202	339000
Minimum	387	470	2161	3963	2673	304000
Standard Deviation	76	587	654	585	5048	8419

PZ-2023-04	Li mg/L	Ca mg/L	Mg mg/L	K mg/L	SO_4^{2-} mg/L	TDS (180°)
Average	462	1096	2799	4165	14814	330500
Maximum	574	2448	3877	5060	33029	352000
Minimum	365	270	2317	2981	2378	318000
Standard Deviation	71	839	483	776	13087	10309
PZ-2023-12 & 12Bis	**Li mg/L**	**Ca mg/L**	**Mg mg/L**	**K mg/L**	**SO_4^{2-} mg/L**	**TDS (180°)**
Average	578	519	3929	4079	15817	318098
Maximum	702	863	4510	5723	19107	333000
Minimum	297	394	2674	2381	8550	268000
Standard Deviation	91	112	425	855	2285	13641
PZ-2023-19	**Li mg/L**	**Ca mg/L**	**Mg mg/L**	**K mg/L**	**SO_4^{2-} mg/L**	**TDS (180°)**
Average	536	553	3635	4186	14529	326611
Maximum	688	1003	4794	5042	17934	336000
Minimum	343	443	1398	3119	7361	313000
Standard Deviation	115	143	1013	531	3235	5337

Figure 56 shows the box plot of de lithium concentration for all the samples collected since 2017. The minimum lithium grade is 169 mg/L, the maximum of 908 mg/L, the arithmetic average is 518 mg/L, and the Standard Deviation of all the samples is 111 mg/L.

Samples with lower concentrations are mostly from shallow wells.

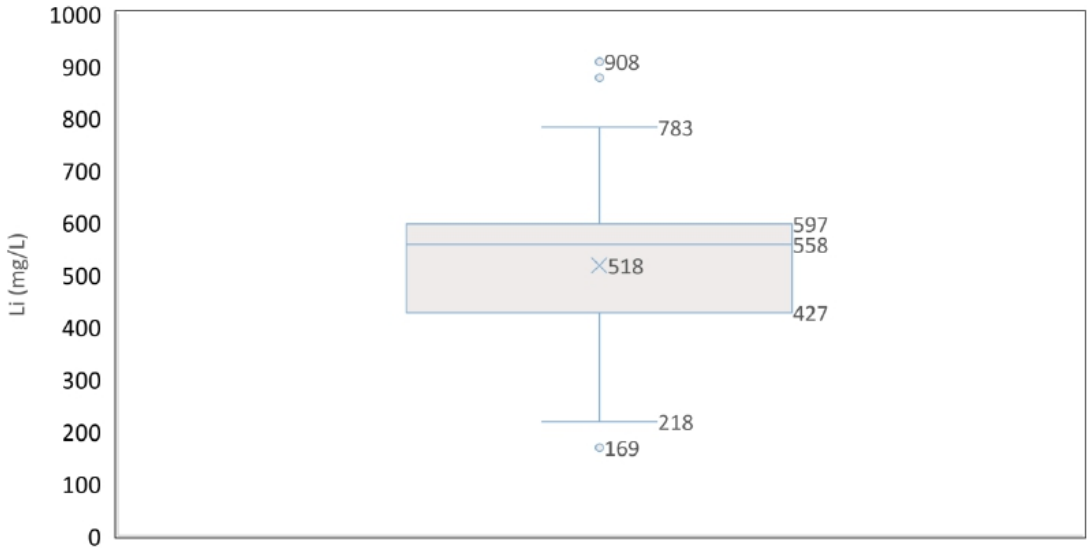

Figure 56: Lithium Concentrations from all the Exploration Samples (Source: Golder, Jan 2025)

To understand the distribution of the lithium grades in the aquifer, the sample dataset was grouped according to its location in the salar: North, Central and South zones.

The Boxplots from Figure 57 to Figure 64 provide a quick visual summary of the variability of values in each zone.

Northern Zone

The graphics of the northern area include the wells PZ-2023-14, PZ-2023-12 and PZ-18-02. The whiskers show anomalies in the lower concentrations as dots below the lower quartile.

In the North of the salar, the statistics show that the Lithium concentration average is similar to the median (Average 569 mg/L and Median 585 mg/L of lithium). The Maximum value of the zone is 702 mg/L.

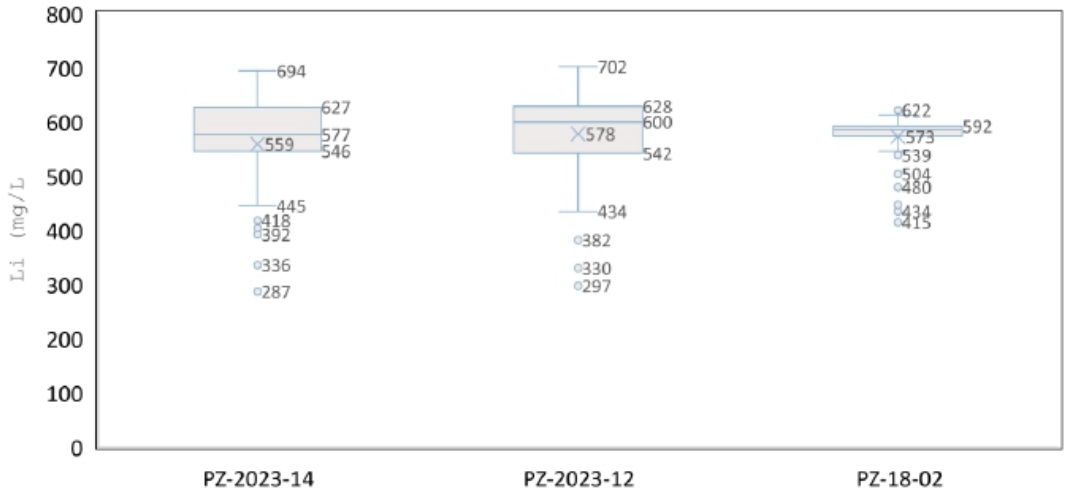

Figure 57: Lithium Concentrations in Northern Drillholes (Source: Golder, Jan 2025)

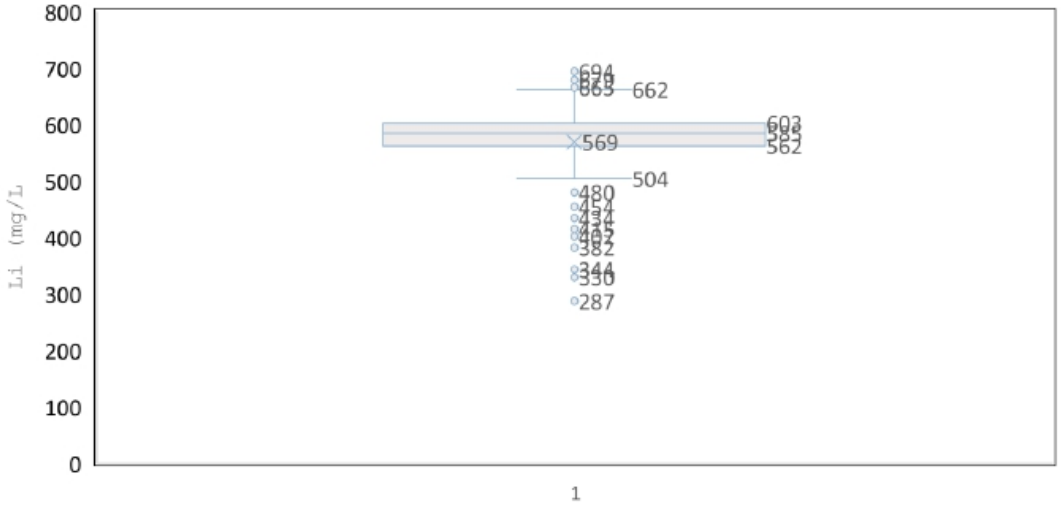

Figure 58: Lithium Concentration in the Northern Zone from Pozuelos (Source: Golder, Jan 2025)

Central Zone

Data from the central zone was divided into two datasets: samples from 2017/2018 and samples from 2023/2024.

The 2017/2018 campaign includes wells SP-2017-02, SP-2017-05, SP-2017-06, SP-2017-07, SP-2017-08, SP-2017-09 and DDH-400.

The lithium concentrations from the shallower drill holes show median values between 242 and 272 mg/L of Lithium. These low values may reflect concentrations of the shallower aquifer. However, SP-2017-02 was drilled to 128 m with a median of 446 mg/L. The well DDH-400 has Lithium grades as high as 522 mg/L, (this well is 322.7 m deep).

The variability of these results could indicate dilution in the upper layers due to the sampling procedures or weather conditions.

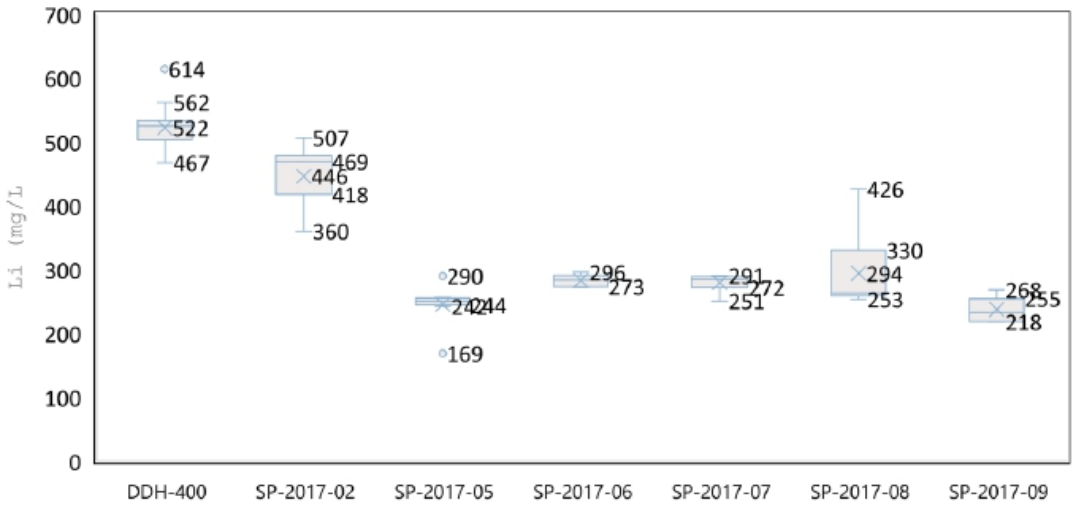

Figure 59: Lithium Concentrations Central Drillholes (2017-2018 exploration) (Source: WSP Golder, Jan 2025)

The 2023-2024 campaign includes Wells PZ-2023-19, PZ-2023-20, PZ-2024-07, PZ-2024-13, PZ-2024-22 and PZ-2024-03.

The well PZ-2023-20 has only one sample.

Data indicates that lithium concentrations increase with depth in the centre of the salar.

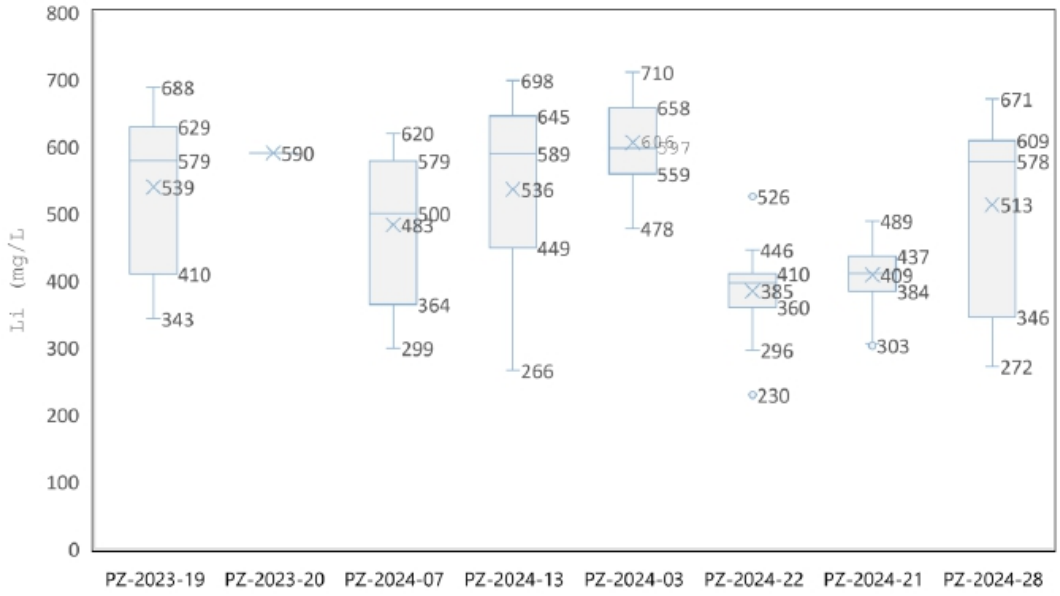

Figure 60: Lithium Concentrations from the Central Drillholes (2023-2024 Exploration) (Source: Golder, Jan 2025)

The median and average of the lithium concentrations show values above 400 and 597 mg/L, except in PZ-2024-22, where the median is 385 and the average is 396 mg/L.

Figure 61 shows the variability of the concentrations for the central zone of the salar.

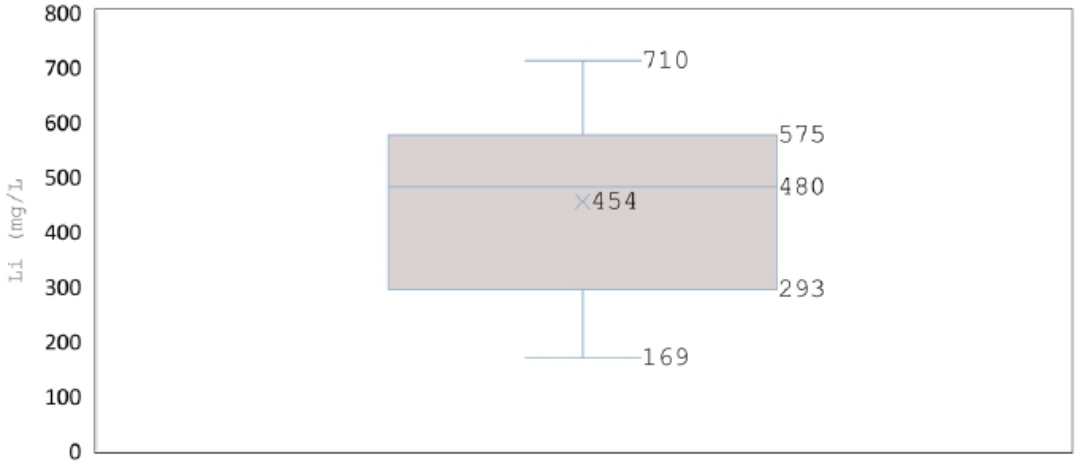

Figure 61: Lithium Concentration in the Central Zone from Pozuelos (Source: Golder, Jan 2025)

Southern Zone

Data from the South zone was also divided into two datasets based on data obtained during the 2017/2018 and 2023/2024 campaigns. The 2017-2018 campaign includes the wells SP-2017-10, SP-2017-11, SP-2017-12, SP-2017-13, SP-2017-14 and SP-2017-15. The dataset was analysed for lithium concentrations, showing a median between 368 and 441 mg/L, a maximum of 576 mg/L and a minimum of 272 mg/L.

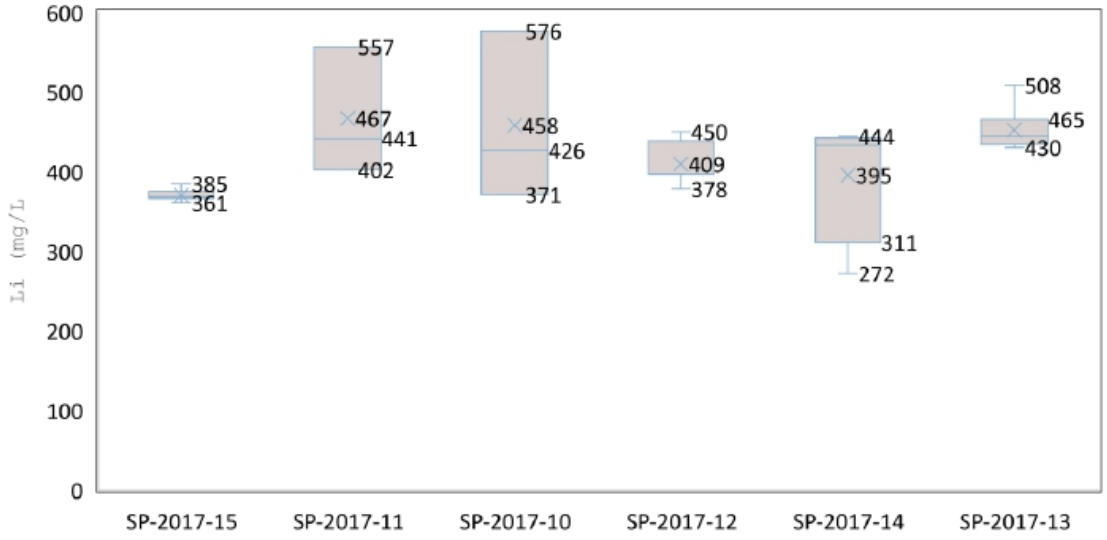

Figure 62: Lithium Concentrations from the Southern Drillholes (2017-2018 Exploration) (Source: WSP Golder, Jan 2025)

The 2023-2024 campaign includes wells PZ-2023-24, PZ-2023-04, and PZ-2023-26. The data show a median of 460 and 586 mg/L of Lithium, a maximum of 908 mg/L, and a minimum of 365 mg/L.

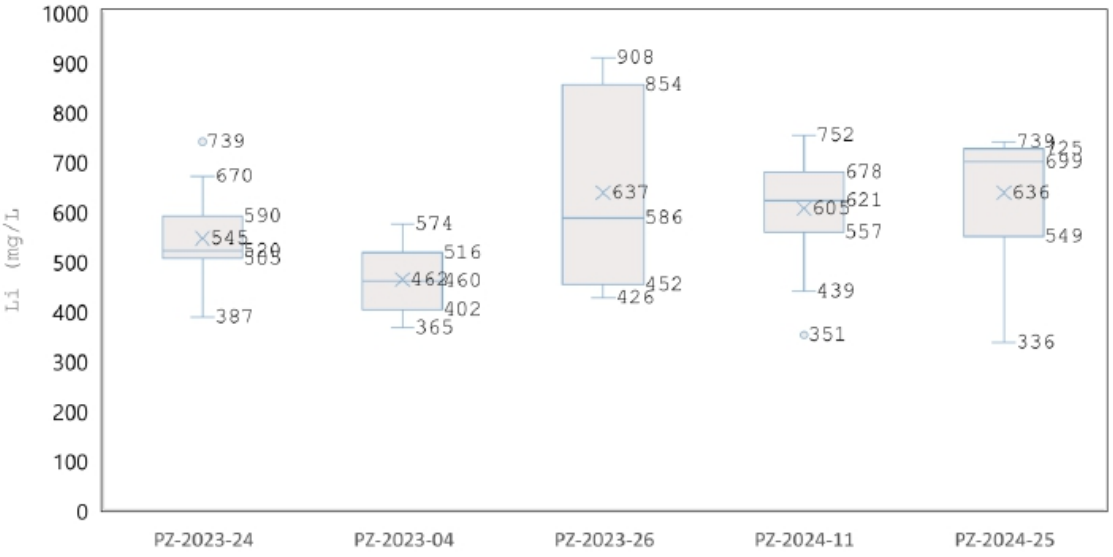

Figure 63: Lithium Concentrations from the Southern Drillholes (2023-2024 Exploration) (Source: WSP Golder, Jan 2025)

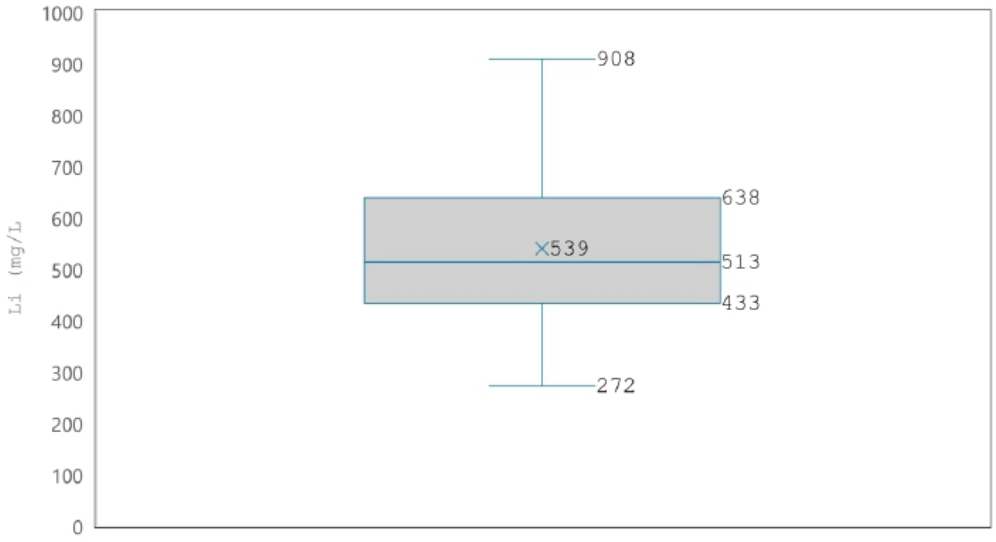

Figure 64: Lithium Concentrations from the Southern Zone from Pozuelos (Source: Golder, Jan 2025)

To verify the distribution of concentrations, the results obtained were grouped in a histogram graphic, divided into seven classes of equal width, to observe the frequency of the lithium concentration in all the datasets.

Figure 65 shows the histogram from the complete dataset. It is a unimodal diagram that includes the mode (546 mg/L), median (561.5 mg/L), and mean (518 mg/L).

The homogeneity of the results provides greater confidence in the concentration used for resource estimation.

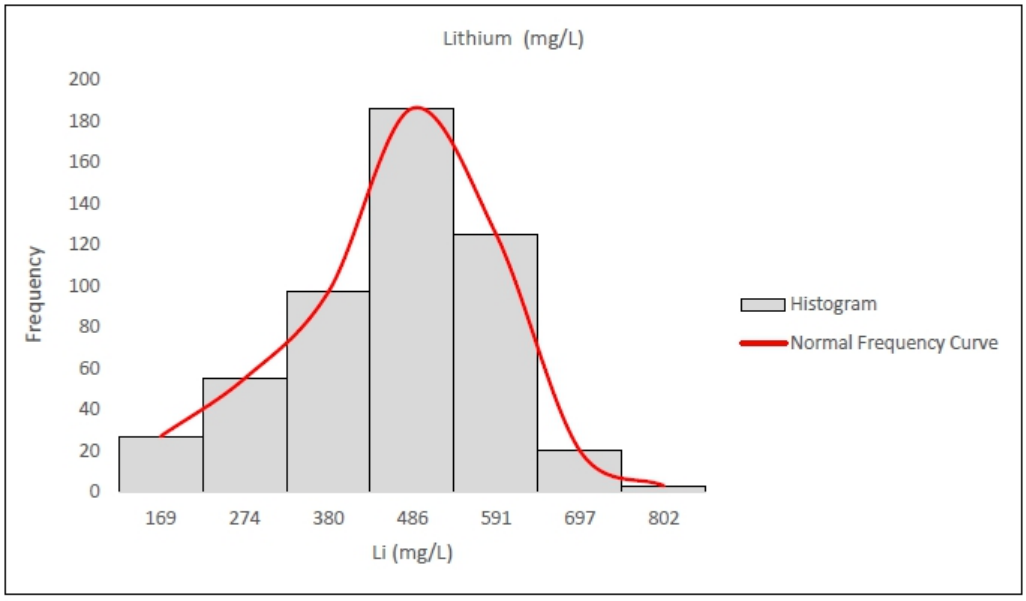

Figure 65: Histogram for Lithium Concentrations of the Complete Dataset of Samples (Source: Golder, Jan 2025)

8.1.2 Drainable Porosity Estimate

The determination of these pore parameters is probably the most challenging aspect of brine resource estimation.

Total porosity (Pt) relates to the volume of pores contained within a unit volume of aquifer material. Except in well-sorted sands, some of the pores are isolated, and only the pores in mutual contact may be drained. This interconnected porosity is known as the effective porosity (Pe). Assuming that the Pe is totally saturated, only part may be drained under gravity during the pumping process. This part of the porosity is known as the specific yield (Sy). A portion of the fluid in the pores is retained as a result of adsorption and capillary forces and is known as specific retention (Sr). The relationship between Sy and Sr depends largely on lithology. In fine-grained sediments Sy << Sr, whereas in coarser-grained sediments Sy >> Sr.

In the Pozuelos project, each operator used different methodologies to estimate the part of the aquifer that may be drained under gravity during the pumping process.

The summary of the efforts in estimating Drainable porosity is listed below:

- **2017-2018**: Core samples from 15 wells drilled in 2017 were sent to D.B. Stephens & Associates (DBSA) in Albuquerque, New Mexico, to determine Relative Brine Release Capacity (RBRC). The results of these tests are analogous to Drainable Porosity.
- **2021:** Neutron log to estimate the Total Porosity (N-Tp) from two wells Li.Pz.RW-11, drilled in the platform of the well PZ-18-02 and Li.Pz.RW-15, drilled in the platform of the well PZ-18-01.
- **2023-2024**: Borehole Magnetic Resonance (BMR) geophysical logging has been received for holes PZ-2024-03, PZ-2023-26, PZ-2023-19, PZ-2023-13 and the production well PZ-2023-16 PW.

Figure 68 shows the location of the boreholes with drainable porosity data.

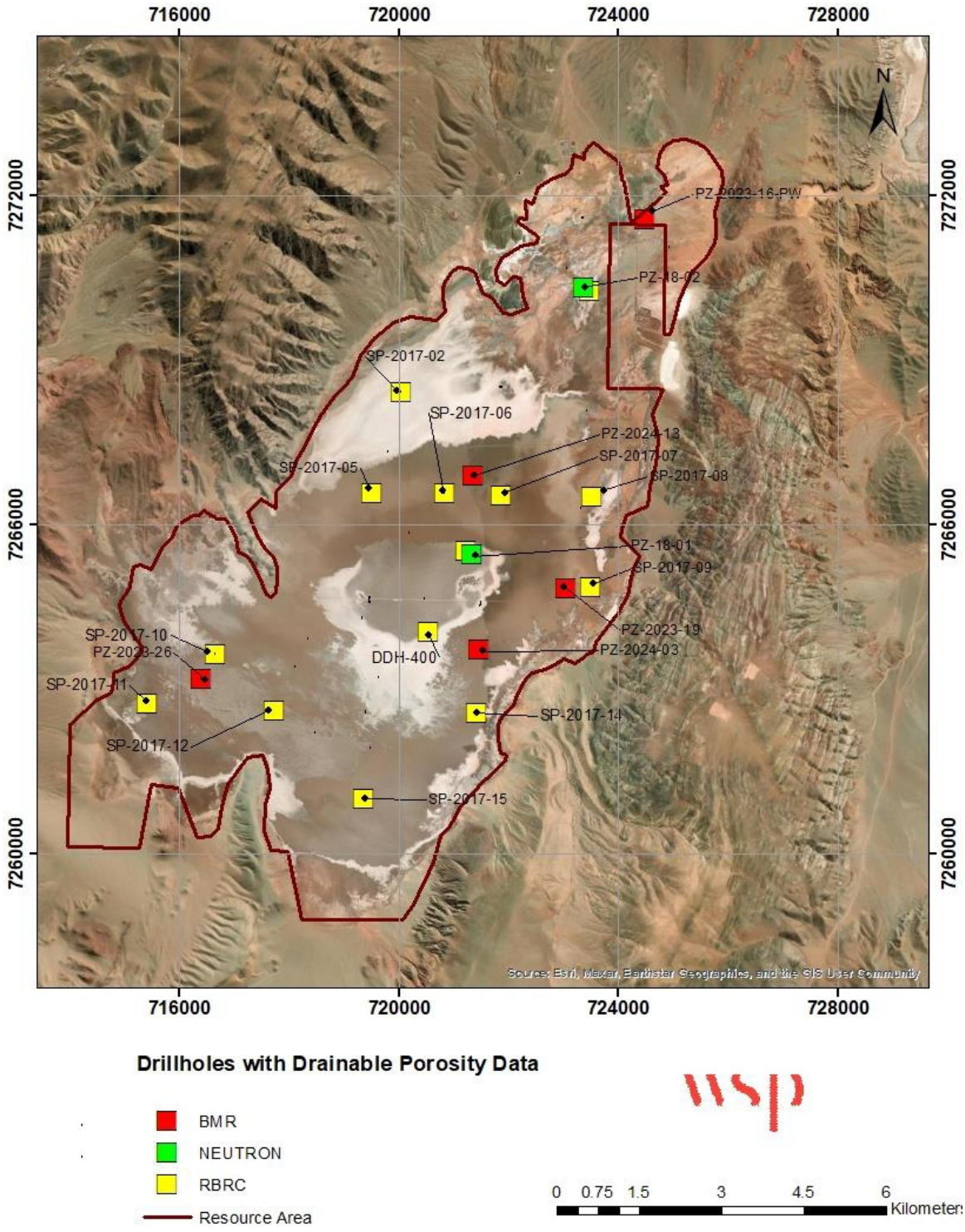

Figure 66: Location of the Wells with Drainable Porosity Data (Source: WSP Golder, Jan 2025)

8.1.3 Core Samples (RBRC)

This method predicts the volume of brine that can readily be extracted from an unstressed geologic sample.

Samples from the site were saturated in the laboratory using a site-specific brine solution. One end of the samples was then attached to a vacuum pump using tubing and a permeable end cap and subjected to a suction of 0.33 bars for 18 to 24 hours. The top end is fitted with a low-flow cap, which allows sufficient drainage while inhibiting continuous atmospheric airflow. The vacuum system permits multiple samples testing simultaneously.

The volumetric moisture (brine) contents of the samples are calculated based on the density of the brine, the sample mass at saturation, and the sample mass at 'vacuum dry'. The difference between the volumetric moisture (brine) content of the saturated sample and the volumetric moisture (brine) content of the 'vacuum dry' sample is the "relative brine release capacity". Data from RBRC for each HSU, from each well is shown in Table 26.

Table 26: Summarizes RBRC Results for Each HSU Unit of the Salar

Hole ID	HSU	RBRC (%, cm^3/cm^3)			# Samples
		Minimum	Maximum	Average	
SP-2017-15	Saline Lake	0.81	13.37	5.47	8
	Sandy Alluvial and/or Colluvial Sediments	-	-	3.84	1
SP-2017-11	Saline Lake	2.62	5.75	3.6	6
SP-2017-10	Saline Lake	2.20	5.46	3.8	4
	Muddy Alluvial and/or Colluvial Sediments	-	-	0.57	1
SP-2017-02	Saline Lake	1.14	5.04	3.53	6
	Muddy Alluvial and/or Colluvial Sediments	2.12	5.31	3.71	2
SP-2017-05	Saline Lake	2.49	9.60	5.23	9
SP-2017-06	Saline Lake	0.36	5.29	3.39	6
SP-2017-07	Saline Lake	1.19	7.98	6.23	7
SP-2017-08	Saline Lake	2.40	4.76	3.93	5
	Muddy Alluvial and/or Colluvial Sediments	1.27	6.19	3.36	3
SP-2017-09	Saline Lake	4.60	14.02	8.3	5
	Mudflat	3.16	16.33	8.3	3
SP-2017-12	Saline Lake	0.8	10.3	4	8
SP-2017-14	Saline Lake	1.5	8	4.81	6
SP-2017-13	Saline Lake	2.55	8.38	5.57	6
PZ-18-01	Saline Lake	2.36	9.38	4.3	7
	Mudflat	0.51	15.31	4.39	14
	Sandy Alluvial and/or Colluvial Sediments	6.71	15.99	11.77	4
DDH-400	Mudflat	0.84	11.99	4.54	10
PZ-18-02	Sandy Alluvial and/or Colluvial Sediments	-	-	2	1
	Muddy Alluvial and/or Colluvial Sediments	1.26	17.66	5.5	8
	Sandy Alluvial and/or Colluvial Sediments	0.79	10.98	4.4	7
	Fractured Aquifer	1.37	4.2	2.83	6

The RBRC results were not used for Resource Estimate because:

- The samples are from the 2017 exploration when the exploration target was shallower. Consequently, the deeper units are not represented,

- Most of the samples are from Halite and Mudflat (77% or 110 samples from a total of 145). Which is limited to the upper units of the salar,
- The average of Sy for the Saline Lake and Mudflat resulted in 5%. This percentage is considered representative and valid, supported by the high density of samples.
- RBRC from the alluvial and colluvial sediments are considered to not characterize enough the HSUs for the lower density of samples,
- It is noted that the RBRC values for the highly fractured, coarse crystalline halite and moderately fractured, porous halite lithologies may be underestimated due to difficulties in obtaining suitable samples. The test method requires samples with reasonable structural competence. Analysis of core photos indicates that RBRC samples within the affected lithologies were generally more competent than the majority of the core within the same overall lithological zone. Thus, the RBRC results may underestimate the true effective porosity of the interval.

8.1.4 Geophysical Hole Logging

Neutron and BMR logs were used to measure porosity and permeability in situ to assist reservoir studies. The data acquisition and processing methodology gives information with a vertical resolution of 1 and 2 cm, respectively, resulting in a continuous log of Sy at depth.

8.1.4.1 BMR Dataset Processing

The Salta-based company, Zelandez, conducted downhole logging in the 2023/2024 exploration. The logging tools used were spectral gamma, resistivity, conductivity, BMR, and a calliper in the wells where the log was performed in an open hole.

The BMR is meant to indicate total porosity; the porewater held immobile by capillary forces within the formation and mobile porewater. The mobile porewater measure is comparable to drainable porosity or specific yield.

The photos of the drilling cores were thoroughly compared against the BMR results at the same depth. According to the visual estimation of porosity, BMR results lower than 1% were considered outliers.

Null (-999) values and Specific Yields greater than 40% and lower than 1% were removed from the data set. The percentage of removed data and the maximum and minimum values are shown in Table 27. (“Uncut” maximum and minimum include outliers, “cut” exclude outliers).

Table 27: Sy Measured with BMR Before and After Processing the Dataset

Drillhole	# Data Points	Sy %	Sy %	# Data Points after removing Outliers	Sy %	Sy %	% Removed
		Minimum (Uncut)	Maximum (Uncut)		Minimum (Cut)	Maximum (Cut)	
PZ-2023-26	9,101	9.14741E-11	38.5	7422	1.0	38.5	18%
PZ-2023-19	41,632	9.45778E-09	47.1	37597	1.0	40.0	10%
PZ-2023-13	15,751	1.11472E-09	70.7	11986	1.0	40.0	24%
PZ-2024-03	18,726	3.11998E-09	31.6	13526	1.0	31.6	28%
PZ-2023-16 PW	17,501	3.17E-03	14.9	11243	1.0	14.9	36%
Total	102,711	-	-	81774	-	-	20%

A possible explanation for the large number of outliers and null values (-999) is that the hole diameter was greater than the investigation radius of the BMR tool. This may explain the higher values up to 70 %. Most of the higher outliers are in the halite, which, due to the solubility, could have been partially dissolved during the drilling process. The lower outliers could be an effect of the cased well or the “mud cake” on the borehole walls since it is impossible to completely clean the well in unstable formations before conducting the geophysical profiles. The dataset from the well PZ-2024-16PW may explain this effect. The uniformity of the data from the Gamma-ray and the resistivity do not indicate any formational change. The specific yield from the BMR shows a quasi-constant value of 3% along the depth of the hole, likely reflecting the Sy of clays or drilling mud. The cutting chips of PZ-2024-16PW show beds of fine and coarse sediments with abundant clay and silt, indicating that the infill in that area of the salar could be interpreted as Muddy Alluvial and Colluvial Sediments. To support that concept, the penetration rates from the well PZ-2023-12BIZ (DDH) were compared with the penetration rate from PZ-2024-16PW (Figure 67). Penetration rates are usually indicative of the consolidation grade of the drilled lithologies.

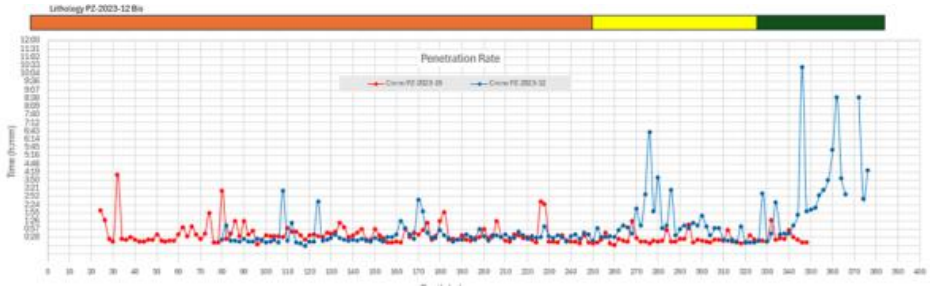

Figure 67: Penetration Rate from PZ-2024-16PW and PZ-2023-12 (Source: Golder, Jan 2025)

The percentages of Sy from each HSU, before and after removing the outliers, are shown in Table 28.

The Sy in the fractured aquifer was discarded because the amount of data is limited, and it is not considered representative.

Table 28: Percentages of Sy Before and After Removing the Outliers

Hole ID	HSU	From (m)	To (m)	Average Sy Uncut (%, m^3/m^3)	Average Sy Cut (%, m^3/m^3)
PZ-2023-26	Saline Lake	0	59	6.42	7.5
PZ-2023-26	Muddy Alluvial and/or Colluvial Sediments	59	206.5	7	7.75
PZ-2023-19	Saline Lake	0	63.5	6.5	7.43
PZ-2023-19	Muddy Alluvial and/or Colluvial Sediments	63.5	288	10.7	10.94
PZ-2023-19	Sandy Alluvial and/or Colluvial Sediments	288	440	9.7	10.39
PZ-2024-13	Saline Lake	0	79.2	7.89	8.76
PZ-2024-13	Mudflat	79.2	234	6.3	7.76
PZ-2024-13	Sandy Alluvial and/or Colluvial Sediments	234	283	5	6
PZ-2024-13	Fractured Aquifer	283	391	2.77	-
PZ-2024-03	Saline Lake	0	75	4.76	5.43
PZ-2024-03	Mudflat	75	132	7.29	7.84

Hole ID	HSU	From (m)	To (m)	Average Sy Uncut (%, m^3/m^3)	Average Sy Cut (%, m^3/m^3)
PZ-2024-03	Sandy Alluvial and/or Colluvial Sediments	132	218	8.04	8.126
PZ-2024-03	Muddy Alluvial and/or Colluvial Sediments	218	309.6	5.33	6.19
PZ-2024-03	Fractured Aquifer	309.6	461	5.47	-

Due to the uncertainties regarding the original data set and the high percentage of outliers, the BMR was not used in the Resource Estimate. Most of the averages tend to be lower than the visual porosity from the cores, and the pumping well results indicate a porous media with higher transmissivity and aquifer elasticity.

Deeper interpretations of the dataset, related to the lithology and calibrations with Sy measured in the laboratory, need to be completed to justify using the BMR in the Resource Estimate.

8.1.4.2 Neutron Downhole Logs

Downhole Neutron logging was run in two production wells located in the north and central area of the salar. Li.Pz.RW-11, drilled in the platform from the DDH well PZ-18-02 and Li.Pz.RW-15, drilled in the platform of the well PZ-18-01.

Litica Resources used these Neutron logs in the 2021/2022 resource estimate. The Neutron measures the total porosity (N-Pt) of the formation. Porosity is highly dependent on lithology. Pt is much higher in finer-grained sediments, whereas the reverse is for Sy due to the high *Sr* in these sediments. The lithology from the Pozuelos aquifer is highly variable at depth, containing halite, sand, and silt-clay mixes, spanning the full spectrum of possibilities.

The raw data from the N-Pt was converted to Sy by Pluspetrol geophysicists in 2021 (Table PHIE from the Leapfrog model)

The QPs interpolated the Sy data points in the Leapfrog model to estimate the mean Sy for each unit.

The Sy from the Mudflat resulted higher than expected for a mix of silts and clays. The QPs used the graphic form Figure 68 to interpolate the N-Pt to obtain an acceptable value of Sy for this HSU. This procedure is considered adequate and is supported by the Sy of this unit measured in lab (RBRC).

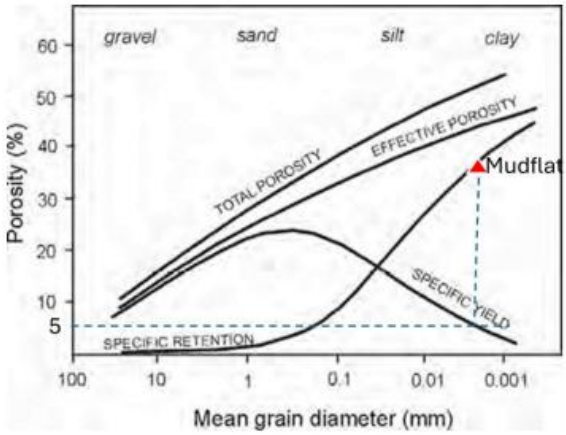

Figure 68: Porosity Relationships for Unconsolidated Material (Source: Johnson 1967)

The averages of the Specific Yield estimated from Neutron downhole logging are shown in Table 29.

Table 29: Average of Specific Yield Estimated from the N-Pt

Hole ID	HGU	PT % (Neutron Borehole Logging)				Sy (%)
		Average	Minimum	Maximum	Median	
Li.Pz.RW-15	Mudflat	37	0.00650	60	38	5
Li.Pz.RW-15	Saline Lake	5	0	36	2	5
Li.Pz.RW-11	Sandy Alluvial and/or Colluvial Sediments	22	0	45	25	16
Li.Pz.RW-11	Muddy Alluvial and/or Colluvial Sediments	21	0	38	20	17
Li.Pz.RW-11	Fractured Aquifer	14	0	35	15	-

8.1.4.3 Sy of the Fractured Aquifer

The Fractured Aquifer Unit is considered to have double (or dual) porosity where the groundwater flows through the matrix as a primary porous system with low hydraulic conductivity and high storage capacity and the fractures as a secondary porous system with high hydraulic conductivity and low storage capacity.

Golder applied an Sy of 10 per cent to the Fractured Aquifer based on the knowledge of these types of lithologies. The Neutron logging from the well does not have enough data to be reliable. Photos of the fractured aquifer in different areas of the salar are shown in Figure 69.

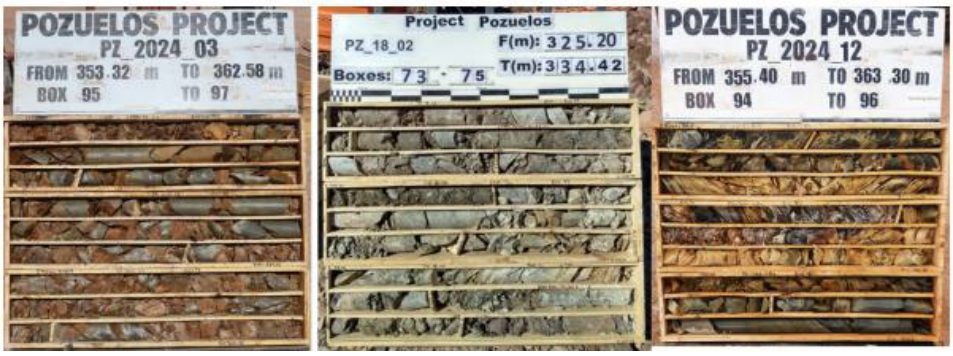

Figure 69: Photographs of the Fractured Aquifer (Source: Golder, Jan 2025)

The average of the drainable porosity or each HSU using BMR, Neutron and RBRC are shown in Table 30.

Table 30: Drainable Porosities Estimated for Each HSU Using RBRC, Neutron Logging and BMR

HSU	BMR Sy (%, m^3/m^3)	Neutron Logging Sy (%, m^3/m^3)	RBRC Sy (%, m^3/m^3)
Saline Lake	7	5	5
Mudflat	8	5	5
Muddy Alluvial and/or Colluvial sediments	8.3	17	5
Sandy Alluvial and/or Colluvial Sediments	8.2	16	6
Fractured Aquifer	10*	10*	-

**Visual estimation. Further work is required to confirm this value.*

The QPs considers that the porosity from the neutron logging is more representative of the lithological because the dataset has less bias than the BMR, and the RBRC is limited to the upper units of the HGU.

Further work needs to be carried out by testing individually the Fractured Aquifer through production tests and a monitoring well to confirm the Sy value.

8.1.5 Analytical Quality Assurance and Quality Control (“QA/QC”)

Litica and Lithea geologists conducted a QA/QC program to monitor the accuracy, precision, and potential contamination of the entire sampling and analytical program. Accuracy was monitored by inserting a reference sample (a well-known concentrated solution). The precision of the sampling and analytical process was monitored by submitting blind field duplicates, and contamination was monitored by inserting stable field blanks.

8.1.5.1 Samples Governance of the Drillholes

A total of 529 brine samples, including a QA/QC program, were sent to the laboratories ASI in Jujuy province, SGS in Salta province, and the site laboratory in Pozuelos.

Details of the samples from 2017-2024, including the QA/QC are in Table 31.

Table 31: Number of Samples (including QA/QC)

Sample Type	Number
Brine Samples	429
Reference Samples	29
Duplicates	30
Blanks	41
Total Samples	529
Total samples for QA/QC	100
Percentage of QA/QC samples	19%

This report only analysed the 2023/2024 performance of the samples inserted for QA/QC purposes. The QA/QC from the samples 2017/2028 were validated and explained in NI 43-101 Pozuelos Technical Report (Hains 2018).

8.1.5.2 Reference Samples Performance

Figure 70 to Figure 72 summarise the performance of the reference samples used by Lithea in the 2023/2024 drilling program. The campaign inserted three Reference Samples: TDS B 3002, TDS D 3001, and TDS D 3004.

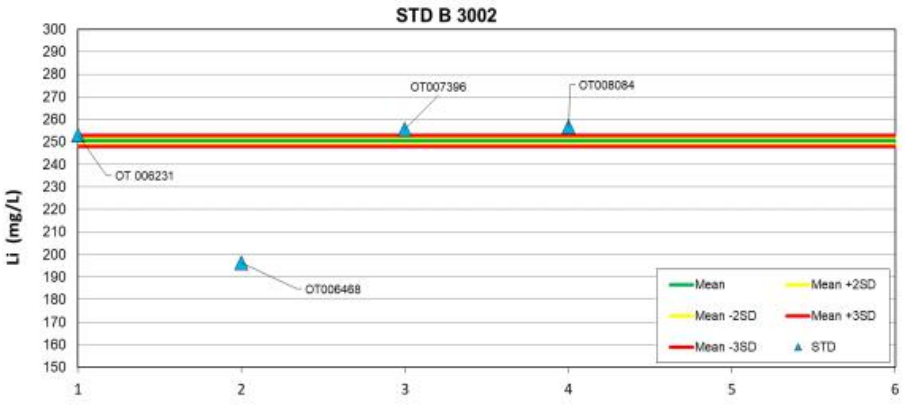

Figure 70: Performance of the Reference Sample TDS B 3002 (Source: Golder, Jan 2025)

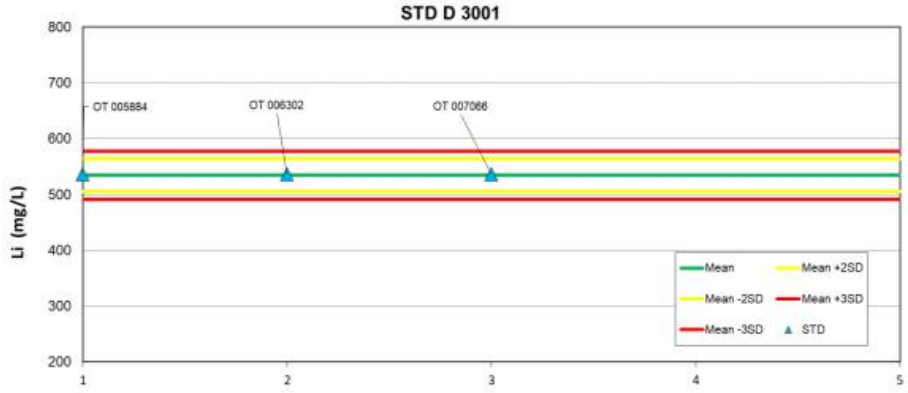

Figure 71: Performance of the Reference Sample TDS D 3001 (Source: Golder, Jan 2025)

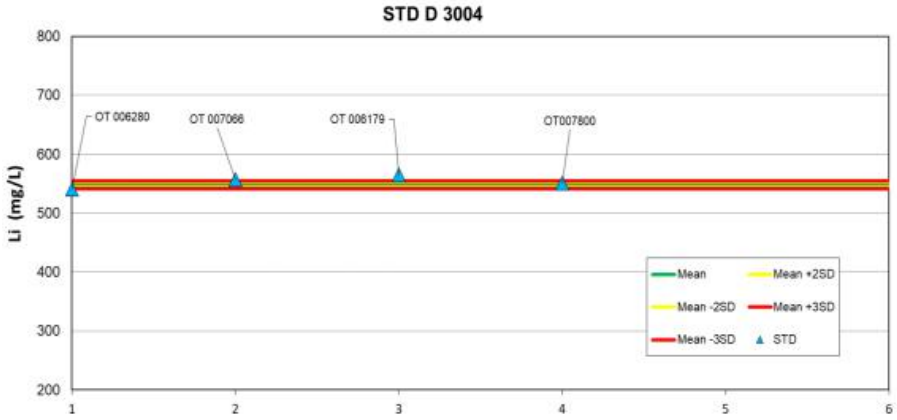

Figure 72: Performance of the Reference Sample TDS D 3004 (Source: Golder, Jan 2025)

It is the QPs' opinion that the results from the reference samples from 2023/2024 do not show a significant analytical drift over the mainstream of samples.

8.1.5.3 Duplicate Performance

Lithium values for the field duplicate samples were plotted in Figure 73 against their original counterparts.

Most samples plot close to their respective 1:1 line. The results show good repetitively. The overall precision of the data is considered acceptable.

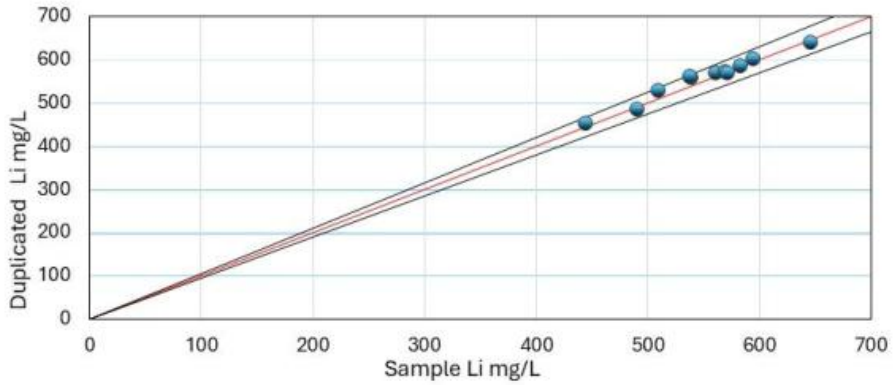

Figure 73: Duplicate Vs Original Samples (Source: Golder, Jan 2025)

8.1.5.4 Blank Field Performance

Lithium results for the field blank samples are shown in Figure 74. The results assess cross-contamination in the laboratory and the field (for example, whether the instrumentation was cleaned sufficiently between analysis of samples). Lithium was not detected in any blank sample. Overall, field blank performance is considered acceptable.

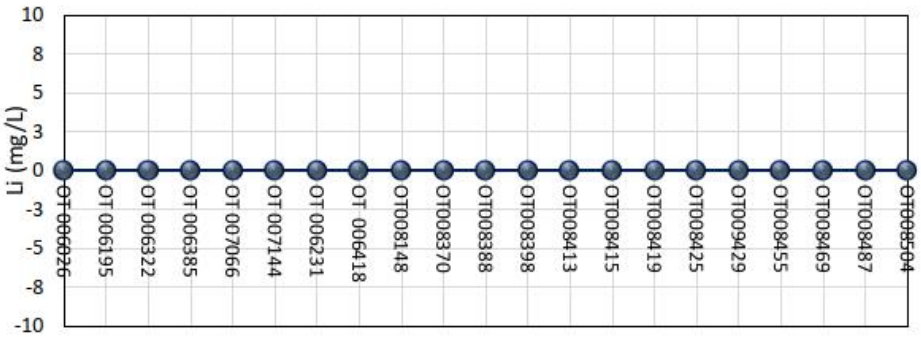

Figure 74: Blanks Performance (Source: Golder, Jan 2025)

Differences between original and duplicate samples and results for standards and blanks are considered within the acceptable range.

The QA/QC procedures and dataset indicate that the chemical analysis of the brine samples does not show significant or systematic bias and is acceptable for use in resource estimate.

8.2 Pastos Grandes

8.2.1 Drainable Porosity

8.2.1.1 Millennial Drainable Porosity Analysis (2016-2019)

Samples were obtained from 'undisturbed' core during the 2016-2019 Millennial drilling programs and analyzed for drainable porosity by Core Laboratories-Petroleum Services in Houston, Texas ("Corelabs"). In addition, rotary drill cuttings were sent to Geosystems Analysis in Tucson, Arizona ("GSA") for repacking, triaxial testing, and drainable porosity analysis.

Both Corelabs and GSA offer advanced petrophysical and geological analysis and interpretation services for core samples. These laboratories operate in compliance with ISO 9001:2008 Certification ensuring that processes and procedures adhere to internationally recognized quality standards. The analytical procedures for determining drainable porosity for each laboratory are further described below.

Corelab drainable porosity analysis is based on centrifuge methodology and involves the following:

- 38 mm (1.5-inch) diameter cylindrical plugs were cut from the sample material.
- Samples were frozen with dry ice to maintain their integrity, if required.
- Sample weight and thickness were measured.
- The plugs were encapsulated in Teflon and nickel foil as required, and nickel screens were placed on the ends of the plugs. The encapsulated samples were then weighed.
- Bulk density was calculated as: (Mass of plug before encapsulation) / (Calliper bulk volume).
- The plugs were placed in brine and saturated under vacuum to ensure full saturation. Corelabs utilized a standard sodium chloride brine with a NaCl concentration of 244,000 ppm with a density of 1.184 gm/cm3.
- The weight of the saturated cores was recorded.
- The samples were desaturated in a high-speed centrifuge for 4 hours. Spin rates were calculated to provide a drainage pressure of 1 pound per square inch (psi) for poorly cemented or loose sands and 5 psi for clay and halite.
- The drainage was collected, and the volume was recorded. The effluent was saved for possible analysis. However, it should be noted that the fluid collected from these cores may not be representative of in situ brine if re-saturation with NaCl was required.
- Plugs were removed from the centrifuge and weight was recorded. Drained fluid volume was calculated as: (saturated plug weight - drained plug weight) /1.184. Drainable porosity was calculated as (Drained fluid volume) / (Calliper bulk volume).
- Total porosity was calculated after drying the samples for 5 days at 115.6 degrees Celsius to record dry weight.
- All weight loss is assumed to be water lost from pore space where volume of water loss is calculated as: ((Drained plug weight) – (Oven-dried plug weight))/ (Water density of 1 g/cc).
- Total porosity is calculated as ((Drained fluid volume) + (Oven drying fluid loss))/ (Calliper bulk volume).

GSA drainable porosity analysis procedures for repacked sediment samples include the following steps:

- All loose and sandy samples were packed into test cells with moderate effort without prior knowledge of bulk density or other consolidation tests. Additional repacking was performed on some samples with minimum and maximum effort to evaluate the effectiveness and variation of hand-packing at higher and lower densities. Bulk densities approximately 0.1 g/cm^3 lower and higher than the initial density was achieved, respectively.

- The sandy material was packed into a stainless-steel ring in several small lifts. The weight and packing height of the first lift were used to guide the subsequent lifts to ensure consistent density packing. Scales were used to track the equipment, cells, and sample weights throughout the process, and the final packed and assembled core weight was recorded.

- Plastic air tubing, approximately 6 inches in length, was inserted into the top of each core to monitor saturation and prevent brine solution spillage. The cores were then assembled and saturated slowly from the bottom up using a provided brine. A combination of gravity feed and vacuum suction was used to achieve the target saturation. If the target saturation could not be reached using gravity feed alone, vacuum suction was applied. The saturation process lasted for up to 24 hours. Once fully saturated, the cores were closed at the bottom with a hose clamp to prevent brine solution loss and disconnect from the saturation setup.

- Each cell assembly underwent three pressure steps after being transferred to a test rack. The first step, at 0 mbar pressure, lasted for 24 hours and was applied to remove excess saturation solution. To approximate the release of brine solution at 120 mbar and 1/3 bar of the brine solution, two sequential pressure steps were used at 120 mbar and 1/3 bar, respectively. The 120-mbar pressure step was maintained for 2 days, and the 1/3 bar was continued for another 2 to 4 days. Weight measurements were taken twice a day to determine the loss of brine solution over time. After the final step the cores were disassembled and samples were oven dried to determine total porosity following the procedure described in MOSA, 2002, Part 4 Ch. 2, 2.3.2.1.

- To estimate the brine solution release volumes at the 120 millibar and 1/3 bar pressure steps, the difference was calculated between the measured total porosity and the moisture retained after the pressure plate measurements as outlined in MOSA (2002), Part 4, Chapter 3, Section 3.3.3.5. The solution's release volume obtained at 1/3 bar was regarded as an approximation of the maximum solution drainage that could occur under gravity or pumping conditions and hence was used to determine the specific yield.

After completing the tests, the estimated particle density and weight data from core samples at various pressure steps were entered into a spreadsheet. The spreadsheet was programmed to automatically calculate the salt weight left in the sample after drying, estimated porosity, and water content change. Furthermore, particle density was optimized during data processing by utilizing all prior test measurements and using a solver in Microsoft Excel. The laboratory report presented the calculated particle density for each sample.

8.2.1.2 AMSA Drainable Porosity Samples (2021-2022)

36 samples from the AMSA 2021-2022 drilling program were sent to GSA for drainable porosity analysis. All samples were tested using the 'Rapid Brine Release' method (Yao et al., 2018) to measure specific yield (Sy) and total porosity (Pt). Brine released drainable porosity was measured at 120 mbar and 333 mbar of pressure, where:

- Brine release at 120 mbar represents drainable porosity from sand dominated sediments and rapid brine release from macropores (Nwankwo et al., 1984).

- Brine release at 333 mbar represents the Sy for intermediate to finer texture sediments (Cassel and Nielsen, 1986).

Brine release values at 120 mbar were provided for reference and 333 mbar values were presented as the estimated Sy (drainable porosity). A subset of paired samples representative of the range in lithology types was selected by AW and GSA for testing using the Relative Brine Release Capacity (RBRC, Stormont et. al., 2011) method by Daniel B. Stephens & Associates, Inc. in Albuquerque, NM (DBSA). The goals of the test were to provide Sy and Pt values for each sample, summary statistics of Sy and Pt by lithological group, and to compare the Sy and Pt values derived for paired core samples using the RBR and RBRC methods.

Table 32 lists the physical properties analyses carried out by GSA. In addition to the RBR testing, physical property tests were run by GSA to assist in lithologic characterization and interpretation of results including bulk density testing (ASTM D2937-17e2) on all RBR samples.

Table 32: Summary of Laboratory Tests Conducted by GSA

Test Type	Sample Type and Number	Test Method	Testing Laboratory	Standard
Physical	36 core samples	Bulk density	GSA Laboratory (Tucson, AZ)	ASTM D2937-17e2
	36 core samples	Estimated Particle Density	GSA Laboratory (Tucson, AZ)	MOSA Part 4 Ch. 2, 2.2
Hydraulic	5 core samples	Relative Brine Release Capacity (RBRC)	DBS&A (Albuquerque, NM)	Stormont et. al., 2011
	36 core samples	Estimated Total Porosity	GSA Laboratory (Tucson, AZ)	MOSA Part 4 Ch. 2, 2.3.2.1
		Estimated Field Water Capacity		MOSA Part 4 Ch. 3, 3.3.3.2
		Rapid Brine Release (RBR)		Modified ASTM D6836-16
				MOSA Part 4 Ch. 3, 3.3.3.5

Three packing methods were used to prepare RBR core samples:

a) Stainless steel rings were pushed into intact sediment cores to preserve the structure and retain the original bulk density and porosity distribution in the sample.

b) Sediment cores with loose sediment and/or disturbed samples were extruded, and voids were filled in using moderate packing effort to eliminate voids in the test samples.

c) Most solid halite and/or rock cores were cut with a rock saw to fit GSA's RBR test cells and then fit into a 6.35 cm diameter ring and sealed as discussed below.

RBR test cells were prepared by placing a pre-wetted micro-pore membrane (rated 1200 mbar air entry value) into the bottom PVC cap. This membrane maintains a permeable saturated bottom boundary for solution flow and prevents air entry under the target air pressures applied during RBR testing. The PVC caps contain gaskets to create an air-tight test cell that maintains constant air pressure and allows continuous solution outflow through the membrane.

The RBR method is based on the moisture retention characteristic method using the Tempe cell design (Modified ASTM D6836-16), whereby Sy is determined by applying pressures equivalent to gravity drainage to the Test Cell and measuring the amount of brine solution released. Pt is also measured in the RBR method, and is equal to the sum of Sy and Sr.

Each saturated RBR Test Cell was transferred to a test rack for the pressure extraction procedure where no pressure was applied for one day to remove any excess brine solution due to core over-saturation. Two sequential pressure steps were used to approximate brine solution release at 120 mbar and 333 mbar of matric potential (MOSA Part 4 Ch. 3, 3.3.3.2).

The 120-mbar pressure step was maintained for at least two days, and the 333-mbar pressure step was continued for another two to four days. Core assemblies were weighed prior to saturation, after saturation, and then two times daily determine brine solution loss over time.

All samples were oven dried for three days at 60°C and one day at 105°C after the final step to determine the specific retention (Sr), dry bulk density, and Pt (MOSA Part 4 Ch. 2, 2.3.2.1), where Sr is the volume of water retained by the sample under 333 mbar soil water potential. This drying approach allowed for quantification of the amount of moisture lost due to crystalline water present in gypsum.

8.2.1.3 LAR Drainable Porosity Samples (2023)

During 2023 LAR drilling campaign (boreholes PGMW23-23 and PGMW23-24) 43 ‘undisturbed’ core samples were collected and sent to GSA for drainable porosity analysis. All samples were tested using the ‘Rapid Brine Release’ method to measure specific yield (Sy) and total porosity (Pt). Brine release drainable porosity was measured at 120 mbar of pressure as described in previous section.

8.2.2 Brine Samples

Depth-specific brine samples were collected during core and rotary drilling by packer-system, bailing, or drive- point sampling. Bulk (compound) brine samples were obtained during pumping tests on selected exploration wells.

- Depth-specific packer sampling was the primary method used to collect brine samples during the drilling programs for Phase II and III (2016-2020). Most samples were obtained during drilling, although some were also taken after drilling had concluded. Samples were considered acceptable and representative of the depth interval only if they showed no, or minimal traces of drilling mud. The intervals were typically 3 m long and determined by the site geologist after inspecting drill cores or at predetermined depths. However, the interval length may vary depending on the specific circumstances of a given hole or interval, such as borehole stability. To ensure accurate sampling, intervals were flushed out multiple times before collecting the actual sample. The flushed brine was then collected in a barrel, and the time taken to fill the barrel was recorded.

- Drive-point sampling: five brine samples were collected using this method where a drive-point was installed onto BT-sized drill rods after removing the core barrel. The drive-point was then lowered past the drill bit with the help of a drop hammer, and an impermeable diaphragm was used to prevent filling of the drill rods during the descent. Once the desired depth was reached, an electric water level sounder was used to confirm that the interior was dry before perforating the diaphragm using a weighted pin lowered with the wireline. This piercing allowed the brine to flow into the drive point and fill the BT rods and collect the samples with the use of a bailer.

- Bailing: the borehole was purged by bailing up to three well volumes of brine from the drill casing as calculated from the water level measurement, prior to collecting the final brine sample from the bottom of the hole. The final brine sample was discharged from the bailer into a 20-liter clean bucket from which one-liter sample bottles were rinsed and filled with brine. Each bottle was taped and marked with the borehole number and depth interval. A small sub-sample from the bucket was used to measure field parameters (density, electric conductivity, pH and temperature) at the wellhead.

- Samples from pumping tests: This method involved collecting samples directly from the discharge pipe at regular intervals during pumping tests. Temperature and density were recorded on internal field sheets.

Regardless of the sampling method, samples were collected in 20-liter containers that were washed with distilled water and rinsed with brine several times prior to filling. The temperature and density were recorded before filling 1-liter sample bottles which were also flushed with brine from the 20-liter container. The sample bottles were then sealed with a secure screw top to prevent leakage and labelled clearly with their identification number. Samples did not undergo any further preparation before being shipped to their respective laboratories.

After the sampling process the site geologist would retain possession of the brine samples until they were delivered to the office for shipment to the assay laboratory. Once at the office, duplicates, blanks, and standards were inserted into the assay batches before being sent to the laboratory. Prior to shipment all samples were kept under controlled temperature conditions.

The chemical analysis of brine was conducted by two reputable laboratories: SGS Argentina S.A and Norlab S.R.L, the later partnered with Alex Stewart Assayers (ASA) in 'ASANOA'. The mentioned laboratories have extensive experience analyzing lithium-bearing brine and hold accreditation to ISO 9001 standards and follow the ISO 17025 guidelines.

For the primary constituents of interest, including boron, calcium, potassium, lithium, and magnesium, ASANOA and SGS utilized Inductively Coupled Plasma Analysis (ICP) as the analytical technique, with samples diluted 100:1 prior to analysis. A summary of the analytical methods employed by each laboratory for each physicochemical parameter and analyte is shown in Table 33.

Table 33: Analytical Methods Used by ASANOA and SGS for Brine Assays

Analysis	ASA Code	ASA Method	SGS Code	SGS Method
Physicochemical Parameters				
Alkalinity	LMFQ167	Volumetric	SM 2320B	Titration
Conductivity	LMFQ01	Potentiometric	SM 2510 B	Resistor Network
Density	LMFQ19	Pycnometer	ASTM D4052-16	Digital Density Meter
Hardness ($CaCO_3$)	LMFQ13	Volumetric	SM 2320B	Titration
PH	LMC128	Potentiometric	SM 4500 H B	Potentiometric
TDS	LMFQ08	Gravimetric	SM 2540C	Gravimetric
Inorganic Parameters				
Chlorides (Cl)	LMC101	Argentometric	SGS.ME.108	Ion Chromatography
Sulphates (SO_4)	LMC107	Gravimetric	SGS.ME.108	Ion Chromatography
Dissolved Metals				
Barium (Ba)	LMMT03	ICP	SGS.ME.113	ICP
Boron (B)	LMMT03	ICP	SGS.ME.113	ICP
Calcium (Ca)	LMMT03	ICP	SGS.ME.113	ICP

Analysis	ASA Code	ASA Method	SGS Code	SGS Method
Iron (Fe)	LMMT03	ICP	SGS.ME.113	ICP
Lithium (Li)	LMMT03	ICP	SGS.ME.113	ICP
Magnesium (Mg)	LMMT03	ICP	SGS.ME.113	ICP
Manganese (Mn)	LMMT03	ICP	SGS.ME.113	ICP
Potassium (K)	LMMT03	ICP	SGS.ME.113	ICP
Sodium (Na)	LMMT03	ICP	SGS.ME.113	ICP
Strontium (Sr)	LMMT03	ICP	SGS.ME.113	ICP

8.2.3 Drainable Porosity QA/QC

Five duplicate samples were sent to DBSA to serve as check samples to test for accuracy within the drainable porosity analysis. Summary statistics for paired samples by GSA lithologic category for Pt and Sy are provided in Table 34 and Table 35 respectively. QAQC testing was run on subsamples from the same core, but not on identical samples. Minor differences in material type (sand/silt/clay content) and core physical structure (bulk density, degree of cementation, rock content, macropore content) may result in discrepancies between laboratory measured values. Correlations between GSA and external laboratory measured values of Pt and Sy are provided in Figure 75.

Variations can likely be attributed to sample heterogeneity within cores which result in subsamples with slightly to significantly different material properties, and differences in laboratory methods such as testing duration. The Sy values measured by GSA were often considerably higher than the Sy values measured by DBSA, particularly for the 333 mbar RBR measurement (Figure 75). Differences were most pronounced for halite samples due to lithological variability within the group (one crystalline sample with large crystals and one massive to crystalline sample with very scarce matrix). In the absence of sample heterogeneity, differences are likely attributable to testing equilibration time and testing methods. DBSA's RBRC method only applied 333 mbar of equivalent pressure for 24 hours and did not use filter paper to prevent air moving through samples, whereas GSA's RBR testing was run at 120 mb for two days and then 333 mbar for two to four days no air was allowed to move through samples. Therefore, the lower Sy values reported by DBSA may be due to the samples not reaching equilibrium over the testing period. This may be most pronounced in materials with a greater predominance of macropores such as sands. It should be noted that Sy values measured at 120 mbar were generally in better agreement with DBSA's measured Sy values for all sediment lithological groups (Table 35 and Figure 75).

Specific gravity was higher for the RBR DD-01 451-451,2 sample (SG=2.29) compared to the RBRC sample (SG=2.13). Comparison of average values by lithological group was also limited due to small sample number. Average Pt values measured using the RBRC method (DBSA) were 7% lower for the clastic material group and 129% lower for the halite group. Average Pt values were considerably higher for the clastic group (0.24), with the halite group having a mean Pt value of 0.02.

There was general agreement between the total porosity data (R2=0.85). Correlation was slightly lower for the specific yield data (R2=0.80). The slope of the line was relatively high, indicating that GSA Sy values were approximately 35% higher than those reported by DBSA. The adjusted correlation coefficient between RBRC Sy and the drainable porosity at 120 mbar was R2=0.80.

All the samples tested for Sy fell below the 1:1 line indicating that GSA measured Sy values were typically higher than DBSA measured Sy values. In contrast, while three Pt points were scattered below the 1:1 line, two clastic material samples were plotted on the 1:1 line meaning the measured Pt values were similar for both laboratories.

Figure 75 compare Pt, Sy, and GSA´s drainable porosity (at 120 mbar) versus DBSA´s Sy (at 333 mbar) respectively, for the 5 check samples. The lithology classification of the plotted data is indicated by color, with green representing clastic material and purple representing halite. The central blue line represents the 1:1 ratio while the two adjacent blue lines indicate the acceptable 33% threshold. The graphs reveal that there is acceptable variation between the laboratories for samples in the clastic material classification, but unacceptable variation for samples in the halite classification.

Table 34: Total Porosity Results for Paired Samples Using GSA Lithologic Classification

Total Porosity Statistics	Clastic material		Halite	
	RBR	RBRC	RBR	RBRC
N	3		2	
Avg	0.26	0.24	0.11	0.02
StdDev	0.02	0.02	0.07	0.02
Average Relative Percent Difference	7%		129%	

Table 35: Specific Yield Results for Paired Samples Using GSA Lithological Classification

Specific Yield Statistics	Clastic material			Halite		
	RBR @ 120	RBR @ 333	RBRC	RBR @ 120	RBR @ 333	RBRC
N	3			2		
Avg	0.10	0.14	0.10	0.02	0.07	0.00
StdDev	0.05	0.04	0.03	0.00	0.01	0.00
Average Relative Percent Difference	2% (120 mbar), 29% (333 mbar)			123% (120 mbar), 177% (333 mbar)		

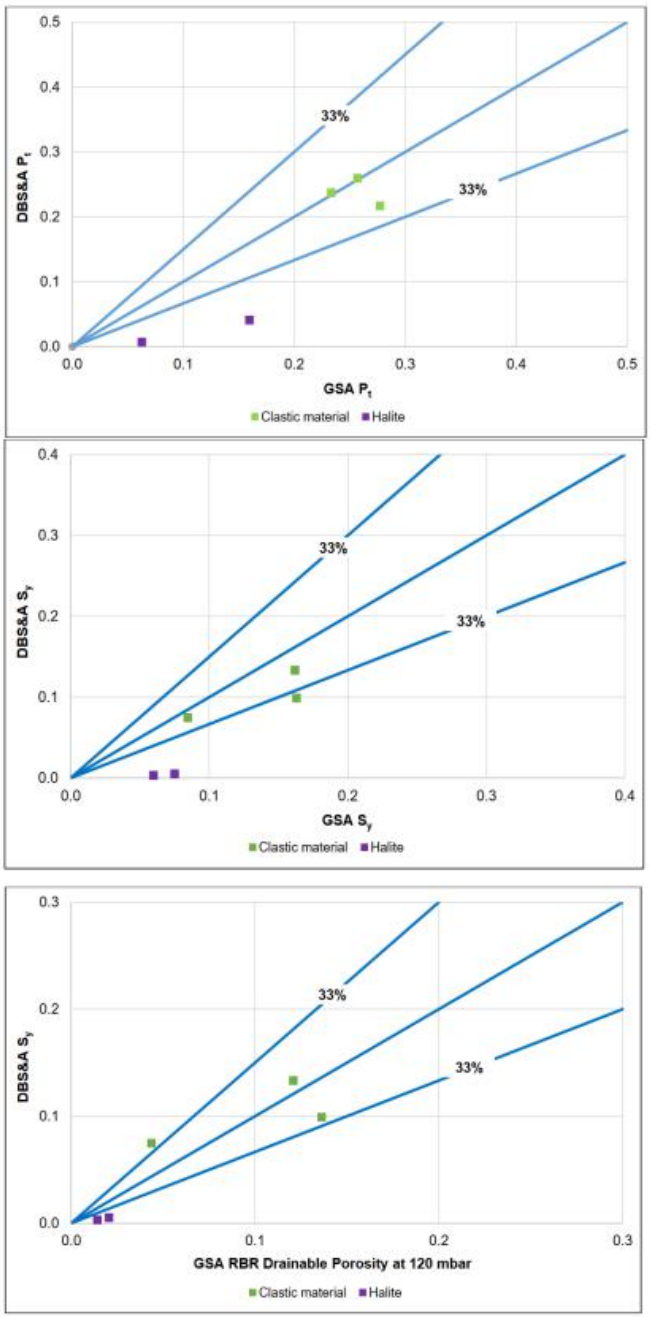

Figure 75: Pt (top), Sy (middle), Sy and RBR (bottom) Comparison for Check Samples DBSA-GSA (Source: AW, Dec 2024)

8.2.4 Brine QA/QC

This section outlines the quality assurance and quality control (QA/QC) procedures implemented for laboratory chemistry analysis of brine samples obtained during drilling and pumping activities. Each QA/QC program involved randomly inserting duplicates, check samples, field blank, and standards, with the following percentage of quality control samples for each party:

- 21% for Millennial
- 21% for AMSA
- 17% for Centaur and
- 25% for Ganfeng

The purpose of each QA/QC program was to confirm the accuracy and precision of the analysis, as well as to detect any potential contamination of the samples.

ASANOA was the primary laboratory used by Millennial while SGS was used as the secondary lab for check samples. This arrangement was in place until August 21, 2017, when ASANOA was replaced by SGS as the main laboratory. No registered secondary lab was used for check samples.

AMSA used SGS as their primary laboratory throughout the 2021/2 campaign, while ASANOA was used as the main lab for Centaur throughout the 2019/9 campaign. The insertion rates for blanks, check samples, duplicates, and standards for each QA/QC program are detailed in Table 36.

Ganfeng Lithium used for the 2023 Exploration Campaign in Pastos Grandes, an internal laboratory located at the Pozuelos Project that carried out tests on brine samples while the laboratory ASANOA was used for control samples.

Table 36: Summary of QAQC Insertion Rates for Each Campaign

Sample Type	Total N°	Millennial	AMSA	Centaur	Ganfeng
Originals	635	452	104	79	34
Duplicates & Checks	66	51	9	6	7
Blanks	43	32	6	5	2
Standards	56	39	12	5	2
Total	800	574	131	95	45

8.2.4.1 Millennial QA/QC

8.2.4.1.1 Duplicate Brine Samples

To ensure the laboratory's precision, duplicate brine samples were submitted to the same facility. Millennial’s Phase II and Phase III exploration programs included a total of 51 duplicate samples, some of these also used as check samples. 16 duplicates and their original samples were submitted to ASANOA, while 35 were submitted to SGS. Table 37 list the main statistics regarding the duplicates versus their original samples for lithium and potassium for each laboratory.

Table 37: Statistical Analysis of Duplicate Samples – ASANOA

ASANOA					SGS			
Statistic	**Li (mg/L)**	**Duplicate Li (mg/L)**	**K (mg/L)**	**Duplicate K (mg/L)**	**Li (mg/L)**	**Duplicate Li (mg/L)**	**K (mg/L)**	**Duplicate K (mg/L)**
Count	16	16	16	16	35	35	35	35
Min	247.1	273.8	2783.2	3300.5	10.0	10.0	15.0	15.0
Max	579.4	570.7	6092.0	6367.8	701.0	758.0	6,660.0	7,170.0
Mean	478.5	471.8	5147.9	5047.5	415.6	416.2	4,340.5	4,362.1
Std Dev	92.0	85.6	926.4	817.1	155.4	162.1	1,574.4	1,653.4
RPD	1.4		2.0		0.2		0.5	

The assay results for duplicate samples at both ASANOA and SGS laboratories demonstrate a high degree of precision and consistency for key parameters of lithium and potassium. The highest Relative Percent Difference (RPD) is only 2% for ASANOA and 0.5% for SGS. This is significantly lower than the commonly accepted 10% cut-off and suggests that the laboratory's analytical procedures are consistently producing results that are in close agreement with each other.

Max-min plots for each laboratory are displayed from Figure 76 and Figure 77. These show the maximum versus minimum values for each pair of samples, and the failure line is represented by a hyperbolic function ($Y^2 = m^2X^2 + b^2$), where m is the slope of the asymptote and b the intersection at the y axis. The failure line was calculated based on a 10% relative error allowance.

The standard threshold for an acceptable number of failures is typically set at 10%. However, given the limited sample size and the observation that there are 2 failures for both lithium and potassium that are marginally beyond the 10% relative error cut-off, a failure rate of 25% is deemed acceptable in this specific instance. If the failures found on the limit of the failure line were deemed to be acceptable, the percentage of failure would change to 6.25% and 12.5% respectively.

Figure 76 and Figure 77 show the max-min plots for SGS, and duplicate samples are considered acceptable for both lithium and potassium, as the percentage of failures for each element falls below the 10% cut-off. It is noteworthy that three registered failures for lithium are only marginally beyond the 10% threshold, indicating high precision within the SGS laboratory.

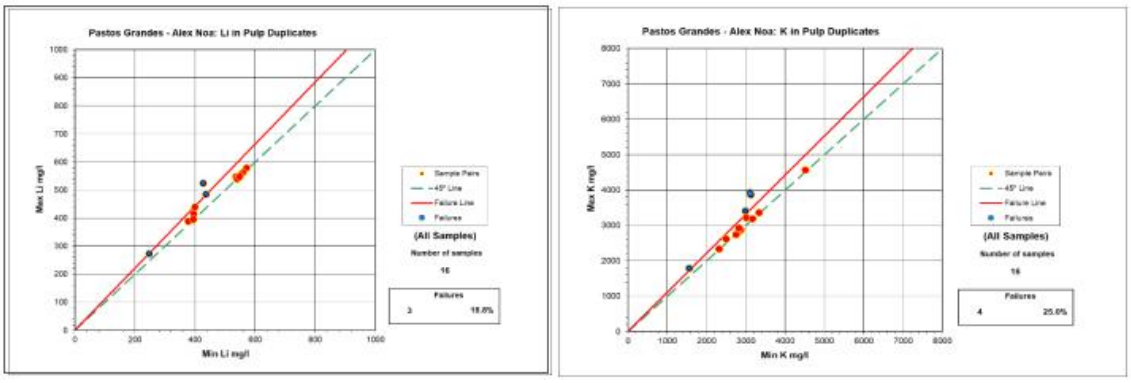

Figure 76: Max-min Plot for Li (left) and K (right) in Duplicates – ASANOA (Source: AW, Dec 2024)

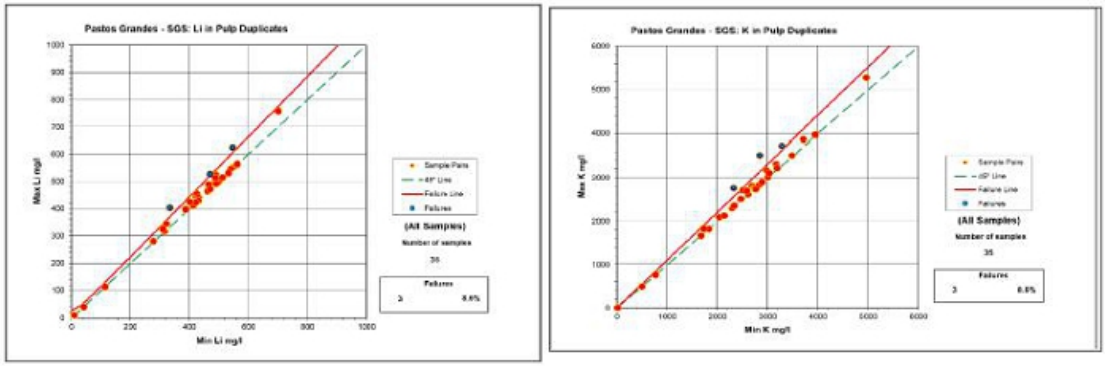

Figure 77: Max-min Plot for Li (left) and K (right) in Duplicates – SGS (Source: AW, Dec 2024)

8.2.4.1.2 Check Samples

To test the laboratory's accuracy, samples were randomly selected and analyzed at a secondary and independent laboratory - SGS. It's important to note that this only occurred before August 21, 2017, when SGS replaced ASANOA as the main laboratory. Since that date, no secondary laboratory has been registered for check samples. Millennial's Phase II and III exploration programs included 29 check samples to both primary and secondary labs. The main statistics regarding the check samples for lithium and potassium are listed in Table 38.

Table 38: Statistical Analysis of Check Samples – ASANOA & SGS

Statistic	ASANOA-Li (mg/L)	SGS-Li (mg/L)	ASANOA-K (mg/L)	SGS-K (mg/L)
Count	29.0	29.0	29.0	29.0
Min	0.5	10.0	2.5	10.0
Max	554.4	714.0	5424.3	7740.0
Mean	468.8	543.9	4779.2	5916.2
Std Dev	104.1	123.8	970.3	1248.8
RPD	14.8		21.3	

The assay results for check samples between ASANOA and SGS fall within a 20% relative difference for lithium, but slightly over 20% for potassium. A RPD over 20% indicates that there may be an issue with the accuracy of one or both laboratories testing methods, but this cannot be determined solely by the RPD value, and further investigation is needed to identify the cause of the discrepancy. The RPD value for lithium of 14.8% is within the accepted 20% cut-off but still suggests there is some difference between the results obtained by the two labs.

Figure 78 present the max-min plots for the check samples of lithium and potassium respectively. Like the duplicate section discussed above, these plots display the maximum versus minimum values for each pair of samples. The failure line is represented by a hyperbolic function ($Y^2 = m^2X^2 + b^2$), where m is the slope of the asymptote and b the intersection at the y axis. The failure line was calculated based on a 20% relative error allowance.

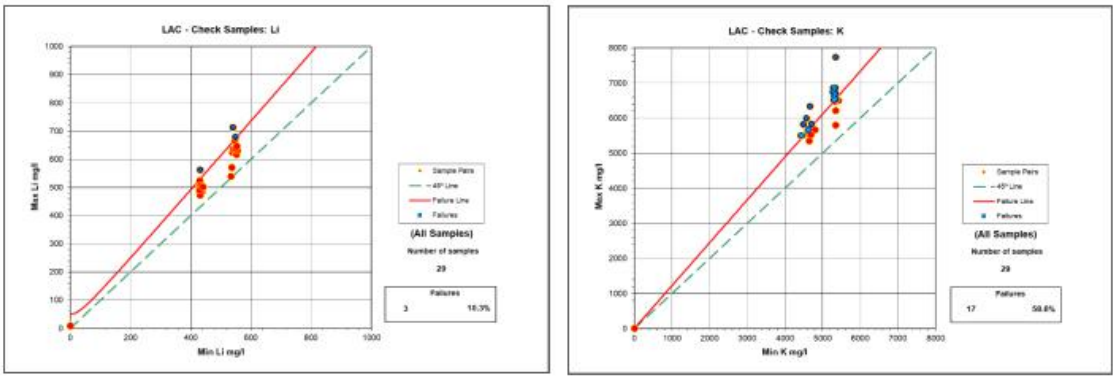

Figure 78: Max-min Plot for Li (left) and K (right) in Check Samples: ASANOA – SGS (Source: AW, Dec 2024)

The check samples for both lithium and potassium show a failure rate that exceeds the accepted 10% cut-off. However, one of the three failures for lithium falls only marginally beyond the failure line, which, if considered acceptable, would result in a failure rate of 6.9%. In contrast, the failure rate for potassium is 58.6%, with several samples falling beyond the failure line, indicating an unacceptable level of variation.

8.2.4.1.3 Field Blanks

To measure potential contamination 32 blank samples consisting of distilled water were inserted into the sample stream and sent to the laboratories for analysis. ASANOA received 10 blanks, while SGS received 22. Neither laboratory detected any lithium in the samples, although traces of potassium were detected by ASANOA. It is important to note that the detected potassium concentrations were below the standard safe limit, which is generally considered to be three times the detection limit.

This data can be visualized with Blank vs Previous graphs where the Y-axis represents the concentrations detected in blanks for each element and the X-axis represents the measured concentration of the same element for the sample assayed just before the blank. Additionally, the graphs feature a regression line for lithium concentrations shown in blue and a red line, representing the safe limit. Figure 79 and Figure 80 display these graphs for both lithium and potassium for each lab.

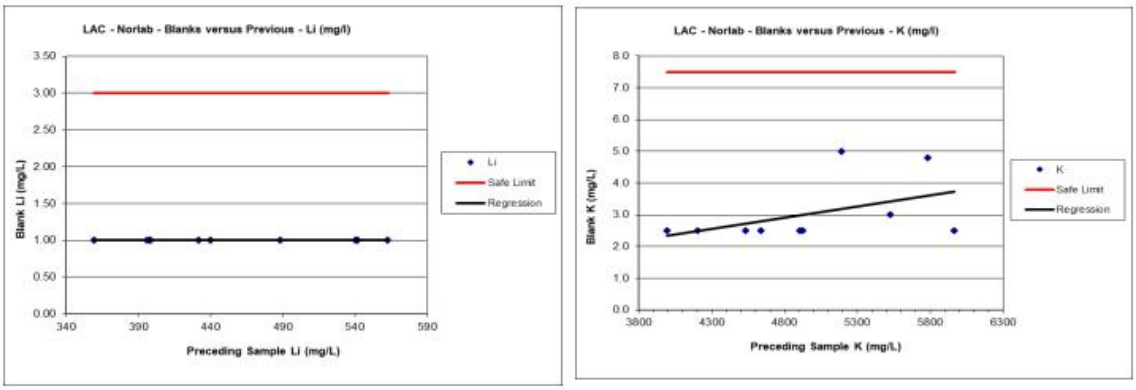

Figure 79: Blank vs Previous Samples for Lithium and Potassium – ASANOA (Source: AW, Dec 2024)

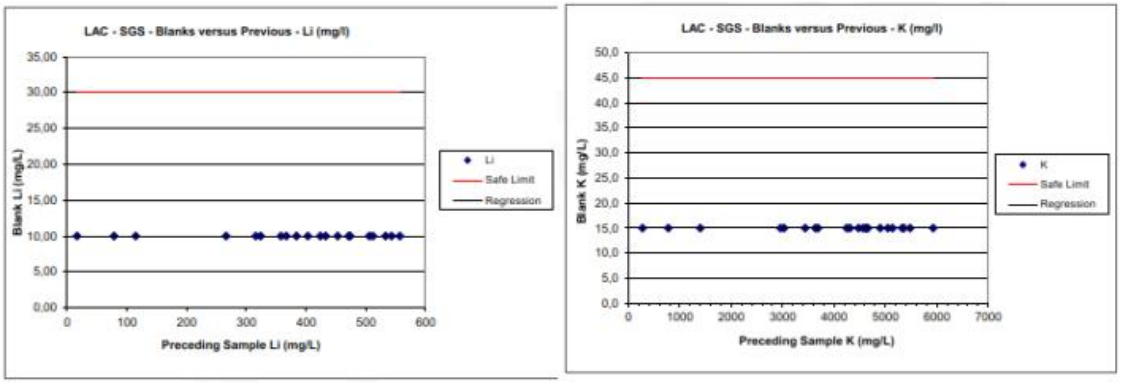

Figure 80: Blank vs Previous Samples for Lithium and Potassium – SGS (Source: AW, Dec 2024)

8.2.4.1.4 Standard Samples

The Millennial sampling program utilized two types of standards. The concentrations (best values) of the standard obtained through the round robin are shown in Table 39.

- The first standard, 'RR', consisted of a large sample of brine collected from the Salar de Pastos Grandes during testing at well PGPW16-01 with the concentrations being obtained from a round robin style quality control check. 5 RR standards were sent to ASANOA for analysis while 26 samples were sent to SGS.
- The second type of standard, INBEMI, consisted of a synthetic solution prepared by the National University of Salta. INBEMI standards were only sent to SGS for analysis, amounting to a total of 6 samples.

Table 39: Element Concentrations (Best Values) for Standard RR – Millennial

Standard	Sample	Li (mg/L)	Ca (mg/L)	Mg (mg/L)	B (mg/L)	Na (mg/L)	K (mg/L)	SO_4 (mg/L)	Density (g/mL)	EC (mS/cm)	TDS (mg/L)
RR	PGS17153	450.2	618.8	3,034	774.9	107,255	4,890	-	1.2	189	334,800
INBEMI	PGS17153	295.0	440.0	189.0	532.0	75,518	3,188	189.0	1.2	-	-

Figure 81 to **Figure 83** present a graphical analysis of the assay results for the samples using both the 'RR' and 'INBEMI' standards for both ASANOA and SGS laboratories. All graphs account for a 95% confidence interval of the mean and display the element concentration on the Y-axis and the date of sampling on the X-axis. The reference value (best value) of the element for each standard is shown with a purple line along with a ± 5% acceptable variation represented by a brown and grey line respectively. The actual data is displayed with black outlined squares while the data's moving average is represented in green. The average plus or minus 2 standard deviations are displayed in yellow lines. In general, a total relative bias higher than ±10% is considered unacceptable.

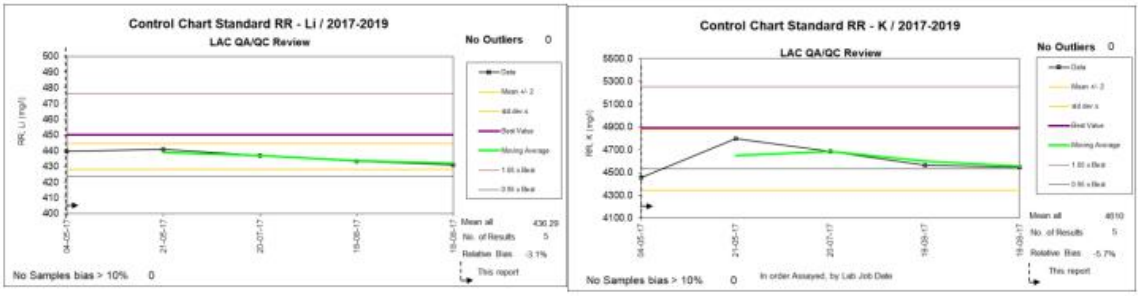

Figure 81: Graphical Analysis of Li (top) and K (bottom) within 'RR' Standards Assayed y ASANOA (Source: AW, Dec 2024)

The RR standards analyzed by ASANOA show that none of the lithium nor potassium values fall outside the ± 2 standard deviations from the mean. Additionally, all lithium values fall within the ± 5% range of the reference values while only one potassium value falls outside this range. There were not enough INBEMI standard samples analyzed by ASANOA to conduct a graphical analysis as the moving average does not have enough data. Notably, a bias check for the assay results revealed a negative bias ranging from -3.1% for Li to -5.7% for potassium indicating that the measured values are consistently lower than the expected or reference values. However, this detected bias is well below the accepted 10% and is not considered to be significant.

The RR standards analyzed by SGS (Figure 82) show that 6 out of 26 samples had a bias over the accepted limit of 10% bias lithium with no outliers and a total relative bias of -1.9% which is considered acceptable. Similarly, the potassium samples present 4 out of 26 values over 10% bias with one outlier, and a total relative bias of -3.1%, also deemed acceptable.

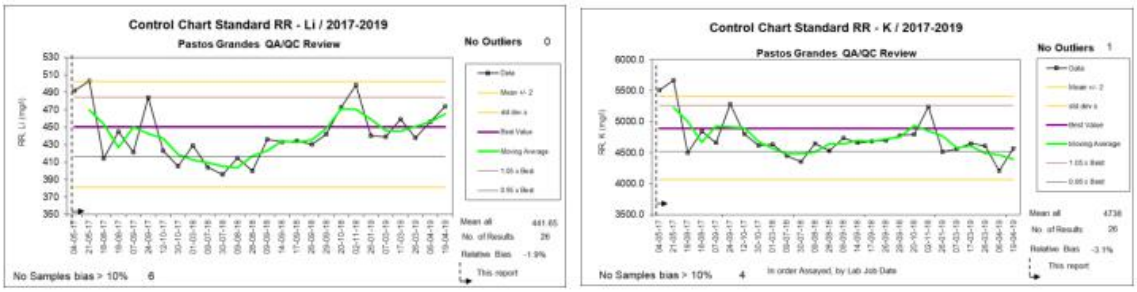

Figure 82: Graphical Analysis of Li (top) and K (bottom) within 'RR' Standards Assayed by SGS (Source: AW, Dec 2024)

Regarding the INBEMI standards analyzed by SGS (Figure 83), 2 out of 6 lithium samples showed a bias over 10% with no outliers and a total relative bias of 0%. For potassium samples show 1 out of a total of 6 had a bias over 10%, with no outliers and a total relative bias of 0%.

In summary, while some individual samples showed a bias beyond the generally accepted 10% limit, the overall bias for both lithium and potassium within the standard samples analyzed by both laboratories is considered acceptable with the highest being -5.7% for lithium within the RR standards assayed by ASANOA.

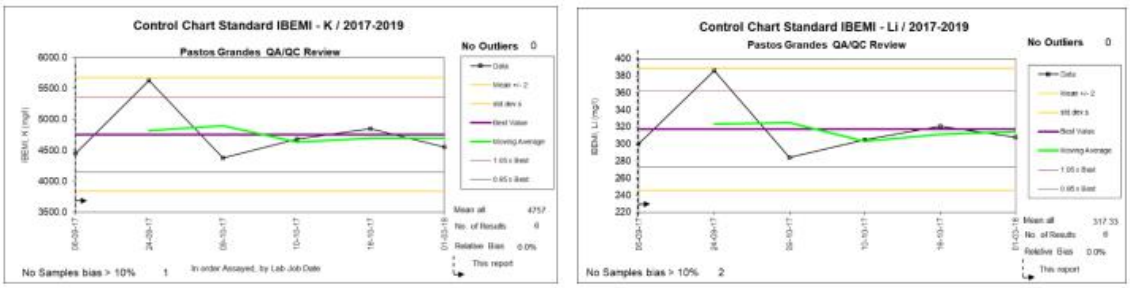

Figure 83: Graphical Analysis of Li (top) and K (bottom) within 'INBEMI' Standards Assayed by SGS (Source: AW, Dec 2024)

8.2.4.2 AMSA Brine Samples QA/QC

8.2.4.2.1 Duplicate Brine Samples

SGS was used as the main assay laboratory by AMSA and to ensure that the precision of the lab was acceptable, a total of 9 duplicate brine samples were submitted. There was no check samples used during the AMSA drilling campaign due to C-19 related issues. Table 40 lists the main statistics regarding the duplicates for lithium and potassium.

Table 40: Statistical Analysis of Duplicate Samples – SGS

Statistic	Li (mg/L)	Duplicate Li (mg/L)	K (mg/L)	Duplicate K (mg/L)
Count	9.0	9.0	9.0	9.0
Min	33.6	31.9	197.0	177.9
Max	658.8	657.8	6022.9	6075.6
Mean	419.1	413.8	3726.1	3686.1
Std Dev	185.0	183.3	1788.9	1757.4
RPD	1.3		1.1	

The assay results for duplicate samples at SGS demonstrate a high degree of precision and consistency for key parameters of lithium and potassium. The Relative Percent Difference (RPD) is low, with values of only 1.3% for lithium and 1.1% for potassium. These are significantly lower than the commonly accepted 10% cut-off and suggest that the laboratory's analytical procedures are consistently producing results that are in close agreement with each other.

Figure 84 display max-min plots for each laboratory, showing the maximum versus minimum values for each pair of samples and the failure line is represented by a hyperbolic function ($Y^2 = m^2X^2 + b^2$), where m is the slope of the asymptote and b the intersection at the y axis. The failure line was calculated based on a 10% relative error allowance.

There were no failures for either lithium nor potassium within duplicates analyzed by SGS. The generally accepted threshold for failure rates is 10%, so duplicates are not only considered acceptable, but the lack of failures suggests high precision within the SGS laboratory for the current project.

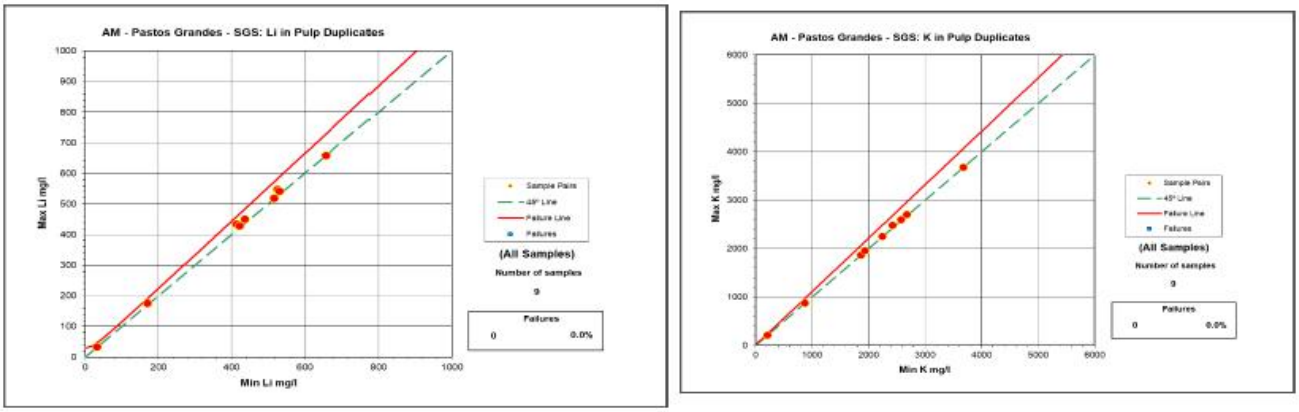

Figure 84: Max-min Plot for Lithium (left) and Potassium (right) in Duplicates – SGS (Source: AW, Dec 2024)

8.2.4.2.2 Field Blanks

To measure potential contamination within the sampling process a total of 6 blank samples consisting of distilled water were inserted into the sample stream and sent to the SGS laboratory for analysis. Neither lithium nor potassium were detected in any samples, therefore all concentrations were below the standard safe limit, which is generally considered to be three times the detection limit.

This data can be visualized with Blank vs Previous graphs, where the Y-axis represents the concentrations detected in blanks for each element, and the X-axis represents the measured concentration of the same element for the sample assayed just before the blank. Additionally, the graphs feature a regression line for lithium concentrations shown in blue and a red line representing the safe limit. Figure 85 display these graphs for both lithium and potassium for each lab.

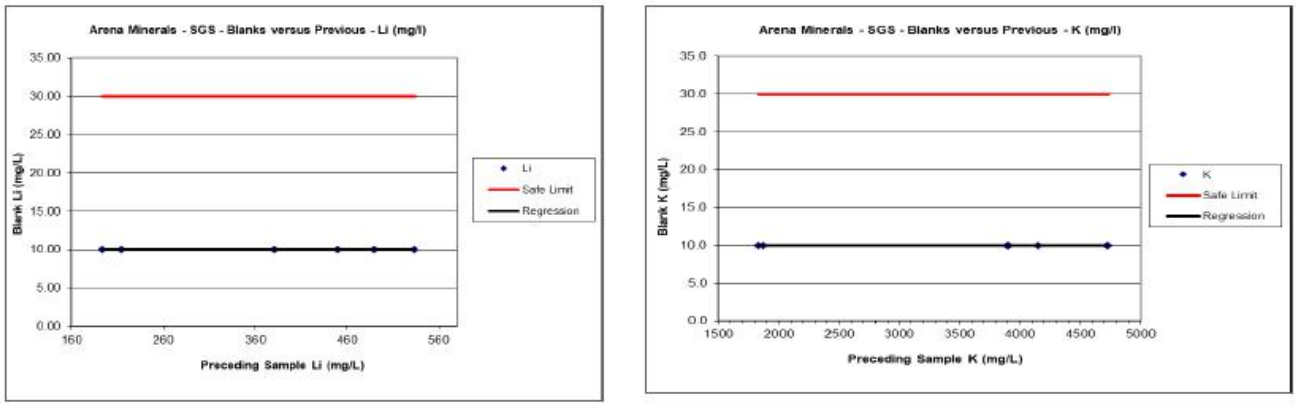

Figure 85: Blank vs Previous Samples for Lithium (left) and Potassium (right) – SGS (Source: AW, Dec 2024)

8.2.4.2.3 Standard Samples

The AMSA sampling program utilized two different standards; both obtained from brine within Salar de Pastos Grandes and named STD-1 and STD-2. Six samples were sent to SGS for analysis for each standard, amounting to a total of 12 standard samples. Their respective concentrations (best values) were obtained from a round robin style quality control check and are shown in Table 41.

Table 41: Element Concentrations for Standards 1& 2 - AMSA

Sample	Li (mg/L)	Mg (mg/L)	Na (mg/L)	K (mg/L)
STD-1	645.7	2,395.5	55,435.8	6,709.8
STD-2	352.6	1,292.0	29,825	3,682.5

Figure 86 and Figure 87 present a graphical analysis of the assay results for lithium and potassium within the samples using both the STD-1 and STD-2 standards. All graphs account for a 95% confidence interval of the mean and display the element concentration on the Y-axis and the date of sampling on the X-axis. The reference value (best value) of the element for each standard is shown with a purple line, along with a ± 5% variation, represented by a brown and grey line respectively. The actual data is displayed with black outlined squares while the data's moving average is represented in green. Finally, the average ± 2 standard deviations are displayed in yellow lines. In general, a total relative bias higher than ±10% is considered unacceptable.

In summary, while some individual samples showed a bias beyond the generally accepted 10% limit, the overall bias for both lithium and potassium within the standard samples analyzed by both laboratories is considered acceptable, with the highest being 7.3% for lithium within the STD-2 standard.

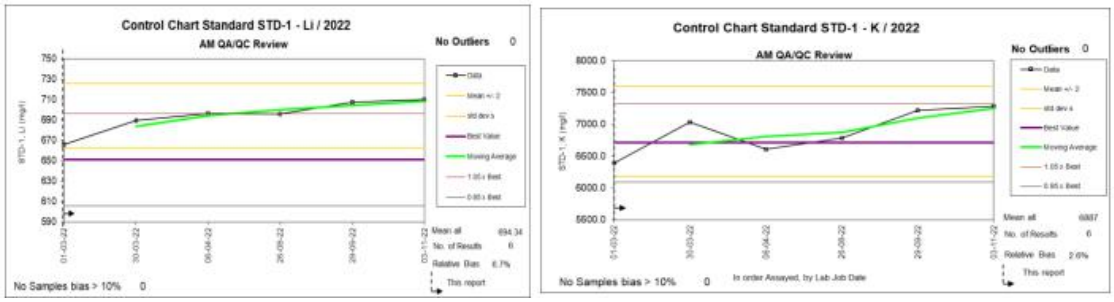

Figure 86: Blank vs Previous Samples for Lithium (left) and Potassium (right) – SGS (Source: AW, Dec 2024)

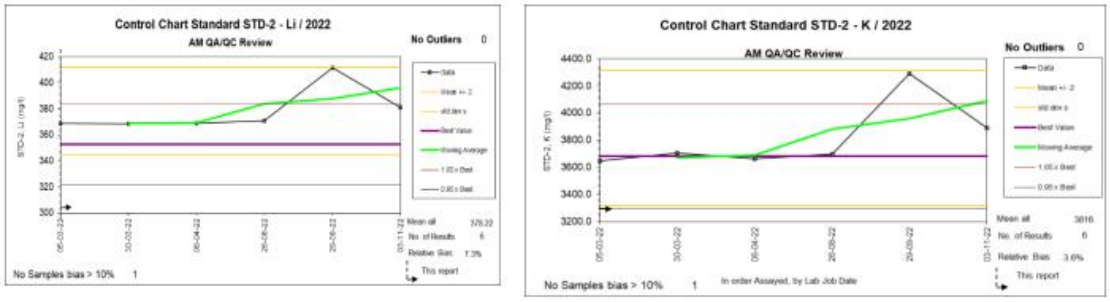

Figure 87: Blank vs Previous Samples for Lithium (left) and Potassium (right) – SGS (Source: AW, Dec 2024)

8.2.4.3 Centaur QA/QC

8.2.4.3.1 Duplicate Brine Samples

ASANOA was used as the main laboratory by Centaur and to ensure acceptable precision within the lab, a total of six duplicate brine samples were submitted to the same facility. Table 42 lists the main statistics regarding the duplicates for lithium and potassium.

Table 42: Statistical Analysis of Duplicate Samples – ASANOA

Statistic	Li (mg/L)	Duplicate Li (mg/L)	K (mg/L)	Duplicate K (mg/L)
Count	6.0	6.0	6.0	6.0
Min	409.6	411.5	2,894.1	2,886.7
Max	548.3	627.9	5,093.1	5,213.7
Mean	507.3	543.2	4257.6	4617.1
Std Dev	52.5	65.8	880.1	824.0
RPD	6.8		8.1	

The assay results for duplicate samples at ASANOA demonstrate a high degree of precision and consistency for key parameters of lithium and potassium. The Relative Percent Difference (RPD) is below the commonly accepted 10% cut-off for lithium and potassium, with values of 6.8% and 8.1% respectively. This suggests that the laboratory's analytical procedures are consistently producing results that are in close agreement with each other.

Figure 88 display max-min plots for each laboratory showing the maximum versus minimum values for each pair of samples and the failure line is represented by a hyperbolic function ($Y^2 = m^2X^2 + b^2$), where m is the slope of the asymptote and b the intersection at the y axis. The failure line was calculated based on a 10% relative error allowance.

The max-min plots showed that out of the six duplicates tested, only one failure occurred for lithium while there were no failures for potassium. This translates to a 16.7% failure rate for lithium and 0% for potassium. The generally accepted failure rate threshold is 10% which means that duplicates are considered acceptable for potassium but unacceptable for lithium. However, it's important to note that the sample size taken under Centaur Resources is limited, with only six duplicates assayed. Therefore, in this case, a single failure surpasses the 10% threshold. Taking this into consideration a 16.7% failure rate is deemed to be acceptable.

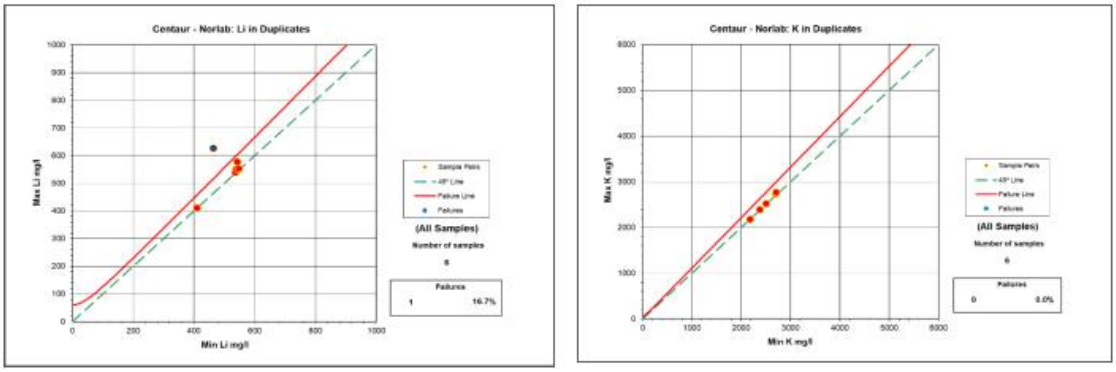

Figure 88: Max-min Plot for Lithium (left) and Potassium (right) in Duplicates – ASANOA (Source: AW, Dec 2024)

8.2.4.3.2 Field Blanks

To measure potential contamination a total of five blank samples consisting of distilled water were inserted into the sample stream and sent to ASANOA for analysis. Neither lithium nor potassium were detected in any samples, which means that all concentrations were below the standard safe limit, generally considered to be three times the detection limit.

This data is presented in Blank vs Previous graphs, where the Y-axis represents the concentrations detected in blanks for each element, and the X-axis represents the measured concentration of the same element for the sample assayed just before the blank. Additionally, the graphs feature a regression line for lithium concentrations shown in blue and a red line representing the safe limit. These graphs are displayed for both lithium and potassium in Figure 89.

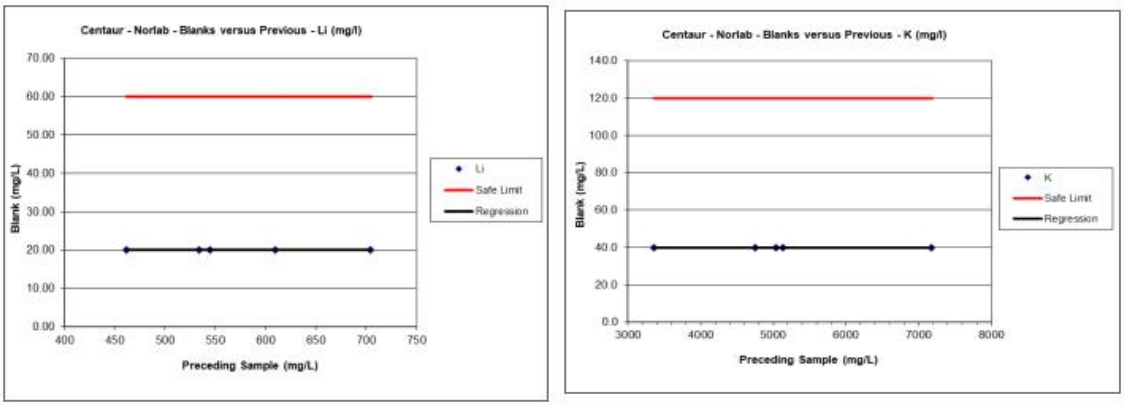

Figure 89: Blank vs Previous Samples for Lithium (left) and Potassium (right) – ASANO (Source: AW, Dec 2024)

8.2.4.3.3 Standard Samples

The Centaur sampling program utilized two different standards both obtained from brine within Salar de Pastos Grandes with their respective concentrations obtained from a round robin style quality control check. These standards were named STD-A and STD-B, and three samples of the former were sent to the lab for analysis while only 2 of the latter were assayed. The concentrations (best values) for each standard obtained through the round robin are shown in Table 43.

Table 43: Element Concentrations (best values) for Standards A & B – Centaur

Sample	Li (mg/L)	Mg (mg/L)	Na (mg/L)	K (mg/L)
STD-A	707.0	4,641.9	111,699.2	7,041.9
STD-B	370.5	2,444.3	58,074.0	3,543.1

Graphical analysis of the assay results for lithium and potassium for the STD-A standards can be seen in Figure 90 while graphical analysis for the STD-B standard was not possible due to a lack of samples. Both graphs account for a 95% confidence interval of the mean and display the element concentration on the Y- axis and the date of sampling on the X-axis. The reference value (best value) of the element for each standard is represented with a purple line, along with a ± 5% variation, represented by a brown and grey line respectively. The actual data is displayed with black outlined squares while the data's moving average is represented in green. Finally, the average ± 2 standard deviations are displayed in yellow lines. In general, a total relative bias higher than ±10% is considered unacceptable.

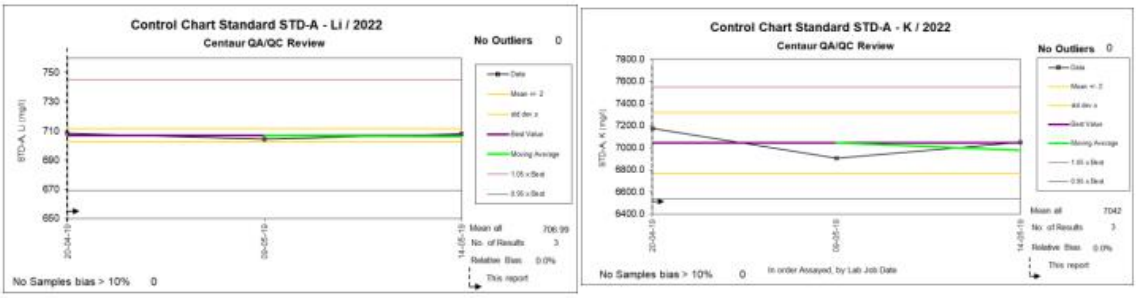

Figure 90: Max-min Plot for Lithium (left) and Potassium (right) in Duplicates – ASANOA (Source: AW, Dec 2024)

8.2.4.4 Ganfeng QA/QC

8.2.4.4.1 Duplicate and Check Brine Samples

To evaluate precision for the primary internal laboratory, duplicate brine samples were submitted to the same laboratory facility. A total of 5 duplicate samples were assayed, and 2 check samples were submitted to ASANOA to confirm the accuracy performance. Table 44 list the main statistics regarding the duplicates versus their original samples for lithium and potassium for main laboratory.

Table 44: Statistical Analysis of Duplicate Samples – Ganfeng

Statistic	Li (mg/L)	Duplicate Li (mg/L)	K (mg/L)	Duplicate K (mg/L)
Count	5	5	5	5
Min	199	200	1886	1903
Max	545	556	5318	5381
Mean	423.7	423.8	4320	4331
Std Dev	118.6	119.2	1235.0	1236.9
RPD	0.038%		0.254%	

Max-min plots for the main laboratory are displayed in Figure 91. These plots show the maximum versus minimum values for each pair of samples, and the failure line was calculated based on a 5% relative error allowance when, typically, 10% is used as tolerance limit.

For each max-min plot, sample pairs (each duplicate and its original) are represented by blue circles, while the failure curve is shown in red, and a 45° line is added in dark gray for reference. All duplicated pairs show good precision.

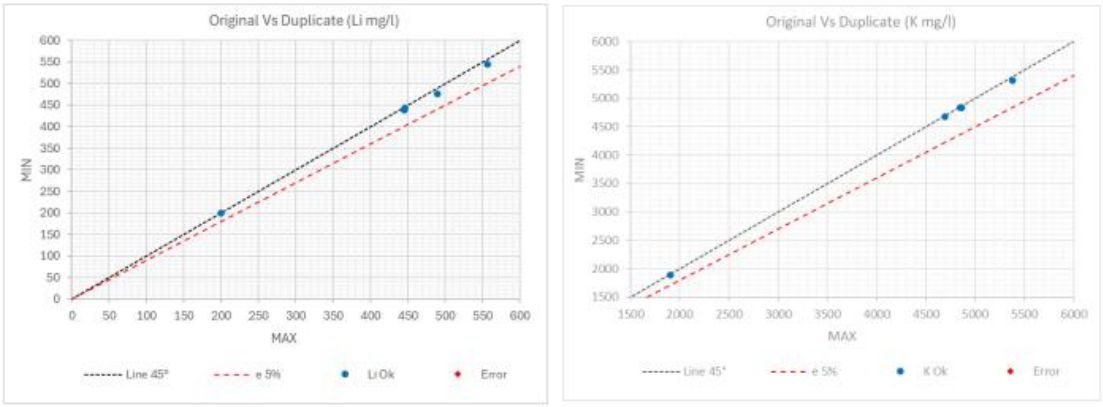

Figure 91: Max-min Plot for Lithium (left) and Potassium (right) in Duplicates – Lab Pozuelos (Source: AW, Dec 2024)

The assay results for duplicate samples at both primary (Pozuelos) and ASANOA laboratories demonstrate a high degree of accuracy and consistency for key parameters of lithium and potassium (Table 45) and suggests that the analytical procedures are consistently producing results that are in close agreement for both laboratories.

Table 45: Statistical Analysis of Check Samples

Hole_ID	Sample	From_m	To_m	Analite	Lab Pozuelos	Lab ASANOA	Error
PG-2023-04	263	238.0	249.0	Li (mg/L)	534	539	0.9%
PG-2023-04	263	238.0	249.0	K (mg/L)	7221	7054	2.3%
PG-2023-03	1010	346.5	363.5	Li (mg/L)	553	523	5.6%
PG-2023-03	1010	346.5	363.5	K (mg/L)	5258	4999	5.1%

8.2.4.4.2 Field Blanks

Distilled water was inserted as a blank sample into the samples batch and sent to the Pozuelos laboratory in order to evaluate contamination. All reports showed concentrations below the quantification limit were usually the safe limit is three to five times the quantification limit.

Figure 92 display the Lithium and Potassium concentrations with acceptable safe limits for blank samples compared to previous samples.

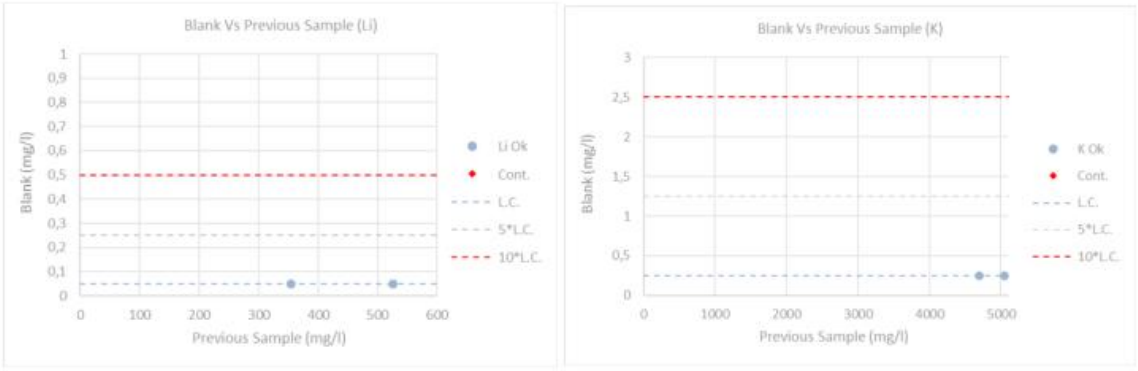

Figure 92: Blank vs Previous Samples for Lithium (left) and Potassium (right) – Lab Pozuelos (Source: AW, Dec 2024)

It is QPs' opinion that sample preparation, security and analytical procedures are adequate and compliant with the requirements of S-K §229.1300.

8.3 Conclusions and Recommendations

In Golder's opinion, the brine sampling methodologies applied during the various drilling campaigns and associated QAQC protocols implemented to verify laboratory accuracy and precision meet industry standards. The quality control data based upon the insertion of standards, field blanks and field duplicates indicate that the analytical data is accurate and precise, and the samples being analyzed are representative of the brine within the aquifer.

Laboratories including Alex Steward International Argentina, Corelabs, GSA, and ASANOA have no relation to Ganfeng or LAR.

The following recommendations are made with regards to QA/QC procedures:

- Exploration samples should continue to be sent to certified laboratories.
- Verification sampling should be conducted prior to updating the Mineral Resource Estimate and Mineral Reserve Estimate in 2025 and beyond.

9.0 DATA VERIFICATION

The QPs were responsible for the oversight and analysis of the QA/QC programs related to brine sampling and laboratory brine chemistry analysis as well as the laboratory porosity analysis. A significant amount of QA/QC protocols were implemented for the brine chemistry and drainable porosity analysis programs that allowed continuous verification of the accuracy and reliability of the results obtained. As described in Section 11 no issues were found with the results of the brine and porosity laboratory analysis.

It is the opinion of the QPs that the information developed and used for the brine resource estimate herein is adequate, accurate and reliable for the purposes used in the technical report.

10.0 MINERAL PROCESSING AND BRINE TESTING

10.1 Introduction

Key metallurgical testing was performed by Ganfeng Lithium to define the technology and engineering parameters required to design a direct extraction process for the PPG Project.

This section was based on the test results and reports provided by Ganfeng Lithium (GF). Frederik Reidel has visited the metallurgical laboratory performing the test work and is confident that the quantity and quality of the test work completed is sufficient to the level of a PEA Study.

10.1.1 Process Overview

It was determined that the brine was only concentred to ~3 g/l lithium to feed a unique solvent extraction process to produce a pure concentrate that will report to the lithium carbonate and hydroxide plants at the Salar de Pozuelos. The process involved pre-concentration in solar ponds, solvent extraction, purification and product recovery.

10.2 Brine Evaporation

To determine the evaporation path of the brine at the Salars de Pozuelos and Pastos Grandes, the QP relied on a traditional modelling commissioned to Adinf with extensive experience in design of solar evaporation ponds throughout Argentina and Chile.

10.3 Purification of Brine

Impurities, such as Ca, and B, will be removed in the several purification steps used in the lithium plant. All purification test-work was performed by GF at its R&D Centre in China. Since these are traditional processes used in industry whether based on chemical precipitation or resin ion exchange, they are not reported in this Chapter but discussed in detail in Chapter 17.

10.4 Solvent Extraction Test Work

The solvent extraction test work was to verify the extractant selectivity for lithium and its efficiency of boron removal. This was achieved with a proprietary and selective solvent formulation. To identify the feasibility of the proposed experimental route and process of extraction method, and the reliability of multi-component synergistic extraction-water stripping. Whether the lithium extraction rate is ≥ 90%, and the content of stripped lithium is ≥19 g/L.

10.4.1 Experimental Principle

When the synergistic extractant is contacted with the brine containing high concentration of Cl^- after being preconditioned with an active agent, lithium can be extracted to form a relatively stable complex. In the stripping stage, due to ion concentration difference, lithium chloride is stripped from the organic phase with water allowing for the regeneration of the organic phase. An aqueous phase rich in lithium chloride is obtained.

10.4.2 Experimental Steps

- Determine the proportion of organic phase and extraction ratio

- Conduct a five-stage continuous extraction cascade experiment to simulate the continuous extraction effect of the mixer-settler
- Carry out operation experiment of mixer-settler

10.4.3 Experimental Summary and Data

10.4.3.1 Determination of Organic Phase and Extraction Ratio

The Extractant #1, the Extractant #2 and the Extractant #3 are preloaded with an active agent.

Preloaded extractants #1, #2, #3 were mixed with PPG Lithium-rich brine at different volume ratios, contacted for 15 minutes, then stripped to obtain the raffinate after single-stage extraction and an Li-loaded organic phase.

Considering the data obtained Extractant#3 was chosen because of the low extraction of impurities and reasonable lithium extraction. The solvent components were:

- 60% of main extractant
- 10% synergistic agent
- 30% diluent

Table 46: Analysis Data of Five-stage Simulated Extraction Experiment

Name	Li	Na	K	Ca	Mg	B	SO_4^{2-}	Fe	Unit
PPG Li-rich brine	3.190	104.11	16.78	0.12	12.68	2.03	67.16	/	g/L
Raffinate 1	0.027	92.96	13.76	0.176	23.12	1.12	68.24	0.031	g/L
Raffinate 2	0.126	103.12	14.24	0.216	12.80	1.68	67.92	0.065	g/L
Raffinate 3	0.361	105.20	14.16	0.184	12.56	1.84	70.00	0.063	g/L
Raffinate 4	0.856	102.32	13.76	0.152	12.32	1.84	68.64	0.050	g/L
Raffinate 5	1.703	102.56	14.56	0.128	12.40	1.84	68.96	0.034	g/L
Preloaded organic phase 1	0.806	1.42	0.082	0.012	0.038	0.178	0.102	/	g/L
Preloaded organic phase 2	0.473	1.58	0.022	0.014	0.038	0.166	0.080	/	g/L
Preloaded organic phase 3	0.221	1.96	0.072	0.019	0.054	0.164	0.136	/	g/L
Preloaded organic phase 4	0.095	1.94	0.038	0.024	0.050	0.150	0.092	/	g/L
Preloaded organic phase 5	0.027	2.40	0.058	0.034	0.132	0.116	0.096	/	g/L

Table 47: Analysis Data of Five-stage Simulated Extraction Experiment

Name	Calculated by raffinate	Based on Li^+ loaded organic phase
Extraction rate of Li^+	99.15%	101.07%
The extraction rate of Fe	99.95%	/
B extraction rate	44.83%	35.07%

The experimental data showed that when using Extractant #3 with the extraction phase ratio O: A of 4:1, the extraction rate of PPG Li-rich brine by five-stage continuous cascade extraction was ≥99%.

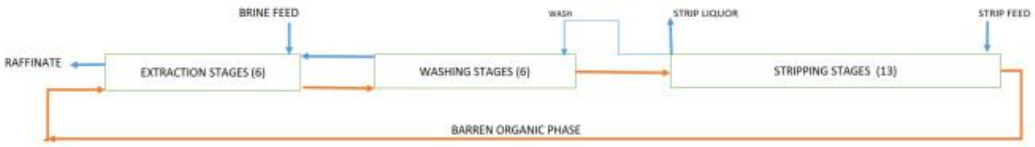

Figure 93: Process Flowsheet for Continuous Extraction Process (Source: Ganfeng, 2024)

10.4.3.2 Operation Experiment of Mixed Clarification Tank

Operating parameters with Extractant#3:

- 6 stages of extraction,
- 6 stages of washing and
- 13 stages of water stripping.

- **Extraction stage:**
  - phase ratio O: A = 4.47 ~ 4.53:1,
  - organic flow rate is about 170 mL/min,
  - brine flow rate is 37.5 ~ 38.0 mL/min.
- **Washing stage:**
  - LiCl recycle 2.5 ~ 3 ml/min, (20% ~ 26% of the total).
  - phase ratio O: A = 56.67 ~ 70:1,
- **Stripping stage:**
  - O: A ratio is 14.78 ~ 20:1,
  - aqueous flow rate is about 8.5 ~ 11.5 mL/min.

10.4.3.3 Experimental Results and Discussion

After one month running time equilibrium was reached and the data analysed.

Table 48: Experimental Data of PPG Li-rich Brine Tank Extraction Operation

Time		Li in Extraction aqueous by stage						Brine Feed	Extraction rate (%)	The aqueous phase of washing section						Wash/Strip	Li in Stripping by stage						Stripping rate (%)
		1	2	3	4	5	6			7	8	9	10	11	12		13	14	24	25	25-O	12-O	
Dec 19	8:40	0.32	0.48	1.00	1.80	2.60	3.15	3.35	90.45	7.25	12.00	15.00	17.50	19.25	19.00	21.50	19.75	18.50	2.75	1.73	0.072	1.12	93.57
	14:00	0.33	0.43	0.75	1.35	2.30	3.05	3.45	90.43	6.40	12.00	14.75	16.75	19.25	18.75	21.25	18.75	16.75	3.60	2.13	0.090	0.84	89.29
Dec 20	8:20	0.30	0.43	0.90	1.65	2.65	3.10	3.40	91.18	6.40	12.00	15.00	17.25	19.50	18.75	21.25	17.75	16.25	2.50	1.20	0.040	0.90	95.56
	15:15	0.30	0.78	1.30	2.35	3.10	3.35	3.45	91.30	6.50	12.25	15.00	17.50	19.75	18.75	20.25	17.75	15.50	1.60	0.95	0.034	1.04	96.73
	21:00	0.34	0.75	1.65	2.55	3.10	3.45	3.35	89.85	6.40	12.00	14.75	17.50	19.25	20.25	21.00	18.00	15.75	1.90	1.18	0.052	/	/
Dec 21	7:50	0.29	0.68	1.50	2.40	3.05	3.35	3.35	91.34	7.40	13.00	15.25	17.50	19.75	20.50	21.00	19.50	17.25	2.25	1.40	0.056	1.18	95.25
Dec 23	12:15	0.37	0.85	2.00	2.85	3.35	3.55	3.40	89.12	7.70	12.75	15.25	17.50	20.00	20.75	21.25	19.00	16.50	2.25	1.35	0.052	0.96	94.58
	17:10	0.36	0.75	1.65	2.55	3.25	3.40	3.40	89.41	7.90	13.75	15.50	18.00	20.25	21.25	21.25	19.00	17.25	2.25	1.40	0.054	/	/
	21:10	0.35	0.73	1.60	2.65	3.15	3.40	3.40	89.71	8.10	13.75	15.50	18.75	20.25	21.25	21.25	19.50	17.75	2.40	1.55	0.068	/	/
Dec 24	14:30	0.34	0.63	1.35	2.25	3.00	3.45	3.40	90.00	8.30	13.50	16.50	18.75	20.25	21.00	21.25	20.00	18.75	2.85	1.72	0.082	1.08	92.41
Dec 26	14:30	0.28	0.45	0.85	1.65	2.65	3.25	3.40	91.76	7.50	14.25	16.00	17.00	19.75	21.00	21.00	19.75	18.75	3.35	2.03	0.068		/
Dec 27	14:30	0.31	0.50	1.05	1.90	2.75	3.15	3.35	90.75	7.60	14.00	15.75	17.00	20.00	21.50	21.25	20.25	18.75	3.60	2.15	0.076	1.16	93.45
Dec 28	14:30	0.46	0.63	1.35	2.30	3.05	3.55	3.45	86.67	7.70	13.75	15.50	17.25	19.75	21.25	21.25	20.25	19.00	3.35	1.98	0.058	1.18	95.08
Dec 29	14:30	0.38	0.70	1.50	2.55	3.10	3.30	3.30	88.48	8.10	14.25	15.75	18.50	20.00	20.75	20.75	20.00	18.75	3.25	1.90	0.062	1.14	94.56
Dec 30	15:30	0.40	0.73	1.60	2.50	3.20	3.55	3.40	88.24	8.30	14.00	16.25	18.50	19.50	21.00	20.75	20.50	19.25	3.25	1.93	0.066	1.10	94.00

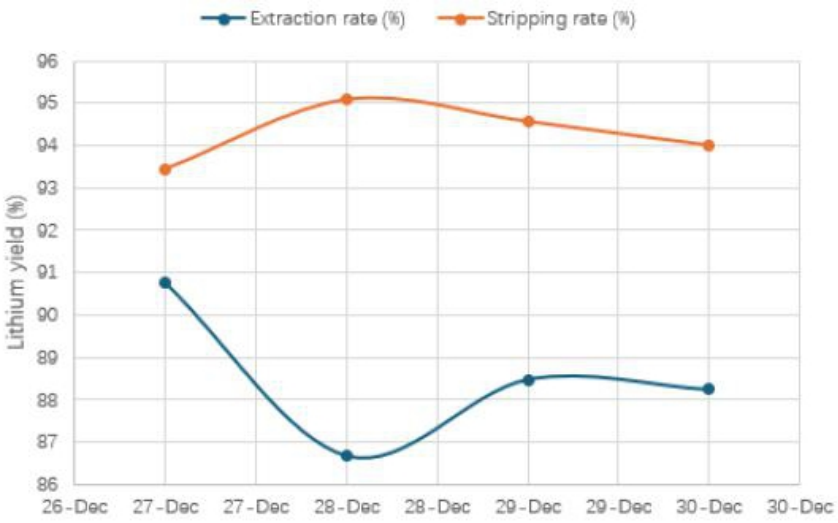

Figure 94: Lithium Yield of PPG Li-rich Brine (Source: Ganfeng, 2024)

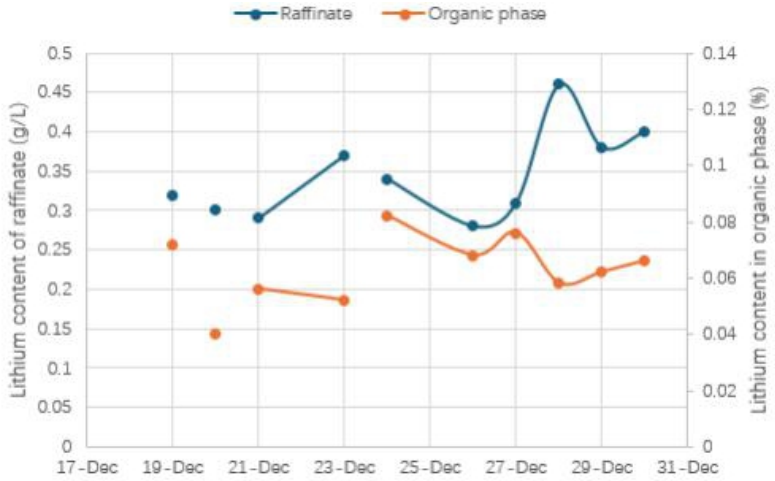

Figure 95: Lithium Content in Raffinate and Organic Phase (Source: Ganfeng 2024)

Table 48 and Figure 94 and Figure 95 show that the average lithium extraction rate was 90% over one-month operation with an average lithium content in the raffinate of 0.34 g/L. Stripping with water reached an average 94.05% efficiency. The average lithium content in the barren organic was 0. 062 g/L, indicating complete stripping.

Table 49: Summary of Experimental Data

No.	Date	Extraction rate	Stripping rate	Flow rate/ (ml/min)						Ratio		
				Organic	Lithium material	Lotion	Stripping water	Stripping solution	Raffinate	Extraction	Washing	Stripping
1	2024/12/19	90.6%	87.6%	170.0	37.0	2.5	12.0	/	/	4.59	68.00	14.17
2	2024/12/20 (Morning)	90.5%	93.8%	170.0	38.0	2.5	12.0	/	/	4.47	68.00	14.17
3	2024/12/20 (evening)	91.5%	91.6%	170.0	37.5	3.0	11.0	/	/	4.53	56.67	15.45
4	2024/12/21	92.4%	91.5%	170.0	37.5	3.0	11.0	/	/	4.53	56.67	15.45
5	2024/12/23	91.1%	90.6%	170.0	37.0	3.0	11.0	9.0	42.0	4.59	56.67	15.45
6	2024/12/24	91.7%	89.4%	170.0	37.0	3.0	11.0	8.3	40.5	4.59	56.67	15.45
7	2024/12/25	92.3%	89.1%	170.0	37.0	3.0	11.0	8.5	41.6	4.59	56.67	15.45
8	2024/12/26	93.2%	89.2%	170.0	37.5	3.0	11.0	8.3	42.7	4.53	56.67	15.45
9	2024/12/27	92.3%	87.5%	170.0	37.5	3.0	11.5	8.3	41.9	4.53	56.67	14.78
10	2024/12/28	89.2%	91.7%	170.0	37.5	3.0	11.5	8.3	41.9	4.53	56.67	14.78
11	2024/12/29	90.4%	90.4%	170.0	38.0	3.0	11.5	8.3	43.7	4.47	56.67	14.78
12	2024/12/30	90.1%	89.0%	170.0	38.0	3.0	11.5	8.2	44.2	4.47	56.67	14.78

Table 49 shows under stable conditions, the extraction O: A is 4.5: 1, the washing O: A is 56: 1, and the strip is 15: 1. The recycled strip is 0.25: 1, which is within the set operating range. The experimental data of simulated counter current extraction is in good agreement with the experimental data from batch operation. The expected results can be achieved by adjusting the flow rate and phase ratio of each phase.

Table 50: Analysis Result of PPG Brine Feed for Extraction Batch Operation

Serial number	Date	Li	Na	K	Ca	Mg	B	SO_4^{2-}	Unit
1	2024/12/19	3.39	88.78	21.21	0.18	17.48	2.56	41.58	g/L
2	2024/12/20 (Morning)	3.37	89.08	24.66	0.17	16.61	2.43	45.32	g/L
3	2024/12/20 (Evening)	3.28	83.06	22.58	0.18	17.69	2.51	38.25	g/L
4	2024/12/21	3.28	83.06	22.58	0.18	17.69	2.51	38.25	g/L
5	2024/12/23	3.26	82.74	21.04	0.18	17.16	2.48	39.17	g/L
6	2024/12/24	3.26	82.74	21.04	0.18	17.16	2.48	39.17	g/L
7	2024/12/25	3.24	82.33	20.59	0.19	17.26	2.41	37.43	g/L
8	2024/12/26	3.24	82.33	20.59	0.19	17.26	2.41	37.43	g/L
9	2024/12/27	3.23	85.51	22.62	0.19	17.77	2.53	37.38	g/L
10	2024/12/28	3.23	85.51	22.62	0.19	17.77	2.53	37.38	g/L
11	2024/12/29	3.23	85.51	22.62	0.19	17.77	2.53	37.38	g/L
12	2024/12/30	3.23	85.51	22.62	0.19	17.77	2.53	37.38	g/L

Table 51: Analysis Result of Raffinate from Extraction Batch Operation

PPG brine raffinate										
No.	Date	Li	Na	K	Ca	Mg	B	SO_4^{2-}	Fe	Unit
1	2024/12/19	0.32	71.22	16.71	0.15	13.54	1.93	34.59	0.70	g/L
2	2024/12/20 (Morning)	0.32	81.68	20.69	0.14	12.53	1.72	35.71	0.92	g/L
3	2024/12/20 (Evening)	0.28	74.31	18.28	0.14	14.74	1.77	38.07	0.29	g/L
4	2024/12/21	0.25	73.81	18.92	0.15	15.75	1.82	33.18	0.14	g/L
5	2024/12/23	0.29	70.35	17.72	0.16	14.5	1.88	31.66	0.27	g/L
6	2024/12/24	0.27	72.12	20.22	0.16	14.41	1.88	32.46	0.25	g/L
7	2024/12/25	0.25	71.84	19.27	0.15	14.97	1.89	32.57	0.32	g/L
8	2024/12/26	0.22	73.63	20.02	0.15	15.58	1.92	33.52	0.20	g/L
9	2024/12/27	0.25	78.99	19.65	0.16	16.13	2.03	33.7	0.18	g/L
10	2024/12/28	0.35	73.79	18.05	0.16	15.18	1.94	31.58	0.37	g/L
11	2024/12/29	0.31	76.38	19.01	0.17	15.87	1.97	33.03	0.19	g/L
12	2024/12/30	0.32	77.83	18.45	0.16	16.19	1.91	32.81	0.19	g/L

Table 52: Analysis Result of Stripping Solution

No.	Li	Na	K	Ca	Mg	B	SO_4^{2-}	Unit
1	19.16	3.55	0.098	0.150	0.080	2.02	3.78	g/L
2	16.02	1.84	0.080	0.110	0.042	2.08	2.66	g/L
3	17.05	2.09	0.110	0.120	0.044	1.99	2.52	g/L
4	18.19	2.04	0.073	0.120	0.044	1.94	2.42	g/L
5	18.54	2.13	0.070	0.130	0.052	1.91	2.34	g/L
6	18.89	2.18	0.090	0.140	0.080	1.88	2.51	g/L
7	19.54	2.04	0.065	0.120	0.051	1.79	2.46	g/L
8	19.57	1.98	0.055	0.120	0.049	1.77	2.41	g/L
9	19.64	2.43	0.073	0.130	0.062	1.87	2.33	g/L
10	19.68	2.37	0.073	0.130	0.060	1.87	2.29	g/L
11	19.79	2.41	0.085	0.130	0.060	1.87	2.29	g/L
12	20.05	2.58	0.120	0.140	0.067	1.86	2.36	g/L

Table 50 to Table 52 show that the lithium content in PPG brine decreased from 3.35 g/L to 0.286 g/L after extraction. Stripping resulted in a product lithium concentration of 18.84 g/L. Lithium concentration can reach over 20 g/L by adjusting the conditions, Na about 2.2 g/L, B 1.9 g/L, sulfte 2.4 g/L, while other impurities are about 0.1 g/L.

Sodium is extracted during the process, particularly when the lithium concentration is low. The recycling of strip solution to organic wash will control the sodium so that it will not affect its quality.

This test work has been running for 694 hours, with no abnormalities.

Figure 96: Continuous Extraction Device Diagram (Source: Ganfeng 2024)

10.4.3.4 Conclusion

During testing, 6-stage extraction, 6-stage washing and 13-stage stripping were adopted and ran for 694 hours. No abnormalities have been found.

- Operating conditions:
  - organic flow rate of 170 ml/min, brine flow rate of 37.5-38.0 ml/min
  - washing solution flow rate of 3.0 ml/min
  - The stripping solution flow rate is 11-11.5 ml/min
  - extraction phase ratio is 4.47-4.53
  - washing phase ratio is 56.67; and
  - the stripping phase ratio is 14.78-15.45.
- Main Results Achieved
  - Extraction efficiency is ≥ 90%
  - stripping efficiency ≥ 94%
  - Strip solution analysis
    - lithium concentration of 19 ~ 20 g/L
    - sodium concentration 0.2 ~ 0.25 g/L
    - iron concentration is about 0.12 ~ 0.20 g/L
  - Lithium concentration of raffinate is about 0.25 ~ 0.35 g/L, and the iron concentration is about 0.2 g/L.

10.5 Lithium Carbonate and Hydroxide

After purification steps, the purified brine is sent to the Li_2CO_3 and $LiOH \times H_2O$ plants.

Again, since these are traditional methods there is no test work. Ganfeng will use their industrial experience to define the design parameters.

10.6 Closing Statement

Solvent extraction of lithium has been extensively tested with a novel extractant formulated for the PPG brine.

A 75% overall lithium recovery efficiency factor has been applied to calculate the final LCE production. The recovery is based on test work carried out to date and assumptions provided by Ganfeng.

11.0 MINERAL RESOURCE ESTIMATES (EFFECTIVE DATE: DECEMBER 31, 2025)

11.1 Pozuelos

11.1.1 Overview

The Resource Estimate was developed using three-dimensional block modelling with Leapfrog Geo (Seequent) software. The modelling was supported by geophysical, geological, and geochemical data and interpretations made by Golder. The resources estimate was prepared in according with the requirements of S-K §229.1300. A 125 mg/l lithium concentration cut-off was applied to the resource estimate.

The modelling method consisted of the following steps:

- The footprint of the resource zone was defined based on the interpreted boundaries of the salt flat and the deposit characteristics.
- The drilling data and MT results were interpreted to identify primary lithologies and their continuity within the resource zone. Data interpolation was conducted to develop a full 3D geological model.
- The 3D geological model was divided into five Hydrostratigraphic Units (HSUs), which are groups of lithologies with similar hydrological properties.
- The drainable porosity data from Neutron logs were used to calculate the amount of lithium-enriched brine available for the Pozuelos project.
- The assays from the brine samples from packer testing were interpolated in the block model to obtain the amount of lithium available to estimate the total resource stated as LCE.

11.1.2 Hydrostratigraphic Model Development

11.1.2.1 Geological Considerations

The Pozuelos project is located in a hypersaline salar corresponding to the topographic low area of the basin. Its resource comprises the brine hosted in clastic and evaporitic sediments beneath the surface.

The evaporitic facies are limited to the upper layers of the salar in the central and southern areas. The evaporitic facies overlie thick beds of clastic sediments that rest over fractured and altered rocks of the Ordovician and Eocene-Oligocene age.

In the northern part of the basin, the brine is hosted in clastic sediments, and there are no visible evaporitic facies. The northern area seems to be isolated from the rest of the basin for Ordovician highs, which acted as barriers.

The HSUs of the salar subsurface are based on lithologies described from the recovered cores, and the author is confident in their continuity assessment.

Evaluation of the resource of a brine deposit within each HSU includes the estimation of two key components:

- The continuity and distribution of Lithium grade and,
- The aquifer portion containing brine, estimated from the Sy. This is relevant to brine deposits because brine resources occupy the pore spaces of rock or sediment.

The continuity of the HSUs was modelled using control points located in areas with data gaps. These control points were used to extend the HSU at depth in areas where the exploration was not deep enough to reach the bedrock.

The control points reflect the author's understanding of the basin. For Instance, the well PZ-2023-19 was drilled to 464 m; however, it was inferred to 629 m because the well PZ-2024-22, located at 1,500 m distance, was drilled to 602 m deep and did not reach the basement. Figure 97 shows the location of the control points used to estimate the continuity of the HSU's.

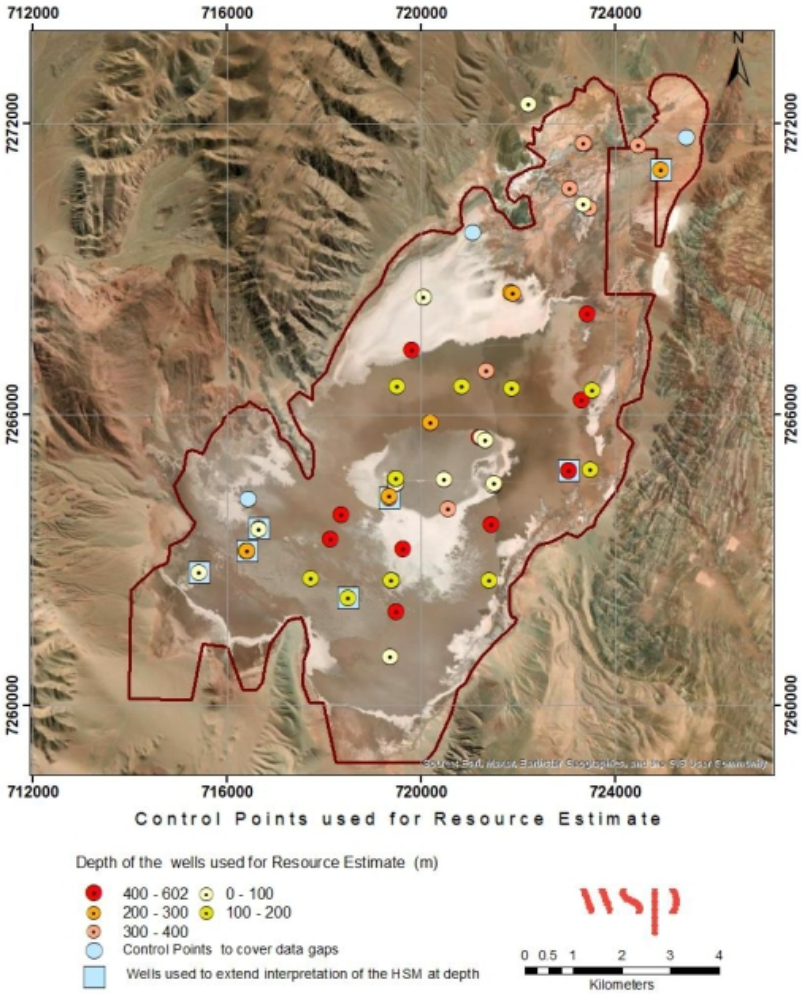

Figure 97: Location of the Control Points (Source: Golder, Jan 2025)

11.1.2.2 Brine Model Development

The footprint of the Resource Zone was defined based on the interpreted boundaries of the salt flat, the deposit characteristics and boundaries of the mining properties. The boundaries definition included the following:

- The East, West and North boundaries were defined as the outer bounds of the salt flat, based on topography,
- The southwest boundary coincides with the limit of the mining property.

- The mining properties from third parties within the salar area were clipped and excluded from the estimation.

The top of the geological model has been restricted to the topography of the Pozuelos saline surface because the static level from the Saline Lake varies from 0.23 m to 0.77 m.

This difference is negligible, considering that the DEM's vertical resolution is 30 m (greater than the difference between the static level and the topography).

The bottom of the resource zone was defined as follows:

- Where the boreholes were not deep enough to encounter the bedrock, the resource was extended according to interpretations of the horizontal continuity of the facies. The extension at depth was based on the interpretation of the continuity of the facies based on deep wells nearby. The uncertainties of extending the resource were addressed with the resource categorisations.

- In the south of the salar (the area around PZ-.2023-24, PZ-DDH17 SP-2017-12 and PZ-2024-28bis), the resource was extended to the top of the Siltstone unit since it was excluded from the estimation.

The delineated resource area covers 7,733.75 Ha. It is shown in Figure 98.

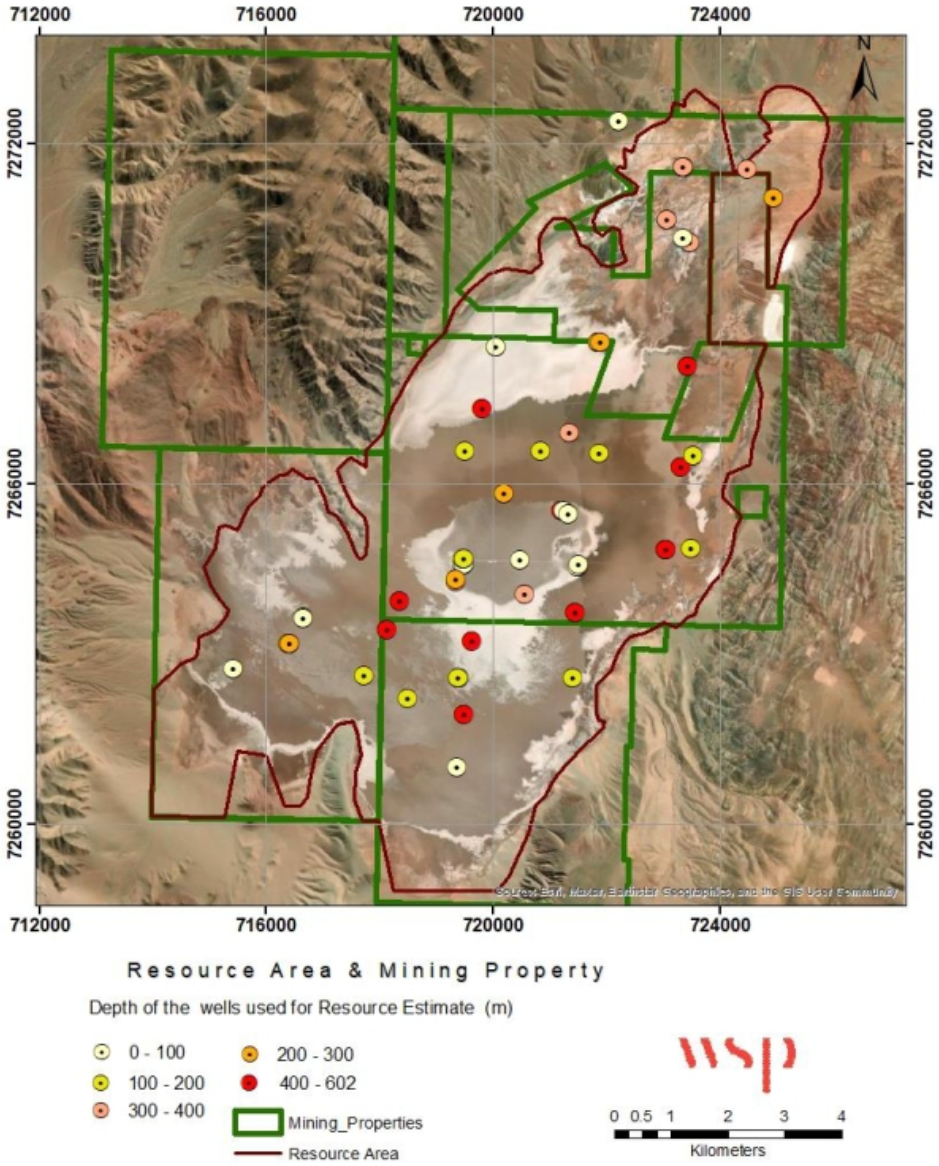

Figure 98: Resource Area vs Mining Properties (Source: Golder, Jan 2025)

11.1.2.3 Percentage of Each HSU in the Total Resource Volume

The volume percentage that each HSU occupies in the Resource Estimate is shown in Table 53.

Table 53: Percentage of Each Hydrostratigraphic Unit in the Total Volume of the Block Model

Unit	Rock volume (m^3) Block Model	Rock volume (km^3)	%
Saline Lake	4,040,736,250	4.04	12.2
Mudflat	4,816,499,375	4.82	14.6
Sandy Alluvial and/or Colluvial Sediments	8,456,065,000	8.46	25.6
Muddy Alluvial and/or Colluvial Sediments	7,548,276,250	7.55	22.8
Fractured Aquifer	8,181,241,875	8.18	24.8
Total	**33,042,818,750**	**33.04**	**100.0**

Figure 99 illustrates the volume of each unit in the HSU.

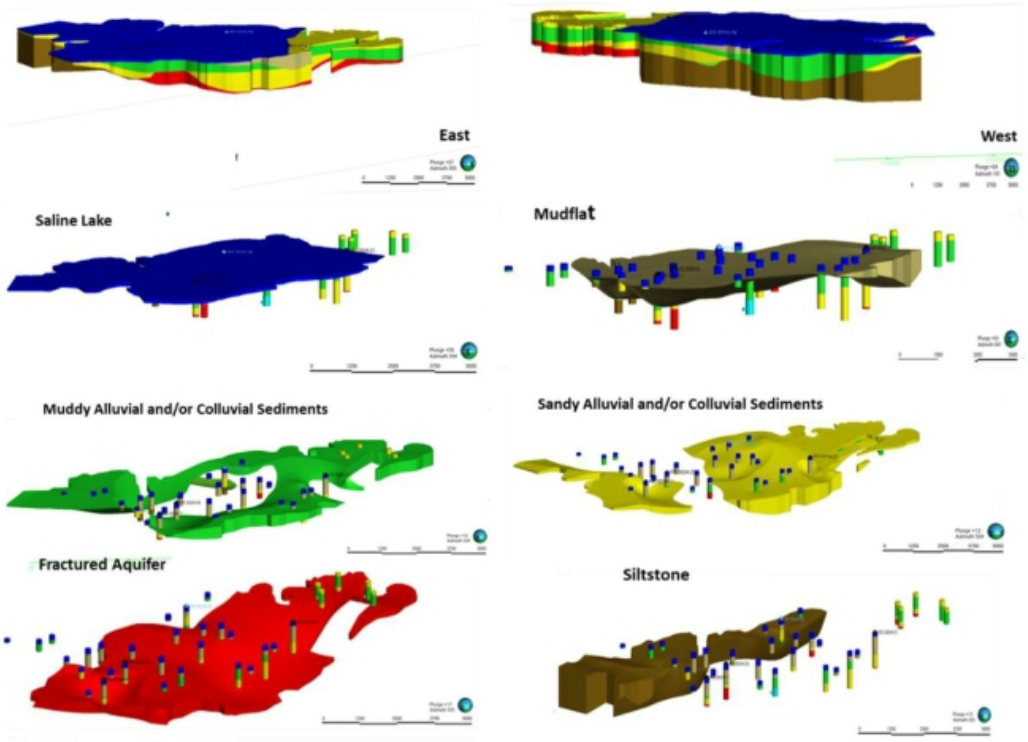

Figure 99: Hydrostratigraphic Units from the Hydrostratigraphic Model (Source: Golder, Jan 2025)

11.1.2.4 Drainable Porosity Assigned to Each Hydrostratigrafic Unit

The QPs assumed that the averages of Sy from the Neutron downhole logging are more representative of the lithologies of the salar. It remains conservative and reasonable, according to the author's experience with similar aquifers.

The drainable porosities used in the Leapfrog model to estimate the amount of drainable brine from each HSU are shown in the Table 54.

Table 54: Averages of Sy Used for the Resource Estimate

Hole ID	HGU	Sy (%)
Li.Pz.RW-15	Mudflat	5**
Li.Pz.RW-15	Saline Lake	5
Li.Pz.RW-11	Sandy Alluvial and/or Colluvial Sediments	16
Li.Pz.RW-11	Muddy Alluvial and/or Colluvial Sediments	17
Li.Pz.RW-11	Fractured Aquifer	10*

** * Estimation from porosity relationships for unconsolidated material (Source Johnson,1967),*
**Visual estimation. Further work is required to confirm this value.*

The use of Neutron logs is accepted by the guidelines published by Huston and others in 2011.

The Histograms of the Sy (PHIEE) for each unit and all the resource model domains are in Figure 100 to Figure 102.

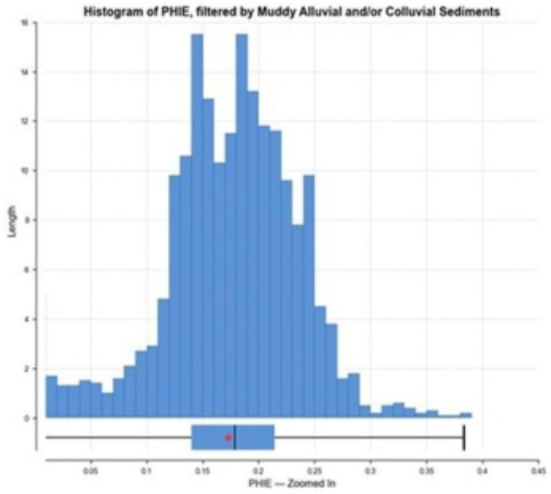

Figure 100: Histograms of the Sy (PHIEE) for the Muddy Alluvial and Colluvial Sediments (Source: Golder, Jan 2025)

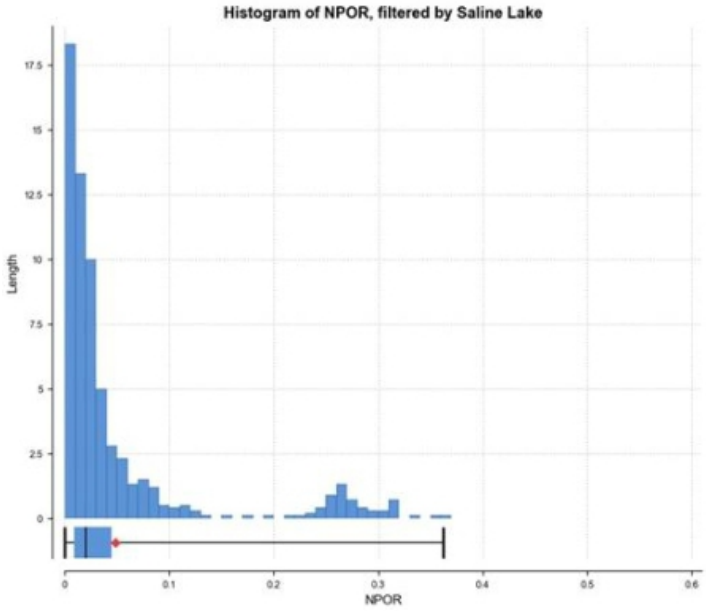

Figure 101: Histograms for Porosities of the Saline Lake (Source: Golder, Jan 2025)

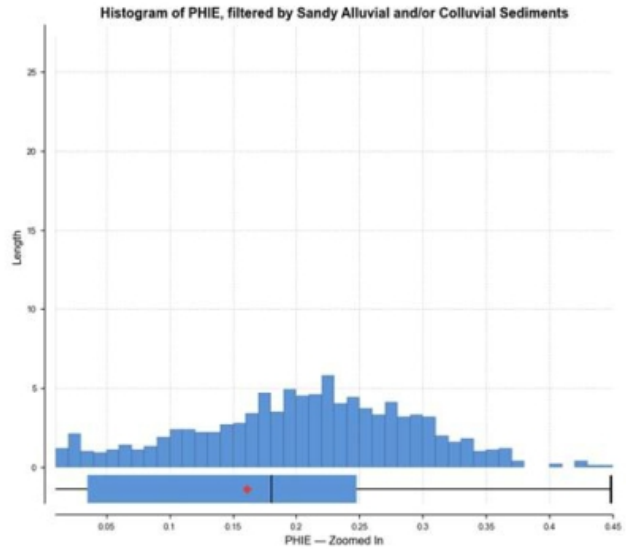

Figure 102: Histograms of the Sy (PHIEE) for the Sandy Alluvial and Colluvial Sediments (Source: Golder, Jan 2025)

11.1.2.4.1 Sy Estimation of the Fractured Aquifer

The high grade of folding and faulting between the Copalayo (Ordovician) and Viscachera formations at the Pozuelos basin may indicate that the Fractured aquifer is a mix of both formations. The lithologies are silts and clays for both formations. The impact is not so significant because both have sediments with similar lithologies and Sy.

As this acts as a fractured aquifer, the voids, which are much better connected than matrix pores, can constitute an effective conduit for groundwater flow.

Secondary porosity is the additional porosity acquired after the original rock formation process. Whether the porosity is primary or secondary, the combined properties are included in the effective porosity. In most cases, the development of secondary porosity increases the effective porosity of a porous material (Hydrogeologic properties of earth materials and principles of groundwater flow / William W. Woessner, Eileen P. Poeter – Guelph, Ontario, Canada, 2020.)

The extensive faulting and folding due to geological processes around the Pozuelos Basin, and the thin stratification layering, facilitated the movement of fluids along the stratification planes of the PZ fractured aquifer increasing the alteration and weathering of the original rock; those processes along with the erosion of sand and silts from Tertiary sediments made the Fractured aquifer a good reservoir with a high fraction of sediments with primary porosity.

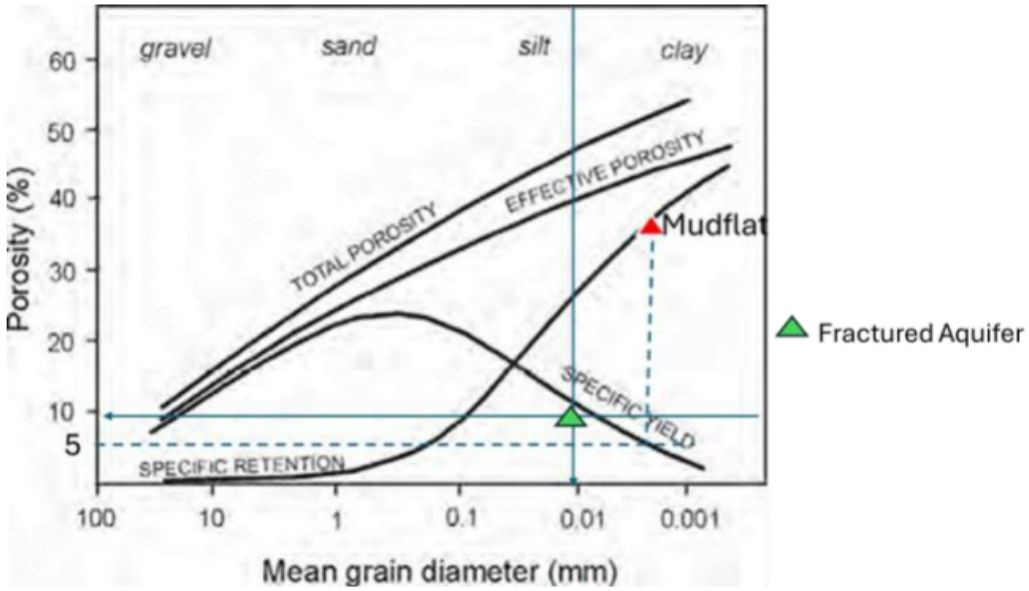

Figure 103: Porosity relationships for unconsolidated material (Source: Johnson 1967)

The value of 10% was assigned based on the following reasons:

- The cores of the lithologies interpreted as Fractured Aquifer Unit, which was interpreted as an aquifer overlying the Ordovician solid bedrock.
- Neutron logging results
- Based on the drainable porosities of the bibliography for the granular facie of silts and clayey silts.

The specific yield used for the Fractured Aquifer is considered conservative and applicable, capable of passing any rational audit. Further work is required to confirm this value.

11.1.3 Block Model

The Lithium concentrations from the samples of the packer test were used to estimate the distribution of the Lithium concentrations within the Block Model.

The size of the cells of the block model that better represents the distribution of the samples is 200 m for the X and Y directions and 1 m along the Z axis.

The lithium distribution within the Block Model was done with an Inverse Distance interpolator, however it was compared with ordinary Kriging.

The Swat Plot from Figure 104 shows the lithium dataset (Yellow dots) and the estimation done with the ordinary kriging (blue dots) and Inverse Distance (purple dots).

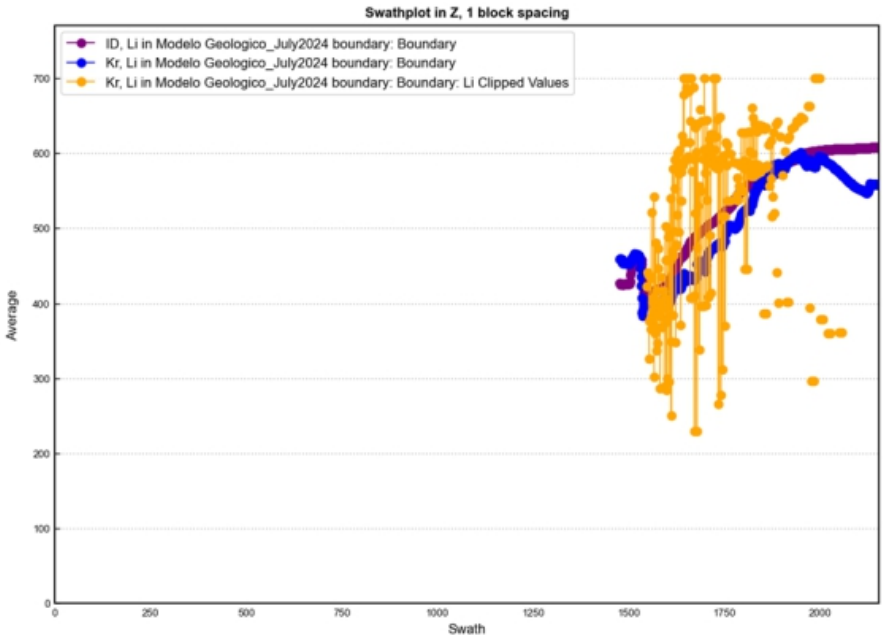

Figure 104: Swat Plot Showing the Concentrations of Lithium from the Samples, Kriging and Inverse Distance Estimator (Source: Golder, Jan 2025)

The author of this report considered that Inverse distance presents a better correlation with the field data and accurately represents higher concentrations. The Swat plot shows that the Ordinary Kriging smooths the higher concentrations, lowering the general average of the lithium concentration of the estimated resource.

The Lithium distribution within the Block Model resulted as it is shown in Figure 105.

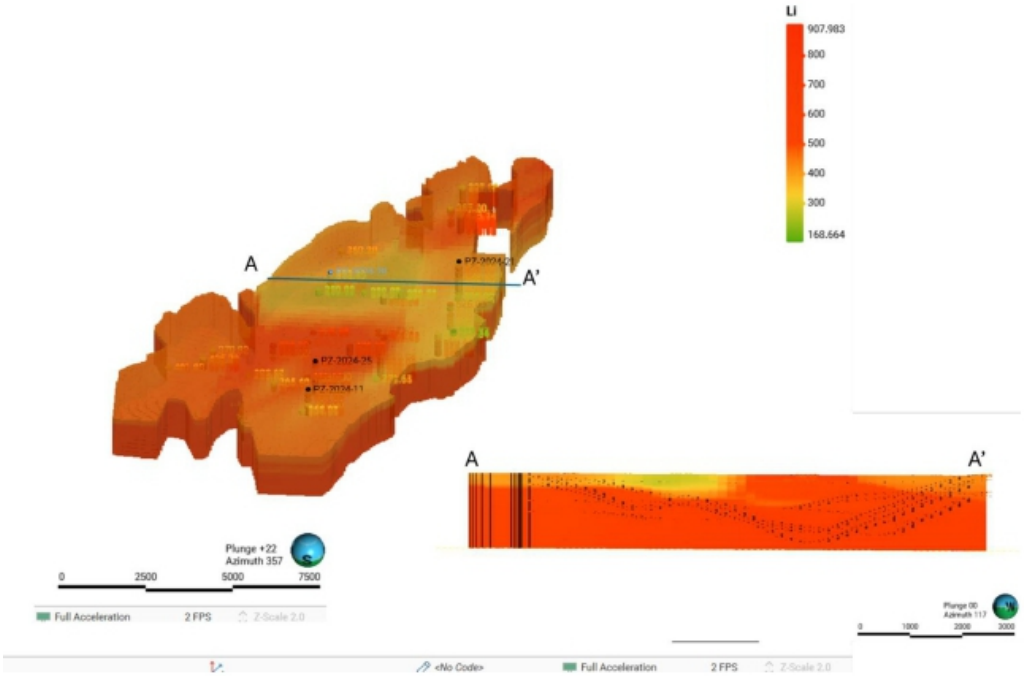

Figure 105: Lithium Distribution from the Block Model (Source: Golder, Jan 2025)

11.1.4 Resource Categorization

Measured, Indicated and Inferred categories were based on the following qualitative assessment of the certainty associated with each Hydrostratigraphic unit.

- Measured Resources were estimated to be a maximum distance of 1,700 m from the nearest samples.
- Indicated Resources were considered between 1,700 m to 2,300 m.
- Inferred Resources were considered at a distance greater than 2,300 m to the limit of the resource area.
- If samples were not encountered between those distances, the author used his criteria to categorize the resource based on the confidence of the continuity of the aquifer.
- The bottom of the Measured resource was 10 m below the existing drillhole, Indicated Resources were extended between 20-30 m below the Measured Resource. In locations with shallow drill holes from 2017, next to deeper drill holes from 2023/2024, the resource was categorized as Measured or Indicated based on the confidence of the author in the continuity of the aquifer
- In the north of the resource area, the uncertainty of the great distances between samples was addressed, categorising the resource as indicated around the well PZ-2024-16PW and Inferred further to the north.
- At the west of the salar where most of the wells did not reach the basement, the resource was categorised as Measured, around the well PZ-2024-28 Bis.

- Below the alluvial sediments from the salar margin, the resource was categorised as Inferred due to uncertainties regarding the porosities and lithium concentration.
- In the northeast of the salar, the Inferred resource was extended towards the north below the indicated resource, assuming the continuity of the facies encountered in the well PZ-2024-22.

For reference, the resource category domains estimated for the Pozuelos Project were compared against the brine deposit borehole density guidelines suggested by Houston et al. (2011). Pozuelos should be conservatively classified as an immature (clastic-dominant) salar, which would suggest for different categories of resources a drill spacing of 2.5 km for the Measured category, 5 km for the Indicated category and 7 to 10 km for the Inferred category.

Leapfrog modelling is considered to be reasonable and appropriate for Resource Estimation according to the S-K regulations.

Figure 106 shows the distribution of the resource categories within the delineated area.

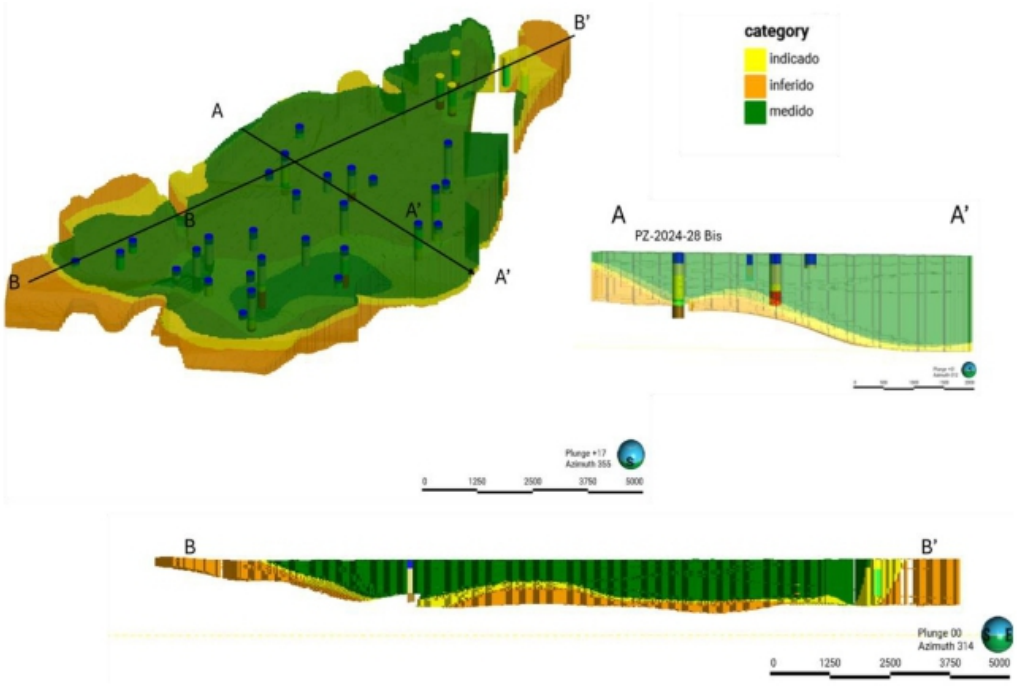

Figure 106: Measured, Indicated and Inferred Resource Distribution (Source: Golder, Jan 2025)

11.1.5 Resource Estimate

The resource estimate for Pozuelos was prepared in accordance with the requirements of S-K §229.1300 and uses the best practices methods specific to brine resources, including a reliance on core drilling and sampling methods that yield depth-specific chemistry and drainable porosity measurements. A 125 mg/l lithium concentration cut-off was applied to the resource estimate.

The Mineral Resource Estimate is detailed in Table 55. A summary of the Measured, Indicated and Inferred Resource Estimate is shown in Table 56.

Table 55: Resource Estimated for Each HSU (Effective Date: December 31, 2025)

Unit	Rock volume (km^3)	Average effective porosity (%)	Brine volume calculated (km^3)	Li (mg/L)	Li Calculated (tonnes)	LCE Calculated (tonnes)
Fractured Aquifer	7.37	10.00	0.74	585.6	431,737	2,296,839
Muddy Alluvial and/or Colluvial Sediments	7.69	17.00	1.31	571.6	728,470	3,875,461
Mudflat	6.06	4.00	0.30	461.4	139,863	744,071
Saline Lake	4.12	5.00	0.21	418.7	86,319	459,219
Sandy Alluvial and/or Colluvial Sediments	8.24	16.00	1.32	510.0	669,450	3,561,475

Table 56: Measured, Indicated and Inferred Resource Estimate for the Pozuelos (Effective Date: December 31, 2025)

Salar	Resource Category	Aquifer Volume (km^3)	Brine Volume (km^3)	Average Lithium Concentration (mg/L)	Lithium (tonnes)	LCE (tonnes)
Pozuelos	Measured Resource	20.45	2.21	490.5	1,097,038	5,836,244
	Indicated Resource	3.54	0.41	528.7	221,877	1,180,384
	Measured + Indicated	**23.99**	**2.62**	**510.0**	**1,318,915**	**7,016,628**
	Inferred Resource	9.50	1.25	581.0	736,924	3,920,437

Notes:

1) S-K §229.1300 definitions were followed for Mineral Resources.

2) Lithium carbonate equivalent ("LCE") is calculated using the Li: LCE factor = 5.322785 multiplied by the mass of Lithium.

3) The Mineral Resource Estimate is not a Mineral Reserves Estimate and has no demonstrated economic viability.

4) Comparisons of values may not be equivalent due to rounding of numbers and the differences caused by use of averaging methods.

5) The Siltstone unit was not included in the resource estimate.

6) Project economics in this report are not based on Inferred Mineral Resource.

7) A cut-off grade of 125 mg/l has been applied to the mineral resource estimates. An FoB price forecast of US$18,000 per metric ton of Li_2CO_3 and US$17,800 per metric ton of coarse particle $LiOH \times H_2O$ for years beyond 2028 is used. A 75% overall lithium recovery efficiency factor has been applied to calculate the final LCE production.

8) The cutoff grade is based on the various inputs and the formula below:

$$Cutoff\ Grade = \frac{\frac{(Total\ capital\ expenditure + Total\ operating\ expense)}{Total\ brine\ extracted}}{(Recovery * Conversion\ from\ Li\ to\ Li_2CO_3 * Projected\ LCE\ Price * (1 - Export\ Duties) * (1 - Royalties))}$$

Where:

Total capital expenditure = US$ 3,301 million

Total operating expenditure = US$ 16,332 million

Conversion from Li to Li_2CO_3 = 5.323

Projected long term LCE price = US$ 18,000 per ton of LCE

Export duties = 0%

Royalties = 3.0%

Calculated recovery = 75%

Resulting in a calculated cut-off grade of 125 mg/l.

Factors that may affect the Brine Resource estimate include: locations of aquifer boundaries; lateral continuity of key aquifer zones; presence of fresh and brackish water which have the potential to dilute the brine in the wellfield area; the uniformity of aquifer parameters within specific aquifer units; commodity price assumptions; changes to hydrogeological, metallurgical recovery, and extraction assumptions; density assignments; and input factors used to assess reasonable prospects for eventual economic extraction. Currently, Mr. James Wang (the QP), does not know any environmental, legal, title, taxation, socio-economic, marketing, political, or other factors that would materially affect the current Resource estimate.

11.1.5.1 Historical Resources Estimate

The previous Lithium Resources Estimate at the Pozuelos corresponds to the work of Hains and Fourie (2018) for LSC Lithium, followed by the internal reports from Litica Resources (2021,2022), and Lithos Consulting Group (April 2024).

11.1.5.1.1 2018 Estimate - Hains and Fourie

The 2018 estimation was carried out using the polygon method with data from 16 boreholes drilled in 2017. The polygon volumes were determined by calculating the surface area of each polygon and the lithological thicknesses for each hole. The final depth of each polygon was established either from the available drill data or from the available seismic profile data. The polygon volume was multiplied by the RBRC value for the respective lithologies to derive the available brine volume for each lithological unit in each polygon, and by the grade or lithium content representative of the polygon.

11.1.5.1.2 2021 Estimate - Litica Resources

In August 2021, a Resource Estimate was carried out using Leapfrog Geo software. The estimation included drilling data from the 2017 and 2018 diamond wells, and the depth of the resource was based on the depth of the drill holes.

Litica Estimation used drainable porosities from the Neutron logs from boreholes Li.Pz.RW-12 and Li.Pz.RW-15. The raw data from the neutron logging was processed and converted to drainable porosity by geophysics from Pluspetrol and given to Litica modelers to use in the estimation.

Porosities used by Litica in 2021 and 2022 are in Table 57.

Table 57: Drainable Porosities from Neutron Logs (Source: Bea., Chanampa 2021/2022)

LITOLOGIAS	DESCRIPCION	RANGOS LITICA	RANGOS BIBLIOGRAFIA (Sander 1998)	RANGOS RBRC	MEDIA	P10	P90
		%	%	%	%	%	%
FHB	Halita fracturada	6-13		0.5-12	4	2	11
MH	Halita compacta	2-9		1-4	4	3	9
LSND	Arena superior	11-30	10-28 (fina), 22-35 (gruesa)		18	13	28
UG	Grava superior	12-26	13-35	4-6	19	15	26
USND	Arena inferior	17-31	10-28, 22-35	1-18	23	18	30
LG	Grava inferior	11-31	13-35	1-16	19	13	27
SI	Limo inferior	6-15	3-19	1-15	5	1	12

The 2022 estimate included the geological unit the Silts (Siltstone) encountered in wells DDH17 and SP-2017-12, which was extended at depth to the basement indicated by the gravity survey from Proingeo. That estimation excluded the fractured aquifer.

11.1.5.1.3 2022 Estimate - Litica Resources

In January 2022, Litica Resources upgraded the resource using the same 2021 drill holes and drainable porositie from the Neutron, but in this estimate, the Silt unit was extended to the basement inferred from the gravity survey from Proingeo (2021). This interpretation increased the volume of the inferred resources considerably without drillhole data or samples. Litica estimation excluded the Fractured Aquifer encountered in DDH-400 and Pz.18-02.

11.1.5.1.4 April 2024 Estimate - Lithos Consulting Group

In April 2024, the Lithos Consulting group estimated the Pozuelos resource using Leapfrog Geo software, incorporating the wells from the 2023 exploration campaign and using the gravity survey as the bottom of the estimation. Drainable porosity from each HSU was arbitrarily quantified from the flow measured in the packer tests.

This estimate excluded the Silt unit and the Ordovician Fractured aquifer because they were considered hydrological basements.

11.1.5.1.5 December 2024 Estimate - Golder

The QPs estimated the resources was described in this report. The estimation followed CIM (Canadian Institute of Mining, Metallurgy and Petroleum) was based on a deep analysis of the existing drainable porosity data collected throughout the project life.

The resource was estimated using the drainable porosities from the Neutron logging, but with lower values because the higher outliers were not included in the Resource Estimate.

All the data, which was reviewed and compared with the photos of the core holes, The QPs concluded that the silt unit (Siltstone) is the hydrogeological basement, hence it was excluded from the estimation.

The Hydrostratigrafic Model included the Ordovician Fractured Aquifer, which has been demonstrated with packer testing to host drainable lithium-enriched brine.

This estimation did not consider the basement from the gravity survey from Proingeo 2021, as explained in Section 7.4. Table 58 summarises the resource estimations done throughout the project life.

Table 58: Historical Resource Estimates for Pozuelos

Year /Author	Hains & Fourie 2018		Litica Resources 2021		Litica Resources 2022		Lithos Consulting 2024	Golder Dec 2024	
Resource Category	M+I	Inferred	M+I	Inferred	M+I	Inferred	Total Resources	M+I	Inferred
Brine Volume (km^3)	0.0057	0.0057	1.40	0.90	1.05	3.34	1.10	2.62	1.25
Lithium Grade (mg/L)	387	340	458	458	480	414	509	510	581
In Situ Lithium (Tonnes)	243,536	93,360	664,782	385,608	500,320	1,904,621	557,770	1,318,915	736,924
LCE (Tonnes)	1,296,000	497,000	3,536,639	2,051,435	2,663,203	7,470,880	2,969,009	7,016,628	3,920,437

11.2 Pastos Grandes

11.2.1 Resource Model Domain and Aquifer Geometry

The resource model domain is constrained by the following factors:

- Upper Boundary: The upper boundary of the model is determined by the highest elevation samples within the dataset, and/or the phreatic brine level.
- Lateral Extent: The lateral extent of the resource model is confined within the boundaries of the mining claims in the Salar. Additionally, the extent can be restricted in some cases by the contact between the Quaternary basin and the underlying basement rock.
- Lower Boundary: The lower boundary of the model domain is set to coincide with the basement from the geological model or the total depth of 660 m when the basement is not present.

11.2.2 Specific Yield

The specific yield values were derived from 115 valid drainable porosity analyses of undisturbed samples, analyzed by GeoSystems Analysis. Unlike lithium concentration data, which shows spatial correlation due to geological processes influencing its distribution, the drainable porosity data exhibits no such spatial correlation. This is evident in Figure 107 which shows the variogram of specific yield with no discernible pattern or trend over distance, indicating a lack of spatial correlation.

This lack of correlation is primarily because the Sy values are highly dependent on the lithology of the project area, resulting in considerable stochastic variability. After conducting exploratory data analysis, it was concluded that assigning representative values to each geological unit would provide more accurate results than using interpolation methods like kriging.

Figure 108 presents a violin plot of the specific yield distribution across different geological model units, highlighting the variability within and between units. It is clear from the figure that different geological units exhibit distinct distributions of specific yield values, reinforcing the decision to assign values based on geological units.

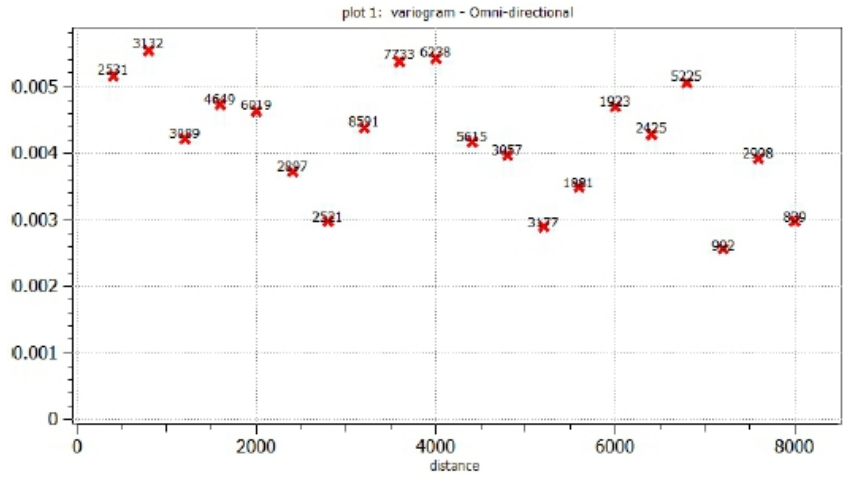

Figure 107: Specific Yield Variogram Showing no Spatial Correlation (Source: AW, Dec 2024)

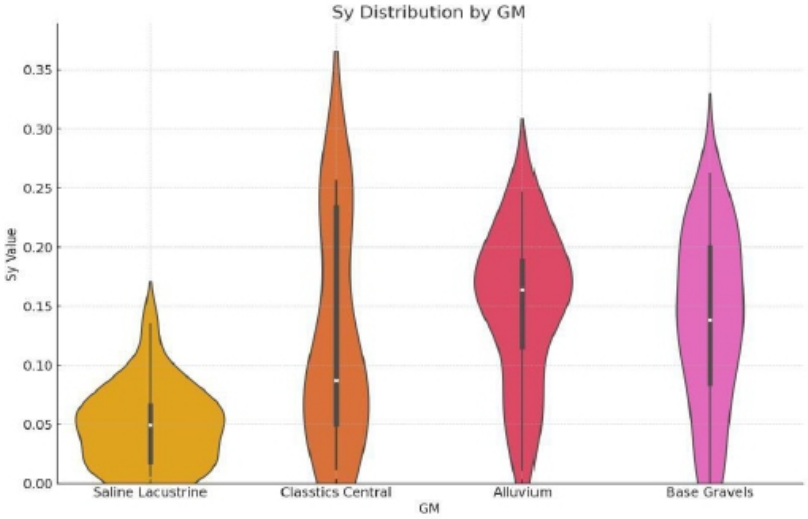

Figure 108: Specific Yield Violin Graph by Different Geological Model Unit (Source: AW, Dec 2024)

Table 59 provides a summary of the drainable porosity statistics for the geological units, based on a total of 115 valid samples. This table further supports the heterogeneity observed across different units.

Table 59: Summary Statistics of Drainable Porosity for Geological Units

Unit	Samples	Average	Standard Deviation
Alluvium	32	14.9%	6.2%
Saline Lacustrine	23	4.6%	3.3%
Central Clastics	13	12.2%	8.6%
Base Gravels	47	13.8%	7.3%
All units	115	12.1%	7.5%

11.2.3 Brine Concentrations

The distributions of lithium and potassium concentrations in the model domain are based on a total of 530 brine analyses (not including QA/QC analyses). Table 60 shows a summary of the brine chemical composition.

Table 60: Summary of Brine Chemistry Composition

Composition	B	Ca	Cl	Li	Mg	K	Na	SO_4	Density
Units	mg/L	mg/L	mg/L	mg/L	mg/L	mg/L	mg/L	mg/L	g/cm^3
Maximum	2460.0	15661.0	196869.0	701.0	5130.2	7221.0	130032.2	13998.0	1.2
Average	564.4	865.8	172164.8	401.0	2340.8	3963.5	102830.7	7706.2	1.2
Minimum	7.0	5.0	116.0	5.0	5.0	7.5	196.0	12.0	0.9

11.2.4 Resource Category

The S-K §229.1300 (September 2020) adopted the following definition standards for minerals resources:

- ***Inferred Mineral Resource*** is that part of a mineral resource for which quantity and grade or quality are estimated based on the basis of limited geological evidence and sampling. The level of geological uncertainty associated with an inferred mineral resource is too high to apply relevant technical and economic factors likely to influence the prospects of economic extraction in a manner useful for evaluation of economic viability. Because an inferred mineral resource has the lowest level of geological confidence of all mineral resources, which prevents the application of the modifying factors in a manner useful for evaluation of economic viability, an inferred mineral resource may not be considered when assessing the economic viability of a mining project, and may not be converted to a mineral reserve.

- ***Indicated Mineral Resource*** is that part of a mineral resource for which quantity and grade or quality are estimated on the basis of adequate geological evidence and sampling. The level of geological certainty associated with an indicated mineral resource is sufficient to allow a qualified person to apply modifying factors in sufficient detail to support mine planning and evaluation of the economic viability of the deposit. Because an indicated mineral resource has a lower level of confidence than the level of confidence of a measured mineral resource, an indicated mineral resource may only be converted to a probable mineral reserve.

- ***Measured Mineral Resource*** is that part of a mineral resource for which quantity and grade or quality are estimated on the basis of conclusive geological evidence and sampling. The level of geological certainty associated with a measured mineral resource is sufficient to allow a qualified person to apply modifying factors, as defined in this section, in sufficient detail to support detailed mine planning and final evaluation of the economic viability of the deposit. Because a measured mineral resource has a higher level of confidence than the level of confidence of either an indicated mineral resource or an inferred mineral resource, a measured mineral resource may be converted to a proven mineral reserve or to a probable mineral reserve.

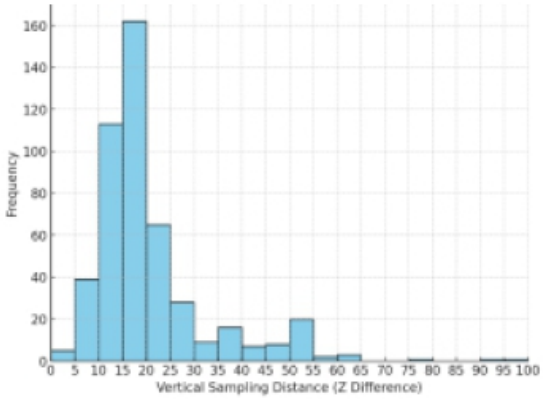

Figure 109: Histogram of Vertical Sampling Distances (Source: AW, Dec 2024)

Figure 109 shows the vertical sampling distribution, which predominantly falls between 15 to 20 m. This, combined with a drill hole spacing between 2 to 3 kilometers, generally provides a strong basis for the measurement and classification of resources. However, when examining the data in more detail, it becomes evident that uncertainty can vary significantly across different areas, not solely dependent on these factors. Below is a more specific analysis of each domain based on the available sampling data:

- The unsaturated zone contains no resources.

- The northern and eastern transitional zones, which show low lithium concentrations and represent the transition between brine and freshwater, were classified as indicated resources.

- The upper zone has a very limited number of samples, with unsampled intervals of up to 200 m. Because of the lack of systematic sampling, this zone is therefore classified as an inferred resource. It is also worth mentioning that several drillholes have unsampled intervals of up to 300 m.
- The central brine zone has the highest sample density and best characterization and was classified as a measured resource.
- The lower zone was incorporated due to lithium samples showing a tendency to improve with depth and was classified as an inferred resource to a depth of 660 m.
- The northern border, situated within the projected high-grade lithium brine volume but lacking direct sampling data, has been categorized as an inferred resource due to the absence of analytical confirmation of the projected high lithium concentrations.

The different zones used in this classification are schematically illustrated in Figure 110.The distribution of the category within the model across various depth sections is shown in Figure 111.

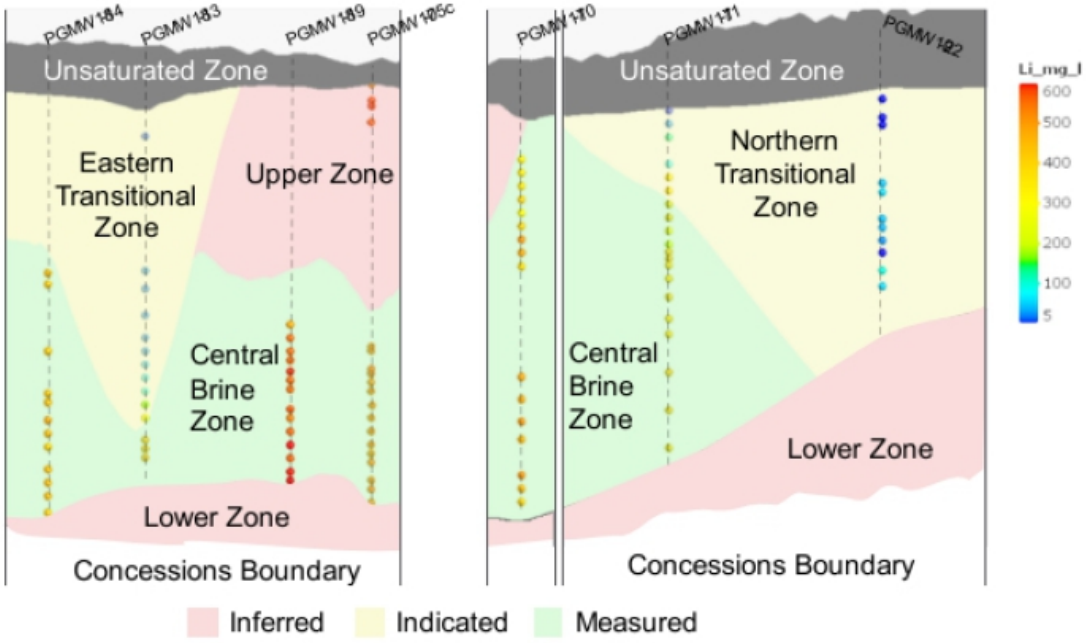

Figure 110: Schematic Section Illustrating Resource Categories Based on Data Density for Different Zones (Source: AW, Dec 2024)

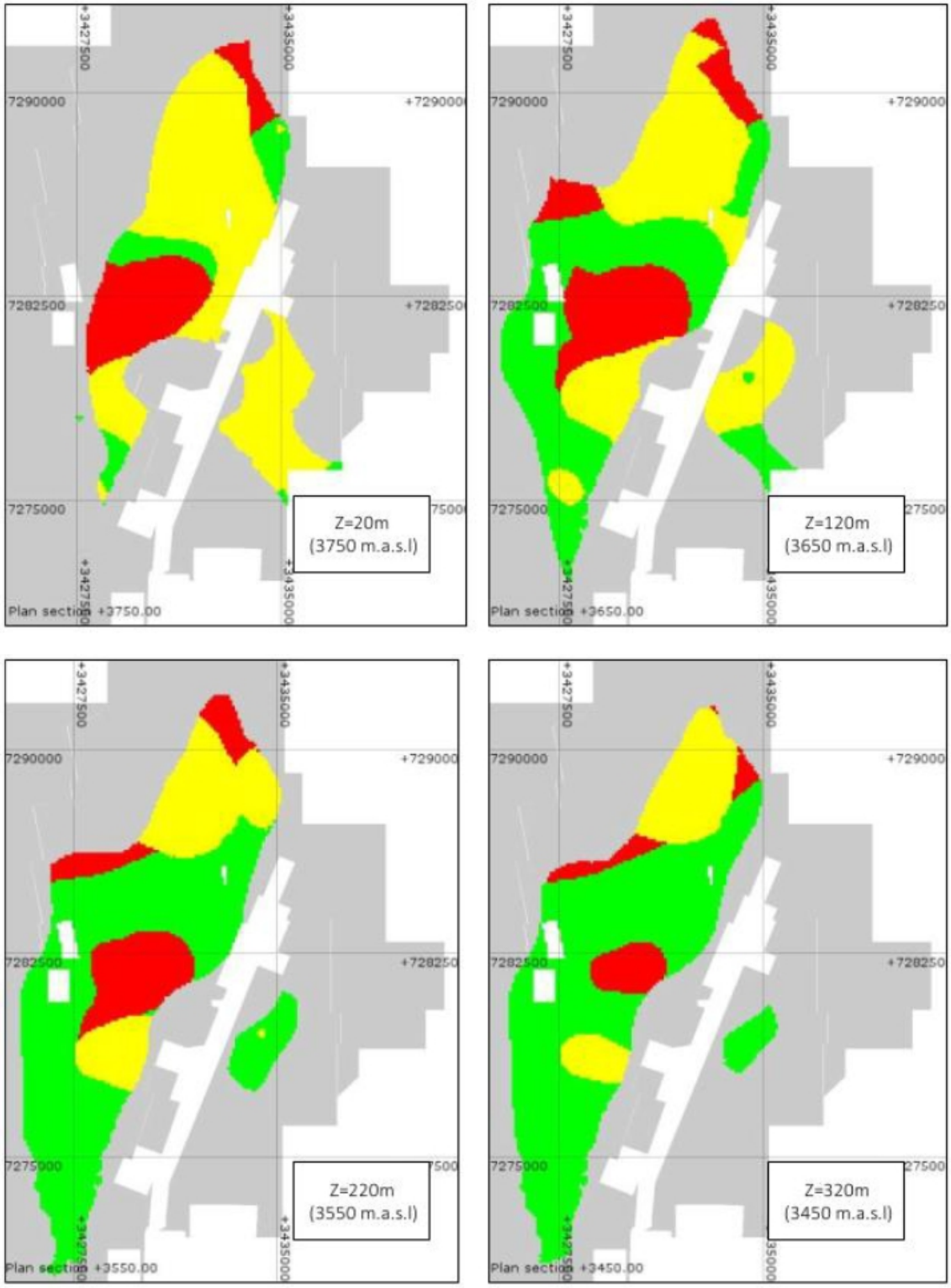

Figure 111: Spatial Distribution of Resource Classification by Depth (Source: AW, Dec 2024)

11.2.5 Resource Model Methodology and Construction

The resource estimation for the Project was developed using the Stanford Geostatistical Modelling Software (SGeMS). Brine concentrations showed two clear groups of data spatially distributed in two regions: Regions I and II. Region I is associated with high concentrations of potassium and lithium, whereas Region II is associated with low concentrations of potassium and lithium. Region II is mostly located close to the boundaries of the reservoir, where brine is affected by mixing with fresh water. The delineation of these two regions was estimated through geostatic indicator kriging. For this the following indicator function is defined:

$$I(\boldsymbol{x}) = \begin{cases} 1 & C(\boldsymbol{x}) \geq 2000\ mg/L \\ 0 & Otherwise \end{cases}$$

The conditional expected value of the indicator function is exactly the probability that the potassium concentration is larger or equal to 2,000 mg/L (or the probability that Region I prevails at that location). Given the high correlation between potassium and lithium concentrations (coefficient of correlation of 0.93), one can delineate the probability that Region I prevails by considering either potassium or lithium concentrations. That is because the ratio between potassium and lithium concentrations is about 10, similar results will be obtained by considering a lithium cut-off of 200 mg/L. Note that the lithium histogram shows two groups of data with a cut-off of 200 mg/L. By definition, the probability of occurrence of a given region is a continuous variable ranging between 0 and 1. In order to separate the data into regions a cut-off in the estimate of the indicator variable must be developed. Ritzi et al. (1994) has suggested to define the boundary between regions by the isoline Prob{C≥2000} = p, where p is estimated as either the global mean of the indicator values or the empirical relative volumetric fraction of the region. In this case, both conditions yield similar results and p=0.8 was selected which is close to the data volumetric fraction. Once the two regions were defined, kriging was applied within each region. Kriging interpolation within each specific region is sequentially performed using the semi-variogram model and the closest primary data samples within the region. The following steps were carried out to calculate the lithium and potassium resources.

- Definition of the block model (1,310,400 blocks) and block size (x=100 m, y=100 m, z=20 m). The block size has been chosen for being representative of the geological model.
- Delineate regions of high and low brine concentrations based on geostatistical indicator kriging. Spatial definition of region I with potassium concentrations larger or equal to 2,000 mg/L and region II with potassium concentrations smaller than 2,000 mg/L.
- For each region, generation of histograms, probability plots and box plots for the Exploratory Data Analysis (EDA) for lithium and potassium. No outlier restrictions were applied, as distributions of the different elements do not show anomalously high values. The experimental variograms were calculated with their respective variogram models for lithium and potassium in three orthogonal directions. Variography revealed that the variogram model is axisymmetric with respect to the z coordinate direction; the variogram model is isotropic in the horizontal direction and anisotropic in the vertical.
- For each region, lithium and potassium concentrations were interpolated for each block in mg/L using ordinary kriging with the variogram models shown in Figure 114 and Figure 115.
- Validation using a series of checks including comparison of univariate statistics for global estimation bias, visual inspection against samples on plans and sections in the north, south and vertical directions to detect any spatial bias.
- Calculation of total resources using the average drainable porosity value for each geological unit, based on the boreholes data and results of the laboratory drainable porosity analysis

11.2.5.1 Univariate Statistical Description

The univariate statistical description of lithium and potassium concentrations are based on histograms, probability plots and box plots. Table 61 presents a summary of the univariate statistics of potassium and lithium. As described in the methodology, these statistics contain information of all geological units. The mean concentration of potassium is about 10 times that of lithium. Both exhibit a similar high degree of variability with coefficients of variation of 39.6 and 39.9 for potassium and lithium, respectively. The concentrations of potassium range between 7.5 mg/L and 7,221 mg/L, and the concentrations of lithium range between 5 mg/L and 701 mg/L.

Table 61: Summary of Univariate Statistics of Li and K

	Li (mg/L)	K (mg/L)
Valid N	530	530
Mean	400	3,963
Minimum	5	7.5
Maximum	701	7,221
Variance	25,463	2,467,880
Upper Quartile	519	5,070
Median	439	4,490
Lower Quartile	358	3,266
CV	39.9%	39.6%

Figure 112 shows the lithium and potassium distribution and their cumulative distribution. Results show that the data do not strictly follow a normal distribution and that the distribution is markedly bimodal. This suggests two different groups of data that should be treated separately: one defined by potassium concentrations larger or equal to 2,000 mg/L (region I), and another associated with potassium concentrations smaller than 2,000 mg/L (region II). From a physical perspective, the first group is located within and nearby the nucleus of the Salar, whereas the second group is close to the boundaries of the resource. In the latter, brine concentrations are relatively low, reflecting the mixing with freshwater at the salar boundaries. Once data is separated into groups, the corresponding histograms of the potassium and lithium concentrations follow a Gaussian shape (see Figure 113). This gives confidence in the kriging estimate of the concentrations, which is known to be the best linear and nonlinear estimator of the concentrations when the data follows a multivariate normal distribution.

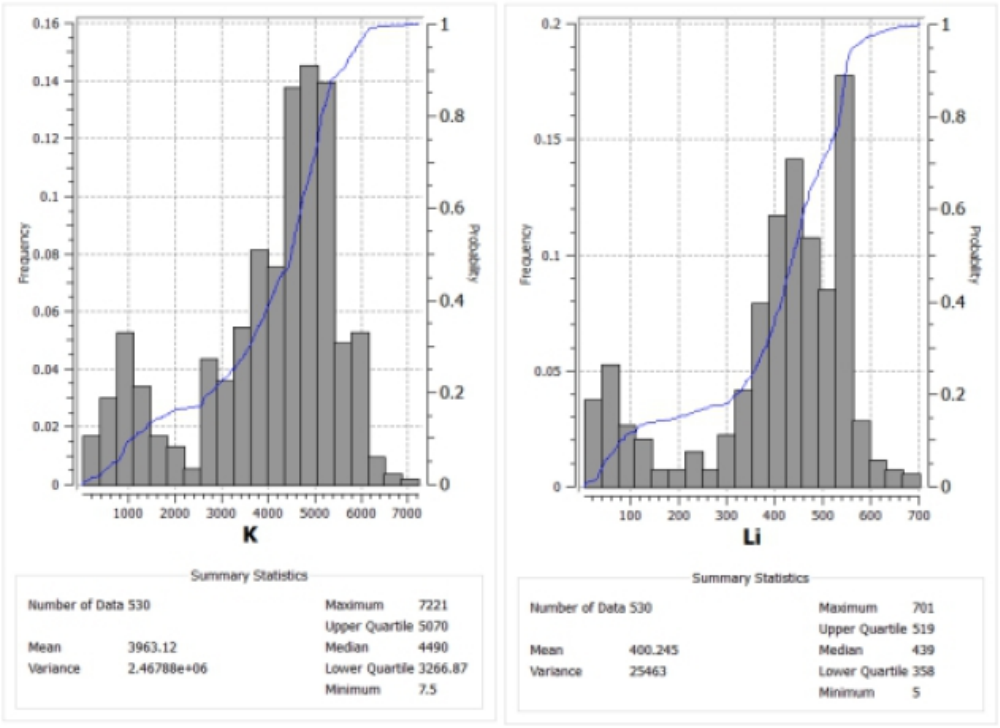

Figure 112: Lithium and Potassium Histograms and Cumulative Distributions (Source: AW, Dec 2024)

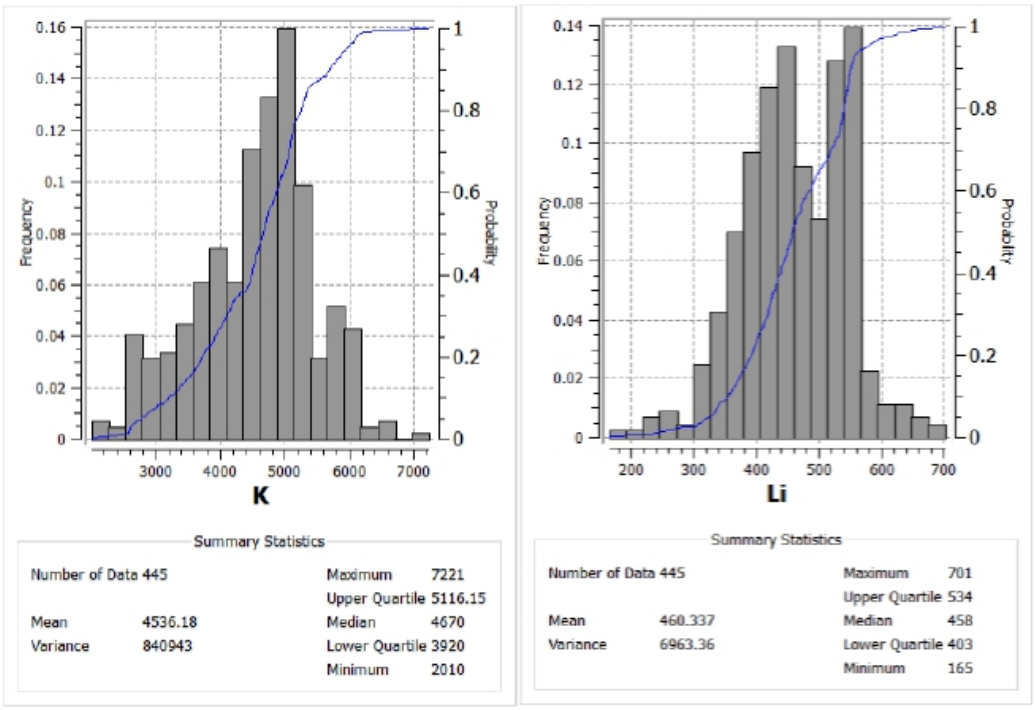

Figure 113: Lithium and Potassium Histograms and Cumulative Distributions for Region I (Source: AW, Dec 2024)

11.2.5.2 Variography

The spatial correlation for the indicator variable I(**x**), defined previously to delineate regions of different concentration groups, was reviewed using experimental variograms with the parameters shown in Table 62. Variogram models are axisymmetric with a simple exponential structure characterized by a horizontal range ah and a vertical range az. Consequently, the spatial variability was modelled using two experimental directions. The horizontal range is ah=10,800 m and the vertical range is az=2,120 m. The anisotropy ratio is about ah/az=5, which suggests that the indicator variable is only slightly stratified. The variogram ranges obtained for the indicator variable are substantially larger (double) than those obtained for the potassium and lithium concentrations, meaning that the indicator variables are more continuous in space compared with concentrations. The experimental variograms for the indicator variable with their respective variogram models are shown in Figure 114 and Figure 115.

$\gamma I = 0.25\ \gamma Exp(ah = 10{,}800\ m,\ az = 2{,}120\ m)$

Table 62: Parameters for the Calculation of the Experimental Variograms of the Indicator Variable

Variogram Parameters				Tolerance	
Lag (m)	Max. No. of Lags	Azimuth (°)	Dip (°)	Bandwidth (m)	Angular (°)
600	50	70	0	50	45
600	50	70	0	50	45
18	50	0	90	100	45

The spatial correlation for the lithium and potassium concentrations for each region were reviewed using experimental variograms with the parameters shown in Table 63. Variogram models are axisymmetric with multiple structures characterized by a horizontal range ah and a vertical range az. Consequently, for each region, spatial variability was modelled using two experimental directions. Lithium and potassium concentrations are expressed in mg/L. The variograms are expressed in mg/L squared. In general, a good correlation was found between the sample concentrations of lithium and potassium in all regions. Consequently, results show that lithium and potassium concentrations can be represented by the combination of similar fundamental structures.

Table 63: Parameters for the Calculation of the Experimental Variograms of the K and Li Concentrations

Variogram Parameters				Tolerance	
Lag (m)	Max. No. of Lags	Azimuth (°)	Dip (°)	Bandwidth (m)	Angular (°)
400	50	70	0	50	45
400	50	70	0	50	45
18	50	0	90	100	45

Region I of the formation characterized by higher potassium concentrations not influenced by fresh water were represented by the sum of two exponential variograms with a different vertical range. In this case, two structures are needed to represent the vertical variability of the concentrations. The first exponential variogram describes the short-scale spatial continuity with a vertical range of az=100 m, which contrasts with a range of ah=3,400 m in the horizontal direction. This means that the ratio of anisotropy is ah/az=34, which expresses that the geological system is highly stratified as typically observed in most sedimentary formations. The second structure reflects the appearance of more variability in the vertical direction at larger scales.

Variogram models for Region I:

$\gamma K(h) = 0.24 \times 10^6 \gamma Exp(ah = 1000\ m, az = 70\ m) + 0.59 \times 10^6 \gamma Exp(ah = 3000, az = 2100\ m)$

$\gamma Li(h) = 2400 \gamma Exp(ah = 400\ m, az = 100\ m) + 6900 \gamma Exp(ah = 3400, az = 2200\ m)$

Variogram models for Region II:

$\gamma Li(h) = 5150\ \gamma Sph(ah = 6600\ m, az = 310\ m)$

$\gamma K(h) = 0.25 \times 10^6 \gamma Sph(ah = 7500\ m, az = 260\ m)$

Region II of the formation characterized by lower potassium concentrations was represented by an anisotropic axisymmetric spherical variogram. The range in the vertical direction is 260 m for potassium and 310 m for lithium which seems to be more continuous in this direction. In the horizontal direction, the range is 6,600 m and 7,500 m for potassium and lithium, respectively. The anisotropy ratio ah/az ranges between 25 and 24 meaning that potassium and lithium have a similar stratification in region I compared to Region II. The variogram contributions are like region I but the vertical variogram model does not reflect multiple structures.

The experimental variograms with their respective variogram models are shown in Figure 114 and Figure 115.

The lithium and potassium concentrations were estimated within each specific region using the corresponding variogram models and the closest concentration data samples within the region. The interpolation methodology for estimating lithium and potassium was Ordinary Kriging (OK). The estimation was carried out separately for each parameter using their respective variogram models as appropriate.

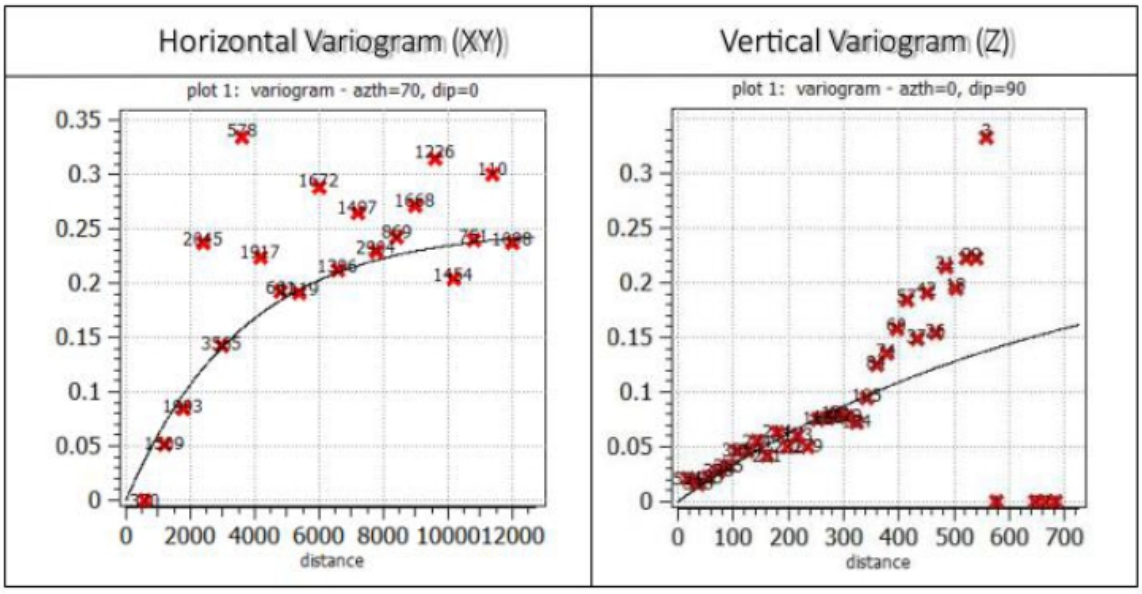

Figure 114: Experimental Variogram and Variogram Model for the Indicator Variable (Source: AW, Dec 2024)

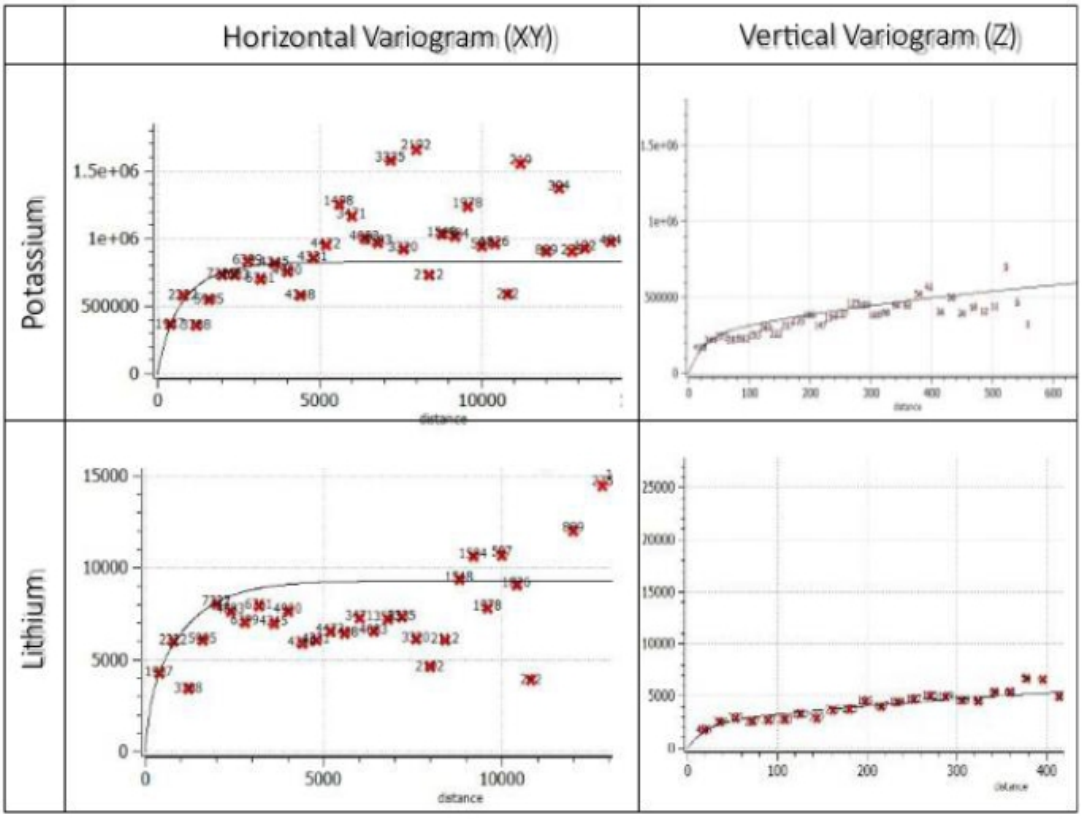

Figure 115: Experimental Variogram and Variogram Model for Potassium and Lithium in Region I (Source: AW, Dec 2024)

11.2.5.3 Grade Estimate

The grade estimates of lithium and potassium in each block inside the model were calculated applying the following operation:

$$Ri = Ci.\ Syi$$

Where: i is the indice of the block, going from 1 to 1,310,400

Ri: Grade value to be assigned (g/m^3)

Ci: Concentration value assigned from the estimation (mg/L)

Syi: Specific yield value assigned from the estimation (%)

Figure 116 through Figure 118 shows N-S, W-E, and SW-NE sections through the resource model showing lithium grade distributions in g/m^3. The resource classification was made within the limits of the block model.

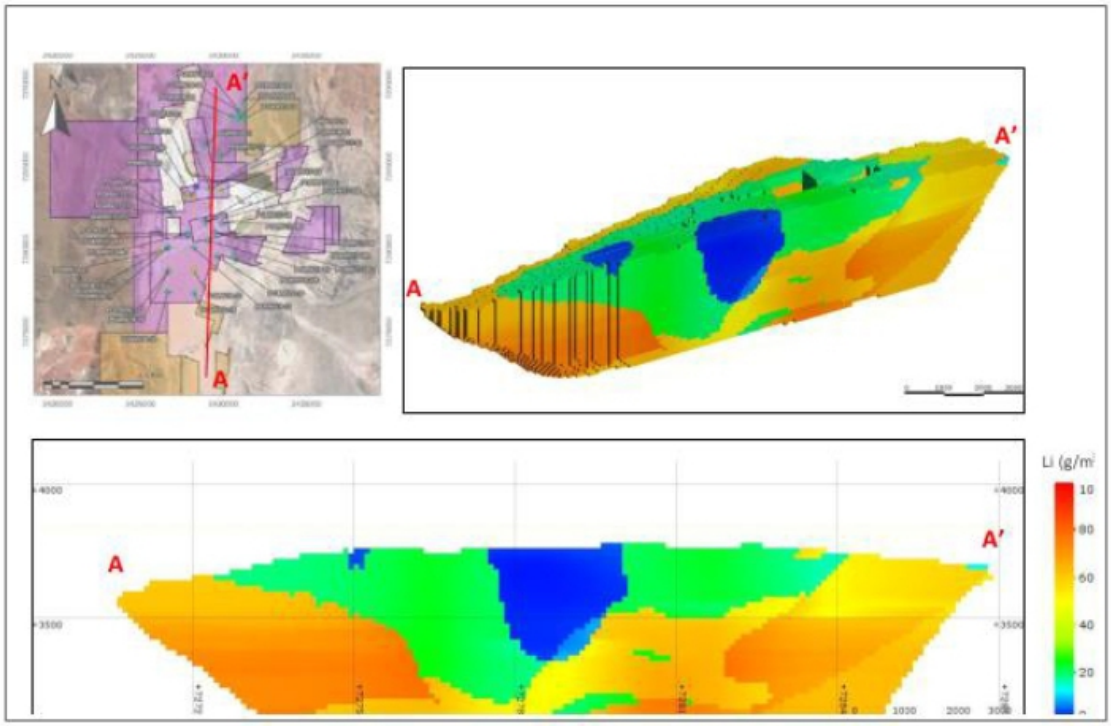

Figure 116: N-S Section through the Resource Model Showing the Lithium Grade Distribution (Source: AW, Dec 2024)

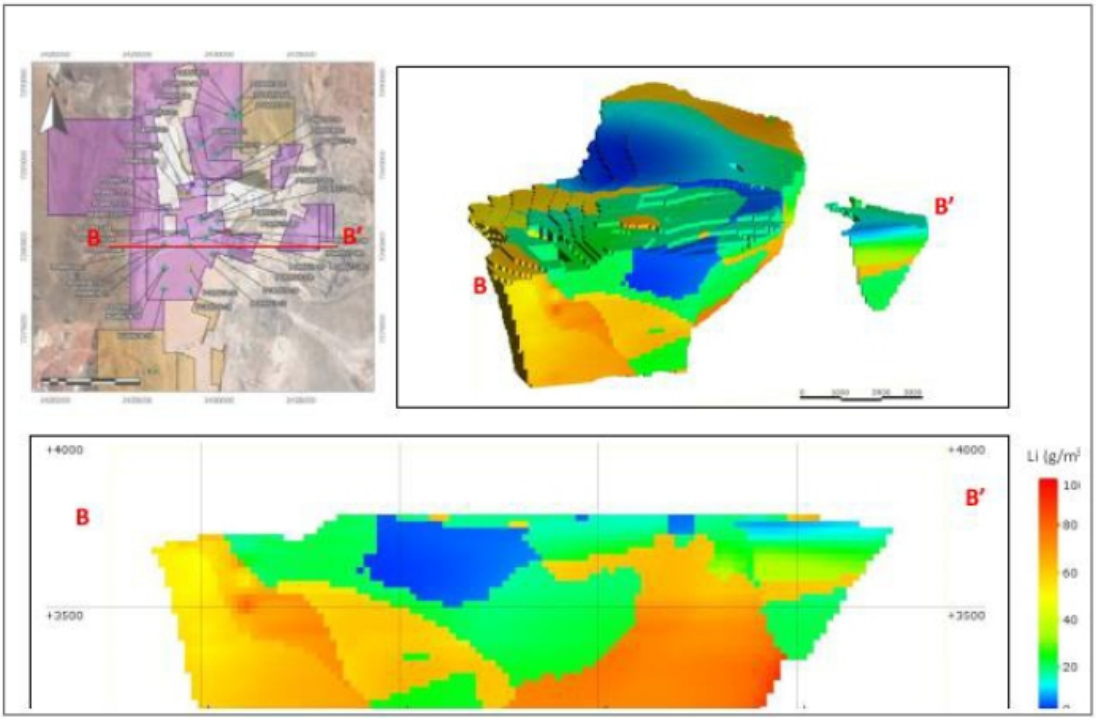

Figure 117: W-E Section through the Resource Model Showing the Lithium Grade Distribution (Source: AW, Dec 2024)

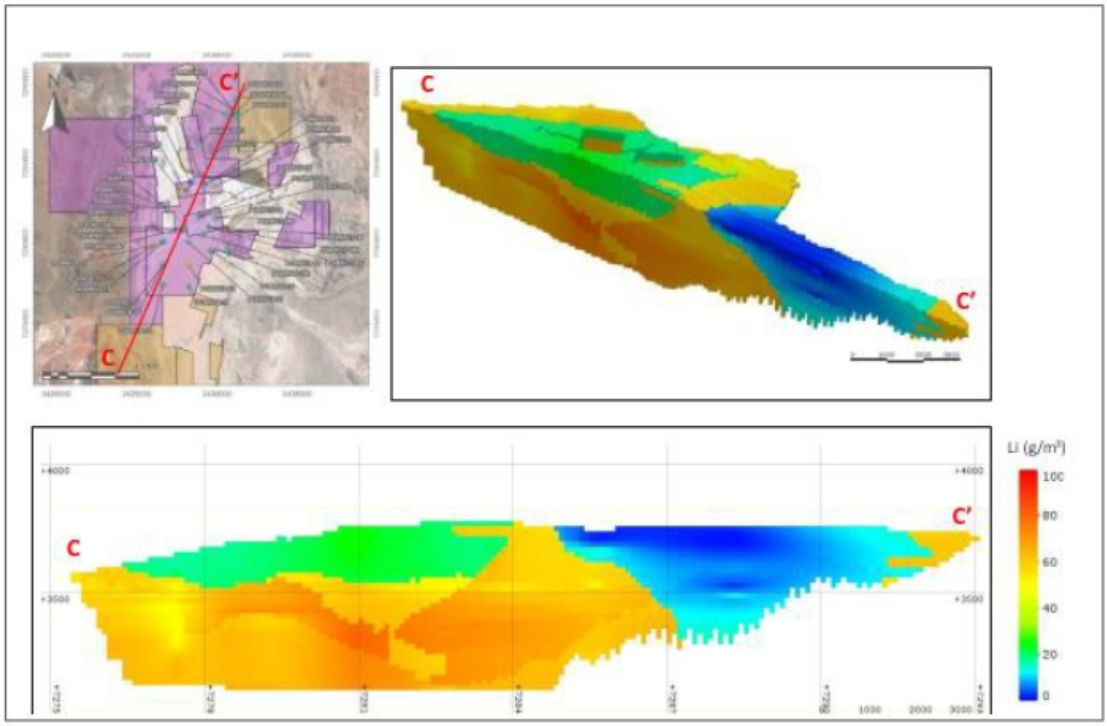

Figure 118: SW-NE Section through the Resource Model Showing the Lithium Grade Distribution (Source: AW, Dec 2024)

11.2.6 Resource Estimate

The resource estimate for the Pastos Grandes Project was prepared in accordance with the requirements of S-K §229.1300 and uses the best practices methods specific to brine resources, including a reliance on core drilling and sampling methods that yield depth-specific chemistry and drainable porosity measurements. A 125 mg/l lithium concentration cut-off was applied to the resource estimate.

Table 64 shows the mineral resources for the Pastos Grandes project expressed as lithium carbonate equivalent (LCE).

It is the opinion of the QPs that the Salar geometry, brine chemistry composition, and the specific yield of the Salar sediments have been adequately characterized to support the Measured, Indicated, and Inferred Resource estimate for the Project herein.

It is the opinion of the QPs that the resources estimated and described in the current report meet the requirements of reasonable prospects for eventual economic extraction, as defined in S-K § 229.601(b)(96). The resource described herein has similar lithium concentrations, chemical composition, and hydraulic parameter values (drainable porosity values between 0.04 and 0.15 and hydraulic conductivities values between 0.5 m/d and 300 m/d) to resources currently in commercial production such as those in Salar de Atacama in Chile or Salar de Olaroz located in the Puna region of Northern Argentina. The hydraulic parameters of the resource area determined from the results of the pumping tests suggests that it is reasonable to expect brine extraction by a conventional production wellfield at a commercially viable rate, while the geochemical characteristics of the brine suggest that conventional processing or DLE techniques may be employed to produce saleable lithium products in an economically profitable manner. The author is not aware of any known environmental, permitting, legal, title, taxation, socio-economic, marketing, political or other relevant factors which could materially affect the mineral resource estimate.

Table 64: Mineral Resources (LCE) for the Pastos Grandes Salar (Effective Date: December 31, 2025)

Salar	Resource Category	Aquifer Volume (km^3)	Brine Volume (km^3)	Average Lithium Concentration (mg/L)	Lithium (tonnes)	LCE (tonnes)
Pastos Grandes	Measured Resource	25.28	3.09	451	1,393,000	7,414,640
	Indicated Resource	1.15	0.17	166	28,000	149,038
	Measured + Indicated	**26.43**	**3.26**	**439**	**1,421,000**	**7,563,678**
	Inferred Resource	26.43	3.26	456	525,000	2,794,462

Note:

1) *S-K §229.1300 definitions were followed for Mineral Resources.*
2) *This table includes resources in all areas of PG and SdlP previously owned by Ganfeng and Lithium Argentina separately.*
3) *Lithium carbonate equivalent ("LCE") is calculated using the Li: LCE factor = 5.322785 multiplied by the mass of Lithium.*
4) *The Mineral Resource Estimate is not a Mineral Reserves Estimate and has no demonstrated economic viability.*
5) *Comparisons of values may not be equivalent due to rounding of numbers and the differences caused by use of averaging methods.*
6) *Project economics in this report are not based on Inferred Mineral Resource.*
1) *A cut-off grade of 125 mg/l has been applied to the mineral resource estimates. An FoB price forecast of US$18,000 per metric ton of Li_2CO_3 and US$17,800 per metric ton of coarse particle $LiOH \times H_2O$ for years beyond 2028 is used. A 75% overall lithium recovery efficiency factor has been applied to calculate the final LCE production.*
7) *The cutoff grade is based on the various inputs and the formula below:*

$$Cutoff\ Grade = \frac{\frac{(Total\ capital\ expenditure + Total\ operating\ expense)}{Total\ brine\ extracted}}{(Recovery * Conversion\ from\ Li\ to\ Li_2CO_3 * Projected\ LCE\ Price * (1 - Export\ Duties) * (1 - Royalties))}$$

Where:

Total capital expenditure = US$ 3,301 million

Total operating expenditure = US$ 16,332 million

Conversion from Li to Li_2CO_3 = 5.323

Projected long term LCE price = US$ 18,000 per ton of LCE

Export duties = 0%

Royalties = 3.0%

Calculated recovery = 75%

Resulting in a calculated cut-off grade of 125 mg/l.

Factors that may affect the Brine Resource estimate include: locations of aquifer boundaries; lateral continuity of key aquifer zones; presence of fresh and brackish water which have the potential to dilute the brine in the wellfield area; the uniformity of aquifer parameters within specific aquifer units; commodity price assumptions; changes to hydrogeological, metallurgical recovery, and extraction assumptions; density assignments; and input factors used to assess reasonable prospects for eventual economic extraction. Currently, Mr. F. Reidel (the QP), does not know any environmental, legal, title, taxation, socio-economic, marketing, political, or other factors that would materially affect the current Resource estimate.

11.3 Mineral Resources for the PPG Project

For the PPG Project, the integrated mineral resources are shown in Table 65.

Table 65: Mineral Resources (LCE) for the PPG Project (Effective Date: December 31, 2025)

Salar	Resource Category	Pozuelos		Pastos Grandes (including SdLP)		Subtotal LCE (tonnes)
		Li (mg/L)	LCE (tonnes)	Li (mg/L)	LCE (tonnes)	
PPG	Measured Resource	490.5	5,836,244	451	7,414,640	13,250,884
	Indicated Resource	528.7	1,180,383	166	149,038	1,329,421
	Measured + Indicated	**510.0**	**7,016,627**	**439**	**7,563,678**	**14,580,305**
	Inferred	581	3,920,437	456	2,794,462	6,714,899

Note:

2) *S-K §229.1300 definitions were followed for Mineral Resources.*

3) *Lithium carbonate equivalent ("LCE") is calculated using the Li: LCE factor = 5.322785 multiplied by the mass of Lithium.*

4) *A cut-off grade of 125 mg/l has been applied to the mineral resource estimates. An FoB price forecast of US$18,000 per metric ton of Li_2CO_3 and US$17,800 per metric ton of coarse particle $LiOH \times H_2O$ for years beyond 2028 is used. A 75% overall lithium recovery efficiency factor has been applied to calculate the final LCE production.*

5) *The Mineral Resource Estimate is not a Mineral Reserves Estimate and has no demonstrated economic viability.*

6) *Comparisons of values may not be equivalent due to rounding of numbers and the differences caused by use of averaging methods.*

7) *Project economics in this report are not based on Inferred Mineral Resource.*

8) *The QPs are not aware of any known legal, political, environmental, or other risks that could materially affect the potential development of the mineral resources.*

11.4 Groundwater Dynamic Modelling at Pozuelos

In September 2024, Atacama Water Consultants completed the simulation of brine abstraction (960 L/s from 24 production wells) from Pozuelos to support an annual production of 50 kt LCE over a 20-year project life, evaluation of water level declines during the operation and water levels recoveries after the operation ceases, and evaluation of the effects of depleted brine infiltration (148 l/s) on lithium concentrations and LCE production targets.

The updated model builds on Ganfeng's original FEFLOW model (spz_reserves_model_2024.fem), prepared in FEFLOW 8.0 and was a single-density flow-and-lithium-transport model designed to produce a preliminary simulation result with and without planned infiltration schemes.

Note that updated resources estimate at Pozuelos (as of February 2025, see Chapter 14) has not been reflected in the September 2024 dynamic model.

11.4.1 Model Construction

11.4.1.1 Finite Element Mesh

A new mesh was created to reduce the obtuse triangles with maximum interior angles greater than 160°. The new mesh is approximately 20% larger than the original mesh, with 1,362,400 activate elements and 722,724 active nodes.

The updated model uses the SAMG solver with a termination criterion of 1×10^{-13}.

The updated model uses the maximum error norm and a target of 10 with 60 iterations.

The transient model uses a first-order accurate predictor-corrector, automatic time-stepping scheme with an initial time step of 1×10^{-5} days, and a maximum time step of 50 days.

The transport model uses the FEFLOW default setting of a convective form of the equation with constant viscosity and linear solute dispersion. The model uses a setting called "Include fluid change in storage component in mass and/or heat transport budgets."

11.4.1.2 Boundary Condition, Lateral Recharge and Extraction Well

Figure 120 shows the boundary condition, lateral recharge and the locations of extraction wells for brine (in the center of the domain in grey-shaded areas) and freshwater (in the purple zone labelled "Outer Alluvium").

The information in the provided fem file was initially edited to be applicable to a single-density model, keeping an exponential decay function, with a maximum evaporation rate of 6.756×10^{-3} m/d and an exponential decay constant of 3. In the early version, the depth to groundwater was computed with a Python script embedded in spz_li_ca_so4.fem, also provided by Ganfeng. However, in the interest of numerical efficiency, the evaporation term was converted to a third-type boundary with a linear reduction in evaporation with water table depth. The extinction depths for brine, brackish water, and freshwater for the linear evaporation function used in the model update are shown in Figure 119.

The model removed the lateral recharge from the southeastern catchments and adjusted the hydraulic conductivity of thin layer of alluvium and bedrock in northward. As shown in Figure 120, the total lateral recharge used in the model is about 612 L/s, not 707 L/s based on the watershed.

Zone	Extinction Depth (m)	Steady State Evaporation Rate (L/s)
Brine	0.5	34
Brackish	1.0	305
Freshwater	2.0	273

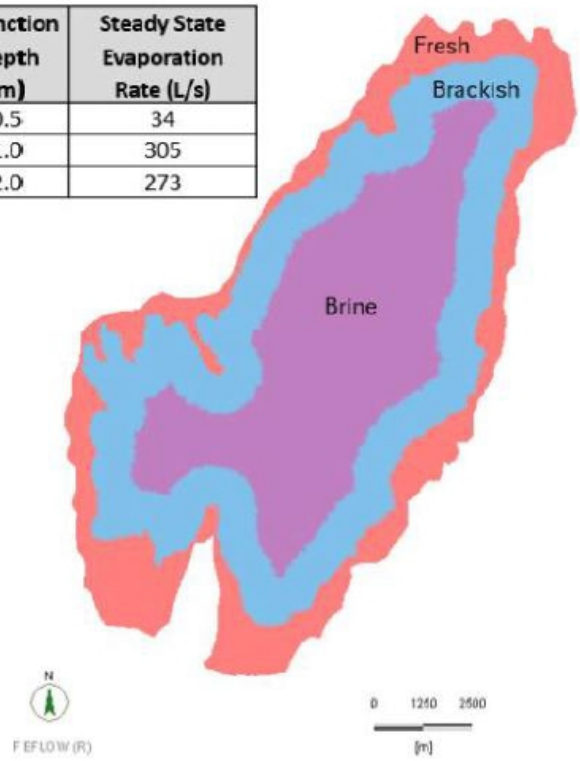

Figure 119: Evaporation Function (Source: AW, September 2024)

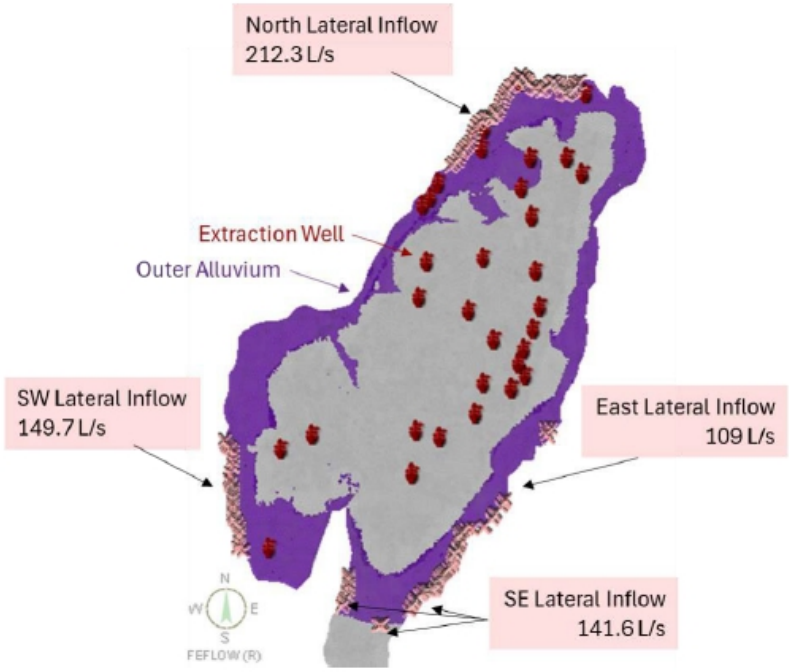

Figure 120: Boundary Conditions for Lateral Recharge and Extraction Wells (Source: AW, September 2024)

11.4.1.3 Parameter Distribution

The parameters applied in the updated model are shown in

Table 66. These parameters are based on the values in the provided FEFLOW file and information from the conceptual model. The generalized parameter distribution is shown in Figure 121.

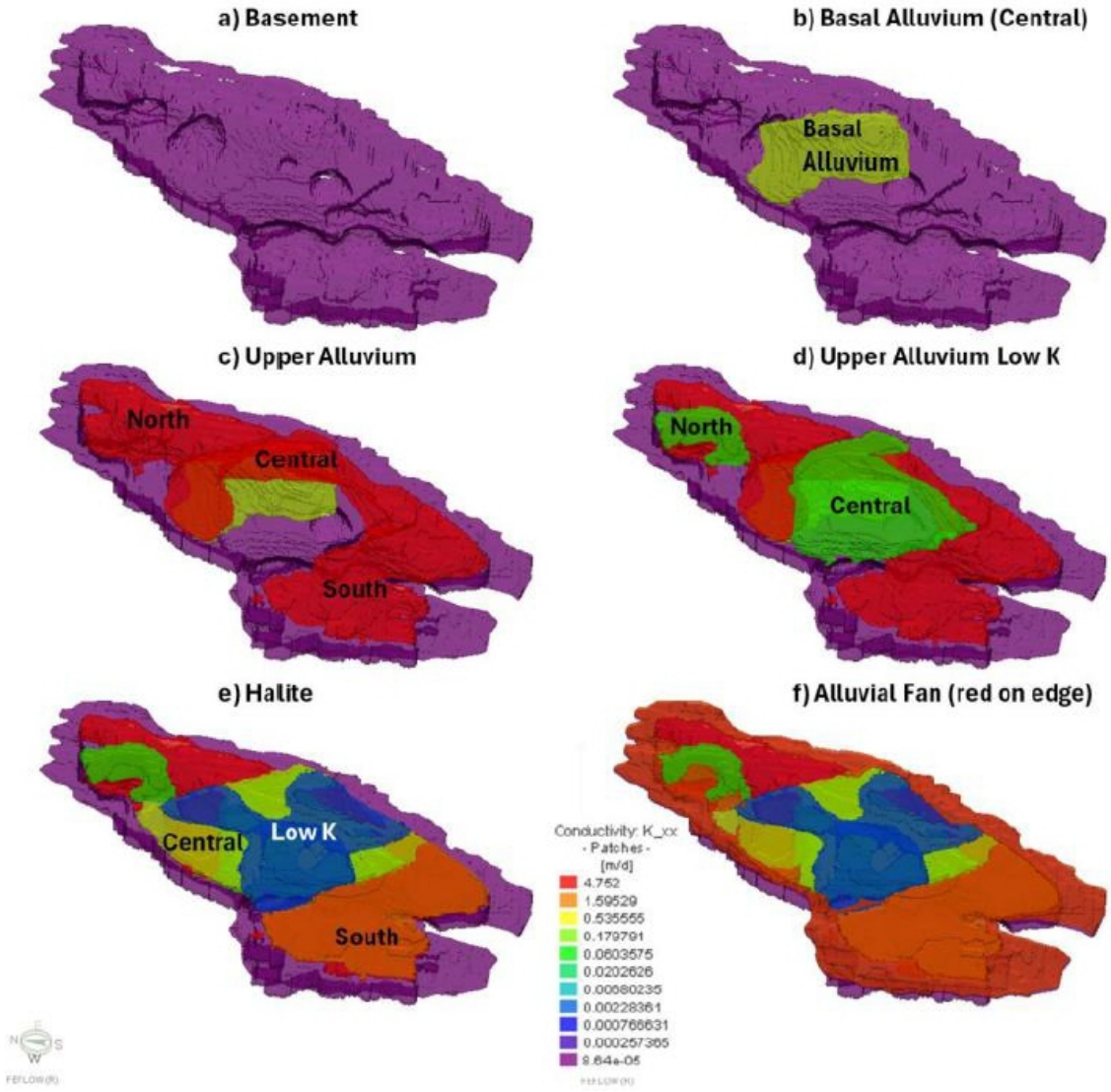

Figure 121: Generalized Hydrostratigraphic Units (built up from bottom to top in images a to f) (Source: AW, September 2024)

The mass porosity was set equal to the specific yield in the runs. A longitudinal dispersivity of 120 m and a transverse dispersity of 12 m was used in the simulations.

Table 66: Updated Model Parameters (Source: AW, September 2024)

Zone No.	Name	K (m/s)	K (m/d)	Sy	Ss (m^{-1})
0	Basement	1×10E-9	8.64×10E−5	0.01	1×10E−6
1	Halite Low Flow	2×10E-8	1.728×10E−3	0.04	1×10E−5
2	Halite South	2×10E−6	1.728	0.06	1×10E−5
3	Halite Central	4×10E−6	0.3456	0.06	1×10E−5
4	Upper Alluvium North	5.5×10E−5	4.752	0.09	1×10E−4

5	Upper Alluvium Central	5.5×10E−5	4.752	0.09	1×10E−4
6	Upper Alluvium South	5.5×10E−5	4.752	0.02	1×10E−4
7	Basal Alluvium Central	3.5×10E−6	0.3042	0.09	1×10E−5
8	Upper Alluvium North Low Flow	1×10E−6	0.0864	0.03	1×10E−4
9	Upper Alluvium Central Low Flow	1×10E−6	0.0864	0.03	1×10E−5
10	Alluvial Fans	3×10E−5	2.592	0.09	1×10E−4

11.4.1.4 Initial Head and Lithium Concentration

Figure 122 shows the hydraulic head and lithium concentration distribution at the top and bottom of the simulated brine wells.

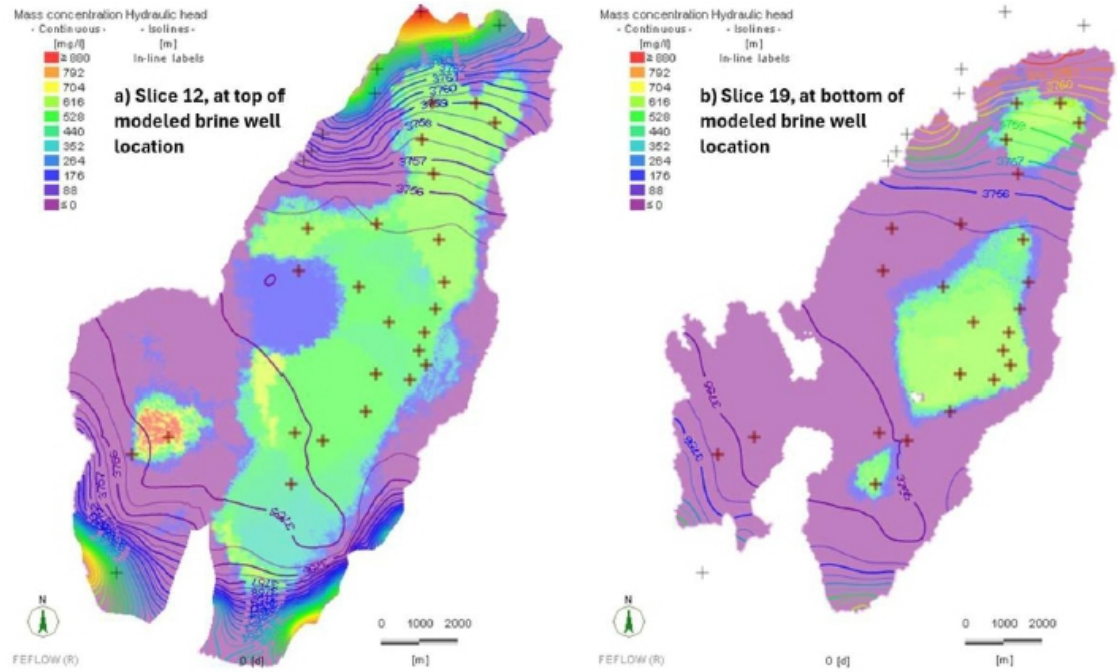

Figure 122: Initial Single-density Head and Lithium Concentration Distribution at the top and bottom of Screens of the Simulated Brine Wells (brown plus signs denote brine well locations) (Source: AW, September 2024)

11.4.2 Predictive Simulations

Four transient, predictive, 20-year operational models were completed, as follows:

- A “Base Case” model, in which the head and lithium evolution was simulated without brine extraction
- “Without Infiltration” model, in which 960 L/s of brine extraction was simulated with up to 24 L/s of freshwater – without infiltration
- “With-Recharge” model, in which 960 L/s of brine was extracted, and 148 L/s was applied to ground surface for recharge, with a concentration of 300 mg/L Li

- "With-Infiltration-Wells" model, in which 960 L/s of brine was extracted, and 148 L/s was modelled as reinjection through 14 gravity wells with long screens (0-230 m below ground surface), with a concentration of 300 mg/L Li

In addition to these runs, the post-pumping recovery period was simulated for Model 2, the "Without Infiltration" model, i.e.,

- "Recovery" model, for a period of 100 years after the end of pumping.

All models were run with a relaxed convergence criterion in order to efficiently assess the feasibility of the infiltration schemes.

11.4.2.1 Base Case Model Results

The primary purpose of the base case model was to evaluate the numerical stability of the model. Over the course of 20 years, the head distribution in the FEFLOW model did not substantially change, as shown in **Figure 123**. In this figure, white areas have head changes that are less than ±0.2 m. The areas with some colours have simulated head changes over 20 years of modelling that were higher than approximately ±0.2 m. It can be seen that all of these areas are located near the model border, in the freshwater zone. These areas do not significantly influence the brine production simulations calculation. Future predictive simulations run will use the head after initial quasi-steady state head run like the Base Case model.

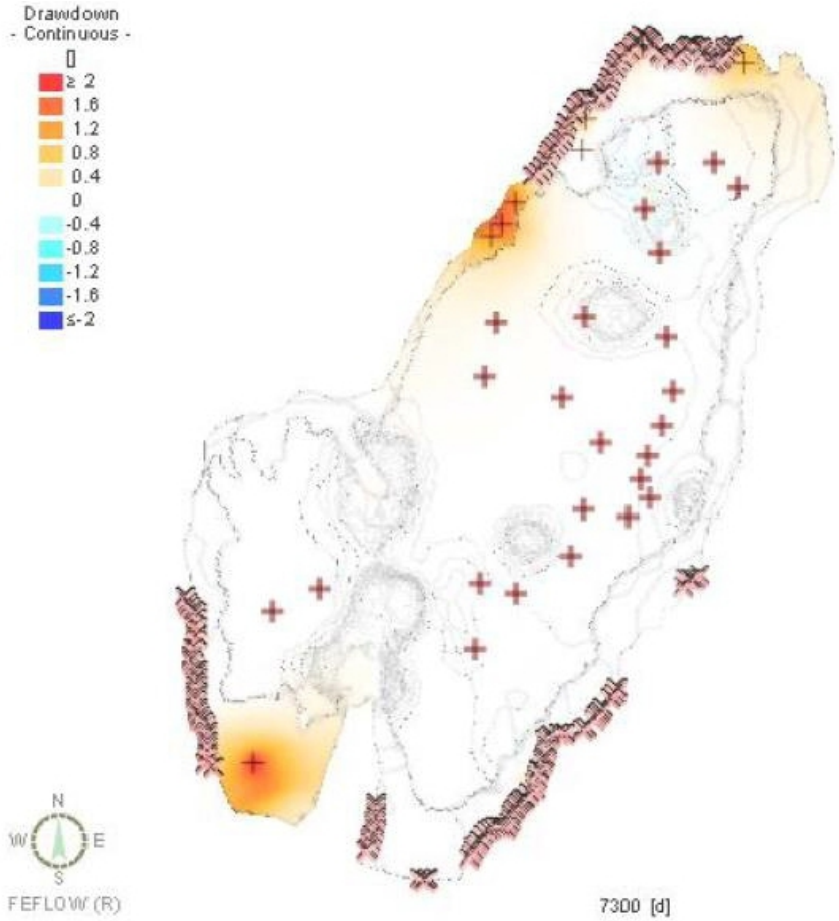

Figure 123: Change in Hydraulic Head during 20-year Base Case Simulation (Source: AW, September 2024)

Figure 124 shows the lithium concentration distribution in three south-to-north cross-sections through the model domain. Four features are important to notice in this figure. First, the overall drawdown (i.e., the initial head minus the final head) over the 20-year simulation period of the Base Case model is generally less than 0.1 m, as denoted by the yellow lines that demarcate the 0.1 m drawdown zone. Second, the lithium concentration in all three sections experiences a decline even without brine extraction. The decrease is greatest in Section A and lowest in Section B. The reason for the dilution of lithium over time is that the lateral recharge is assigned a zero-lithium concentration in the numerical model. Due to this inflow of freshwater at the model boundaries, the model is a conservative prediction tool with regard to lithium production. Third, it can be seen that the bottom two-thirds of the numerical model includes low-permeability, zero-lithium concentration bedrock with a thickness on the order of 500 m to 600 m. Finally, the figure shows that there are small numerical instabilities (undershoot) in the lithium concentration within this bedrock unit. Future version of the model can use higher dispersivity values to minimize the undershoot of the solute concentration.

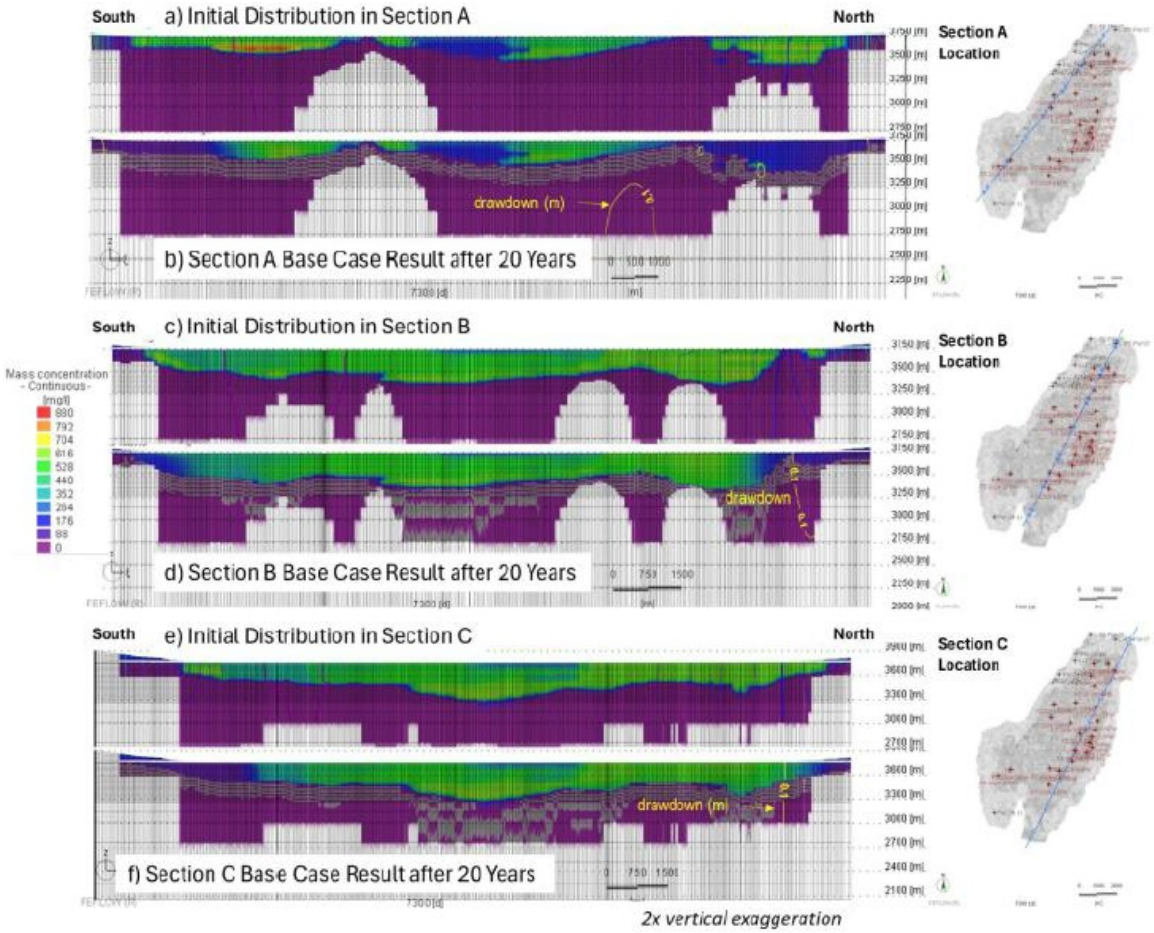

Figure 124: Lithium Concentration Distribution at Beginning and End of Base Case Run, Sections A to C (Source: AW, September 2024)

11.4.2.2 Without Infiltration Model Results

In the simulated runs, the initial pumping rates were adjusted based on the hydraulic conductivity of the geological units intersecting the well screens. In other words, if the hydraulic conductivity around a well screen is low, it may not be able to pump a high volume of water. In order that all wells continue to pump for 20 years, some of the pumping rates were adjusted downward in low-permeability zones and upward in higher permeability zones, maintaining the specific total extraction rate of 960 L/s. Table 67 summarizes the pumping rates applied in the FEFLOW model. The well screens for the brine wells were assigned based on the model mesh to be at approximately the same depth as the design configuration.

Total 24 production wells were designed to achieve the above extraction rate.

Table 68 shows the screen depths and pumping rates of the freshwater wells. The screens of these wells were adjusted to be shallower than originally proposed in order to intersect higher permeability units. The freshwater pumping rates were also revised based on the hydraulic conductivity of the material around the well screens.

Table 67: Brine Well Extraction Rates

ID	Coordinates_POSGAR 94 Argentina 3		Coordinates_WGS84_ 19S		Screen Locations (masl)		Screen Length (m)	Pumping Rate (L/s)
	X (m)	Y (m)	X (m)	Y (m)	Bottom	Top		
PZ-2023-PW12	3419721	7274025	723363	7271587	3449	3679	230	55
PZ-2023-16PW	3420847	7274023	724489	7271560	3449	3679	230	55
PZ-2023-19PW	3419557	7267280	723051	7264740	3449	3679	230	55
PZ-2024-02PW	3416496	7270801	720068	7268431	3449	3679	230	10
PZ-2024-03PW	3417998	7266126	721467	7263727	3449	3679	230	15
PZ-2024-05PW	3418596	7268388	722115	7265975	3449	3679	230	55
PZ-2024-06PW	3419512	7268126	723090	7265671	3449	3679	230	55
PZ-2024-07PW	3418276	7270916	721850	7268510	3449	3679	230	15
PZ-2024-08PW	3419754	7272206	723356	7269768	3449	3679	230	55
PZ-2024-09PW	3421332	7273524	724963	7271051	3449	3679	230	55
PZ-2024-10PW	3416894	7265379	720347	7263004	3449	3679	230	22
PZ-2024-11PW	3416073	7264260	719502	7261903	3449	3679	230	60
PZ-2024-13PW	3417825	7269296	721364	7266900	3449	3679	230	32
PZ-2024-14PW	3419449	7273089	723070	7270657	3449	3679	230	55
PZ-2024-15PW	3420025	7269421	723566	7266977	3449	3679	230	55
PZ-2024-17PW	3419135	7266908	722621	7264406	3449	3679	230	55
PZ-2024-18PW	3418255	7267057	721745	7264652	3449	3679	230	15
PZ-2024-21PW	3419890	7270516	723455	7268075	3449	3679	230	55
PZ-2024-22PW	3419799	7268729	723325	7266290	3449	3679	230	55
PZ-2024-25PW	3416170	7265582	719628	7263223	3449	3679	230	10
PZ-2024-26PW	3412944	7265472	716400	7263183	3449	3679	230	22
PZ-2024-27PW	3411996	7265023	715442	7262755	3449	3679	230	22
PZ-2024-28PW	3416268	7269714	719816	7267352	3449	3679	230	22
PZ-2024-29PW	3419371	7267656	722874	7265226	3449	3679	230	55

Table 68: Freshwater Well Extraction Rates

ID	Coordinates_POSGAR 94 Argentina 3		Coordinates_WGS84 _19S		Screen Locations (masl)		Screen Length (m)	Pumping Rate (L/s)
	X (m)	Y (m)	X (m)	Y (m)	Bottom	Top		
Li-PZ-FW-08	3419413	7276376	723106	7273945	3704	3800	96	4
Li-PZ-FW-12	3418226	7274278	721874	7271873	3704	3766	62	1
Li-PZ-FW-11	3416609	7272786	720224	7270416	3704	3770	66	3
Li-PZ-FW-07	3421449	7276026	725134	7273550	3704	3792	88	3
FW-24-18	3418295	7274904	721956	7272497	3704	3776	72	4
FW-24-13	3416397	7272535	720007	7270170	3704	3773	69	1
FW-24-16	3411604	7261979	714983	7259618	3704	3790	86	4
FW-24-05	3416885	7273226	720510	7270850	3704	3769	65	4

The brine extraction wells were simulated as multi-layer wells with the FEFLOW default parameters (well radius of 0.25 m, specific storage of 1E-4 m^{-1}). The freshwater wells were simulated as discrete features with a specified head boundary condition with a flow constraint. Using these pumping rates, the LCE production, not considering process efficiency factors, is shown in Figure 125. The figure shows in blue bars that all of the brine extraction wells are able to extract the specified rates shown in Figure 125.
Figure 125 shows the average lithium concentration extracted by the wells and the total mass of lithium extracted on an annual average basis. The average lithium concentration is simulated to decline from 520 mg/L to 320 mg/L through the life of mine (20-year life), with an average concentration of 420 mg/L. The lithium extracted ranges from 15.7 kilotonnes per year (kpy) to 9.6 kpy, with an average of 12.7 kpy.

Based on the above dynamic modelling of 2024 AW, it indicates that PZ salar can support the production capacity of 50 kpy with 20 years of LOM.

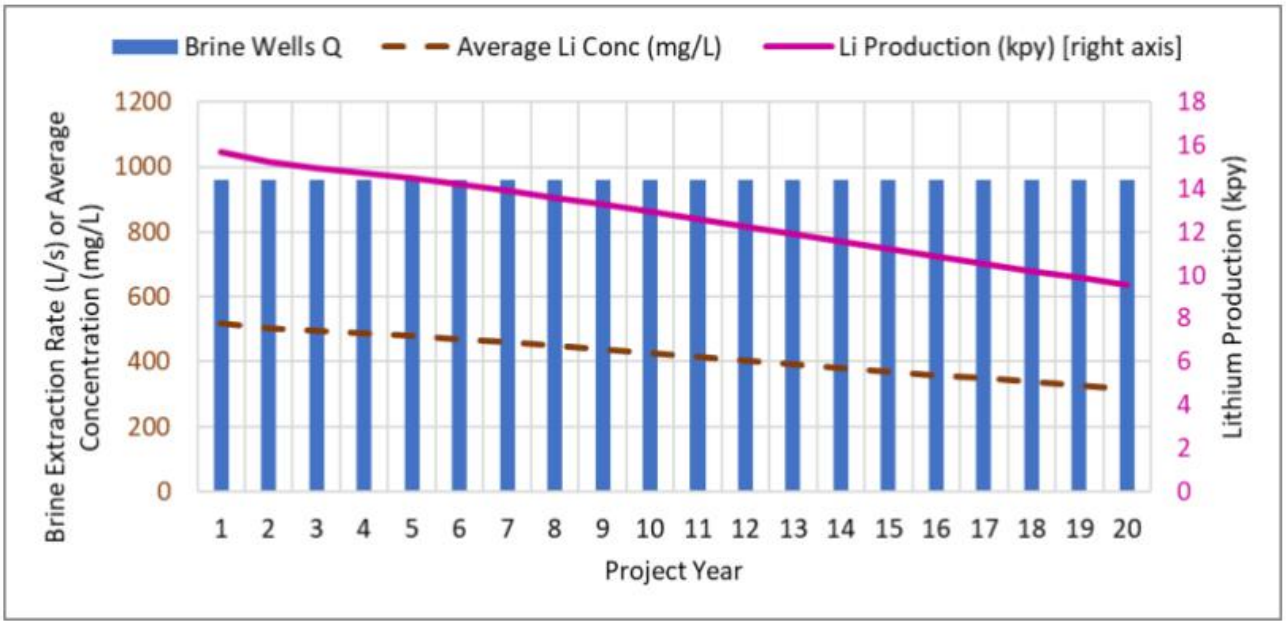

Figure 125: Lithium Production Estimate (Source: AW, September 2024)

The simulation predicts that the freshwater extraction rate will decline during operations, as the water table declines. Additional analysis of the freshwater extraction rates is recommended in future revisions of the model.

The predicted drawdown at the end of brine production is shown in Figure 126. The figure shows that the drawdown is highest in the center-eastern part of the Salar. Lower drawdown is predicted for the southern area, where there are only three brine extraction wells, and in the northwestern area, where lateral recharge enters the domain.

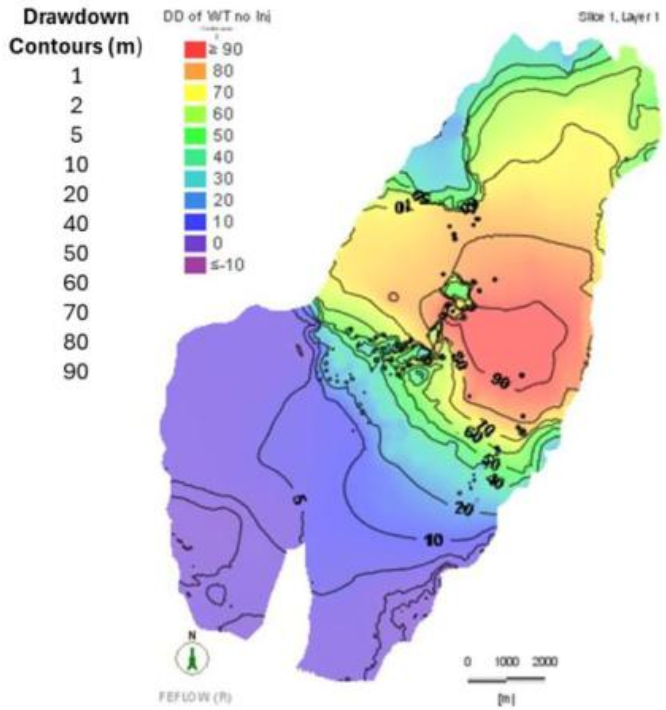

Figure 126: Simulated Drawdown without Infiltration (Source: AW, September 2024)

11.4.2.3 Infiltration Scenarios

Two simulations were completed with infiltration of 148 L/s of spent brine at a lithium concentration of 300 mg/L. Infiltration was modelled as reinjection of spent brine, bypassing the unsaturated zone, adding spent brine directly into the aquifer. These simulations are a conservative way to show how infiltration of spent brine would affect the water table and Li concentration. This, given the short time constraints and the fact that GF's FEFLOW model is not implemented in the vadose zone.

The simulated scenarios are: With-Recharge and With-Infiltration-Wells. The first scenario attempts to show the effects of the surface infiltration (trenches), while the second scenario attempts to show the effects of the gravity wells (shallow wells). The simulated configuration does not conform to the proposed infiltration infrastructure, from the study carried out in parallel, named "Evaluation of alternatives of depleted brine management for Salar de Pozuelos". Future evaluations of the surface infiltration (trenches) and gravity wells could be done with a variably saturated FEFLOW model configuration.

In the With-Recharge Model, the 148 L/s of spent brine was distributed on an area shown in pink in Figure 127, applied to the uppermost active layer. Recharge was applied in selected zones with low Li concentration and proper permeability. The larger area in the western part of the model domain was used at first. However, some surface ponding of water was noted during the first two years, and the area was reduced to the darker zone. The same recharge rate was used for the entire duration of the operation period.

Figure 127 shows that the drawdown in the central area is reduced with the application of recharge. This area has predicted drawdowns greater than 90 m in the Without-Infiltration model and greater than 70 m in the With-Recharge model.

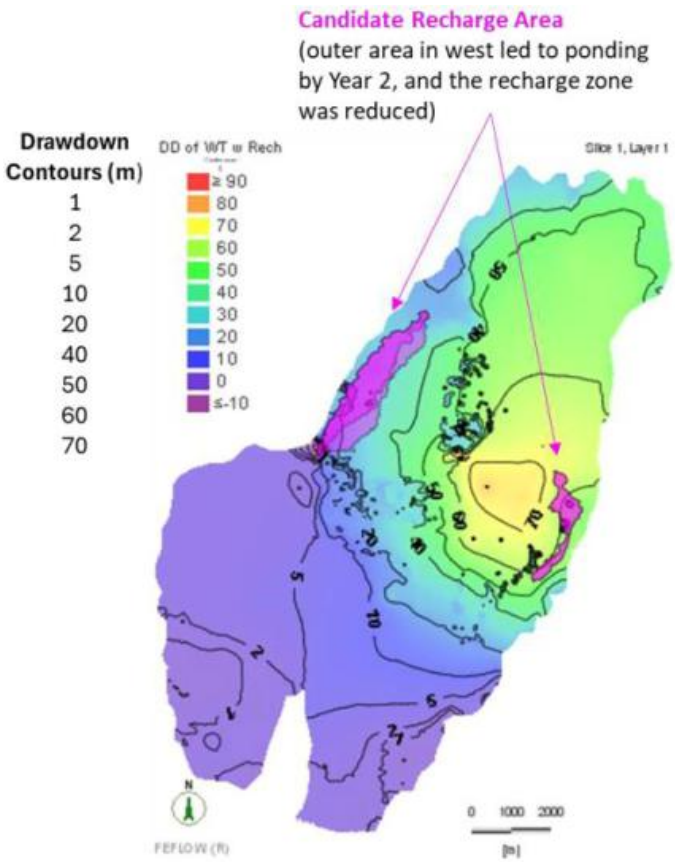

Figure 127: With-recharge Configuration and Drawdown at end of Operations (Source: AW, September 2024)

In the With-Infiltration-Wells Model, the 148 L/s of spent brine was injected through 14 wells below the water table, as shown on Figure 128. Wells were located to the north of the Salar de Pozuelos, where important drawdown is predicted due to production and permeable layers are present. The injection below the water table was required due to the phreatic setting of the FEFLOW model. The injection began at a depth of 10 m below ground surface and was lowered to 50 m at the end of the run.

Like the infiltration wells, the lateral recharge must also be applied below the water table in the phreatic FEFLOW configuration. The lateral recharge zones in the north and east of the model are in areas where the drawdown was significant (greater than 40 m) at the end of the simulation. As a result, the model did not fully converge at these borders at the end of the run. A confirmatory run was completed with a constraint on these borders, but the overall drawdown did not significantly change. To better maintain the lateral inflow in a numerically stable fashion, future runs should: (1) redistribute the lateral recharge, (2) raise the hydraulic conductivity of the shallowest layers of bedrock, and (3) use the variably saturated option in FEFLOW.

Figure 128 shows that the simulated drawdown for the With-Infiltration-Well scenario is lower than the Without-Infiltration scenario. While the With-Recharge model simulates significantly lower drawdown in the western and eastern area, the With-Infiltration-Wells model shows a reduction in drawdown in the eastern and northern area.

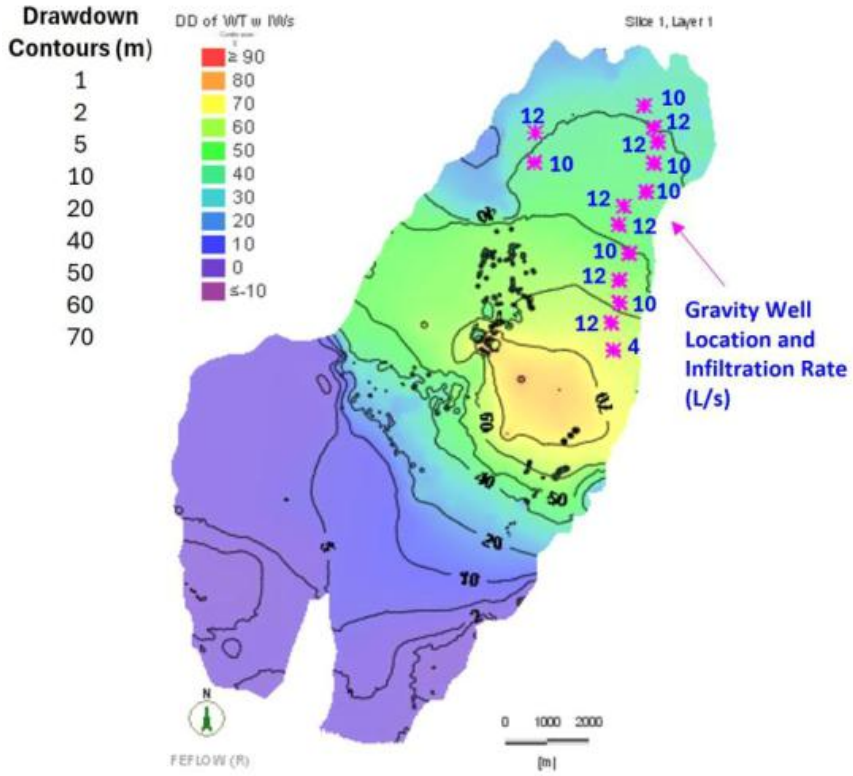

Figure 128: With-infiltration-well Configuration and Drawdown at end of Operations (Source: AW, September 2024)

Table 69 summarizes the effect of the Infiltration schemes on the lithium extracted via the brine wells. The table shows that Infiltration does not significantly change the simulated brine production.

Table 69: Effect of Infiltration on Li Production (Source: AW, September 2024)

Model	Average Li Produced by Brine Wells (kpy)			Average Lithium Concentration(mg/L)	
	Year 1	Year 20	20-Year Average	Year 1	Year 20
Without Infiltration	15.7	9.6	12.7	520	310
With Recharge	15.7	9.5	12.6	520	310
Infiltration Wells	14.1	9.7	12.6	500	320

11.4.2.4 Recovery After Operations

The Without Infiltration Model was continued after the end of brine extraction to evaluate the time required for water table recovery. The results are presented in Figure 129 and Figure 130. Figure 129a shows that the model predicts approximately 57% recovery by 10 years after the end of operations and 90% recovery by 20 years after the end of operations Figure 129b shows that the area of the model domain with simulated drawdowns greater than 40 m drops rapidly within the first 3 years after operations. The area with drawdowns greater than 20 m is predicted to disappear within 20 years. The lower-drawdown areas are predicted to recover more slowly.

a) Average Nodal Drawdown on Slice 1*

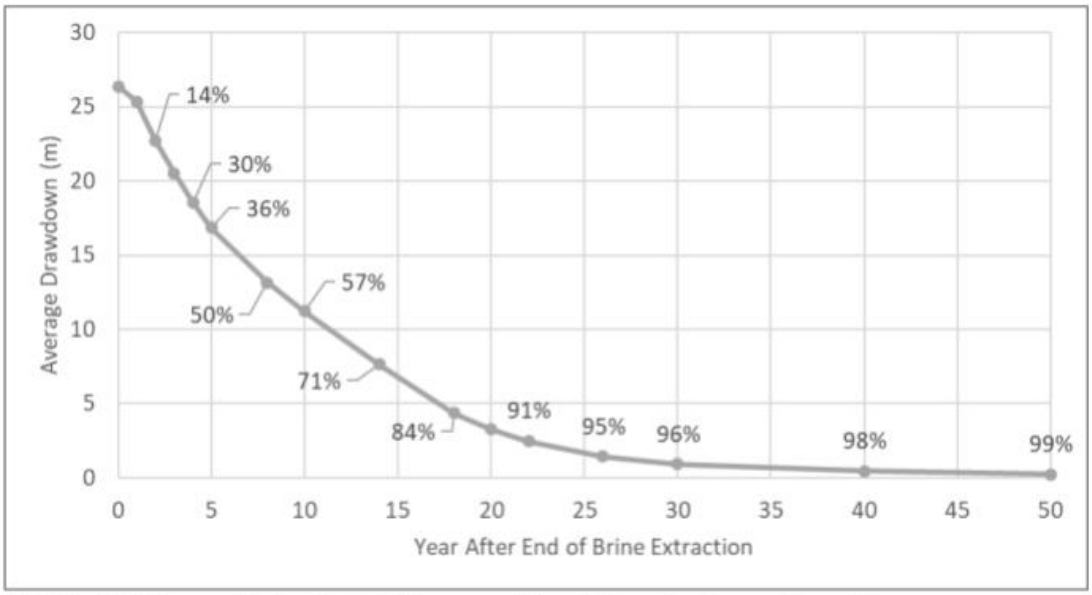

* Note that the nodal density is higher around the brine extraction wells, so these averages may be overestimated.

b) Area with Drawdown Greater than 5, 10, 20, and 40 m

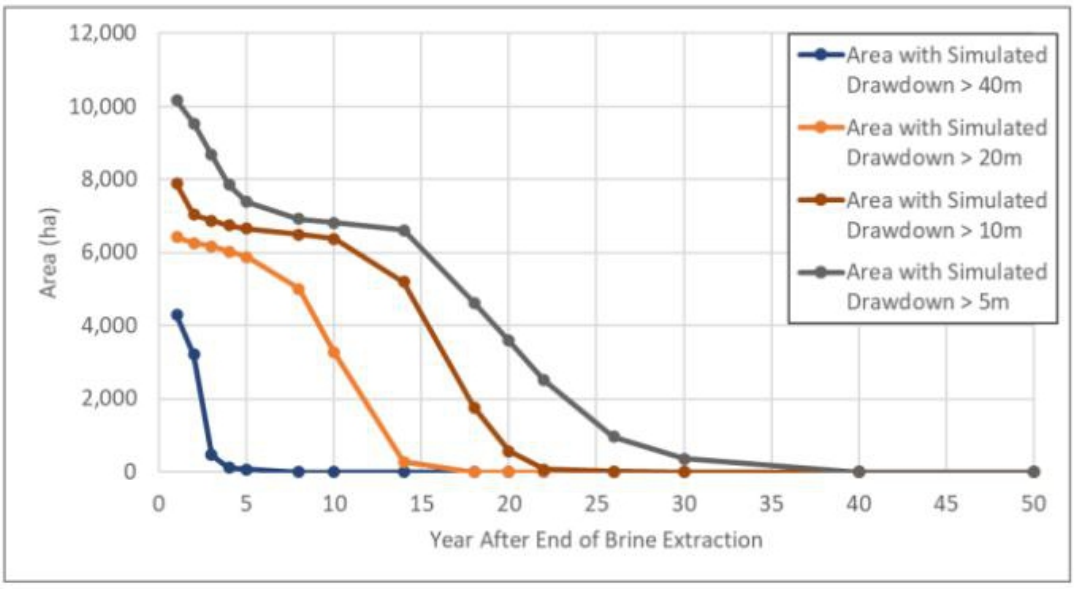

Figure 129: Average Drawdown and Area of Drawdown Impact after Operations (Source: AW, September 2024)

Figure 130 shows the simulated drawdown maps from which Figure 129 was computed. The color scale is different from the drawdown figures above. The figure shows that the predicted recovery of the water table in the southern part of the Salar is the most rapid. This area has a lower simulated drawdown than the northern and eastern areas. The northern area is simulated to recover more slowly than the southern area but is predicted to recover within approximately 20 years. By 20 years after the end of pumping, most of the areas adjacent to lateral recharge zones (compare with Figure 120) have fully recovered.

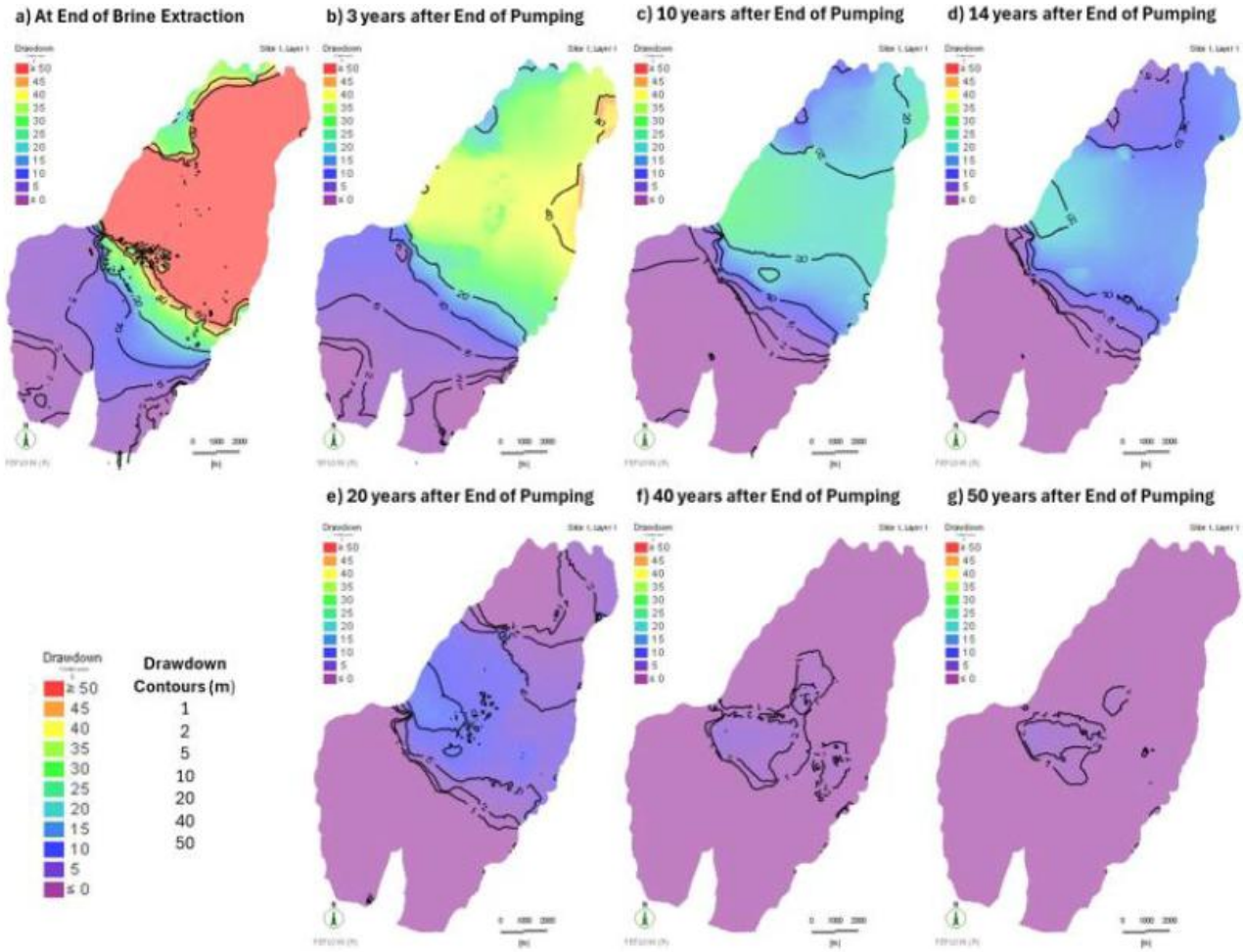

Figure 130: Simulated Drawdown after End of Brine Pumping (Source: AW, September 2024)

The last area predicted to return to pre-mining water levels is the low-permeability halite in the center of the Salar. On the other hand, the low-permeability halite is the zone most likely to be hydraulically disconnected from the deeper brine-filled sediments. Adding anisotropy to the halite or using a different FEFLOW model configuration (i.e., variably saturated instead of phreatic) could reduce the simulated drawdown in this area during operations. In addition, adding recharge of precipitation on the ground surface would result in faster water table recovery in the central, low-permeability halite.

11.4.3 Summary

These preliminary models show that, with the conceptual values of hydraulic conductivity, specific yield, and lateral recharge, the proposed total brine pumping rate of 960 L/s for a period of 20 years appears to be feasible.

The preliminary run suggests that the freshwater well locations may not be sufficient to meet the 24 L/s of freshwater required for the project which will have to be sourced from Pastos Grandes. With 960 L/s of total brine extraction, the model predicts drawdowns of greater than 80 m in areas, with an average drawdown on the order of 26 m at the end of operations. The modelling shows that changing the pumping rates at individual wells or including infiltration of 148 L/s (modelled as reinjection) can reduce the drawdown in local areas within the Salar. The infiltration can also improve freshwater capture by reducing drawdown along the Salar margins. The modelling shows that applying infiltration to the Pozuelos does not significantly affect the simulated brine production.

The recovery after operations model predicts approximately 57% recovery by 10 years after the end of operations and 90% recovery by 20 years after the end of operations. The simulated water table recovery after the end of operations is fastest in the south, followed by the north and Salar margins. The low-permeability halite in the center of the Salar is predicted to recover more slowly that the other areas. However, if there is any direct precipitation onto the Salar, this area could recover more quickly than modelled.

11.4.4 Limitations

It should be noted that this preliminary model did not include a calibration phase and is characterized by relatively poor water budgets. These choices were necessary to efficiently evaluate the feasibility of infiltration. However, the results presented here should not be used for purposes beyond the specific objectives of the model.

The analysis presented here is subject to limitations and uncertainties. There are uncertainties inherent to the numerical simulation of groundwater flow. The accuracy of the model depends on the quality and quantity of data and the time frame over which the data were collected. These data include the hydraulic conductivity, specific storage, specific yield, lateral recharge, and evaporation inputs, all of which are subject to uncertainty. Additional uncertainties arise from potential future events. For instance, future groundwater flow will be influenced by changes in climate dynamics, including precipitation rates, temperatures.

11.4.5 Recommendations

The next phase of modelling should include a calibration phase and some model adjustments to improve the numerical stability of the solutions. Although subject to a different set of potential challenges, a variably saturated configuration would be beneficial to address some of the numerical problems of the current model, including the difficulty of accurately simulating the gravity Infiltration wells and the challenge of introducing lateral recharge when the simulated water table dropped into the lower-permeability bedrock.

The next phase of modelling should also include an uncertainty analysis to explore the influence of model assumptions.

The improved model can be used to assess an optimization of the well field, including well location and pumping rates.

11.5 Groundwater Dynamic Modelling at Pastos Grandes

A numerical groundwater flow and transport model have been developed in December 2024. The modelling work was carried out by DHI in Lima, Peru under close supervision of Atacama Water and the QP.

The calibrated dynamic model is used to simulate a brine extraction system over a 20-year project life. It is assumed that the Project has an overall lithium recovery efficiency of 75%.

This section describes the construction and calibration of the numerical model and summarizes the results of the brine production simulations and the estimate results.

11.5.1 Model construction

11.5.1.1 Model Domain

The model domain shown in Figure 131 encompasses the unconsolidated sediments of the Pastos Grandes basin. The topographic elevation of the model domain ranges from 3,768 m above sea level (masl) at the Salar to 3,922 masl in the northeast corner of the domain. The base of the model has an elevation of 2,200 m, for a maximum thickness beneath the salar of 1,500 m.

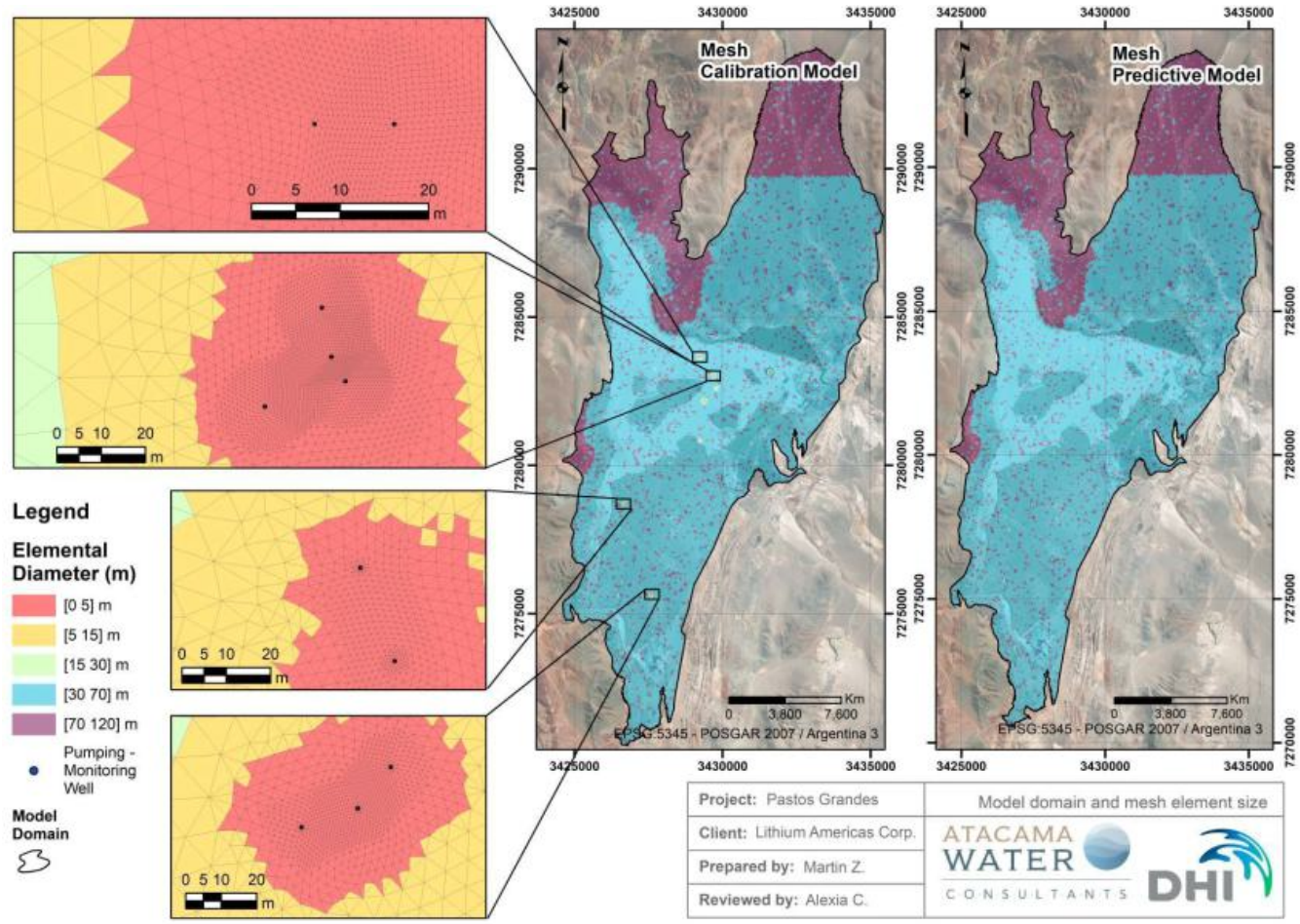

Figure 131: Model Domain and Meshes Element Size (Source: AW, Dec 2024)

11.5.1.2 Meshing and Layering

During the modelling process, two different meshes were developed:

- Calibration mesh: included finer refinement both vertically and horizontally in the vicinity of the pumping test. This refinement was essential to accurately simulate the localized effects of the pumping test during the calibration phase.
- Prediction mesh was designed without the localized refinements to ensure a more uniform mesh size throughout the model.

In both meshes, the horizontal refinement consists of triangular prism elements with an approximate size of 50 m across most of the model domain. In the northern part of the model, element size increases to 100 m (Figure 131). For the calibration mesh, additional local refinement is applied around the pumping wells, resulting in element sizes ranging from 5 m to as small as 1 m.

Figure 132 present the layering for both the calibration and prediction meshes. Considering only the active parts of the meshes:

- The calibration mesh comprises 1,322,885 active nodes, 2,489,470 active elements, and 34 partially or fully activated layers.
- The prediction mesh comprises 540,039 active nodes, 959,392 active elements, and 19 partially or fully activated layers.

The prediction mesh features 61% fewer active elements compared to the calibration mesh, optimizing computational efficiency while maintaining accuracy for predictive simulations.

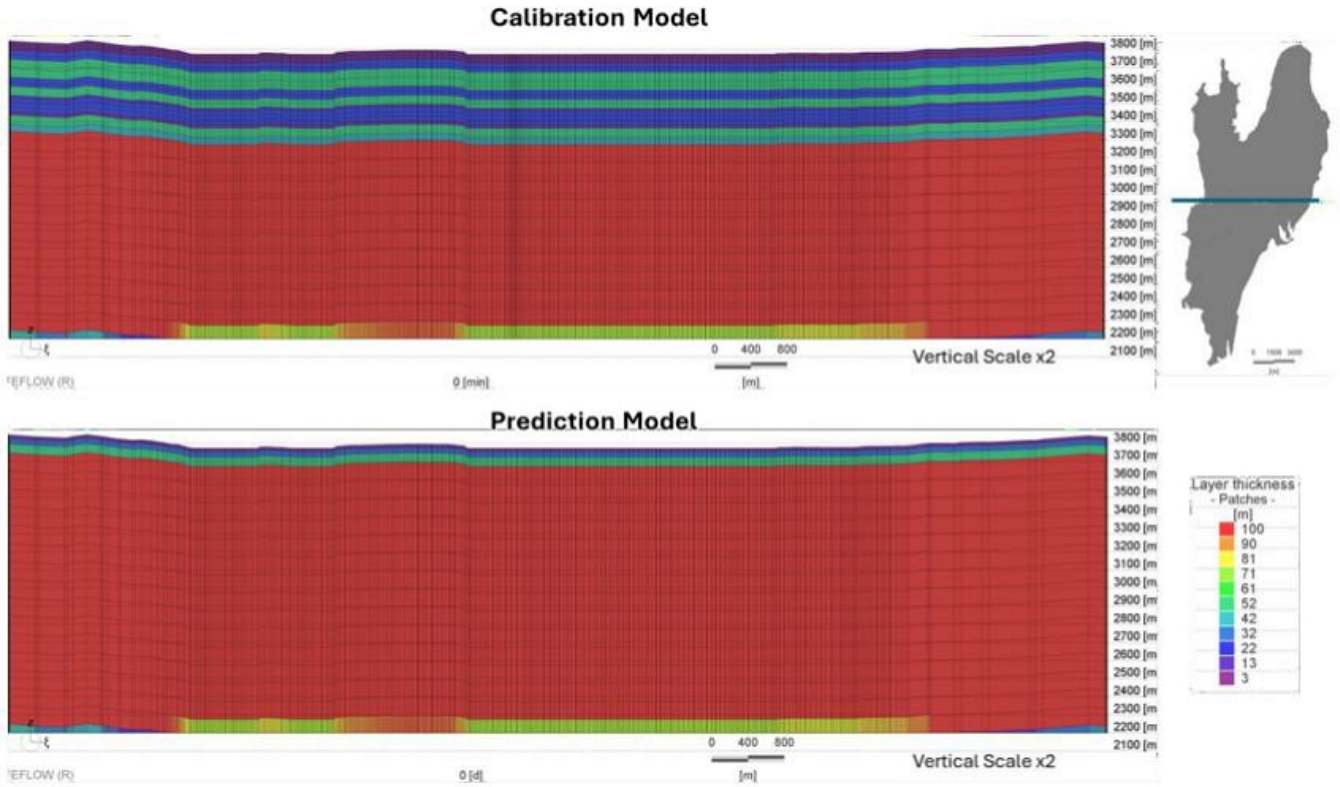

Figure 132: Mesh Vertical Extension (Source: AW, Dec 2024)

11.5.1.3 Flow Boundary Conditions

The regional boundary conditions are presented in Figure 133. Two primary groundwater inflow processes occur in the Pastos Grandes salar as surface recharge by direct precipitation and lateral recharge from the surrounding catchments. The groundwater natural outflow occurs at lower elevations only through evapotranspiration or evaporation.

The lateral recharge boundary conditions were applied to the outer boundaries in all the slices of the model, except for the inactive basement elements. Where a lateral recharge boundary is not defined, the model edge is treated as a no-flow boundary. Evapotranspiration and surface recharge boundary conditions were applied to Layer 1. The bottom of the model domain was treated as a no-flow boundary.

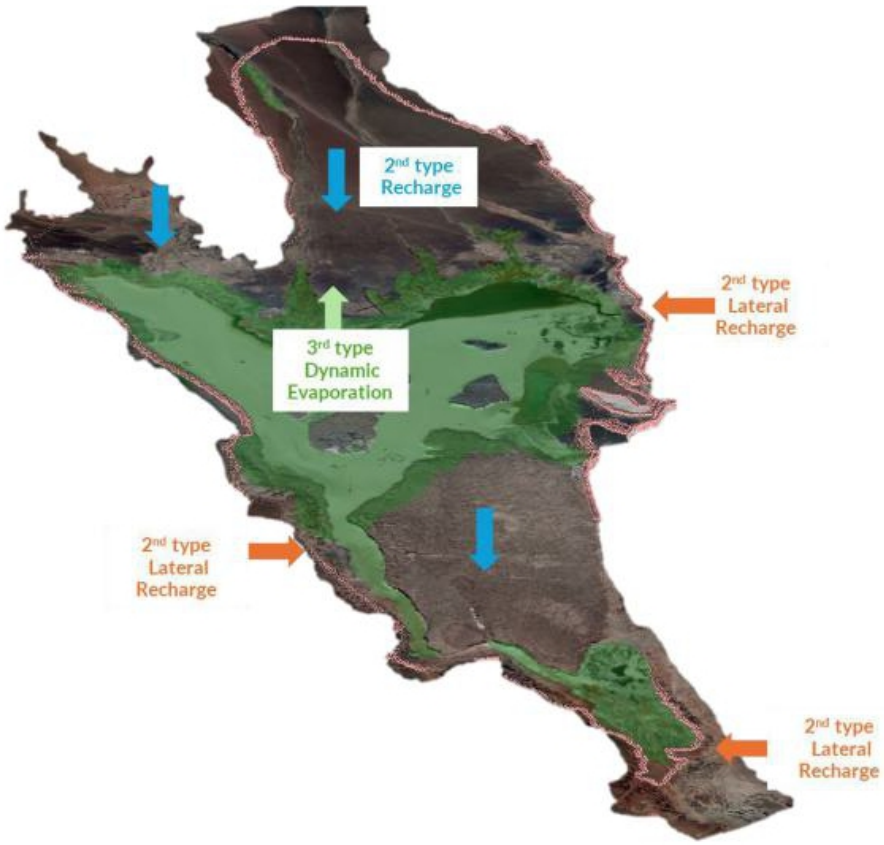

Figure 133: Model Boundary Conditions (Source: AW, Dec 2024)

- **Direct Recharge through precipitation:** Direct recharge from precipitation was applied across the topography. A 2nd type boundary condition (specified flux) was assigned outside the zones dominated by evaporation processes, which correspond to areas of groundwater discharge. The recharge rate varied depending on the outcropping geology. For higher-permeability alluvial deposits, a recharge rate of 90 mm/year was applied, while for clay and lacustrine units, a lower rate of 10 mm/year was used. This resulted in a total recharge of 105 L/s across the model domain.

- **Catchment Inflows:** the Pastos Grandes Salar receives indirect recharge as lateral groundwater recharge that is generated by the seven upstream catchments surrounding the Pastos Grandes Basin (Figure 134). The catchment inflows were treated as flux (2nd type) boundary conditions. Inflow rates range from 3 L/s from the western catchments to 227 L/s from the Pastos Grandes catchment at the North. The total inflow in the model as lateral recharge is 580 L/s.

- **Evaporation and Evapotranspiration groundwater discharge:** using a fluid-transfer boundary condition (third-type boundary). A head reference, maximum flow constraint, and transfer rate were applied to represent dynamic evaporation rates. These rates were set to match the maximum evaporation rate when the water table reached ground elevation and decreased linearly to zero when the water table dropped to or below the extinction depth of 2.5 m. The steady-state evaporation magnitude was calibrated using target evaporation fluxes derived from the conceptual water balance.

- **Pumping wells:** pumping wells were implemented using the Multilayer Well Boundary Condition (4th type boundary). Figure 142 illustrates the spatial distribution of wells for both transient calibration and prediction simulations. In the transient calibration simulation, the wells correspond to those used in the pumping test, while in the prediction simulation, they represent brine and freshwater extraction wells.

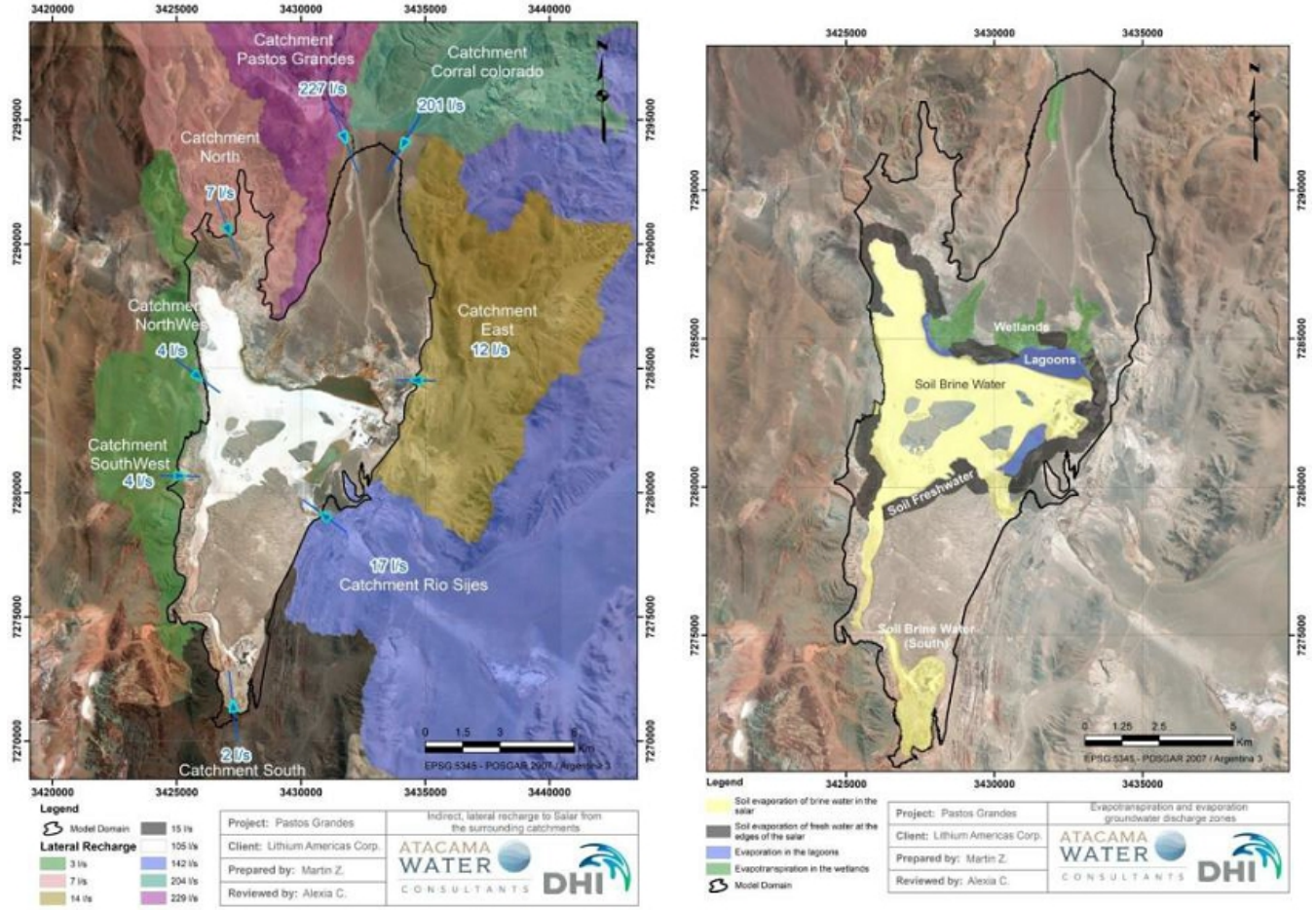

Figure 134: Indirect, Lateral Recharge (Left) and Evapotranspiration and Diffuse Groundwater Discharge Zones (right) to Salar Pastos Grandes (Source: AW, Dec 2024)

11.5.1.4 Mass Boundary Conditions

The only mass boundary conditions in the model are applied at the nodes of lateral recharge entry. These nodes use Mass Concentration Boundary Conditions (1st type) with a prescribed concentration of 0 mg/L. This implementation ensures that no mass enters the model, adopting a conservative approach suitable for LCE production scenarios.

11.5.1.5 Hydrogeological Units and Parameters

The five main hydrogeological units from the Leapfrog geological model were incorporated into the numerical model:

- Fluvial/Alluvial Unit: alluvial and fluvial sediments surrounding the Salar. For calibration purposes, this unit is divided into 6 different zones in the model.
- Upper Clay Unit (Blanca Lila Fm): clay-dominated units in the center-south of the basin as well as in the western margin. For calibration purposes, this unit is divided into 6 different zones in the model.
- Saline/Lacustrine Unit: massive and compact halite body with presence of interstitial clastic material and occasional intercalations of finer levels of clay located below the Blanca Lila Fm and in the north- central part of the Salar at surface. For calibration purposes, this unit is divided into 3 different zones in the model.
- Central Clastic Unit consists of clay and clayey sands and occurs within the central sector of the basin underneath the halite deposits. For calibration purposes, this unit is divided into 4 different zones in the model.
- Base Breccia/Gravels Unit: a sedimentary breccia unit of coarse fragments of silicified conglomerate and ignimbrites. It contains intermixed levels of sand and gravel with a thickness of 200 m on the western edge of the basin and deepens towards the north-central limit of the resource area. For calibration purposes, this unit is divided into 3 different zones in the model.

The basement unit is not considered in the simulation and is inactivated. A total of 22 hydrogeological property zones is defined in the model. The main hydrogeological zones are shown in Figure 135 and Figure 136.

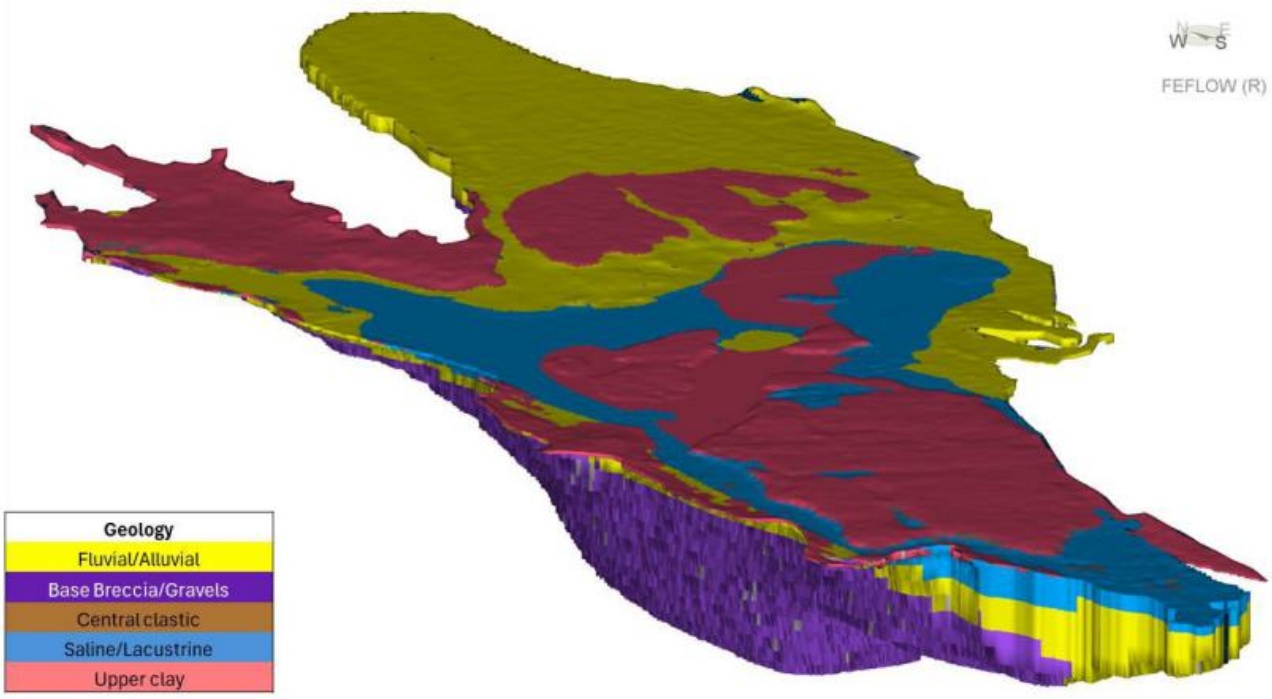

Figure 135: 3D View of the Hydrogeological Units in the Mmodel (Source: AW, Dec 2024)

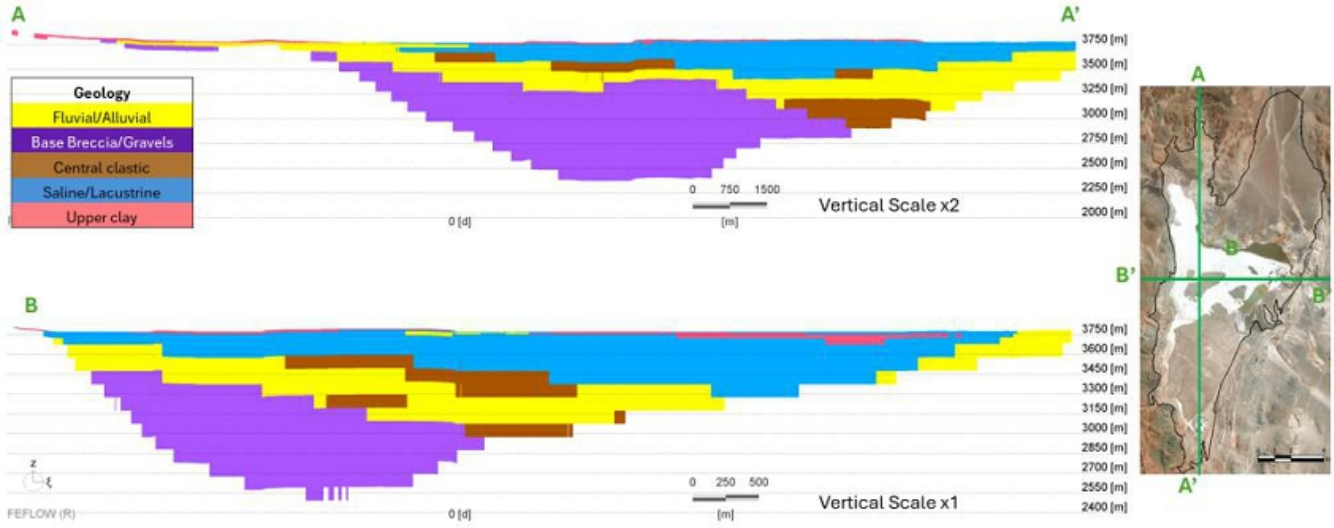

Figure 136: Hydrogeological Units in Cross Sections (Source: AW, Dec 2024)

11.5.1.6 Flow Parameters

For each hydrogeological unit, the hydraulic conductivity and specific storage are considered during the calibration process. The parameters used in the Feflow model are shown in Table 70. Also shown in the table is the conceptual specific yield values range for each hydrogeological unit. Total porosity is a calibration parameter that is adjusted to fit the conceptual specific yield.

Table 70: Unsaturated Parameter Values

Hydrogeological units	Specific Yield Sy (-)		Total Porosity	Sr	Alpha	n	m	Delta
	Conceptual Min	Conceptual Max	(-)	(-)	(1/m)	(-)	(-)	(-)
Base Gravels	1.0E-01	1.7E-01	0.20	0.20	2.50	1.45	0.40	1.50
Central Clastic	8.0E-02	1.7E-01	0.18	0.20	2.50	1.45	0.40	1.50
Saline/Lacustrine	3.0E-02	6.0E-02	0.12	0.10	0.50	1.35	0.25	4.00
Upper Clay	5.0E-02	7.0E-02	0.30	0.60	0.10	1.19	0.70	1.50
Upper Clay (outside salar)	5.0E-02	7.0E-02	0.30	0.60	0.10	1.19	0.70	1.50
Alluvial	1.2E-01	1.8E-01	0.20	0.20	2.50	1.45	0.40	1.50

11.5.1.7 Lithium Transport Parameters

In addition to groundwater flow, the FEFLOW model also considers mass to simulate the transport of lithium. Specific model parameters such as longitudinal and transverse dispersivity were defined as follows: longitudinal dispersivity was set to a constant value of 20 m and the horizontal and vertical transverse dispersivity values were set to 10 m. In addition, unwinding process is activated. The effective porosity for the mass transport simulations was based on the conceptual specific yield and consistent with the value used for the resource estimate as it is shown in Table 71.

The initial concentration of lithium for the simulations was based on resource model (Section 14) and is shown in Figure 137.

Table 71: Effective Porosity for Transport Simulations

Hydrogeological units	Effective Porosity (-)
Base Gravels	0.138
Central Clastic	0.122
Saline/Lacustrine	0.046
Upper Clay	0.120
Alluvial	0.149

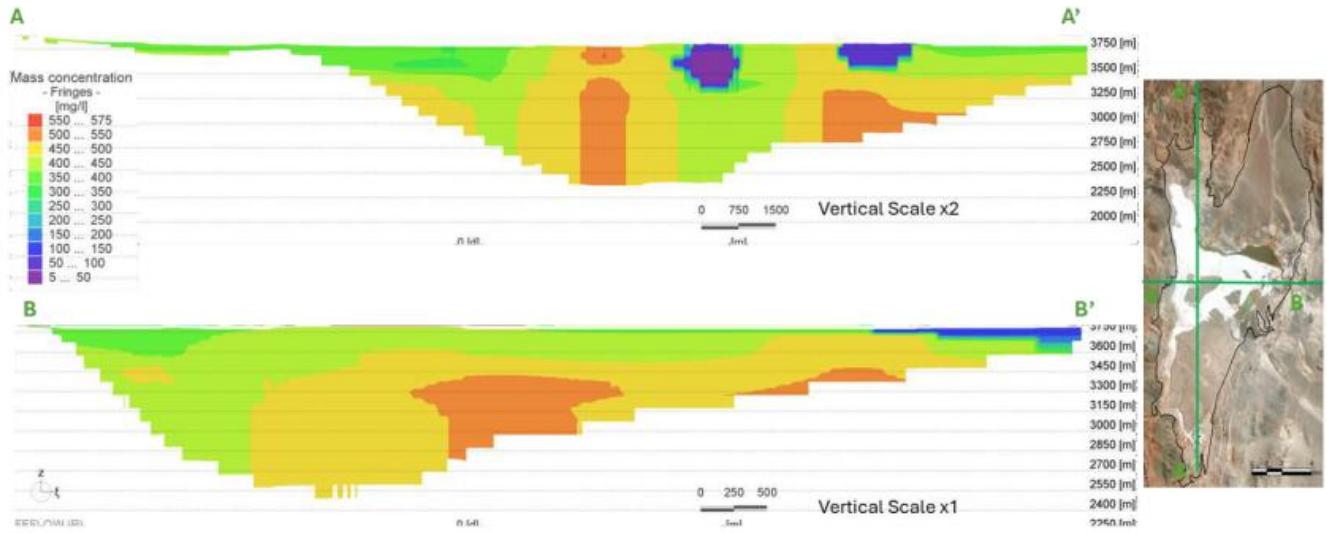

Figure 137: Initial Distribution of Lithium Concentration (Source: AW, Dec 2024)

11.5.2 Model Calibration

The flow model was calibrated for steady state and transient conditions to (1) fit the static water levels, (2) match the conceptual water balance, and (3) simulate head drawdowns from different pumping tests. A combination of manual and automated calibration was completed for both calibration processes. For the automated calibration, Feflow's built-in version of the PEST parameter optimization program, FePest, was applied.

11.5.2.1 Steady State Calibration

In the steady state calibration, the hydraulic conductivities and the transfer coefficients used to simulate evapotranspiration and evaporation discharge were calibrated to fit the observed heads and the conceptual flow values for evaporation.

A total of 49 parameters were calibrated for the steady state head and flow solution: 44 parameter zones were applied for calibration of saturated hydraulic properties and 5 zones for the out- transfer rate that affects the evapotranspiration outflow. Each parameter was restricted by the conceptual ranges. The hydraulic properties parameters were later further calibrated in the transient calibration.

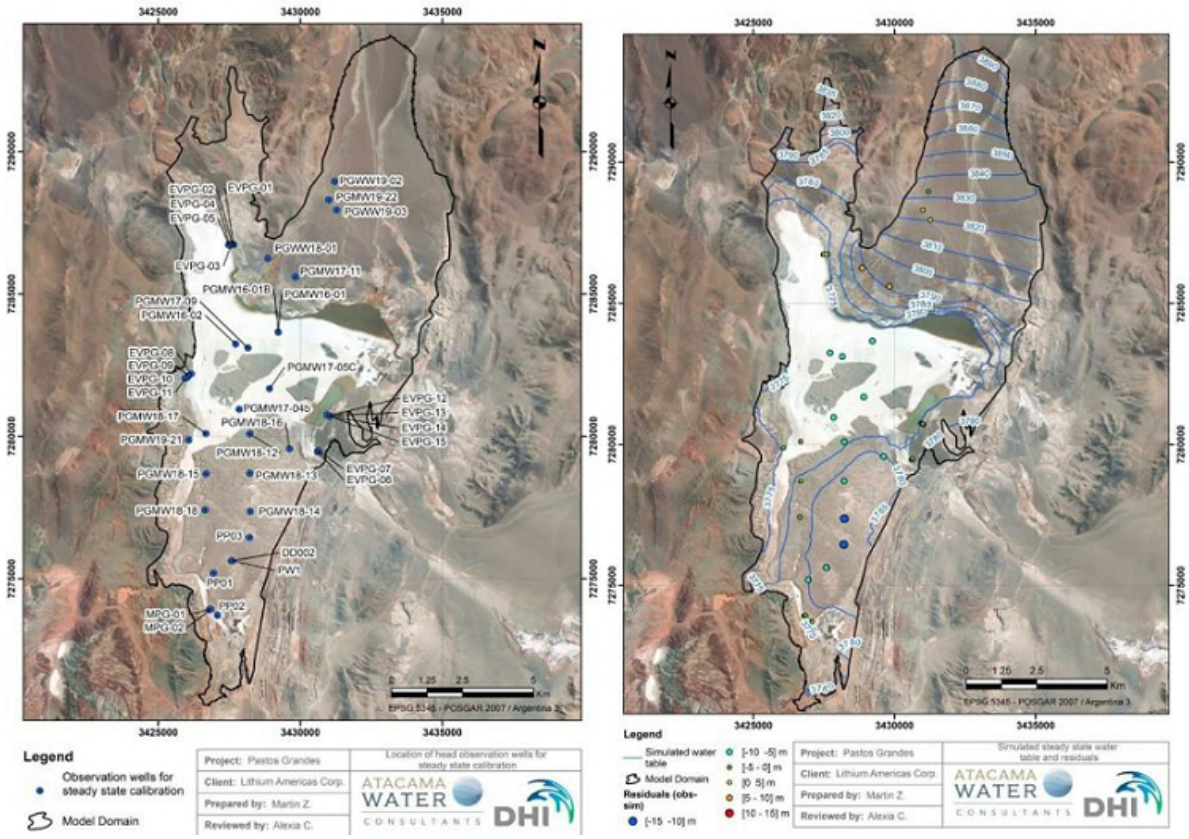

Figure 138: Location of Head Observation Piezometers (left) and Simulated Steady State Water Table and Residuals (right) (Source: AW, Dec 2024)

Figure 138 shows the simulated steady state water table and a map-view of the calibration residuals. Figure 139 and Table 72 display the calibration statistics. The mean residual head for the steady state calibrated model is -2.5 m and the mean absolute residual (MAE) is 4.2 m. The head error as the normalized root means squared error (NRMSE) is 8.6%.

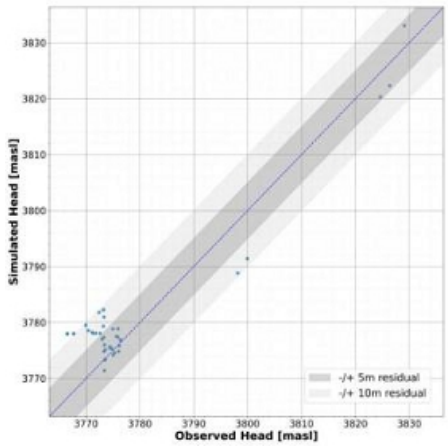

Figure 139: Observed vs. Simulated Water Levels (Source: AW, Dec 2024)

Table 72: Steady Sate Calibration Statistics

Number of piezometers	41
Normalized Root Mean Squared Error NRMSE (%)	9.7%
Root Mean Squared Error NRMSE (m)	6.0
Residual Mean (m)	-3.6
Mean Absolute Residual MAE (m)	4.9

The calibrated water balance components are shown in Table 73. The simulated total inflow/outflow is 581 L/s which is within the conceptual range of 200 to 900 L/s. The simulated lateral recharge rate of 477 L/s is lower than the conceptual estimate due to the reduced simulated inflow from the Rio Sijes basin.

Table 73: Simulated Water Balance

Components		Conceptual Target (L/s)		Calibrated Value (L/s)
		Value	Range	
Inflow	Lateral Recharge	617	150 - 750	477
	Direct Recharge by Precipitation	105	50 - 150	104
	Total	722	200 - 900	581
Outflow	Soil Evaporation	439	100 - 500	334
	Lagoons Evaporation	140	50 - 200	95
	Wetlands Evapotranspiration	143	50 - 200	152
	Total	722	200 - 900	581

11.5.2.2 Transient Calibration

Pumping tests from production wells PGPW1815, PW1, PG2023-03PW and PGPW16-01 were used for the transient calibration of hydraulic conductivity and storage parameters. Several other pumping tests were considered inappropriate for the transient calibration process. Summary details of each pumping test are as follows:

- Pumping test PGPW1815: 3-day pumping test at a constant rate of 24.1 L/s. Monitoring well PGPM1815 is located 22 m from the pumping well. Both pumping and monitoring wells have long screen intervals across the lacustrine, alluvial and base gravels units.
- Pumping test PG2023-03PW: 1-day pumping test at a constant rate of 17.5 L/s. Monitoring wells PG-2023-03 and Li.PG.RW-06 are located 9 m and 1,910 m from the pumping well, respectively. The pumping well and PG-2023-03 are screened in the clastic and alluvial units, while Li.PG.RW-06 is in the lacustrine unit.
- Pumping test PGPW16-01: 15-day pumping test at a constant rate of 30.2 L/s. 2 monitoring wells are used for the calibration process: SWPG03-01 and PGMW16-01. The pumping well is screened in the lacustrine and alluvial units. Monitoring wells PGMW16-01B and SWPG03-02 are discarded from the calibration due to small drawdown amplitude that is difficult to breakdown from residual noise and for consistency from previous study (Dworzanowski et al., 2018).

- Pumping test PW-01: 10-hour step test with rate increasing from 13.2 L/s to 24.8 L/s. The monitoring wells DD-02 and M-01 are located 17 m and 31 m respectively from the pumping well. Both pumping well PW-01 and monitoring well DD-02 are screened in the alluvial unit. Monitoring well M-01 is screened in the lacustrine unit.

The drawdown in the pumping wells was not calibrated. As part of the calibration process, the observation points of the monitoring wells and the screen elevation of the pumping well may have been adjusted.

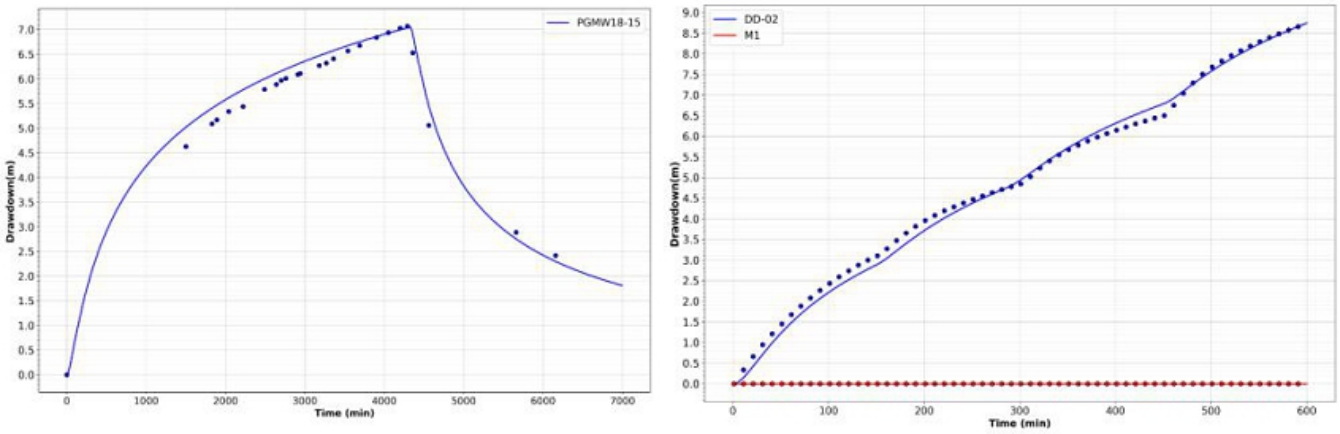

Figure 140: PGPW1815 (left) and PW1 (right) Pumping Test Simulated and Observed Drawdowns (Source: AW, Dec 2024)

In PGPW1815 and PW1 pumping test, the observed and modelled water level responses are shown in Figure 140. The calibrated drawdown shows a good fit to the measured data, representing both the maximum drawdown and the global trend of the monitoring wells.

For PG-2023-03PW and PGPW16-01 pumping test, the observed and modelled water level responses are shown in Figure 141. The calibrated drawdown shows the same trend as the measured data, although the model overestimated the maximum drawdown in PG-2023-03 and PGMW16-01 by 0.2 m and 0.6 m, respectively.

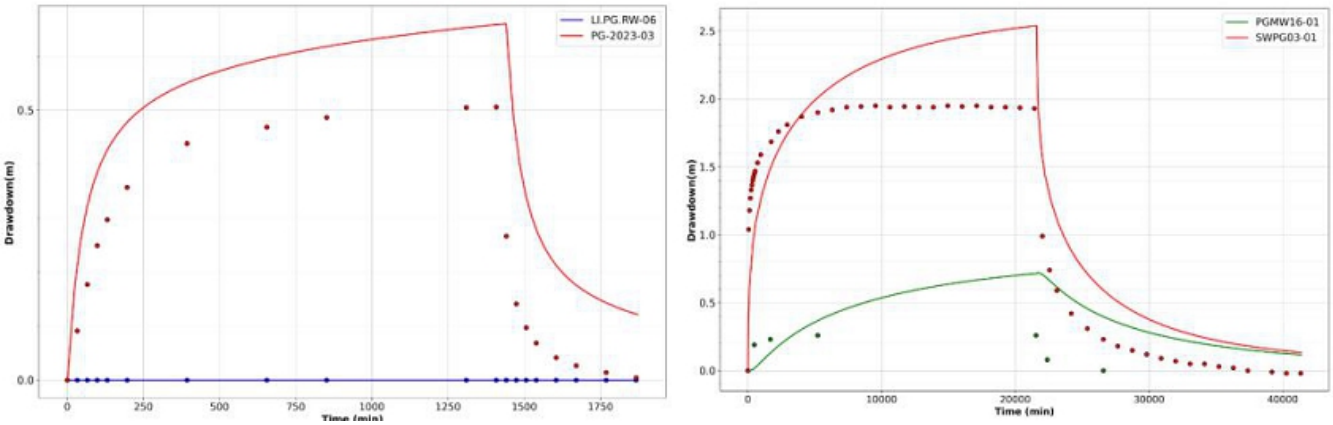

Figure 141: PG-2023-03PW (left) and PGPW16-01 (right) Pumping Test Simulated and Observed Drawdowns (Source: AW, Dec 2024)

Table 74: Pumping Test Maximum Simulated and Observed Drawdown Values

Pumping well	Monitoring well	Maximum observed drawdown (m)	Maximum simulated drawdown (m)
PGPW18-15	PGMW18-15	7.1	7.0
PW01	DD-02	8.8	8.8
	M1	0.0	0.0
PG-2023-03PW	PG-2023-03	0.5	0.65
	LI.PG.RW-06	0.0	0.0
PGPW1601	PGMW16-01	1.9	2.7
	SWPG03-01	0.2	0.8

11.5.3 Predictive Simulations

The numerical model, calibrated to steady state and transient flows and heads, was used to simulate brine extraction over a 20-year period. The simulation utilizes transient groundwater flow and lithium mass transport beginning with the initial steady state head distribution (Figure 138) and the initial lithium concentration distribution (Figure 137) from the brine resource estimate (Section 14). The analysis assumes an overall efficiency of 75% to estimate LCE production. A freshwater wellfield with a total flow rate of 150 L/s is included in the simulation.

11.5.3.1 Wellfield Layout

Figure 142 shows the well locations for the brine production and freshwater wellfield.

The freshwater wellfield configuration includes 10 wells located at the north of the salar, which can provide enough resource for Phase I and II of the Project. Each well has a constant pumping rate of 15 L/s for a total of 150 L/s over the 20-year Project life.

The brine wellfield production rate is 977 L/s for a period of 20 years, distributed among 47 production wells with a constant rate varying between 7 L/s and 25 L/s. The production wells are screened in moderate to high permeable units, below the lacustrine.

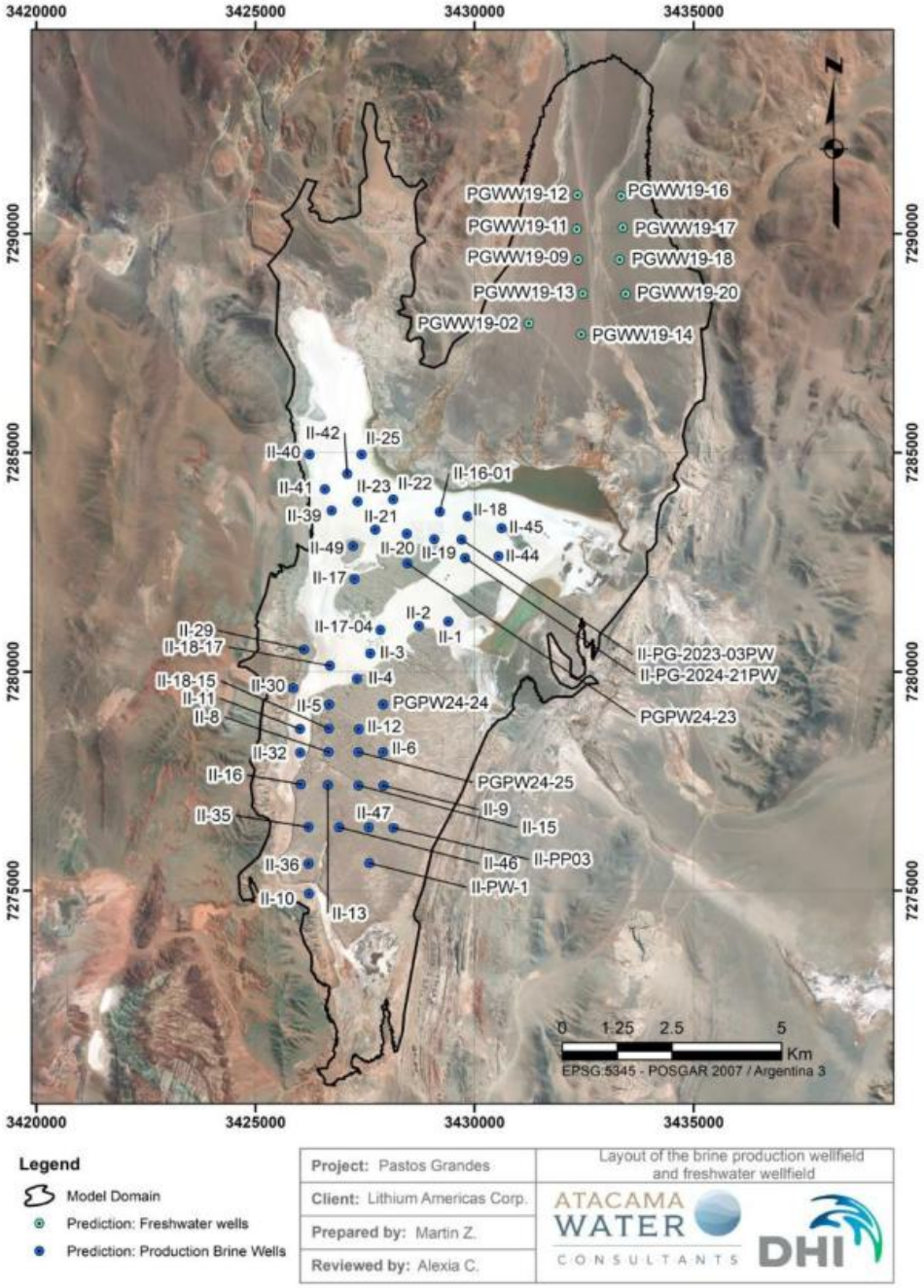

Figure 142: Layout of the Brine Production Wellfield and Freshwater Wellfield (Source: AW, Dec 2024)

11.5.3.2 LCE Production

The model simulations predict that 1,395 kt of LCE is contained in the brine pumped to the evaporation ponds over the 20-year period, resulting in a final LCE plant production of 1,045 kt considering an overall 75% efficiency. The annual production profile of LCE contained in the pumped brine is shown in Figure 143. The yearly average over the 20-year period is 52.3 kt/year.

The lithium concentration in the produced brine evolves over the 20-year period as shown in Figure 143. The average lithium concentration is predicted to range between 435 mg/L and 415 mg/L.

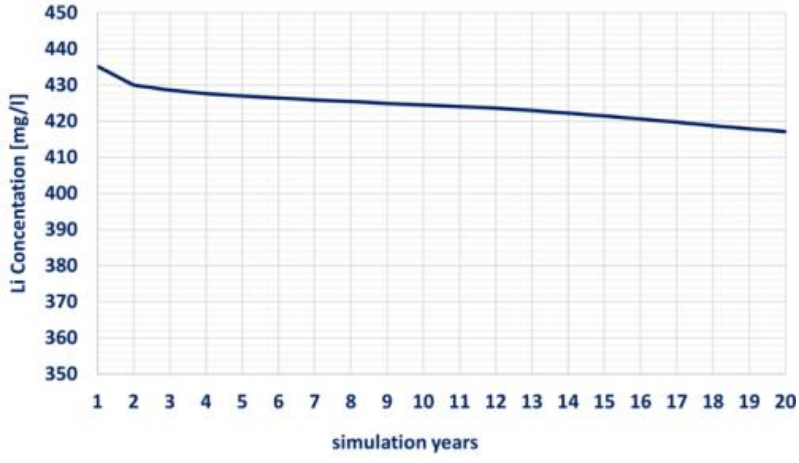

Figure 143: Average Lithium Concentration of Wellfield Production (top) (Source: AW, Dec 2024)

11.5.3.3 Water Table Predictions

The simulated water level responses after 20 years of brine production are shown in Figure 144. The drawdown at the water table is predicted to be around 15 m in the freshwater wellfield at the north of the salar. The water table declines in the brine wellfield are between 20 and 30 m at the end of operation. Drawdown up to 80 m is predicted to occur on the west side of the brine production wellfield, where the low permeability Lacustrine unit is not present.

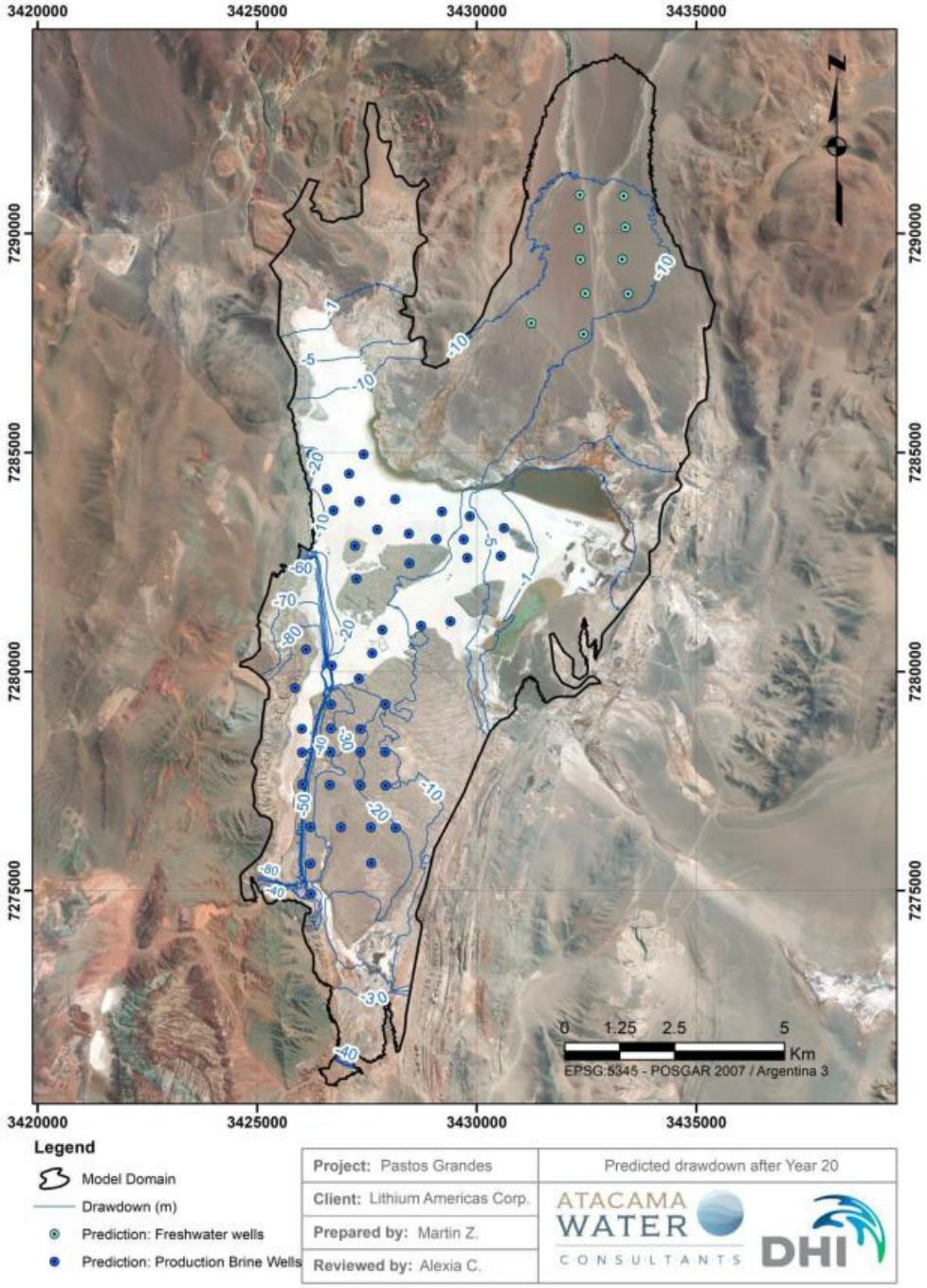

Figure 144: Predicted Drawdown after Year 20 (Source: AW, Dec 2024)

11.5.4 Model Result

The lithium dynamic model was carried out based on a FEFLOW multi-species simulation. Each resource type is a species in the model. Four species were defined for characterizing the Measured, Indicated and Inferred Resources and any brine coming from outside the resource model domain.

The brine for pumping to ponds is summarized in Table 75. The brine production, assuming a 75% overall recovery efficiency, is shown in Table 76.

Table 75: Simulated Water Balance

Year	Brine Volume (Mm^3)	Average Lithium Conc‘ (mg/L)	Li Metal (tonnes)	LCE (tonnes)
1-7	216	429	93,000	493,000
8-20	402	422	169,000	902,000
1-20	**618**	**424**	**262,000**	**1,395,000**

Table 76: Brine Production for Lithium Carbonate Production (Assuming 75% of Overall Lithium Recovery Efficiency)

Year	Brine Volume (Mm^3)	Average. Lithium Conc’ (mg/L)	Li Metal (tonnes)	LCE (tonnes)
1-7	216	429	70,000	371,000
8-20	402	422	127,000	674,000
1-20	618	424	197,000	1,045,000

Notes to the estimate:

- *The current brine wellfield layout and pumping schedule is not optimized and approximately 27% of the total mass of Li is derived from Inferred (13%) and outside mass (14%).*
- *No cut-off grade has been applied to the simulation*
- *Lithium is converted to lithium carbonate (Li_2CO_3) with a conversion factor of 5.32.*
- *Numbers may not add due to rounding or averaging effects.*

12.0 MINERAL RESERVE ESTIMATE

No reserve has yet been defined for the PPG Project. Two updated groundwater models have been developed for Pozuelos and Pastos Grandes Salars with the results of drilling and testing to date and this will be used to develop a maiden reserve for the PPG Project.

13.0 MINING METHODS

Mineral brine, occurring as groundwater within the salars, is to be used as the primary raw material for lithium carbonate production. A total of about 10,500 m^3/h of raw brine feed is the design rate to support a lithium carbonate production in three phases each of 51,000 TPA LCE.

The brine extraction wellfields will be located within the respective Salars and will be accessible by interconnected roads and in the case of Pozuelos from the solar evaporation ponds.

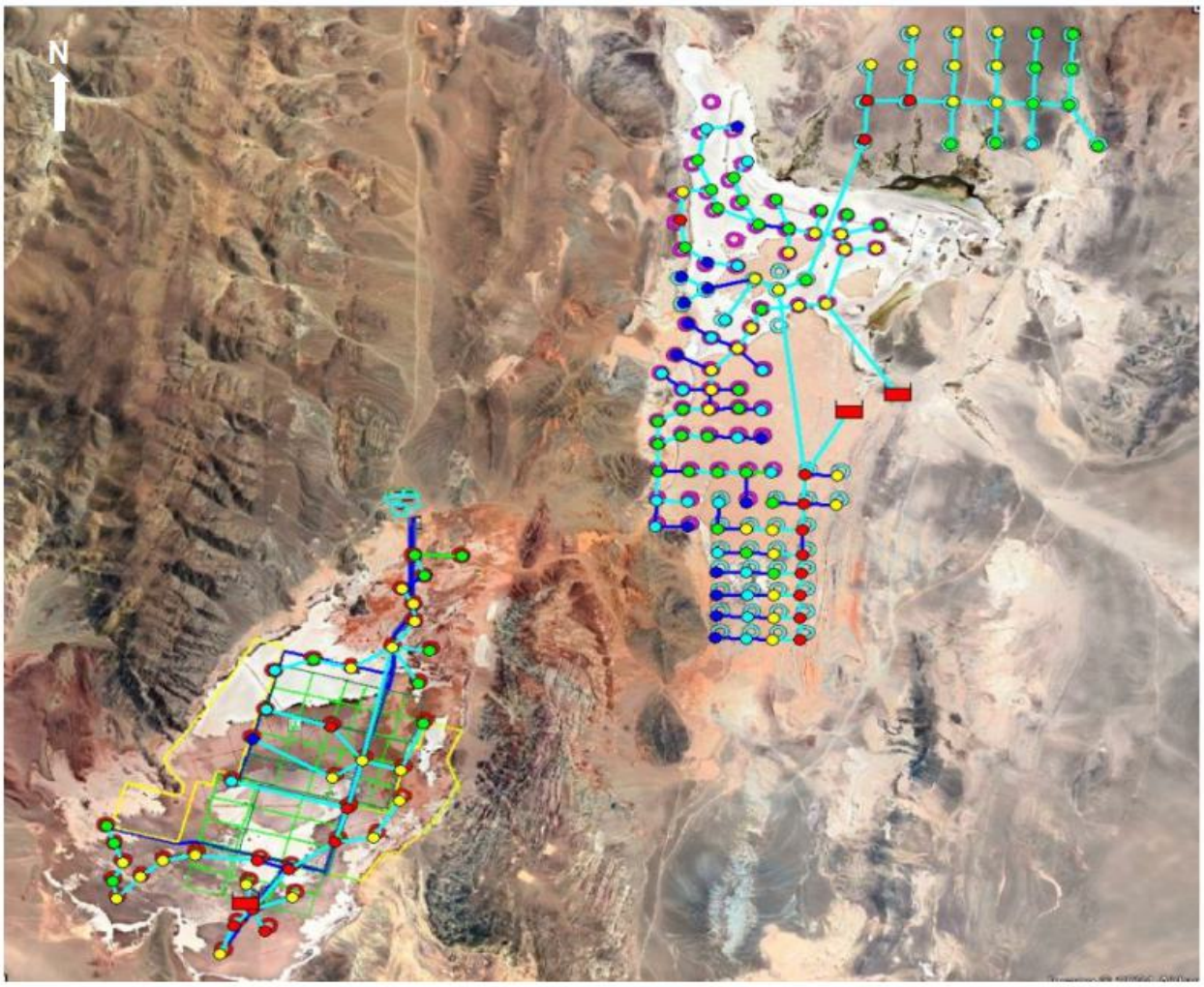

Figure 145: Production Wells for Three Phases

13.1 Brine Wellfield

Phase 1 wellfield is consisted of 34 production wells, while Phases 2 and 3 will include 60 and 61 wells respectively including spares and redundant wells. The brine production wells will be completed with a 12-inch-diameter stainless steel production casing and be equipped with 380V submersible pumping equipment. The well depth will vary from 420 m to 640 m for the different phases of the project. The power to the wellfield and individual wells will be delivered via a medium voltage power line.

The brine production wellfield will be operated during the three phases to support a production of approximately 51,000 TPA LCE for each phase.

The power to each pump and to the well field will be delivered via a medium voltage power line. The brine feeding to solar evaporation ponds is transported by pipelines to a series of solar evaporation ponds, for each phase.

The coordinates and parameters for the wells are shown in Table 77 to Table 79. A simplified general layout of the wells is depicted in Figure 146. For 51,000 TPA 34 wells will be built for the Pozuelos (Phase 1) and 60&61 wells for Pastos Grandes during Phases 2&3, including auxiliary and spares providing 80-90% availability of all operational wells.

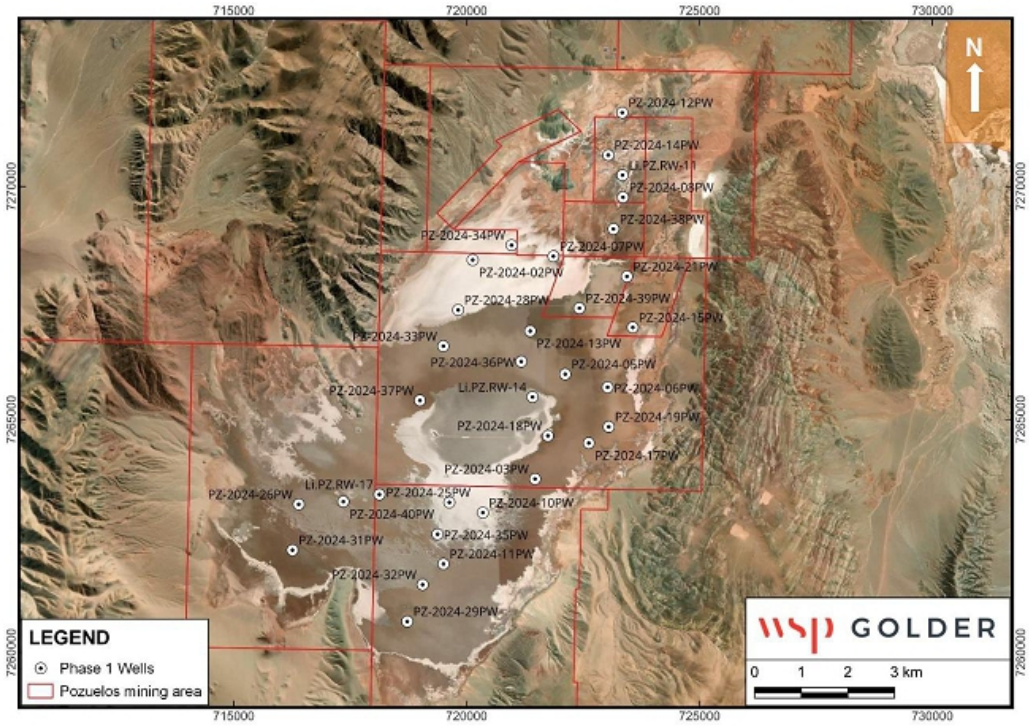

Figure 146: Production Wells for Phase 1

Table 77: Pozuelos Wells (Phase 1)

No.	Wells Phase 1	X	Y	Depth		No.	Wells Phase 1	X	Y	Depth
1	Li.PZ.RW-11	723345	7270242	372		18	PZ-2024-05PW	722115	7265975	600
2	Li.PZ.RW-14	721415	7265485	424		19	PZ-2024-15PW	723566	7266977	600
3	Li.PZ.RW-17	718126	7263394	162		20	PZ-2024-21PW	723440	7268070	400
4	PZ-2024-03PW	721467	7263727	404		21	PZ-2024-25PW	719628	7263223	500
5	PZ-2024-06PW	723025	7265693	500		22	PZ-2024-28PW	719816	7267352	400
6	PZ-2024-07PW	721862	7268504	270		23	PZ-2024-29PW	718725	7260670	400
7	PZ-2024-10PW	720347	7263004	460		24	PZ-2024-30PW	716015	72640180	400
8	PZ-2024-12PW	723341	7271585	380		25	PZ-2024-31PW	716260	7262200	400

No.	Wells Phase 1	X	Y	Depth		No.	Wells Phase 1	X	Y	Depth
9	PZ-2024-14PW	723040	7270674	392		26	PZ-2024-32PW	719055	7261460	400
10	PZ-2024-17PW	722622	7264497	500		27	PZ-2024-33PW	719497	7266575	400
11	PZ-2024-19PW	723051	7264846	639		28	PZ-2024-34PW	720963	7268741	400
12	PZ-2024-26PW	716395	7263183	220		29	PZ-2024-35PW	719375	7262542	400
13	PZ-2024-08PW	723356	7269768	400		30	PZ-2024-36PW	721173	7266246	400
14	PZ-2024-11PW	719502	7261903	400		31	PZ-2024-37PW	718996	7265410	400
15	PZ-2024-13PW	721364	7266900	400		32	PZ-2024-38PW	723152	7269089	400
16	PZ-2024-18PW	721745	7264652	550		33	PZ-2024-39PW	722419	7267390	400
17	PZ-2024-02PW	720130	7268425	400		34	PZ-2024-40PW	717350	7263240	400

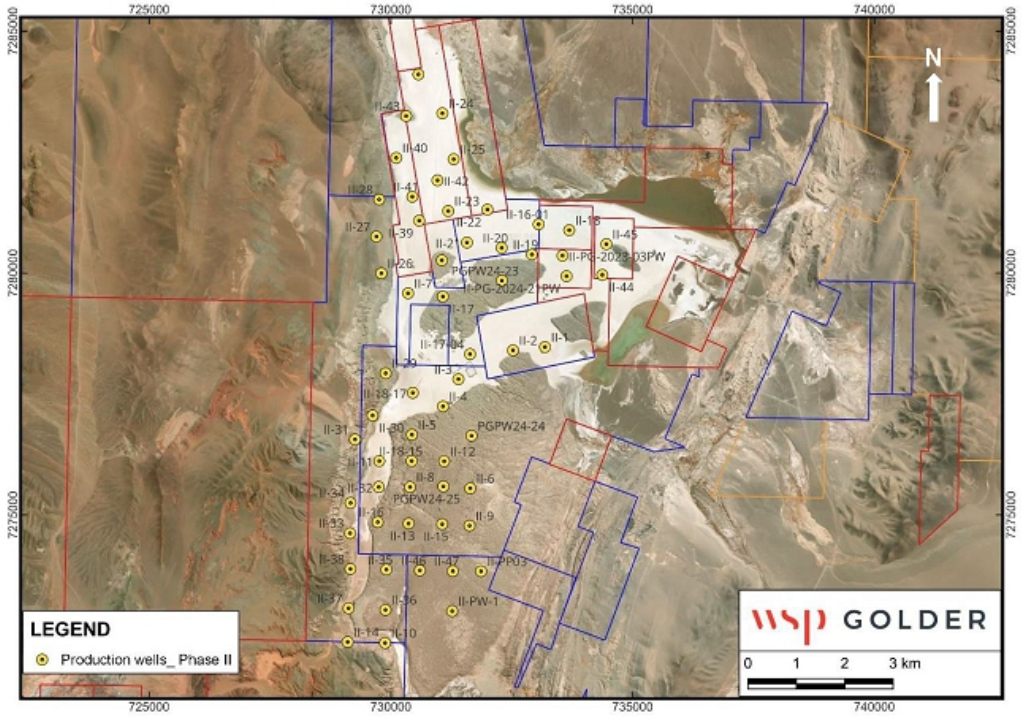

Figure 147: Proposed Production Wells for Phase 2

Table 78: Pastos Grandes Wells (Phases 2)

No.	WELLS	X	Y	Depth	Flow Rate (L/s)		No.	WELLS	X	Y	Depth	Flow Rate (L/s)
1	II-1	3429388	7281126	650	25		31	II-31	3425506	7279127	650	17.5
2	II-2	3428731	7281038	650	25		32	II-32	3426019	7278155	650	17.5
3	II-3	3427616	7280419	650	17.5		33	II-33	3425445	7277188	650	17.5
4	II-4	3427316	7279851	650	17.5		34	II-34	3425443	7277813	650	17

No.	WELLS	X	Y	Depth	Flow Rate (L/s)		No.	WELLS	X	Y	Depth	Flow Rate (L/s)
5	II-5	3426680	7279250	650	17.5		35	II-35	3426213	7276453	650	17
6	II-6	3427913	7278166	650	17.5		36	II-36	3426212	7275619	650	12
7	II-7	3428436	7279255	650	17.5		37	II-37	3425449	7275638	650	12
8	II-8	3426665	7278168	650	17.5		38	II-38	3425470	7276450	650	17.5
9	II-9	3427919	7277397	650	17.5		39	II-39	3426734	7283676	650	25
10	II-10	3426219	7274935	650	17.5		40	II-40	3426231	7284963	650	25
11	II-11	3426017	7278692	650	17.5		41	II-41	3426581	7284167	650	25
12	II-12	3427351	7278691	650	17.5		42	II-42	3427094	7284516	650	25
13	II-13	3426651	7277414	650	17.5		43	II-43	3426416	7285831	650	25
14	II-14	3425445	7274939	650	17.5		44	II-44	3430544	7282638	650	25
15	II-15	3427349	7277417	650	17.5		45	II-45	3430614	7283275	650	25
16	II-16	3426031	7277431	650	17.5		46	II-46	3426906	7276451	650	17.5
17	II-17	3427258	7282119	650	25		47	II-47	3427587	7276451	650	17.5
18	II-18	3429840	7283546	650	25		48	PGPW24-23	3428464	7282469	650	25
19	II-19	3429079	7283026	650	25		49	PGPW24-24	3427910	7279258	650	17.5
20	II-20	3428450	7283151	650	25		50	PGPW24-25	3427344	7278173	650	17.5
21	II-21	3427731	7283245	650	25		51	II-16-01	3429204	7283655	500	25
22	II-22	3428139	7283935	650	25		52	II-17-04	3427845	7280941	600	12.5
23	II-23	3427329	7283887	650	25		53	II-18-15	3426687	7278707	600	17.5
24	II-24	3427165	7285904	650	25		54	II-18-17	3426680	7280117	600	17.5
25	II-25	3427420	7284960	650	25		55	II-PW-1	3427592	7275625	600	17.5
26	II-26	3425976	7282570	650	25		56	II-PP03	3428171	7276461	600	7
27	II-27	3425855	7283328	650	25		57	II-PG-2023-03PW	3429712	7283019	514	17.5
28	II-28	3425895	7284095	650	25		58	II-PG-2024-21PW	3429804	7282595	504	17.5
29	II-29	3426109	7280509	650	17.5		59	II-48	3426654	7286701	650	12.5
30	II-30	3425860	7279630	650	17.5		60	II-49	3427214	7282856	650	12.5

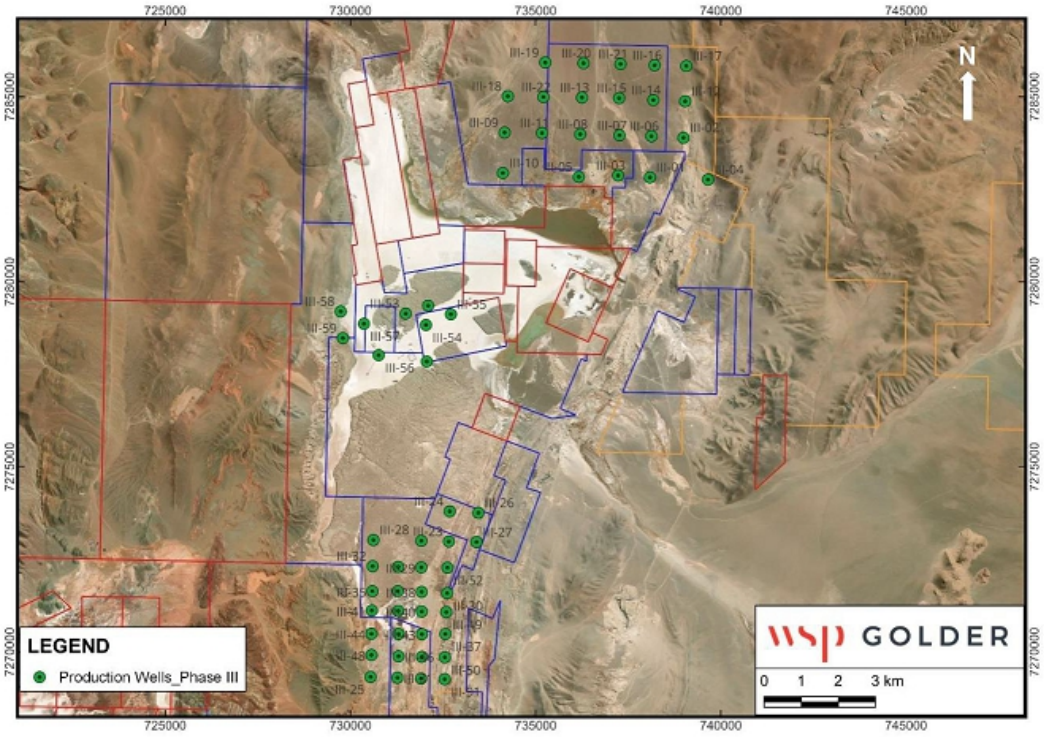

Figure 148: Proposed Production Wells for Phase 3

Table 79: Pastos Grandes Wells (Phases 3)

No.	Wells Phase3	X	Y	Depth (m)	Flow Rate (L/s)		No.	Wells Phase3	X	Y	Depth (m)	Flow Rate (L/s)
1	III-01	3434191	7285577	650	25		32	III-32	3426937	7274913	650	17.5
2	III-02	3435073	7286665	650	25		33	III-33	3427628	7274913	650	17.5
3	III-03	3433331	7285607	650	25		34	III-34	3428237	7275628	650	17.5
4	III-04	3435759	7285549	650	25		35	III-35	3426945	7274237	650	17.5
5	III-05	3432270	7285548	650	25		36	III-36	3427634	7274255	650	17.5
6	III-06	3434207	7286690	650	25		37	III-37	3428941	7273126	650	17.5
7	III-07	3433345	7286694	650	25		38	III-38	3428275	7274248	650	17.5
8	III-08	3432285	7286700	650	25		39	III-39	3427653	7273722	650	17.5
9	III-09	3430243	7286702	650	25		40	III-40	3428289	7273719	650	17.5
10	III-10	3430220	7285607	650	25		41	III-41	3426941	7273715	650	17.5
11	III-11	3431254	7286712	650	25		42	III-42	3427678	7273098	650	17.5
12	III-12	3435097	7287653	650	25		43	III-43	3428308	7273107	650	17.5
13	III-13	3432311	7287692	650	25		44	III-44	3426945	7273087	650	17.5
14	III-14	3434238	7287667	650	25		45	III-45	3428311	7271907	650	17.5

No.	Wells Phase3	X	Y	Depth (m)	Flow Rate (L/s)		No.	Wells Phase3	X	Y	Depth (m)	Flow Rate (L/s)
15	III-15	3433313	7287699	650	25		46	III-46	3427688	7272496	650	17.5
16	III-16	3434251	7288608	650	25		47	III-47	3428319	7272496	650	17.5
17	III-17	3435107	7288606	650	25		48	III-48	3426958	7272513	650	17.5
18	III-18	3430309	7287684	650	25		49	III-49	3428951	7273717	650	17.5
19	III-19	3431300	7288616	650	25		50	III-50	3428941	7272498	650	17.5
20	III-20	3432332	7288621	650	25		51	III-51	3428949	7271905	650	17.5
21	III-21	3433331	7288620	650	25		52	III-52	3428957	7274916	650	17.5
22	III-22	3431270	7287684	650	25		53	III-53	3427682	7281755	650	12.5
23	III-23	3428978	7275626	650	17.5		54	III-54	3428235	7281459	650	12.5
24	III-24	3428985	7276441	650	17.5		55	III-55	3428900	7281764	650	12
25	III-25	3426947	7271921	650	17.5		56	III-56	3426976	7280615	650	12
26	III-26	3429760	7276417	650	17.5		57	III-57	3426561	7281455	650	12
27	III-27	3429726	7275627	650	17.5		58	III-58	3425926	7281772	650	12
28	III-28	3426943	7275621	650	17.5		59	III-59	3426000	7281056	650	12
29	III-29	3428252	7274910	650	17.5		60	III-60	3428238	7282013	650	12.5
30	III-30	3428963	7274229	650	17.5		61	III-61	3428275	7280470	650	12.5
31	III-31	3427673	7271918	650	17.5		-					

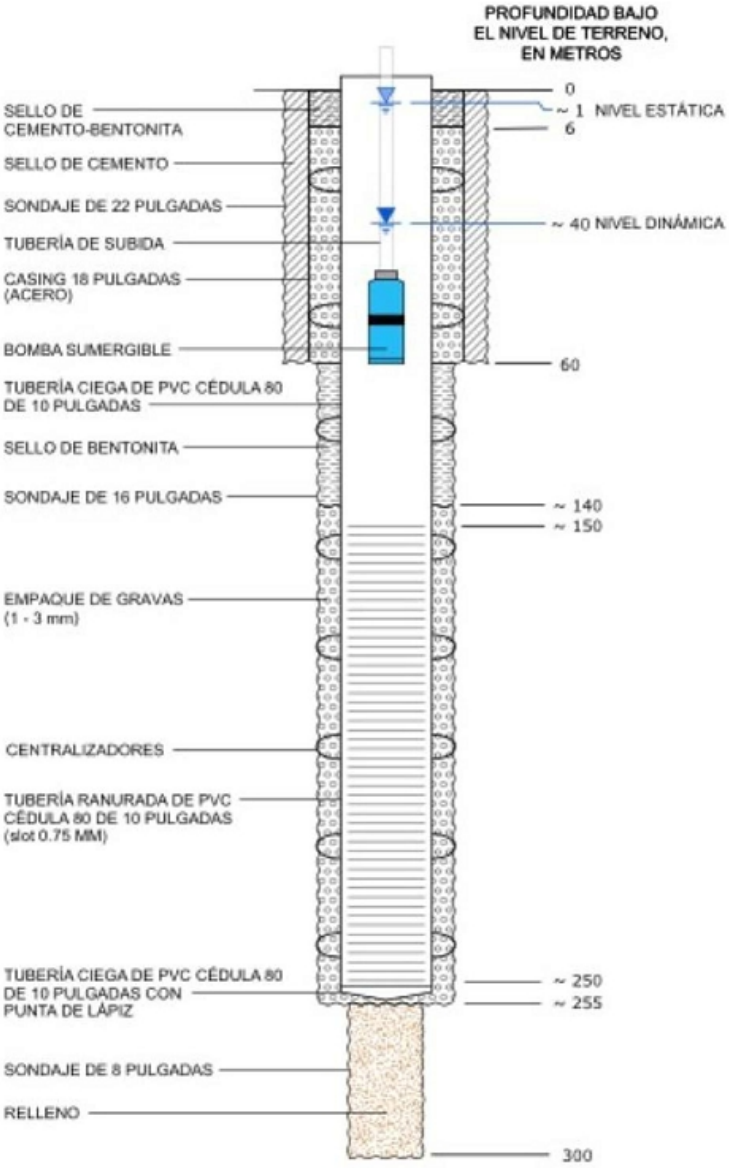

Figure 149: Construction Drawing of Production Well

The current design of the brine wellfields is subject to change, as continuous long-term pumping will have a cumulative effect on salt flat groundwater level and water quality.

The well piping designed is shown in Table 80.

Table 80: Design Properties of Wells Piping

Material	Schedule	DN		Internal Diameter (mm)
		(pulg)	(mm)	
HDPE ISO4427 PE100	PN10 (SDR17)	3	90	79
		4	110	97
		6	160	141
		8	200	176
		10	250	220
		12	315	278
		14	355	313
		16	400	353
	PN 16 (SDR11)	8	200	164
	PN 20 (SDR9)	6	180	139,8
ASTM A312	5S	8	219,1	214

13.1.1 Uncertainty Assessment

Risk pertaining was identified during the risk assessment conducted by the project team, as shown in Table 81. With the implementation of a risk treatment plan, the risk is reduced to low.

Table 81: Summary of Well Management Risks and Remedies

Risk Description	Existing Controls	Initial Risk	Risk Treatment Plan	Residual Risk
Maintaining constant brine feed to plant	Wellfield simulations used for design	Moderate	Construct backup production well	Low
Additional cost associated with low-yield wells	Wellfield simulations used for design	Moderate	Using pumping test results to improve well design during well construction	Low
Maximize lithium grade	Evaluation of test chemistry used to help well design	Low	Monitor well chemistry during production and possibly redesign future wells	Very Low
Minimize water level drawdown	Wellfield simulations to minimize drawdown	Low to Moderate	Monitor future drawdown and plan for well rehabilitation to improve efficiency	Low to Very Low
Minimize potential impacts to surface water	Wellfield simulations to locate wells to minimize surface water impacts	Moderate	Field monitoring to identify possible impacts, and then additional modelling to relocate or change pumping for the wells	Low

13.1.2 Well Utilization Philosophy

The goals of wellfield management for the project are as follows:

- Ensure an uninterrupted supply of brine to the processing plant
- Minimize the number of wells required to save costs
- Maximize lithium grade in the brine feed water
- Minimize water level drawdown at individual wells to reduce energy costs associated with pumping

- Prevent or minimize environmental impacts to surface water areas that may occur as a result of production pumping

To realize the wellfield goals as stated above, the existing, calibrated groundwater flow model was used for initial design of the wellfield and pumping regimen. In addition to initial planning, flexibility in wellfield operation is important to account for unanticipated changes in wellfield conditions or initial assumptions. Periodic monitoring of pumping rates and quantities, brine chemistry, and water levels in the wellfield and in the surrounding area is important for facilitating recalibration of the model, and to allow updated simulations and projections during the life of the mine.

The following remedies for achieving the goals above are summarized in Table 81.

Ensure an uninterrupted supply of brine to the processing plant. We recommend always having an extra well in the wellfield that is not pumped. If eight production wells are recommended for production, nine wells should be constructed. The extra well should be available in case of pump or well failure at one of the operating wells, or during maintenance, cleaning, and/or pump replacement. Cycling the production wells to give each well a "rest" is recommended during long-term production pumping.

Minimize the number of wells required to save costs. If possible, operating fewer wells at larger pumping rates may be cost beneficial regarding initial capital expenses and also operating expenses. The groundwater flow model can assist with an optimal design. Larger yield wells tend to more cost-effective than low-yield wells.

Maximize lithium grade in the brine feed water. This optimization is important for increasing total output of final product. In this recommendation, it is important to ensure that the pumping design minimizes potential future dilution of brine with fresh water, as well as target higher grade aquifer zones for increased lithium grade during production pumping.

Minimize water level drawdown at individual wells to reduce energy costs associated with pumping. During production well construction, it is important that the production wells are properly designed and developed to have the highest efficiency as possible. This initial efficiency will be reduced over time naturally, resulting in increased pumping lift and increased pumping costs. Therefore, periodic rehabilitation (cleaning) of the well screen to improve transmissivity of the well is recommended. In addition, determining the optimal/maximum distance between the wells is important to avoid interference effects which increase water level drawdown at the wells, or positioning wells too close to no-flow boundaries, which can also increase water level drawdown over time.

Prevent or minimize environmental impacts to surface water areas that may occur as a result of production pumping. The groundwater flow model is an important tool to predict potential impacts to nearby surface water and/or environmentally sensitive areas that may occur as a result of water level drawdown due to wellfield pumping. Model simulations may suggest optimal initial well locations and well design to minimize potential future impacts to surface water. If environmentally sensitive areas have been identified, a long-term monitoring program should be developed and implemented to measure potential impacts to these areas.

13.2 LCE Production Schedule

The project will have the capacity to produce 153,000 TPA LCE of Li_2CO_3 and $LiOH \times H_2O$, and it is planned to be developed and constructed in 3 Phases, each with a capacity of approximately 51,000 TPA LCE:

- **Phase 1:** 40,000 TPA Li_2CO_3 + 12,500 TPA $LiOH \times H_2O$
  - Brine from Pozuelos
  - 34 wells planned in Pozuelos
  - Starting production: Q1 2029
- **Phase 2:** Additional 40,000 TPA Li_2CO_3 + 12,500 TPA $LiOH \times H_2O$
  - Brine from Pastos Grandes
  - 60 wells in Pastos Grandes planned
  - Starting production: Q4 2031
- **Phase 3:** Additional 40,000 TPA Li_2CO_3 + 12,500 TPA $LiOH \times H_2O$
  - Brine from Pastos Grandes + Sal de la Puna + Pozuelos
  - 61 wells in Pastos Grandes + Sal de la Puna planned
  - Starting production: Q4 2035

Golder are comfortable with using 37% of measured and indicated (M+I) resources for production planning. It is common to apply 37% of aquifer efficiency factor to measured and indicated resources to estimate pumpable resources for mine life planning in the lithium brine industry. The predictive groundwater flow and transport model simulations carried out for Pozuelos and Pastos Grandes support that the application of the 37% efficiency factor is reasonable.

Table 82 shows that, if only M+I resources are included and 37% of M+I resources are considered pumpable, the PPG Project has a nominal production life of 30 years for Phase 1, 28 years for Phase 2, and 24 years for Phase 3. It is planned that all 3 phases will end in the same year. A 75% overall lithium recovery efficiency factor has been applied to calculate the final LCE production. This recovery is based on previous work and assumptions delivered by Ganfeng.

Table 82: LCE Production Schedule

	M+I	Pumpable**	Recovered*	Phase 1 @ 30 years (consumed)	Phase 2 @28 years + (consumed)	Phase 3 @ 24 years (consumed)	Remaining resources
Unit	**(kt, LCE)**	**(kt, LCE)**	**(kt, LCE)**	**(kt, LCE)**	**(kt, LCE)**	**(kt, LCE)**	**(kt, LCE)**
Pozuelos	7,017	2,569	1,947	1,492	-	387	68
Pastos Grandes	7,563	2,798	2,099	-	1,345	754	-

Note:

1. *Units: k (1,000) tons LCE.*
2. ** An overall recovery rate of 75% is used for all phases.*
3. *** Assuming 36% of M+I resources can be pumped out and go into production.*
4. *Annual production rate of ~51,000 TPA of LCE is assumed for each phase (40,000 TPA of Li_2CO_3 plus 12,500 TPA of $LiOH \times H_2O$).*

14.0 PROCESSING AND RECOVERY METHODS

14.1 General

Lithium recovery is based on a direct extraction process using brine pre-concentration followed by solvent extraction. Purification steps follow in order to produce lithium carbonate and lithium hydroxide. The target of 153,000 tons production is accomplished in three phases. For each phase, 51,000 tons of lithium carbonate equivalent comprising 40,000 tons lithium carbonate and 12,500 TPA lithium hydroxide monohydrate per year will be produced. The following sections cover the details for the phased production.

Process engineering and design for the ponds and the process plants were completed by Santiago, Chile based Adinf and Jiangxi, China based Ganfeng Lithium, respectively, based on their respective experience and test work results.

The construction of the PPG Lithium Plant will be in three stages. Each stage (phase) is designed to process 3,383,884 m^3/y of pre-concentrate brine feed and produce 51,000 TPA battery grade Lithium Carbonate Equivalent.

14.2 Process Description

The main activities involved in the process include:

- Extraction of brine from wells
- Pre-concentration of the brine in solar ponds
- Solvent extraction of the pre-concentrated brine
- Raffinate treatment
- Primary purification
- Secondary purification
- Lithium hydroxide and lithium carbonate precipitation

A simplified overall flowsheet of the process is shown in Figure 150.

Notes:

- *Please note that industrial grade lithium carbonate was not included in this report.*
- *Lithium carbonate flow scheme as developed in 2024 may show different recycles as compared the 2025 LiCl.*

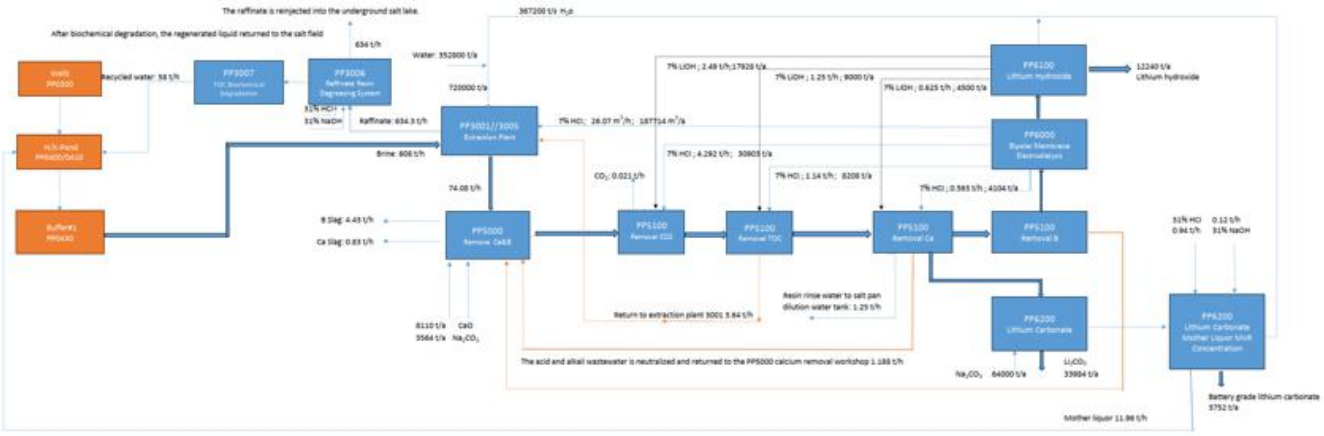

Figure 150: Simplified Overall Process Flowsheet for Each Phase (Source: Ganfeng, 2024)

14.3 Pre-concentration Ponds

The design of the evaporation ponds process considers the entry of brine from the wellfield to the first pond of each string. Water evaporation occurs along the string, formed by 8 ponds in series, in which the even ponds is separated by baffles and not by walls, in such a way that the use of transfer pumps is avoided and the flow of dilution water injected into the system is reduced. The string ends with a smaller pond, which also functions as a buffer. In this last pond, the final concentration of 3.09 g/L of lithium is reached. The concentrated brine is transferred to covered reservoirs, from where it is sent to the plant. The target lithium concentration for the plant has been defined as 3.05 g/L, which is obtained from the concentration of 3.09 g/L plus the dilution water added for transport to the plant. The concentration process is carried out in 4 parallel strings, with the same characteristics for each phase.

It is necessary to harvest the salts that precipitate in the ponds, as a result of the concentration and saturation of different brine compounds. The execution of the harvest determines that the area available for evaporation is slightly less than the area actually built. It is estimated that the availability is 90%, considering that at all times there is 10% of the built area that is out of service (not evaporated), while the salt harvest is carried out. During this activity, the recovery of impregnated brine is also carried out, in such a way as to minimize lithium losses at each stage. The evaporation system includes the addition of dilution water at each transfer to prevent incrustations formed by brine concentration.

The brine extracted from the production wells is pumped to the pre-concentration ponds, where lithium is concentrated to 0.246% Li.

Salt precipitation occurs as a result of evaporation and the saturation of salts according to chemical equilibrium, removed and disposed into a TMA (Tailings Management Area) stockpile. The location of the pre-concentration ponds, TMA are shown in Figure 152 and Figure 153.

The basic criteria for the ponds design are shown in Table 83. The process and design pond areas for each stage are shown in Table 84 and Table 85, where a pond availability of approximately 90% has been considered, due to the need to harvest, with the pond operating time of 365 days per year.

Table 83: Design Criteria for the Pre-concentration Ponds for All Stages

Parameter	Unit	Phase 1	Phase 2	Phase 3
Evaporation rate	mm/day	7 (referred to water)	7 (referred to water)	7 (referred to water)
Seepage	mm/m2	0.05	0.05	0.05
Entrainment	%w/w	10%	10%	10%
Feed Li Concentration	%w/w	0.0462	0.0355	0.0355
Flow Rate	TPD	67,070	87,347	87,347
Concentrated brine (Li)	%w/w	0.246	0.246	0.246
Flow Rate	TPD	11,635	11,635	11,635
Dilution Water	%	1%	1%	1%
Wells	N	34	60	61

Table 84: Preconcentration Ponds Areas for Stage 1**

Phase 1 PONDS 50KTPA (4 Strings)		
Pond Lines	Design Area (m^2)	Area each line (m^2)
PC1	1,743,744	435,936
PC2	2,076,928	519,232
PC3	2,076,928	519,232
PC4	1,845,888	461,472
PC5	1,845,888	461,472
PC6	1,383,808	345,952
PC7	1,383,808	345,952
PC8	994,688	248,672
R	28,000	7,000
Totals	**13,379,680**	**3,344,920**

** see note

The areas shown above represent the first phase of the project for a production to 51,000 TPA.

Table 85: Preconcentration Ponds Areas for Stage 2&3

Phases 2&3 PONDS 50KTPA each (4 Strings)		
Ponds Lines	Design Area (m^2)	Area each line (m^2)
PC1	2,120,704	530,176
PC2	2,643,584	660,896
PC3	2,643,584	660,896
PC4	2,290,944	572,736
PC5	2,290,944	572,736
PC6	1,763,200	440,800

Phases 2&3 PONDS 50KTPA each (4 Strings)		
PC7	1,763,200	440,800
PC8	1,357,056	339,264
R	28,000	7,000
Totals	**16,901,216**	**4,225,304**

The areas shown above represent each phase of the project to reach 51,000 TPA nominal **.

The pre-concentration pond systems are divided into four (4) independent strings each with 8 areas. Once the brine reaches the target lithium concentration, it is pumped to a Buffer Pond for storage, from where it will be transferred to the processing plant designed to process 11,635 tons per day of brine at 0.246% Li over 300 days operating time, same for each of the 3 Phases of production.

Ponds configuration is shown in Figure 151.

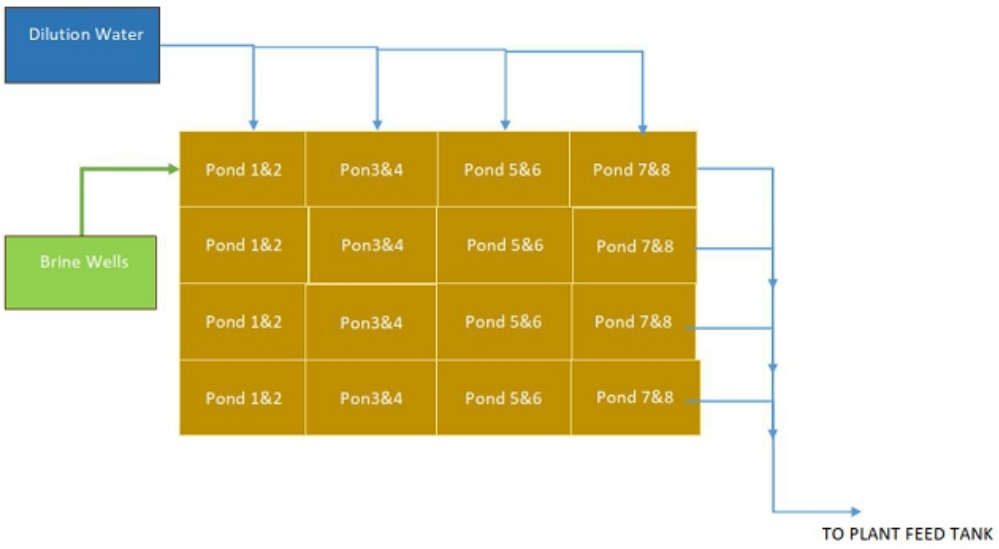

Figure 151: Ponds Simple Conceptual Configuration (Source: Ganfeng, 2024)**

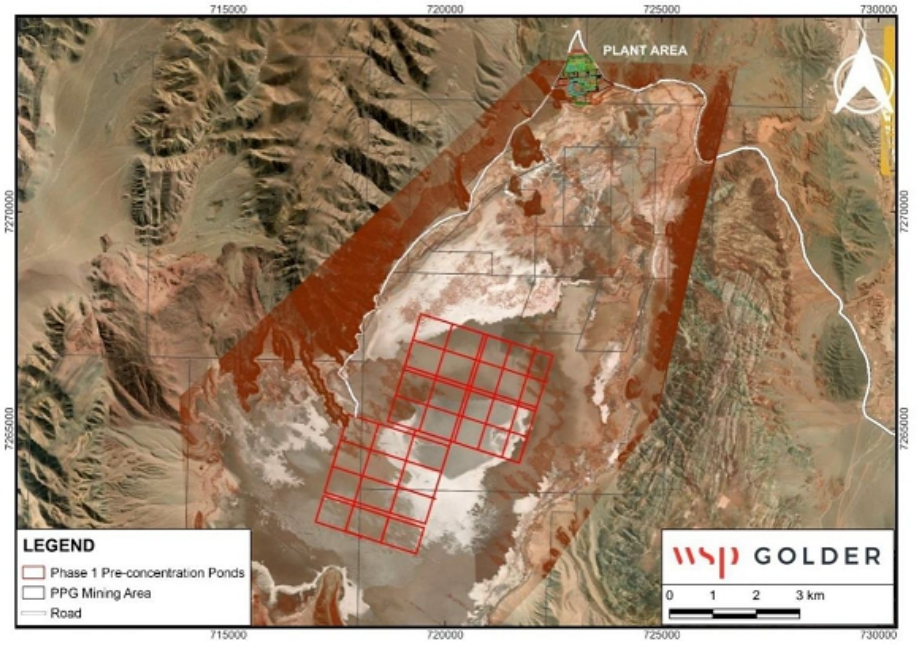

Figure 152: Phase 1 Ponds Layout

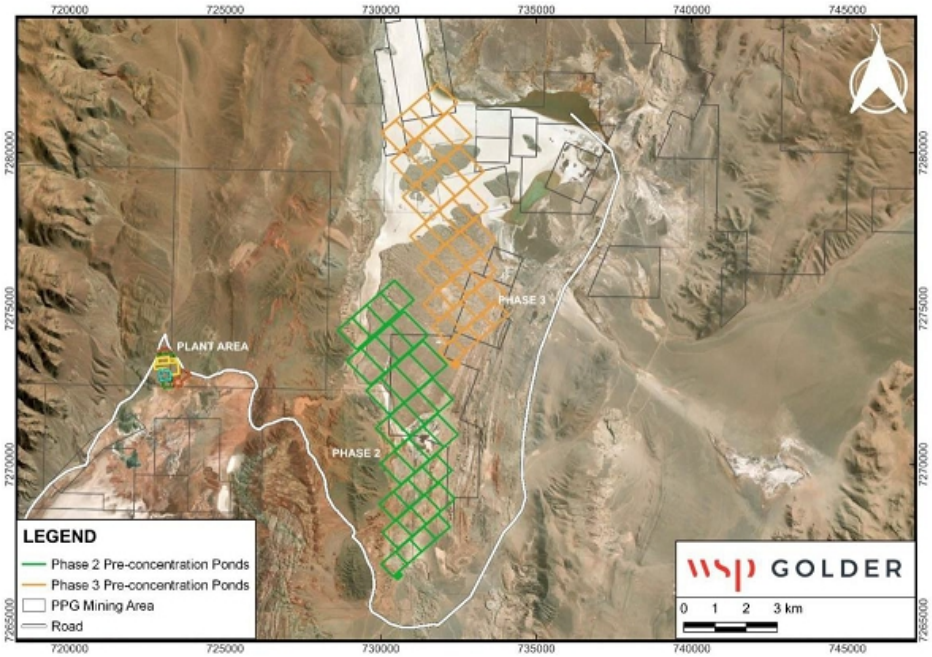

Figure 153: Phase 2 and 3 Ponds Layouts

The figure (Figure 152 and Figure 153) above shows the location of the ponds at the Phases 1, 2 and 3 of the project. It is QP's opinion that the geotechnical and topographic studies should be conducted in next engineering phase.

**These layouts are considered preliminary (based on the design criteria chosen) at this stage in project development and may change during final engineering based on additional information such as topographical, geotechnical and value engineering studies.

14.3.1 Salt Harvesting

The crystallized salts, mainly sodium chloride, are collected every 1 to 2 years to maintain the appropriate volume capacity of the ponds. This collection is known as harvesting, and it is conducted according to the steps listed below:

- The flow of brine entering the pond is stopped and the harvesting area inside the pond is isolated by baffles.
- Brine remaining in the pond is pumped out and directed to the closest pond of the string.
- Salt cords are formed with the crystallized salts, using a front loader or a backhoe tractor.

A second extraction of the remaining brine is conducted between the salt cords:

- Crystallized salts are removed from the pond and transported to a stockpile with backhoe tractors and trucks.
- The process is repeated in the remaining areas of the pond until all areas have been harvested.
- The pond is re-filled with brine.

Pond design and operation make it necessary to remove the salt deposits formed at the bottom of the ponds after a period of time. For this purpose, typical earthmoving machinery will be used, such as bulldozers, front end loaders and dump trucks. This service will be sub-contracted.

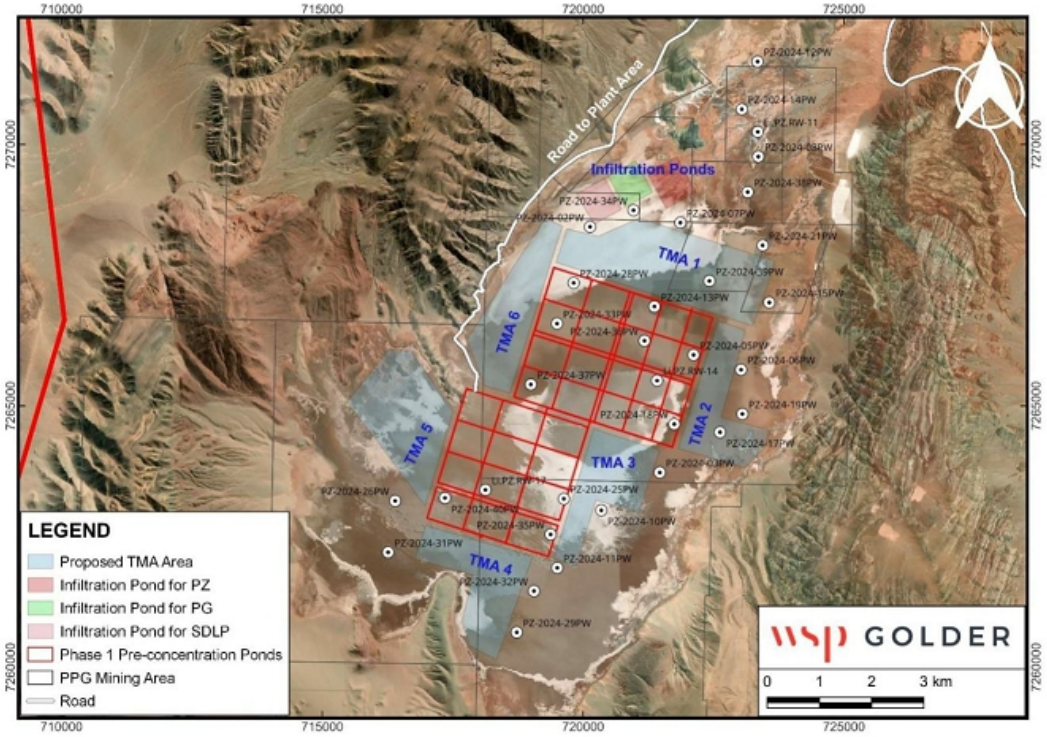

Figure 154: Proposed TMA and Infiltration Ponds for Phase 1

14.3.1.1 Waste Salts Quantities and Areas

All waste salts will be discharged to a Tailing Management Area (TMA) salts stockpile. Yearly quantity of salt from each area is shown in Table 86.

Table 86: Salt Quantity for the Three Phased 51 KTPA Production

SALT QUANTITY AND STORAGE			
30 years basis	Area (m^2)	TPA	m^3/year
PHASE 1	7,504,603	5,153,241	3,680,886
PHASE 2	7,144,873	4,921,674	3,515,481
PHASE 3	7,144,873	4,921,674	3,515,481

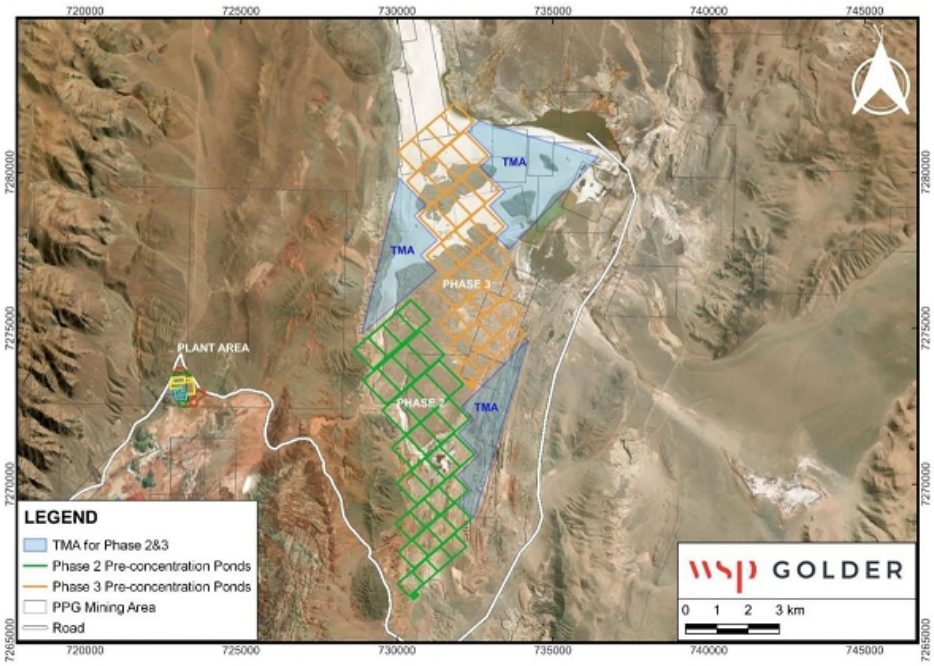

Figure 155: TMA Locations for Phase 2&3

A simplified process diagram for the pre-concentration ponds is presented in Figure 156 below.

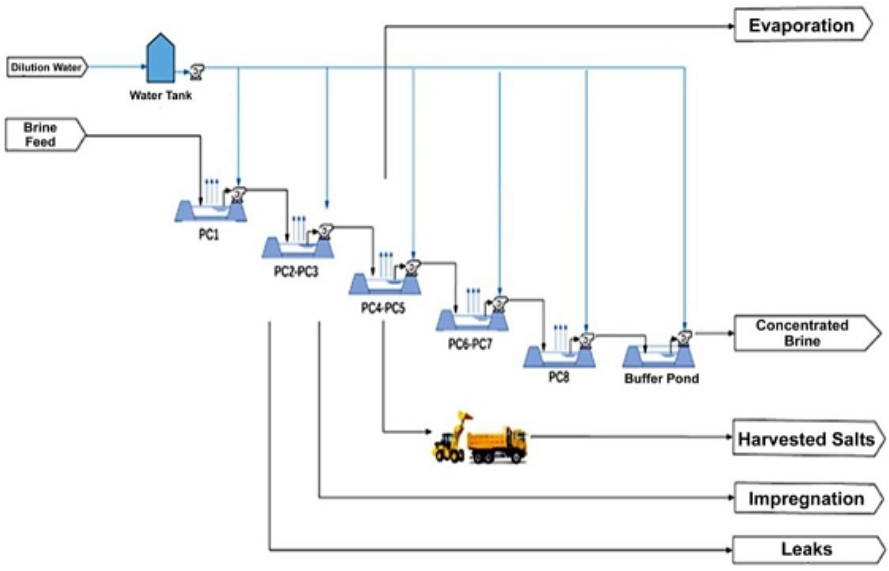

Figure 156: Simplified Process Diagram for the Pre-concentration Ponds (Source: Ganfeng 2024)

14.3.1.2 Analyses of Brine

Table 87 shows the average analyses of the incoming and product brine.

Table 87: Raw Brine Analysis*

RAW BRINE Phase 1								
Element (%)	**Li**	**Na**	**K**	**Mg**	**Cl**	**Ca**	**B**	**Density**
Phase 1	0.046	9.37	0.37	0.3	15.07	0.05	0.050	1.21
RAW BRINE Phase 2								
Element (%)	**Li**	**Na**	**K**	**Mg**	**Cl**	**Ca**	**B**	**Density**
Phase 2	0.036	7.48	0.394	0.18	12.94	0.053	0.051	1.21
RAW BRINE Phase 3								
Element (%)	**Li**	**Na**	**K**	**Mg**	**Cl**	**Ca**	**B**	**Density**
Phase 3	0.036	7.48	0.394	0.18	12.94	0.053	0.051	1.21
PRECONCENTRATED BRINE								
Element	**Li**	**Na**	**K**	**Mg**	**Cl**	**Ca**	**B**	**Density**
%	0.25	8.2	1.5	1.3	16.5	0.01	0.2	1.26

*Numbers may differ because of rounding.

14.3.2 Mass Balance

The mass balance for the pond systems for 51 KTPA production is presented in Table 88.

Table 88: Mass Balance for Phase 1 Pond System

Item	Unit	PZ	PC1	PC2	PC3	PC4	PC5	PC6	PC7	PC8 to Reservoir	Reservoir to Plant
Flow Design	**ton/day**	67,072	60,295	51,996	43,007	35,449	27,175	21,382	15,470	11,635	12,972
Density	**Kg/m³**	1,212	1,218	1,220	1,223	1,226	1,229	1,234	1,244	1,255	1,253
Flow	**m³/day**	55,338	49,513	42,620	35,165	28,910	22,103	17,329	12,437	9,271	10,355
Water Dilution (Inflow)	**m³/day**	111	495	0	352	0	221	0	124	92	103
Flow Design	**m³/day**	55,338	49,513		35,165		22,103		12,437	9,271	10,355
Availability	**%**	100%	100%		100%		100%		100%	100%	100%
Operating hours	**Hours**	24	12		12		12		12	12	12
Total Flow Design	**m³/h**	2,306	4,126		2,930		1,842		1,036	773	863
Number of Shifts	**-**	24	4		4		4		4	4	4
Flow by each Shift	**m³/h**	96	1,032		733		460		259	193	216
Water Dilution	m³/h	0.2	10.3		7.3		4.6		2.6	1.9	2.1
Water Dilution by Shift	m³/day	4.6	123.8		87.9		55.3		31.1	23	25.6
% Water Dilution	%	0.20%	1.00%		1.00%		1.00%		1.00%	1.00%	1.00%

The summary mass balance for the three phases is presented in Table 89.

Table 89: Summary of Mass Balance for Three Phases

	Brine In	% Li	Brine Out	% Li	Salts TPA
Phase 1 TPA	24,480,424	0.0462	4,246,775	0.246215	5,269,808
Phase 2 TPA	31,881,483	0.0355	4,246,775	0.246215	4,921,674
Phase 3 TPA	31,881,483	0.0355	4,246,775	0.246215	4,921,674
TOTALS	**88,243,390**	-	-	-	-

14.4 Plant Location and the Plant Layout

The processing plant is located at the Salar de Pozuelos with short distance from the concentration ponds and includes:

- Processing modules for the three phases of production
- Camp
- Warehouses and Maintenance shops
- Fuel Storage
- Spare parts workshop
- Waste Yard
- LNG storage and re-gasification
- Emergency Generators

Figure 157: Process Plants Layout for Three Phases (Source: Golder, 2024)

14.4.1 General

The lithium in concentrated brine is extracted by a solvent, and transferred into a rich LiCl solution with a concentration of 19 g/L.

The process consists of a three-step solvent extraction cycle: extraction, washing and stripping. There will be 5 production lines with a capacity of ~10,000 TPA each, thus completing a production of ~50,000 TPA.

The organic solution is prepared, consisting of TIAP (Tri Isoamyl phosphate), P507 (2-Ethylhexyl 2-Ethylhexyl phosphate).

The processes and tables described below are applicable to all 3 Phases of production and utilize the same criteria and equipment.

14.4.2 Process Description

The brine with a nominal lithium concentration of 3.05 g/L from the evaporation ponds is filtered and acidified to pH=1 with recycle 7% HCl. The filtrate after acidification is sent to a storage tank and then pumped to the solvent extraction plant. The extractant and diluent are mixed in a certain proportion to form an organic phase, which joins the acidified brine to extract lithium. The rich organic phase containing lithium is separated. The organic phase is then washed and stripped with water to obtain a lithium chloride product solution. The rich lithium chloride solution is then purified to remove calcium, boron, and ferrum while the spent lithium raffinate is sent to a resin adsorption system to remove any entrained organic solvent and finally returned to the salar. The resin regeneration liquid from resin adsorption is sent to a wastewater treatment station for biochemical degradation, with clear wastewater is recycled for dilution of the brine during preconcentration.

14.4.3 Iron Pre-loading

The project uses 5 extraction production trains, each with a capacity of 10,000 TPA; each extraction line uses 26-stage extraction tanks (6-stage extraction, 6-stage washing, 13-stage stripping). Ferric chloride is pre-loaded on the extractant before being pumped into the solvent extraction system.

The mass balance of the extraction system is shown in Table 90 below.

Table 90: Mass Balance of the Extraction System

Item	Name	Flow (tons/day)	Fe (g/L)	P (t/m^3)
Inflow	Brine*	15,375	ND	1.212
	Extractant	11,478	ND	0.90
	$FeCl_3$	598	99%	/
	Total	27,451	204.05	/
Outflow	Brine	15,375	ND	1.212
	Extractant (+Fe)	12,070	15.55	0.92
	Solids	6.58	ND	/
	Totals	27,451	204.05	/

* Brine feed includes HCl consumption.

14.4.4 Solvent Extraction Process

The lithium extraction process includes an extraction cycle consisting of three process sections: extraction-washing-strip extraction. The acidified brine is pumped into the lithium extraction process, and a lithium chloride stripping solution is obtained after extraction. Five identical extraction production lines are designed for a lithium carbonate production capacity of 51,000 TPA (nominal), and the production capacity of each extraction production line is 10,000 TPA (nominal).

Table 91: Basic Parameters of Solvent Extraction

Item	Units	Value	Comment
DESIGN TPA	LCE	40,000	-
	LHM	12,500	-
Concentrated Brine	g/L Li	3.05/3.09	Average
Recovery	%	90	Extraction
Annual brine treatment	10,000 m^3	361.19	Brine plus adjustment
Extraction Stages	LINE	5	-
Extraction	O/A	4	-
Washing	O/A	40 to 66.7	-
Stripping	O/A	20	-

The extraction is accomplished in a multi-stage mixer settler system where brine is mixed with the iron-loaded extractant TIAP/P507/sulfonated kerosene-Fe(III). Lithium is coextracted with iron to form a complex $[Li(TIAP)_2][FeCl_4]$.

After water stripping, a lithium chloride solution with a pH of 1 and a lithium content of ≥19 g/L is obtained. Part of the stripping solution is recycled as washing liquid for the extraction section.

$Li + FeCl_4^- + 2TIAP = [Li(TIAP)_2][FeCl_4]$

$[Li(TIAP)_2][FeCl_4] + HL_2 = [FeCl_2\ L.(HL).\ 2TIAP] + LiCl + HCl$

Table 92: Analysis of Main Solvent Extraction Streams

Element g/l	Li	Mg	Ca	Na	K	B	Cl	pH	TOC	Density
Feed Brine	3.05	15.77	0.16	98.99	18.29	2.5	199.8	6.5	0.033	1.212
Raffinate	0.3	15.02	0.15	94.27	17.41	2	190.2	0.5-1	50	1.194
Strip Solution	19.34	0.007	0.03	0.172	0.014	1.96	91.37	0.5-1	0.078	1.055

The solvent extraction flowsheets are shown below and the material balance in Table 93.

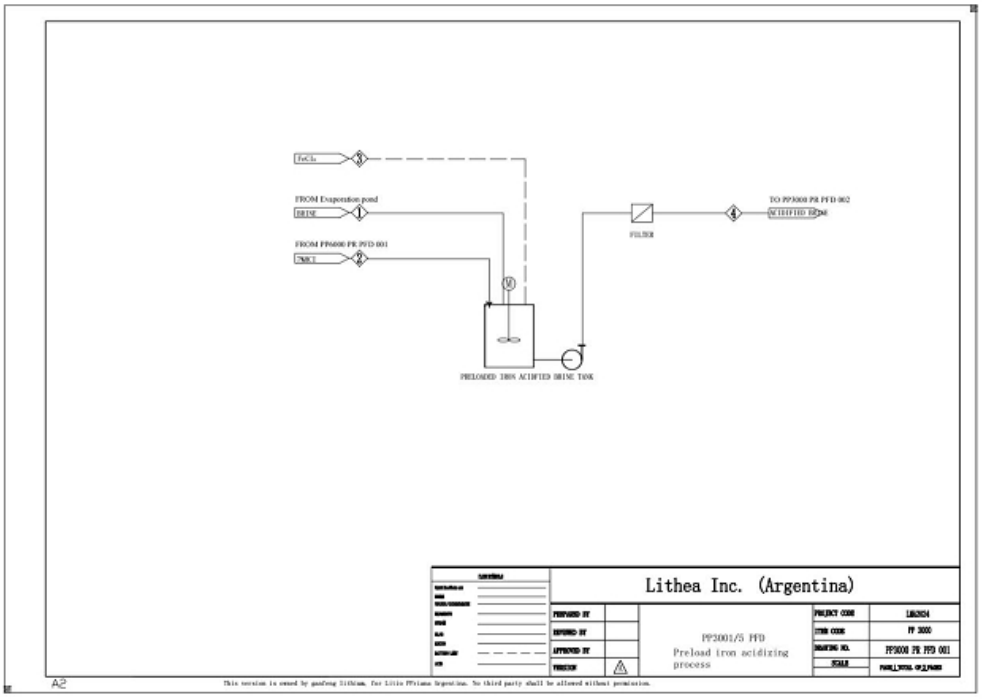
FeCl3
FROM Evaporation pond
BRINE
FROM PP6000 PR PFD 001
TMCl
TO PP3000 PR PFD 002
FILTER
PRELOADED IRON ACIDIFIED BRINE TANK
Lithea Inc. (Argentina)
PP3001/5 PFD
Preload iron acidizing process
A2

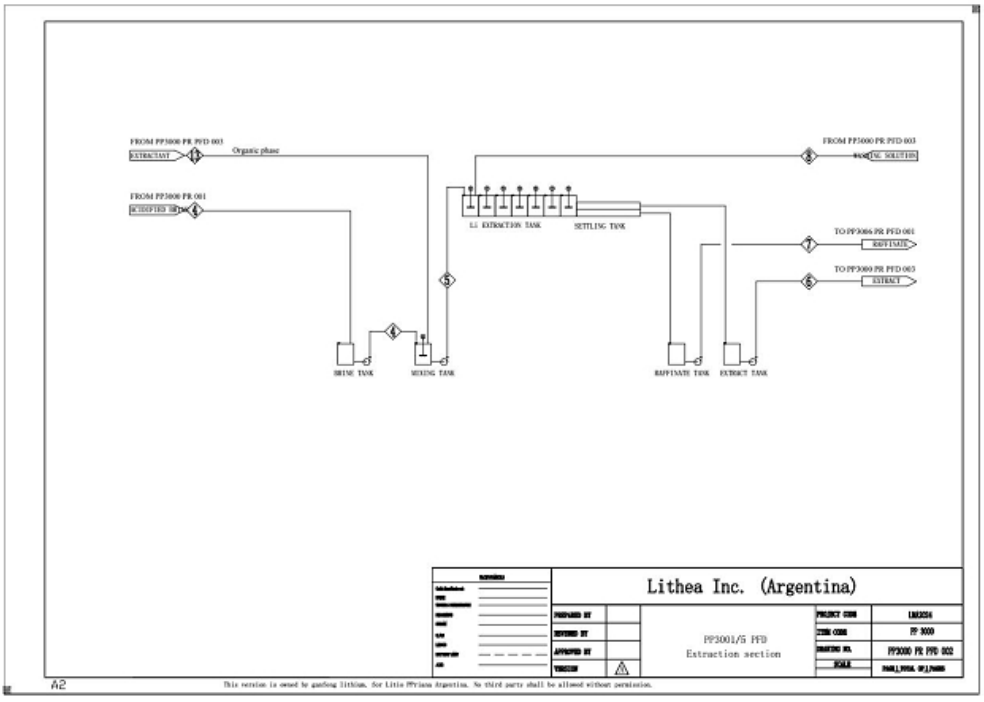
FROM PP3000 PR PFD 003
EXTRACTANT
Organic phase
FROM PP3000 PR PFD 003
FROM PP3000 PR 001
LI EXTRACTION TANK
SETTLING TANK
TO PP3006 PR PFD 001
RAFFINATE
TO PP3000 PR PFD 003
EXTRACT
BRINE TANK
MIXING TANK
RAFFINATE TANK
EXTRACT TANK
Lithea Inc. (Argentina)
PP3001/5 PFD
Extraction section
A2

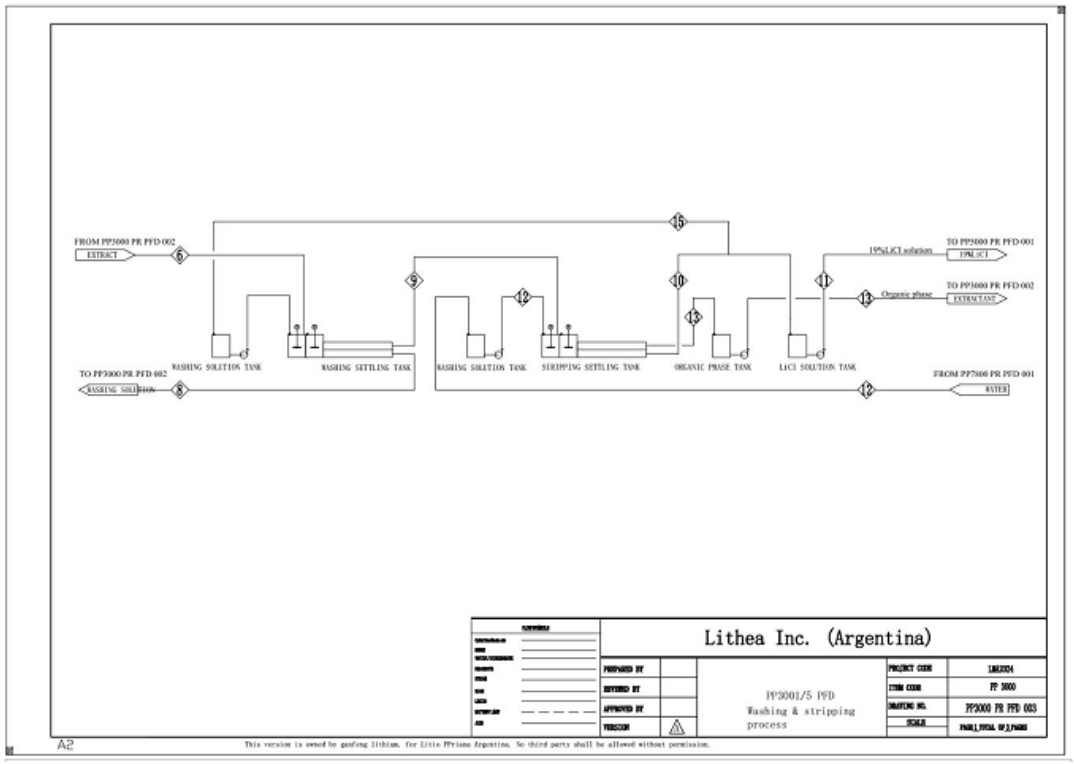

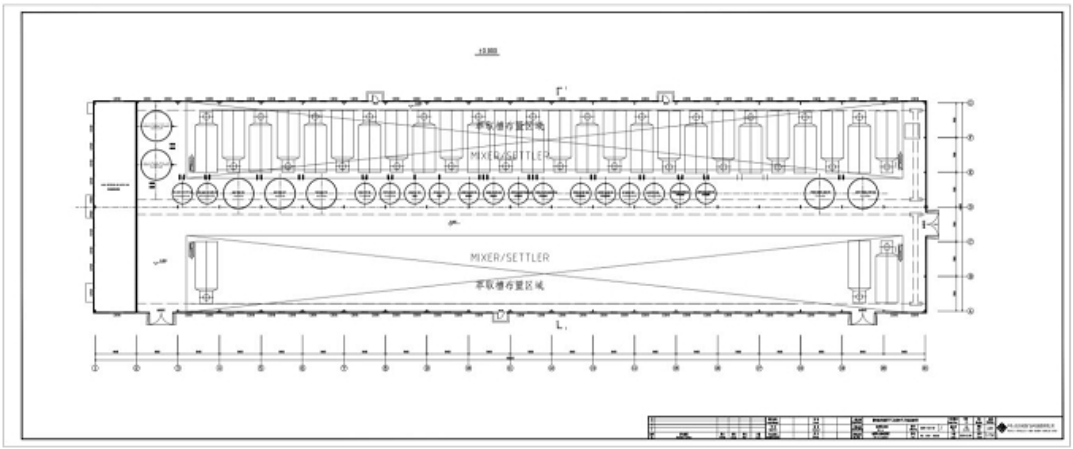

Figure 158: Solvent Extraction Flowsheets (Source: Ganfeng, 2024)

Table 93: Material Balance Table for Lithium Extraction

No	Stream	Quantity	Li	Na	K	B	Ca	SO_4^{2-}	Mg	Fe	ρ
		t/h	g/L	g/L	g/L	g/L	g/L	g/L	g/L	g/L	t/m3
Inflow	Preconcentrated Brine	608	3.05	98.99	18.29	2.5	0.05	0.06	15.77	ND	1.212
	Organic	1848.08	0	0	0	0	0	0	0	15.55	0.92
	Water strip	100.3	0	0	0	0	0	0	0	0	1
	Totals	**2556.38**	**1.53**	**49.66**	**9.18**	**1.25**	**0.02**	**0.03**	**7.91**	**31.23**	**-**
Outflow	Raffinate	660.37	0.3	93.38	17.26	2.07	0.045	0.043	14.88	0.05	1.193
	Strip Solution	74.08	19.5	0.2	0.011	2.16	0.005	0.06	0.01	0.2	1.055
	Barren Organic	1848	0	0	0	0	0	0	0	15.53	0.92
	Totals	**2556.38**	**1.53**	**49.66**	**9.18**	**1.25**	**0.02**	**0.03**	**7.91**	**31.23**	**-**

14.4.5 Raffinate Treatment Process

The depleted brine (Raffinate) obtained from the lithium extraction plants is pumped into 8-stage of resin adsorption to remove entrained organic. The raffinate is first adjusted to pH 7 with NaOH, the entrained organic is removed, reducing the TOC (Total Organic Carbon) to ≤30 ppm. The wastewater generated from the removal of total organic carbon (TOC) originating from the ion exchange (IX) process is subjected to a biochemical degradation process. The following table summarizes the mass balance showing the inflow and outlet streams of the plant, followed by the process flow diagram.

The raffinate organic removal system is comprised of a pH adjustment to 7 with NaOH and a resin adsorption. After the TOC is reduced to less than 30 ppm, the raffinate is sent to waste disposal in the salar assumed to utilize pond/infiltration/evaporation for this report. Atacama Water has issued a trade-off analysis comparing two alternatives that could be evaluated further before final design is enacted.

Following pH adjustment any iron contained in the raffinate will precipitate as hydroxide once it reaches pH=4

$Fe^{3+} + 3OH^- = Fe(OH)_3$

The adsorption resin is regenerated with an alkaline solution, whose TOC is further controlled through a biochemical treatment system before being discarded at a maximum of 30 ppm (See Figure 159).

The regenerated degreased resin solution from PP3006 enters the PP3007 biochemical wastewater treatment system. After passing through the first stage of a Fenton reactor, the second stage catalytic oxidation reactor, the first stage anaerobic treatment, and the first stage contact oxidation treatment, it is returned to the salt field dilution water system when the COD is less than 20 ppm.

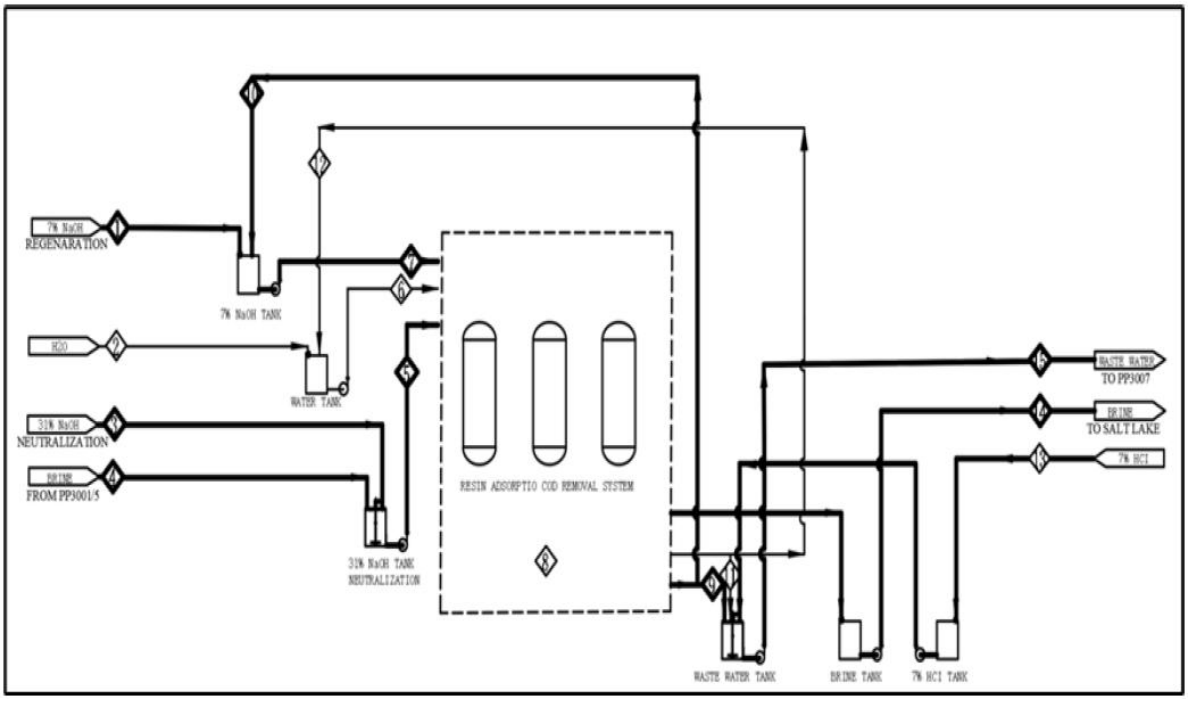

Figure 159: Process Flow Diagram of Raffinate Resin Organic Removal (Source: Ganfeng, 2024)

Table 94: Material Balance of the Raffinate Resin Organic Removal Process

No	Material	QTY	Li	Na	K	B	Ca	SO_4^{2-}	Mg	TOC	PH	ρ
		t/h	g/L	g/L	g/L	g/L	g/L	g/L	g/L	ppm	-	t/m^3
Inflow	Raffinate	660.37	0.30	93.38	17.26	2.07	0.045	0.043	14.88	50	7	1.19
	Resin Wash Water	20									9	1.0
	7% NaOH	20		3.51								
	7% HCI	18.25										
Outflow	Raffinate	660.37	0.30	93.38	17.26	2.07	0.045	0.043	14.88	20	7	1.19
	Recycle wastewater	58.25		10.29						300		1.0

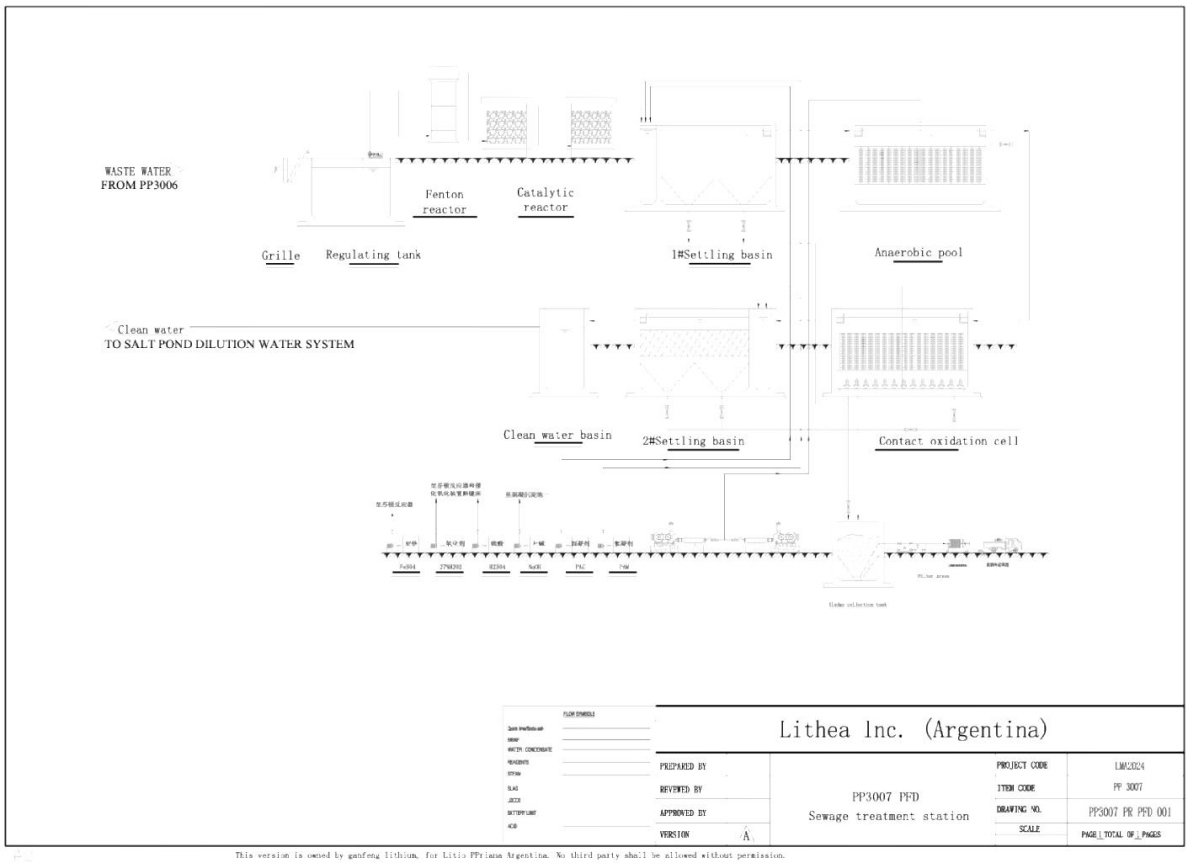

Figure 160: Process Flow Diagram of Sewage Treatment Station (Source: Ganfeng, 2024)

14.5 Primary Purification

14.5.1 Primary Purification Plant

The LiCl-rich solution from solvent extraction undergoes primary purification, consisting of boron and calcium removal.

14.5.1.1 Boron Removal

The solvent extraction strip solution enters the liming plant to remove B at a temperature between 70 to 80 °C. Calcium oxide reacts with boron in a molar ratio of 1.2: 1 with the concentration of boron decreasing from less than 3 g/L to 0.31 g/L, and a loss of lithium of less than 0.5%. The solid waste, calcium borate, is sent to the storage yard. Due to the addition of CaO for the reaction, the pH of removal B solution is pH=12 and ferrum hydroxide solid precipitates.

$2Ca(OH)_2+2H_3BO_3 \rightarrow Ca_2B_2O_5 \cdot H_2O \downarrow +4H_2O$

$2CaO+2H_3BO_3 \rightarrow Ca_2B_2O_5 \cdot H_2O \downarrow +2H_2O$

$Fe^{3+} +3OH^- \rightarrow Fe(OH)_3$

Table 95: Boron Removal Mass Balance

Items	Name	Qty	Li	Na	K	B	Ca	SO_4^{2-}	Mg	Fe
		t/h	g/L	g/L	g/L	g/L	g/L	g/L	g/L	g/L
Inflow	Feed Strip Solution	74.1	19.50	0.20	0.01	2.16	0.005	0.06	0.01	0.20
	Lime	1.48	0	0	0	0	61.4%	0	0	0
	Fresh water	2.96	0	0	0	0	0	0	0	0
	Total	**78.44**	**1.37**	**0.01**	**0.0007**	**0.15**	**0.91**	**0.00**	**0.00**	**0.01**
Outflow	De-boronized Strip Soln	74.1	19.11	0.2	0.011	0.31	2.54	0.043	0.01	0.00
	Waste Solids (wet)	4.431	0.37%	0.01%	0.01%	2.91%	16.50%	0.02%	0.01%	0.31%
	Total	**78.54**	**1.37**	**0.01**	**0.0007**	**0.15**	**0.91**	**0.004**	**0.00**	**0.01**

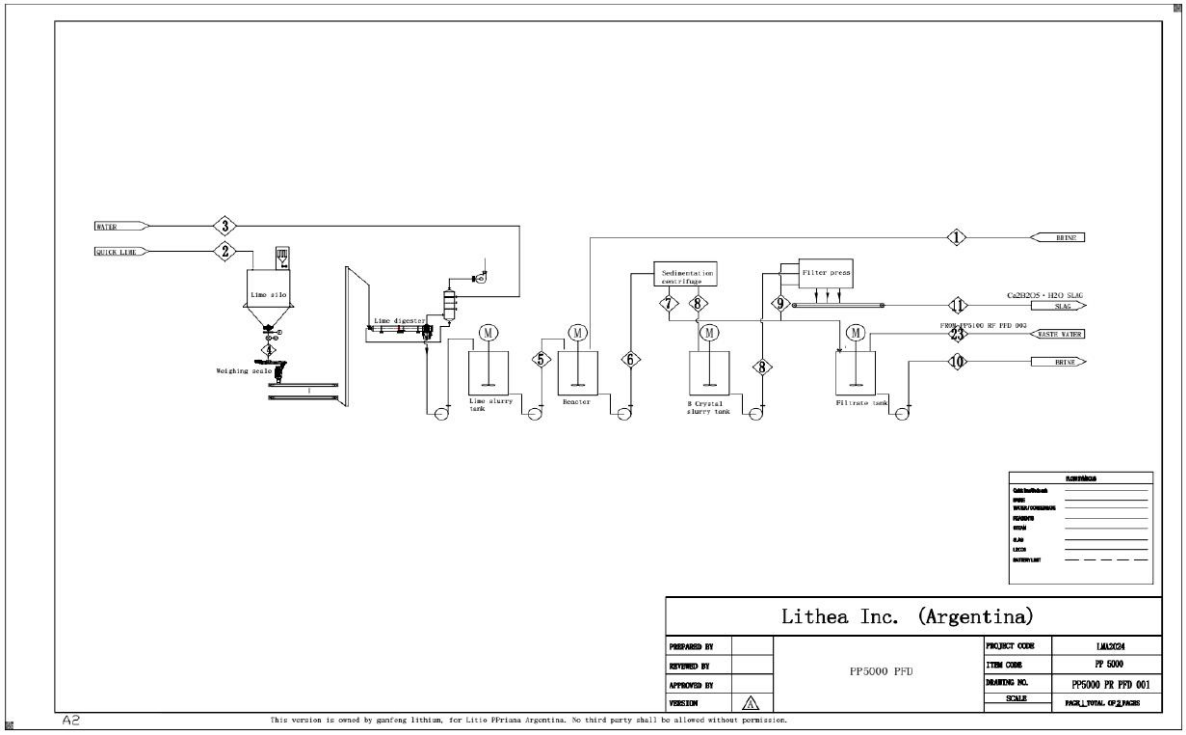

Figure 161: Process Flow Diagram of Boron Removal in Primary Purification Plant (Source: Ganfeng, 2024)

14.5.1.2 Calcium Removal

The solution after boron removal is then reacted with sodium carbonate at a temperature of 75 °C to reduce the Ca concentration down to 10 ppm. Solid calcium carbonate residue is disposed of in the storage yard.

The solid waste obtained from this plant, corresponding to the boron and calcium sludge, will be collected in an area as close as possible to the plants.

This area will have a maximum height of 10 m, composed of 2 overlapping platforms. It covers an approximate area of 7,916 m^2 to cover a storage volume of approximately 36,000 m^3. Below is an image with the location of this deposit.

$Na_2CO_3 + Ca++ = CaCO_3 + 2Na+$

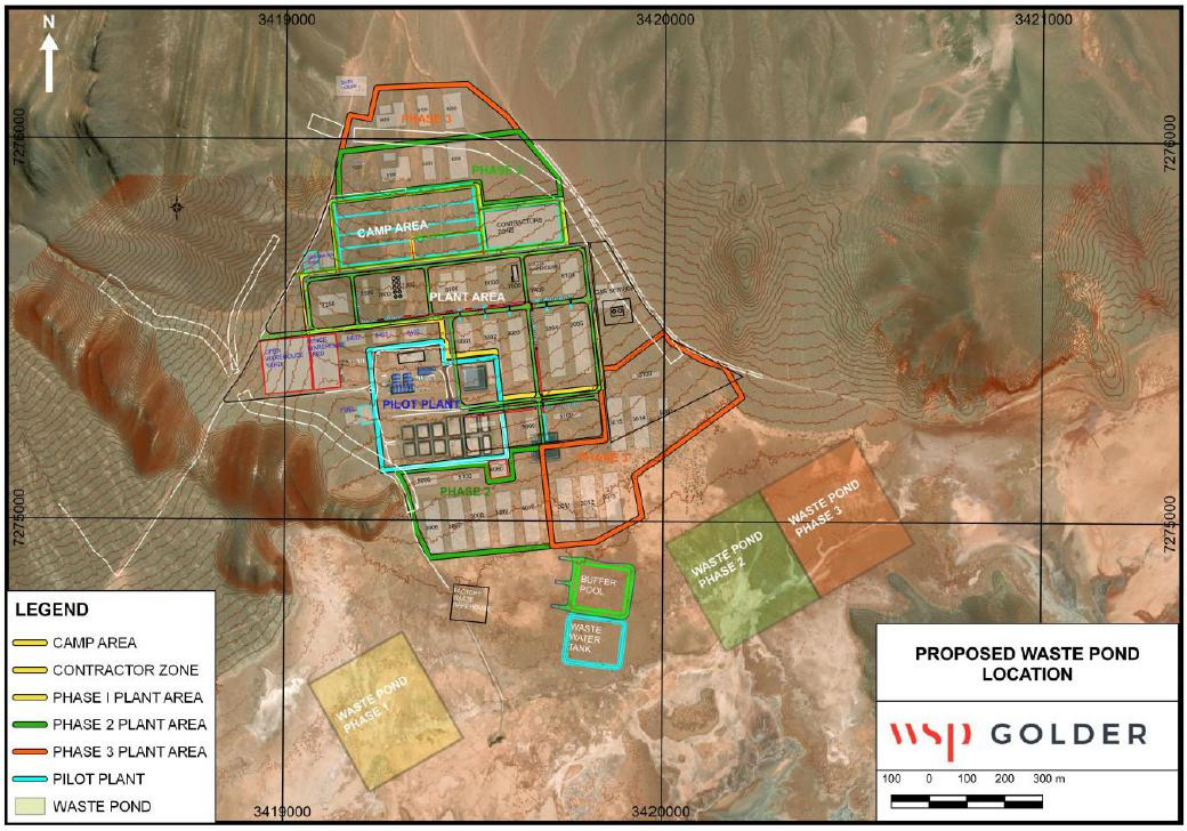

Figure 162: Location of the Plant's Solid Waste Deposit (Source: Golder, Jan 2025)

After removing B, the brine is reacted with sodium carbonate, to remove calcium down to 10 ppm.

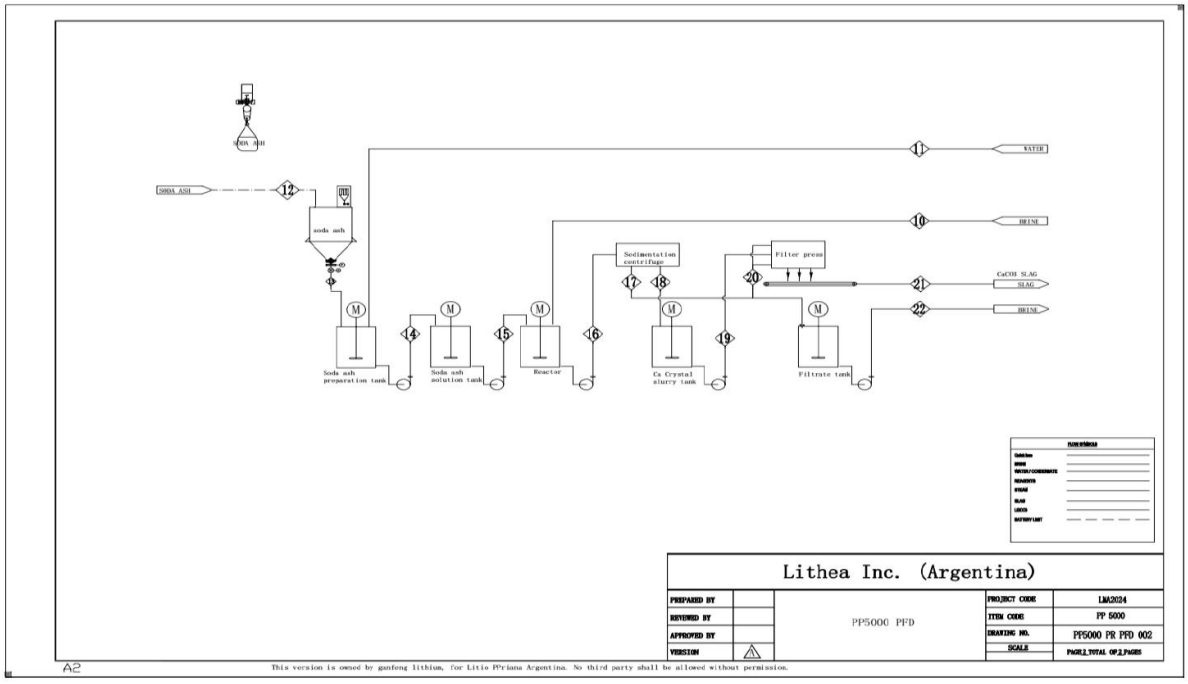

Figure 163: Flowsheet for Ca Removal Process (Source: Ganfeng, 2024)

Table 96: Mass Balance for Ca Removal

	Material name	Flow	Li	Na	K	B	Ca	SO_4^{2-}	Mg	CO_3^{2-}	ρ
		t/h	g/L	g/L	g/L	g/L	g/L	g/L	g/L	g/L	t/m^3
Inflow	B free Brine	74.1	19.48	0.2	0.011	0.31	2.54	0.043	0.01	0	1.057
	Na_2CO_3	0.495	--								
	Water	2.16	0	99.81	0	0	0	0	0	130.19	/
	Total	**76.75**	**1.34**	**0.229**	**0.001**	**0.022**	**0.178**	**0.003**	**0.001**	**0.28**	**/**
Outflow	Ca free solution	75.82	18.98	3.08	0.011	0.302	0.009	0.024	0.0005	0.39	1.053
	$CaCO_3$ wet slag	0.832	0.74%	0.79%	0.01%	0.01%	21.34%	0.09%	0.04%	30.28%	/
	Total	**76.65**	**1.34**	**1.34**	**0.001**	**0.022**	**0.178**	**0.003**	**0.001**	**0.28**	**/**

14.6 Secondary Purification

The solution from the previous stage is acidified and then it enters in a resin system for organic removal and continues through the chelating resin calcium removal system and enters through a boron removal resin process. Finally, the solution obtained is divided into two streams, one going to the lithium carbonate plant and the other further purified before reporting to bipolar membrane electrodialysis plant.

14.6.1 Process Description

The brine from primary purification plant is acidified to remove carbonate and then neutralized to pH 7 before entering an organic removal resin adsorption system, to reduce TOC down to 10 ppm. The effluent brine enters then a chelating resin to remove calcium down to 1 ppm. The brine is then divided into two streams:

- One enters additional purification (brine removal by resin), before reporting to the electrodialysis plant; and
- The other goes to the lithium carbonate plant.

14.6.2 Carbonate Removal

The brine from the primary purification plant is acidified to pH 1 with recycle 7% HCl and then neutralized to pH 7 with 7% NaOH recycle.

Table 97: Secondary Purification Feed Specifications

Material name	Flowrate	Li	Na	K	B	Ca	SO_4^{2-}	Mg	CO_3^{2-}	TOC	PH
	t/h	g/L	g/L	g/L	g/L	g/L	g/L	g/L	g/L	ppm	
The primary purified brine	75.82	18.98	3.08	0.011	0.302	0.009	0.024	0.0005	0.39	30	11

14.6.2.1 Material balance of Carbonate Removal

Material balance of the acidizing process in carbonate removal˙ is shown in the following table (Table 98 and Table 99).

Table 98: Material Balance of the Acidizing Process in Carbonate Removal

	Material name	Flowrate	Li	Na	K	B	Ca	SO_4^{2-}	Mg	CO_3^{2-}	TOC	PH	ρ	T
		t/h	g/L	g/L	g/L	g/L	g/L	g/L	g/L	g/L	ppm		t/m^3	(℃)
Inflow	Primary purified brine	75.82	18.98	3.08	0.011	0.302	0.009	0.024	0.0005	0.39	50	11	1.053	70
	7% HCI	4.292	0.477	0.08										
Outflow	Brine after Removal CO_3^{2-}	80.09	17.99	3.06	0.01	0.30	0.009	0.023	0.0004	0	50	1	1.053	50
	CO_2	0.021												

Table 99: Material Balance of Neutralization Process in Carbonate Removal

	Material name	Flow	Li	Na	K	B	Ca	SO_4^{2-}	Mg	CO_3^{2-}	TOC	PH	ρ	T
		t/h	g/L	g/L	g/L	g/L	g/L	g/L	g/L	g/L	ppm		t/m^3	(℃)
Inflow	Brine after B-removal	80.09	17.99	3.06	0.01	0.30	0.009	0.023	0.0004	0	50	1	1.053	50
	7% LiOH	2.49	21.50	3.46										
Outflow	Brine after CO_3^{2-} Removal	82.58	18.11	3.07	0.01	0.30	0.009	0.023	0.0004	0	50	7	1.053	50

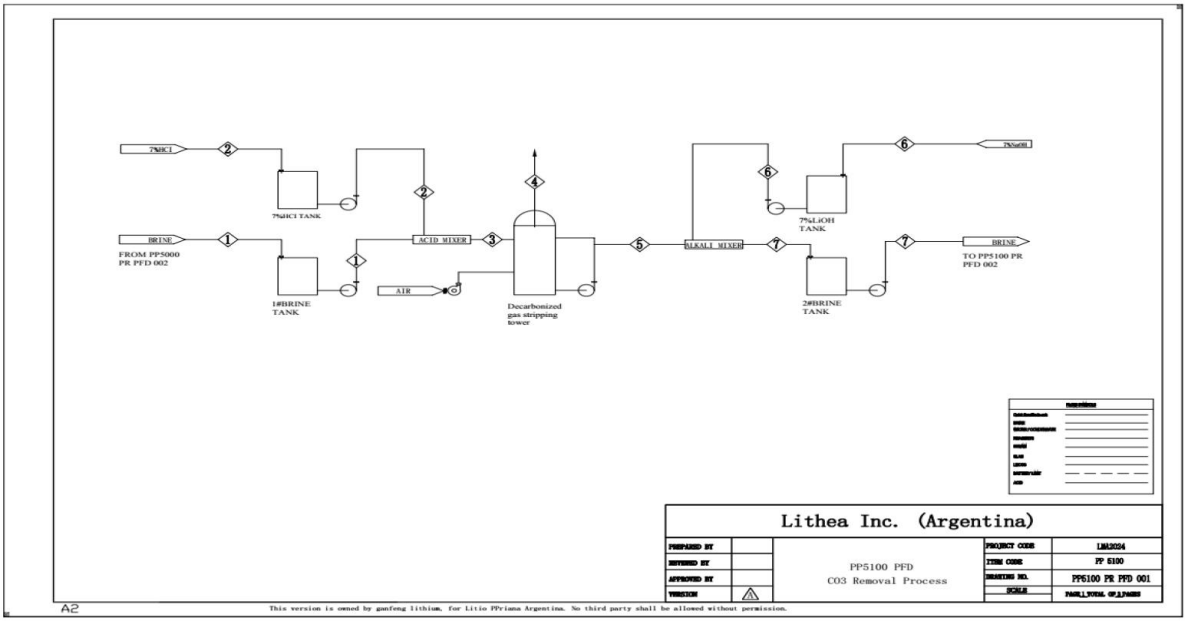

Figure 164: Flowsheet for Carbonate Removal Process (Source: Ganfeng, 2024)

14.6.3 TOC Removal Process

14.6.3.1 Description of the Process

Resin adsorption is used to remove organic entrainment from solvent extraction; each adsorption system consists of three resin columns connected in series; each filled with 10m^3 of resin.

The primary purification brine organic is adsorbed from the resin columns and the TOC of the brine reduced to 10 ppm.

After adsorption the resin is regenerated with 7% sodium hydroxide solution, and the regeneration liquid is neutralized with 7% hydrochloric acid and sent to the TOC biochemical treatment (*). Once regeneration is complete, the resin adsorption columns are reintroduced into the system for use.

(*) Ref. 2024 General Flowsheet

14.6.3.2 Material Balance for TOC Removal Processes

Material balance of the TOC removal is shown in the following table.

Table 100: Material Balance for TOC Removal Process

N°	Material	Quantity	Li	Na	K	B	Ca	SO_4^{2-}	Mg	TOC	PH	ρ	T
		t/h	g/L	g/L	g/L	g/L	g/L	g/L	g/L	ppm		t/m^3	℃
Inflow	Carbonate Free Brine	82.58	18.11	3.07	0.01	0.30	0.009	0.023	0.0004	50	7	1.053	50
	Resin Wash	1.25	/								7	1.0	
	7% NaOH	1.25	21,5	3.51									
	7%HCl	1.14	0.477	0.08									

N°	Material	Quantity	Li	Na	K	B	Ca	SO_4^{2-}	Mg	TOC	PH	ρ	T
		t/h	g/L	g/L	g/L	g/L	g/L	g/L	g/L	ppm		t/m^3	℃
Outflow	TOC Free Brine	82.58	17.60	2.84	0.01	0.30	0.009	0.023	0.0004	0	7	1.053	50
	Regeneration waste liquids	3.64	5,61	10.29						55		1.0	

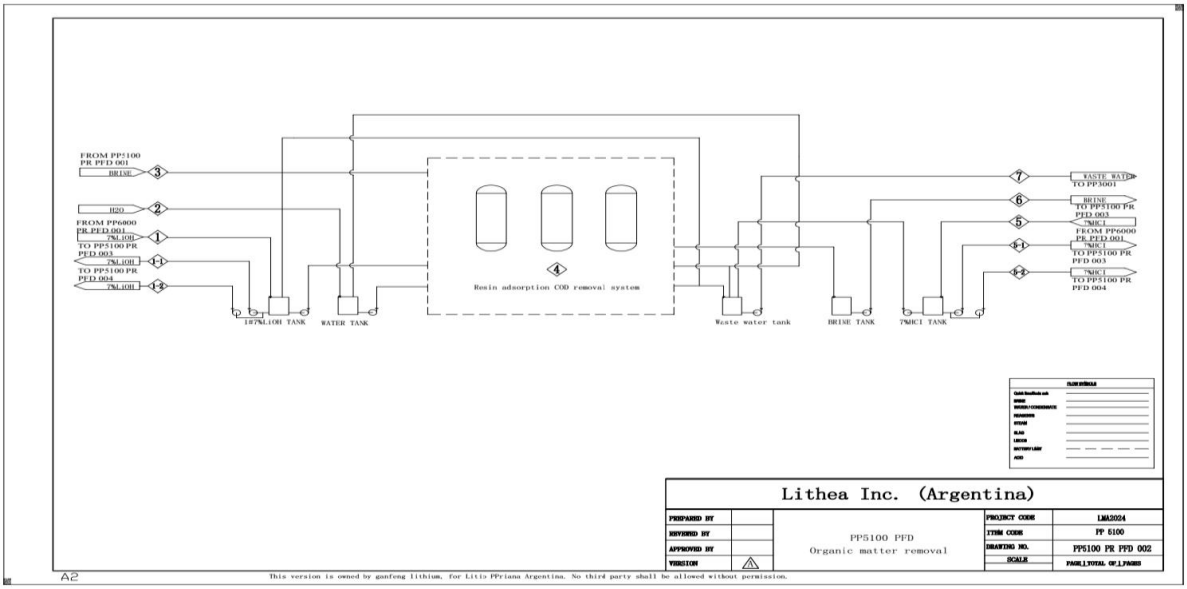

Figure 165: Flowsheet for TOC Removal Process (Source: Ganfeng, 2024)

14.6.4 Ca Removal

The brine from the TOC removal process in PP5100 plant is filtered before entering the ion exchange Ca removal system.

Chelating resin utilizes its special functional groups to form chelates with calcium ions, which can remove calcium and magnesium ions from high salt content solutions.

Table 101: Brine Specification for Ca Ion Exchange

Material name	Flowrate	Li	Na	K	B	Ca	SO_4^{2-}	Mg	PH	ρ	T
Unit	t/h	g/L	g/L	g/L	g/L	g/L	g/L	g/L		t/m^3	℃
Brine after TOC Removal	82.58	17.60	2.84	0.01	0.30	0.009	0.023	0.0004	7	1.053	50

Table 102: Mass Balance for Ca Ion Exchange

ID	Material name	Qty	Li	Na	K	B	Ca	SO_4^{2-}	Mg	PH	ρ
		t/h	g/L	g/L	g/L	g/L	g/L	g/L	g/L		t/m^3
Inflow	Brine after Removal TOC	82.58	17.60	2.84	0.01	0.30	0.009	0.023	0.0004	7	1.053
	Resin wash water	1.25	/							9	1.0
	7% LiOH	0.625	21.5	3.51							
	7% HCl	0.563	0.477	0.08							

	Material name	Qty	Li	Na	K	B	Ca	SO_4^{2-}	Mg	PH	ρ
		t/h	g/L	g/L	g/L	g/L	g/L	g/L	g/L		t/m^3
Outflow	Ca free brine	82.58	17.60	2.84	0.01	0.30	0	0.023	0	7	1.053
	Wastewater	1.188	2.80	5.20							1.0

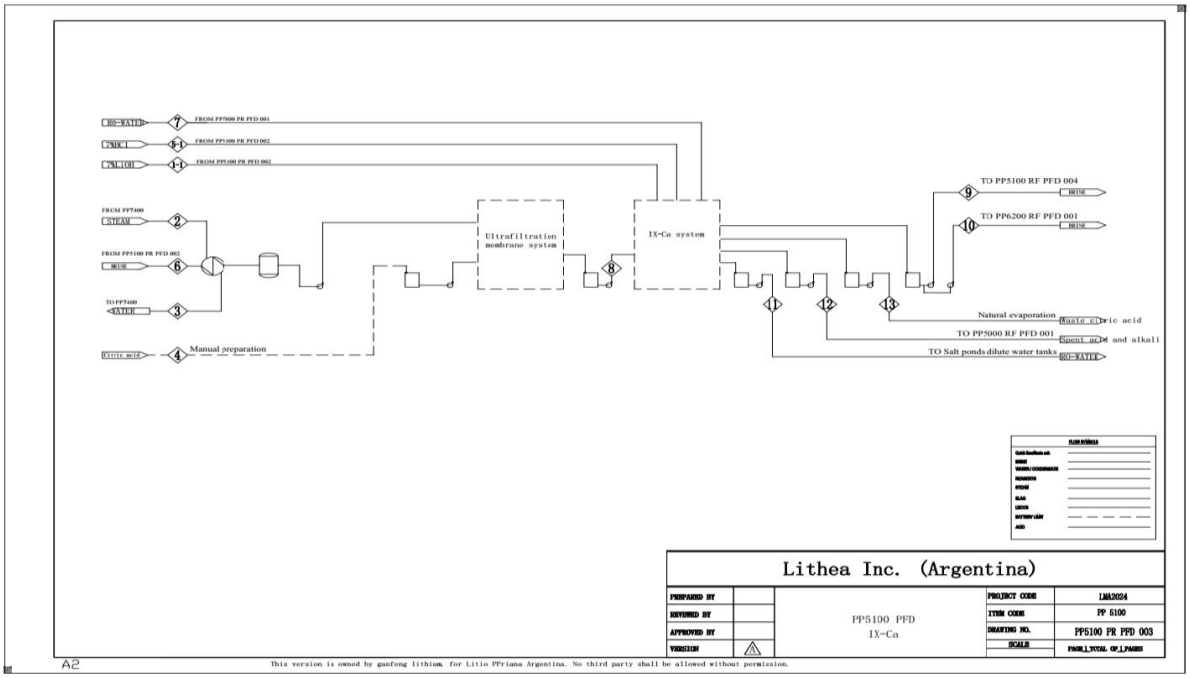

Figure 166: Flowsheet for Ca Removal Process (Source: Ganfeng, 2024)

14.6.5 Boron Removal

Boron is removed from the brine by a resin process with 3 columns in series.

The brine from the Ca ion exchange resin is sent to the 5100 resin B removal process with a flow rate of 82.58t/h. After B removal, it is divided into two streams: one streams enters the PP6000 bipolar membrane electrodialysis plant, with the flowrate of 25.16 t/h; the other path enters into the 6200-lithium hydroxide plant to produce lithium hydroxide, with a flow rate of 57.42 t/h.

The boron resin adsorption is designed with 2 columns in series 1 standby, with 2 resin towers running in series at the same time, another tower for regeneration process or standby.

The regeneration process is divided into five stages:

- The displacement stage, in which the lithium chloride solution remaining in the upper part of the resin layer inside the tower is discharged from the tower and returned to the raw material regulator tank for further boron removal to reduce the loss of lithium chloride solution.
- The first water washing stage, pure water is used for counter-current backwashing.
- The desorption stage: carried out in two steps. 7% hydrochloric acid is used for desorption, and the desorption liquid at the beginning stage is sent into the recovery tank as boric acid solution. At the end of the desorption stage, the desorption solution is collected and reused to reconfigure the desorption solution to reduce the amount of acid.

- The second stage of water washing: pure water is used for counter current backwashing. The purpose of the 2nd water washing is to replace the residual desorption liquid in the tower body, and the backwashing water at this stage is reused for the configuration of the desorption liquid.
- In the transformation and regeneration stage, 7%LiOH solution is used to recycle and soak the resin in the resin tower for regeneration. The purpose of this step is to regenerate the resin to restore the resin exchange ability. After the completion of the 5 stages, the regeneration of the resin adsorption tower is completed.
- The regeneration liquid is sent to the ponds.

Table 103: Brine Components to Boron Removal Resin

	Flow	Li	Na	K	B	SO_4^{2-}	PH	ρ	T
Unit	t/h	g/L	g/L	g/L	g/L	g/L		t/m^3	℃
Purified brine after Ca removal	20.78	17.60	2.84	0.01	0.30	0.023	7	1.053	40

Table 104: Mass Balance for Boron Removal

ID	Material name	Flow	Li	Na	K	B	SO_4^{2-}	PH	ρ
		t/h	g/L	g/L	g/L	g/L	g/L		t/m^3
Inflow	Ca free brine	20.779	17.60	2.84	0.01	0.30	0.023	7	1.053
	Resin wash water*	4.0	/					9	1.0
	7% LiOH	0.452	21.5	3.51					
	7% HCI	0.585	0.477	0.08					
Outflow	B free brine	20.779	17.60	2.84	0.01	0	0.023	7	1.053

* The regeneration liquid is sent to the ponds.

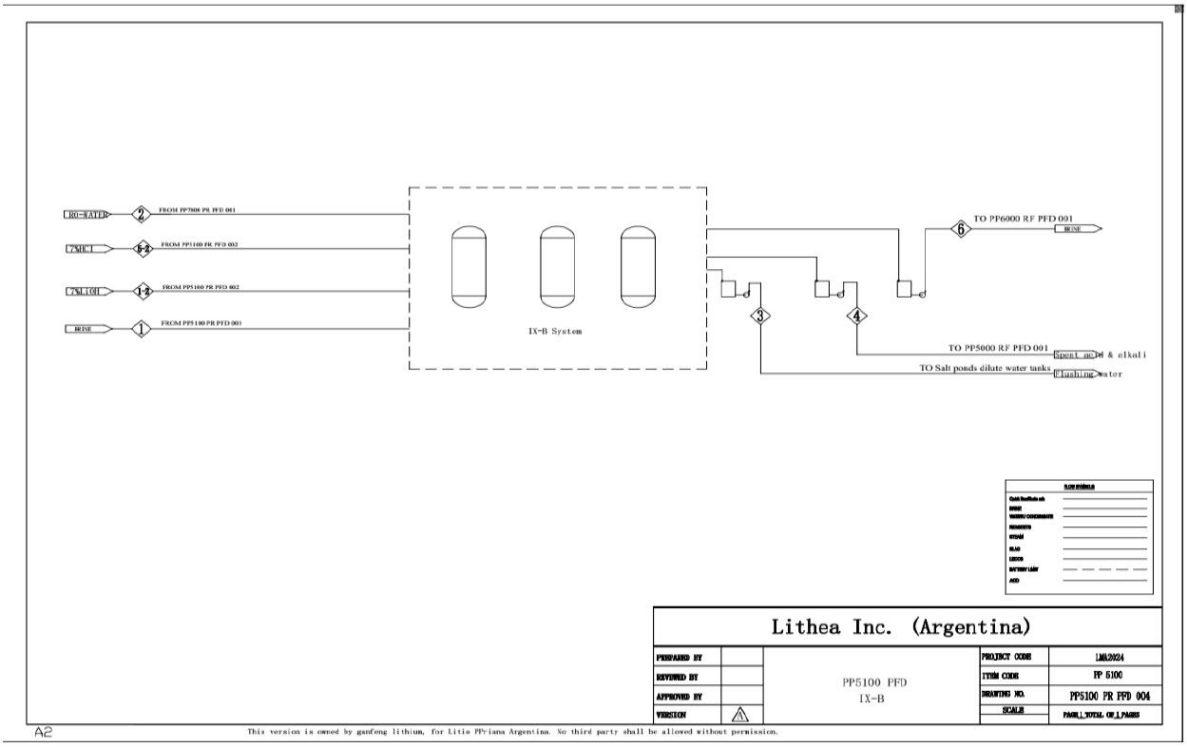

Figure 167: Flowsheet for Boron Removal Process (Source: Ganfeng, 2024)

14.7 Bipolar Membrane Electrodialysis

14.7.1 Process Description

When lithium chloride solution enters the bipolar membrane chamber, chloride ions migrate through the anion membrane to the acid chamber combining with hydrogen ions to form hydrochloric acid. The cathode surface of the bipolar membrane rejects hydroxide ions, that combine with lithium ions (in the alkali side) to form lithium hydroxide. Lithium chloride is transformed to hydrochloric acid and lithium hydroxide.

The cation-exchange membrane only allows cations to pass through and blocks anions; The anion-exchange membrane only allows anions to pass through.

Electrode reaction in bipolar membrane system: once the positive and negative electrodes of the electrodialysis device are connected to a direct current, an electrochemical reaction will occur on the positive and negative electrode plates. This system uses about 3% sodium hydroxide solution as the electrode solution.

In this system, a 3 - 5% sodium sulfate solution is employed as the electrolyte at the anode, and a 5% sodium chloride solution is utilized as the electrolyte at the cathode.

Overall Electrochemical Reaction:

$$LiCl + H_2O \xrightarrow{ED} LiOH + HCl$$

Table 105: Bipolar Membrane Electrodialysis

	Flowrate	Li	Na	K	SO_4^{2-}	PH	ρ	T
Unit	t/h	g/L	g/L	g/L	g/L		t/m^3	℃
Purified brine after Removal B	20.779	17.60	2.84	0.01	0.023	7	1.053	40

The lithium hydroxide solution from the bipolar membrane electrodialysis plant enters the MVR evaporator for evaporation and crystallization after preheating, and the crystal slurry is dried and packaged after centrifugal separation.

14.7.2 Mass Balance

The lithium hydroxide solution enters the MVR evaporator crystallizer evaporation and crystallization chamber for evaporation, concentration and crystallization. The steam generated in the evaporation chamber is pressurized and heated by the compressor and enters the heating chamber. The crystal slurry in the evaporation and crystallization system is discharged and pumped into the cooling cylinder. The crystal slurry discharged from the bottom of the cooling barrel is pumped to a curved screen for separation and then flows into the crystal slurry tank and centrifuged; the solid lithium hydroxide monohydrate is dried and packaged; the mother liquor is sent to the front-end of the process.

Table 106: Mass Balance for Bipolar Membrane Electrodialysis

	Material Name	Flowrate	Li	Na	K	SO_4^{2-}	ρ	T
		t/h	g/L	g/L	g/L	g/L	t/m^3	(℃)
Inflow	Purification brine after Removal B	20.779	17.60	2.84	0.01	0.023	1.053	40
	Pure water	23.07						
Outflow	7% HCI	27.45	0.477	0.08	/	/	1.053	50
	7% LiOH	16.40	21.50	3.46	/	/	1.053	0

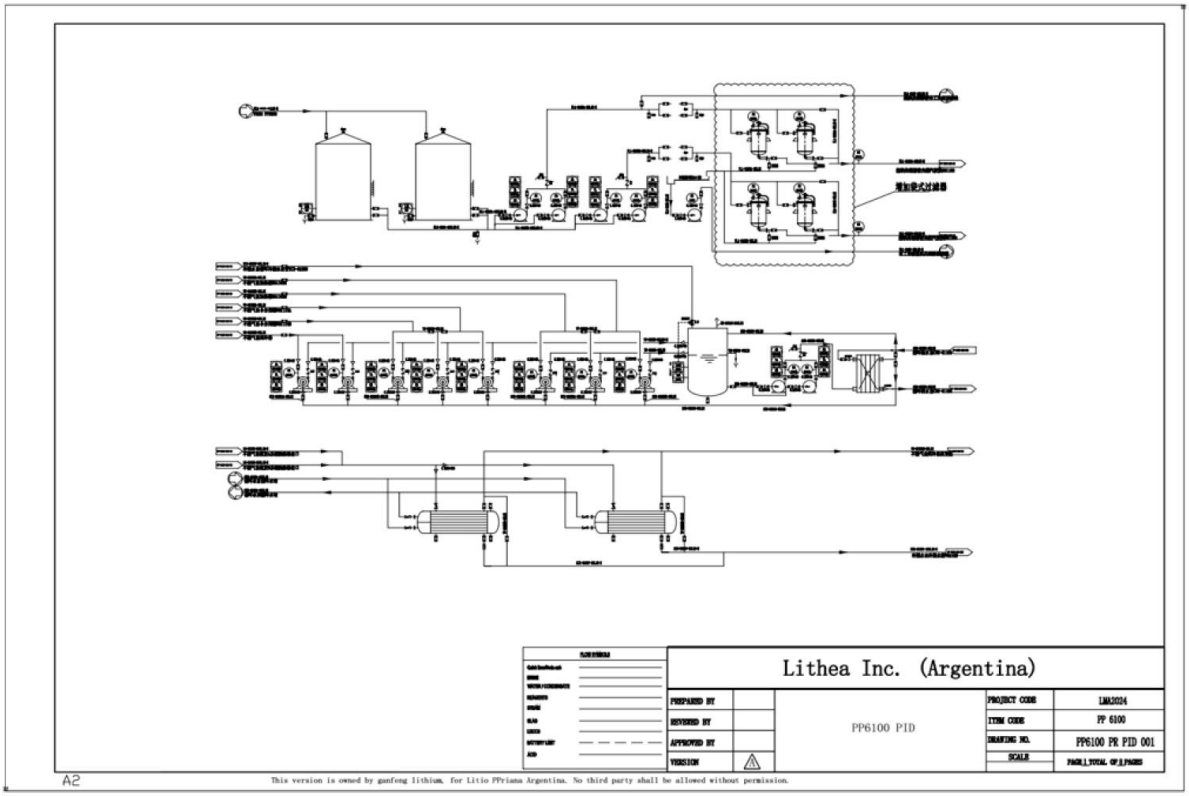
Lithea Inc. (Argentina)
PP6100 PID
PP6100 PR PID 001
A2

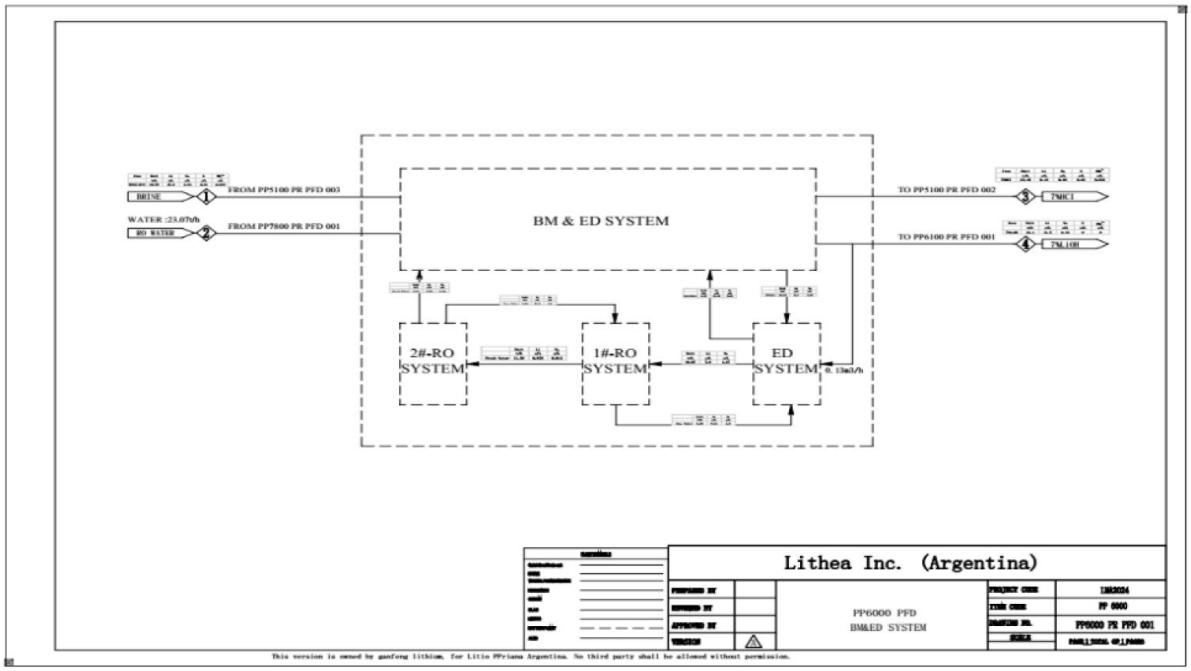
BRINE
FROM PP5100 PR PFD 003
WATER :23.07t/h
RO WATER
FROM PP7800 PR PFD 001
BM & ED SYSTEM
TO PP5100 PR PFD 002
TO PP6100 PR PFD 001
2#-RO SYSTEM
1#-RO SYSTEM
ED SYSTEM
Lithea Inc. (Argentina)
PP6000 PFD
BM&ED SYSTEM
PP6000 PR PFD 001

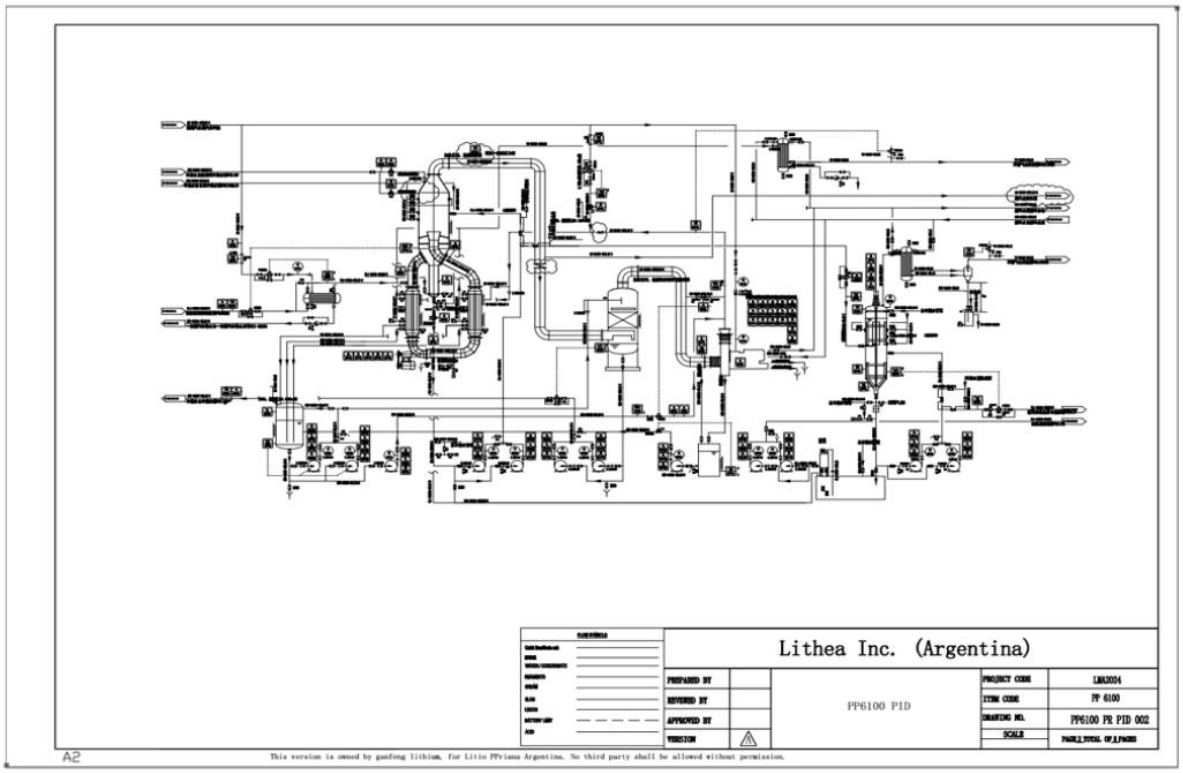

Figure 168: Flowsheet for Bipolar Membrane Electrodialysis (Source: Ganfeng, 2024)

14.8 Lithium Carbonate Plant

Soda ash is dissolved in water to prepare a 220 g/L solution, which is preheated to 80 ℃.

The sodium carbonate solution and the lithium chloride solution from the calcium removal process react at 85°C with a molar ratio of LiCl: Na_2CO_3 = 1: 0.525 (mol), resulting in lithium carbonate. After centrifugal separation, drying, and micronization, the lithium carbonate product is obtained.

$$2LiCl + Na_2CO_3 = Li_2CO_3 *+2NaCl$$

* Only battery grade Li_2CO_3 is envisioned in this report.

The mother liquor after lithium precipitation is acidified and neutralized to remove carbonate ions.

Finally, the mother liquor will be recycled into the process to leverage overall lithium recovery.

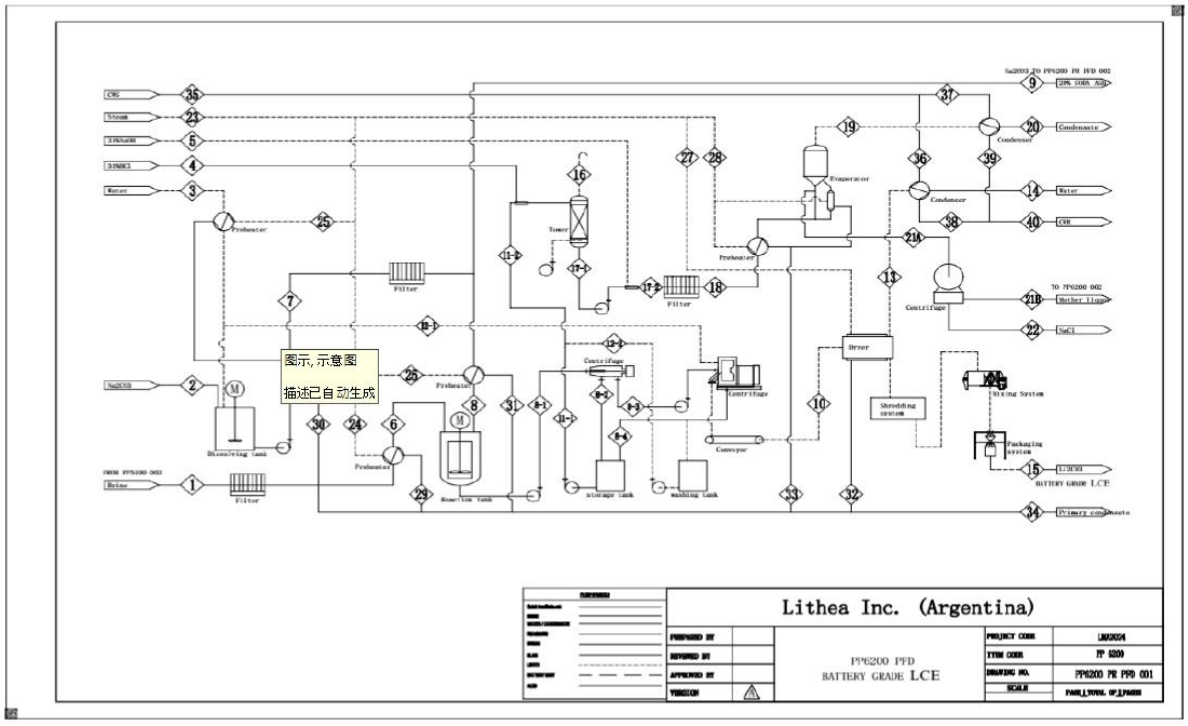

Figure 169: Flowsheet for Lithium Carbonate Plant (Source: Ganfeng, 2024)

15.0 INFRASTRUCTURE

15.1 General

Infrastructure at the Salar site consist of an electric power line, LNG, power distribution, water, and ancillary facilities such as camp, waste treatment and buildings for warehouses, truck shops, office buildings, reagents and fuels storage.

The details of the planned infrastructure for each of the two Pozuelos and Pastos Grandes Sites are presented in the following sections.

15.2 Utilities

15.2.1 Power

The PPG Project will have its main source of electrical energy, a new high voltage line at 345 kV connected to the Argentine interconnection system (SADI) from the ET La Puna located approximately 70 km from the property along Route 51.

This “New High Voltage Line” together with the necessary modifications and extensions to the “ET Puna” (switching sector, disconnectors, switches, metering systems, protection relays, communication systems, SMEC metering system, etc.), are part of the “YPF-LUZ Project” that some companies are carrying out together with the electricity distributor. These companies together with the distributor are going to finance the installation of the power line in La Puna. This will not involve a CapEx cost, except for the last section within the Lithea property, about 30 km (US$425,000/km) long.

This financing will be accounting for in the OpEx. The cost is around US$135/MW plus a fee of US$8/MW.

It is understood that this expansion in the “ET Puna” will be carried out with funds from the joint venture, but its maintenance and operation will be the responsibility of the concessionaire of the generation park.

The line that will connect to the Project site will be built with aluminium conductors with steel core on reticulated structures and average spans of 500 m; the safety strip from the axis of the line to its sides is 15 m and the minimum height at the lowest point of the span will be 7.5 m to the natural terrain and/or crossings of provincial and national roads. The estimated number of pickets to be installed for this section is 150 units between terminal structures, retention and suspensions.

The electric company has proposed to provide a new LAT connection through a transformer station in which the Volage is reduced to 33kV and from there will enter the project with medium voltage overhead lines to carry out the internal distribution at the salars, processing plants and auxiliary areas of the property.

To comply with this, 2 transformers of 345/33 kV 60MW (75MVA) of power will be installed, with oil insulation in accordance with IRAM 2250 Standard and will be PCB free. The system will include:

- Installation and connection of 33 kV subway cables composed of Cu unipolar cables within the ET premises that allow linking the outputs of the power transformers with the transformer input cubicles.
- Supply and assembly of 33 kV shielded GIS type indoor switchgear and its connection to the power transformers according to single-line electrical diagrams.
- Supply and assembly of the Alternating Current and Direct Current Auxiliary Services. It includes the supply of two (2) 33/0.4 kV Transformers and the electrical panels TGSACA and TGSACC, chargers and Ni-Cd battery banks.

- Supply and assembly of command and protection panels / cubicles for the 345 kV Overhead Line Output, Transformer and Coupling fields.
- Supply and assembly of the Command and Telecontrol system for the new ET.
- Supply and assembly of the SMEC Metering System in 33 kV and backup in 345 kV.
- Supply and installation of the Communication System of the ET. OPGW system (fibre optic) recommended.
- In addition to complying with all the requirements and regulations established for this type of facility, it must have a SCADA system for monitoring the entire station and operation of the 33 kV output circuit breakers from the Lithea Production Plant.
- Construction of a building for Control, Protection, Measurement, Tele-control, Communications, Auxiliary Services and 33 kV gas insulated switchgear type GIS.
- Execution of all complementary works that include filling and leveling the land, provision and assembly of porticos, posts and pedestals, foundations, pipelines, grounding mesh, access roads and internal to the Station, whether main or secondary, sewers, lighting, perimeter fence, gate, etc
- The approximate dimensions of the EETT will be 100 x 150 m.

From the transformer station, the 33kV lines for internal power distribution will go first to the medium voltage distribution centre (CD-MV) in the process plant (15 km from the EETT) and the second will travel 12 km to reach the production wells located in Salar de Pastos Grandes. From the CD-MV, a 33 kV line will be installed channelled by trays to the transformation centres of the production plant where the CCM and low voltage distribution systems will be installed for the different terminal circuits; from the same CD-MV the laying of a 33 kV medium voltage overhead line will be carried out; approximately 15 km to energize the production wells and evaporation ponds located in the Pastos Grandes Salar, where each well will have a dedicated transformation centre that will energize the pumps. The project is planned to be developed in 3 stages:

- The “Medium Voltage Distribution Centres” are very similar to each other; the main difference is the total power they handle and the number of output cells at 13.2kV.
- The “Medium Voltage Distribution Centre 1 will have 2 transformers of 25MVA (each) to reduce the voltage level from 33kV to 13.2kV and distribute it to the different consumption points. In addition, there will be a 13.2kV to 0.4kV - 315kVA transformer for the “auxiliary services” of the Electrical Room of the Distribution Centre.
- The “Medium Voltage Distribution Centre 2 will have 2 transformers of 30MVA (each) to reduce the voltage level from 33kV to 13.2kV and distribute it to the different consumption points. In addition, there will be a 13.2kV to 0.4kV - 315kVA transformer for the “auxiliary services” of the Distribution Centre Electrical Room.
- The “Medium Voltage Distribution Centre 3 will have 2 transformers of 10MVA (each) to reduce the voltage level from 33kV to 13.2kV and distribute it to the different consumption points. In addition, there will be a 13.2kV to 0.4kV - 315kVA transformer for the “auxiliary services” of the Distribution Centre Electrical Room.

15.2.1.1 Internal Overhead Lines

For the 33kV main power supply of the PZ-PG project, 3 Medium Voltage Lines will be used, as described above, which will use aluminium conductor with steel alloy, with section and number of terns to be determined in the detailed engineering stage. The average span will be 70 m, where the minimum distance to the natural ground, at the point of maximum sag, will be 7 m high and an easement strip from the central axis of the line will be 12.5 m for both sides, the terminal columns, suspensions and retentions will be of pre-cast H°A° and their bases will be of H°A° with diagonal orientation to the longitudinal axis of the line; the route of this line will be prioritized following the internal roads of the property.

Table 107: Internal Overhead Lines

Overhead Power Line	Starting Point	Destination	Voltage Level	Distance
Main Line 1	ET#1 – SPG	CD-MV1	33 kV	30 km
Main Line 2	ET#2 – SPG	CD-MV2	33 kV	30 km
Main Line 3	ET#3 – SPG	CD-MV3	33 kV	30 km

15.2.1.2 Emergency Generation

As an emergency system, critical equipment will be connected to diesel generators.

These generators deliver low voltage (0.4 kV), so at the output of each of them they will be connected to a 0.4 to 13.2 kV step-up transformer of 2 MVA at 4,000 masl and from there to a common 13.2 kV busbar in a Synchronism and Transfer electrical room (located in the area near the generators, but opposite to the fuel storage tanks for the generators) to then take that energy to the corresponding Medium Voltage Distribution Center.

The use of this Emergency Generation System will be on an eventual basis for maintenance tasks or extreme contingencies of the main connection line to the SADI; its location will be close to the plant so as to cover the basic needs of the process and the permanent camp; in a first approximation this System will deliver 12 MW of electric power.

Figure 170: PPG Project Electric Line from La Puna

This “New High Voltage Line” together with the necessary modifications and extensions in the “ET Puna” (shunting yard, addition of disconnectors, switches, measurement systems, protection relays, communication systems, SMEC measurement system, etc.), are part of the “YPF-LUZ Project” that is being carried out by some companies together with the electric distributor.

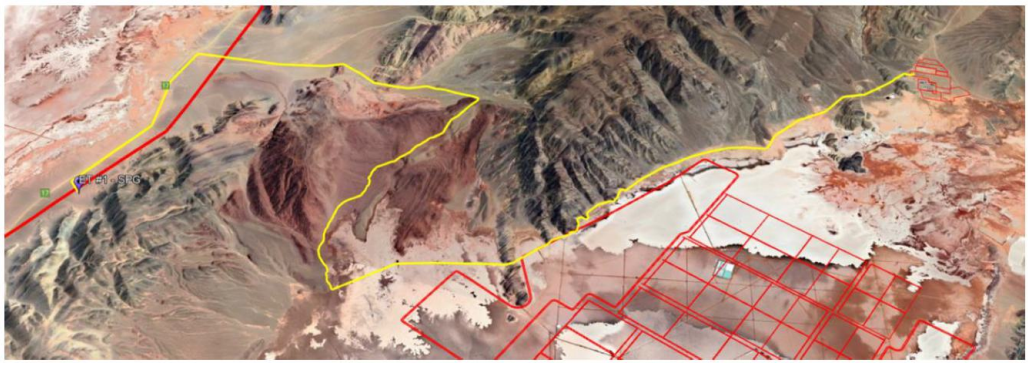

Figure 171: PPG Project Electric Line to the Plant

This financing will be paid in OpEx. The price is around 65 USD/MW + 36,448 USD/MW-month (15-year fixed fee of around 49.9 USD/MW).

15.2.1.3 Electrical Load

Total operating electrical energy for the Project is estimated below, which includes the required energy for brine extraction wells, evaporation ponds, processing plants, infiltration ponds, worker´s camp etc.

Table 108 shows the anticipated power consumption for each area and for each stage of the project.

Table 108: Power Consumption for 50K Production and 150K Production

PROJECT AREA	Power Consumption (kw) for Phase 1			Power Consumption (kw) for Phase 2			Power Consumption (kw) for Phase 3		
	Load kw	Operating	kw/year	Load kw	Operating	kw/year	Load kw	Operating	kw/year
Brine Well Field	5,250	80%	45,990,000	7,240	80%	63,422,400	7,240	80%	63,422,400
Ponds	9,000	100%	78,840,000	10,280	100%	90,052,800	10,280	100%	90,052,800
SX	7,455	78%	53,676,000	7,455	78%	53,676,000	7,455	78%	53,676,000
Primary Purification	857	90%	6,170,400	857	90%	6,170,400	857	90%	6,170,400
Raffinate Treatment	515	55%	3,708,000	515	55%	3,708,000	515	55%	3,708,000
Raff Water Treat	210	89%	1,512,000	210	89%	1,512,000	210	89%	1,512,000
Ancillary Facilities (Camp, Offices, Sewage Treatment, water treatment)	1,222	100%	8,028,540	1,222	100%	8,028,540	1,222	100%	8,028,540
Second Purification	696	63%	5,011,200	696	63%	5,011,200	696	63%	5,011,200
Electrodialysis	7,635	95%	54,972,000	7,635	95%	54,972,000	7,635	95%	54,972,000
LHM Plant	3,161	66%	22,759,200	3,161	66%	22,759,200	3,161	66%	22,759,200
LCE Process Plant	7,253	96%	52,221,600	7,253	96%	52,221,600	7,253	96%	52,221,600
Utilities	2,690	100%	19,368,000	2,690	100%	19,368,000	2,690	100%	19,368,000
Operating Power Demand	45,944	42,906	352,256,940	49,214	45,778	380,902,140	49,214	45,778	380,902,140

- The new 345 kV YPF Line (from the Puna power plant) does not have a start-up date (we do not know it).
- The new 345 kV EETT on the Lithea property may have a construction time of approximately 14 months, plus when adding the time for purchasing, equipment manufacturing, import, transfers, testing and start-up, that time will not be less than 28 months.
- Based on the above, it is clear that for almost all of Stage 1 and perhaps part of Stage 2 we will have to provide electricity to the Project through own or rented generation.
- Taking this into account, we assume that the 12 MW planned for Emergency would be used as the main source of energy until YPF energy is available, enough to supply the camp with all the water wells and RO plant, the operation of the PZ brine wells and the PZ ponds, A supply of natural gas may be needed to generate electricity for the critical components. This should be studied in detail over the next stage.

15.2.2 Natural Gas

Heat and steam for the process has been assumed to be supplied by brackets around Liquefied Natural Gas (LNG) trucked to site, stored, re-gasified and distributed to the respective users as summarized in table below (Table 109).

Table 109: Saturated Steam Usage

Saturated Steam Usage		
No.	Item	tons per hour
1	PP5000 Removal B process	8.07
2	PP5100 ion-exchange for removal Ca	3.24
3	PP6100	3.088
	LiOH workshop	
4	PP6200	17.82
	Battery grade Li_2CO_3 workshop	
TOTAL with contingency		**32.22**

To use the LNG as fuel for heating, it must be converted back to gaseous state. This process takes place at a local plant terminal where the carrier discharges the LNG cargo. At the terminal, the gas is stored at liquid state in tanks, and re-gasified before it is transferred as natural gas to the end users through a pipeline gas network.

The on-site facility to handle LNG will comprise a dedicated plant module to effectively transform liquid LNG into its gaseous form. This service is included in the supplier's unit cost for LNG without additional re-gasification capital required.

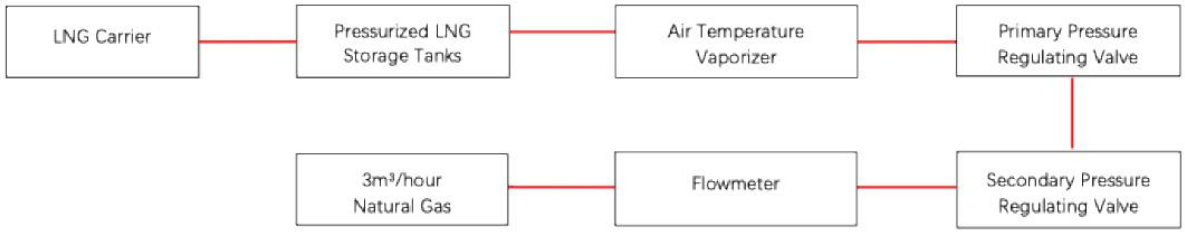

Figure 172: The Process Flow for LNG (Source: Ganfeng 2025)

15.2.3 Water Supply

The water supply system for the project will consist of wells distributed in the salars of Pozuelos and Pastos Grandes. All the wells will be connected to aqueducts to transport water to the points of consumption. To meet the requirements of dilution water for ponds, process water for plants, services and camp, the pipelines will be distributed taking into account the distances to optimize the routing of pipes.

Below is the location of the various wells in the salars.

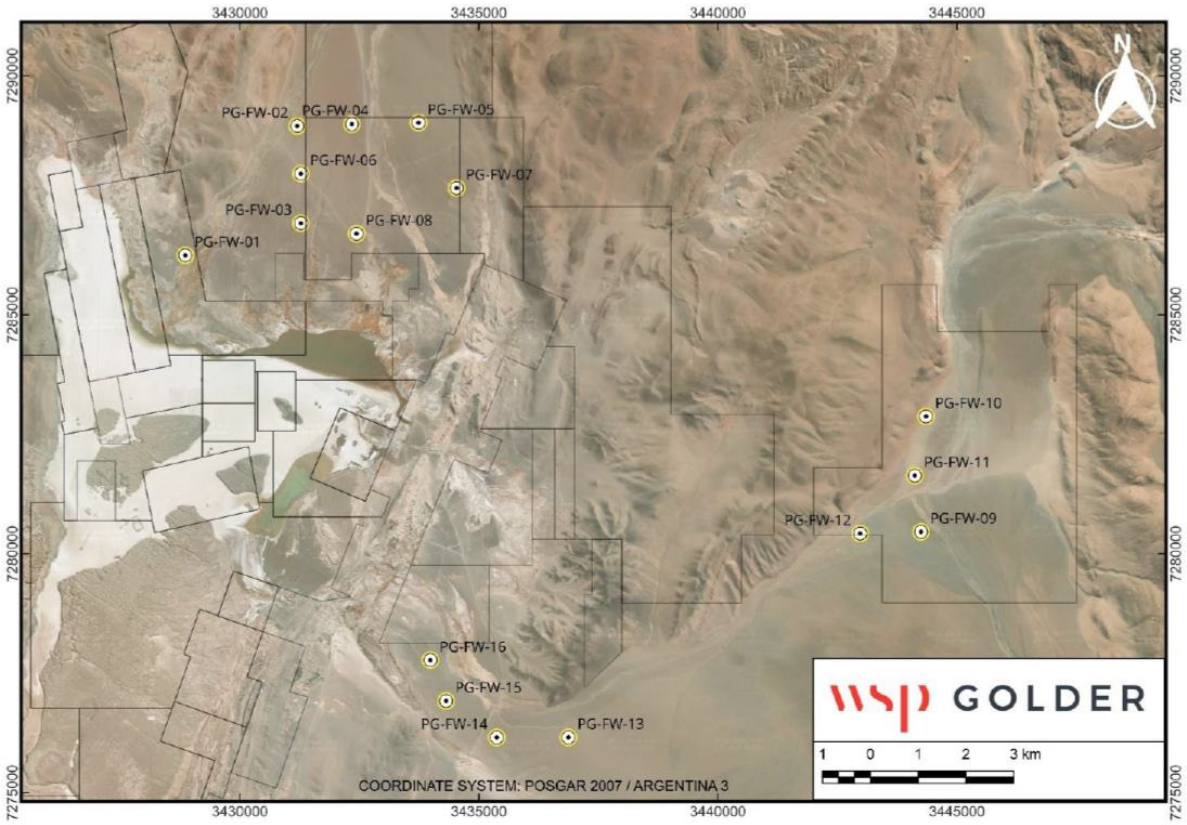

Figure 173: Location of Fresh Wells at Pastos Grandes

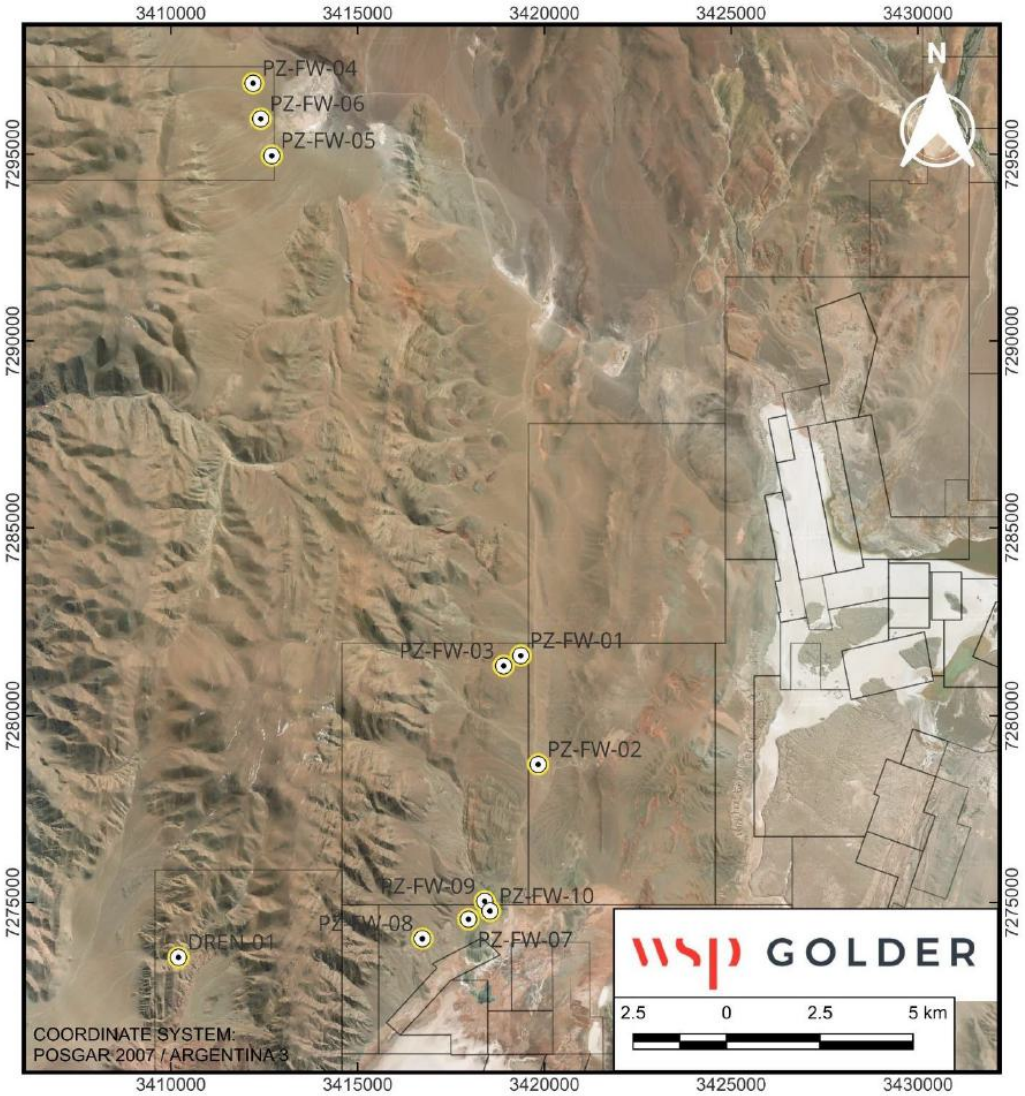

Figure 174: Location of Fresh Wells at Pozuelos

Table 110: Fresh Well Coordinates at Pozuelos and Pastos Grandes

No.	Pozuelos	X (Posgar 07)	Y (Posgar 07)		No.	PG	X (Posgar 07)	Y (Posgar 07)
1	PZ-FW-01	3419368.92	7281611.45		1	PG-FW-01	3428857.50	7286244.54
2	PZ-FW-02	3419833.32	7278698.44		2	PG-FW-02	3431201.65	7288952.58
3	PZ-FW-03	3418909.73	7281335.57		3	PG-FW-03	3431278.91	7286917.24
4	PZ-FW-04	3412199.60	7296898.73		4	PG-FW-04	3432343.86	7288989.42
5	PZ-FW-05	3412700.66	7294962.31		5	PG-FW-05	3433738.19	7289019.73
6	PZ-FW-06	3412403.24	7295948.00		6	PG-FW-06	3431278.38	7287953.24

No.	Pozuelos	X (Posgar 07)	Y (Posgar 07)
7	PZ-FW-07	3417968.57	7274555.29
8	PZ-FW-08	3416731.76	7274036.20
9	PZ-FW-09	3418404.08	7275037.85
10	PZ-FW-10	3418545.81	7274775.92
11	DREN-01	3410202.75	7273534.47

No.	PG	X (Posgar 07)	Y (Posgar 07)
7	PG-FW-07	3434536.93	7287652.11
8	PG-FW-08	3432442.03	7286694.43
9	PG-FW-09	3444251.12	7280459.04
10	PG-FW-10	3444355.44	7282875.11
11	PG-FW-11	3444121.51	7281634.11
12	PG-FW-12	3442979.00	7280423.30
13	PG-FW-13	3436873.36	7276159.27
14	PG-FW-14	3435374.43	7276157.53
15	PG-FW-15	3434314.75	7276922.39
16	PG-FW-16	3433987.07	7277778.23

15.2.3.1 Water Consumption

Water will be consumed for the operation, service, and drinking etc. at the site. The main consumption of the raw (fresh) water is for the process plants. Based on the empirical experience, 1% of brine dilution or 1% of the transfer brine flow rate is enough to maintain the adequate operation of the pump. Total water requirement at the site is summarized in Table 111.

The water requirements for the project will be met by regionally available water wells. It is projected that the available water sources will supply the temporary facilities during the construction stage as well as the permanent industrial facilities.

Table 111: Raw Water Consumption for the Three Phases of Production

Water Consumption Phase 1		
Description	**Usage m^3/day**	**Water Usage TPA**
Process Plants	3,712	1,113,598
General Services	1,367	498,984
Potable water	92	33,682
Evaporation Ponds	1,498	546,770
Total Water	**6,669**	**2,193,034**
Water Consumption Each Phases 2 & 3		
Description	**Usage m3/day**	**Usage TPA**
Process Plants	3,712	1,113,598
General Services	1,367	498,984
Potable water	92	33,682
Evaporation Ponds	1,572	573,780
Total Water	**6,743**	**2,220,044**

15.2.3.2 Water Distribution

To supply the water required for the three Phases, considering the well locations, aqueducts are used to connect several wells and transport them in pipelines.

Figure 175 shows the aqueducts proposed to connect the wells located both in Pastos Grandes and in the northern area of the project. These are divided into the Northern Aqueduct (Green), the PG-PZ Main Branch Aqueduct (Magenta) and the PG-PZ Secondary Branch Aqueduct (Yellow). Figure 176 shows the Southern Aqueduct (Blue).

15.2.3.2.1 Northern Aqueduct

To transport water from the northern sector of the project, an aqueduct of approximately 32 km is proposed. This will collect water from ten wells located both in the northern sector and along the route. Given the geography of the terrain, it is proposed that transport be by gravity; the route and elevation profile are shown in the figures.

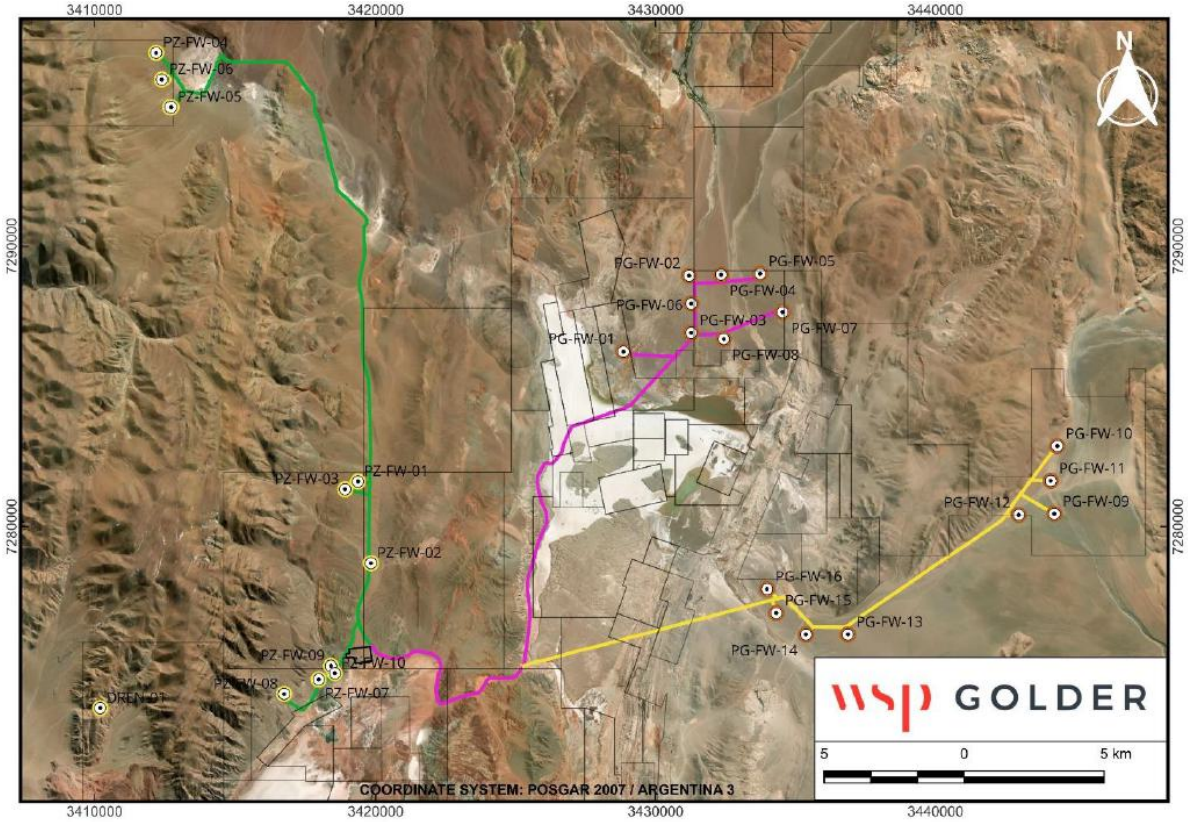

Figure 175: Northern Aqueduct Wells and Route

15.2.3.2.2 Pastos Grandes – Pozuelos Aqueduct (PG-PZ)

To transport water from the Pastos Grandes salt flat to Pozuelos, the aqueduct is divided into two branches that group the wells distributed in the area.

Transport will be done either by gravity or by pumping depending on the elevation profile.

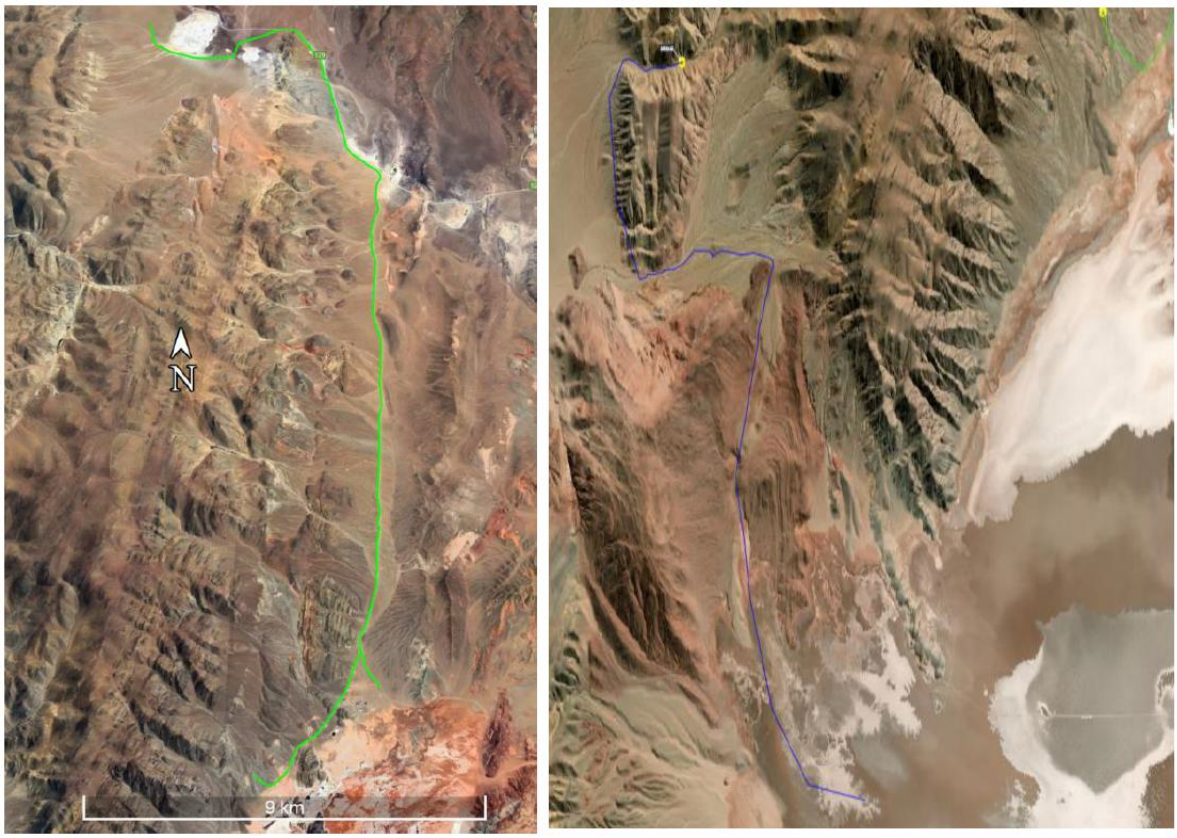

Figure 176: Southern Aqueduct Wells and Route

15.2.3.3 Water Treatment

Raw water in the area is rich in chlorine, sulphate, boron and magnesium etc., thus water treatment required to obtain the water quality needed by all applications.

A water treatment system is utilized for producing portable water and high-quality water for the steam boiler. The system consists of ultrafiltration and two-stage Reverse Osmosis (RO) process.

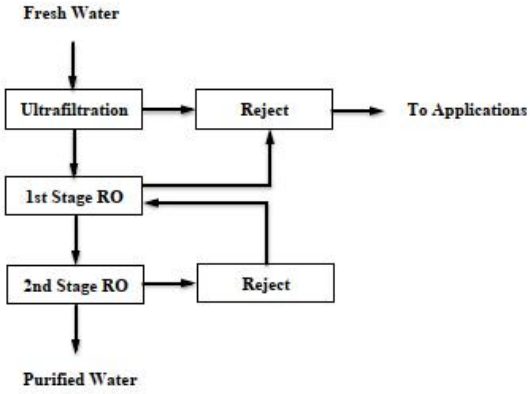

Figure 177: Simplified Block Flow Diagram for the Purification System (Source: Ganfeng, 2024)

Raw water will be diverted to a surge tank from the reservoir to supply feed to the system. Purified water will be stored in additional tanks and distributed to the applications. A simplified block flow diagram for the system is illustrated in Figure 177.

Table 112: Analyses of the Water Treatment System

	Cl	SO_4^{2-}	Li	Mg	Ca	B	pH
	ppm	ppm	ppm	ppm	ppm	ppm	ppm
Raw water	50.20	105.00	0.00	5.62	57.46	0.36	7.38
Purified water	0.20	0.03	0.00	0.00	0.01	0.15	7.00
Reject	389.00	233.5	0.00	3.80	160.10	2.30	7.93

15.2.3.4 Steam

Steam for the process will be supplied by a 35 tons per hour boiler fuelled with natural gas (LNG) for each Phase of production.

15.2.4 Ancillary Facilities^^

^^ The infrastructure description below refers to all of the three phases of the project. The breakdown for each Phase is shown in the distribution used later in this report (Table 127 Infrastructure and energy capital).

15.2.4.1 Truck Shops

Two truck shops consist of maintenance workshops for heavy and light machinery.

The shops will have bays for heavy equipment and for light equipment; equipped with lubricants, greases, refrigerants, compressed air, water, energy, drain, epoxy floor, tools and lifting equipment systems.

The work to be carried out in the Truck Shops will be scheduled maintenance and emergency repairs of all the mobile equipment of the project. The area is covered, built in ASTM-A36 structural steel frames with insulating panels. They will be 50mm for its walls and 30mm for the roof with double sheet metal and PIR filling. For the interior divisions, 150 mm thick drywall with double plating and 100mm thick glass wool insulation is foreseen. Micro-perforated tape and interior putty will be used to take joints, in turn galvanized edge-bands will be used to cover the corner joints and the final plaster will be carried out for finishing. The Shops will have 2 bays for semi-heavy equipment that will have pits with a depth of 1.6 meters, 2 bays for light equipment equipped with vehicle lifts of up to 4.5 Tn and 1 bay for washing equipment; It will be equipped with lubrication systems, greases, refrigerants, compressed air, water, energy, drainage, epoxy flooring, tools and lifting equipment.

The following were considered for the workshop:

- One locker per sector. Each sector will have two working tables.
- Three storage tanks
- An electrical workshop
- A furnished office
- Bathrooms
- Laundry room with wash water recovery and filtration system
- Fire detection system. With evacuation zones
- Both lubrications, greasing and refrigeration systems will have integral circuits that allow the collection and storage of maintenance waste.
- The drainage system will be centralised in a chamber for subsequent effluent treatment.
- Disused tyres will be placed in suitable and defined areas for subsequent collection/recycling.
- Disused batteries will be placed in suitable areas with a containment trough for classification and collection.
- Solid waste will be disposed of in suitable and defined areas for classification and collection.

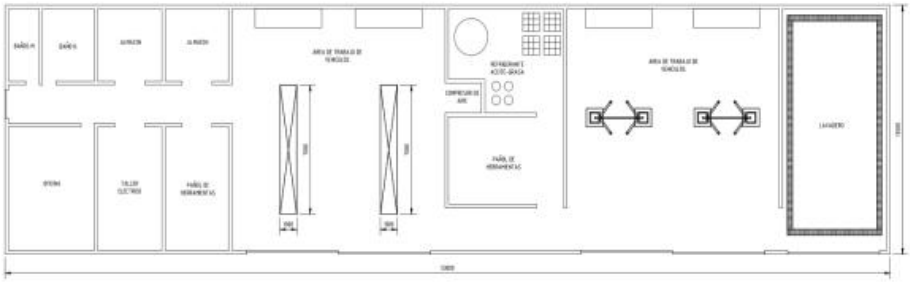

Figure 178: Typical Layout of Truck Shop (Source: Ganfeng, 2024)

15.2.4.2 Warehouses

The warehouse sector is located to the east of the processing plant on a site of approximately 35,000 m^2. There are 5 sectors for indoor and open warehouses to accommodate spare parts, machineries, products, general materials and geomembrane,

Two warehouses have an approximate area of 2,160 m^2 each (Figure 179), built with ASTM-A36 structural steel frames covered with insulating panels. The walls will be 50 mm thick, and the roof will be 30 mm thick, with double-sided sheet metal and filled with PIR.

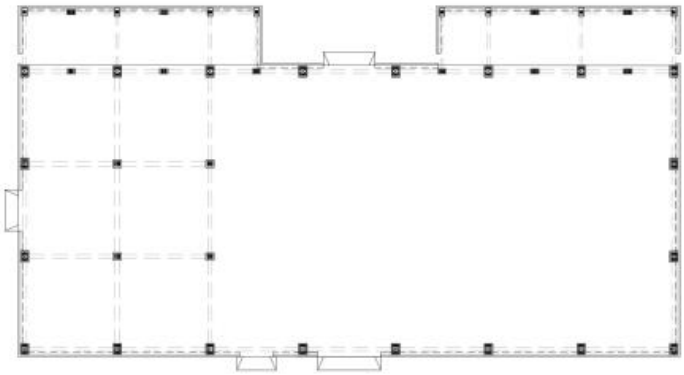

Figure 179: Typical Layout of a 2,160 m^2 Warehouse (Source: Ganfeng, 2024)

Another warehouse, shed style with an approximate area of 1,960 m^2, built with ASTM-A36 structural steel frames covered with insulating panels (Figure 180). The walls will be 50 mm thick, and the roof will be 30 mm thick, with double-sided sheet metal and filled with PIR. For the interior partitions, 150 mm thick double-plastered partition walls and 100 mm thick glass wool insulation are foreseen. Micro-perforated tape and interior mastic will be used for joint sealing, galvanized edge banding will be used to cover the corner joints, and the final finish will be applied.

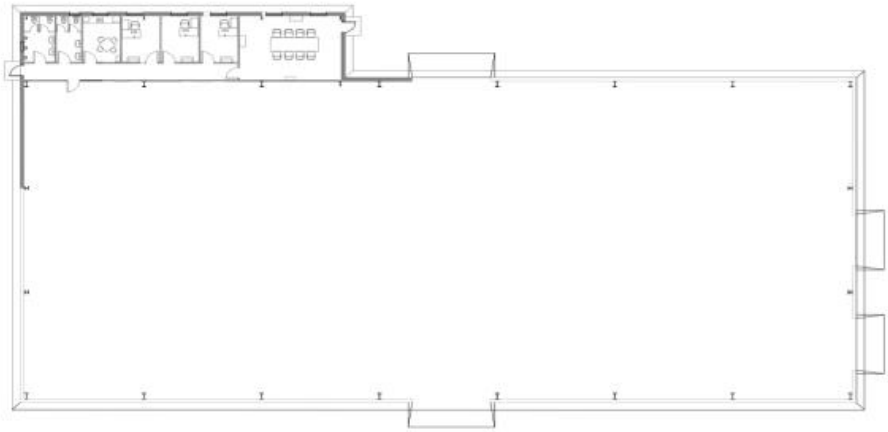

Figure 180: Typical 1,960 m^2 Warehouse Layout (Source: Ganfeng, 2024)

15.2.4.3 Storage Yards

There will be two storage yards. The first one will have an area of 9,800 m^2 for various supplies, with a perimeter fence made up of standard 13-gauge x 2 ½" diamond-shaped wire and 1.80 m high, 3-row galvanized barbed wire, supported by 11x11cm concrete posts 3.20 m high with a 45º upper elbow for a 2.40 m fence every 4 m, buried 0.9 m. The tensioning of the fence will use 1"x3/16" planks 1.80 m long, 3/8" x 9" wire pulling hooks and No. 7 turnstiles to ensure the correct placement of the wiring before it is cast in a 0.20 m x 0.30 m perimeter plinth of plain concrete.

The second yard of 17,640 m^2 for the storage of supplies that can be contaminated, will have a 1.5 mm geomembrane made of HDPE whose joints will be made by thermos-fusion to guarantee the correct sealing.

15.2.4.4 Offices

The administration building areas includes:

- Management offices
- Supervisory offices
- Locations for administrative personnel
- Men and women's washrooms
- Kitchen
- Meeting room

15.2.4.5 Camp

The camp sector is divided into 4 terraces for maximum peak of 2,000 people (Table 113). In order to comply with such requirement, the layout of the terraces is as follows:

On the first terrace, the camp's maintenance and infrastructure areas will be located:

- GEOLOGY DEPOSIT - 228.8 m^2 (in project)
- LAUNDRY - 136.9 m^2 (in project)
- WATER PLANT - 428.2 m^2 (in project)
- PROVISORY WATER TANKS - 300 m^2 (in project)
- RECREATION ROOM – 1,581 m^2 (in project)

On the second and third terraces, the following residential and office modules are already assembled on site:

- CAMP 4, 2-FLOOR MOD. - 321.49 m^2 each. **Capacity: 288 people.**
- CAMP 2 MOD. 1 FLOOR - 237.90 m^2 each. **Capacity: 48 people.**
- IT OFFICE - 66.36 m^2

The following are planned to be built in the future:

- CAMP 12 MOD. 2 FLOOR - **Capacity: 960 people.**
- NURSING - 216 m^2
- CAMP OFFICE - 73.87 m^2
- OFFICES 6 MOD. - 162 m^2 each. Workspaces: 168
- PARKING - 1112.56 m^2
- CAMP 12 MOD. 1 FLOOR 237.90 m^2 each. **Capacity: 192 people.**

And in the last one, the dining room and living modules:

- DINING & KITCHEN – 3,294.15 m^2
- GAS TANKS
- SUPPLIES DOWNLOAD ZONE
- TEMPORARY WASTE YARD
- CAMP 2 MOD 1 FLOOR - 237.90 m^2 each **Capacity: 48 people.**

- CAMP 6 MOD 2 FLOOR 543.40 m^2 each **Capacity: 464 people**.
- PARKING – 2,479.20 m^2

To the east of the camp there is a space reserved for contractors of 21,392.59 m^2 and to the west the electrical park that supplies the camp, along with the fuel tanks (996.31 m^2).

Table 113: Population in Terrace 2, 3 and 4 in Camp Sectors

Zone	Population	Levels per module (Beds per level)	Number of modules
TERRACE 2 and 3	288	2 levels (36 seats per level)	4
	48	1 level (24 places per level)	2
	960	2 levels (40 places per level)	12
	192	1 level (16 places per level)	12
Zone	**Population**	**Levels per module (Beds per level)**	**Number of modules**
TERRACE 4	48	1 level (24 places per level)	2
	464	2 levels (40 places per level)	6

The value of 464 on terrace 4 is obtained by adding the 96 modules required and the additional 368 modules needed to complete the total population previously mentioned (2,000 people).

15.2.5 Reagents and Fuels

15.2.5.1 Reagents

Reagents used in the plant are lime, hydrogen peroxide, sodium carbonate, sodium hydroxide, hydrochloric acid and miscellaneous reagents and products used in solvent extraction and brine purification.

Table 114 shows the annual requirement for those reagents.

Table 114: Annual Consumptions of Reagents

REAGENTS USAGE SUMMARY Phase 1	
	TPA
Lime	10,656
27.5% H_2O_2	1,258
NaOH (100%)	18,239
HCl 32%	2,881
Sodium Carbonate	67,788
Other Chemicals	Various
AFTER PHASE 3	TPA
Lime	31,968
27.5% H_2O_2	3,774
NaOH (100%)	54,718
HCl 32%	8,643

Sodium Carbonate	203,364
Other Chemicals	Various
OTHER REAGENTS (EACH PHASE)	TPA
H_2SO_4	640
PAM	4
PAC	0.252
$FeSO_4$	838
Oil adsorbing resin	54
IX resin Ca	6
IX resin B	6
Na_2SO_4	0.378
NaCl	0.792

15.2.5.2 Fuels and Lubricants

The fuel plant will be located in the southwest sector of the plant (Figure 181).

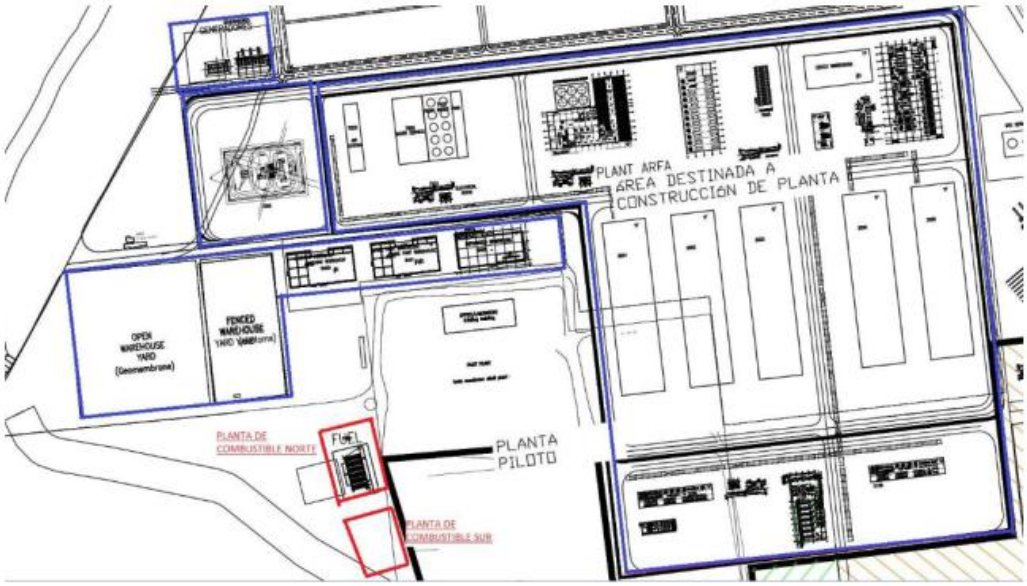

Figure 181: South-west Fuel Plant Location (Source: Ganfeng, 2024)

15.2.5.2.1 Fuel Unloading

The fuel (diesel) discharge will be carried out by means of a 3 (HP) APEX three-phase explosion-proof electric pump. The meter (flow meter) will be of 3", with inductive sensor, and a maximum flow of 30,000 L/h (500 L/min).

As for accessories, the following will be taken into account:

- 3" filter (with manual vent): Constructed with a stainless-steel mesh, washable, which ensures fuel cleanliness and care of the flowmeter.
- Jefferson solenoid valve or similar.
- Electronic equipment of national manufacture, installed in a cast aluminium box, certified under IEC standard with IP 66 protection degree, APEX.
- Metal dispenser box, with TC 5,700K square box, IP 68, APEX, housing a 10" touch screen for accessing the operating system.

15.2.5.2.2 Fuel Storage

For the storage of fuel (Gasoil), 2 areas located in adjacent sectors will be contemplated, complying with resolutions 76/2002 - 655/2003.

The North plant foresees 1 tank of 60 m^3, and 2 tanks of 40 m^3, arranged as follows: 60 m^3 tank in the middle, and 40 m^3 tanks on each side (north and south of the plant). A valve box will be included to load only one, or the 3 simultaneously with a maximum flow of 30,000 L/h (500 L/min). In the South plant, 1 tank of 60 m^3 and 1 tank of 40 m^3 are foreseen. A valve panel will be included to load only one, or both simultaneously with a maximum flow of 30,000 L/h (500 L/min).

The following considerations will be taken into account for the tanks:

- Constructed with SAE 1010 quality carbon steel plate, with a minimum thickness of 3/16".
- Exterior and interior double welding procedure under IRAM IAS U 500 Standard.
- The tank must be delivered with a hydraulic test certificate of 800 gr/cm^2 or higher.
- Both the tank and the pan must be finished with dual purpose white polyurethane paint with a minimum thickness of 80 µm.
- The tank shall have a level measurement system.
- The tanks must be delivered with all the necessary documentation for the qualification at the secretary's office.

15.2.5.2.3 Fuel Loading

The fuel (Diesel) will be loaded by means of a 3 HP APEX three-phase explosion-proof electric pump. The meter (flow meter) will be of 2", with inductive sensor, and a maximum flow of 24,000 L/h (400 L/min).

As for accessories, the following will be taken into account:

- Filter 2" (with manual vent): Constructed with a stainless-steel mesh, washable, which ensures the cleanliness of the fuel and the care of the flow meter.
- Electronic equipment of national manufacture, installed in a cast aluminium box, certified under IEC standard with IP 66 protection degree, APEX.
- Metal dispenser box, with TC 5700K square box, IP 68, APEX, housing a 10" touch screen for accessing the operating system.

15.2.5.2.4 Fuel Distribution

The distribution corresponds to the consumption of fuel (diesel) for each stage of the project (construction, operations) is shown in Table 115.

Table 115: Fuel Distribution for Each Stage

Item	Construction Phase (L/h)	Stage of Operation (L/h)
Plant Generation	N/A	5,360**
Generation Camp	100	N/A
Remote Zone Generation	300	300
Light Vehicles	1,680	560

Item	Construction Phase (L/h)	Stage of Operation (L/h)
Heavy Vehicles	2,500	240
Total by stage	4,580	7,710**

*Note: ** Considered in an emergency situation, not for normal daily consumption for the project.*

The fuel plant will supply light equipment, trucks, emergency generators, etc. Estimated consumptions of fuel and lubricant are shown in Table 116.

Table 116: Estimated Fuel Consumption

Equipment	Description	Daily consumption (L/day)
Vans	20 Units	125
Trucks	10 Units	1,000
Diesel Generation	2 Gen of 3.3 Kva - backup (*)	39,600
Stand-alone Generators	5 Gen of 350 Kva - 4 hrs/day of use	1,750
	Lubricants L/Y	720

15.2.6 Waste Storage

For waste management, two containment sites were defined, an enclosed one and an openair one with an approximate area of 941 m^2 and 1,424 m^2, respectively. The area will have perimeter grids to prevent contaminants from leaking into the soil. Including pumping circuit for subsequent containment.

The waste to be found in this sector is that which comes from the industrial activity itself. Industrial wastes can be hazardous or non-hazardous according to their characteristics, which are subclassified into:

- RI from production: wastes that come directly from production processes and lithium carbonate production activities or generation of reagents. Examples: calcium sulphate cakes, calcium and magnesium carbonates, etc.
- Non-production IR: waste that is not directly related to production, but to other general site operation activities. Example: scrap metal, raw material packaging material, pallets, discarded PPE, maintenance waste.

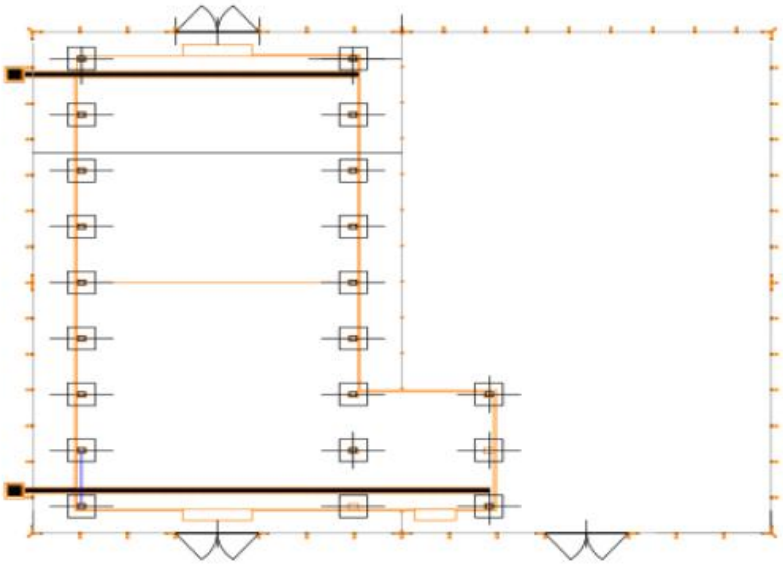

Figure 182: Layout of Waste Warehouse (Source: Ganfeng, 2024)

For waste similar to urban waste or household waste, an open-air yard was considered, in which the topsoil must be cleaned. Subsequently, the perimeter of the site must be fenced off for greater security.

15.2.6.1 Hazardous Waste

The hazardous waste generated by the Project is mainly used in oils and lubricants, paint remains, solvents, material contaminated with hydrocarbons, among others. It is estimated that less than 200 kilograms of hazardous waste will be generated per month.

The hazardous waste will be temporarily stored in the waste yard until it is removed by a company authorized for transport, treatment and/or disposal. The different waste storage sectors will have Olympic perimeter fencing, signage with legends of the types of waste found on site and waterproofing in the case of critical waste to prevent direct contact of the containers with the ground.

16.0 MARKET STUDIES

This section provides a summary of the supply and demand of lithium and price forecasts. Material presented in this chapter is primarily from the Lithium Quarterly Market Review October 2024, Benchmark Minerals, iLiMarkets and U.S. Geological Survey, Mineral Commodity Summaries, January 2024.

16.1 Lithium Applications

Lithium has unique properties that enables its use in many applications. This metal, the lightest known, combines high electrochemical potential with exceptional heat and electricity conductivity. Its role in the battery industry is critical, as lithium, while just one component, is indispensable for battery functionality.

Lithium-ion batteries are the most suitable technology for energy storage and the most electrochemically mature due to their high energy capacity. The largest applications for lithium chemicals are rechargeable batteries, but lithium chemicals are also used in the glass, lubricating greases, metallurgy, pharmaceutical, and polymer industries.

Lithium-ion batteries are advanced energy storage devices that rely on electrochemical processes to function. Their key components include the anode and cathode, which serve as electrodes where electrochemical reactions take place, and the electrolyte, a medium that facilitates the movement of lithium ions between the anode and cathode during charge and discharge cycles. This design enables efficient energy storage and transfer, making lithium-ion batteries a cornerstone of modern energy solutions.

Among the various types of cathodes used are lithium cobalt oxide (LCO), lithium iron phosphate (LFP), lithium nickel manganese cobalt oxide (NMC), lithium manganese spinel (LMO), lithium nickel cobalt aluminum oxide (NCA), and Lithium Manganese Iron Phosphate (LMFP). Each of these cathode types offers distinct advantages and disadvantages in terms of safety and specific energy.

When comparing LFP and LMFP, LMFP offers improved energy density over LFP, while still maintaining a low-cost structure, making it an attractive option for a range of applications. Currently, LMFP technology is primarily being pioneered in China, although initial variants are not pure LMFP, but a compound combined with NMC. Key optimization decisions being made in the early stages of development focus on refining the production process and selecting the appropriate manganese chemical feedstock to maximize performance and cost-efficiency.

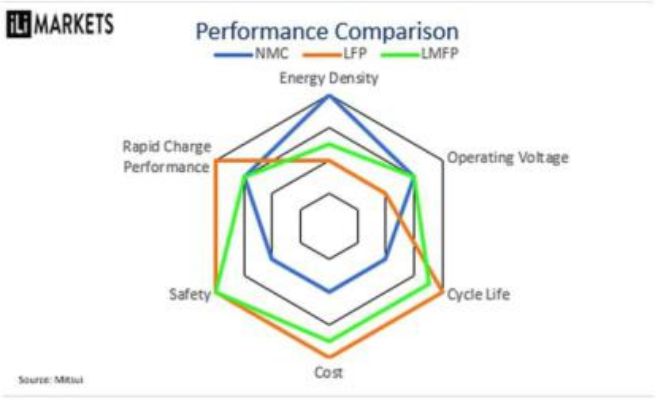

Figure 183: LFP, LMFP, and NCM Comparison (Source: Lithium Quarterly Market Review October 2024 from iLiMarkets.)

Just as potential improvements in battery cathodes have been studied, efforts have also been dedicated to refining the anode and the electrolyte.

The battery raw materials cost is presented in the following figures. The commercial used of Li anode means that Li intensity will double in the battery.

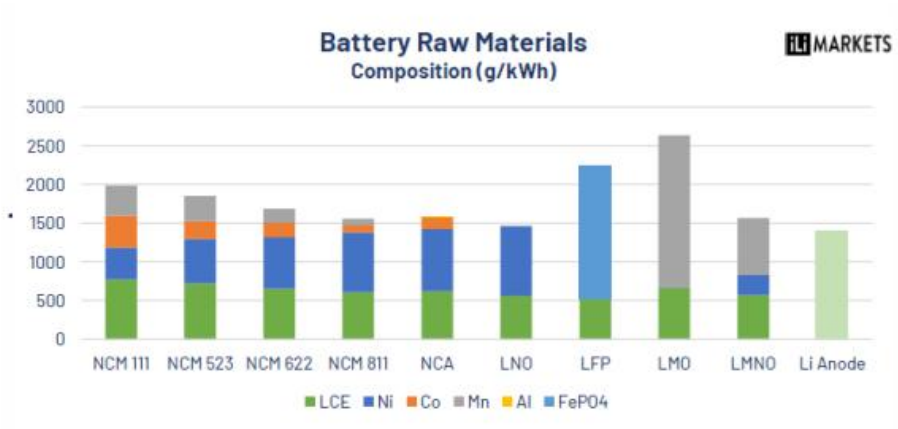

Figure 184: Battery Raw Materials Cost (Source: Lithium Quarterly Market Review October 2024 from iLiMarkets)

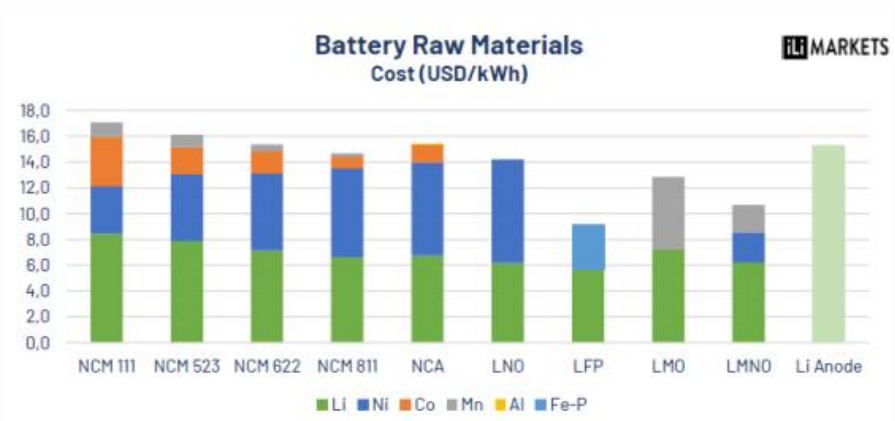

Figure 185: Battery Raw Materials Cost (Source: Lithium Quarterly Market Review October 2024 from iLiMarkets.)

16.2 Lithium Demand

Lithium average demand growth through 2030 is expected to be 250-300 kMT/y with a CAGR of 18%. Lithium demand for batteries was projected to reach 3.4 million MT LCE in 2033, electric vehicles (EVs) accounting for 64% of lithium demand and Battery Energy Storage System (BESS) representing 24% (Figure 186).

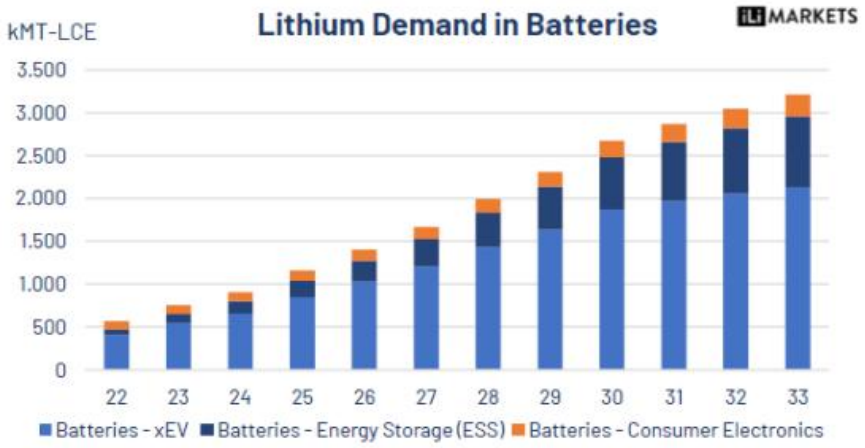

Figure 186: Lithium Demand in Batteries (2024) (Source: Lithium Quarterly Market Review October 2024 from iLiMarkets.)

The outlook for lithium demand is positive, driven by the development of electromobility and the growing need for batteries in the electronics industry (Figure 19.3). Lithium has been listed as one of the critical elements by the U.S. Department of Energy based largely on its importance in rechargeable batteries. Lithium-ion battery is the preferred form for high-density applications like EVs and portable electronics. A full-electric EV can require over 50 kg of LCE in the battery. By 2033, it is estimated that energy storage could represent 95% of global lithium demand.

Lithium consumption is expected to increase significantly in the coming years driven by a rapid increase in demand for EVs. According to Lithium Quarterly Market review from iLiMarkets issued on October 2024, EV sales have grown by 3.5 -4.0 million EVs per year over the last three years, which represents between 150-200 kMT-LCE incremental demand year on year. The EV main players in EV battery manufacturing are represented in the following Figure 187.

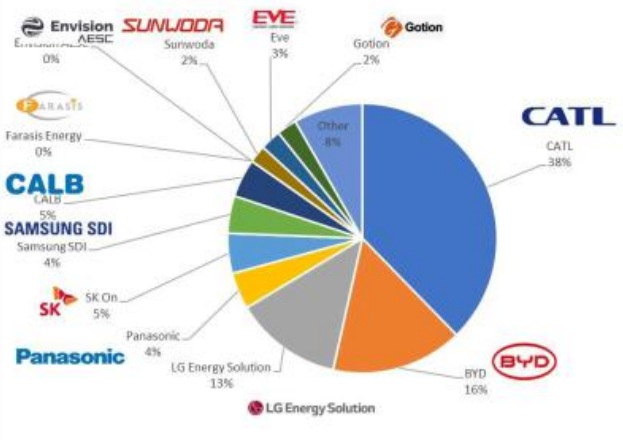

Figure 187: Lithium EV Main Players (Source: Lithium Quarterly Market Review October 2024 from iLiMarkets.)

The EV sales forecast for the region is presented in Figure 188 and the EV penetration rate forecast is presented in Figure 189.

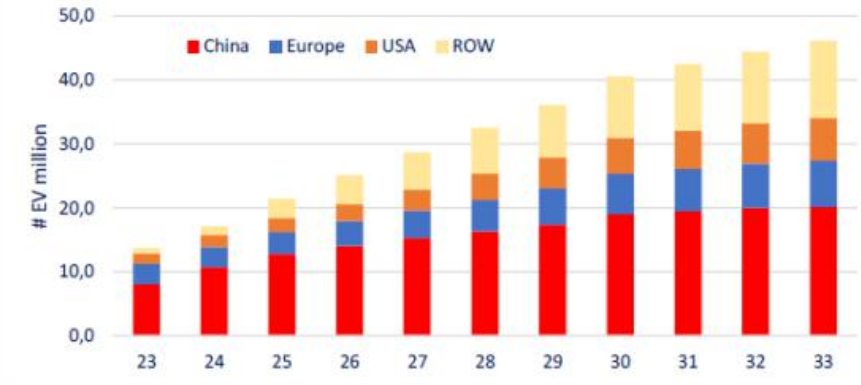

Figure 188: EV Sales Forecast per Region (Source: Lithium Quarterly Market Review October 2024 from iLiMarkets. Horizontal axis label is in years.)

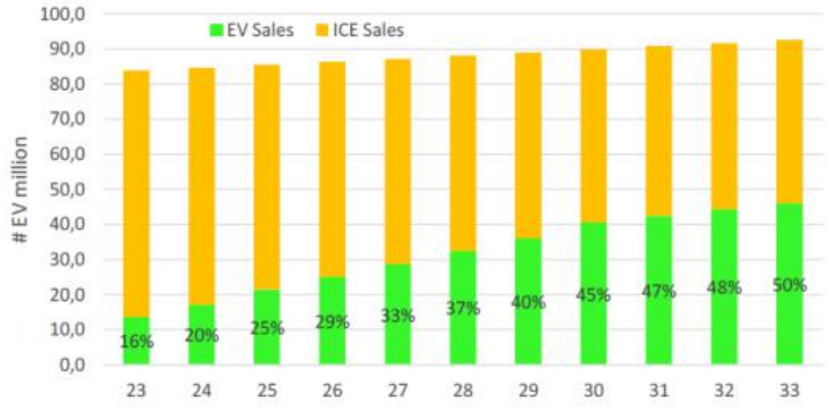

Figure 189: EV Penetration Rate Forecast (Source: Lithium Quarterly Market Review October 2024 from iLiMarkets.)

16.3 Lithium Supply

Lithium occurs in the structure of pegmatitic minerals, the most important of which is spodumene (hard rock) and due to its solubility as an ion, is also commonly found in brine and clays. Pure lithium does not occur freely in nature, only in compounds. Starting in the 1980s, brine-based lithium chemicals provided most of the supply; however, in recent years' hardrock forms have surpassed brine as the largest feedstock for lithium chemical production.

The US Geological Survey estimates global lithium reserves of 147 MT of lithium carbonate equivalent (LCE) (USGS, January 2024).

The world's largest known lithium reserves are in Chile, which accounts for 34% of lithium reserves, followed by Australia with 22%, and Argentina in third place, accounting for 13% of global reserves. Lithium production is summarized in Figure 190.

China is a global leader in lithium refining and battery production, with a highly advanced and integrated supply chain. It imports raw lithium minerals, mainly from Australia and South America, and then processes it into battery-grade lithium compounds, such as lithium hydroxide and lithium carbonate.

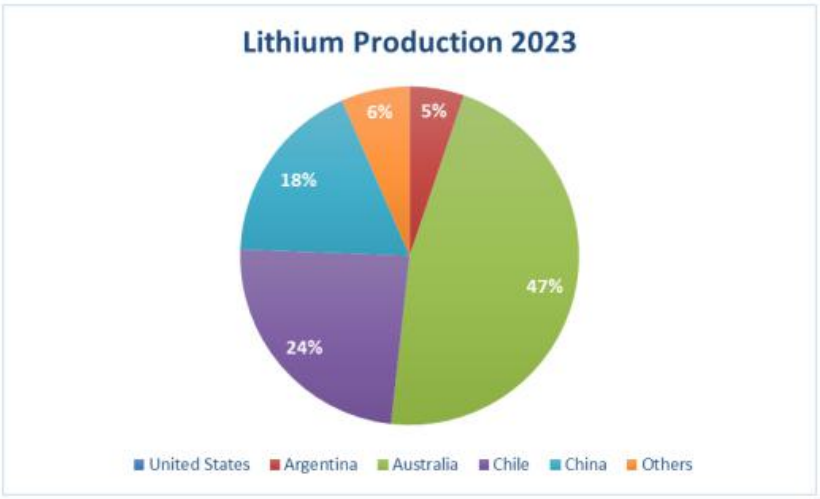

Figure 190: Lithium Production (2023) by Country (Source: U.S. Geological Survey, Mineral Commodity Summaries, January 2024. It excludes US production.)

Minerals are expected to play a key role in meeting the growing demand for critical resources in the coming years, contributing the majority of the incremental supply. The global lithium production is largely driven spodumene operations in Australia, brine operations in Chile and Argentina. Over the last 12 months, Australia's lithium exports were approximately 400,000 t of LCE, Chile's lithium exports were about 250,000 t of LCE, and Argentina's lithium mineral exports reached approximately 60,000 t of LCE. The lithium supply forecast per resource type is presented in Figure 191 and per country in Figure 192.

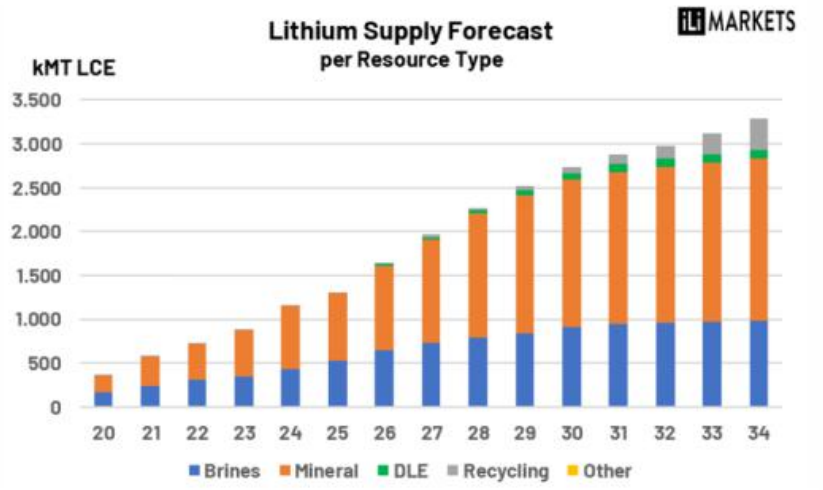

Figure 191: Lithium Supply Forecast per Resource Type (Source: Lithium Quarterly Market Review October 2024 from iLiMarkets.)

Currently, Argentina has four active lithium projects, collectively exporting approximately 60,000 metric tons of LCE. Production is projected to reach 450,000 t of LCE by 2034, driven by the expansion of existing operations and the development of new projects. This growth highlights Argentina's increasing role in the global lithium market as demand for critical resources continues to rise.

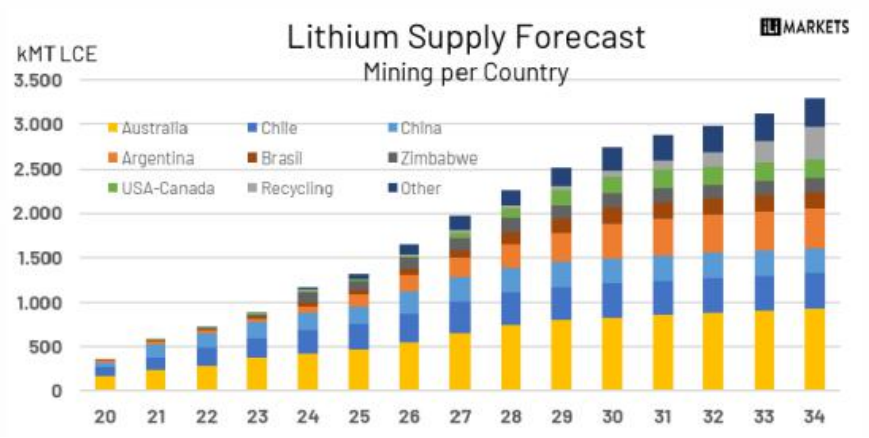

Figure 192: Lithium Supply Forecast per Country (Source: Lithium Quarterly Market Review October 2024 from iLiMarkets)

16.4 Lithium Suppliers Leading Companies and Their Market Shares

Market cap of leading lithium players is shown in the following figure (Figure 193).

Figure 193: Market cap/sum LCE Mined (24-28) (Source: Lithium Quarterly Market Review October 2024 from iLiMarkets)

16.4.1 Competitive Strategies

Due to the high competitiveness in the market, there are various strategies that lithium suppliers can adopt to differentiate themselves. The main ones are detailed below.

- **Pricing Strategies:** In the lithium carbonate market, pricing plays a critical role in maintaining competitiveness. Companies often adopt dynamic pricing models based on production costs, market demand, and competitor benchmarks. Long-term contracts with fixed or indexed pricing provide stability, while spot pricing allows for flexibility in responding to short-term market fluctuations. Competitive pricing is particularly crucial in regions with high production costs or significant logistical challenges.

- **Innovation as a Differentiator:** Innovation is a key driver of competitive advantage in the lithium industry. Investments in advanced extraction technologies, such as direct lithium extraction (DLE), enable companies to reduce environmental impact and enhance efficiency. Additionally, breakthroughs in battery technology, including higher energy density and faster charging capabilities, can open new market opportunities and strengthen partnerships with downstream industries. Companies that prioritize research and development are better positioned to adapt to evolving market demands.

- **Sustainability as a Core Strategy:** Sustainability has become a pillar of competitive strategies in the lithium carbonate market. Producers are increasingly focusing on reducing their carbon footprint, optimizing water usage, and adopting renewable energy sources for operations. Transparent reporting on environmental, social, and governance (ESG) metrics appeals to environmentally conscious investors and customers. Companies that integrate sustainability into their operations not only meet regulatory requirements but also build long-term trust and resilience in a rapidly changing market.

- **Regulations and Legal Aspects:** The lithium carbonate industry operates under a complex framework of regulations and legal requirements that vary across regions. Environmental regulations are particularly stringent, with a focus on minimizing the ecological impact of mining and processing activities. Companies must comply with strict water usage policies, waste management protocols, and carbon emission standards. Non-compliance can lead to hefty fines, operational delays, or loss of permits, posing significant risks to business continuity. Adhering to evolving regulations can also present opportunities. Compliance with high environmental and social standards enhances a company's reputation and can provide a competitive edge in securing contracts with environmentally conscious clients. Additionally, favorable government policies, such as tax incentives or grants for sustainable practices, can reduce operational costs. Companies that proactively engage in legal risk assessment and align with global sustainability frameworks are better positioned to thrive in a highly regulated market.

16.5 Lithium Supply Demand Balance

Whereas in 2010, the world´s two largest producers supplied 68% of the global lithium market, by 2024 their share has shrank to 33% and it will continue decreasing. On the demand side, in 2010 the world´s two largest consumers accounted for around 5% of global demand. By 2024 their share has grown to 36% and it will continue increasing. With this large market share, the capability to control market dynamics is huge.

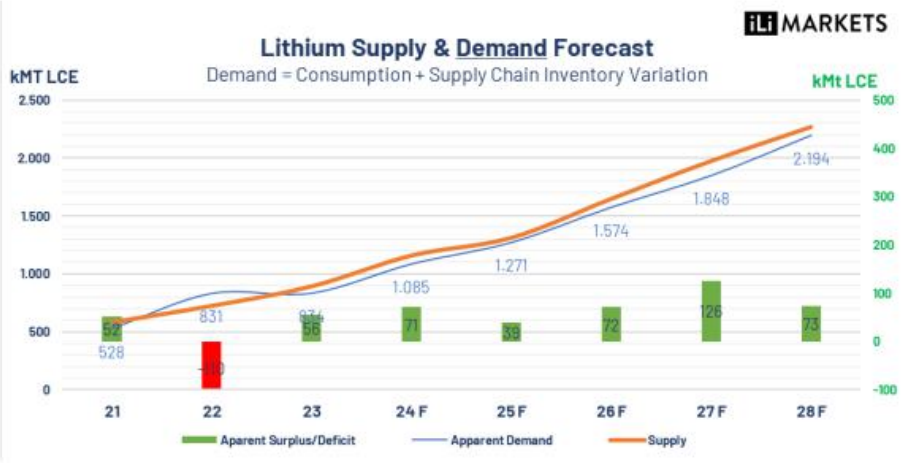

Figure 194: Lithium Supply & Demand Forecast (Source: Lithium Quarterly Market Review October 2024 from iLiMarkets)

16.5.1 Market Projections: Risk Assessment and Identification of Opportunities

The lithium carbonate market faces various risks that could impact future projections, including fluctuations in raw material availability, regulatory changes, and evolving technological requirements. Environmental concerns and stricter sustainability standards may also pose challenges for producers, requiring significant investment in greener extraction and processing methods. Additionally, the volatility of global demand for electric vehicles and energy storage solutions presents uncertainty, making accurate market forecasting essential.

Despite these risks, the market offers numerous opportunities for growth. Increasing global investments in renewable energy and the transition to electric mobility drive demand for lithium carbonate. Emerging technologies, such as solid-state batteries, could further boost the market, creating opportunities for innovation. Furthermore, the development of localized supply chains and strategic partnerships in key regions may enhance market stability and competitiveness, positioning companies to capitalize on future growth.

16.5.2 Economic Factors and Price Volatility

Lithium carbonate prices are heavily influenced by various economic factors, including supply and demand dynamics, global economic conditions, and the pace of technological advancements in battery and renewable energy sectors. A key driver of price volatility is the cyclical nature of demand from electric vehicle manufacturers and energy storage markets, which can lead to sharp fluctuations. Additionally, geopolitical factors and shifts in production levels in major lithium-producing countries further contribute to market instability.

16.5.3 Impact of Logistics and Tariff Costs

Logistics and tariff costs significantly impact on the final price of lithium carbonate. Transportation challenges, including limited infrastructure in remote mining regions and the rising costs of shipping, add to the overall expenses. Moreover, tariffs and trade restrictions between countries can increase costs for exporters and importers, creating regional price disparities. These factors, combined with exchange rate fluctuations, play a crucial role in shaping the competitiveness and accessibility of lithium carbonate in global markets.

16.6 Price Forecast

As the transition towards sustainable energy solutions accelerates, lithium has become a critical raw material. Over the past decade, supply constraints and oversupply at different times have contributed to significant price fluctuations. In recent years, prices saw dramatic increases between 2021 and 2023, peaking for a short period of time at around US$84 per kg, before seeing a significant decline and downward trend continue through 2025.

Investments in lithium extraction technologies, such as direct lithium extraction (DLE), and the expansion of mining capacity could impact the future supply/demand balance and pricing landscape.

Market analysts predict that lithium prices may stabilize in the coming years as supply chains adapt to growing demand and new production methods are developed.

A range of projected prices to 2040 is presented in Figure 195.

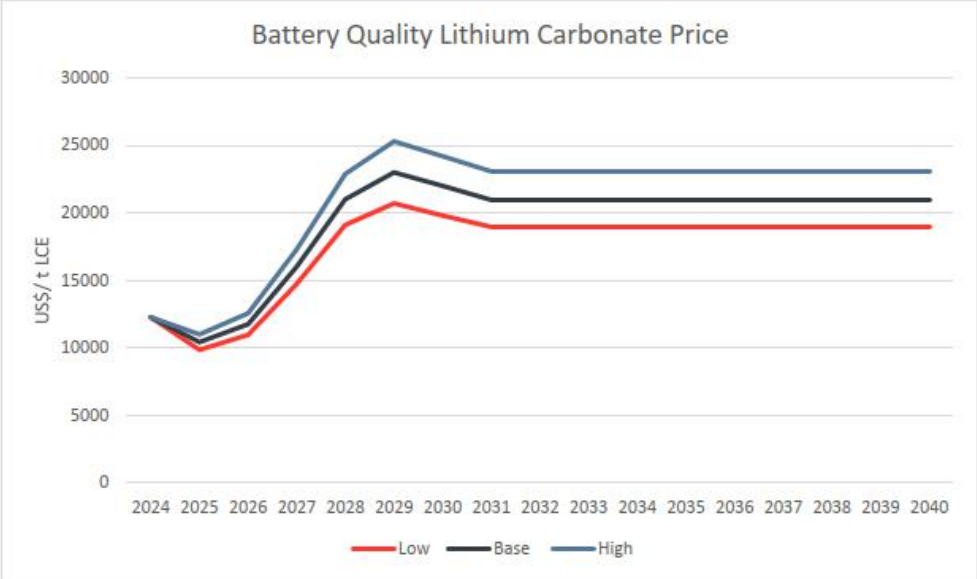

Figure 195: Projected Pricing for Battery-Quality Lithium Carbonate Used in Economic Model (Source: "Lithium Price Forecast," Benchmark Mineral Intelligence, Q1 2025.)

Table 118 reflects Benchmark Minerals market price expectations for battery quality lithium, which was presented in the Benchmark Mineral Intelligence Lithium Price Forecast report dated Q1 2025.

The QP looked at the trailing 3-year and 5-year average spot price of battery grade LCE as support for projected average LCE price over the next 5 to 10 years. The average prices are shown in Table 117 below. Most stock exchanges allow the use of either the 5-year or the 3-year trailing averages for valuation of mineral assets.

Table 117: 3-year and 5-year Average Spot Price of Battery Grade LCE

LCE Price	From	To	LCE (CNY/T)	LCE (USD/T)
Average over the last 5 years	2020-10-31	2025-10-31	150,858	21,629
Average over the last 3 years	2022-10-31	2025-10-31	135,625	19,127

The QP believes an FoB price forecast of US$18,000 per metric ton of Li_2CO_3 for years beyond 2028 is a reasonable figure for this Scoping Study.

Figure 196 below shows that the average spot price for $LiOH{\times}H_2O$ (micronized) is about 20% higher than Li_2CO_3. Typically, coarse particle $LiOH{\times}H_2O$ price takes about 5-10% discount off the price for micronized $LiOH{\times}H_2O$.

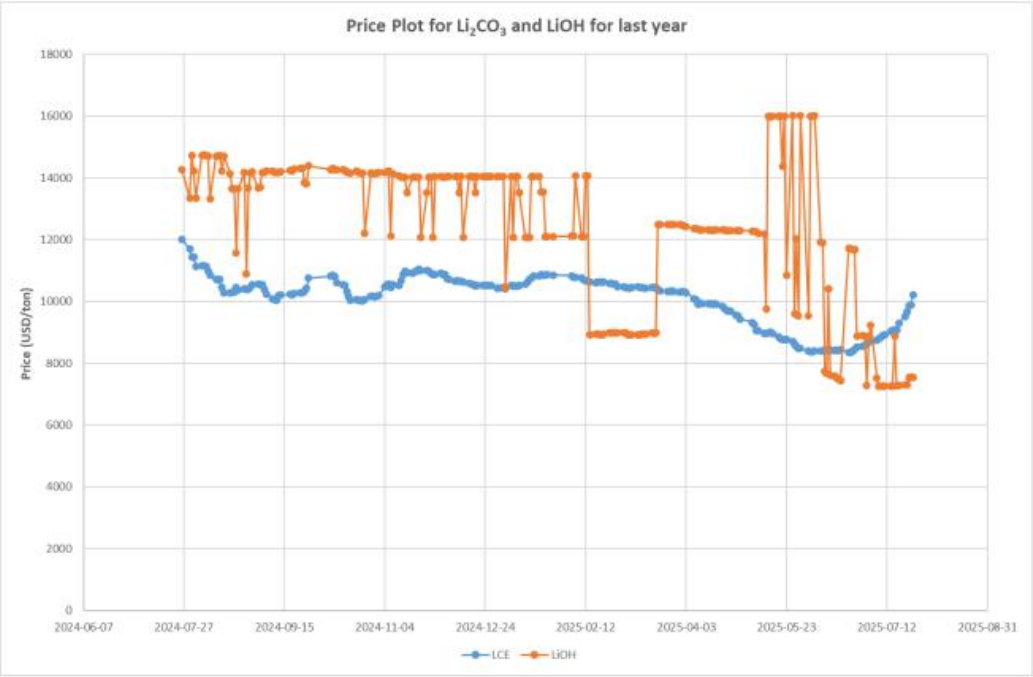

Figure 196: Spot Price Comparison for Li_2CO_3 and $LiOH*H_2O$ (micronized) over the 1-year Period between July 2024 and July 2025

The QP believes an FoB price forecast of US$17,800 per metric ton of coarse particle $LiOH*H_2O$ for years beyond 2028 is a conservative (as compared to Li_2CO_3) figure for this Scoping Study.

Table 118: Benchmark Minerals Market Price Expectations for Battery Quality Lithium

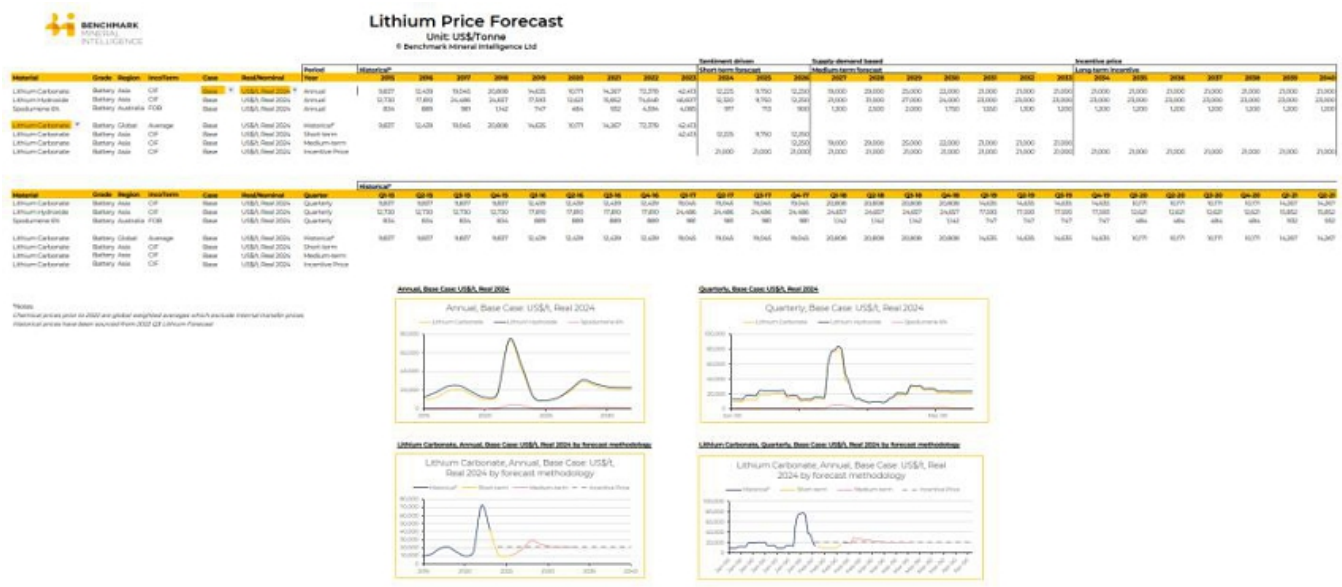

17.0 ENVIRONMENTAL STUDIES, PERMITTING AND SOCIAL OR COMMUNITY IMPACT

The environmental and social studies for both Pozuelos and Pastos Grandes Salars required for the project are described in this section.

Ganfeng and LAR is committed to preserving the natural environment of the Puna region. All exploration activities are under the auspices of an approved Environmental Impact Statement (EIR) by the Provincial Argentine regulator. These are referred to locally as Declaración De Impacto Ambiental (DIA) and are issued for the exploration activities. Resolution 440 for activities at Pastos Grandes was approved in December 2017 and Resolution 034 was passed in February 2018 for advanced exploration activities at Pozuelos.

There are no known environmental liabilities. The Company has already submitted an Environmental Study for the pipeline corridor which allows the transport of brine from Pastos Grandes to Pozuelos. The EIR/EIS for Phase 1 (Pozuelos) was approved by the Province of Salta in November 2025.

The description of the existing Environmental Situation allows us to recognize the environmental and social components that will be potentially affected by the project. The justification of the importance of these components in the environmental and social system arises from the baseline carried out in the project area.

In turn, the description of the activities proposed for this period makes it possible to define the impacting actions.

From the environment-project interactions it is possible to define the environmental and social impacts and characterize them by applying the polynomial proposed by the methodology.

The development of the PPG Project will cause impacts on the environment, which need to be quantified, and actions shall be taken to avoid, minimize or compensate these impacts. The Environmental Impact Study provides the framework for this process. The Environmental and Social Impact Study aims to establish a balance between the development of the project and the environment, including the potential effects on the hydrological system of the basin, human life, fauna, flora, soil, air, climate, landscape, historical and the environment.

Baseline surveys show that the natural subsystem generally preserves its quality in relation to mining activities generally preserves its quality in relation to the mining activities developed in the area, with a biodiversity similar to that of other environments activities developed in the area, with a biodiversity similar to that of other Puna environments. From the socioeconomic point of view, the mining activity contributes to local and regional contributions to local and regional development, generating direct and indirect jobs and indirect jobs, and interacting with the community through solidarity actions and participation in empowerment projects participation in empowerment projects.

The analysis of the environmental impacts derived from the development and production actions of the Development and Lithium Production of the Pozuelos - Pastos Grandes Project was oriented to the identification and valuation of the main impacts according to on the different components of the three subsystems of the environment. Environmental subsystems. To facilitate the analysis, the Conesa-Fernández Vittora matrix was used detailing the components of the environment and the level or intensity of the impact, as well as the level or intensity of the impact. the level or intensity of the impact, the latter evaluated fundamentally in terms of the area affected, its intensity the affected area, its intensity, the persistence over time of the disturbance caused and the possibility of environmental recovery. The evaluation also considered that all the tasks are carried out in accordance with the environmental procedures established by Lithea and current legislation, i.e., the impacts are the current legislation, i.e. the impacts are reduced or mitigated by programmed prevention measures already programmed, such as the use of oil containers for the replacement of oils in the maintenance of machinery maintenance.

The most significant impacts are related to the transformation of the landscape, derived from the modification of the environment, the installation of infrastructure and the extraction of water for the processing of lithium brine. Although the visual basin is extensive, the number of landscape users is small, no new mining areas will be opened and the water supply for the project will come from drilling in Pozuelos and Pastos Grandes, considering that there are sufficient water resources to supply the demand for a 100 kt lithium carbonate production project in both salt flats. Finally, given that no serious or critical negative impacts (those that cause a permanent loss of environmental conditions) were identified and considering that it is possible to implement corrective or mitigation measures during the production stage, it can be concluded that the project is environmentally viable.

Baseline Studies

An environmental and social baseline refers to a set of initial data and conditions that describe the state of the environment and social conditions in an area prior to the implementation of a project, program or activity. This baseline serves as a starting point for assessing and monitoring potential impacts and changes that could occur over time due to human intervention, whether in terms of air quality, water, biodiversity, or the well-being and social dynamics of affected communities.

In other words, it is a detailed analysis that includes both environmental aspects (such as flora, fauna, natural resources, etc.) and social aspects (such as living conditions, employment, community structures, etc.), in order to identify previous conditions and have a reference against which to measure the alterations or improvements generated by the project.

The general objectives of the Environmental Baseline Studies were the following:

- Characterize the current state of air, soils and bodies of surface water present in the area that may be influenced by mining activities.
- Make a description of environmental zones within the study area, based on their physiognomy and vegetation, characterizing the different types of ecosystems.
- Analyse the richness and diversity of the flora and fauna of local vertebrates
- Identify:
    - Areas of special biological relevance and protected areas in accordance with Argentine law.
    - Critical periods (nesting, migration, breeding, mating)
    - Species that have a biological interest in terms of conservation or exploitation
- Analyse demographic and quality of life aspects of the populations included in the area of direct and indirect influence of the project.
- Describe the archaeological and cultural heritage in the area, recognizing areas of special interest for conservation.

In order to achieve these objectives, the environmental baseline includes the study of biodiversity and the quality of the environment in the project area, specifically the recording of the data to observe in which state the studied environmental components are found such as air, soil, water, climate, fauna and flora, and other elements such as the quality of life of the inhabitants or the cultural heritage of the area.

Potential Impacts

The identification, description and assessment of potential environmental and social impacts, both positive and negative, will be performed for the construction, operation and closure stages of the Project.

Initially, actions that could cause impacts were identified, and a classification of the environment was made, providing Environmental Units to each of the factors that will be affected by the Project.

During the construction and operation stages of the Project, there is the potential for moderate impacts to the environment, some of which can be reversed or mitigated in the short, medium and long term. The following are the key potential impacts that were identified:

- Changes to landscape and topography due to occupation of physical spaces (evaporation ponds, lithium plant and salt stockpiles).
- Noise level increased caused by the use of pumps at the wellfield sites and mobile equipment near the evaporation ponds.
- Alteration to flora and fauna habitats due to infrastructure footprint and movement of mobile machinery.
- Greenhouse gas emissions, in particular, related to the project use of natural gas for electricity and steam production.
- Noise and dust impact related to traffic for project reagent supply and product export

Environmental Monitoring Plan

An Environmental Monitoring Plan has been developed for the project, which is a management tool designed to collect information continuously over time. This plan provides the necessary knowledge for decision making, with the objective of optimizing the management of the impacts identified during the Environmental Impact Statement (EIS) process. The baseline studies detailed below present the initial state of the environment, serving as a starting point for this monitoring.

Impact prevention involves the implementation of protective, corrective or compensatory measures, which may include modifications in location, technology, size, design or materials, adapting to project forecasts or incorporating new elements.

The Environmental Management Plan is a dynamic document that will be updated at each biannual renewal of the Operation AAI, in accordance with current legislation, to include aspects not previously considered or in response to significant changes that may arise during the life of the project.

Social and Communities

Ganfeng has continued to commit to the highest environmental and social standards and maintain a constant and active dialogue with all stakeholders in the provinces, including the local communities, National, Provincial and respective Municipal Administrations, and their representatives in the various government departments. The PPG Project is within the direct influence of the community of Santa Rosa de los Pastos Grandes, located in close vicinity to Salar Pastos Grandes. The community of Pocitos, located approximately 60 km north of Pozuelos is also considered to be within the project as an indirect area of influence.

In general, Pozuelos and Pastos Grandes are relatively unencumbered by communities and, the Pozuelos area, in particular, hosts no people in its vicinity. Nevertheless, Ganfeng is committed to ensuring a positive impact on local host communities through a range of initiatives which include:

Employing individuals from local communities and contracting local suppliers.

- Actively participating with other lithium companies in associated CSR programs.
- Ganfeng actively participates in local events and meetings in the communities surrounding Pastos Grandes, Salinas Grandes and San Antonio de los Cobres.

During construction and operations staff will be employed and trained preferentially from local communities.

17.1 Environmental And Social Studies Performed – Pastos Grandes

17.1.1 Baseline

Ausenco (2018) previously prepared the Environmental Baseline Study in the ecosystem of Pastos Grandes Salar, with the goal of characterizing the following environmental components:

- Physical components: geology and geomorphology, seismology, climate, soils, air quality and noise, hydrology and hydrogeology, water quality and landscape.
- Biological components: flora, fauna, limnology, ecosystem characterization and protected natural areas.
- Cultural components: archaeology.
- Social components: social and economic features of the study area and the project social perception.

The studies of the different environmental disciplines were carried out within the basin of Salar de Pastos Grandes. The study covers Quebrada Quirón, Pastos Grandes river sub-basin and the river entrance into the salar of the Sijes river sub-basin (see Figure 197 and Figure 198). The hydrological and hydrogeological studies cover the entire Salar de Pastos Grandes basin. The social studies take into account the communities of San Antonio de los Cobres (department head) and Santa Rosa de los Pastos Grandes, the main populations near the project. The smaller communities of Cóndor Huasi and Ciénago Ancho were also surveyed.

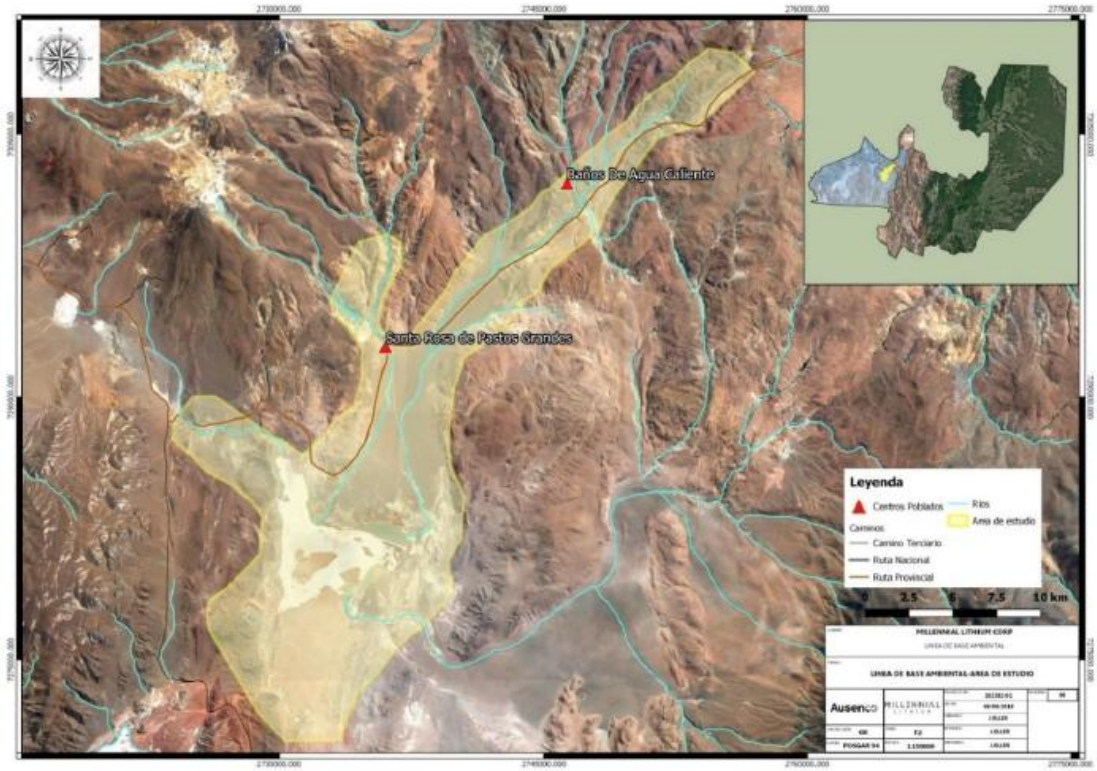

Figure 197: Environmental Baseline Study Area (Source: Ausenco, 2018)

The Baseline report is structured as a series of partial reports covering the different disciplines in autonomous sections. The sections for each discipline include objectives, applied methodologies, results and conclusions.

The studies of fauna, flora and limnology were executed in two steps, one at the end of the dry winter season, and the other at the end of the humid summer season to verify the seasonal characteristics of the disciplines studied.

The Geology and Geomorphology reports were developed mostly from published data and from information provided by Millennial.

From seismic available data catalogues, seismicity of the Pastos Grandes basin was assessed using probabilistic and deterministic approaches. The project area is located within zone 2 of INPRES (Instituto Nacional de Prevención Sísmica), which is categorized as having potential for moderate seismic activity.

Soils and landscape were studied in detail. In the case of soil, these units were described and mapped based on their physical and chemical composition. The heavy metal contents of upper soil unit horizons were also analysed following international standards.

The final report was submitted by Ausenco to Millennial and approved in July 2018. The report was later used by Ausenco to prepare the Environmental Impact Assessment. The following items summarize the findings for the most relevant environmental factors.

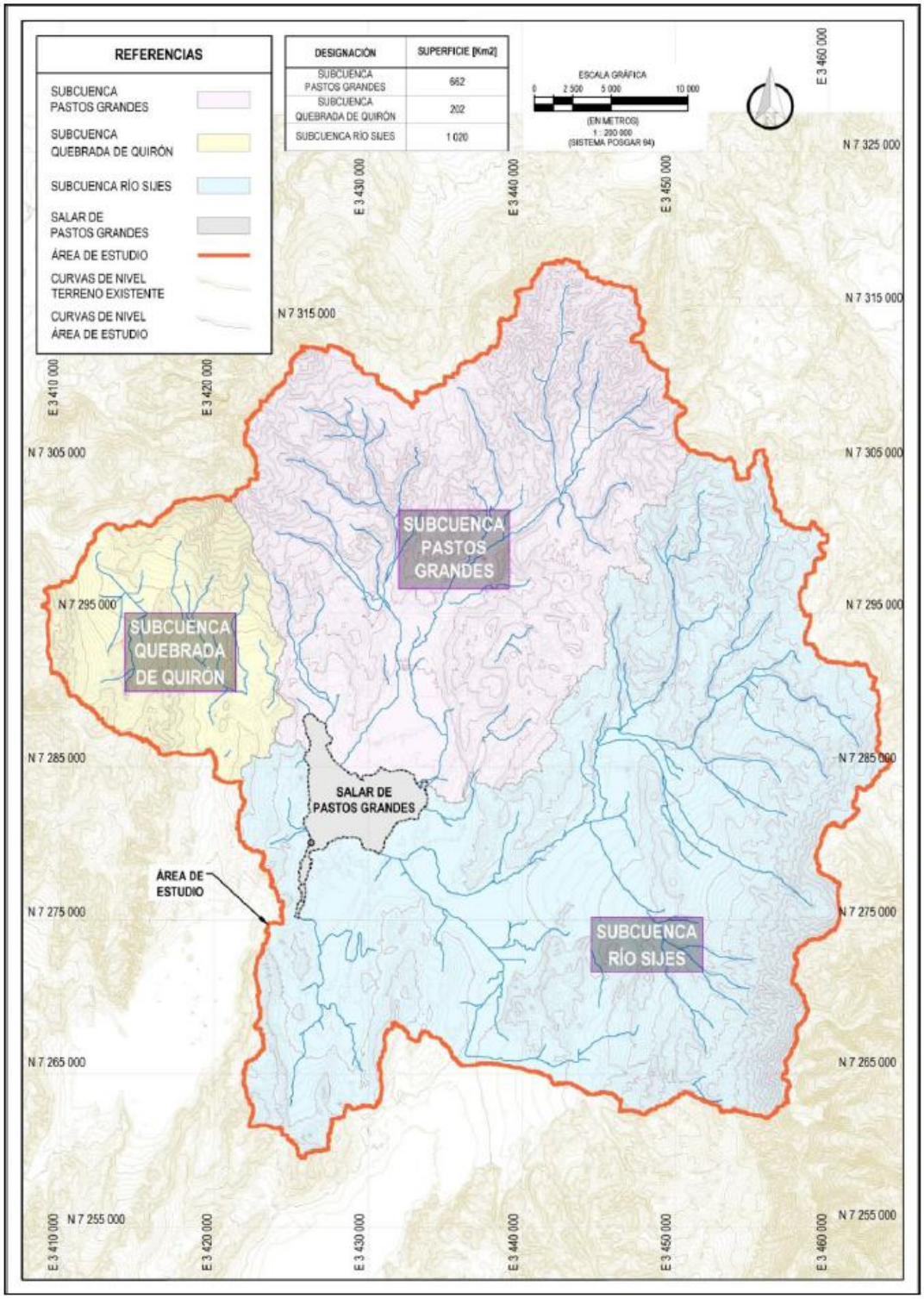

Figure 198: Salar de Pastos Grandes Basin and Sub-Basins (Source: Ausenco, 2018)

17.1.1.1 Water Quality

Water, particulate material and gas analyses for the evaluation of air quality were performed by internationally certified laboratories incorporating respective chains of custody.

Surface water sampling was carried out following the Standard Methods for the Examination of Water and Wastewater (Eaton,1995) guidelines. The results were compared with compliance concentration levels established by Law Nº24,585 and the Código Alimentario Nacional (CAA). Most of water bodies showed a high content of Total Dissolved Solids (TDS); this is a common characteristic for those that bodies that are located near saline and brackish water-bearing, finer grained formations. Most of the water samples show concentrations of TDS, B, As, Zn and Be greater than allowable limits for water usage for human consumption as defined by law.

17.1.1.2 Air Quality

Air quality sampling for concentrations of CO_2, NO_2, Pb, H_2S, O_2 and PM^{10} particulate material were analyzed following the USA-CFR, ASTM, NIOSH and OSHA methodologies. The analytical results were compared with the concentration levels established by Law 24,585. All parameter concentrations were measured to be below the guideline levels of the environmental regulations.

17.1.1.3 Noise

The basal noise level study was carried out at selected locations within the project area and included noise pressure level (NPL) measurements. The obtained values were compared with the IRAM 4062:2001-05 regulation in force in the Argentine Republic and the General Guide of Environment, Health and Security of the International Financial Cooperation (IFC) World Bank Group. The study concluded that the measuring point located in Santa Rosa de los Pastos Grandes had values above the allowable base level. The registered noise level is related to the nearby population activities. Other measuring points are below guideline levels of environmental regulations.

17.1.1.4 Soil Quality

To evaluate soil quality, samples were taken at 2 points of the Salar de Pastos Grandes, located the first in proximity to the site where the future camp will be located and the second at the east end of the salar.

The results of the soil analysis of the samples from the Salar de Pastos Grandes indicate that the quality of the soil is good, and the concentrations of the elements analyzed are below the reference values established by Law 24585 for industrial soils.

17.1.1.5 Hydrology and Hydrogeology

Based on a study by University of Massachusetts (2024), a salar water budget of Pastos Grandes basin was included and the results are presented in this section.

Salar de Pastos Grandes is in the East Puna, with the basin floor 3,770 m above sea level (m. asl). Mountains surround the salar, with Quevar Volcano as the highest peak, reaching 6,200 m. asl. The basin is at high elevation with intense topographic relief. The basin catchment is about 1,700 km^2 with surficial geology dominated by thin veneers of alluvial sediment with numerous volcanic and older sedimentary rock outcrops.

This region is arid, with average annual precipitation of 115 mm/yr (McKnight et al. 2023), although higher elevations of the basin could experience precipitation rates up to 200-300 mm annually. Most of this precipitation occurs in the summer months. In 2023-24 significant rainfall occurred in the months of February and March.

Within the basin, there are five streams that have perennial flow. The two largest inflows are Rio Pastos Grandes and Rio Corral Colorado. These streams are located in the north sub-basins and originate near the basin divide. The north sub-basins exhibit the greatest elevation relief, and precipitation is most common in the northern mountainous region. Both streams are first gauged about 20 km from the basin floor, about 4,000 masl. They are also gauged at specific sites downgradient toward the basin floor. Streamflow measurements are made weekly in Rio Pastos Grandes and Rio Corral Colorado, and other locations of perennial flow.

Throughout the basin there are key areas of ephemeral flow, not solely driven by episodic precipitation but from seasonal changes in water yield from upgradient watershed areas. In Rio Pastos Grandes, Rio Corral Colorado and Rio Ochaky here are perennial flows that are lost before feeding into the basin floor. Areas of localized groundwater emergence along low elevations of the basin (springs) are found in the East, Central and West Vegas with minimal flows (<10 L/s) that directly recharge to the salar.

Utilizing field observations and analysis of collected water budget data, we have documented that there is an unsaturated zone that separates the surface flow from the freshwater aquifer. Drilling and geophysical data collected in the north alluvial fan area has mapped a large freshwater aquifer system with a hydraulic gradient directed towards the salar floor. Unsaturated sediment under the streambed enables high infiltration rates and hinders groundwater contribution to streams. This is supported by temperature array observations, geochemical data and streamflow gauging.

The hydrogeology of the basin provides a framework for conceptualizing the components of the water budget. Our approach was informed by observations and a critical analysis of the factors driving hydrologic processes within the basin.

17.1.1.5.1 Water Budget Summary

A water balance for the Pastos Grandes Subbasin was prepared as part of the conceptual hydrogeological model and is summarized in Table 119. The range of the water balance components presented here takes into account the data presented in the following documents:

· "Salar Water Budget-Pastos Grandes", prepared by UMAss/UAA Lithium Solutions for Lithium Americas in 2024

The water budget for the Pastos Grandes Basin is presented and applied to the Atacama Water (AW) FeFlow model boundary conditions and model design (Kleeberg & Rediel November 24, 2022, *Modelo Hidrogeológico Salar de Pastos Grandes*). The calculations were focused on balancing inflows to the model domain with the outflow of salar area evapotranspiration estimated using remote sensing and meteorological methods (e.g. EEFlux). The inflows are comprised of direct precipitation; alluvial fan recharge and lateral recharge applied to the AW groundwater flow model domain. Weekly streamflow measurements guide the lateral inflow magnitude and their spatial distribution. Additionally, the amount of modern water in the basin and how this impacts the current water budget was evaluated. Main water budgets (and their ranges) are as shown in Table 119.

Table 119: Main Water Budget in Pastos Grandes

	Water Budget Component	Flow (L/s)
Inflow	Direct Salar Precipitation	98
	Alluvial Fan (diffuse) Recharge	7
	Lateral Inflows	953 (769 – 2123)
Outflow	Salar Evapotranspiration	1058 (831 – 2185)

The mean values are close to the best measured or inferred fluxes to the basin over the long-term modern climate average. Upper and lower ranges, while plausible given uncertainty in methods, could be used to optimize the groundwater flow model or be used in scoping purposes. Spatial distribution of inflows to the model domain are presented in Figure 199.

Key Water Budget Definitions:

- Direct Salar Precipitation: Water that falls directly onto the salar surface that rapidly becomes incorporated into the shallow water table and/or is quickly evaporated.

- Focused recharge: Rapid subsurface water infiltration through localized areas where perennial or ephemeral surface water accumulates (e.g. streambed infiltration). Rates can be very high especially in perennial streambeds with losing conditions to the aquifer.
- Diffuse recharge: Groundwater recharge across broad surfaces from direct precipitation onto the soil/sediment surface. Rates are low (< 5 mm/yr) because of evaporative losses from soil and low soil moisture conditions.
- Lateral Inflows: Fluxes applied to lateral boundaries of groundwater flow model. The water that makes up these flows consists of a combination of recharge such as mountain block/front, focused, diffuse, and event driven processes from rain, snow or ice.
- Seasonal Average Flow: This defines the flow for perennial surface water streams within the Pastos Grandes basin for the purpose of defining an average flow for water budget calculations. It is a combination of winter and summer baseflow excluding event driven increases in streamflow.

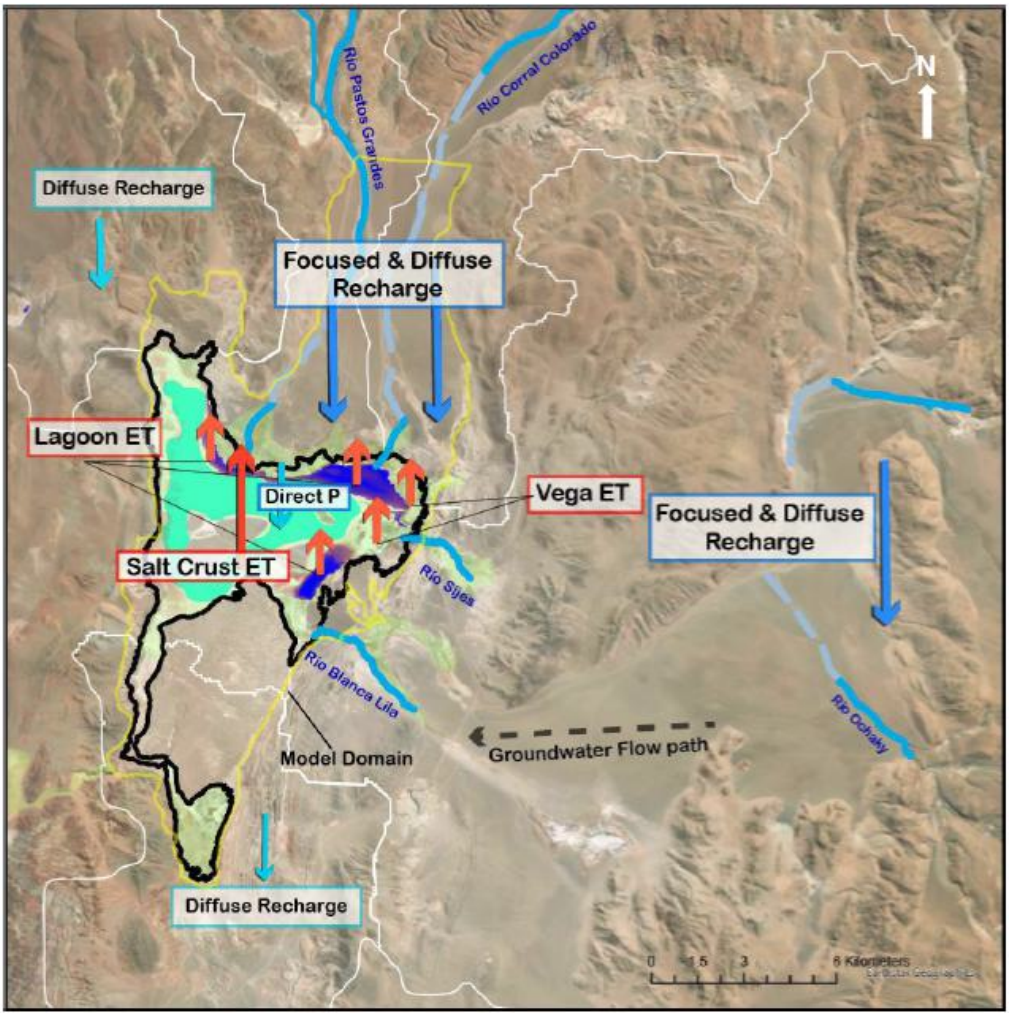

Figure 199: Inflows and Outflows Considered in Water Budget (Source: UMAss/UAA, 2024)

Note: Blue arrows are inflows and orange arrows are outflows. Dark blue arrows represent focused and diffuse recharge likely from streambed infiltration, snowmelt, precipitation, and other hydrologic processes. The dark blue arrows are larger because sub-basins with perennial streams contribute a larger recharge flux. Light blue arrows represent diffuse processes and are smaller than the dark blue arrow, because their recharge flux is smaller. The yellow line defines the AW groundwater flow model domain.

17.1.1.6 Flora

The Altiplano of the Central Andes extends through Argentina, Bolivia, Chile and Peru, between 3,500 and 4,500 meters above sea level (Cabrera and Willink, 1973). It is a cold and arid region, exposed to intense solar radiation, strong winds and great daily thermal amplitude. The average annual temperatures are around 8.5 to 9.5 ºC, and the scarce rainfall is almost exclusively summer and decreases from North to South and from East to West.

The characterization of vegetation in the project area was carried out by studying the flora composition, richness, abundance and coverage of identified species, as well as determining the index of diversity. The study covered an area of 280 km^2.

The vegetation and the flora compositions were defined by two categories corresponding to dry environments and humid environments. Dry environments develop into alluvial fans and piedmonts, corresponding to the Puneña Province locally referred to as “Estepa de Tolilla”, “Chijua” and “Añagua” (Cabrera, 1994), where 28 species were cataloged.

Humid environments, called. Edaphic Communities of “Festuca”, “Pajonal de Chillagua” and “Pasto de Vega” (Cabrera, 1994) are restricted to the Salar border and vegas. For the humid environments, 12 species were cataloged. Conditions in the humid areas demonstrate greater plant density.

Although humid environments are recognized as more fragile than the dry environments, there are no threatened species recognized in either environment. Figure 200 shows the sampled zone map and floristic units identified.

17.1.1.7 Fauna

The area of the fauna study covers the same 280 km^2. Three well-defined environments were recognized: vegas, lagoon and dry environments. Figure 200 is a map of observation transects and sampling points (mouse traps and odoriferous stations) that were used for observation during both the dry part of the year (autumn and winter seasons), and the humid part of the year (rainy summer season). Fauna richness observed during the dry period included 56 species distributed as follows: 47 bird, 6 mammal, 2 reptile, and 1 amphibian. During the rainy season, 58 species were observed: 46 birds, 10 mammals, 1 reptile, and 1 amphibian.

“Categorización de las Aves de la Argentina (MAyDS, Aves Argentinas, 2017) was used as a reference to understand the state of conservation at a national level for birds. For mammals, the “Libro Rojo de los Mamíferos Amenazados de la Argentina” (SAREM, 2015).

At an international scale, conservation categories proposed by the IUCN (2017) (International Union for Conservation of Nature) and the employed by CITES (The Convention on International Trade in Endangered Species of Wild Fauna) were used.

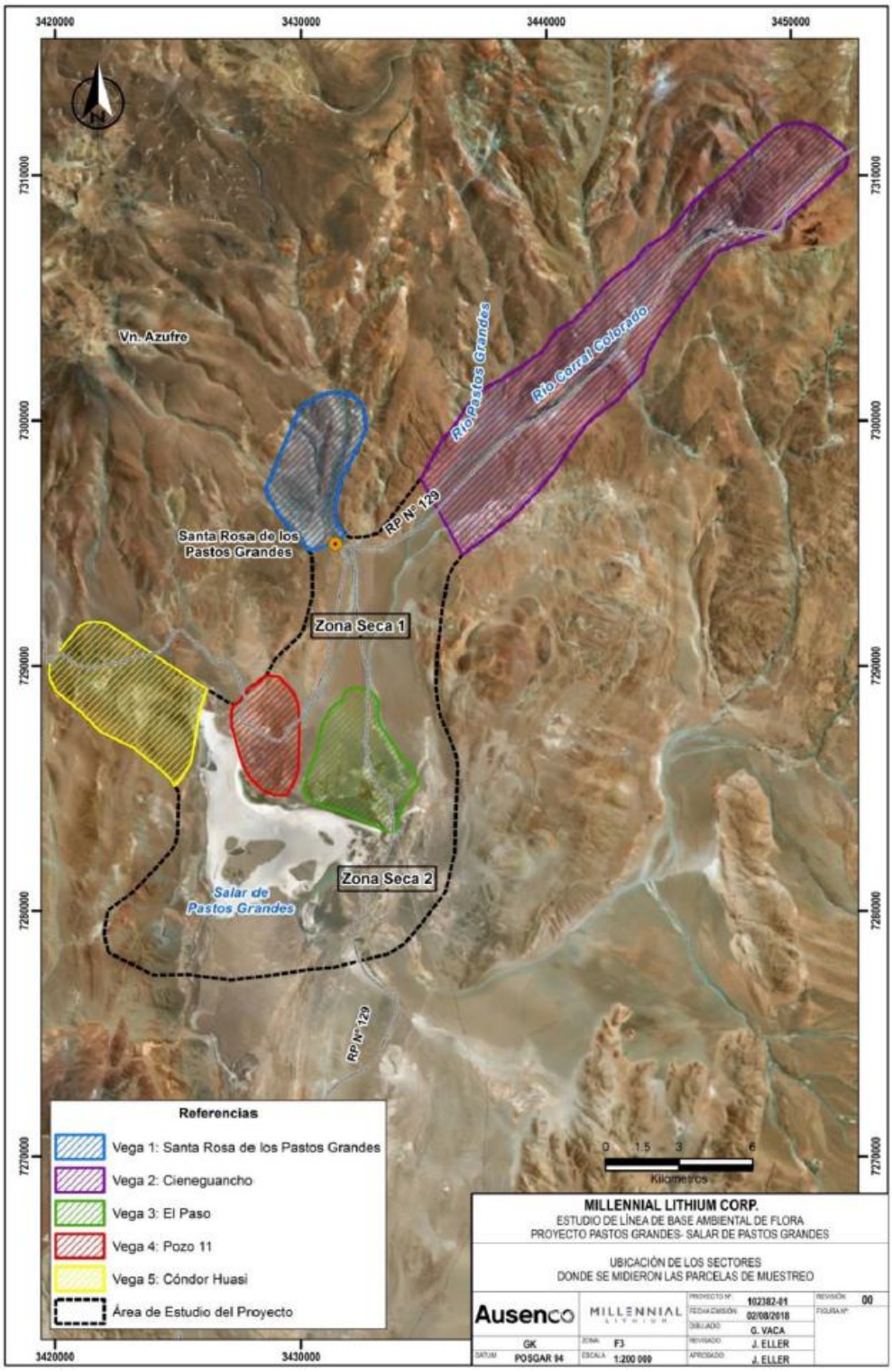

Figure 200: Areas Sampled for Flora and Floristic Units (Source: Ausenco, 2018)

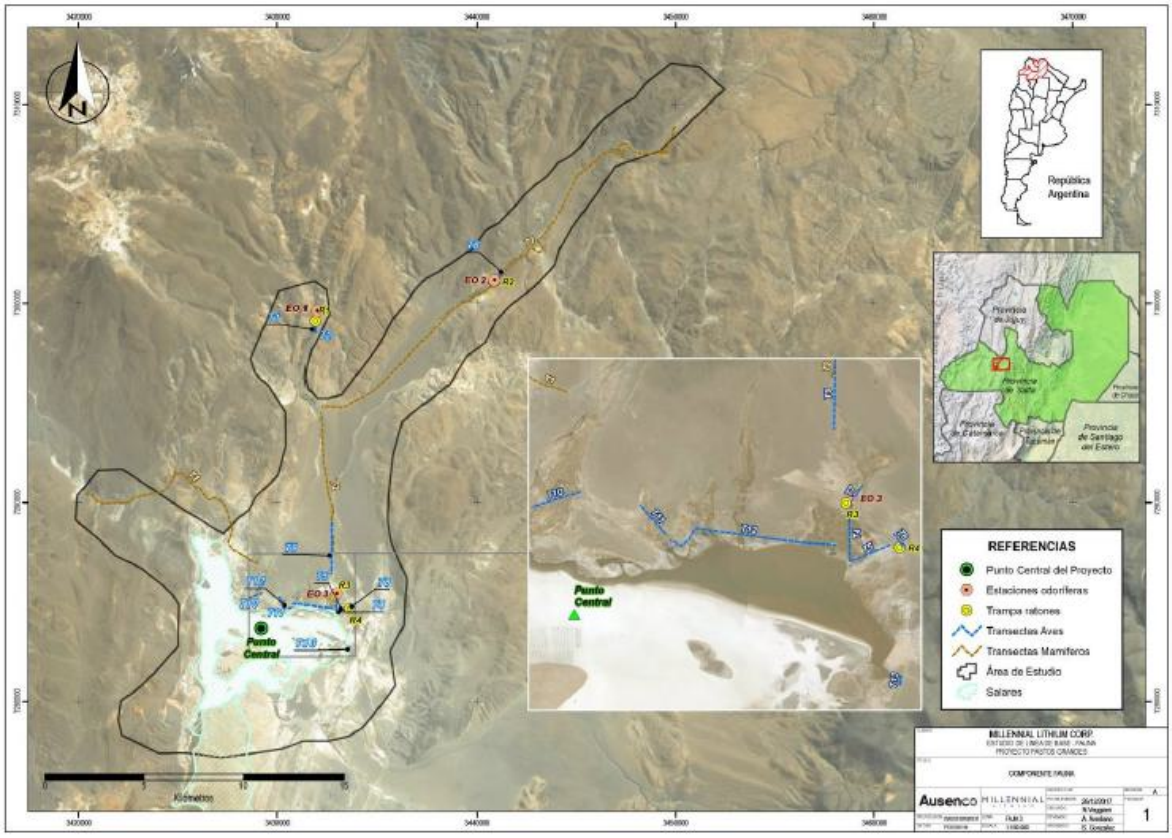

Figure 201: Bird and Mammal Observation Transects and Mouse Trap Locations (Source: Ausenco, 2018)

- Dry period: at national level, 85% of species are included in the Non-threatened category, 6% in the Vulnerable category and 9% within the Threatened category. At the international scale, 92% of species are included in the Least Concern (LC) category, 6% are considered to be Near Threatened (NT) and 2% in the Vulnerable (VU) category.

- Humid period: at national level, 87% of species are included in the Non-threatened category, 4% in the Vulnerable category and 9% in the Threatened category. At the international level, 94% of species are included in the LC category, 4% are considered to be NT and 2% in the VU category.

The conservation state of mammal species is distributed as follows:

- Dry period: at national level, 83% of species are included in the LC category, 13% are in the NT category. At international scale, 6 species are within the LC category.

- Humid period: at national level, 90% of species are included in the LC category and 10% are in the Near Threat (NT) category. At international level, 10 species are considered to be within the LC category.

Of the mammal species observed in the study area, only the vicuña population is included in the Convention on International Trade in Endangered Species of Wild Fauna and Flora (CITES) list which regulates animal populates based on their conservation.

17.1.2 Limnology

Limnologic characterization of the vega, lagoon and stream channel environments were carried out. Phyto benthos, phytoplankton, zooplankton and benthonic micro-invertebrates were sampled. Sampling sites included Vega Santa Rosa, Vega Ciénago Ancho, Salar Pastos Grandes, Salar Artificial and Sijes River (Figure 202). The biologic classification was done identifying groups of related organisms called a taxon (“taxa” plural). Similar to the Fauna and Flora studies, two sampling steps were done, one in dry season and other in humid season.

From these studies, 9 taxa of benthonic micro-invertebrates were identified, 5 taxa of zooplankton, 3 taxa of Phyto benthos and 37 taxa of phytoplankton. A comparative study was performed in each site for abundance and diversity. It was recommended that additional studies of entomofauna should be carried out to have a more complete register of biodiversity in the zona.

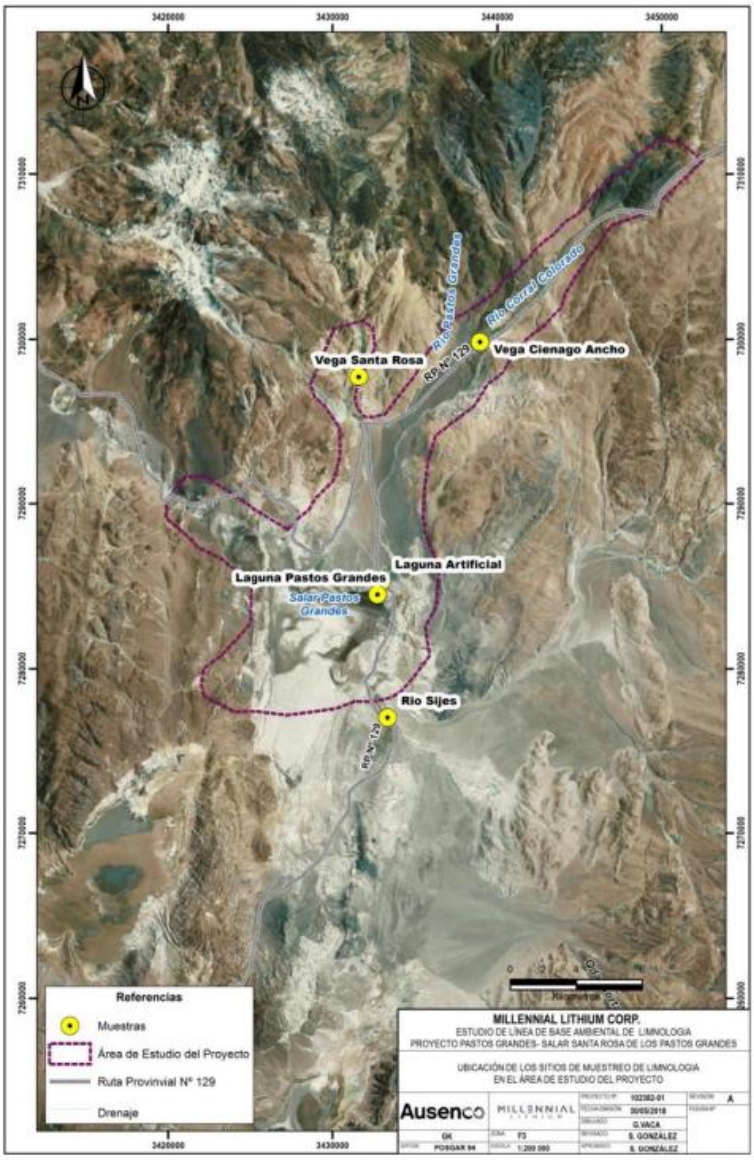

Figure 202: Limnologic Sampling Site Locations (Source: Ausenco, 2018)

17.1.3 Ecosystem Characterization

The zone of the Salar de Pastos Grandes basin presents two types of well-defined habitats: Humid and Dry, as described below.

- **Humid Habitat**
  - Are those found nearby water bodies, which can be lentic (Salar de Pastos Grandes) or lotic (Vegas El Paso, Condor Huasi, Pastos Grandes and Ciénago Ancho); where well-defined flora communities are found, for example, the halophyte and hydrophilic grass, with pigmy vegetation at a lower substrate and an herbaceous shrub at a higher substrate.
  - Many species of avifauna frequent these habitats, such as the flamingos, gallaretas among the most observed. Considering the register of migratory species like the small gull, it can be inferred that it is an important site for migratory species.
- **Dry Habitat**
  - Are those considered as “Dry” due to the interaction of factors from arid environments, such as the Puna region, in which their species are adapted to these conditions. Flora communities present two well-defined substrates, one shrubbery and other herbaceous.
  - The fauna component presents a wide range of distribution due to the scarce vegetal coverage, with a tendency to inhabit caves due to the lack of a substrate that provides shelter characteristics to the local fauna. Among the most common mammals, stand out the vicuñas and guanacos, with individuals of lone habits such as the red fox (Zorro Colorado).

From the cultural point of view, the populated village of Pastos Grandes has been the main focus for the development of activities and agriculture and cattle projects, in order to generate opportunities to widen the amount of job possibilities for the local population. Among the most highlighted projects are “Proyecto Quinoa” and “Feria de la llama”, which led to changes in the social dynamics.

Ausenco (2018) recommended systematic monitoring, preferably in each season of the year, in order to better understand natural variations in the complete annual cycle, especially the highly dynamic and migratory populations, including birds.

17.1.4 Social-Economic Characterization

The socio-economic characterization of Pastos Grandes area was carried out through the analysis of the following data: population dynamics, administrative and community organization, residence, public service infrastructure, communication channels and access, education and educational infrastructure, health, economical structure and employment, unsatisfied basic needs, public security, tenure and ownership of land, tradition and customs, historical and tourism sites. Figure 203 shows a map of the locations for the communities.

The population directly related to the Project is rural and it is self-described as descendants from the Kolla ethnic group. In general, they carry out activities associated with a pastoral economy with limited interaction with other communities or tourists. A large part of their everyday practices and their intra- and inter-ethnical relations include management of animals. This economic practice continues to date, despite the fact that some community workers have become involved in mining activities.

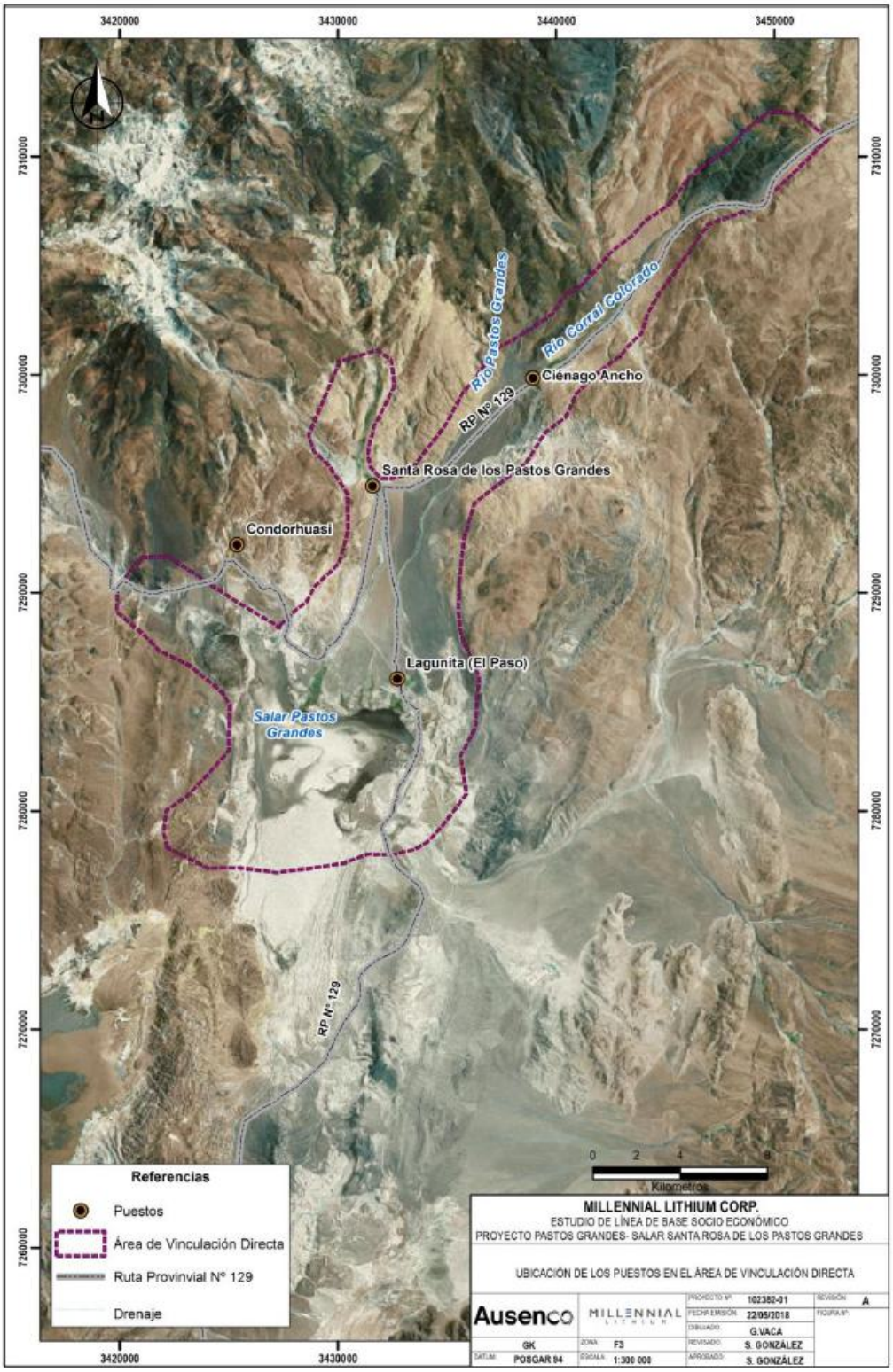

Figure 203: Location of Social Communities (Source: Ausenco, 2018)

17.1.5 Social Perception

Through interviews, the inhabitants´ opinion of the Project was investigated. The interviewers gathered information about the knowledge of the Project from the communities, and its acceptance. In addition, the interviews focused on mining activities, perceived benefits and impacts of mining activity in the region, the community's main concerns, and communication.

Social perception about mining activity in general is positive, due to the potential for direct or indirect job generation. The monetary income obtained from employment allows the acquisition of necessary or desired goods for the families' members. It represents a possibility for the community to initiate small businesses for satisfying the needs of mining companies and contractors (accommodation and dinners, for example) or efforts that can be oriented to the developments of new productive options, parallel to the mining industry.

The possibility of Vega contamination that may affect animals and human beings is considered by the locals to be the main negative impact that mining activities may produce. Furthermore, the communities were concerned about the long-term effects that could occur after mining is completed.

To prevent negative impact to the environment and the community, they argue that it is important that the government monitors activities and ensures that the companies fulfill their obligations to environment protection and prevent negative impact on the socio-economic practices of the local population. For the community, it is important that Millennial maintains clear, transparent and fluid conversation with the locals, informing them not only of the progress of the operations, but also the mechanisms and techniques employed in each stage of the project. They indicated that most of the time, their mistrust is the result of the lack of accurate information. The community requests more information and, as much as possible, opportunities to visit the operation sites so as to understand what is explained to them during meetings.

LAR currently maintains fluent communication with the communities, which is coordinated by the Community Relationship Program and CSR (Corporate Social Responsibility) that the company implemented. A summary of the activities that take place in the Community Relations Plan that Millennial implements in the project's influence area is incorporated.

Finally, from the interviews, it was also clear that they are worried about the potential incorporation of foreign practices to the community's culture, as well as the permanent installation of foreign people to the community within Santa Rosa village.

17.1.6 Archaeological Survey

The field survey tasks were carried out during the month of June 2018, by ARQUEOAMBIENTAL Archaeological Consultants. The objective was to evaluate the archaeological situation of the study area, so that the results are used as basic information for the development of future work. This will allow to have a previous knowledge of the location and characteristics of the archaeological heritage, in order to achieve a harmonious relationship between this and these works.

It is worth mentioning that the preparation of this study was authorized, upon formal presentation, by the Museum of Anthropology of Salta (MAS), under the direction of Ms. Mirta Elsa Santoni -dependent General Directorate Cultural Heritage – Ministry of Culture – Ministry of Tourism and Culture-, acting as the enforcement authority of National Law No. 25743 and Provincial Law No. 6,649.

The selected methodology was based on a strategy of random probabilistic sampling, alternated with targeted sampling, mainly to geoforms where the antecedents show a recurrence of findings such as edges of lagoons, channels, meadows, outcrops, among others.

The survey method consisted of the implementation of a transect system taking as origin the sampling points, with different orientations.

The area of the Salar de Pastos Grandes has had archaeological research since the first decade of this century. The surveys were carried out in sectors of streams, meadows, the salar in question and areas near the town of Santa Rosa de los Pastos Grandes. As a result, archaeological sites of different functionality were recorded, which range from periods related to hunter-gatherer groups, to those with the presence of early pottery.

Near Santa Rosa, the sites of Quebrada Chica, Cerro Pozos and Picadero were surveyed with findings of circular and semicircular structures, with corresponding ceramic fragments, lithic artifacts and remains of camelids.

The site called "Alero Cuevas" was dated between 10,000- and 600-years BP, with evidence of occupation throughout the Holocene.

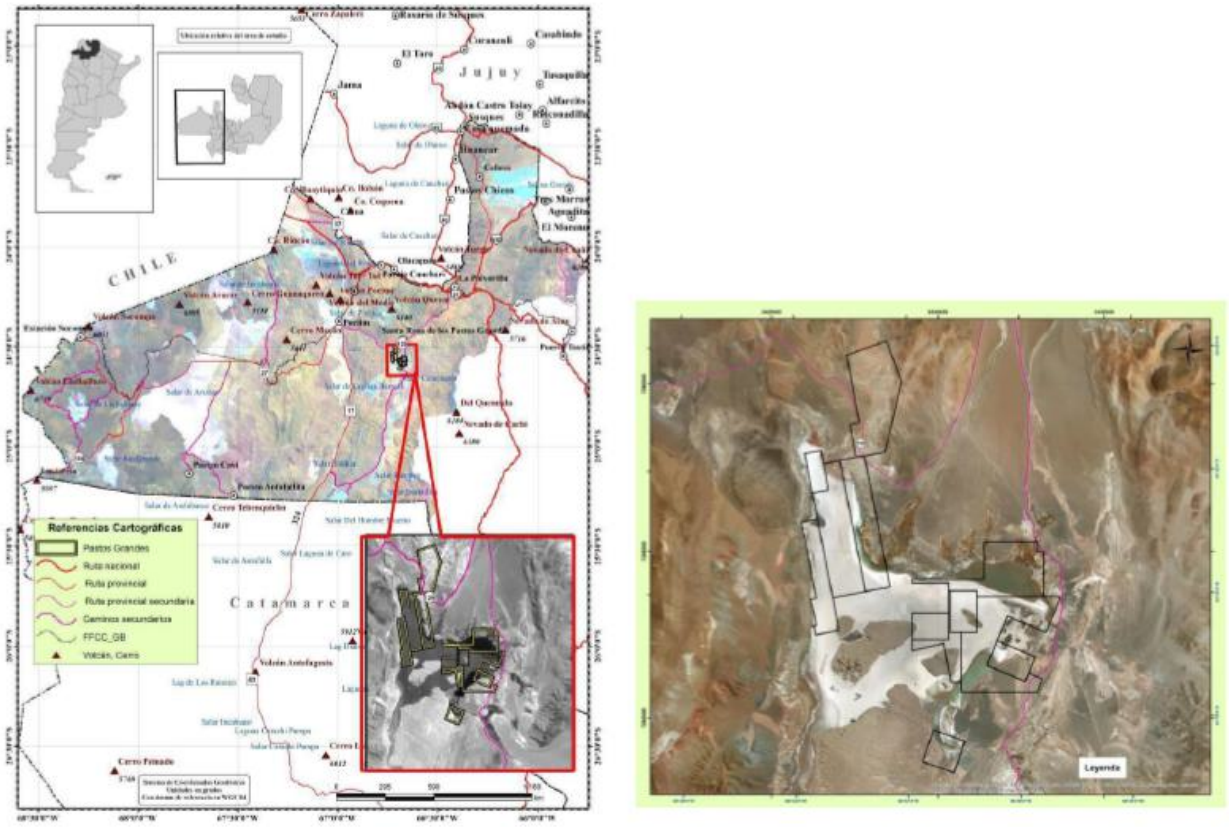

Figure 204: General Location of Large Pastures in Pastos Grandes (Source: Ausenco, 2018)

Another study was carried out by LAR with Ausenco. As part of the study, 42 sampling sites were surveyed according to the methodology described. Of the 42 locations, nine findings were catalogued. Four more findings are included based on previous findings described in earlier studies nearby the Salar. The 13 findings are grouped in three categories: sets of stone structures, rocky shelters, and sets of lithic material.

From the archaeological perspective, the surveyed sites are characterized as two cultural systems. One related to hunter-gatherer group (extractive economy) and other to an agricultural group (extractive-productive economy).

- The hunter-gatherer groups mainly occupied the Vega borders, channel terraces, stream creeks and lagoons. The hunter-gatherer groups are mainly associated with lithic material and rocky shelters

- The agricultural groups associated with stone structures were related to agricultural activity and more prolonged occupation structures needed for harvesting and production.

The overall state of the archaeological findings and sites is reported to be in good condition of conservation. However, there exists evidence of modifications from anthropic origin, due to the continued habitation of the area by people. Modifications to some of these sites has been caused by pastoral and farming practices, and by general mining industry activities.

Finally, Ausenco (2018) recommended measures to prevent further damage to the surveyed archaeological sites that could result due from future mining activities.

17.1.7 Protected Natural Areas

The project study area is located within the Natural Reservation Los Andes and the zone of La Vicuña reservation (Figure 205). The categorization of the reservation permits the development of activities, including mining, with the condition that natural resources are used in a sustainable way, and the conservation and the usage are of mutual benefit. Protection of the ecosystem, and economic development, must be integrated and must benefit each other through the implementation of proper management practices.

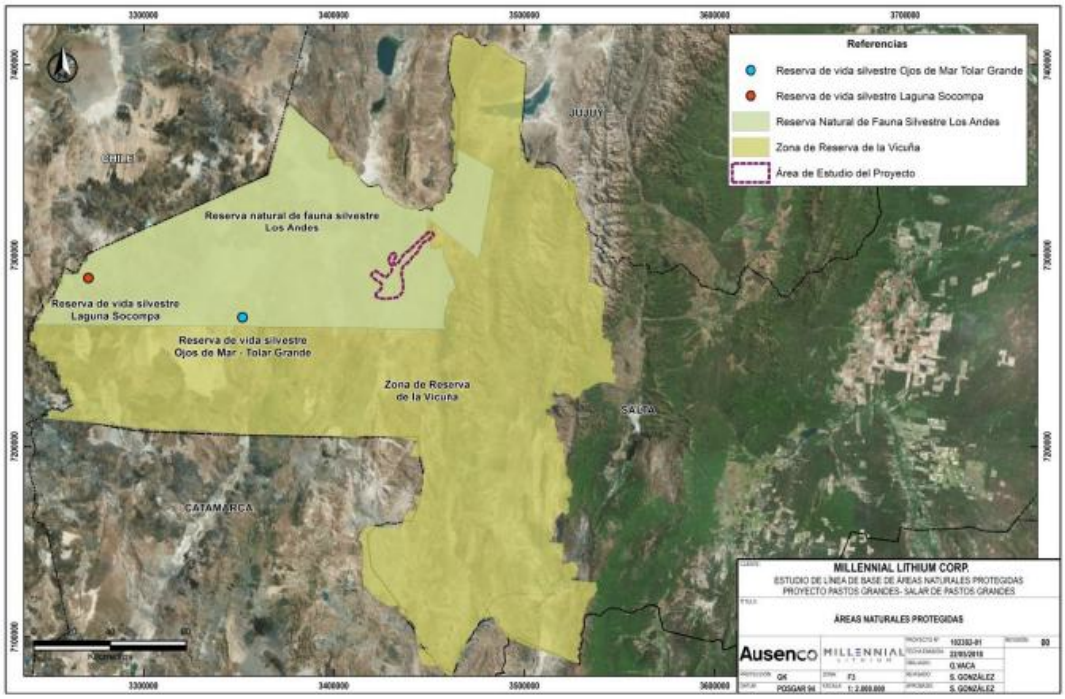

Figure 205: Distribution of Natural Protected Areas (Source: Ausenco, 2018)

17.1.7.1 Los Andes Provincial Reserve

This Reserve, created by Decree 308/80, is located in the Department of Los Andes, with an approximate surface of 1,440,000 hectares. It is bordered to the north by the province of Jujuy and the Department of La Poma, to the east by the Department of La Poma, and to the west by the Republic of Chile. The southern limit of the reserve is defined by the 24º 45' S parallel.

Los Andes Reserve was created because of the need to adequately manage the high Andean ecosystems in order to guarantee their conservation and to generate local development alternatives compatible with the particularities of this environment. It represents 60% of the surface of the Provincial System of Protected Areas and 80% of the provincial high Andean ecosystems. It harbors not only unique natural values, but also important cultural values.

The Secretariat of the Environment of the Province of Salta obtained international financing to carry out the participatory preparation of the Comprehensive Management and Development Plan for the Los Andes Wildlife Nature Reserve (RNFSLA), which was proposed under Component 4 of the Program (IDB 2835/OC-AR), as part of the objective of consolidating the conservation of protected areas in the Province of Salta.

The same instrument recategorizes the “Reserva Natural de Fauna Silvestre Los Andes” as a “Reserva Natural de Uso Múltiple”, under the terms of sections 17º, paragraph g); 25º; 35º paragraph c) and concordant sections of Law 7.107 and section 25 and ccdtes. of Decree 2019/10, under the denomination of “Reserva Natural de Uso Múltiple Los Andes”. Likewise, it establishes a term of one year for its effective implementation and that it must be reviewed and updated every five (5) years, as from the same.

17.2 Environmental And Social Studies Performed – Pozuelos

17.2.1 Pozuelos Baseline

Pozuelos is located in the Puna of Salta, northwest Argentina, approximately 230 km west of the city of Salta and 150 km east of the border with Chile.

Access to the area from the city of Salta is via RN 51 until reaching the town of Olacapato, 228 km away, and after approximately 10 km take RP 27 towards the southwest towards the Salar de Pocitos, 50 km away. km. From the town of Pocitos, along RP 17 and then RP 129, travel 30 km to access via a mining road to the Salar de Pozuelos. Alternatively, along the RN 51 you can travel from Salta Capital approximately 170 km, meeting the RP 129 near the La Poma mine, where turning southwest along the RP 129, you reach the town of Santa Rosa de los Pastos Grandes, 75 km away. From there and continuing along the same RP 129, access to the Salar de Pozuelos is reached. The closest town to the property is the aforementioned town of Santa Rosa de Pastos Grandes, 40 km to the northeast.

RN 51 is almost entirely paved until the town of San Antonio de los Cobres, head of the Los Andes Department, 150 km from Salta Capital, and from there the roads are mostly gravel, with the provincial routes being maintained by Provincial roads and by the mining companies themselves. The estimated driving time to the Salar de Pozuelos is approximately 4 and a half hours.

The baseline information gathered for Pozuelos is summarized in the sections below.

17.2.1.1 Air Quality

To evaluate the presence of gaseous emissions and particulate matter, a sampling program was carried out. During the sampling of air quality parameters, meteorological data (temperature, atmospheric pressure, relative humidity, wind speed and direction) were recorded using a WS 3200 meteorological station.

17.2.1.2 Soil Quality

To evaluate the quality of the soil, samples were taken at 2 points in the Salar de Pozuelos, the first located near the site where the future camp will be located and the second at the southern end of the salar.

The analysed parameters and the reference values for them correspond to those referred to in Table 7 of Law 24585 with Quality Guide Levels for Soils for Industrial Use.

17.2.1.3 Surface Water Characterization

To evaluate the quality of the surface water, samples were taken at 2 points at Salar de Pozuelos, one located in a meadow located close to the future camp, from where it is expected in the future to take water for sanitary use there, and the second at a point where water is currently taken for road construction.

17.2.1.4 Flora

In order to achieve the work objectives proposed for the characterization of the Flora, the following tasks were carried out:

- Phytogeographic and phytosociological characterization of the vegetation of the study area and surroundings.
- Map of vegetation units.
- Definition of environmental and vegetation units and their physiognomic and floristic description; dominance and rare species in each vegetation unit.
- Determination of diversity, coverage in each vegetation unit.
- Protected species.

In the Salar de Pozuelos, 5 units were distinguished, one with bare soil, (the salar), two belonging to shrub steppes, the environments associated with meadows, located at the head of the runoff from the hills to the salar, and those at the edge of the salar. Sparse shrub-steppes with low soil cover largely predominate the study area. Along the mining access road to the area, there are sectors of herbaceous steppes and mixed shrub steppes.

The study area shows a richness of 36 species to date, all of different genus, distributed in 13 families, typical of the region. No invasive species were found.

It was found that the taxonomic richness remains similar to other studies conducted for the area (Pacha environmental consultant, 2022), reporting on this occasion 36 plant species for the entire study area. The most representative families are Asteraceae followed by Poaceae, coinciding with the existing literature for the region (Cabrera 1994). The zonal sector's corresponding to steppe environments were the most diverse in terms of species.

Regarding the conservation status of the species, most are endemic to this ecoregion; however, at the national level, many are still in the process of being classified from the conservation point of view. Considering international regulatory bodies, only Maihueniopsis boliviana is listed in Appendix II of CITES.

17.2.1.5 Fauna

The reptiles that inhabit the Puna are represented by 42 species of lizards and one species of snake. The group of lizards represents a very important biological resource for the Puna region due to its particular endemism, with species little known to science. The field survey also recorded 17 species of birds Characteristic among mammals is the vicuña, typical of the Puneña Province; Among the felines are the Andean cat and the grassland cat, and among the canids, the red fox that inhabits the steppes and open areas. Most of them are species included in some protection category such as the Andean cat and the vicuña.

Rodents are the most abundant animals, with about half of them being endemic species, which are observed in the foothills and valleys. The vicuña is distributed in several areas of the province of Salta.

Figure 206: The Fauna Observed at Pozuelos

Regarding the fauna, a total of 82 native species is reported present for the groups studied: 14 native mammal species (3 exotic species). 64 species of birds according to the database obtained so far and current surveys (Pacha 2018 a and b, 2019, 2021, 2022). As for reptiles, 3 species have been identified so far (Pacha 2018 a and b, 2019, 2021, 2022, EC and Associates 2023), and as for amphibians, 2 species have been recorded present in the area, *Rhinella spinulosa* and *Telmatobius cf atacamensis*. Finally, only 1 species of fish that is an invasive exotic. These findings are of great importance to understand the biological diversity of the region and provide a solid basis for decision making regarding the project and its impact on the natural environment.

17.2.2 Social Aspects

The social, economic and cultural characteristics of the population and infrastructure for the area of influence of the Project were compiled using descriptive-exploratory methodology, based on qualitative and quantitative information from primary and secondary sources.

The stages of the work were the following:

- Descriptive Analysis: the background information comes from sources such as the 2010 Population and Housing Census and the Statistical Yearbooks of each Province.
- The information collected were Population, Education, Health. Housing. Property ownership. Economic dynamics. Employment. Service infrastructure. Main access roads. Transport networks and Cultural Heritage
- Exploratory Analysis: in this stage, field survey techniques were used to collect updated information regarding interviews with local authorities. In parallel, a photographic and georeferenced record was taken of the state of the area of direct social influence of the Project. Aspects to be highlighted:
    - Opinion of the interviewees about mining activity in general.
    - Knowledge by interviewees about the project
    - Communication routes Company - Community.
    - Expectations and fears in relation to the Project
    - Opinion on the content of the Relationship Plan

17.2.3 Social and Community Aspects

At the time of the survey in Santa Rosa de los Pastos Grandes, the health authority and the secondary school teachers could not be interviewed.

It is important to mention that at the time of the field work, a large part of the people who appear statistically as residents in Santa Rosa de los Pastos Grandes, (Area of Influence, 40 km away), for various reasons was not present. However, it was possible to obtain information from community members that allowed the necessary data to be collected, also using information from interviews carried out in May 2017 (Pacha Consultora Ambiental, 2017).

17.2.4 Archaeological Survey

The field surveys were carried out during the month of June 2018, by ARQUEOAMBIENTAL Archaeological Consultants. The objective of this study was to evaluate the archaeological baseline situation for the area.

The preparation of this study was authorized, by the Museum of Anthropology of Salta (MAS)3.

The field survey did not yield a positive result in terms of new findings. However, it does include a record product of previous surveys conducted in the framework of environmental studies on an initial phase of the same Project and other adjacent ones (Ambasch and Andueza, 2016a, 2018a-c, 2020a, 2023a, López et al., 2004; Patané Araoz, 2017).

Thus, a total of fifty (50) findings is considered within the present analysis, which maintain their coding and description (review) under textual citation of the original studies.

Archaeologically, the surveyed area can be characterized through two scenarios related to extractive and productive economies. In functional terms, the simple structures would possibly be related to hunting strategies or as improvised shelter against inclement weather. Another possibility refers to them being rest stops for travellers and caravans of llamas in transit.

On the other hand, those groups of structures would be related to longer-term occupations in pursuit of the capture/production of some resource, related to practices that imply a certain sedentary lifestyle, such as camelid breeding.

Based on the concept of archaeologically sensitive area used for this study, the existence of one (1) area – located on the W margin of the Salar – called AS(SPo)-1 was determined, which is considered to be of Medium Sensitivity.

Poor management could cause severe and irreversible impacts. It is worth clarifying that several of the findings, even though they are located within the Project properties, are related to public communication routes.

17.2.5 Prevention/mitigation Measures

Based on the conclusions presented, the following measures are recommended. Their correct application will minimize the risk of negative impacts on the archaeological heritage.

- Restrict the movement - on foot or motorized - of personnel through the discovery sectors and/or defined sensitive areas.
- Prohibit the collection and/or manipulation of archaeological material, understanding this situation as one of the most severe impacts.
- In the event of any discoveries that may arise by chance, the “Procedure Plan” attached here must be immediately applied, which aims to mitigate possible damage to the heritage (See Annex VIII).
- Informative meeting with those responsible for the personnel involved in the works plan to be executed.

- Delivery of a training course aimed at personnel in general, and particularly those directly involved in field activities.
- Incorporate the information resulting from this report into the general logistics of the Project. The objective of this action is to ensure that knowledge about the related archaeological situation is available during the planning and development of future work.
- Generate fluid communication - understood as an open space for discussion - with the archaeology team in the event of doubts and concerns that may arise during the development of the works plan.
- Promote respect for cultural manifestations of all types, since they can be an active part in the worldview – be it symbolic, religious, domestic, productive, etc. – of certain social actors of the "place".
- Provide a space for participation to indigenous peoples in decision-making about their natural and cultural heritage (Reference to the National Law on Indigenous Affairs No 23,302).

17.3 Ecological and Environmental Aspects

17.3.1 Waste and Tailing Disposals

Tailings produced by the project are mainly the salts precipitated in the various stages of evaporation ponds and other waste produced by brine processing. The largest quantities are NaCl (halite) harvested from the evaporation ponds.

The TMA quantities are expected to be about 15 million tons/year when all phases are in full production. The facility will be lined, and run-off will be caught and returned to the evaporation ponds.

17.3.2 TMA and Solid Tailings

The solid/semi-solid effluents for 3 phases are list in Table 120.

Table 120: Solid/semi-solid Effluent for 3 Phases

Waste Name	Moisture (%)	Rate (TPA)	Area	Disposal Site
Phase 1 salts	10-15%	5,269,808	P1 ponds	TMA stockpile
Phase 2/3 salts	10-15%	9,843,348	P2/3 ponds	TMA stockpile
Waste Cake (all Phases)	10-15%	113,681	Brine Purification	Waste disposal

The main effluents to be generated during the construction and operation stages of the project will be as follows:

- Maintenance shop effluents from washing vehicles and equipment.
- Used oils and lubricants produced by maintenance tasks.
- Cleaning effluents and sewage liquids.
- Laboratory effluents, acids, reagents, etc.

Figure 207: Efluentes Plant Location (Source: Ganfeng, 2024)

17.3.2.1.1 Effluents from Truck Shop Washing Vehicles and Equipment

In the truck shop the washing operation will be carried out in a specially arranged area. The washing area will have a concrete pad to avoid contact of the washings with the ground, and to allow their separation and collection.

The vehicles wash area will be covered and thermally insulated, with electric power and water mains and will have a gutter to convey used waters to a degreasing chamber. Washing is restricted to the bodies of vehicles and equipment and not to the engines with an estimated frequency of twice a week.

Washing trucks, equipment and all mobile machinery is an activity that will be carried out during the preventive maintenance of these and will be carried out regularly during the operation stage. It consists of a surface wash with water, to remove dust and salts attached, as well as fats and oils, from the different parts and parts of the truck and machineries in general. As part of this operation, a liquid residue containing suspended solids and oil residues will be generated.

It is important that effluents containing greases or oils are handled independently of domestic waters and that hydrocarbons are separated from the mainstream, as both oils and grease can interfere with disposal systems or accumulate in unwanted areas.

The purpose of hydrocarbon separators is the separation of water from lighter substances that tend to float. The material collected on the surface of these tanks includes greases, oils, soaps, etc.

This separator tank shall consist of a reservoir where floating matter rises and remains on the surface of the water until it is collected, while the liquid will continuously exit from the bottom behind baffles.

Decanted solids shall be temporarily deposited in a drying area, to reduce the water content by evaporation and then tagged as hydrocarbon-contaminated waste.

Greases and oils recovered will be put in containers in the oil waste storage area for final disposal offsite.

The treated liquid from the decanter shall be sent to the waste liquid treatment system.

17.3.2.1.2 Waste Oils and Lubricants

Oils and lubricants from the equipment maintenance, that will remain in the Project area will be stored in identified containers; for this purpose, the maintenance workshop will have drum groups of 200 liters capacity to deposit the daily waste generated. These will be black, labelled with the identification of the waste current they contain. These tanks will also store waste oils and hydraulic fluids that are recovered during maintenance of other machinery, such as electric generators, motors, etc. And then they are sent to final disposal where the legislation so provides.)

Depending on the activities provided for in the project, hazardous liquid waste might distinguish:

- Residues of Hydrocarbons: composed of hydrocarbons and/or mixtures, such as burnt oil, mixtures of water and oil or fuels, etc. They correspond to categories Y8 and Y9.

- Liquid chemicals: these are those generated by the laboratory, chemicals, mixtures of substances and chemical compounds or remnants of expired chemical. They correspond to categories Y34 or Y35.

The drums with the liquid waste generated will be transferred and stored in a differentiated area within the Hazardous Waste Yard: a separate area with a waterproof base, containment dams, signage and all required safety measures.

17.3.2.1.3 Cleaning Effluents and Sewage Liquids

Sewage effluents are considered to originate from the domestic activities of the staff (toilets, kitchens, laundry rooms). These liquids will be collected and sent for subsequent treatment in a centralized system.

In the Operation Stage, effluents will be treated at the sewage treatment plant, which will consist of a system with appropriate capacity for the maximum number of personnel who will reside in the camp during the operation stage.

The average volume of sewage estimated for the different stages is detailed in the Table 121**.**

Table 121: Details of Sewage

Parameter	Values
Flow (m^3/d)	400
Equivalent Population	2000
Endowment (ltr/hab*d)	200
Equalized Flow Rate (m^3/h)	16
Organic Load Per Capita	60
DBO Concentration (mg/l)	300
Height (msnm)	3800
Liquid Design Temperature (ºC)	15

(*) Calculations based on a generation of 200 litres/day/person and a staff of 2000 people for the construction stage and 1700 people for the operation stage.

The system to be installed for the treatment of sewage is an aerobic treatment system, modular and able to grow according to the needs of the plant. It will be designed to achieve an effluent of acceptable quality.

It is assumed that the raw effluent corresponds to an effluent suitable for biological treatment, which must meet the following requirements:

- There is sufficient micronutrient available to satisfy the minimum biological requirements, according to the following ratio: 100 BODS: 5-10 N: 1-3 P.

- Stable pH between 6.8 – 8.5 as an acceptable range. Between 7 – 8 as an optimal range.
- DBO & DQO are easily biodegradable.
- It must not contain toxic or inhibitory compounds.
- Concentration of fats and oils less than 30 ppm (must be removed prior to entering the plant).
- Water temperature less than 37°C.

As requested, and in accordance with Resolution 11/2001 of the Department of Environment and Sustainable Development of Salta, the effluent treated by the plant will comply with the following discharge limits into an open storm drain or directly into a surface water course (closed basins and non-permanent water channels are excluded).

Table 122: Composition of Treated Effluents

TREATED EFFLUENT	
Parameters	**Values**
Ph	6.5 -10
Sedimentable Solids in 2 HS (ml/L)	≤ 1
DQO (mg/L)	≤ 250
FATS (SSEE) (mg/L)	≤ 50
DBO5 (mg/L)	≤ 50
Fecal Coliforms (NMP/100mL)	≤ 2000

To comply with the discharge parameters, it is important that the plant is operated according to the recommendations of the operation and maintenance manual. Avoiding the entry of grease, oils, non-biodegradable cleaning products, laundry detergents, and bathroom and kitchen cleaners in excess (must be diluted or used), which can generate excess foam or are bactericidal.

The Project will consider 4 stages of growth. Each treatment module corresponds to a capacity of 100 m^3/day, equivalent to 500 inhabitants. The modules were designed completely independent of each other. Each module for 500 inhabitants contemplates the following:

- A pumping well with 2 - 100% stand-by submersible pumps built in ¼" SAE 1010 F-24 A°C° sheet metal. External reinforcing ribs for rigidity, upper angle at the crown for mounting the cover with reinforcements and 3 (Three) hinged sub-stages for lifting centrifugal pumps, and a solids retention basket.
- Characteristics:
    - The upper cover made of expanded metal, painted with Epoxy paint.
    - Total volume: 10 m^3 total.
    - Useful volume: 6 m^3
    - Width and length: 1.5 meters
    - Depth: 4.5 meters
    - Connection flange for effluent inlet, diameter 160 mm

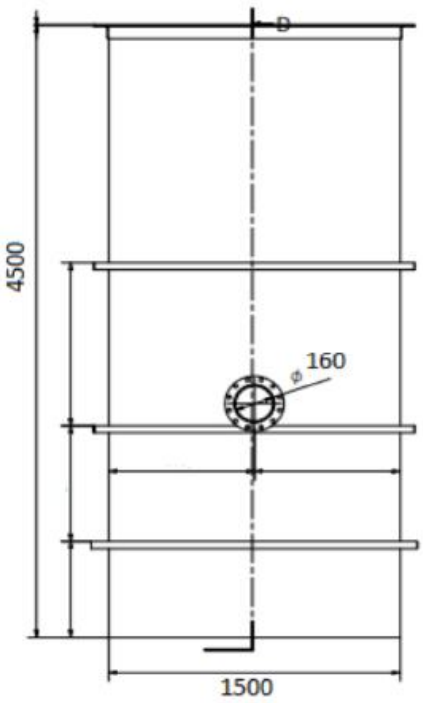

Figure 208: Pumping Well Details (Source: Ganfeng, 2024)

The pumping group is made up of 2 submersible sewage pumps, 1 in service and 1 in reserve, which will work automatically and alternately to ensure even wear. When the peak hourly flow of the plant is reached, both pumps can start working at the same time.

- A 100% standby pumping system equalizer tank for each reactor tank located inside a 40'HC container. The equalizer will serve to cushion and homogenize the flow and organic load values. An air insufflation system must be incorporated into this tank through diffusers arranged at the bottom. And a pumping group will be installed in it that sends the effluents at a regulated flow to the biological reactor. The Equalizer then works as a hydraulic lung to cushion the significant flow peaks that are expected in the generation. The pumping group is made up of 2 submersible sewage pumps for each biological module (4 for each plant with 500 inhabitants), 1 in service and 1 in reserve, which will operate automatically and alternately to guarantee even wear.

- Two activated sludge treatment plants with extended aeration, each located inside a 40'HC container. The Biological Treatment module is made up of a compact unit in which four functional enclosures are delimited: Aerobic Reactor, Sedimenter, Chlorination Chamber and Sludge Digester.

- The raw effluent is initially sent to the corresponding Aerobic Reactor where the bacteria are in continuous movement capturing the contaminants that enter, giving rise to the biodegradation of the contaminating organic matter. To do this, the required air is provided in sufficient quantity to ensure a dissolved oxygen concentration of 1 to 2 mg/L. For the incorporation of air, fine bubble membrane diffusers are used by means of 2 100% stand-by.

- The biological degradation process that takes place in the reactor is based on the following:

    - Substrate (organic load) + O_2 + Bacteria ➔ CO_2 + H_2O + Residual sludge

    - The treatment module will have an electrical panel with protection and automatisms.

    - The modules will be provided with a ladder to access the upper part of them and protective railings. All openings will be covered with removable access holes to facilitate the operation and routine maintenance of the system components.

    - The sludge that accumulates in the system as a result of the purification process will be extracted with the necessary frequency directly from the sludge digester by an authorized transporter, in order to dispose of it in an authorized dump.

17.3.2.2 Installation Details

The following are planned for the installation of the equipment:

- 12 reinforced concrete slabs (3 per stage) of 0.25 m thickness, 14 m x 3 m with their corresponding reinforcement, for which a 0.7 m deep earth movement will be carried out. With its subsequent filling and compaction, to avoid possible settlements during the assembly or subsequent process stage.
- In addition, 4 ponds (1 per stage) must be built to concentrate the sewage flows from the camp and from the different wings of the project. For subsequent pumping to the treatment tanks.
- For the collection of sewage, approximately 1 km of line will be channelled from the camp with a slope of approximately 1%, divided by 30 inspection chambers, for possible inconveniences and to collect lines coming from the different wings of the plant.

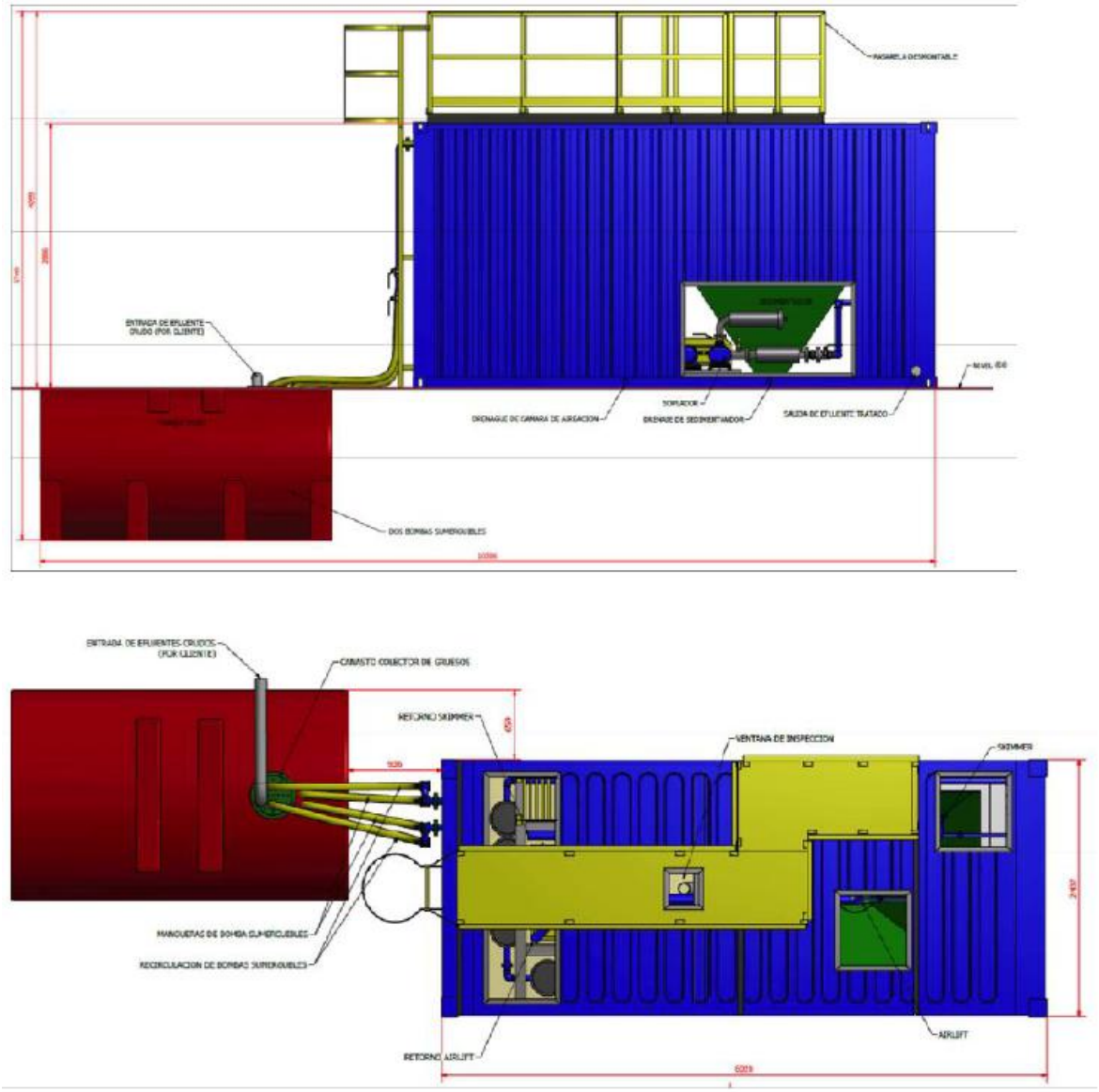

Figure 209: Views of the Wastewater Treatment System (Source: Ganfeng, 2024)

For the water leaving the wastewater plant, a system of infiltration tunnels in the ground was designed. For these, an infiltration test must be carried out to consider the permeability of the ground. The use of approximately 3,100 infiltration tunnels in the ground is planned, for which a 2 m deep excavation must be made to house the tunnels in an area of 2,900 m^2. A 5 cm layer of gravel must be placed on the entire excavation surface, and then the tunnels must be placed and their surface covered with a geotextile mesh.

After the tunnels are assembled, the ground over them must be filled and compacted.

Figure 210: Infiltration Duct (Source: Ganfeng, 2024)

17.3.2.3 Special Effluents

For the operation stage, the construction of a laboratory with equipment for routine control of brine by ICP and atomic absorption is planned, as well as analysis of sewage effluents and process water.

The liquid waste generated will be diluted solutions corresponding to glassware washing water that will be treated jointly with sewage liquids.

The waste from analytical tests and solutions will be sent to neutralization tanks stored temporarily until they are collected in tanker trucks for final disposal according to current requirements.

The volume of general liquid waste is estimated at 0.25 m^3/day.

The volume of waste and solutions from the laboratory is estimated at 0.1 m^3/d maximum.

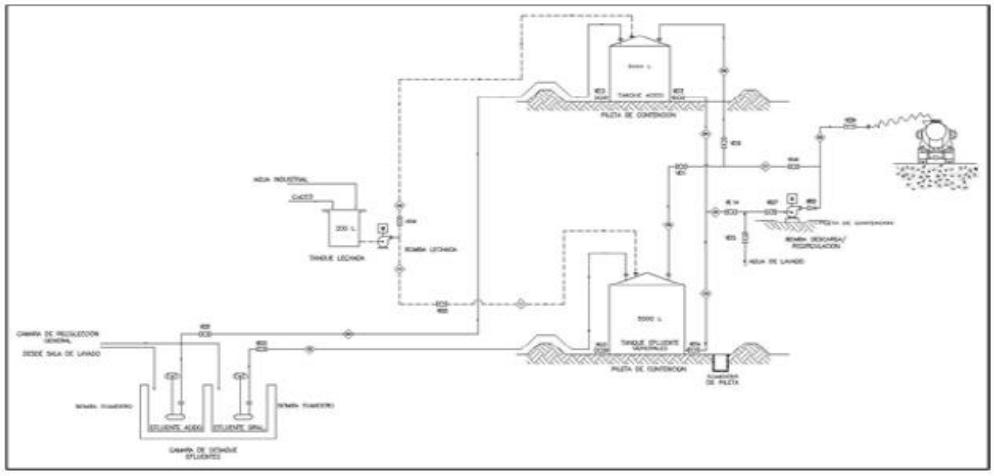

Figure 211: Acid Effluent Neutralization System (Source: Ganfeng, 2024)

17.3.2.4 Waste Yard

Figure 212: Layout of Warehouse and Waste Yard (Source: Ganfeng, 2024)

17.3.2.4.1 Description

For waste management, two containment sites were defined, an enclosed warehouse and an openair yard.

The warehouse for waste containment will have an approximate area of 941 m^2 covered and 1,424 m^2 fenced around it. It will be built with ASTM-A36 structural steel frames covered with 22-gauge trapezoidal sheet metal.

For proper ventilation, there will be ceiling extractors.

It will be divided into 3 modules, separated to avoid mixing of the different wastes.

The warehouse will have perimeter grids to prevent contaminants from leaking into the soil. Including pumping circuit for subsequent containment.

The waste to be found in this sector is that which comes from the industrial activity itself. Industrial wastes can be hazardous or non-hazardous according to their characteristics, which are subclassified into:

- RI from production wastes that come directly from production processes and lithium carbonate production activities or generation of reagents. Examples: calcium sulfate cakes, calcium and magnesium carbonates, etc.

- Non-production IR: waste that is not directly related to production, but to other general site operation activities. Example: scrap metal, raw material packaging material, pallets, discarded PPE, maintenance waste.

For waste similar to urban waste or household waste, an open-air yard was considered, in which the topsoil must be cleaned. Subsequently, the perimeter of the site must be fenced off for greater security.

Table 123: Classification of Wastes National Hazardous Waste Law 24051

Ranking	Description	Type
Dangerous	SEMI SOLIDS / LIQUIDS:	Y8 and Y9
	Used oils	
	Fuels / solvents used in cleaning.	
	SOLIDS	Y48
	Sand/soil contaminated with hydrocarbons. Used oil and fuel filters	
	Contaminated membranes	
	Rags, cloths and Personal Protective Equipment contaminated with hydrocarbons	
Non dangerous	Scrap, pallets, membrane remnants and packaging material	
	Rags, cloths and Personal Protective Equipment contaminated with hydrocarbons	
HOUSEHOLD/ URBAN ASSIMILABLES		
Dangerous	Nursing waste from medical care (Y1) and waste from drugs and pharmaceuticals (Y3)	Y1 and Y3
Non-hazardous	ORGANICS	
	Kitchen and toilet waste	
	INORGANICS	
	Plastics, Glass, Metals, Paper and cardboard	

17.3.2.4.2 Waste Management

Waste management includes handling, transport, storage and disposal or treatment of waste generated in the project area, including contractors and consultants.

- **Waste like urban to domestic waste**

In all sectors (dining room, offices, bedrooms, plant) the company will place differentiated basket to deposit household waste. They will be signposted for the separation of fractions.

The staff shall collect waste from the baskets and arrange them in drums or maxi bags according to the type of waste and following the colour classification detailed above.

Internal transport will be carried out by removing the contents of the temporary storage containers of the plants; biodegradable waste three time a week and for recyclable waste when the container capacity is completed.

Daily waste production is estimated to be 0.7 kg/person/day in operation.

- **Hazardous waste**

The hazardous waste generated by the Project is mainly used in oils and lubricants, paint remains, solvents, material contaminated with hydrocarbons, among others. Hazardous waste generation is estimated to be less than 200 kilograms per month.

Hazardous waste shall be temporarily stored in the waste yard until its disposal by a company authorized for transfer and treatment. The different areas of waste storage will have Olympic perimeter enclosure, signage with legends of the types of waste and waterproofing to avoid direct contact with the soil.

- **Disposal of spent brine**

The direct extraction system generates a waste or depleted brine by-product resulting from the lithium extraction process. This by-product must be properly managed for treatment or disposal, using various technologies or techniques. In this context, a series of alternatives are proposed for the management and discharge of the spent brine.

With this objective in mind, Lithea asked the consultant AW to prepare a technical memo to identify suitable sites for the storage of spent brine, estimate the volumes that can be recharged to groundwater or evaporated, and describe the technologies and sequencing of the systems to be used.

The primary treatment for disposal of the depleted brine (Alternative 2 Ataca Waters Report), as described, will be its management through evaporation ponds located in the southern sector of the Salar de Pozuelos.

Surface recharge and gravity wells (Alternative 1) are presented as secondary disposal methods. The sequencing of the use of the proposed alternatives will be defined prior to the start of the operation.

17.4 Closure and Reclamation Plans

Closure and reclamation for the PPG Project have followed legislative requirements and best practice guidance. The legislative requirements for mine closure were outlined under Law 7070 and Decree 3097/00 (as amended by Decree 1587/03) in Salta Province.

A conceptual mine closure plan was included in both the Pozuelos and Pastos Grandes IIAs (Initial Investment Analysis).

On completion of mining operations at the Project, Ganfeng and LAR are committed to restoring the area to its pre-mining use state where practical and applicable. For the purposes of this study, The QP conservatively estimated closure costs by applying a 5% factor to initial CapEx. The closure costs are included in the sustaining CapEx in the technical economics model for the project.

We recommend a detailed mine closure plan within the next 5 years. Development of a mine closure plan is not a one-time event but a continuous process, evolving from a conceptual stage during project development to a detailed plan during operations.

18.0 CAPITAL AND OPERATING COSTS

The cost estimate for the Project is divided into Capital Expenditures (CapEx) and Operational Expenditures (OpEx). Sustaining capital expenditures over the life of mine (LoM) are included in the cash flow. These will be discussed in the following sections. All estimated costs have been based on recent Argentinian and international prices for similar lithium Projects.

The CapEx has an estimated accuracy of -15% to +25% compliant with a Class 3+ Study defined in American Association of Cost Engineers (AACE) International Recommended Practice.

These are generally prepared for budget authorization, and funding. Typical engineering completion is from 10% to 40% comprising the following: process flow diagrams, some P&IDs, plot plans, layout drawings, and process and utility equipment lists. Estimates usually involve more deterministic estimating methods, usually involving unit cost line items, although these may be at an assembly level of detail rather than individual components. Factoring and other stochastic methods may be used to estimate some areas of the project. Many of the above-mentioned drawings used for cost estimate are included in this report.

18.1 Capital Cost Estimate

Capital and Operating Cost estimates developed by the QP are based on an average capacity of 51,000 TPA LCE per each phase of the project. It covers three sites: Pozuelos, Pastos Grandes and SdlP salars and central plant areas. A simple breakdown structure was developed to facilitate cost allocation of the different elements to the Salars and the facilities.

Civil, structural, piping and mechanical costs were partially derived from available engineering, and the remaining costs are factored. Electrical and instrumentation costs were quantified and priced according to the operating philosophy. Equipment and construction prices were obtained from either equipment manufacturers, Ganfeng/Lithea or in-house pricing for similar installations.

Capital Operating Cost estimates developed by Golder are in conformance with the requirements of § 229.601(b)(96) .

Project CapEx is shown in Table 130 and Figure 213. These estimates incorporate direct and indirect costs for the implementation of the entire Project, including:

- Brine production well-field and pipeline delivery system
- Evaporation ponds and liners
- Solvent extraction Plant
- Purification plants
- Lithium carbonate and lithium hydroxide plants
- General services
- Infrastructure; and utilities
- Indirect and Owner’s Costs.

No provision has been included to offset future cost escalation since estimated expenses, as well as expected revenue, are expressed in constant dollars. The capital expenditure for the PPG Project, including equipment, materials, indirect costs and contingencies during the construction period, is estimated to be:

- Phase 1 – US$1,124,293,717

- Phase 2 – US$1,108,130,936
- Phase 3 – US$1,068,784,553

These values exclude interest expense that might be capitalized during the same period but include the following:

- Direct Project Costs
- Indirect Project Costs
- Project Contingencies
- Owners Costs
- VAT Taxes

18.1.1 Basis of Estimate

The Basis of Estimate (BoE) is a description of how a cost estimate was obtained for each Work Breakdown Structure (WBS) element for which a cost is estimated.

For the FS of the PPG Project, the BoE is as follows:

- Product specifications: Lithium carbonate (battery grade) and Lithium Hydroxide Monohydrate (battery grade).
- Process flowsheets were prepared. Some P&ID drawings prepared.
- Brine extraction method is based on modelling of pumping wells.
- Production schedules are estimated to form the basis of process facilities capacity.
- Some factoring has been used derived from historical data or modelling. These factors are capacity factored estimates.

For calculation of Direct Cost, estimated percentages have been used for labour, materials and subcontracts that represent the installed costs for similar facilities. The Indirect Costs are factored as percentage (%) of Direct Cost to account for EPCM, Commissioning, freight, taxes, Owner Costs and other miscellaneous field costs.

- For evaporation ponds and wells, Take-off quantities were calculated for each discipline and unit costs applied to labour materials and subcontracts.
- Process plants costs were factored from the estimated CIF equipment cost for each process plant.
- A similar methodology was used for infrastructure items although some budget quotations were obtained by Ganfeng.
- Percentage factors are used for estimating contractor’s field overhead costs, construction shops, construction camp, contractor’s profit, and EPCM costs.
- Engineering, project management, project controls, procurement and contracting, and site construction management (EPCM) costs have been developed from first principles based on the developed schedule and expected engineering deliverables.
- Engineering support labour costs for commissioning has been developed from first principles based on the developed schedule. Support from PPG operations and maintenance staff has been assumed.

- Owner’s costs were assumed at 4% of direct costs and include field staffing, travel, general expenses, basic office costs, and insurance. No allowance has been made for pre-production operating costs.
- Contingency refers to costs that will likely occur based on past experience, but with some uncertainty in regard to precisely how and where it will be spent. Contingency, used as a percentage of total direct and indirect costs, ranged from 15-25%.
- Mine closure costs were assumed at 5% of capital investment.

Table 124 summarized the estimate methodology used for the main areas for the three Phases of the project.

Table 124: Summary of the Estimate Methodology Used for Main Areas for All Three Phases

Project Area	Data Used	Direct Cost Details	Indirect costs details	Contingency	VAT
Wellfields	Take-off quantities	Unit Costs and benchmarks	Unit Costs and benchmarks	15%	Calculated
Ponds	Take-offs	Unit Costs and benchmarks	Unit Costs and benchmarks	15%	Calculated
Infiltration Ponds	Take-offs	Unit Costs and benchmarks	Unit Costs and benchmarks	15%	Calculated
Infrastructure	Take-offs + Client driven	Unit Costs and benchmarks	Unit Costs and benchmarks	15%	Calculated
Process Plants	Ganfeng	Equipment cost Factored	Factored from direct costs	25%	Calculated
Utilities	Take-offs + Client driven	Unit Costs and benchmarks	Unit Costs and benchmarks	15%	Calculated

This methodology fits the level of estimate described at the beginning of this chapter.

18.1.2 Exclusions and Assumptions

The following items are specifically excluded from the estimate at this level of study:

- Allowances for special incentives (schedule, safety or others)
- Cost changes due to currency fluctuation and escalation
- Force majeure issues
- Owner’s costs prior to project approval
- Finance charges and interest during construction
- Sunk costs
- Environmental mitigation costs
- Delays and redesign work associated with any antiquities

- All costs associated with weather delays including flooding or resulting construction labour stand-down costs.

The following assumptions underlie this estimate:

- Suitably qualified and experienced construction labour will be available at the time of execution of the project
- No extreme weather will be experienced during the construction phase and as such no allowances are included for flooding or construction-labour stand-down costs

18.1.3 Brine Well Field

The cost of the brine field was estimated based on drilling, subcontract and materials. The total Costs for the well fields were estimated as follows for each stage of the project exclusive of owners' costs and VAT but inclusive of indirect costs and 15% contingency.

- Phase 1: US$103,431,233
- Phase 2: US$188,999,721
- Phase 3: US$208,999,993

18.1.4 Evaporation Ponds

The CapEx for the evaporation ponds was estimated based on take-off quantities and is shown in Table 125 for the 3 Phases of the project. The cost of evaporation ponds is inclusive of the evapo-infiltration ponds for the lithium depleted brine from solvent extraction.

Table 125: Evaporation Ponds and Wells

Wells, Pipelines and Ponds Capital Estimate			
	Phase 1	**Phase 2**	**Phase 3**
Production wells (Pozuelos)	$ 68,621,980	-	-
Production wells (Pastos Grandes)	-	$ 126,214,650	-
Production wells (PG + SdlP)	-	-	$ 140,884,621
ALL Ponds	$ 174,467,119	$ 219,903,917	$ 214,836,346
Monitor Wells	$ 8,513,700	$ 14,735,250	$ 14,980,838
SUBTOTAL DIRECTS	**$ 251,602,799**	**$ 360,853,817**	**$ 370,701,805**
Contractor Fees	$ 12,580,140	$ 18,042,691	$ 18,535,090
Construction Camp	$ 5,032,056	$ 7,217,076	$ 7,414,036
Start-up Assistance	$ 5,032,056	$ 7,217,076	$ 7,414,036
Consumables	$ 5,032,056	$ 7,217,076	$ 7,414,036
EPCM	$ 14,089,757	$ 20,207,814	$ 20,759,301
SUBTOTAL INDIRECTS	**$ 41,766,065**	**$ 59,901,734**	**$ 61,536,500**

Wells, Pipelines and Ponds Capital Estimate						
SUBTOTALS	**$**	**293,368,864**	**$**	420,755,551	**$**	**432,238,304**
Contingency	$	44,005,330	$	63,113,333	$	64,835,746
TOTALS	**$**	**337,374,193**	**$**	483,868,883	**$**	**497,074,050**
Owners' costs	$	10,064,112	$	14,434,153	$	14,828,072

18.1.5 Process Plants

The estimate for the processing plants, as shown in Table 126, is based on the process design and costs provided by Ganfeng. The tables below represent the cost for each of the 3 phases planned for the project.

The cost for the Process Plants is estimated at US$459,108,440 for each stage of production inclusive of indirect and 25% contingency but exclusive of owners' costs.

Table 126: Process Plants for Each Stage

SX and Raffinate Plants Capital		
Total Equipment Cost	$	46,246,200
Earthwork	$	11,561,550
Concrete	$	12,486,474
Structures	$	18,498,480
Piping	$	19,423,404
Electrical	$	6,936,930
Painting	$	1,387,386
Instr.&control	$	6,936,930
Installation& assembly	$	16,186,170
Subtotal Indirect Costs	**$**	**139,663,524**
Field Exp	$	8,324,316
Constr. Supplies	$	5,549,544
Start up	$	2,312,310
Temp Facilities	$	2,774,772
Constr. Equipment	$	2,774,772
Craft Benefits	$	2,312,310
EPCM	$	8,185,577
Subtotal Indirect Costs	**$**	**32,233,601**
Directs + Indirect Costs	**$**	**171,897,125**
Contingency	$	42,974,281
TOTAL COSTS	**$**	**214,871,407**

Purification Plants Capital		
Equipment Cost	$	11,011,000
Earthwork	$	2,752,750
Concrete	$	2,972,970
Structures	$	4,404,400
Piping	$	4,624,620
Electrical	$	1,651,650
Painting	$	330,330
Instr.&control	$	1,651,650
Equipment setup & assembly	$	3,853,850
Subtotal Direct Costs	**$**	**33,253,220**
Field Exp	$	1,651,650
Constr. Supplies	$	1,321,320
Start up	$	550,550
Temp Facilities	$	660,660
Constr. Equipment	$	660,660
Craft Benefits	$	550,550
EPCM	$	1,932,431
Subtotal Indirect Costs	**$**	**7,327,821**
Directs + Indirect Costs	**$**	**40,581,041**
Contingency	$	10,145,260
TOTAL COSTS	**$**	**50,726,301**

LCE Plant Capital		
Equipment Cost	$	20,836,200
Earthwork	$	5,209,050
Concrete	$	5,625,774
Bldgs&Structures	$	8,334,480
Piping	$	8,751,204
Electrical	$	3,125,430
Painting	$	625,086
Instruments &control	$	3,125,430
Equipment setup & assembly	$	7,292,670
Subtotal Direct Costs	**$**	**62,925,324**
Field Exp	$	3,125,430
Constr. Supplies	$	625,086
Start up	$	1,041,810
Temp Facilities	$	666,758
Constr. Equipment	$	833,448
Craft Benefits	$	625,086
EPCM	$	3,492,147
Subtotal Indirect Costs	**$**	**10,409,766**
Directs + Indirect Costs	**$**	**73,335,090**
Contingency	$	18,333,772
TOTAL COSTS	**$**	**91,668,862**

LHM and AUXILIARY Plants		
Total Equipment Cost	$	23,148,510
Earthwork	$	5,787,128
Concrete	$	6,250,098
Bldgs&Stru	$	9,259,404
Piping	$	9,722,374
Electrical	$	3,472,277
Painting	$	694,455
Instr.&control	$	3,472,277
Assembly	$	8,101,979
Subtotal Direct Costs	**$**	**69,908,500**
Field Exp	$	3,472,277
Constr. Supplies	$	694,455
Start up	$	1,157,426
Temp Facilities	$	740,752
Constr. Equipment	$	925,940
Craft Benefits	$	694,455
EPCM	$	3,879,690
Subtotal Indirect Costs	**$**	**11,564,996**
Directs + Indirect Costs	**$**	**81,473,496**
Contingency	$	20,368,374
TOTAL COSTS	**$**	**101,841,870**

18.1.6 Infrastructure and Energy

Infrastructure and Energy costs for the 3 phases were estimated based on input from Lithea/Ganfeng, internal estimating, and quotations from vendors. These costs are included in Table 127.

Infrastructure and Energy Capital Expenditures

Table 127: Infrastructure and Energy Capital Costs

Infrastructure and Energy Capital Expenditures			
	Totals _ Phase 1	**Totals _ Phase 2**	**Totals _ Phase 3**
Fresh Water Supply	$ 46,038,941	$ 12,038,941	$ 10,032,451
Transformers (Salars)	$ 23,071,108	$ 21,367,122	
Workshop/truck shop	$ 6,501,765		
Warehouses	$ 16,280,416		
Office Buildings	$ 2,880,000		
Camp	$ 45,600,000	$ 23,589,458	
Effluent Plant	$ 1,617,644	$ 2,106,840	$ 2,106,840
Waste Yard	$ 5,786,068		
Subtotal	$ 147,775,941	$ 59,102,361	$ 12,139,291
Contingency (15%)	$ 22,166,391	$ 8,865,354	$ 1,820,894
Subtotal Infrastructure	**$ 169,942,333**	**$ 67,967,715**	**$ 13,960,185**
Phase 3 Power Lines	$ 29,172,653		
PZ Power Lines	$ 22,831,428		
Phase 2 Power Lines	$ 20,232,511		
Fuel Plant	$ 2,718,199		
Emergency Generation	$ 23,477,027		
Contingency (15%)	$ 7,353,998	$ 3,034,877	$ 4,375,898
Subtotal Energy	**$ 56,380,653**	**$ 23,267,387**	**$ 33,548,551**
ALL TOTALS	**$ 226,322,985**	**$ 91,235,102**	**$ 47,508,735**

Note: All internal roads, and brine pipelines are included in the evaporation ponds estimates.

18.1.7 Tailings Management (TMA and Plant Residues)

A costing methodology based on a unit cost of storage area is applied to the Tailings Management Area (TMA), as shown in Table 128. Site levelling preparation, liner installation and a perimeter protective berm is included in the estimate. The TMA cost for the salts at the different phases of production is estimated for the first five (5) years of operation. The remaining 25 years of operation will require construction of additional storage every five years. The cost of expansion of the TMA after the first five years is included into the Cash Flow as sustaining capital. Storage of the Plant residues instead is based on a 20-year operation, and its cost is also included in the Cash Flow.

Table 128: CapEx for The TMA and Gypsum Disposal

CAPITAL COST SUMMARY TMA and PROCESS WASTE

5-YEAR CAPEX Phase 1

DIRECT COSTS	EARTHWORK QUANTITY M3	LINERS QUANTITY M2	LABOR COST	MATERIAL COST	TOTALS
SALT STOCKPILE	1,499,126	0.00	$ 13,492,131		$ 13,492,131
$Ca_2B_2O_5$ DEPOSIT	284,253	125,352	$ 1,749,569	$ 626,761	$ 2,376,330
$CaCO_3$ Waste					
TOTAL DIRECT COSTS	1,783,378	125,352	$ 15,241,701	$ 626,761	$ 15,868,461
INDIRECT COSTS					$ 2,023,820
SUBTOTAL					$ 17,892,281
CONTINGENCY					$ 4,473,070
TOTAL CAPEX					**$ 22,365,351**

CAPITAL COST SUMMARY TMA and PROCESS WASTE

5-YEAR CAPEX Phases 2 and 3

DIRECT COSTS	EARTHWORK QUANTITY M3	LINERS QUANTITY M2	LABOR COST	MATERIAL COST	TOTALS
SALT STOCKPILE	1,400,090	0.00	$ 12,600,8144		$ 12,600,814
Ca_2B2O5 DEPOSIT	284,253	125,352	$ 1,749,569	$ 626,761	$ 2,376,330
CaCO3 Waste					
TOTAL DIRECT COSTS	1,684,343	125,352	$ 14,350,384	$ 626,761	$ 14,977,144
INDIRECT COSTS					$ 1,890,122
SUBTOTALS					$ 16,867,266
CONTINGENCY					$ 4,216,817
TOTAL CAPEX					**$ 21,084,083**

The 5-year Cost for the Tailings Management Area (TMA) and process waste is estimated at:

- Phase 1: US$22,365,351
- Phase 2: US$21,084,083
- Phase 3: US$21,084,083

18.1.8 Sustaining Capital

Sustaining capital expenditures (S-CapEx) are investments for replacement of large equipment not covered by maintenance costs required to keep all equipment for the operation in good shape (e.g. replacement of a main pipeline section on the brine field). The estimate is based on an estimation of the average aggressiveness of the environment and the expected lifetime of main equipment.

Sustaining CapEx is estimated as a percentage of the direct CapEx. At the process plants and on-site supporting facilities, the S- CapEx is taken as 1.5%. For the brine field the S- CapEx is taken as 2.5%. For evaporation ponds, the S- CapEx is taken at 1.0%.

The five (5) year TMA expansion costs are estimated based on the annual tonnage of waste to be deposited to the TMA facilities. The initial CapEx covers the TMA for the first five (5) years of operation. Following the first five (5) years, an expansion of TMA will be required at each subsequent five (5) years. The sustained capital costs are allocated to these years of operation.

Table 129: Sustaining Capital

Sustaining CapEx	%	Direct CapEx $	Phase 1	Direct CapEx $	Phase 2	Direct CapEx $	Phase 3
Brine Field	2.50%	77,135,680	1,928,392	140,949,900	3,523,748	155,865,459	3,896,636
Evaporation Ponds	1.00%	174,467,119	1,744,671	219,903,917	2,199,039	196,304,149	1,963,041
Process Plants	1.50%	305,750,568	4,586,259	305,750,568	4,586,259	305,750,568	4,586,259
On-site Infrastructure	1.50%	147,775,941	2,216,639	59,102,361	886,535	12,139,291	182,089
Energy Infrastructure	3.00%	49,026,654	1,470,800	20,232,511	606,975	29,172,653	875,180
SUBTOTAL (Annual)	-	**Phase1**	**11,946,760**	**Phase2**	**11,802,556**	**Phase3**	**11,503,205**
TMA (Included in DCF)		**20,880,145**	**20,880, 145**	**19,598,877**	**19,598,877**	**19,598,877**	**19,598,877**

The estimated annual cost of sustaining capital S-CAPEX is approximately US$12 million per year for each phase exclusive of TMA.

18.1.9 Owner's and Indirect Costs

Indirect Costs are estimated at percentages of Direct Costs for each of the areas according to standard estimating practices. These costs are listed in the various tables presented above. Owner costs estimated at 4% of direct costs were included in Indirect Costs.

18.1.10 Engineering, Procurement and Construction Services

The EPCM services are estimated at a percentage (5-6%) of Direct costs.

18.1.11 Contingency

A contingency of 15 to 25% was applied across the project depending on the area. This level of contingency allowance is in line for an AACE estimate of this class, where typical method of factored capacity, parametric model, judgment or analogy is used.

18.1.12 CapEx Summary

The CapEx summary for the 3 phases of production is presented in Table 130.

Total CapEx for all 3 phases including contingency, owners' cost, and VAT is estimated to be US$3,301,209,207**.**

Table 130: Capital Cost Summary for the 3 phases

CAPEX FOR PHASE 1		PHASE 2	PHASE 3	TOTALS
COST AREA_ TOTAL INSTALLED COST				
WELLFIELD	$ 103,431,233	$ 188,999,721	$ 208,999,993	$ 501,430,948
EVAPORATION PONDS	$ 233,942,960	$ 294,869,162	$ 288,074,056	$ 816,886,179
TMA AREAS (Initial)	$ 22,365,351	$ 21,084,083	$ 21,084,083	$ 64,533,517
SOLVENT EXTRACTION	$ 214,871,407	$ 214,871,407	$ 214,871,407	$ 644,614,220
PURIFICATION PLANTS	$ 50,726,301	$ 50,726,301	$ 50,726,301	$ 152,178,902
ELECTRODIALYSIS&LHM PLANTS	$ 85,706,660	$ 85,706,660	$ 85,706,660	$ 257,119,979
UTILITIES PLANTS	$ 16,135,210	$ 16,135,210	$ 16,135,210	$ 48,405,631
LCE PLANT	$ 91,668,862	$ 91,668,862	$ 91,668,862	$ 275,006,586
ENERGY	$ 56,380,653	$ 23,267,387	$ 33,548,551	$ 113,196,591
INFRASTRUCTURE	$ 169,942,333	$ 67,967,715	$ 13,960,185	$ 251,870,232
VAT ADD ON	$ 47,140,956	$ 22,520,849	$ 15,050,802	$ 84,712,607
OWNERS COSTS	$ 31,981,793	$ 30,313,580	$ 28,958,444	$ 91,253,816
TOTAL CAPITAL EXPENDITURES	**$ 1,124,293,717**	**$ 1,108,130,936**	**$ 1,068,784,553**	**$ 3,301,209,207**

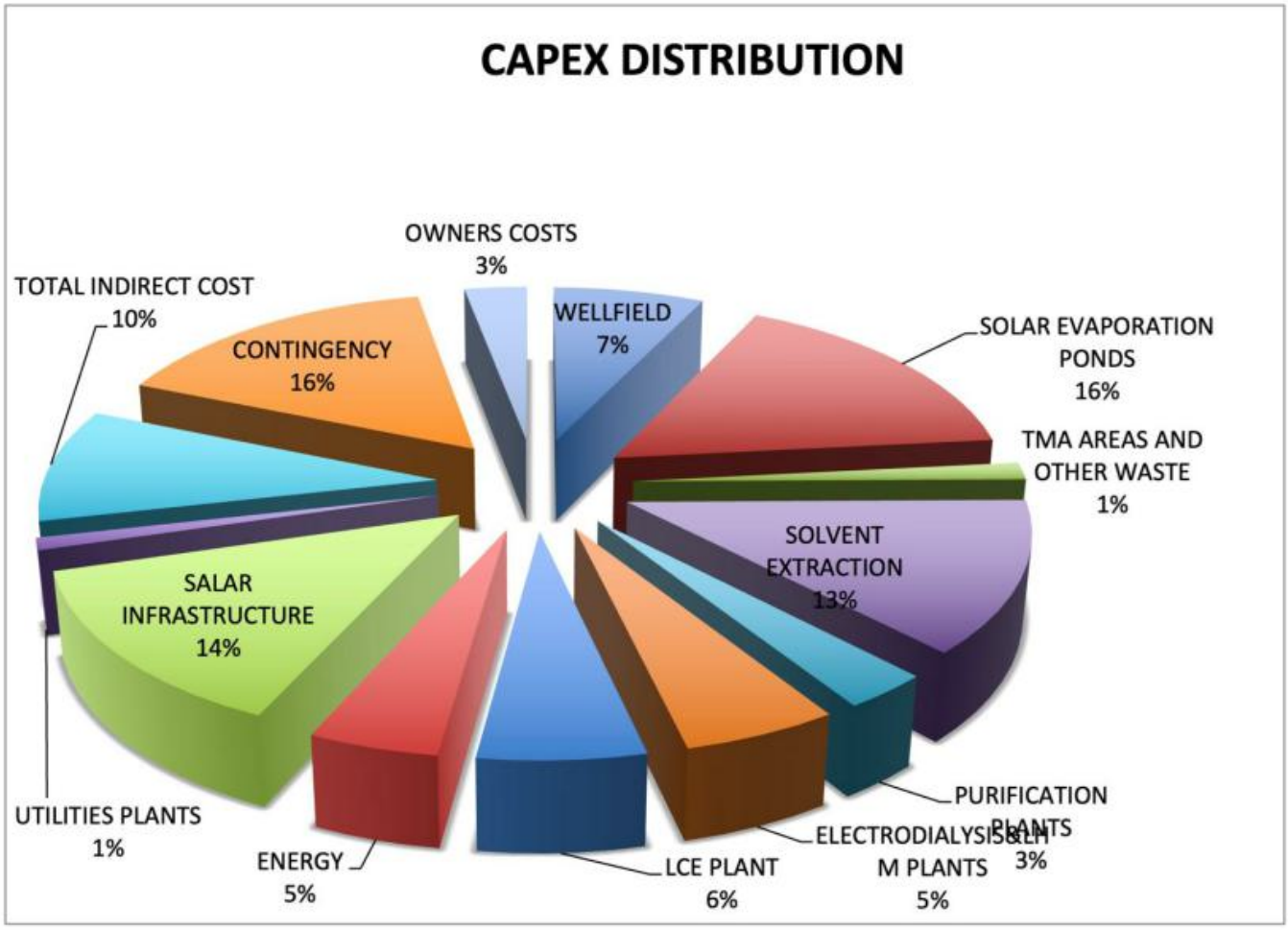

Figure 213: Capital Cost Distribution for Phase 1

18.2 Operating Costs Estimate

18.2.1 Basis of Estimate

The operating cost estimate has been made with quantities developed by the QP and unit prices provided by Lithea. The QP considers it to have an accuracy of ±15%. The estimate includes all site-related operating costs associated with the production of high purity lithium carbonate and lithium hydroxide but expressed as a total LCE. The operating costs were developed by the QP in conjunction with Ganfeng.

Table 136 summarizes the overall PPG operating costs assuming steady state operation after ramp-up. Potential cost increases annually due to reductions in lithium feed grade is not included. Note that the operating costs are based on steady-state operation and an estimated average brine grade for the 30-year operation period.

Exclusions

- Exploration costs
- All withholding taxes and other taxes
- All sunk costs
- Any impact of foreign exchange rate fluctuations
- Any escalation from the date of the estimate
- Any contingency allowance
- Any land compensation costs
- Any rehabilitation or closure costs
- Any license fees or royalties, government permits, legal fees, insurances
- Government monitoring/compliance costs
- Business interruption
- Project finance costs
- Interest charges
- Corporate overheads
- Political risk insurance
- Maintenance cost of hauls and plant access roads
- Union fees
- Contract labour

Estimate Basis

- All costs are as of Q4 2025
- Consumables costs have been established using Golder’s database.
- Reagent consumption rates are determined from the average consumption outlined in the mass balance.

- Reagent costs were supplied by the client.
- Average throughput, availability, grades align with the Process Design Criteria and mass balance prepared by Ganfeng and Lithea.
- Power unit costs are derived from rates provided by the client.
- Maintenance costs have been factored using similar sized plants within the Golder's database
- Labour unit costs were advised by the client.

The operating expenditures (OpEx) are comprised of the following components:

- Manpower
- Electric power
- Reagents
- Consumables & miscellaneous
- Camp operation & personnel transport
- Product transportation
- G&As

Dollar inflation has a significant impact on the plant's OpEx, particularly on the local cost components. This OpEx does not account for the effects of inflation. Certain inputs and services required for operations are sourced from the local market, and their prices were presented in U.S. dollars in our OpEx estimate to mitigate the impact of currency exchange rate fluctuations.

18.2.2 Manpower

Manpower classification and unit counts were provided by Lithea. Salary and wage estimates are based on data given by Lithea.

Annual personnel costs for the various plant personnel have been estimated according to the staffing requirements of each area, considering two- or three-shift system needed for different unit operations. The salaries and number of personnel for the different categories are listed in Table 131 and Table 132.

The manpower requirement listed in the tables below include the Salar sites, and the office in the city of Salta for management and administration.

Table 131: Personnel List at Site

	N°	N°	N°
Management	3	4	5
Plants Supervisors	14	28	56
Wells and Ponds operators	44	88	100
Extraction Plant Operators	36	72	96
Purification plant operators	28	46	68
Electrodialysis Plant Operators	28	35	58
LiOH Plant Operators	28	40	54

	N°	N°	N°
LCE Plant Operators	30	46	68
Services	30	46	64
Control Room	12	24	36
Laboratory Management	3	5	7
Laboratory Analysts	30	36	42
Quality Product	4	4	4
Maintenance	70	90	110
Safety & Health	16	20	24
HR	4	5	6
Warehouse	36	46	51
IT	10	14	16
Community relations	2	2	2
Camp	28	28	28
Finance	2	2	2
Logistics	21	41	51
Property Security & Personnel Transport	4	6	8
Environment	5	5	5
Techniques & Processes	20	20	20
Total Personnel	**508**	**753**	**981**

The manpower cost estimate is based on labour rates and roster structures provided Lithea. Labour cost estimate is based on:

- Shift workers work operate on 12-hour shifts with two shifts per day.
- Day workers work 8-hour shifts, 5 days per week.
- A benefit burden of 33% of the base salary is included to cover overtime, sick leave, annual leave, public holidays, and 13th-month payroll. An additional 10% bonus allowance was also included.

All workers are based in Argentina. No allowances have been included for expatriate staff or international travel.

Table 132: Personnel and Cost During Phase 1

Labour Type	PPG Site	Salta Staff	Totals
Management	17	20	37
Operations	269	28	297
Maintenance	70	0	70
Services	148	0	148
Total Labour	**508**	**45**	**553**
Total Cost	**$ 27,608,232**	**$ 4,729,450**	**$ 32,337,683**

Personnel or staffing requirements for the various parts of the operation are discussed in the following sections. The personnel have been classified in various groups with different salary levels, based on the required skill sets.

18.2.2.1 Management and Production Personnel

Management covers senior personnel responsible for supervising the three different locations and operation sections.

Production personnel include staff assigned to the brine field, evaporation ponds, tailing management area, and the processing plants inclusive of the facility. The estimate presented here is based on Lithea Argentina's provided data regarding headcount, respective salaries, and labour rates.

During the engineering, construction, startup and operation acceleration period, additional personnel will be required. These temporary staffing costs are not included in the direct operating cost.

18.2.2.2 General and Admin Costs

General and administrative (G&A) costs include software license, training, consultants, legal permits, insurance, community support, communications etc.

18.2.3 Electric Power

Energy will be supplied through a combination of electric power and LNG for steam generation. Photovoltaic power may be used for back up and emergency, so it is not included in this report. Unit costs for both LNG and electricity were provided by LAR.

A summary of electrical energy consumption is provided in Table 133.

Table 133: Electricity Consumption for the 3 Phases of Production

PROJECT AREA	Power Consumption Phase1			Power Consumption Phase 2			Power Consumption Phase 3		
	Load kw	Operating	Kw/year	Load kw	Operating	Kw/year	Load kw	Operating	Kw/year
Brine Well Field	5,250	80%	45,990,000	7,240	80%	63,422,400	7,240	80%	63,422,400
Ponds	9,000	100%	78,840,000	10,280	100%	90,052,800	10,280	100%	90,052,800
SX	7,455	78%	53,676,000	7,455	78%	53,676,000	7,455	78%	53,676,000
Primary Purification	857	90%	6,170,400	857	90%	6,170,400	857	90%	6,170,400
Raffinate Treatment	515	55%	3,708,000	515	55%	3,708,000	515	55%	3,708,000
Raff Water Treat	210	89%	1,512,000	210	89%	1,512,000	210	89%	1,512,000
Ancillary Facilities (Camp, Offices, Sewage Treatment, water treatment)	1,222	100%	8,028,540	1,222	100%	8,028,540	1,222	100%	8,028,540
Second Purification	696	63%	5,011,200	696	63%	5,011,200	696	63%	5,011,200
Electrodialysis	7,635	95%	54,972,000	7,635	95%	54,972,000	7,635	95%	54,972,000
LHM Plant	3,161	66%	22,759,200	3,161	66%	22,759,200	3,161	66%	22,759,200
LCE Process Plant	7,253	96%	52,221,600	7,253	96%	52,221,600	7,253	96%	52,221,600
Utilities	2,690	100%	19,368,000	2,690	100%	19,368,000	2,690	100%	19,368,000
Operating Power Demand	**45,944**	**42,906**	**352,256,940**	**49,214**	**45,778**	**380,902,140**	**49,214**	**45,778**	**380,902,140**

18.2.4 Reagents, Fuel and Consumables

This budget line includes reagents and other additives required for brine concentration and in the lithium carbonate production process.

Reagents needed for production include lime, hydrogen peroxide, sodium hydroxide, hydrochloric acid and sodium carbonate. The cost summary is provided in Table 134. The estimated annual cost of production reagents at the 153,000 TPA LCE production level is US$220,872,345**.**

Table 134: Reagents Cost Summary

REAGENTS COST SUMMARY 51K Production			
	Unit Cost	TPA	Total Cost
Lime	$ 399	10,656	$ 4,251,744
27.5% H_2O_2	$ 1,210	1,258	$ 1,522,180
NaOH (100%)	$ 883	18,239	$ 16,015,037
HCl 32%	$ 387	2,881	$ 1,114,947
Sodium Carbonate	$ 726	67,788	$ 49,214,088
Other Chemicals	Various		$ 1,415,825
Total Reagents Cost			**$ 73,623,821**
REAGENTS COST SUMMARY (153K)			
	Unit Cost	TPA	Total Cost
Lime	$ 399	31,968	$ 12,755,232
27.5% H_2O_2	$ 1,210	3,774	$ 4,566,540
NaOH (100%)	$ 883	54,718	$ 48,315,994
HCl 32%	$ 387	8,643	$ 3,344,841
Sodium Carbonate	$ 726	203,364	$ 147,642,264
Other Chemicals	Various		$ 4,247,474
Total Reagents Cost			**$ 220,872,345**

18.2.5 Ponds Harvesting and TMA

Additional costs apply to evaporation pond harvesting and TMA operations. These are based on the equipment and manpower required for harvesting, storing and loading salts from the evaporation ponds, and the equipment to operate the TMA. An annual cost of approximately US$44 million was calculated based on the total combined estimated salt produced from pre-concentration for 3 phases of production case.

18.2.6 Water

The cost of process and domestic water is based on water supply from an on-site desalination plant, which treats brackish water from local springs. These costs are included under the relevant equipment and operating personnel. Water consumption is shown in Table 135.

Table 135: Water Use

Water Consumption (Phase 1)		
Description	**Usage m^3/day**	**Water Usage TPA**
Process Plants	3,712	1,113,598
General Services	1,367	498,984
Potable water	92	33,682
Evaporation Ponds	1,498	546,770
Total Water	**6,669**	**2,193,034**
Water Consumption (Phases Each 2&3)		
Description	**Usage m^3/day**	**Usage TPA**
Process Plants	3,712	1,113,598
General Services	1,367	498,984
Potable water	92	33,682
Evaporation Ponds	1,572	573,780
Total Water	**6,743**	**2,220,044**

18.2.7 Camp

Camp operation costs are estimated using “all-inclusive” charges from a contracted camp operator, based on a monthly room-and-board rate per person derived from data from other projects. Camp construction costs are included in CapEx.

The estimated annual camp operation cost during the PPG phases is based on an average 12-month cost of US$13,887,000 (with VAT) for up to 500 people, inclusive of the following services:

- Food, cleaning, and maintenance
- Disinfection
- Transportation

Camp costs for the additional phases will reach US$39,750,716 after Phases for 981 people.

18.2.8 Product Transportation

The products transportation cost estimate is based on the following:

- Lithium products will be delivered to destination (FOB) via the port of Antofagasta. Products will be packed according to their respective UN numbers.
- Transport from the Salar sites to the plant will use a brine pipeline.

The estimated annual cost of transporting lithium products to market has been included in this report based on other projects data.

18.2.9 Other Costs (General and Maintenance Supplies)

Other costs included in the OpEx were estimated as a percentage of the overall cost. These costs include:

- General Supplies
- Maintenance materials
- Catering
- Security, cleaning service etc. (included in G&A)

18.2.10 OpEx Summary

Annual operating cost summaries for the three production stages are provided in **Table 136**.

Table 136: Annual Operating Cost Summary

OPERATING COST Phase 1		OPERATING COST Phase 2	OPERATING COST Phase 3
PRODUCTION TPA LCE	51,006	102,012	153,018
	$/YEAR	$/YEAR	$/YEAR
LABOUR +CAMP	$ 32,337,683	$ 45,106,523	$ 58,305,580
REAGENTS	$ 73,623,821	$ 147,247,642	$ 220,872,345
POWER & ENERGY	$ 72,225,910	$ 149,408,298	$ 226,590,686
G&A	$ 7,859,050	$ 11,453,100	$ 15,047,150
MEMBRANE	$ 2,017,000	$ 4,034,000	$ 6,051,000
SALTS DISPOSAL	$ 15,538,911	$ 30,057,790	$ 44,576,669
CONSUMABLES	$ 9,705,600	$ 17,470,080	$ 24,264,000
PRODUCT TRANSPORTATION	$ 10,500,000	$ 21,000,000	$ 31,500,000
MAINTENANCE	$ 21,888,841	$ 43,777,681	$ 65,666,522
SERVICES	$ 13,886,999	$ 20,584,469	$ 39,750,716
CONTINGENCY	$ 12,979,663	$ 24,507,924	$ 36,632,607
TOTAL ANNUAL COSTS	**$ 272,563,478**	**$ 514,647,507**	**$ 769,257,275**
COST/T LCE	**$ 5,344**	**$ 5,045**	**$ 5,027**

A total production cost of US$5,027 per ton LCE is estimated after Phase 3 is in full production. VAT has been included in the cost of reagents, and consumables.

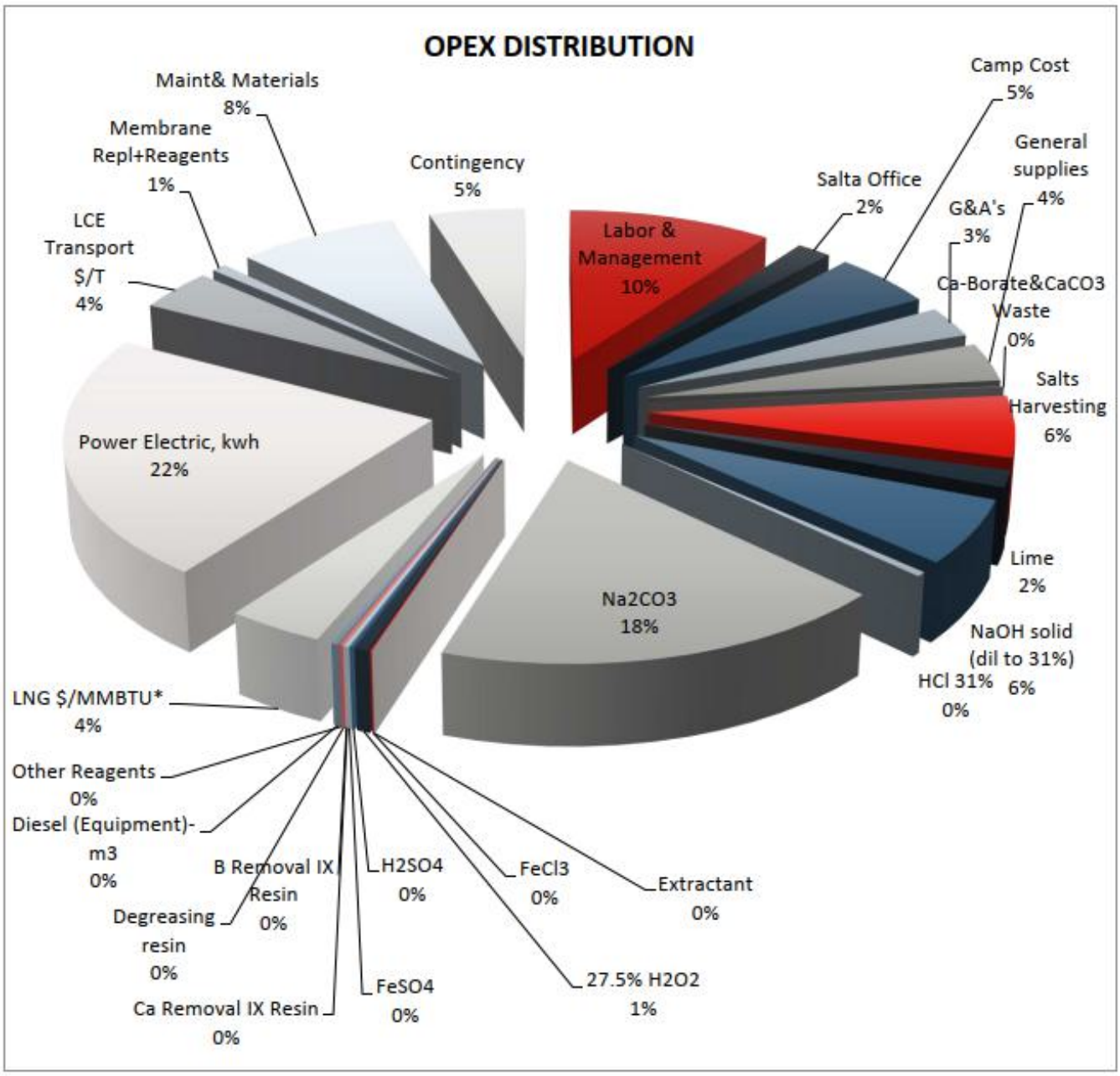

Figure 214: Operating Cost Distribution Phase 1

19.0 ECONOMIC ANALYSIS

Discounted Cash Flow (DCF) analysis was based upon scheduling of the currently available measured and indicated (M+I) resources with the assumptions that 37% of M+I resources are pumpable as brine feed to the evaporation ponds and an overall lithium recovery efficiency of 75%.

The economic analysis was based on measured and indicated resources. Unlike minerals reserves, mineral resources do not have demonstrated economic viability.

19.1 Main Assumptions

A financial analysis of the project was carried out using a discounted cash flow (DCF) approach. This method of valuation requires projecting yearly cash inflows, or revenues, and subtracting yearly cash outflows, such as operating costs, capital costs, and taxes. The resulting net annual cash flows are discounted back to the date of valuation and totalled to determine the NPV of the project at selected discount rates.

The analysis was prepared using an economic model and assesses both before-tax and after-tax cash flow scenarios. Capital (CapEx) and Operational (OpEx) Expenditures presented in previous sections have been used in this analysis. Prices for lithium carbonate and hydroxide was estimated by Golder. The results include Net Present Values (NPV) for 10% discount rate, Internal Rate of Return (IRR) and sensitivity analysis of key inputs.

Cautionary Statement

The results of the economic analysis represent forward-looking information that are subject to a number of known and unknown risks, uncertainties, and other factors that may cause actual results to differ materially from those presented here. Forward-looking information includes Mineral Resource estimates; commodity prices; the production plan; projected recovery rates; use of a process method, infrastructure construction costs and schedule; and assumptions that project environmental approval and permitting.

19.2 Evaluation Criteria

The following criteria have been used to develop the economic model:

- Project life: Life of mine (including construction and operation) is estimated to be 33 years.
- Pricing for lithium carbonate of US$18,000 and LHM (lithium hydroxide monohydrate) of US$17,800 per ton was used.
- Final production rate of 153,000 TPA LCE after all three phases of production reach full operation 9 years after the start of phase 1.
- Final Production for 40,000 TPA lithium carbonate and 12,500 TPA LHM were used for each cumulative phase according to the ramp-up table below (**Table 137**).

Table 137: Assumed Production Schedule

Phase	Years	Li_2CO_3 TPA	LiOH TPA	Ramp-up
Phase 1	1	20,000	6,250	50%
Phase 1	2	30,000	9,375	75%
Phase 1-2	3	45,000	14,063	100%+Q4 Start
Phase 2-3	7	85,000	26,563	100%+Q4 Start

- Discounted Cash Flow (DCF) analysis was based upon scheduling of the currently available measured and indicated (M+I) resources with an assumption of 37% of M+I resources is pumpable that goes into production.
- A discount rate of 10% was used.
- The Discounted Cash Flow (DCF) economic evaluation was carried out on a constant money basis so there is no provision for escalation or inflation on costs or revenue.
- For DCF evaluation purposes, it has been assumed that 100% of capital expenditures, including pre-production expenses, are financed with owners' equity.
- Pre-construction costs are not included in DCF analysis.
- VAT is included for both CapEx and OpEx.
- Lithium grades and recoveries stay constant for 30 years with no dilution.
- Add RIGI benefits applied as assumption for the economic model.
- The key inputs to the economic analysis are shown in Table 138.

Table 138: The Key Inputs to the Economic Analysis (including RIGI benefits)

Economics Overview	Units	Phase 1	After Phase 3
LCE Production	TPA	51,006	153,018
Li_2CO_3	TPA	40,000	120,000
LHM	TPA	12,500	37,500
Mine Life (nominal)	years	30	30
Capital Cost (CapEx)	US$	1,124,293,717	3,301,209,207
Operating Cost (OpEx)	US$/t LCE	5,344	5,027
Average Selling Price (LCE/LHM)	US$/t	18,000/17,800	18,000/17,800
Annual Revenue	US$	942,500,000	2,827,500,000
Discount Rate	%	10	10
Net Present Value (NPV) Pre-Tax	US$	-	7,881,378,524
Internal Rate of Return (IRR) Pre-Tax	%	-	37%
Net Present Value (NPV) Post-Tax	US$	-	5,766,032,301
Internal Rate of Return (IRR) Post-Tax	%	-	32.7%

19.3 Tax

The following taxes and royalties have been applied to the economic analysis of the Project.

19.3.1 Provincial Royalty

Argentinian provinces can charge up to 3% of the value of the mineral "mine of mouth" according to the Federal Mining Legislation in place (Act. N° 24196). A rate of 3% of sales is applied to the DCF model.

19.3.2 Export Refund

No export refund is applied for this evaluation.

19.3.3 Tax on Debits and Credits Accounts

In Argentina, the tax on debits and credits on bank accounts considers 0.6% on debits, plus another 0.6% on credits. A company is permitted to book 34% of the tax paid on credit accounts as a credit for income tax; thus, the net effective rate on both debit and credit accounts is approximately 0.996%. Due to the insignificant value, this item in not included in the DCF economic model.

19.3.4 Aboriginal Programs

The economic model has accounted for anticipated development contributions to local aboriginal groups. The cost of engagement in community programs is included in the Owners' Costs.

19.3.5 Capital Allowance

Investments are eligible for an accelerated amortization incentive, which includes the following:

- 60% of the total amount of the infrastructure cost can be depreciated in the 1st year fiscal year of operation.
- 40% can be depreciated in equal portions in two subsequent years.
- Investment made in machinery, equipment, vehicles and facilities can be depreciated over three years from the start of operation; and
- Provision for an accelerated depreciation of assets in the first three (3) years of operation is included in the DCF.

19.3.6 Corporate Taxes & VAT

The standard corporate tax rate is 35%. VAT rebates are included in the model.

RIGI benefits were applied to the cash flow model which reduces the corporate tax rate (see Section 22.4 below).

19.4 RIGI

19.4.1 About the RIGI

This project can benefit from the Incentive Regime for Large Investments (RIGI, for its acronym in Spanish). The RIGI is a special framework introduced in Argentina under the "*Bases and Starting Points for the Freedom of Argentines Act*" (commonly known as the Bases Law), enacted in 2024. Its primary objective is to attract and promote large-scale, long-term investments by providing legal and fiscal stability, along with tax, customs, and foreign exchange incentives.

19.4.2 Beneficiaries

The RIGI applies to single project vehicles ("SPV") organized as companies or branches of foreign companies (sec.169) investing in certain sectors, including mining, energy and infrastructure (sec.167). If a company already has other projects, the project to be subject to RIGI should be isolated in a dedicated branch (sec.170) which will be considered as a different taxpayer with separate accounting.

19.4.3 Investment

- The minimum amount for an investment to qualify within the regime will be US$200 to US$900 million, as determined for different industries by the regulations (sec. 173).
- The investment must be made in eligible assets, which include all those related to the development of the project, including shares of companies with eligible assets.
- At least 40% of the minimum amount must be invested in the first two years. This percentage can be reduced up to 20% in certain circumstances (sec.173)

19.4.4 RIGI Benefits

The RIGI Benefits applied to the project cash flow model are as follows:

- Reduction of the Corporate Income Tax rate from 35% to 25%.
- Accelerated depreciation schemes (differentiating equipment, plants, and mines with different systems).
- Tax exemptions on VAT (corresponding to the CapEx of the investment presented under RIGI), deduction of debit and credit tax from corporate income tax, indefinite carry forward of tax losses, and exemption from export duty starting in the 3rd year after 40% of the committed investment has been paid.

There is no guarantee that the PPG Project will secure RIGI eligibility.

19.5 Capital Expenditures

The economic model assumes that all capital investment will occur before start of each production phase. However, the actual spend schedule may be done in according to **Table 139**.

Table 139: Capital Expenditures Schedule

AREA	CAPITAL EXPENDITURES SPEND SCHEDULE			
	PHASE 1			
	Y-2	Y-1	Y0	TOTAL $
Wells & Ponds	$ 67,474,839	$ 185,555,806	$ 84,343,548	$ 337,374,193
Process Plants	$ 73,487,915	$ 202,091,767	$ 91,859,894	$ 367,439,577
LCE Plant	$ 18,333,772	$ 50,417,874	$ 22,917,215	$ 91,668,862
Infrastructure and Power	$ 45,264,597	$ 124,477,642	$ 56,580,746	$ 226,322,985
Owners Costs	$ 6,396,359	$ 17,589,986	$ 7,995,448	$ 31,981,793
VAT	$ 9,428,191	$ 25,927,526	$ 11,785,239	$ 47,140,956
FACTORS	20%	55%	25%	
TMA (Initial)				$ 22,365,351
TOTAL	$ 220,385,673	$ 606,060,601	$ 275,482,092	**$ 1,124,293,717**

AREA	CAPITAL EXPENDITURES SPEND SCHEDULE			
	PHASE 2			
	Y2	Y3	Y4	TOTAL $
Wells & Ponds	$ 188,708,864	$ 266,127,886	$ 29,032,133	$ 483,868,883
Process Plants	$ 143,301,435	$ 202,091,767	$ 22,046,375	$ 367,439,577
LCE Plant	$ 35,750,856	$ 50,417,874	$ 5,500,132	$ 91,668,862
Infrastructure and Power	$ 35,581,690	$ 50,179,306	$ 5,474,106	$ 91,235,102
Owners Costs	$ 11,822,296	$ 16,672,469	$ 1,818,815	$ 30,313,580
VAT	$ 8,783,131	$ 12,386,467	$ 1,351,251	$ 22,520,849
FACTORS	39%	55%	6%	
TMA (Initial)				$ 21,084,083
TOTAL	$ 423,948,273	$ 597,875,769	$ 65,222,811	**$ 1,108,130,936**

AREA	CAPITAL EXPENDITURES SPEND SCHEDULE			
	PHASE 3			
	Y6	Y7	Y8	TOTAL $
Wells & Ponds	$ 193,858,879	$ 273,390,727	$ 29,824,443	$ 497,074,050
Process Plants	$ 143,301,435	$ 202,091,767	$ 22,046,375	$ 367,439,577
LCE Plant	$ 35,750,856	$ 50,417,874	$ 5,500,132	$ 91,668,862
Infrastructure and Power	$ 18,528,407	$ 26,129,804	$ 2,850,524	$ 47,508,735
Owners Costs	$ 11,293,793	$ 15,927,144	$ 1,737,507	$ 28,958,444
VAT	$ 5,869,813	$ 8,277,941	$ 903,048	$ 15,050,802
FACTORS	39%	55%	6%	
TMA (Initial)				$ 21,084,083
TOTAL	$ 408,603,183	$ 576,235,259	$ 62,862,028	**$ 1,068,784,553**

19.6 Operating Costs

Operating cost assumptions are covered in Section 18.2. For the financial model, yearly constant operating costs are assumed for the life of mine without regard to potential fluctuations in lithium grades, brine flowrate and recoveries that could change over time and that will impact the operating cost.

19.7 Production Revenues

Production revenues have been estimated based on a price scenario for lithium carbonate of US$18,000/ton and LHM of US$17,800/ton.

No attempt has been made to project product pricing beyond the first year. The same gross revenue per year (at design production) has been used for the duration of the project.

19.8 Cash Flow Projection

Table 140 summarizes the Discounted Cash Flow (DCF) for the assumed Base Case price and production level scenario.

Table 140: Discounted Cash Flow Summary (including RIGI benefits)

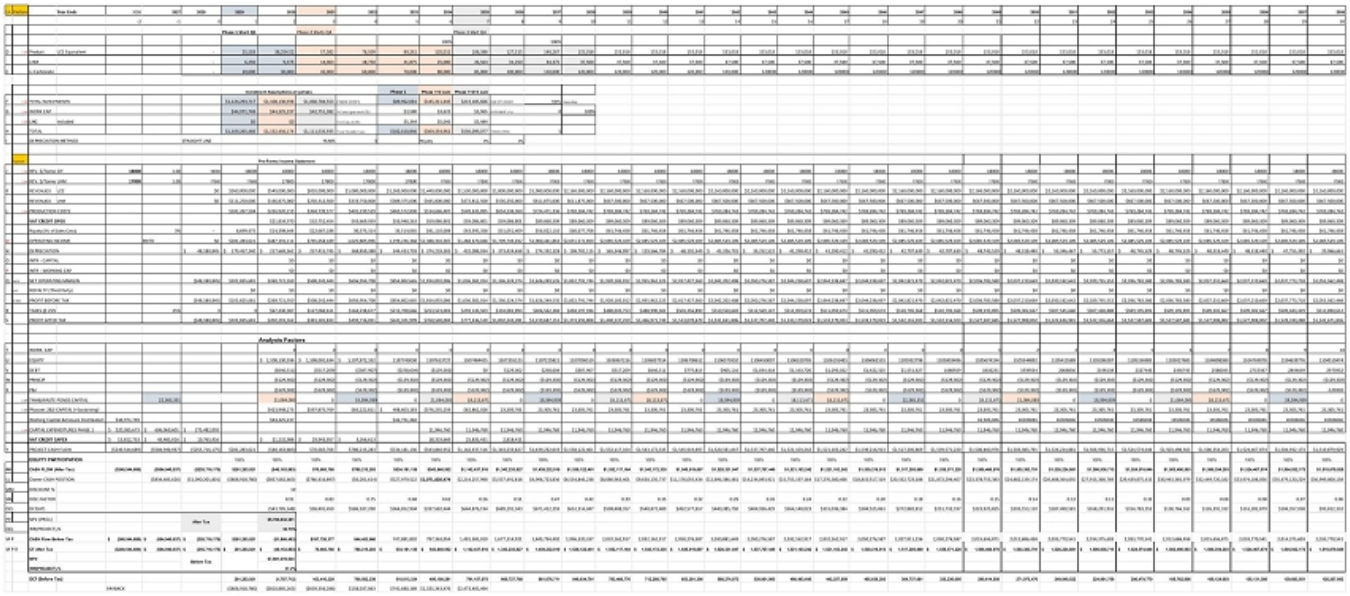

19.9 Economic Evaluation Results

The project is currently estimated to have a payback period of five years. The economic analysis indicates an after-tax Net Present Value (NPV), discounted at 10%, of approximately US$5.77 billion with an Internal Rate of Return (IRR) of approximately 32.7%.

The Project economics, resulting from the assumed commodity price scenario and discount rate used in the economic model, are presented in Table 141.

Table 141: Economic Evaluation – Base Case (including RIGI benefits)

Overview	Initial	W/Expansions
Production (LCE)	51,006	153,018
Capital Cost (CapEx)	$ 1,124,293,717	$ 3,301,209,207
Operating Cost (OpEx)	$ 272,572,927	$ 769,284,742
Average Selling Price LCE per ton	$ 18,000	$ 18,000
Average Selling Price LHM per ton	$ 17,800	$ 17,800
Annual Revenue	$ 942,500,000	$ 2,827,500,000
Discount Rate %	10	10
Net Present Value (NPV) Pre-Tax	-	$ 7,881,378,524
Internal Rate of Return (IRR) Pre-Tax	-	37%
Net Present Value (NPV) Post-Tax	-	$ 5,766,032,301
Internal Rate of Return (IRR) Post-Tax	-	32.7%

19.10 Sensitivity Analysis

A sensitivity analysis was conducted to illustrate the impact of changes in key variables on the Project's NPV and IRR (Table 142).

Sensitivity of NPV, IRR to OpEx increase and decrease from the Base Case is shown in Table 142.

Table 142: Sensitivity Analysis

Overview		Case 1 Base Case	Price -20%	Price -15%	Price +15%	Price +20%
Production (LCE)		100%	100%	100%	100%	100%
Capital cost (CAPEX)	US$	$ 3,301,209,207	$ 3,301,209,207	$ 3,301,209,207	$ 3,301,209,207	$ 3,301,209,207
Operating Cost (OPEX)	US$	$ 769,284,742	$ 769,284,742	$ 769,284,742	$ 769,284,742	$ 769,284,742
Av. Salling price LCE	US$/t LCE	18000	14400	15300	20700	21600
Discount rate	%	10%	10%	10%	10%	10%
NPV Post Tax	MMUS$	$ 5,766	$ 3,735	$ 4,243	$ 7,289	$ 7,797
IRR Post Tax	%	33%	26%	28%	37%	39%

Overview		Case 1 Base Case	OPEX -20%	OPEX -15%	OPEX +15%	OPEX +20%
Production (LCE)		100%	100%	100%	100%	100%
Capital cost (CAPEX)	US$	$ 3,301,209,207	$ 3,301,209,207	$ 3,301,209,207	$ 3,301,209,207	$ 3,301,209,207
Operating Cost (OPEX)	US$	$ 769,284,742	$ 615,427,794	$ 653,892,031	$ 884,677,454	$ 923,141,691
Av. Salling price LCE	US$/t LCE	18000	18000	18000	18000	18000
Discount rate	%	10%	10%	10%	10%	10%
NPV Post Tax	MMUS$	$ 5,766	$ 6,335	$ 6,193	$ 5,339	$ 5,197
IRR Post Tax	%	33%	35%	34%	31%	31%

Overview		Case 1 Base Case	CAPEX -20%	CAPEX -15%	CAPEX +15%	CAPEX +20%
Production (LCE)		100%	100%	100%	100%	100%
Capital cost (CAPEX)	US$	$ 3,301,209,207	$ 2,640,967,366	$ 2,806,027,826	$ 3,796,390,588	$ 3,961,451,049
Operating Cost (OPEX)	US$	$ 769,284,742	$ 769,284,742	$ 769,284,742	$ 769,284,742	$ 769,284,742
Av. Salling price LCE	US$/t LCE	18000	18000	18000	18000	18000
Discount rate	%	10%	10%	10%	10%	10%
NPV Post Tax	MMUS$	$ 5,766	$ 6,151	$ 6,055	$ 5,477	$ 5,381
IRR Post Tax	%	33%	38%	37%	30%	29%

After-Tax sensitivity of NPV and IRR to variations in CapEx, OpEx and Price is shown on Figure 215 and Figure 216.

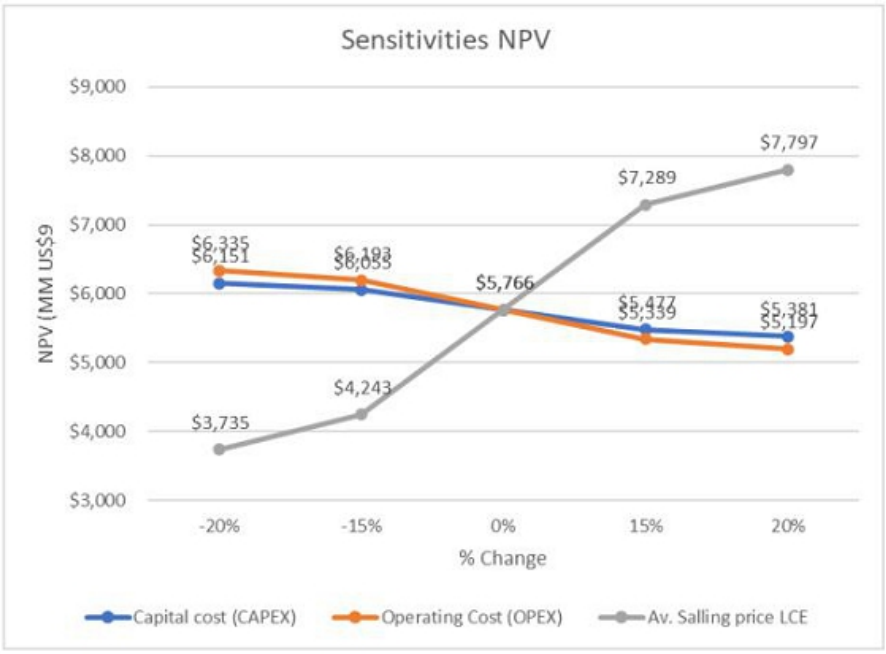

Figure 215: After-Tax NPV Sensitivity to CapEx, OpEx and Price Variation

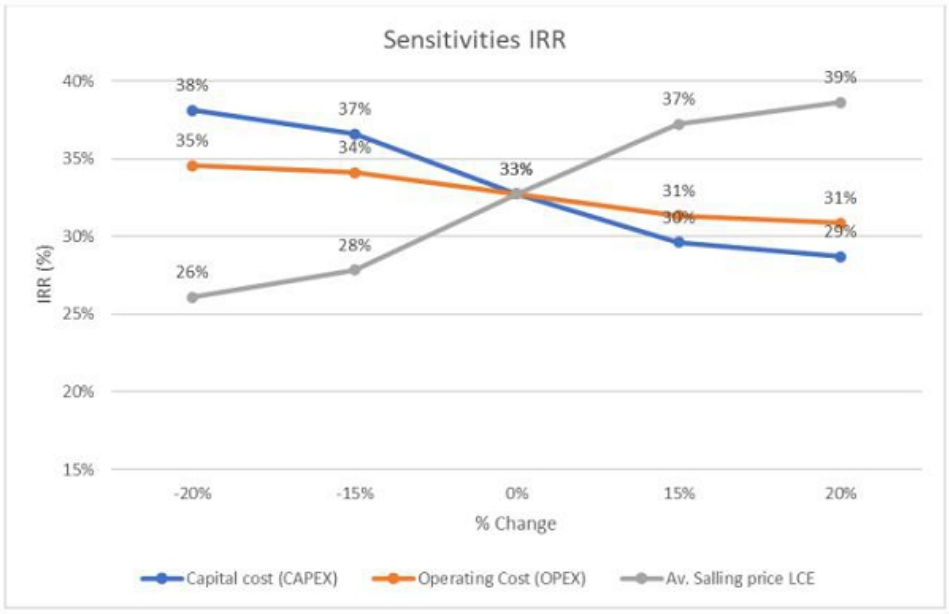

Figure 216: After-Tax IRR Sensitivity to CapEx, OpEx and Price Variation

The Project's IRR results are most sensitive to changes in product pricing. For this reason, the sensitivity of NPV and IRR to specific price scenarios has been evaluated and is presented in Table 143 and Figure 217.

Table 143: Sensitivity Analysis for Different Price Scenarios

Overview		Case 1 Base Case	Case 2 Price: 12 Kus$/t	Case 3 Price: 16 Kus$/t	Case 4 Price: 20 Kus$/t	Case 5 Disc. Rate 8%
Production (LCE)		100%	100%	100%	100%	100%
Capital cost (CAPEX)	US$	$ 3,301,209,207	$ 3,301,209,207	$ 3,301,209,207	$ 3,301,209,207	$ 3,301,209,207
Operating Cost (OPEX)	US$	$ 769,284,742	$ 769,284,742	$ 769,284,742	$ 769,284,742	$ 769,284,742
Av. Salling price LCE	US$/t LCE	18000	12000	16000	20000	18000
Discount rate	%	10%	10%	10%	10%	8%
NPV Post Tax	MMUS$	$ 5,766	$ 2,381	$ 4,638	$ 6,895	$ 8,057
IRR Post Tax	%	33%	21%	29%	36%	33%

Figure 217: Sensitivity Analysis for Different Price Scenarios

19.11 Discussion And Conclusions

Project economics resulting from assumed price scenario used in the economic model are presented in Table 141. A sensitivity analysis was conducted to illustrate the impact of changes in key variables on the Project's NPV and IRR (Figure 215 and Figure 216).

CapEx: Capital investment for the 153,000 TPA LCE Project, including equipment, materials, indirect costs and contingencies during the construction period is estimated to be US$3.301 billion before VAT. This total excludes interest expense that might be capitalized during the same period but includes owner's cost.

Main CapEx components are wells and pond construction and the Process plants, representing about 80% of total Project capital expenditures. Pond investment is driven by two variables, namely, evaporation rate, and pond construction unit cost.

OpEx: The operating cost for the 153,000 TPA LCE Project is estimated at US$769 million annually after phase 3 is in full production. This figure includes ponds and plants, chemicals, energy, labour, salt waste removal, maintenance, camp services, and transportation.

Sensitivity Analysis: Sensitivity analysis indicates that the Project is highly profitable.

Project strengths are as follows:

- Brine: The Project pumps subsurface brine to extract lithium, which is a proven and cost-effective method compared to hard rock mining.
- Lithium: The PPG Project has over 15,077,000 tons of measured and indicated (M+I) LCE resources, enough to support a production rate of 153,000 TPA LCE for a nominal 30-year life.
- Convenient accessibility and available utilization: The Project site is located 70 km away from energy pipeline. The flat and featureless ground over which the feeder pipeline is to be built reduces pipeline construction cost and complexity.
- Pricing Estimate: Sensitivity analysis indicates that the Project is economically viable even under unfavorable pricing conditions.
- Low operation costs.
- SX (DLE) strengths vs conventional process
- The application of RIGI results in a US$0.9 billion increase of NPV, compared with the case without RIGI, and an IRR improvement of 7.6%.

Some project risks list as follows:

- **Location:** Elevation: The Project site is at a high elevation, approximately 4,000 m above sea level, which can result in difficult work conditions for those not accustomed to high altitudes. Medical oxygen tanks are readily available for staff travelling to and working at the mine site.
- **Weather Dependence:** Unpredictable weather, including heavy rains and long winters in recent years, could affect the evaporation cycle in the ponds.
- **Process Implementation:** The process is specialized to the type of brine in the salar and there is no other industrial operation running the same process configuration. Mitigation measures include dedicated steps for removing impurities and purifying the solution.
- **Process System Design and Supplier Expertise:** Equipment and facilities are custom-designed for this unique process and the high-altitude, high-wind environment. Tests at additional suppliers and a pilot plant are recommended before placing equipment orders.

20.0 ADJACENT PROPERTIES

20.1 Other Properties in Pozuelos

There is one other tenements within the greater Pozuelos area. The borate mine named Mina San Mateo (file 64005) is located in the northeastern portion of the Pozuelos. According to the Land Registry Records Office (March-2022), Mina San Mateo is owned by Minera Santa Rita, which is a holding group dedicated to the extraction, production and international marketing of borates, that operates the property intermittently.

Figure 218 illustrates the location of the Mina San Mateo tenements relative to the PPG tenements.

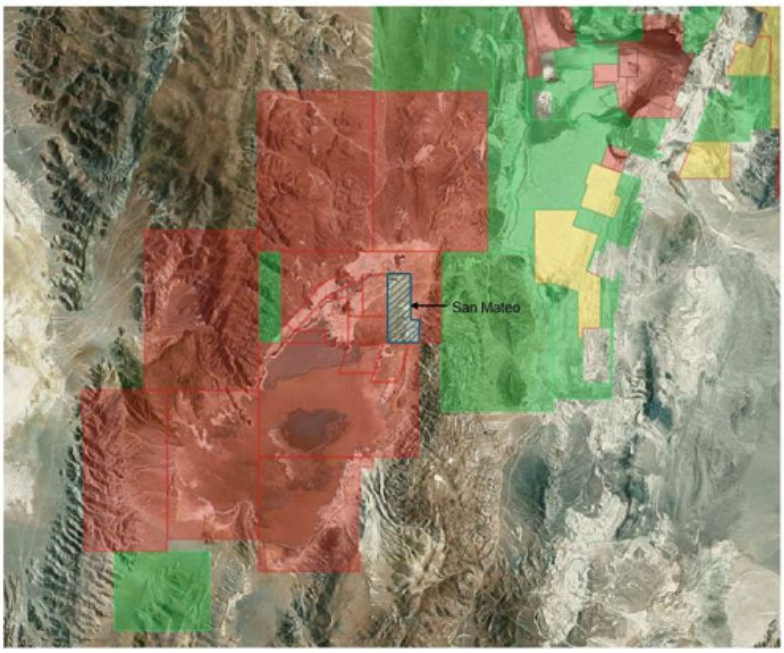

Figure 218: San Mateo Property in Pozuelos (Source: Ganfeng 2024)

20.2 Other Properties in Pastos Grandes Salar

Third-party ownership of mining properties in the vicinity of the Project is shown in Figure 219. Third-party owners include Ganfeng Lithium Co dedicated to lithium production and Borax Argentina S.A. and ULEX S.A focused on borates production.

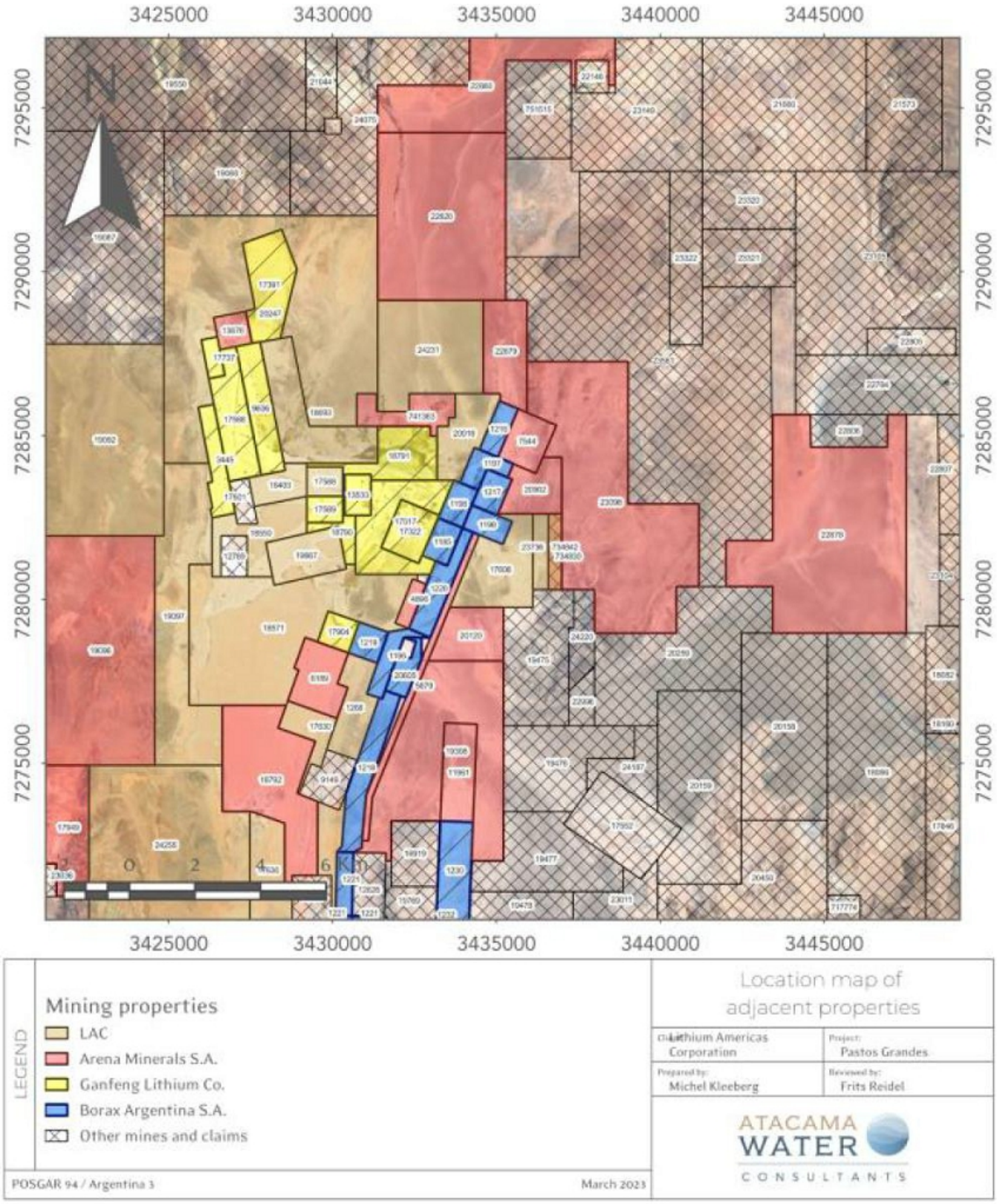

Figure 219: Other Properties in Pastos Grandes Salar (Source: AW, 2023)

21.0 OTHER RELEVANT DATA AND INFORMATION

21.1 Project Schedule

A Level 3 Project Schedule has been prepared considering main project activities (Figure 220). Production can start Q1 2029, however, it assumes that detailed design is completed by Q1 2027, procurement by H2 2026 and construction Q2 2028.

The schedule and the project management plans will be developed together, for the next phase of the Project. Information provided by Ganfeng and its engineering consultants have been utilized to determine the project schedule. The activities and tasks included in the schedule could be conducted in parallel.

The schedule considers government requirements, availability of key resources, project management information systems, and development plans. It follows Argentinean regulations and includes consideration of productivity factors, weather conditions, seasons, etc. The schedule assumes that sufficient workforce and equipment are available to accomplish the activities as scheduled.

From 2026 through 2028, the following activities will be carried out:

- Detailed engineering design
- Definition and negotiation/finalization of construction and installation contracts.
- Acquisition of major equipment and materials
- Completion of camp construction
- Construction of the pre-concentration ponds
- Construction of processing plants (Phase 1) and facilities
- Installation of pumping wells and construction of wellfield (Phase 1)

21.2 Management of Depleted Brine

Options for the management of depleted brine discharge from the PPG process plants include:

- Evaporation facilities (ponds)
- Infiltration through trenches and/or gravity wells
- Reinjection

Initial work on the feasibility of evaporation ponds and infiltration infrastructure to manage 167 L/s of depleted brine discharge has been started in both the Salar de Pozuelos during 2024 and included:

- Selection of potential suitable site for infiltration through trenches or gravity wells
- Preliminary estimates of infiltration rates and long-term infiltration capacity of each site
- Analytical modelling of mounding using MOUNDSOLVE software
- Evaluation of potential impact from infiltration on the Mineral Reserves dilution using the existing Pozuelos FeFlow model.
- Evaluation of infiltration to mitigate drawdown from the brine abstraction.

It is planned that future infiltration test work including pilot scale testing will be continued during 2026/2027 to evaluate the feasibility of the most suitable options for the management of the depleted brine stream.

	Name	Duration	Start	Finish
1	FS 43101	30 d	4/1/25, 08:00	5/12/25, 17:00
2	EIA Approval	6 mo	5/27/25, 08:00	11/10/25, 17:00
3	Finalize Agreements	34 d	10/30/25, 08:00	12/16/25, 17:00
4	Prueba completada	44 d	10/30/25, 08:00	12/30/25, 17:00
5	**Detailed Engineering**	**16.95 mo**	**12/17/25, 08:00**	**4/5/27, 17:00**
6	Wells Design and Roads	4 mo	12/17/25, 08:00	4/7/26, 17:00
7	Pre-concentration Ponds	6 mo	12/17/25, 08:00	6/2/26, 17:00
8	Early infrastructure, roads, services	3 mo	12/17/25, 08:00	3/10/26, 17:00
9	Solvent Extraction Plant	6 mo	12/17/25, 08:00	6/2/26, 17:00
10	Purification Plants	4 mo	12/22/25, 08:00	4/10/26, 17:00
11	Salar main access roads	3 mo	1/20/26, 08:00	4/13/26, 17:00
12	Water Infrastructure	12 mo	5/5/26, 08:00	4/5/27, 17:00
13	Salts disposal areas (TMA)	4 mo	2/11/26, 08:00	6/2/26, 17:00
14	Electrodialysis Plant	8 mo	12/24/25, 08:00	8/4/26, 17:00
15	Purification 2 Plants	7 mo	12/24/25, 08:00	7/7/26, 17:00
16	Lithium Hydroxide Plant	8 mo	1/20/26, 08:00	8/31/26, 17:00
17	Lithium Carbonate Plant	10 mo	1/26/26, 08:00	11/3/26, 17:00
18	Buildings, services, etc.	4 mo	9/1/26, 08:00	12/21/26, 17:00
19	Almacen	4 mo	1/20/26, 08:00	5/11/26, 17:00
20	Brine piping and electrical	7 mo	8/5/26, 08:00	2/16/27, 17:00
21	**Procurement and Contracts**	**17.2 mo**	**10/30/25, 08:00**	**2/23/27, 17:00**
22	Drilling Contract	2 mo	12/30/25, 08:00	2/23/26, 17:00
23	Ponds Contract	3 mo	10/30/25, 08:00	1/21/26, 17:00
24	Main Plants equipment	4 mo	2/11/26, 08:00	6/2/26, 17:00
25	Additional Equipment Plants	4 mo	11/4/26, 08:00	2/23/27, 17:00
26	Foundations Contract Plants	2 mo	10/30/25, 08:00	12/24/25, 17:00
27	Buildings Contract	3 mo	10/30/25, 08:00	1/21/26, 17:00
28	Electrical Line Contract	3 mo	10/30/25, 08:00	1/21/26, 17:00
29	Installation Contracts Plants	4 mo	9/1/26, 08:00	12/21/26, 17:00
30	LNG Gasification Contract	1 mo	10/30/25, 08:00	11/26/25, 17:00
31	**Construction**	**26.55 mo**	**6/30/26, 08:00**	**7/11/28, 17:00**
32	Early Works	12 mo	6/30/26, 08:00	5/31/27, 17:00
33	Wells Drilling	25 mo	6/30/26, 08:00	5/29/28, 17:00
34	Preconcentration Ponds and Piping	24 mo	6/30/26, 08:00	5/1/28, 17:00
35	Extraction Plants	22 mo	7/29/26, 08:00	4/4/28, 17:00
36	Purification Plants	19 mo	7/1/26, 08:00	12/14/27, 17:00
37	Brine Piping and Electrical	17 mo	6/30/26, 08:00	10/18/27, 17:00
38	Salar infrastructure electrical substation, transformers, power line	15 mo	6/30/26, 08:00	8/23/27, 17:00
39	Water Supply	5 mo	4/6/27, 08:00	8/23/27, 17:00
40	Brine wells and piping	18 mo	6/30/26, 08:00	11/15/27, 17:00
41	Salts residues areas (TMA) and piping	16 mo	6/30/26, 08:00	9/20/27, 17:00
42	Truck shop, office buildings, services etc.	6 mo	9/1/26, 08:00	2/15/27, 17:00
43	Electrodialysis Plants	18 mo	2/24/27, 08:00	7/11/28, 17:00
44	Lithium Hydroxide Plants	15 mo	2/24/27, 08:00	4/18/28, 17:00
45	Lithium Carbonate Plant	17 mo	2/24/27, 08:00	6/13/28, 17:00
46	Ponds Commissioning	8 mo	5/2/28, 08:00	12/11/28, 17:00
47	Plants Commissioning and startup	6 mo	8/25/28, 08:00	2/8/29, 17:00

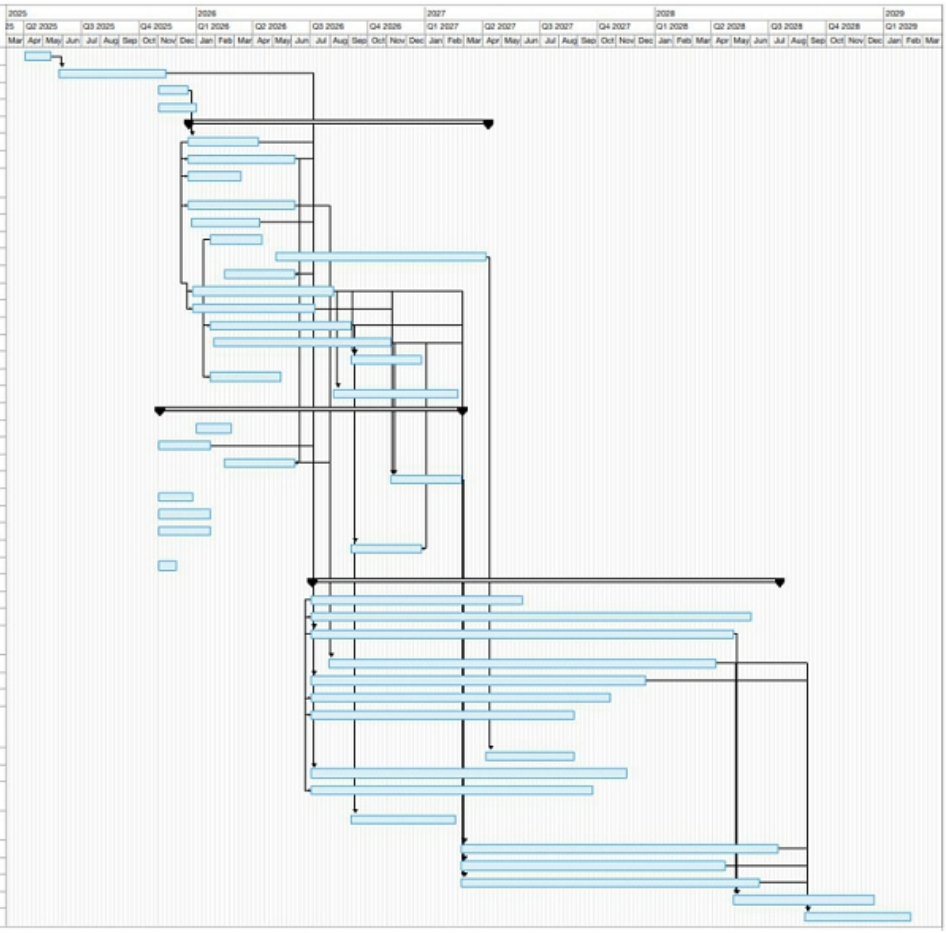

Figure 220: Project schedule for 3 Phases

22.0 CONCLUSIONS AND RECOMMENDATIONS

22.1 Geology and Mineral Resources

Evaluation of the exploration programs and results as of the effective date of this report indicate the following:

- The geological setting is sufficiently well understood to support the estimation of mineral resource presented in this report.
- The database includes all relevant drilling data collected to date and has been structured for resource estimation.
- QA/QC with respect to the results received for exploration programs to date is acceptable and protocols have been sufficiently documented.
- As of December 31, 2025, the Pozuelos deposit is estimated to contain a Measured and Indicated (M+I) resource of 7.02 million tonnes of LCE at an average grade of 510 mg/L, with the cutoff grade of 125 mg/l applied.
- As of December 31, 2025, the Pastos Grandes salar deposit (including SdlP) is estimated to contain a Measured and Indicated (M+I) resources of 7.56 million tonnes LCE at an average grade of 332 mg/L, with the cutoff grade of 125 mg/l applied.
- An FoB price forecast of US$18,000 per metric ton of Li_2CO_3 and US$17,800 per metric ton of coarse particle $LiOH \times H_2O$ for years beyond 2028 is used. A 75% overall lithium recovery efficiency factor has been applied to calculate the final LCE production.
- The PPG salars contain adequate lithium mineral resources to develop an extraction operation and supply a brine for a period of at least 30 years.

22.2 Hydrologic Dynamic Modelling

22.2.1 Pozuelos

In September 2024, Atacama Water Consultants completed the simulation of brine abstraction (960 L/s) from Pozuelos to support an annual production of 50,000 TPA LCE over a 20-year project life, evaluation of water level declines during the operation and water levels recoveries after the operation ceases, and evaluation of the effects of depleted brine infiltration (148 l/s) on lithium concentrations and LCE production targets.

The updated model was built on Ganfeng's original FEFLOW model (spz_reserves_model_2024.fem), prepared in FEFLOW 8.0 and was a single-density flow-and-lithium-transport model designed to produce a preliminary dynamic model with and without planned infiltration schemes.

These preliminary models show that, with the conceptual values of hydraulic conductivity, specific yield, and lateral recharge, the proposed total brine pumping rate of 960 L/s for a period of 20 years appears to be feasible.

The preliminary run suggests that the freshwater well locations may not be sufficient to meet the 24 L/s of freshwater required for the project which will have to be sourced from Pastos Grandes. With 960 L/s of total brine extraction, the model predicts drawdowns of greater than 80 m in areas, with an average drawdown on the order of 26 m at the end of operations. The modelling shows that changing the pumping rates at individual wells or including infiltration of 148 L/s (modelled as reinjection) can reduce the drawdown in local areas within the Salar. The infiltration can also improve freshwater capture by reducing drawdown along the Salar margins. The modelling shows that applying infiltration to the Pozuelos does not significantly affect the simulated brine production.

The recovery after operations model predicts approximately 57% recovery by 10 years after the end of operations and 90% recovery by 20 years after the end of operations. The simulated water table recovery after the end of operations is fastest in the south, followed by the north and Salar margins. The low-permeability halite in the center of the Salar is predicted to recover more slowly that the other areas. However, if there is any direct precipitation onto the Salar, this area could recover more quickly than modelled.

Hydrologic modelling estimates at Pozuelos as of September 2024 is presented in Table 69 in Section 0.

Note that updated resources estimate at Pozuelos (as of February 2025, see Chapter 14) has not been reflected in the September 2024's dynamic modelling work.

The next phase of modelling should include a calibration phase and some model adjustments to improve the numerical stability of the solutions. Although subject to a different set of potential challenges, a variably saturated configuration would be beneficial to address some of the numerical problems of the current model, including the difficulty of accurately simulating the gravity Infiltration wells and the challenge of introducing lateral recharge when the simulated water table dropped into the lower-permeability bedrock.

The next phase of modelling should also include an uncertainty analysis to explore the influence of model assumptions on the reserve estimate.

The improved model can be used to assess an optimization of the well field, including well location and pumping rates.

22.2.2 Pastos Grandes Salar

A numerical groundwater flow and transport model have been developed in December 2024 for the Pastos Grandes Salar. The modelling work was carried out by DHI in Lima, Peru under close supervision of Atacama Water and the QP.

The numerical model, calibrated to steady state and transient flows and heads, was used to simulate brine extraction over a 20-year period. The simulation utilizes transient groundwater flow and lithium mass transport beginning with the initial steady state head distribution and the initial lithium concentration distribution from the brine resource estimate. The analysis assumes an overall efficiency of 75% to estimate the LCE production. A freshwater wellfield with a total flow rate of 150 L/s (10 wells) is included in the simulation enough to source Phase I and II of the Project.

The brine wellfield production rate is 977 L/s for a period of 20 years, distributed among 47 production wells with a constant rate varying between 7 L/s and 25 L/s.

The model simulations predict that 1,395 kt of LCE is contained in the brine pumped to the evaporation ponds over the 20-year period, resulting in a final LCE plant production of 1,045 kt considering a 75% overall lithium recovery efficiency. The yearly average over the 20-year period is 52.3 kt/year. The average lithium concentration is predicted to range between 435 mg/l and 415 mg/l. Dynamic model results at PG as of December 2024 are presented in Table 75 and 78 in Section 11.5.

22.3 Mining Method

The brine extraction well fields will be located within the respective Salars and will be accessible by interconnected roads. The production process starts when brine is pumped from the aquifers beneath the Salars, using electrical pumps, placed in bores (wells) that are completed in the Salars. The extracted brine is pumped from each well to a main distribution pipeline and then to the evaporation ponds.

Phase 1 of the project will include the installation and operation of a brine production wellfield comprising 34 production wells, while Phases 2 and 3 will include 60 and 61 wells respectively including spares and redundant wells. The brine production wells will have a 12 in-diameter stainless steel production casing and be equipped with 380V submersible pumping equipment. The well depth will vary from 420 m to 640 m for the different phases of the project.

Brine production wells are designed for the three Phases of production to obtain approximately 51,000 TPA LCE of each phase.

A total of about 8,000 m^3/h of raw brine feed is the design rate to support a lithium carbonate production of 51,000 TPA LCE for each phase.

Based on the operational experience of similar installations, wells availability of 80-90% can be achieved.

The power to each pump and to the well field will be delivered via a medium voltage power line. The brine feeding to solar evaporation ponds is transported by pipelines to a series of solar evaporation ponds, for each phase.

The detailed well field design is consistent with the hydrogeological characteristics of mineralized zone.

The extraction plan includes a suitable estimate for hydraulic control pumping.

22.3.1 LCE Production Schedule

The project will have the capacity to produce 153,000 TPA LCE of Li_2CO_3 and $LiOH \times H_2O$, and it is planned to be developed and constructed in 3 Phases, each with a capacity of approximately 51,000 TPA LCE:

- **Phase 1:** 40,000 TPA Li_2CO_3 + 12,500 TPA $LiOH \times H_2O$
  - Brine from Pozuelos
  - 34 wells planned in Pozuelos
  - Starting production: Q1 2029
- **Phase 2:** Additional 40,000 TPA Li_2CO_3 + 12,500 TPA $LiOH \times H_2O$
  - Brine from Pastos Grandes
  - 60 wells in Pastos Grandes planned
  - Starting production: Q4 2031
- **Phase 3:** Additional 40,000 TPA Li_2CO_3 + 12,500 TPA $LiOH \times H_2O$
  - Brine from Pastos Grandes + Sal de la Puna + Pozuelos
  - 61 wells in Pastos Grandes + Sal de la Puna planned
  - Starting production: Q4 2035

The QPs are comfortable with using 37% of measured and indicated (M+I) resources for production planning. It is common to apply 37% of aquifer efficiency factor to measured and indicated resources to estimate pumpable resources for mine life planning in the lithium brine industry. The predictive groundwater flow and transport model simulations carried out for Pozuelos and Pastos Grandes support that the application of the 37% efficiency factor is reasonable.

Table 144 shows that, if only M+I resources are included and 37% of M+I resources are considered pumpable, the PPG Project has a nominal production life of 30 years for Phase 1, 28 years for Phase 2, and 24 years for Phase 3. It is planned that all 3 phases will end in the same year. A 75% overall lithium recovery efficiency factor has been applied to calculate the final LCE production. The recovery is based on test work carried out to date and assumptions provided by Ganfeng.

Table 144: LCE Production Schedule

	M+I	Pumpable**	Recovered*	Phase 1 @ 30 years (consumed)	Phase 2 @28 years + (consumed)	Phase 3 @ 24 years (consumed)	Remaining resources
Unit	**(kt, LCE)**	**(kt, LCE)**	**(kt, LCE)**	**(kt, LCE)**	**(kt, LCE)**	**(kt, LCE)**	**(kt, LCE)**
Pozuelos	7,017	2,596	1,947	1,492	-	387	68
Pastos Grandes	7,563	2,798	2,099	-	1,345	754	-

Note:

1. *Units: k (1,000) tons LCE.*
2. ** An overall recovery rate of 75% is used for all phases.*
3. *** Assuming 37% of M+I resources can be pumped out and go into production.*
4. *Annual production rate of ~51,000 TPA of LCE is assumed for each phase (40,000 TPA of Li_2CO_3 plus 12,500 TPA of $LiOH \times H_2O$).*

22.4 Process Information and Design

The plant is to produce 40,000 TPA of lithium carbonate and 12,500 TPA of lithium hydroxide monohydrate starting from brine extraction at the Salars de Pozuelos and Pastos Grandes sites. The brine will be concentrated to approximately 3 g/L Li by standard solar evaporation ponds. A lithium carbonate equivalent (LCE) of 51,000 TPA will be produced for each of the three phases planned for a total of 153,000 TPA LCE at the end of the third phase.

Process engineering and design for the ponds and the process plants were completed by Santiago, Chile based Adinf and Jiangxi, China based Ganfeng Lithium, respectively, based on their respective experience and test work results.

The construction of the PPG Lithium Plant will be in three stages. Each stage (phase) is designed to process 3,383,884 m^3/y of pre-concentrate brine feed, to produce 51,000 TPA battery grade Li_2CO_3 equivalent.

The use of recycle streams generating from the electrodialysis plant serves also the purpose of decreasing dependence from purchasing additional caustic and hydrochloric acid.

Phases 2 and 3 involve adding duplicate process trains, to be constructed for production in Years 4 and 8, to treat for a combined production total of 153,000 TPA LCE, at the end of the last phase.

22.4.1 Process Description

The main activities involved include:

- Pre-concentration of the brine
- Solvent extraction
- Raffinate treatment

- Primary purification
- Secondary purification
- Lithium Hydroxide and Lithium Carbonate processing

Extraction of brine from wells is the first step to provide the feed for the ponds. The brine wells are located within the above mentioned salar, and the brine is transported by surface run pipelines to a series of solar evaporation ponds (pre-concentration ponds), which are also located within the salar.

After the brine is concentrated to approximately 3 g/L lithium in the ponds, it's sent to solvent extraction circuits where lithium is selectively extracted and concentrated to 19 g/L.

22.4.2 Solar Evaporation Ponds

The pre-concentration pond systems are divided into four (4) independent strings each with 8 areas. Once the brine reaches the target lithium concentration, it is pumped to a Buffer-pond for storage, from where it will be transferred to the processing plant designed to process 11,635 tons per day of brine at 0.246% Li over 300 days operating time, for each of the 3 Phases of production.

The crystallized salts, mainly sodium chloride, are collected (harvested) every 1 to 2 years to maintain the appropriate volume capacity of the ponds. For this purpose, typical earthmoving machinery will be used, such as bulldozers, front-end loaders, and dump trucks.

All waste salts will be discharged to a Tailing Management Area (TMA) located on the salar.

22.4.3 Brine Processing

The lithium in concentrated brine is extracted by a solvent, and transferred into a rich LiCl solution with a concentration of 19 g/L.

The process consists of a three-step solvent extraction cycle: extraction, washing and stripping. There will be 5 production lines with a capacity of ~10,000 TPA each, thus completing a production of 51,000 TPA LCE.

The lithium rich solution from solvent extraction undergoes primary and secondary purification steps designed to remove excess boron and calcium and CO_2 removal. The purified and adjusted stream is split and sent to the lithium carbonate plant and the membrane electrodialysis plant to produce the lithium hydroxide feedstock. Lithium hydroxide monohydrate is obtained after further evaporation and crystallization while lithium carbonate is produced with the conventional process by addition of soda ash.

22.4.4 Evaluation of Process Configurations and Final Product Optionality

Different process configurations are being evaluated with the objective of optimizing the balance between plant operability, the supply of critical reagents, and the project's technical-economic risk profile. In particular, this analysis focuses on the strategic definition of the final product and the sourcing of reagents such as HCl and NaOH. Currently, three main alternatives are under consideration to be defined in the next study phase:

- **Maintain the current process scheme**, with a bipolar membrane electrodialysis plant for the production of lithium hydroxide (LiOH), which would also enable internal generation of HCl.
- **Implement a scheme with lower integration**, in which reagents are supplied by third parties, focusing production on battery-grade lithium carbonate and avoiding the installation of a LiOH production plant.

- **Evaluate the incorporation of an electrolysis plant** for internal generation of HCl and NaOH, based on proven technology, as an alternative to installing a lithium hydroxide (LiOH) production plant.

This approach enables adjustment of the project scope based on market conditions, feedstock availability, and risk assessment, while keeping both pathways open until the studies are completed and the final base case is defined.

22.5 Evaluation of Energy Supply Alternatives

The current base case for the project considers energy supply through liquefied natural gas (LNG) and electricity sourced from the grid. In parallel, an alternative is being assessed that involves self-generation using renewable energy sources, primarily through the installation of a photovoltaic solar plant.

The objective of this evaluation is to reduce the risk of external energy dependency, improve the environmental performance of the asset by reducing CO_2 emissions, and assess the economic benefits associated with lower OpEX.

The final decision regarding the energy supply scheme will be made upon completion of comparative studies between the alternatives and any other configurations that may arise during the analysis process.

22.6 Closure and Reclamation Plans

Closure and reclamation for the PPG Project have followed legislative requirements and best practice guidance. The legislative requirements for mine closure were outlined under Law 7070 and Decree 3097/00 (as amended by Decree 1587/03) in Salta Province.

A conceptual mine closure plan was included in both the Pozuelos and Pastos Grandes IIAs (Initial Investment Analysis).

On completion of mining operations at the PPG Project, Ganfeng and LAR are committed to restoring the area to its pre-mining use state where practical and applicable. For the purposes of this study, the QPs conservatively estimated closure costs by applying a 5% factor to initial CapEx. The closure costs are included in the sustaining CapEx in the technical economics model for the project.

We recommend a detailed mine closure plan within the next 5 years. Development of a mine closure plan is not a one-time event but a continuous process, evolving from a conceptual stage during project development to a detailed plan during operations.

22.7 Economic Analysis

The analysis was prepared using an economic model and assesses both before-tax and after-tax cash flow scenarios. Capital (CapEx) and Operational (OpEx) Expenditures presented in previous sections have been used in this analysis. Prices for Lithium carbonate and hydroxide was estimated by Golder. The results include Net Present Values (NPV) for 10% discount rate, Internal Rate of Return (IRR) and sensitivity analysis of key inputs.

The following criteria have been used to develop the economic model:

- Project life: Life of mine (including construction and operation) is estimated to be 33 years.

- Pricing for lithium carbonate of US$18,000 and LHM (lithium hydroxide monohydrate) of US$17,800 per ton was used.
- Final production rate of 153,000 TPA LCE after all three phases of production reach full operation 9 years after the start of phase 1.
- Discounted Cash Flow (DCF) analysis was based upon scheduling of the currently available measured and indicated (M+I) resources with the assumptions that 37% of M+I resources is pumpable as brine feed to the evaporation ponds and an overall lithium recovery efficiency of 75%. A cut-off grade of 125 mg/l has been applied to the mineral resource estimates.
- A discount rate of 10% was used.
- The Discounted Cash Flow (DCF) economic evaluation was carried out on a constant money basis so there is no provision for escalation or inflation on costs or revenue.
- For DCF evaluation purposes, it has been assumed that 100% of capital expenditures, including pre-production expenses, are financed with owners' equity.
- Pre-construction costs are not included in DCF analysis.
- VAT is included for both CapEX and Opex.
- Lithium grades and recoveries stay constant for 30 years with no dilution.
- The key inputs to the economic analysis are shown in Table 138.

CapEx: Capital investment for the 153,000 TPA LCE Project, including equipment, materials, indirect costs and contingencies owner's cost, and VAT has been estimated to be US$3.301 billion**.**

Main CapEx components are wells and pond construction and the Process plants, representing about 80% of total Project capital expenditures. Pond investment is driven by two variables, namely, evaporation rate, and pond construction unit cost.

OpEx: The operating cost for the 153,000 TPA Project is estimated at US$769 M annually after phase 3 is in full production. This figure includes ponds and plants, chemicals, energy, labour, salt waste removal, maintenance, camp services, and transportation.

Sensitivity Analysis: Sensitivity analysis indicates that the Project is highly profitable.

Project strengths are as follows:

- Brine: The Project pumps subsurface brine to extract lithium, which is a proven and cost-effective method compared to hard rock mining.
- Lithium: The PPG Project has over 15,077,000 tons of measured and indicated (M+I) LCE resources, enough to support a production rate of 153,000 TPA LCE for a nominal 30-year life.
- Convenient accessibility and available utilization: The Project site is located 70 km away from energy pipeline. The flat and featureless ground over which the feeder pipeline is to be built reduces pipeline construction cost and complexity.
- Pricing Estimate: Sensitivity analysis indicates that the Project is economically viable even under unfavorable pricing conditions.
- Low operation costs.
- SX (DLE) strengths vs conventional process.

- The application of RIGI results in a US$0.9 billion increase of NPV, compared with the case without RIGI, and an IRR improvement of 7.6%.

The following Project weaknesses are also identified:

- The Project location presents certain challenges. As with most salar, the Project is located above 3,800 masl. This elevation can be difficult for some workers. Location disadvantages have been partially addressed by moving some of the operating facilities to a lower altitude.
- Difficulty for owners to construct the Project in a timely fashion.

22.8 Project Risks

The key aspects of the project presenting most execution risk is described in following sections.

22.8.1 Process Plant

The chemical process utilized for treating the brine is unique and proprietary and may present challenges in the following areas:

The solvent utilized to contact the brine may not be as selective for lithium and more impurities may end up in the strip product which will require additional reagents to remove the said impurities to the meet the specification for battery grade products particularly for lithium hydroxide.

Several recycle streams are noted to be an integral part of the process making lithium hydroxide. Although such recycles in some cases decrease dependence from purchasing additional chemicals (namely caustic and hydrochloric acid) nonetheless may present a problem when such circuits do not operate at design or are inoperable.

22.8.2 Infrastructure

The FS study has shown that the infrastructure required for the project can be delivered. The key aspects of the project presenting most delivery risk for the infrastructure is:

- Further geotechnical and topography work needs to be completed in PG to select the best pond locations
- Additional infiltration/shallow injection of spent brine preliminary and pilot tests would help to reduce costs and derisk these disposal techniques
- Successful finalization of contracts for the power stations and electrical lines. A delay will also delay the completion of the project, particularly commissioning, or have a detrimental economic impact if alternate power and fuel sources need to be secured.
- Electrical loads need reconfirming prior to finalization of contracts being finalized in the event any change in electrical demand.
- Securing of the water supply for a yet to be determined water pipeline route. If sufficient water cannot be secured it can reasonably be expected to delay the execution of the project unless a design change occurs. This may have a detrimental cost impact and may result in additional permitting requirements
- Securing of land access and permits for the bore field. An inability to secure access to water can be expected to cause significant delays.

22.8.3 Environmental

Work to-date has demonstrated that project can expect to receive all necessary environmental permits and licenses. The key risks that may impact the project include:

- Delay of water rights approval to the project may delay the start of operations.
- There is sufficient time for an application to be submitted, and approved, prior to construction.

22.8.4 Time to Market (Schedule)

- The schedule for construction and operation of the project is considered “fast track” and quite aggressive as it assumes that the materials procurement is implemented without any delays and that the plants start-up will occur in accordance with the ramp-up provided herein.
- There is a risk of delays both in procurement and production which will push the schedule by several months which will impact the presented cash flow negatively.

22.8.5 Others

- **Location:** Elevation: The Project site is at a high elevation, approximately 4,000 m above sea level, which can result in difficult work conditions for those not accustomed to high altitudes. Medical oxygen tanks are readily available for staff travelling to and working at the mine site.
- **Weather Dependence:** Unpredictable weather, including heavy rains and long winters in recent years, could affect the evaporation cycle in the ponds.
- **Process Implementation:** The process is specialized to the type of brine in the salar and there is no other industrial operation running the same process configuration. Mitigation measures include dedicated steps for removing impurities and purifying the solution.
- **Process System Design and Supplier Expertise:** Equipment and facilities are custom-designed for this unique process and the high-altitude, high-wind environment. Tests at additional suppliers and a pilot plant are recommended before placing equipment orders.

23.0 REFERENCES

Allmendinger, R.W., Jordan, T.E., Kay, S.M., and Isacks, B.L., 1997, The evolution of the Altiplano-Puna plateau of the Central Andes: Annual review of earth and planetary sciences, v. 25, p. 139–174.

Antoine Lefaivre, Lawrence D. Henchel, Report for LCS Lithium – Preliminary Economic Assessment (PEA) – Pozuelos – Pastos Grandes Project, GHD Chile, January 2019.

Benson, T.R., Boutt, D., Butler, K.L., Deshong, T., Gibbons, L., Hatton, K., Jenckes, J., McCaffrey, O., Mesbah, N., Munk, L.A., Rasbury, T., Seggiaro, R., Villagrán, A. and Wooton, K., 2026. The timing and origin of lithium brine deposits in the central Andean Mountains. Geology, [under review].

Canadian Institute of Mining, Metallurgy and Petroleum (CIM), 2012: Best Practice Guidelines for Resource and Reserve Estimation for Lithium Brines.

Canadian Institute of Mining, Metallurgy and Petroleum on the Valuation of Mineral Properties (CIMVAL), by CIM Council on November 20, 2019.

Canavan, R.R., Carrapa, B., Clementz, M.T., Quade, J., DeCelles, P.G., and Schoenbohm, L.M., 2014, Early Cenozoic uplift of the Puna Plateau, Central Andes, based on stable isotope paleoaltimetry of hydrated volcanic glass: Geology, v. 42, p. 447–450.

Carrapa, B., Huntington, K.W., Clementz, M., Quade, J., Bywater-Reyes, S., Schoenbohm, L.M., and Canavan, R.R., 2014, Uplift of the Central Andes of NW Argentina associated with upper crustal shortening, revealed by multiproxy isotopic analyses: Tectonics, v. 33, p. 1039–1054.

Carrapa, B., Trimble, J.D., and Stockli, D.F., 2011, Patterns and timing of exhumation and deformation in the Eastern Cordillera of NW Argentina revealed by (U-Th)/He thermochronology: Tectonics, v. 30.

Chen, J., Kufner, S., Yuan, X., Heit, B., Wu, H., Yang, D., Schurr, B., and Kay, S., 2020, Lithospheric delamination beneath the southern Puna plateau resolved by local earthquake tomography: Journal of Geophysical Research: Solid Earth, v. 125, p. e2019JB019040.

De Silva, S., Zandt, G., Trumbull, R., Viramonte, J.G., Salas, G. and Jiménez, N., 2006. Large ignimbrite eruptions and volcano-tectonic depressions in the Central Andes: a thermomechanical perspective. Geological Society, London, Special Publications, v. 269, p. 47-63.

Frits Reidel, Lithium Resources Update, Pastos Grandes Project Salta Province, Argentina NI 43-101 Report prepared for Lithium Americas Argentina Corp, 2023.

Frits Reidel, Rodrigo Uribe, RE: Pastos Grandes Updated Mineral Resource Estimate, Atacama Water, August 15, 2024.

Frits Reidel, Jean Cho, Carolina Gomez, Technical Memorandum of Evaluation of Salar de Pozuelos Groundwater Flow and Transport Model, Atacama Water, 13 September 2024.

Frits Reidel, CPG, NI 43-101 Technical Report, Lithium Resources and Reserves for Pastos Grandes Phase 2 Project, Salta Province, Argentina, by Atacama Water, December 15, 2024.

Ganfeng, Process Design Report for LMA 40kt LCE & 12.5 kt $LiOH \times H_2O$, 14 September 2024.

Ghosh, P., Garzione, C.N., and Eiler, J.M., 2006, Rapid uplift of the Altiplano revealed through 13C-18O bonds in paleosol carbonates: Science, v. 311, p. 511–515.

Hains, D.H., Foutie, L.F. Technical Report on Pastos Grandes Project. Prepared for LCS Lithium Corporation. Dated October 25, 2018.

Hardie, L.A. y Eugster, H.P. 1970. The evolution of closed-basin brines. Mineralogical Society of America, Special Paper 3: 273-290, New York.

Houston, J. 2006. Evaporation in the Atacama Desert: An empirical study of spatio-temporal variations and their causes. Journal of Hydrology, 330(3-4), 402-412.

Lithium Argentina, New Conceptual Geological Models for PZ and PG, Jan 2025

LIENPZ-0000-GE-MDC-001_B General Description Memo

Montgomery & Associates (M&A), Salar de Pastos Grandes Water Balance. Pastos Grandes Project, Salta, Argentina. Prepared for Millennial Lithium Corp, 2018.

Montgomery & Associates (M&A), Phase III, Measured, Indicated, and Inferred Lithium and Potassium Resource Estimate, Pastos Grandes Project, Salta Province, Argentina. Report NI 43-101 prepared for Millennial Lithium Corporation, 2019.

Petrinovic, I.A., Martí, J., Aguirre-Diaz, G.J., Guzmán, S., Geyer, A., and Paz, N.S., 2010, The Cerro Aguas Calientes caldera, NW Argentina: an example of a tectonically controlled, polygenetic collapse caldera, and its regional significance: Journal of Volcanology and Geothermal Research, v. 194, p. 15–26.

Pingel, H., Alonso, R.N., Bookhagen, B., Cottle, J.M., Mulch, A., Rohrmann, A., and Strecker, M.R., 2023, Miocene surface uplift and orogenic evolution of the southern Andean Plateau (central Puna), northwestern Argentina: Proceedings of the National Academy of Sciences, v. 120, p. e2303964120.

Proingeo, Realizacion de estudios geofisicos mediante Magnetotelluria en el Salar de Pastos Grandes, Salta, Internal Report, 2021.

Richards, J. P., and Villeneuve, M., 2002, Characteristics of late Cenozoic volcanism along the Archibarca lineament from Cerro Llullaillaco to Corrida de Cori, northwest Argentina. Journal of Volcanology and Geothermal Research, v. 116, p. 161-200.

Seggario, R.E., 2015. Hoja Geologica, 2366-III, Susques, Provincias de Jujuy y Salta. Servicio Geologico Minero Argentino, Instituto de Geologia y Recursos Mineral.

Seggiaro, R.E., Guzmán, S.R., and Apaza, F.D., 2017, Control estructural sobre el magmatismo en los alrededores de San Antonio de los Cobres, sector oriental de la Puna Central, in Proceedings of the XX Congreso Geológico Argentino, San Miguel de Tucumán, Argentina, p. 7–11.

Seggiaro, R.E., Guzmán, S.R., and Martí, J., 2019, Dynamics of caldera collapse during the Coranzulí eruption (6.6 Ma)(Central Andes, Argentina): Journal of Volcanology and Geothermal Research, v. 374, p. 1–12.

UMass/UAA Lithium Solutions, Salar Water Budget - Pastos Grandes, July 2024 Update.

UMass/UAA Lithium Solutions, Preliminary Pozuelos Freshwater Availability Assessment, September 2024.

Golder, Measured, Indicated and Inferred Resource Estimate for Pozuelos Project, Salta, Argentina, GP69507A R.002_Rev 2, 8 January 2025.

24.0 RELIANCE ON INFORMATION PROVIDED BY THE REGISTRANT

Although copies of the tenure documents, operating licenses, permits, and work contracts were reviewed, an independent verification of land title and tenure was not performed. Golder has not verified the legality of any underlying agreement(s) that may exist concerning the licenses or other agreement(s) between third parties but has relied on the client's law firm to have conducted the proper legal due diligence for the claims discussed in Section 3.2.

Details on lithium market were obtained by iLiMarkets, who are global commodity experts, in a report titled iLi Markets Lithium Quarterly Market Review, dated October 2024. This information was used in Section 16.0.

Any statements and opinions expressed in this document are given in good faith and in the belief that such statements and opinions are not false and misleading at the date of this Report.

Signature Page

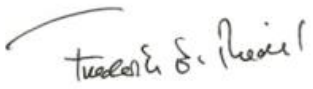

Frederik Reidel, QP, P. Geo.

James Wang, QP, P.Eng.